Detailed Technical Report on

Limestone
Calcined
Clay
Cement

LC³

Prepared by

Team IIT Delhi

Sponsor

Schweizerische Eidgenossenschaft
Confédération suisse
Confederazione Svizzera
Confederaziun svizra

Swiss Agency for Development and Cooperation SDC

Data from

EPFL ★TARA

Preface

Limestone calcined clay cement (LC^3) has been developed as a more sustainable alternative to other contemporary cements. It is a family of cement that can contain as low as 50% clinker ground with crushed limestone and calcined clay for structural applications. Compared to OPC, the production of LC^3 emits 30% less CO_2, consumes 18% less power and conserves limestone resources. With cement production accounting for 7% to 8% of the CO_2 emissions in India, just the replacement of 30% of cement in India by LC^3 can reduce the national CO_2 emissions by 0.5% to 1%. Additionally, the production of LC^3 can be more economical than fly ash based PPC in many scenarios that exist in India, supporting a faster development of the nation.

The development of LC^3 has been spearheaded by an international group of researchers from Switzerland, Cuba and India and it has been found that in most applications, LC^3 gives a better performance than other commercially available cement, despite the lower clinker content. With India making the largest contribution to the research and development, the cement has been extensively studied and found to be suitable for the country. IIT Delhi has played a leading role in the development of LC^3.

With standard already been accepted by the Bureau of Indian Standards, the standard for LC^3 is in advanced stages of acceptance by the standardization body. Internationally as well, the research from India has contributed to the acceptance of standards, such as by ASTM and EN. A wide support for the cement has also been received from the industry, that is preparing to start production of the cement once standards are in place.

Introduction

Asia being the largest producer of cement has the highest CO_2 emission contributions in the world. LC^3 presents a unique opportunity for the cement producers to reduce their CO_2 emissions by as much as 30%. LC^3 is seen as an especially attractive product for developing markets since it allows the growth of production with a relatively moderate capital expenditure. This document describes the policy support sought towards the acceptance of this more sustainable solution for the construction industry.

LC^3 International research team

LC^3 is a product from a collaborative relationship between the École Polytechnique Fédérale de Lausanne (EPFL) and the Centro de Investigación y Desarrollo de Estructuras y Materiales (CIDEM) of the Universidad Central "Marta Abreu" de Las Villas in Cuba. IIT Delhi, IIT Madras and TARA, the partners in India, played a major role in the development of the cement and its commercialization around the world. This project has been partially funded in all its stages by the Swiss Development Cooperation, SDC (www.eda.admin.ch/sdc).

What is LC^3?

LC^3 (Limestone Calcined Clay Cement) is a cement that is a product of a collaborative relationship between the École Polytechnique Fédérale de Lausanne (EPFL) and the Centro de Investigación y Desarrollo de Estructuras y Materiales (CIDEM) of the Universidad Central "Marta Abreu" de Las Villas, funded by the Swiss Development Cooperation, SDC (www.sdc.ch). This new family of cements can reduce up to 30% of CO_2 emission to the atmosphere using a blend of clinker, calcined clay, limestone and gypsum, the most common proportions being : 50% clinker, 30% calcined clay, 15% limestone and 5% gypsum.

The major innovation in LC^3 is to combine the around 30% substitution of relatively abundantly available low-grade kaolinite clay with a further 15% of crushed limestone, which can maintain the

same mechanical and long-term performance as the reference Portland cement. This is due to the synergy between the three key components of LC^3, as shown in the figure below.
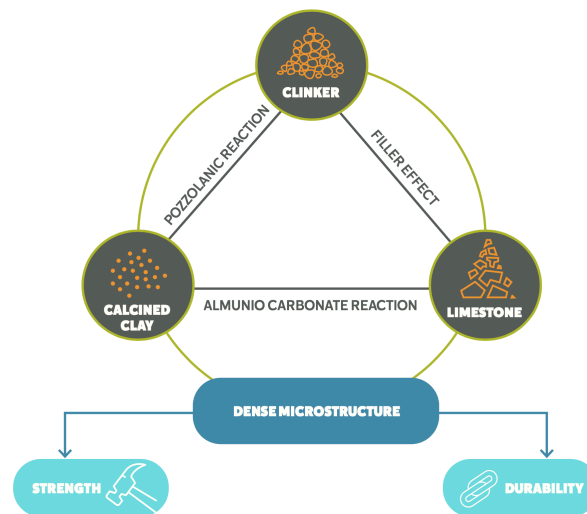
Reduced clinker content, decreased fuel consumption for calcination compared to clinker plus the fact that the added crushed limestone does not need to be heated contribute to lower production costs. The lower cost of production and the lower clinker content are expected to be the main drivers for the uptake of the LC^3 technology. It is important that LC^3 can be produced with existing manufacturing equipment, leading to only marginally increased investments for calcining equipment. LC^3 also helps in ecological conservation by allowing the utilisation of lower grade raw materials.

The rapidly growing interest of the cement industry in the LC^3 technology attests to its economic attractiveness and its feasibility as a driver of sustainable development.


LC^3 experience in India

The work on LC^3 started in 2005, through a collaborative research project funded by the SNSF-SDC in two phases (2005-2008 and 2009-2011), which led to the development of a new ternary binder based on the synergy between calcined clay and limestone

An industrial trial of 130 tonnes was carried out as early as in 2013 in Cuba, and it has proven the potential of producing LC^3 with a clinker content of approximately 50% even in challenging technical conditions. The initial work in India focussed around understanding the calcination of clays and the production of the cement. In 2013, as a first trial, around 10 tonnes each of four batches of the cement were produced in a small cement mill in West Bengal. The clay had earlier been calcined using furnaces used by the ceramics industry. These trials were carried out without any support from the cement industry, leading to a relatively sub-optimal production. Despite this, the cement displayed excellent performance and usability, as was demonstrated by the structure built by TARA at its premises in Orchha in 2014. This demonstration cemented the high potential of LC^3 to serve as a sustainable alternative to existing technologies. Since then, with the support of SDC, a large volume of research has been produced put together by a of researchers, both in India and internationally in Switzerland

and Cuba. The development of LC^3 witnessed a tremendous boost as it gained recognition around the world and researchers from outside the core team also started working on the subject. A quick analysis of research carried out on "calcined clay cement" using the tool Scopus shows an exponentially increasing interest in the subject.
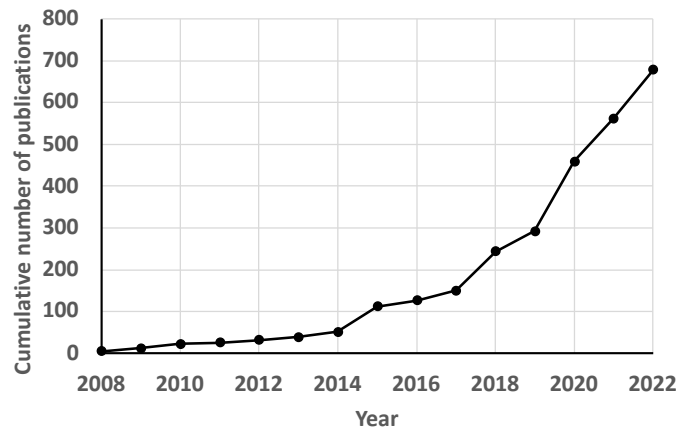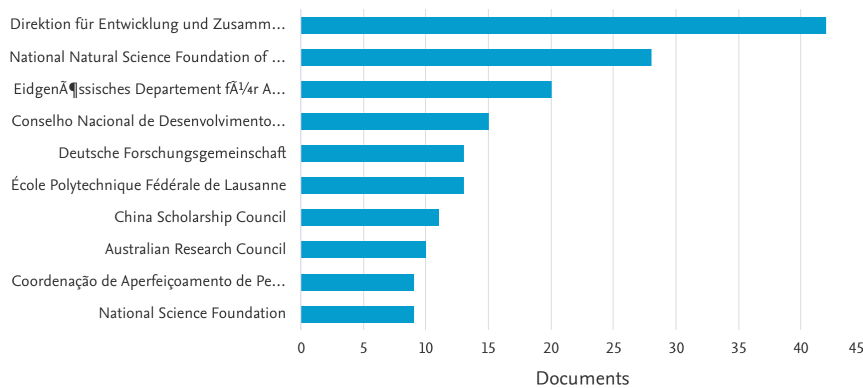

(Data from scopus.com)

While India leads the number of publications on the subject, research on LC^3 is being increasingly taken up by researchers around the world, as can be seen in the graph below.
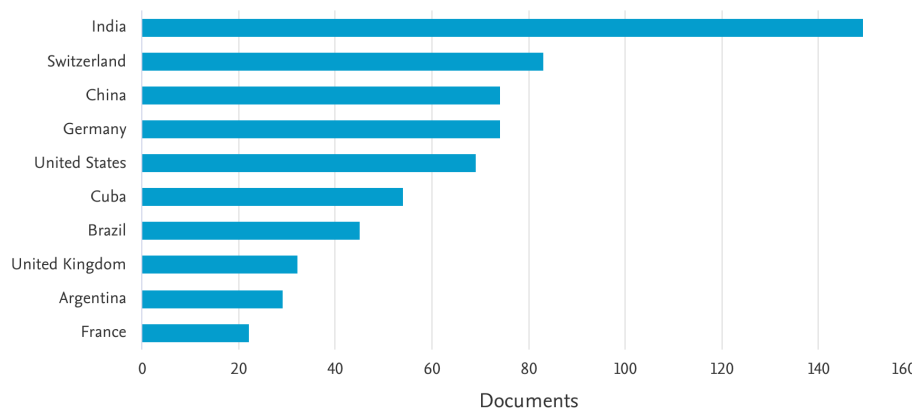
(Figure from scopus.com)

In addition to the above, the subject has been attracting funding from several sponsors other than SDC as well.

(Figure from scopus.com)

The data above clearly shows how scientific research, coupled with field experience, has driven the acceptance of the cement by the industry. As a testament to this, a detailed report on LC^3 compiled by IIT Delhi, detailing the work carried out by all the Indian partners, including IIT Bombay, IIT Madras and TARA, was accepted by the Bureau of Indian Standards (BIS). The BIS released a draft standard on LC^3, that would eventually allow the commercial production of LC^3 in India. The quick acceptance of LC^3 by various stakeholders is exemplary. Draft cement standards like for Portland limestone cement have been in the process of standardisation for more than 15 years with little to show in terms of progress.

Thousands of tonnes of LC^3 has now been produced in India on a trial basis. The calcination of clays and the production of LC^3 using various types of technologies is now well understood by the LC^3 team in India. The LC^3 India team, now possesses the expertise and resources required to support the uptake of LC^3 by the cement and construction industry, not only in India, but also abroad.

Relevance of LC^3 to cement companies

World cement production accounts for 8% of worldwide CO_2 emissions; concrete, made of cement, is the second most used material after water. The negative impact of cement industry mainly comes from:

- Decarbonation of limestone
- Fuel burned to heat the raw materials in a kiln to 1450°C to form clinker.
- The use of the electrical energy to grind the raw materials and clinker

Therefore, many cement producers are pursuing alternatives to reduce CO_2 in a context where fly ash and coal are severely questioned because of their impact on CO_2 emissions, with the incentive of green funds supporting new green initiatives and green taxes punishing CO_2 emissions. In additional, the supplies of good quality fly ash continue to reduce with time. In this context LC^3 appears as a very attractive option, offering a reduction of 30% of CO_2 emissions with minimal capital investments and an improved performance at early ages in comparison with average cements.

The feasibility of the new material is based on:

Low Carbon: LC^3 can reduce up to 30% of CO_2 emissions per tonne of cement.
Low Cost: LC^3 requires less energy and can be made using fairly low grade and low-cost clays.
Low Capital: LC^3 does not require substantial capital investment and can be produced in existing plants with lower operational costs.

Properties and performance of LC^3

With the support of the Swiss Agency for Development and Cooperation, a very large research programme has been implemented by the research partners. Considering that a lot of our knowledge of other cements relies on data that was obtained decades ago on materials that were very different from the ones used today, LC^3 is one of the best understood cements today. From our current understanding, LC^3 is seen to be economically and technically superior to other alternatives in many realistic scenarios. A summary of the key properties of LC^3 is listed below.

- The capital expenses for plants required for the production of LC^3 are significantly lesser than plants of similar capacity for producing other cement types. LC^3 can help in achieving faster growth of the cement industry at lower capital expenses.
- The operational expenses for the production of LC^3 can be significantly lesser than those for other cement types in most scenarios.
- LC^3 can be produced using lower grades of limestone and clays that are often available as waste materials.

- Raw materials required for the production of LC^3 are abundantly available throughout India. Their easy availability in regions where other supplementary cementitious materials like fly ash are not available is especially interesting.
- The production of LC^3 emits 30% to 40% less CO_2 and consumes 20% to 30% less energy than other cements.
- LC^3 can be used in the same manner as other cements currently available, without the need for any special training of the workforce. In fact, LC^3 has been found to be less vulnerable to many poor construction practices.
- Despite the lower clinker content (currently proposed to be 50% and expected to be as low as 35% in the future), LC^3 gains similar compressive strength as other cements.
- LC^3 has been shown to meet durability requirements in most environmental conditions present across India. Concrete produced with LC^3 is seen to be more durable than other cements in environments with chlorides, sulphates and alkalis, as is common across India.

This document summarises the key aspects of the knowledge currently available on LC^3. Subjects from the production of the cement to the durability of concrete and the economy of production of cement are covered. At the end, the report also presents short papers on specific subjects that are important to understand the technical performance of LC^3.

Despite the extensive knowledge available today on LC^3, it is expected that further research will continue to be required to answer questions new research questions that will come with the increased uptake of the cement.

Summary
This document presents the history of development of LC^3, along with its properties, performance, and the value that the cement offers. LC^3 offers a unique opportunity for India since it is a technology that is not only sustainable but also commercially attractive. A major part of the research on LC^3 having taken place in India, LC^3 has been shown to be a cement that is suitable for production and use in the country.

This document has been compiled by the team at the Indian Institute of Technology Delhi, including Aastha Singh, Bharati Thakur, Mehnaz Dhar, Aayush Gupta, Akash Mishra, Amit Kumar, Ashirbad Sathapathy, Gopala Rao D., Lav Singh, Lupesh Dudi and Shashank Bishnoi. This report has also taken excerpts from the earlier detailed report that was compiled at IIT Delhi by Anuj Parashar, Arun C Emmanuel, Srijeeth Krishnan, Vineet Shah and Shashank Bishnoi.

The chapters in this document detail work that has been jointly carried out by EPFL Switzerland, UCLV Cuba, TARA, IIT Delhi and IIT Madras.

Table of contents

1.1 Introduction

For thousands of years, cements of various forms have contributed to the development of civilisation. Historical monuments made using cements composed of simple dried clays to relatively more sophisticated lime or gypsum are to be seen around the world. The cements used in these monuments are a good testimony of the geology of the region and the technology available at the time of construction. For example, while a mixture of lime and volcanic ash, primarily composed of siliceous and aluminous materials, was commonly used in the Roman Empire, a similar mixture of lime and surkhi (a red-coloured burnt clay) is widely found in monuments in India. It is remarkable that over the centuries, most of those technologies slowly converged and the cements used around the world today are reasonably similar. It was in the 19th century that Portland cement established itself as the most widely used binder in construction. This was mainly due to the easy availability of the materials and technology required to produce cements in this family. With the advent of Portland cement, the role of clays in cements, other than as a source of silica and alumina, all but receded to the background. With the development of Limestone Calcined Clay Cement (LC³), clays offer a promising solution to several challenges being faced by the cement industry today. This chapter discusses how cements have evolved over time, the important role they play in the world today, the challenges faced by the industry and possible solutions to these challenges.

1.2 Portland Cement

While gypsum and lime based cements have been historically used as binders, they were known to not be particularly resistant against erosion in water mainly due to the relatively high solubility of the calcium compounds, such as hydrated calcium sulphate and calcium hydroxide, that formed on the hydration of these cements. It was found that the addition of alumino-silicates like clays significantly improved their water-resistance. While some clays, like volcanic ashes, could be directly mixed with the cements, others had to be calcined to achieve reactivity. Although it was not well understood then, the addition of alumina-silicates produced a new class of products known as calcium alumino-silicate hydrates, which are practically insoluble, and thus resistant against water.

In the early 19th century, Portland Cement, also known as Ordinary Portland Cement (OPC), a hydraulic cement, inherently resistant against water, was developed and popularised. As this cement was produced by firing lime, silicates and aluminates together at high temperatures, calcium-silicate hydrate (C-S-H), was one of the main products of its reaction with water. However, since OPC still contains large amounts of calcium, significant quantities of calcium hydroxide (CH) are also formed as hydration product. CH, along with the other alkalis in cement, maintains a high pH and provides alkaline reserves in cement pastes. A further conversion of this remaining CH to C-S-H by the addition of reactive silica is accompanied with an increase in strength and reduction of porosity of cements. This is achieved by the addition of Supplmentary Cementitious Materials (SCMs) to Portland cement. By the end of 20th century, Portland cements blended with SCMs such as blast-furnace slag and fly ash, became the most widely used cements. Apart from improving the performance of cements, these cements also help in reducing the environmental impact of cement production.

It is estimated that over 4 billion tonnes of cement is produced globally. Although this cement is used for a wide-range of purposes such as binding of bricks, stabilisation of soil, production of building materials, etc., plain and reinforced concrete account for the majority of its consumption. Today, concrete accounts for more than 50% of all man-made materials produced annually. Such large quantities are only possible due to the versatile nature of concrete since it can be produced with locally available materials and technology. Additionally, most of the materials can be used in almost their virgin form, without much processing. This makes concrete a low cost, low embodied energy and environment-friendly material. Cement is the only major component of concrete that has a high embodied energy since it is produced by converting stable natural materials into reactive phases.

Furthermore, the production involves the conversion of calcium carbonate in limestone to calcium oxide, releasing mineral CO_2 into the atmosphere. Cement production is responsible for over 7% of global anthropogenic emissions. Still, as cement only makes around 15% of the concrete's volume, the latters embodied energy and CO_2 footprint is significantly lower than many other construction materials like bricks, steel and even timber.

There have been many efforts to look for alternatives to concrete, however, as discussed above, since concrete can be produced from a wide range of locally available materials without significant amounts of processing, it is difficult to find alternatives with a lower embodied energy and cost. Even replacing the binder in concrete is difficult due to the limited materials available in the earth's crust. Oxygen, silicon, aluminium, iron, calcium, sodium, potassium and magnesium make more than 97% of the earth's crust. Therefore, any material that is produced in such large quantities as cement can only be produced from a combination of these elements. It is after thousands of years of trials with various other combinations of these elements that Portland cement became the preferred cement. It must be recognised that the fact, that a material that makes 50% of the total production produces only 7% of the emissions, attests to the environment friendliness of the material.

Still, several possibilities to further improve the environment-friendliness of cement exist. While elaborate techniques such as carbon capture, storage and sequestration are often touted as solutions, their practical limitations, cost-implications, focus on the symptom and failure to address the root problem are often overlooked. It must be recognised that any solution that can reduce the environmental footprint of cement production must be possible for implementation at such a scale that matches the scale of cement production. SCMs offer the only such solution.

1.3 Supplementary Cementitious Materials and LC³
Blast-furnace slag, fly ash, silica fume, calcined clay (clays processed at high temperatures) and limestone are some of the most commonly used supplementary cementitious materials. While slag, arguably, has the highest potential to reduce the energy and CO_2 intensive clinker content in cements, it is available in limited quantities world-wide since the production of steel is much less than cement production. Most of the usable slag today is already consumed by the cement industry. On the other hand, despite the wide availability of fly ash, it can only replace 25% to 35% of clinker. Other materials such as silica fume and rice husk ash, though good potential local solutions, are available in minor amounts compared to the global cement production.

Clays are alumino-silicates that are usually stable in neutral and alkaline conditions. Calcined clays are produced by thermally treating clays to temperatures typically between 600˚C and 900˚C. At these temperatures, there is a loss of hydroxyl groups bound in the chemical structure of the mineral kaolinite, rendering it highly reactive in alkaline conditions. Although Illite, montmorillonite and other minerals in clays are also known to become reactive when processed at slightly higher temperatures, they are rarely used as SCMs. When clays of high purity kaolinite are calcined, they are known as metakaolin. Metakaolin is significantly finer and more reactive than normal calcined clay and its replacement is generally limited to 10% to 15% of weight of cement.

Supplementary cementitious materials (SCMs), although unreactive with water on their own, hydrate in the alkaline environment of cement paste and produce new hydration products in the cement microstructure. Most SCMs are amorphous or poorly crystalline alumino-silicates that dissolve in high pH solutions when hydroxyl ions attach themselves to their silicate chains. SCMs have been used in construction for thousands of years with the oldest available references being of a volcanic ash from the region of Pozzoli, known as pozzolana, which was

widely used in combination with lime in the Roman Empire. For this reason, SCMs are also popularly known as pozzolanic materials and the cements using them are known as Portland Pozzolanic Cements (PPCs). Typical composition ranges of commonly used SCMs are diagrammatically represented in the ternary CaO-SiO_2-Al_2O_3 phase diagram below (Figure 1.1).
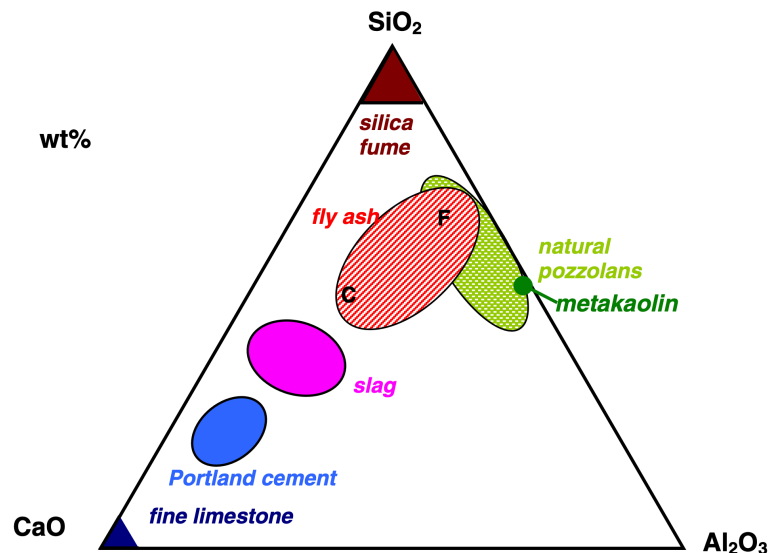
Figure 1.1: Ternary phase diagram of OPC and SCMs (Lothenbach et al. 2010)

Due to the limited quantities and geographical availabilities of natural pozzolanic materials, today industrial by-products such as blast-furnace slag and fly ash are more commonly used as SCMs. Although most SCMs start to react only after sufficient reserve alkalinity is built up in the paste, they start to influence hydration from the start. The influence of the SCMs on the initial rate of hydration depends on their physical and chemical properties. While SCMs like metakaolin and silica fume tend to accelerate hydration, fly ash and slag tend to retard the process. SCMs with high alkali contents also tend to accelerate hydration. The formation of secondary hydration products such as C-S-H and C-A-S-H from the pozzolanic reaction leads to a further development of the mechanical and transport properties of cement paste.

Calcined clays are more reactive than fly ash and slag and known to increase water demand in concretes. Their replacement is generally limited to 25% to 35% of the weight of cement. At the early age, calcined clays accelerate the hydration of clinker and increase the heat of hydration. The aluminates of the calcined clay also participate in the early hydration. Replacement by calcined clay leads to an increase in the early and long-term strength of concrete due to the formation of secondary C-A-S-H, AFm and AFt phases. The permeability and chloride penetration in concrete are known to reduce due to the refinement of the pore-structure from these secondary products. Like other SCMs, calcined clays also reduce the reserve alkalinity of concrete, leading to an increase in the rate of carbonation.

SCMs are used both as additives in commercially available cements and as admixtures for concrete. The addition of SCMs directly to the cement ensure a better compatibility between the clinker and the SCM and also allows for a more homogenous blending of the powders due to processes such as grinding or air-blending. Ensuring a proper distribution of the particle sizes may at times be difficult when clinker is interground with an SCM with a different

hardness, as is common in the case of slag. This is usually overcome by separately grinding one of the components, either partially or fully, and then blending the components together. The use of SCMs as a mineral admixture in concrete allows greater flexibility and adaptation to the application. The proportions of cement and SCM in different concrete mixes can be adjusted in order to achieve the required performance parameters such as workability, strength, permeability, etc. This also allows an easier adjustment of the mix design to site and weather conditions.

Table 1.1 below summarises the main aspects of the use of SCMs including the typical amounts mixed with cement, their influence on strength and durability and their usual availability.

Table 1.1: Summary of commonly used SCMs with cement

Parameters	GGBS	Fly ash	Silica fume	Calcined clay
Replacement level	40-70%	25-35%	2-10%	10-35%
Strength at 3days	Reduced	Reduced	Increased	Increased
Strength at 28 days	Reduced or no effect	Reduced or no effect	Generally increased	Generally increased
Permeability	No effect	Reduced	Reduced	Reduced
Chloride Ingress	Reduced	Reduced	Reduced	Reduced
Carbonation	Increased	Increased	Reduced	Increased
Availability	Limited	Abundant in come countries, limited in others	Very limited	Abundant (manufactured)
Remarks	Excellent in performance but limited availability	Abundantly available, but limited replacement level.	High cost, low replacement possible.	Limited usage

As can be seen in the table above, each of the SCMs has pros and cons for use in concrete. However, the choice of SCM in most applications depends more on the availability since the availability of most SCMs is much less compared to cement production, especially in high cement consumption economies.

SCMs also affect the economy and sustainability of cement production. The partial replacement of clinker by SCMs in cement allows an increase in the cement production capacity of cement plants without significant additional investment. Additionally, reduced operational expenses result from the lower production or procurement cost of SCMs compared to clinker production costs. Depending on their hardness, some SCMs may also reduce the energy required for grinding of the cements. However, slags and high-crystalline content fly ashes are known to increase grinding energy and wear of mills. Since SCMs require less processing than clinker and do not require the calcination of limestone, their use in cement also reduce the energy requirement and CO_2 emissions associated with cement production.

1.4 Limestone cements

Apart from being used as the raw material in clinker production, limestone is also used as a partial replacement of clinker and is ground along with it in cement. Replacement of up to 30% of clinker by limestone is now common. Limestone is known to reduce water demand in concrete and increase its cohesion. At the early ages, limestone slightly increases the rate of hydration of the clinker phases. Although it was earlier assumed that limestone is inert and does not react in the cement paste, it was later found to react with aluminate phases and form carbo-aluminate phases. It has also been observed that the presence of carbonates in the solution prevents the conversion of ettringite to monosulphate by themselves reacting with aluminates upon the exhaustion of excess sulphates in the solution. Due to these chemical processes, limestone can also be considered to be an SCM. The replacement of clinker by limestone allows the consumption of lower grade limestones that are not suitable for clinker production and the reduction of energy and emissions from cement production. Limestones containing both siliceous and dolomitic impurities can be ground along with clinker. The presence of magnesium in an uncalcined form does not lead to unsoundness of the cement, which is known to occur due to the presence of calcined magnesium oxide (periclase) in clinker. It has been reported that there is little loss in mechanical and durability performance of cements up to 10% to 15% of replacement of clinker with limestone or dolomite, however a reduction in performance has been observed at higher replacement levels. Because of this, many standards allow the inclusion of 5% to 10% of ground limestone in OPC. The production of Portland Limestone Cement (PLC), with up to 30% limestone content, is also permitted by many standards.

1.5 Ternary cements

The use of ternary blended cements, where two SCMs are used together, is increasing around the world. Ternary blends allow a more efficient utilisation of clinker, at the same time allowing cements to be tailored to specific applications. The two SCMs are generally chosen in such a way that they complement each other's properties and do not negatively interfere with each other. Although sometimes the blends could be based on synergistic interactions between two SCMs, this is not always the case. One common type of ternary cement contains a mixture of fly ash and slag along with clinker. While finely ground fly ash partially compensates for the low early-strength due to slag, slag compensates for the low calcium content in fly ash. Such combinations allow the reduction of clinker contents below those possible using only a single SCM and to improve the performance of the cement. In another example, a blend of fly ash and silica fume can be used where fly ash compensates for the high heat of hydration due to silica fume and silica fume can compensate the relatively slower strength development in fly ash cements. No chemical synergy is expected in such a blend and fly ash and silica fume compete for the same Portlandite for their reaction. The synergy between limestone and calcined clay in LC^3 is discussed in the next section.

1.6 Synergy between limestone and calcined clay

It is possible to design ternary blends such that the two SCMs used reinforce each others effects. One such blend is of limestone with calcined clay. Calcined clays and limestone are the only two materials available in the large quantities that are required for cement production. However, more than 10% to 15% of replacement of clinker by limestone leads to a significant loss in performance. Similarly, the replacement of more than 20% to 25% of clinker by calcined clay can significantly increase water demand and reduce performance. It

has been found that when used in combination, limestone and calcined clay can replace more than 50% of clinker in cement, without any loss in performance. This technology has the potential to not only tremendously reduce the energy consumption and CO_2 emissions associated with cement production, but also to allow more efficient utilisation of natural resources. Most importantly, this is possible at capital and operational costs that are lower than those that exist currently in the industry.

As has been discussed above, while limestone has been observed to react with aluminates in cement, the relatively small amount of aluminate in clinker limits this reaction. The presence of calcined clay along with limestone provides additional aluminates that are required to react with limestone. A chemical synergy is thus achieved between the components of this ternary cement, as is shown in the figure 1.2 below.
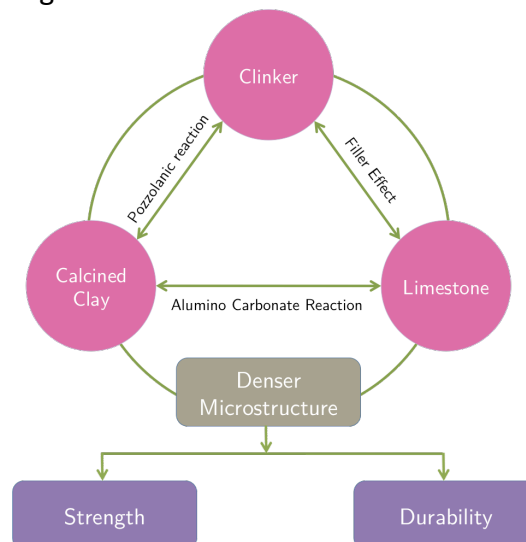
Figure 1.2: synergy between clinker, limestone and calcined clay

The alkaline environment provided by the clinker phases increases the dissolution of both calcined clay and limestone. While some of the alumino-silicates from the calcined clay react with the Portlandite that is produced from the hydration of clinker phases to produce C-A-S-H, the remaining aluminates react with the carbonates to produce carbo-aluminate phases. The limestone also reacts with the aluminates in clinker completing the three-way nature of the reaction. While the reactions occurring in this system are quite complex, a simplified unbalanced representation of the reactions is shown below where C-A-S-H and monocaroaluminate ($C_4A\bar{C}H_{11}$) are formed.

$$AS_2 + C\bar{C} + CH \rightarrow C\text{-}A\text{-}S\text{-}H + C_4A\bar{C}H_{11}$$
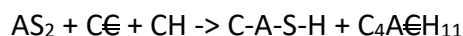
Additionally, as discussed earlier, the presence of carbonates prevents the conversion of ettringite formed from the hydration of the aluminates in the clinker and the calcined clay to monosulphate. Since both ettringite and carbo-aluminate phases occupy space and reduce porosity, their formation leads to an increase in the strength of concrete. Due to the synergistic effect of limestone and calcined clay, the 28-day compressive strength of limestone-calcined clay cements (LC^3) made using less than 50% clinker has been observed to be of the same order as that of OPC made using the same clinker (Figure 1.3 below).
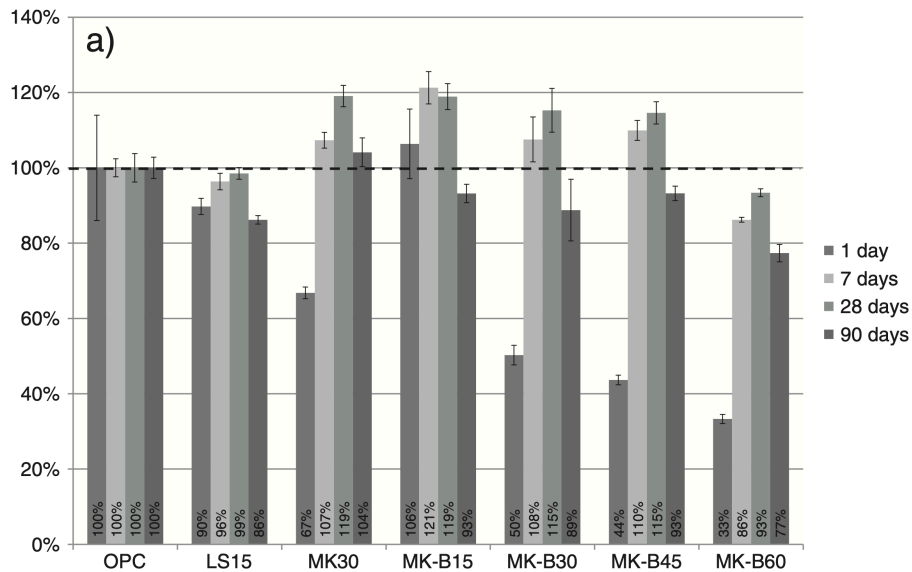
Figure 1.3: Comparison of strength between OPC and LC³ with various replacement levels (Antoni et al. 2012)

In addition to the above, calcined clay and limestone also have complementary physical properties. Limestone partially compensates for the increased water demand of calcined clays allowing high replacement levels without significant increase in water demand. Furthermore, the presence of three components with different hardness in the cement allows for a wider particle size distribution, resulting in a better packing of the cement. This results in improved mechanical and transport properties of concrete.

This report presents the technology behind the production and usage of Limestone Calcined Clay Cement, or LC³ in short. This cement presents a unique opportunity for the cement industry to reduce their energy consumption, CO_2 emissions, capital investment and operational costs using a single technology.

Chapter 2: Clay Minerology, Identification and Locations

2.1 Clay Minerology

Clay minerals are constituents of the earth crust and formed by weathering and chemical modifications of alumino-silicate minerals in hydrothermal environment. They have hydrated aluminosilicate structure in which water molecule is either loosely bound between layers or strongly held by hydroxyl group. It belongs to phyllosilicate group and imparts plastic property to the clay at appropriate water content. There is no well-defined criteria of size as geologist commonly define clay minerals as particles with size of 2 μm and below, while soil scientists describe 4 μm and below size (Moore et al. 1989 and Alujas et al. 2022). Clays are composed of fine-grained fraction of rocks like shales, mudrocks, claystone, siltstone and sediments. They are broadly classified on the basis of particle size distribution and plasticity limit.

Clay minerals are the natural weathering product of many of the most common rock-forming silicates. During weathering, the content of feldspar is distorted by hydrolysis process results in formation of clay minerals such as kaolinite as shown in figure 2.1. Clay can incorporate with one or more clay minerals even in presence of minute quantities of quartz (SiO_2), metal oxides (Al_2O_3, MgO etc.) and organic matter. They typically form as a product of the interaction of silicates and water at ambient or near-ambient conditions. As such clay minerals slowly accumulate at or near the surface of atmospherically exposed rock bodies or in the shallow subsurface. Clay minerals also form in hydrothermal settings by alteration of aluminosilicate parent rocks. Usually formed as loose, fine grained particles, clay minerals are easily eroded and transported by water or air and, when redeposited, can form thick layers of clay sediments. Clay rocks make up about 70% of the sedimentary rocks and about a third of the rocks outcropping at the surface of continents. In sedimentary environments clay minerals may still undergo further chemical and mineralogical transformation during burial. Clay deposits formed by in situ alteration of parent rocks are termed primary, and deposits formed by accumulation of eroded and redeposited clays are classified as secondary.
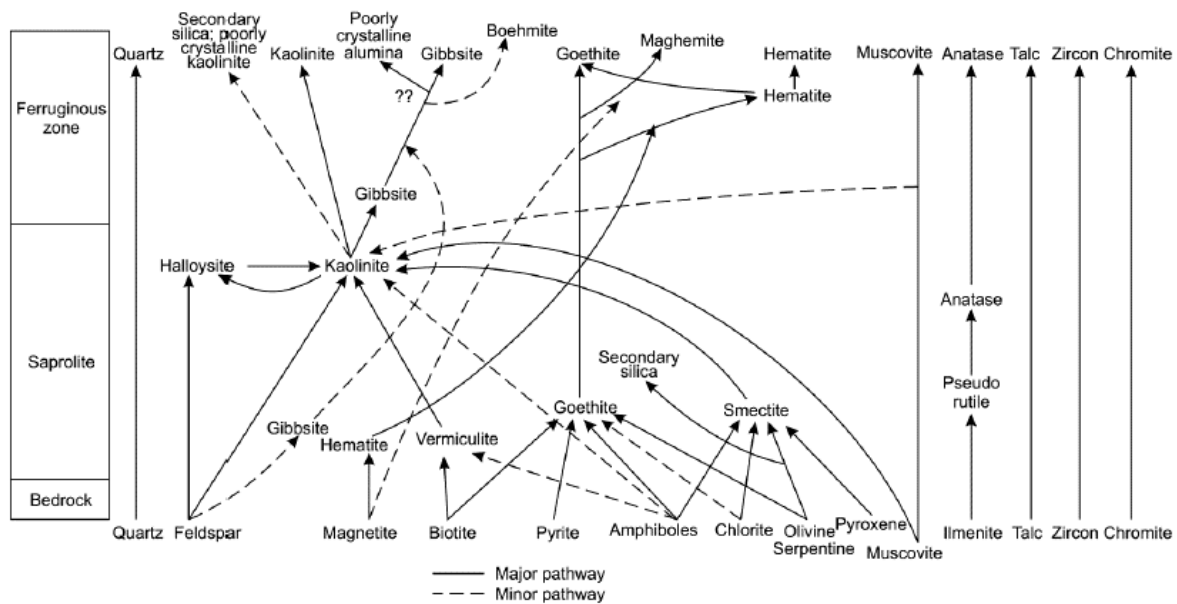

Figure 2.1: Common weathering pathways for clay formation (Alujas et al. 2022).

While hydrothermal alteration may be important for clay mineral formation at a local scale, the global distribution of clay minerals is mainly dictated by weathering mechanisms. The two most used clays

as raw materials for SCMs, kaolinites and smectites, are also the most common end-products of weathering of non-sedimentary rocks. Prevailing climatic conditions over long periods of time determine weathering intensity; therefore, there is a direct link between relative abundance of clay minerals and regional climate. Weathering mechanism associated with cold climates favor the formation of illite and chlorite, while in wet tropical and equatorial climatic conditions, clay minerals from kaolinite group and Al–Fe (hydr)oxides are the main components of the fine fraction of soils. The association and spatial distribution of clay and non-clay minerals in a given clay deposit depend, to a large extent, on the complex chemical reactions between the parent rock and the surrounding environment. Kaolinite is typically formed as an end-product of the intense weathering of aluminosilicates.

Alteration reactions of rock-forming aluminosilicates result from either surface weathering or circulation of ground or hydrothermal waters in the underground. Surface weathering may produce soil profiles enriched in kaolinite that can be tens of meters in thickness. In addition, kaolinite can be formed from a wide range of common aluminosilicate rocks, ranging from more acidic (granites, etc.) to more basic (basalts, etc.). A relatively acidic pH, a moderate silica activity and low amounts of (earth)-alkalis are required conditions to precipitate kaolinite. Such conditions typically develop in tropical soils where a combination of organic acid derived from organic matter and intense rainfall cause extensive leaching of alkali and earth-alkali metals (Blatt et al. 1972 and Pruett 2016). The global distribution of the most abundant clay minerals is given in figure 2.2. Clearly, kaolinite is very abundant in tropical, humid regions over the entire soil profile. In cooler but also in arid regions kaolinite is much less abundant indicating the need for suitable conditions for chemical weathering.
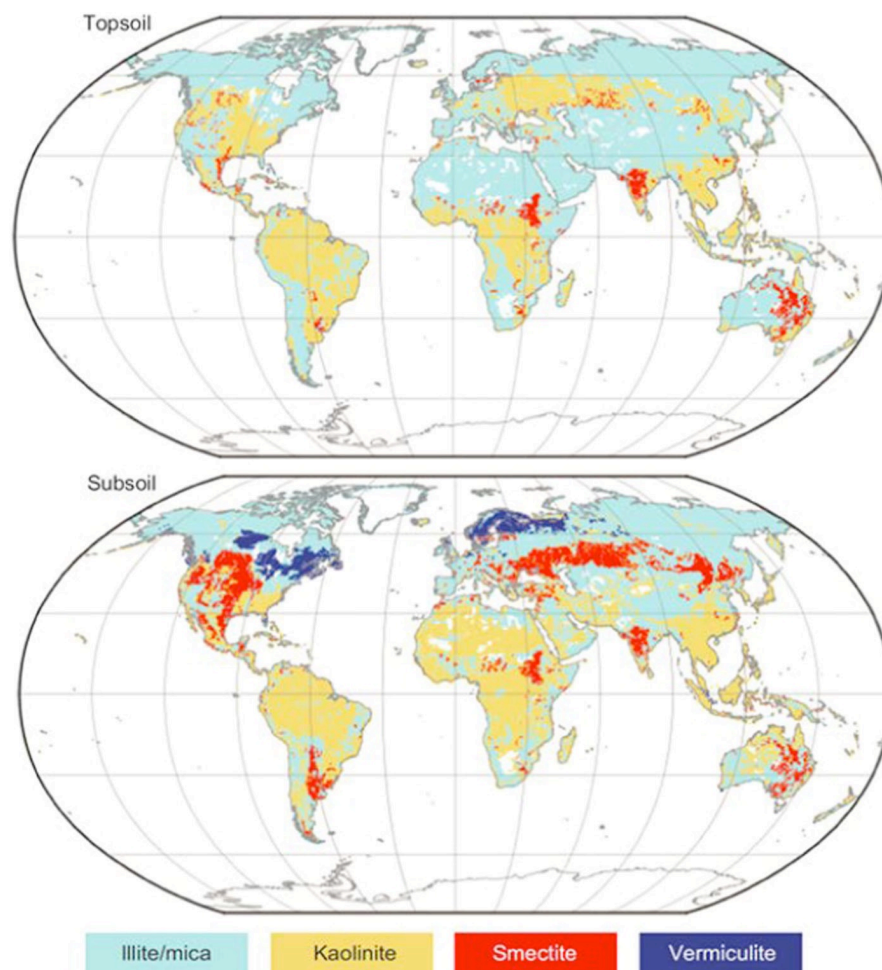

Figure 2.2: Global distribution of most abundant clay minerals (Alujas et al. 2022).

Structure and chemical composition of clay minerals

The properties that define the composition of clay minerals are derived from chemical compounds present in clay minerals, symmetrical arrangement of atoms and ions and the forces that bind them together. The clay minerals are mainly known as the complex silicates of various ions such as aluminium, magnesium and iron. On the basis of the arrangement of these ions, basic crystalline units of the clay minerals are of two types:

a. silicon – oxygen tetrahedron consists of silicon surrounding by four oxygen atoms and unite to form the silica sheet.

b. aluminium or magnesium octahedron consists of aluminium surrounding by six hydroxyl units and combine to form gibbsite sheet or brucite sheet.

Tetrahedral sheet

The basic building block of tetrahedral sheet is a unit of Si atom surrounded by four oxygen atoms known as silica tetrahedra. The tetrahedral sheet is formed by sharing of three oxygen of each tetrahedra with three nearest tetrahedra as shown in figure 2.3. These oxygen atoms are known as basal oxygen which connect pairs of all tetrahedra together (more or less) in one plane whereas the fourth oxygen atom remain free and form the bond with other polyhedral elements known as apical oxygen. Apical oxygens are all in a separate plane and provide a link between both tetrahedral and the octahedral sheet. As only one apical oxygen is present per tetrahedron therefore, each tetrahedron shares a corner with an octahedron in the octahedral sheet. The tetrahedral sheet can carry negative charge due to the isomorphous substitution of Al^{3+} in place of Si^{4+} that generates the charge deficiency in tetrahedral sheet. Common tetrahedral cations are Si^{4+}, Al^{3+}, and Fe^{3+}.
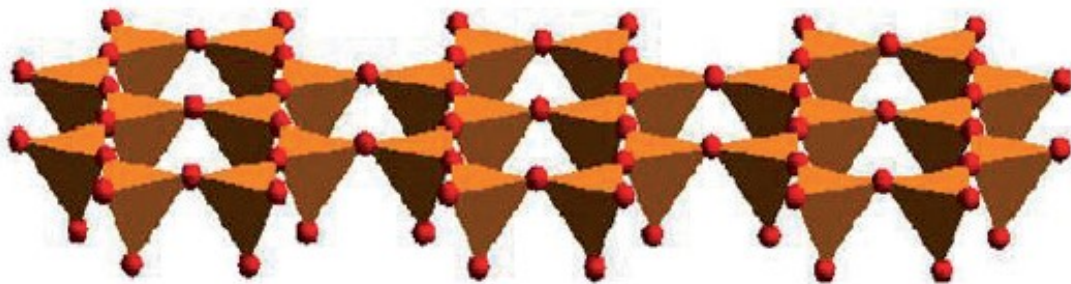
Figure 2.3: Arrangement of tetrahedral unit to form the tetrahedral sheet

Octahedral sheet

The main dominating atom in octahedral sheet is alumina cation that are surrounded by six oxygen atoms or hydroxyl group that give rise to eight-sided building block known as octahedron. Since, octahedral sheet is present in two forms: dioctahedral or trioctahedral sheet. When aluminium having three positive valences present in the octahedral sheet, only two-thirds of the sites are filled so that the charges will be balanced which results in formation of dioctahedral sheet. When magnesium having two positive charge valences is present, all three positions are filled to balance the charge which results in formation of trioctahedral sheet. Therefore, for di – octahedral sheet, Al^{3+} is the main dominating atom with $Al_2(OH)_6$ a unit cell formula where two Al^{3+} atoms coordinated with six oxygen/or hydroxyl ions. In tri – octahedral sheet, Mg^{2+} is the main dominating atom where three Mg^{2+} atoms are coordinated with six oxygen/or hydroxyl ions having a unit cell formula of $Mg(OH)_2$. Gibbsite ($Al_2(OH)_6$) and brucite ($Mg(OH)_2$) are the minerals which are generally present. The octahedral sheet is formed by sharing of two oxygen of each octahedra when various octahedra linked together horizontally as shown in figure 2.4.
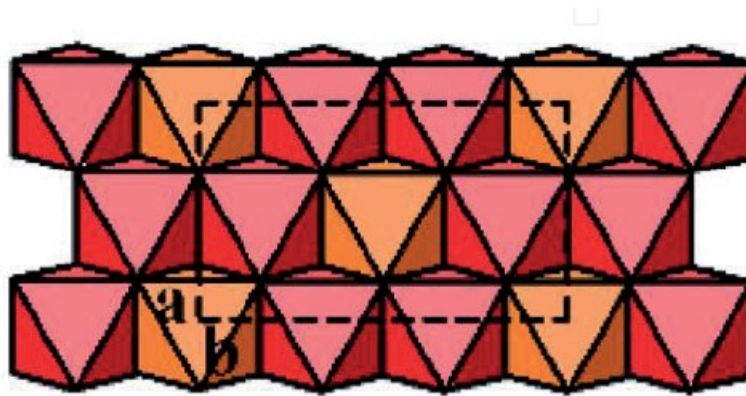
Figure 2.4: Arrangement of octahedral unit to form the octahedral sheet

The difference in the composition of clay minerals occurs very frequently when substitution of ions takes place within the mineral structure. The substitution of Si^{4+}, Al^{3+}, and Mg^{2+} takes place with other cations with comparable ionic radii in their respective tetrahedral and octahedral sheets due to weathering. Consequently, in the centre of the tetrahedron, replacement of Si^{4+} by Al^{3+} without changing the basic structure of the crystal takes place. Moreover, in octahedron, Al^{3+} and Mg^{2+} cations are replaced by the ions such as $Fe^{3+/2+}$ and Zn^{2+}. This process is known as isomorphous substitution where one structural cation is replaced by another of similar size and this kind of replacement signifies the primary cause of both negative and positive charges in clay minerals. For example, the substitution of one Al^{3+} for a Si^{4+} in the tetrahedral unit creates one negative charge. Alternatively, replacement of a lower valence cation by a higher valence (Fe^{2+} by Fe^{3+}) cation results in a gain of one positive charge. The net charge of the clay mineral is determined by after balancing electron loss and gain within the structure. In most soils, the net negative charge exceeds by a positive charge after substitution.

Classification of clay minerals
The aluminosilicate layers comprise of the basic structural units of phyllosilicates which is formed by the combination of tetrahedral and octahedral sheets bound by shared oxygen atoms. Both the tetrahedral and octahedral sheets are the main components of phyllosilicates and are bounded together by sharing of oxygen atoms into different layers. Phyllosilicate are the most common clay minerals that consists of Si dominating tetrahedral unit and Al dominating octahedral unit which are arranged in to sheet form. Based on number of tetrahedral and octahedral sheets and their arrangement, the phyllosilicates are divided into following categories including layer and chain silicates, sesquioxide and other inorganic minerals:
Clay can be classified depending on the way that the tetrahedral and octahedral sheets are packed into layers. The major groups of clay minerals present in the soil environment include layer and chain silicates, sesqui-oxides, and other inorganic minerals as shown in Figure 2.5.
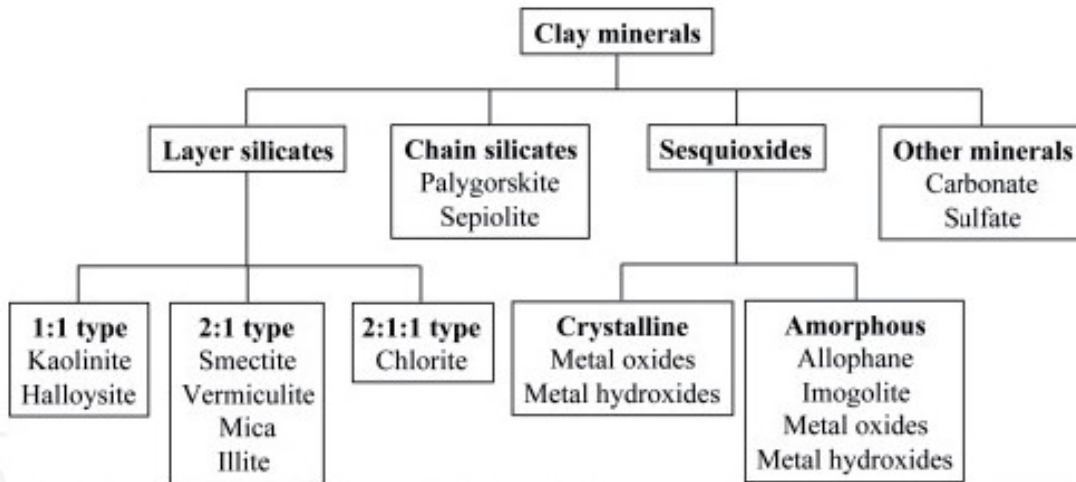
**Figure 2.5: Classification of clay minerals (Huang et al. 2016).**

Layer silicates

It comprises of tetrahedral and octahedral sheets that are bound together and two-dimensional layer structure is built from different stacking combinations. Layer clay silicate minerals can be present either in dioctahedral or trioctahedral state. On the basis of the structure of repeating unit, layer silicates are categorized into 1:1, 2:1 and 2:1:1 type.

a) 1:1 type

It is made up of one tetrahedral and octahedral unit connected by sharing of apical oxygen atoms. All these clay minerals are dioctahedral as two octahedral positions are occupied by trivalent cations like Al^{3+}, Fe^{3+} and one position is vacant. Kaolinite, Halloysite, Nacrite and Dickite are common examples of this type. They are found naturally by hydrothermal, sedimentary and weathering process. In hydrothermal deposits, modifications occur in silica rich rocks like granite due to hydrothermal fluids. The extend of the alteration depends on the temperature, composition of the original rock and pH of the fluid. These deposits have zoning pattern and clay minerals such as nacrite and dickite are commonly found. Weathering is the most common process and large deposits can be found in tropical and sub-tropical areas. These deposits often consist of iron and alumina hydroxide in substantial amount and has low value for the industrial applications. In addition to this, 1:1 clay mineral can be formed by the sedimentary process. The composition is found to be highly variable and mixed with organic rich material.

Kaolinite is most common 1:1 clay mineral with 7 A° thickness and chemical formula of Al_2O_3 $(SiO_2)_2$. $2H_2O$. Hydrogen bond is present between the oxygen atoms of tetrahedral and hydroxyl group of octahedral layers. Theoretically, it is composed of 46.3 % silica, 39.8 % of alumina and 13.9 % of water. Ideal crystal structure makes the kaolinite electrically neutral. However, some charge can be present on surface because of very limited isomorphous substitution and broken bonds. The cation exchange capacity is low as compared to other clay minerals due to presence of only slight charge on lattice. Likewise, kaolinite also shows less adsorption due to lower specific surface area and charge density in comparison with other clay minerals (Martirena et al. 2011 and Diaz et al. 2020). Kaolinite has fixed configuration due to the hydrogen bonding which makes them exhibit low shrinkage and swelling characteristics. It shows well defined sharp crystalline peaks and exhibit hexagonal morphology as shown in figure 2.6. This can be compared with the other minerals in figure 2.7. Kaolinite clays exhibit high flow property which is useful for paper coating industries with low viscosity when dispersed in solution. This is mainly because of broad particle size distribution and deficient charge of crystal structure.
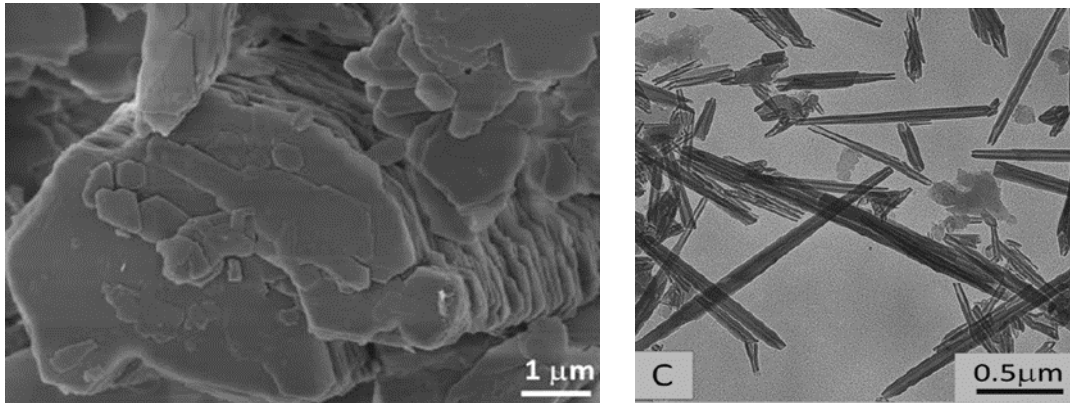
Figure 2.6: Images of (a) Kaolinite and (b) halloysite clay minerals (Lazaro 2015)

Kaolin is hydrophilic in nature and gets easily dispersed in solution. This dispersion property is essential for raw material of paints and paper coating industry. Kaolinite clays are white or off-white in color due to hydrated alumino silicate composition. This characteristic feature makes it an excellent choice for the ceramics industries. High grade kaolin is commonly referred as China clay, flint clay and refractory clay. Kaolinite clays are subjected to thermal treatment for specific applications. The calcination temperature is decided based on the requirement of final material. For example, kaolinite is heated just above dehydroxylation temperature to get metakaolin, which is pozzolanic material and used for blended cements. While, kaolinite clays are heated well above dehydroxylation temperature to obtain mullite and cristobalite, which has high light scattering property and useful for paints industries. For practical use as supplementary cementitious material, low amount of kaolinite content along with other clay minerals are also accepted. This is because of the lower activation temperature, wide activation window and above all the formation of most reactive meta clay. Recent studies have reported that substitution of 30 % clinker by low grade clays with kaolinite content of 40 % is good enough as it displays mechanical performance similar to ordinary Portland cement after seven days.

Halloysite also has same chemical composition as that of kaolinite, except that each repeating unit is separated by single layer of water molecules. The formula of halloysite is $Al_2O_3 (SiO_2)_2. 4H_2O$. It has been observed that upon heating at 150 °C, halloysite gets irreversibly converted to kaolinite. Thickness of each layer of halloysite is 10 A°, which decreases to 7.2 A° for dehydrated halloysite. The difference of roughly 2.9 A° corresponds to the thickness of monolayer of water molecules. Chemical analysis reveals that composition is variable and significant amount of substitution by iron is found to occur which can be as high as 13 %. Halloysite generally shows tubular morphology as shown in figure 3 with length varying between 0.0 2 µm to 30 µm and width less than 0.2 µm (Mackenzie 1975 and Lazaro et al. 2015).

Dickite and Nacrite are other two polytypes of kaolinite clay mineral having repetition of double layer of 1:1 clay type. The average thickness of unit layer is 14 A° and differentiate themselves by stacking pattern of double layer of 1:1 clay mineral. Each 1:1 clay mineral can be distinguished from XRD and IR spectroscopy (Neeraj 2021 and Snelling et al. 2022).

b) 2:1 type
Most of the layer silicate clays are commonly found in soils and based on the mica structure in which a single octahedral sheet sandwiched between two tetrahedral sheets and form an individual composite layer. Therefore, they are referred as 2:1-layer silicates in which Talc and Pyrophyllite signifies the trioctahedral and dioctahedral members. In dioctahedral and trioctahedral layer silicates, two and three octahedral sites are occupied respectively out of the three available sites in the half-unit cell.

These types of clay minerals consist of one octahedral layer sandwiched between two tetrahedral layers. They are further characterized into two categories:

A. Expanding clay minerals: Smectite group and Vermiculite
B. Non – expanding clay minerals: illite (mica groups)

A. **Expanding clay minerals:** This group includes mainly smectite group of clay minerals and vermiculite clay mineral. They are known for their interlayer expansion which happens during their swelling behaviour when they are wet. In case of smectite clays, some sites of alumina in the octahedral layer are occupied by magnesium or iron, and similarly silica are replaced by alumina ions from tetrahedral sheet. This replacement of ions is known as isomorphous substitution and give rise to negative charge on surface. The magnitude of charge depends on the degree of replacement and the type of substituted cation. The charge is balanced by the exchangeable cations (alkali or alkaline earth metals) which have a density of 0.2 to 0.6 per unit cell. The structural formula of smectite is $(Na, Ca)_{0.33}$ $(Al, Mg)_2$ Si_4O_{10} $(OH)_2$ $(H_2O)_N$. Slight attractive forces are present between the top of one tetrahedral unit and bottom of another tetrahedral unit. The space between molecules gets occupied up by the exchangeable cations and water molecules. They have an expanding lattice with the size ranging from 9.6 A° to 20 A° (Odom et al. 1984). Saponite, montmorillonite and bentonite are common clay minerals from smectite family. Bentonite is impure form of phyllosilicate with 98 % montmorillonite and produced by the weathering of rocks in presence of water. It is composed of tetrahedral silicate layer which has some substitution by trivalent aluminate cation present between the two octahedral layers with substitution of divalent cation like calcium or magnesium. Bentonites can have sodium and calcium as dominant ionic species. Sodium bentonite expands around ten times to its dry volume when mixed with water which is highest among other types of bentonites. Calcium bentonite has good absorbent capability and can be transformed into sodium bentonite by ion exchange process using soluble sodium salt such as sodium carbonate. Because of treatment, calcium bentonite can exhibit some characteristics of sodium bentonite. The quantity of cations required to balance the charge deficiency induced by these substitutions is referred to as the cation exchange capacity (CEC). The CEC for Montmorillonite ranges from 80 to 100 milliequivalent per 100 grams. Montmorillonite clays have very poor thermal stability. These minerals show some prominent characteristics like high cation exchange capacity, swelling and shrinkage capacity (Drits et al. 1995 and Garg et al. 2014).

Vermiculite is also 2:1 clay mineral which lies in the category of expanding clays. They are formed by hydrothermal or weathering process of mica clay. In tetrahedral sheets, silica is mostly replaced by alumina which results in the generation of high negative charge. While, alumina is present at most of the locations having dioctahedral structure. The charge density per unit formula is between 0.6 to 0.8 which is much higher than the smectite group. Vermiculite has structural formula of (Mg, Fe^{2+}, Fe^{3+}) $3(Si\,Al\,(Mg, Fe^{2+}, Fe^{3+})3(Si\,Al)4O_{10}\,(OH)\,24H_2O$. The interlayer molecular sheets are occupied by water and divalent cations instead of monovalent ions present in mica. Due to which, layers are held together tight which results in less expansion than the mica clays. The cation exchange capacity of Vermiculite is very high (100–150 meq/100 g). Vermiculite clays are weathered micas where the potassium ions are replaced by magnesium and iron ions between the molecular sheets.

B. Non- expanding clays: It mostly includes mica or illite clay minerals and formed by the weathering and hydrothermal treatment of muscovite and feldspar. They are commonly found in low grade metamorphic and sedimentary rocks. Finely grained mica minerals (muscovite and biotite) are also present with illite clay mineral. The idealized formula of illite structure is (K, H_3O) $(Al, Mg, Fe)_2(Si, Al)$ $4O_{10}[(OH)_2\,(H_2O)$. Silicate is partially substituted by alumina in tetrahedral sheets and also alumina is substituted by divalent cations like Mg^{2+} and Fe^{2+}. This results in high negative charge on illite (0.8 to 0.9) and muscovite (-1). This is balanced by the potassium cations which act as a bridge between two

alternate layers and prevents the expansion. The thickness of each unit cell is 10 A°. Volumetric changes of this clay are found to be much less than vermiculite but slightly higher than 1:1 clay mineral. The adsorption capacity, swelling, shrinkage capacity is less than Montmorillonite and Vermiculite but more than Kaolinite interstratified layers are present. The cation-exchange capacity (CEC) of illite is smaller than that of smectite but higher than that of kaolinite, typically around 20–30 meq/100 g.
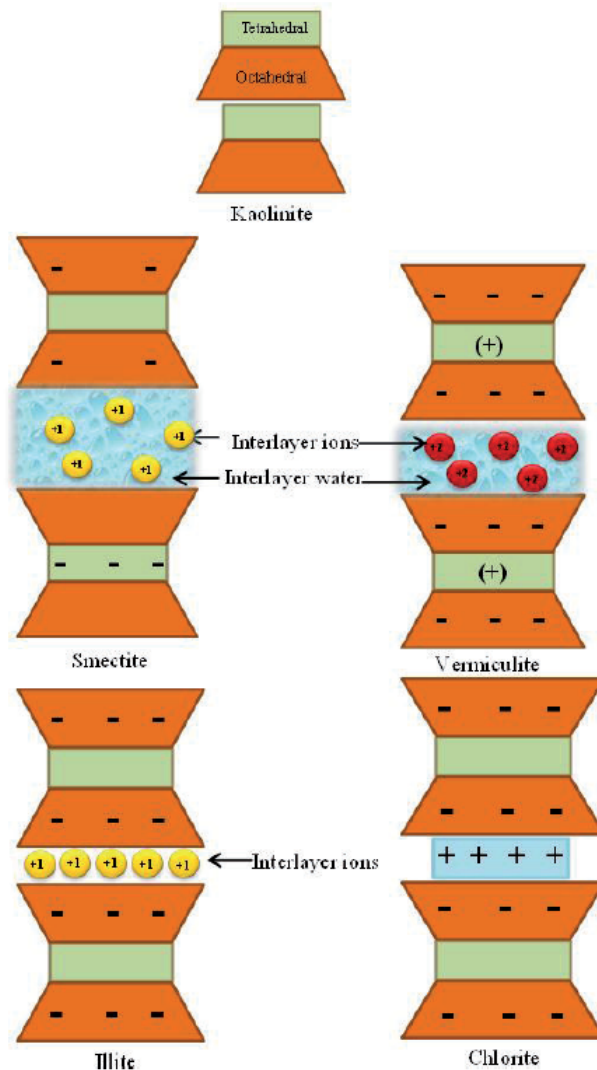
Figure 2.7: Different types of clay minerals (Huang et al. 2016).

c) 2:1:1 type
Chlorite mainly belongs to 2:1:1 silicate group which are basically iron magnesium silicates with some aluminium atoms. The typical chlorite clay crystal composed of 2:1 layer as represented in figure 2.8, such as in vermiculites clay mineral alternate with a magnesium dominated tri-octahedral sheet (also known as brucite) giving rise to 2:1:1 ratio. All the octahedral positions in chlorite are occupied by magnesium ions as in the brucite layer. The negative charge of chlorites is less than smectite or vermiculites but about the same as that of fine-grained mica. There is no water adsorption between the layers responsible for the non – expanding nature of this crystal. The interlayer spacing is about 14 Å. Chlorites having a muscovite-like silicate layer and an aluminium hydroxide sheet are called donbassite. In many cases, the aluminium ions present in octahedral layer are partially replaced by magnesium ions as in magnesium-rich aluminium dioctahedral chlorites called sudoite.
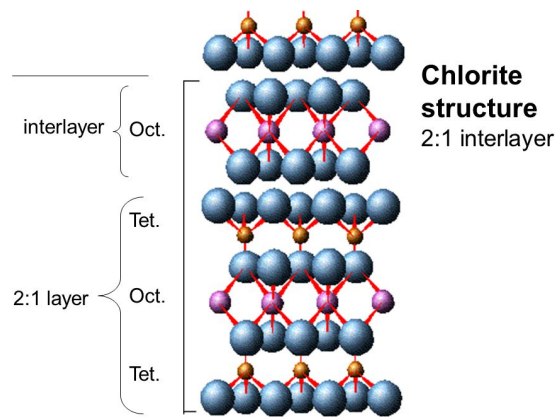
Figure 2.8: Structure of 2:1:1 clay type

Chain silicates

Palygorskite and Sepiolite are two common minerals of chain silicates type with structure formula of Mg Al $S_8 O_{20} OH_3 (OH_2)_4$ X $[M^{2+} (H_2O)_4$ and $Mg_8 Si_{12} O_{30} OH_4 (OH_2)_4$ X $[M^{2+} (H_2O)_8]$ respectively where X refers to octahedral sites. They also have aluminate and silicate as building blocks similar to 2:1 clay mineral with some difference. Firstly, tetrahedral layer undergoes inversion and form narrow ribbon type structure. Secondly, the octahedral layer has irregularity with some amount of isomorphous substitution by magnesium. These alternate layers are connected at corners through the apical oxygen atoms of silica and form rectangular channel like structure which can be filled by zeolite and water molecules. Since, silica does not have layered structure, outer surface has fibrous morphology. Both the clay minerals have almost similar structure and only width of the ribbons differentiates them. It has been found that palygorskite has more width than the sepiolite (Shi et al. 2022 and Alujas et al. 2022).

Sesquioxide

Sesquioxide is clay mineral that is formed through leaching process of alumino-silicates and consists of oxides which has three atoms of oxygen and two of any another element. It can occur in crystalline phase in the form of metal oxides and hydroxides like $Al(OH)_3$, Fe_2O_3. They are not adhesive in nature and do not swell in presence of water. They have ability to hold large amount of phosphate as they have tendency to hold phosphorous tightly make them unavailable for absorption by plants. They have low CEC. They are found in both crystalline and amorphous form. Crystalline Sesquioxide are either metal oxide or hydroxide whereas amorphous Sesquioxide are Allophane and Imogolite.

A. **Imogolite** is an aluminosilicate having the composition of $SiO_2:Al_2O_3$.$5H_2O$. Electron-optical observations of imogolite suggest a unique morphological feature with smooth and curved threadlike tubes differing in diameter from 10 to 30 nanometres which can further extend upto several micrometres in length. The shape of imogolite is cylindrical consisting of a modified gibbsite sheet where the hydroxyl of one side of a gibbsite octahedral sheet loses protons which form bond with silicon atoms located at vacant octahedral cation sites of gibbsite. Thus, three oxygen atoms and one hydroxyl present around silicon atom make up an isolated SiO4 tetrahedron as in orthosilicates which make a planar array on the edge of a gibbsite sheet. Because of shorter bond length between silicon-oxygen bonds than aluminium-oxygen bonds sheet change into curve shape results in a tube-like structure with inner and outer diameters of about 6.4 Å and 21.4 Å, respectively, and with all hydroxyls exposed at the surface.

B. **Allophane** are considered as a group of naturally occurring hydrous aluminosilicate minerals. They are not totally amorphous but are short-range (partially) ordered. Allophane are described by the dominance of Si-O-Al bonds where most of the aluminium atoms are tetrahedrally coordinated. Unlike imogolite, the morphology of allophane varies from fine, rounded ring-shaped particles to irregular

aggregates which indicates that the ring-shaped particles may be hollow spherules or polyhedrons. Despite their indefinable structure, their chemical compositions surprisingly fall down in a relatively narrow range as the $SiO_2:Al_2O_3$ ratios are mostly found to be in between 1.0 and 2.0. In general, the ratio of $SiO_2:Al_2O_3$ allophane is higher than that of imogolite (Achparaki 2012 and Neeraj 2021).

Kaolinitic clay as source of SCM

The development of selection criteria is usually among the first stages for the industrial use of any mineral resource. Although there are currently no specified kaolinitic clay characteristics for use as a source of SCMs a minimum content of clay minerals from the kaolinite group of 40 wt% has been proposed as mineralogical selection criteria. This threshold criterion corresponds to the content of reactive material needed to obtain a mechanical performance at seven days comparable to Portland cement by a 30% substitution with calcined kaolinitic clay, or by a 50% substitution of clinker by a calcined kaolinitic clay-limestone blend in a limestone-calcined clay cement.

A mineralogical classification scheme for the main industrially used kaolinitic clay ores is depicted in figure 2.9. The area for kaolinitic clays that can be used as SCMs (clay minerals from the kaolinite group [40 wt%) is indicated (area 5). As observed, this area comprises all sources currently used for main industrial applications of kaolinitic clays, such as the paper, ceramic or refractories industries, but also mineralogical compositions that reach far beyond specifications for currently used kaolinitic clays. This is especially important for kaolinitic clays with a relatively high content of iron-rich phases, which are relatively abundant but find little use in most of the traditional applications of kaolin industry.
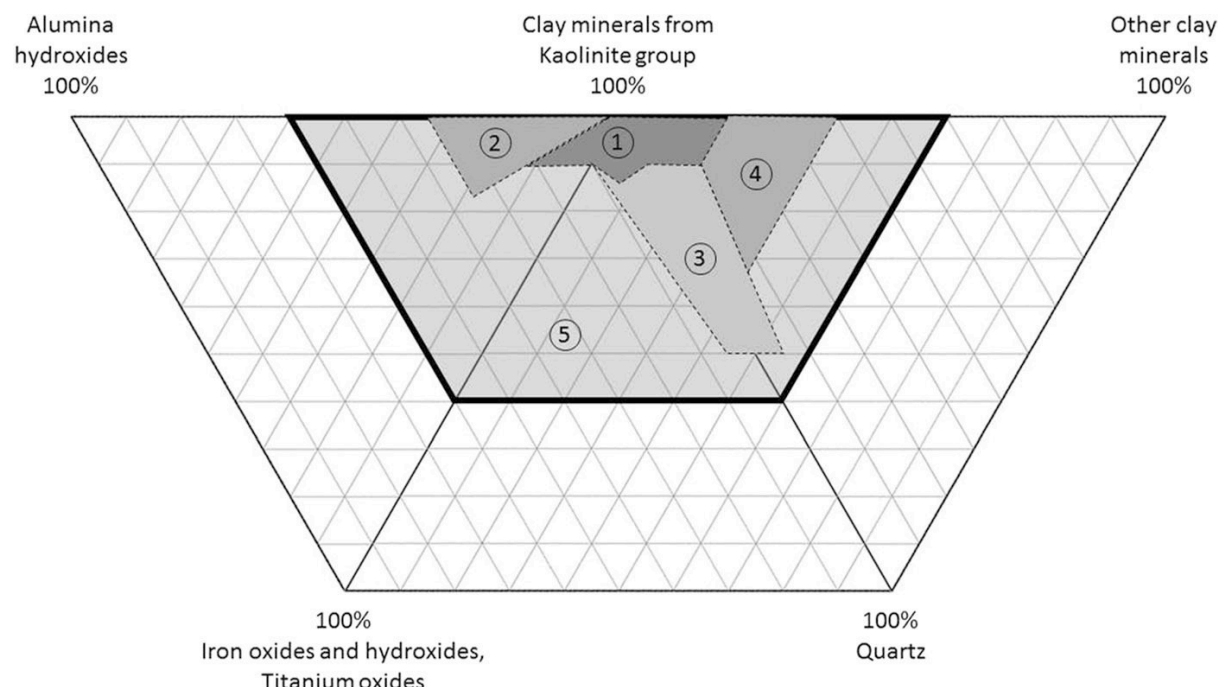
Figure 2.9: Three ternary diagrams used for classification of kaolinitic clay ores (Alujas et al. 2022)

The relationship between mineralogical and chemical composition has been successfully used in the past to establish chemical selection criteria for a given mineral resource and a specific technological application. Clay minerals from the kaolinite group are distinguished from other clay or non-clay minerals by their relatively high Al_2O_3 content and LOI, and by their relatively high Al_2O_3 to SiO_2 ratio. Considering this, recent research based on the chemical and mineralogical analysis of clay samples has derived that, clays with a kaolinite content > 40 wt.% should fulfil the following chemical criteria: Al_2O_3 > 18.0 %; Al_2O_3/SiO_2 > 0.3, LOI > 7.0 %. On the other hand, while iron-rich phases are undesirable for most traditional applications of high-grade kaolin because of the reddish colour of final calcination products, their content varies significantly independent of the kaolinite content and has little influence

on the pozzolanic reactivity given its low solubility in alkaline environments. The chemical criteria used for current main industrial applications of kaolinitic clays and the proposed chemical criteria and mineralogical criteria (kaolinite content) for their use as a source of SCMs are summarized in Table 2.1.

Table 2.1: Requirements for the industrial application of 1:1 clay mineral

	Ceramic Industry	Paper coating	Filler	Refractories	SCM
SiO_2	< 50	< 48	< 48		< 60
Al_2O_3	> 36	> 38	> 36	> 20	> 18
Fe_2O_3	< 1.10	< 2	< 1	< 3	
TiO_2	< 1.10	< 1.5	< 1.5		
LOI	> 11	> 13	> 12	> 5	>7
Kaolinite content	> 75	> 90	> 85		>40

From this comparison it could be observed that lower contents of Al_2O_3 are required for kaolinitic clays as source of SCMs while no upper limit is imposed for other elements commonly associated to impurities, such as Fe_2O_3 and TiO_2. Therefore, chemical criteria for kaolinitic clays intended as source of SCMs are less stringent than the requirements for kaolinite resources suitable for the ceramic, painting, refractories or paper industry. The mineralogical requirements regarding content of clay minerals from the kaolinite group, is also lower as compared to what has been established for current main industrial applications of kaolinitic clays. However, it is important to emphasize that chemical criteria based on chemical composition, although allowing identification of potential candidates and discarding most of the non-compliant clays, are not conclusive per se and should be regarded as a screening tool rather than a binding specification. Further quantitative mineralogical analysis by X-ray diffraction and/or thermal analysis is needed to complete the selection process, once the preselected candidates have been narrowed down to a reasonable number.

Identification of kaolinitic clays across India
The methodology adopted for identification of calcined clay is as follows:

1 Desk research or literature review to collect the information from the secondary sources about the existing integrated cement plants, large scale grinding units and district wise kaolinitic clay deposits on a pan India scale.
2 Field work or technical survey to collect the location of each kaolinitic clay deposit and gather the longitude and latitudes of each mine using GPS. In this activity, the focus was to collect the data of all commercial and working mines.
3 Post field work for creation of database, graphical user interface mapping, plotting the collected information.

As a first step, location of all the major integrated cement plants and grinding units were plotted in GIS map. The data of cement plants and grinding units were collected from Cement Manufacturing Association. In addition, all the locations of the cement units were individually verified from the respective locations given in the cement plant website. This information was cross-checked with the respective cement companies to avoid any discrepancy. Figure 2.10 shows the location of the cement plants in India. The green dots are the integrated cement plants, green colour representing the large grinding units and magenta colour representing the blending units. It was decided to include major cement plants and grinding units since they contribute around 97 % of the total cement production in

the country. The rest 3 % are from mini cement plants and grinding units. These plants are in a cluster and market their products locally. Therefore, these were not surveyed and plotted in the map.

Kaolinitic clays were collected from several states in India. The utilization of clay as supplementary cementitious material requires several stages of pre- processing using various available techniques. The process starts with the identification of clay mines and extraction of virgin clay. Once the clay deposits are identified, top soil or overburden soil lying above it is removed to expose the clay deposits. Overburden soil consists of various clay minerals with high organic content. Common procedure employed in mining is the extraction of clay from slope as it results in homogenization of various layers. Afterwards, clays undergo drying and grinding treatment process. The extent of drying process depends on type of clay. The selection of grinding tool is determined by the size of raw feed and requirement of final particle size. For example, coarse crusher is suitable for large clay lumps in which final raw material obtained has size less than 100 mm. Similarly, blade mills can be used to obtain the size of clay particle in the range of 30mm to 50mm. For achieving much finer particles of size 2-3mm, jaw crusher and pulverizer can be adopted.
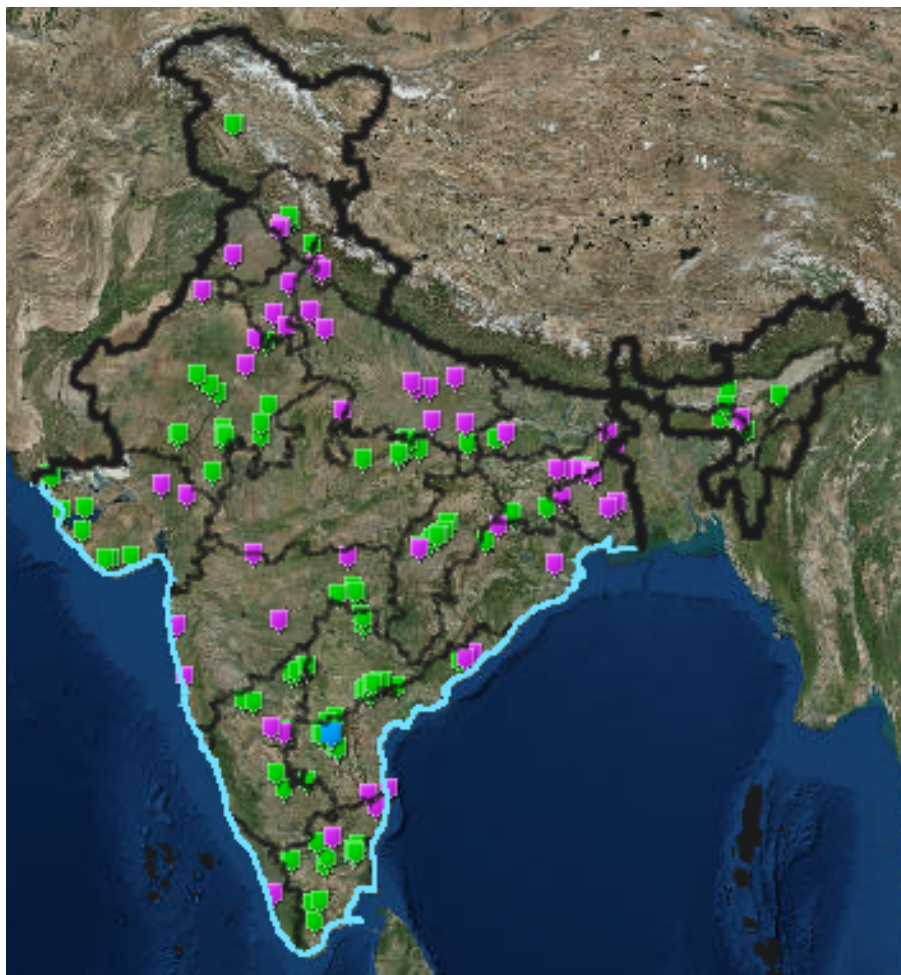
Figure 2.10: Location of major integrated cement plants and grinding units.

Sampling was done based on mine feedback, color and geology of samples and strata and from each of the mines. Pictures of different kaolinitic clay mines are shown in figure 2.11. At each location, multiple number of samples were collected including a mixed type sample to get an idea on types of clay available in that specific mine.

Figure 2.11: Pictures of clay mines

A GPS meter was also used to capture coordinate of the mines. Figures 2.12 to 2.14 show examples of locations where kaolinitic clays were found in Gujrat, Rajasthan and West Bengal. Kaolinite clays were also collected from North-East. In this area, there are several small hills containing outcrops of kaolinite clay and it was not possible to visit each and every hill, clay was collected from the surface outcrop of only one hill. Samples were collected from several places within a single area. All the various samples were collected and analysed for suitability. Figure 2.15 shows the locations of kaolinitic clay sampling in North-East. Figures 2.16 and 2.17 show the locations of kaolinitic clay sampling in Jharkhand and Odisha respectively.
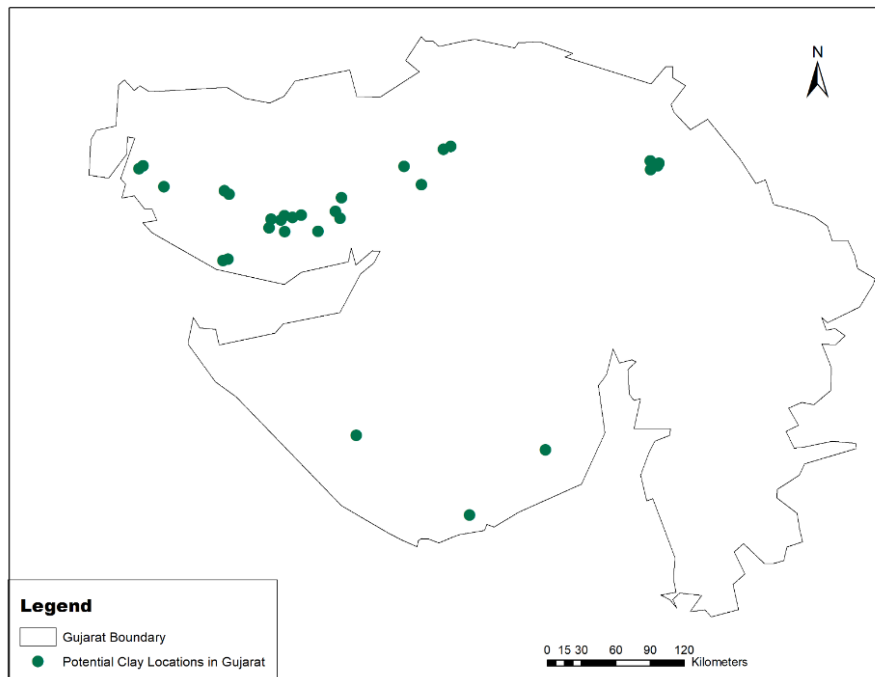
Figure 2.12: Kaolinitic clay sampling locations in Gujrat
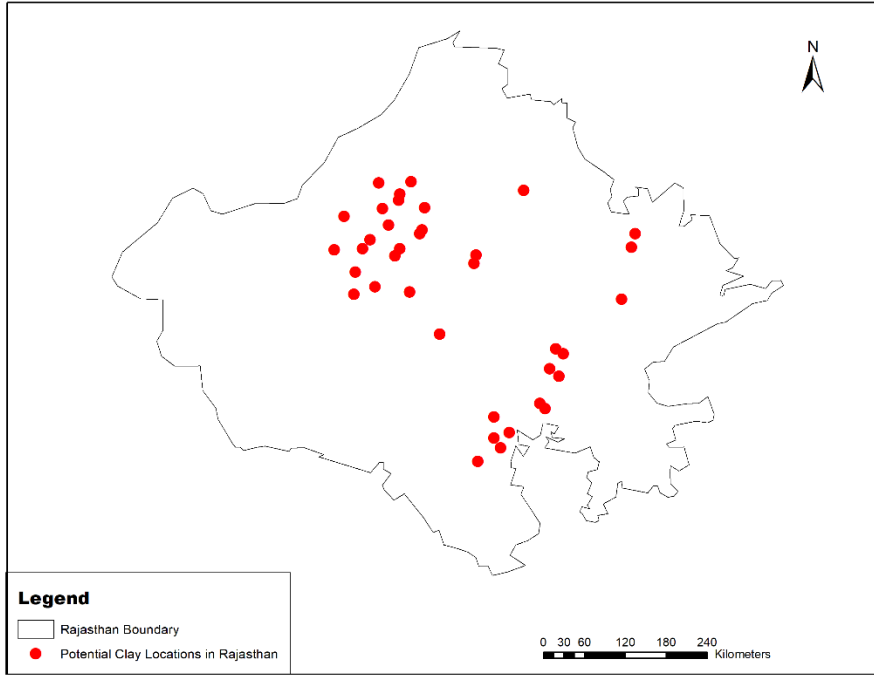
Figure 2.13: Kaolinitic clay deposits in Rajasthan
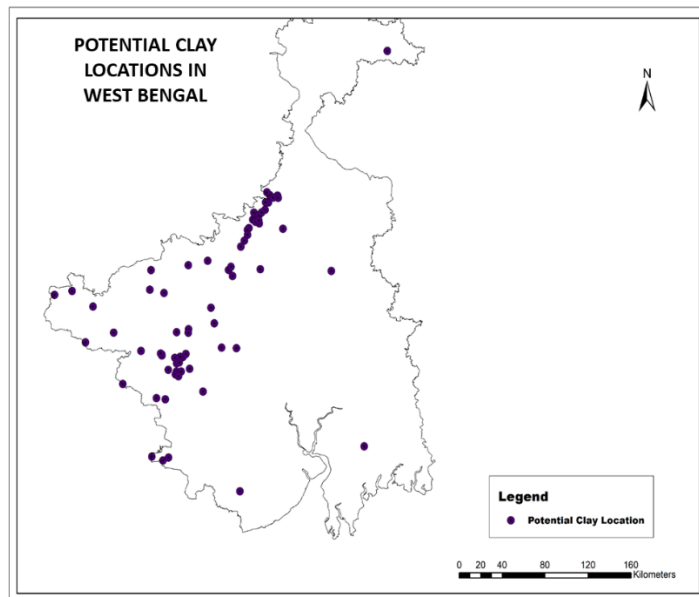
Figure 2.14: Kaolinitic clay deposits in West Bengal
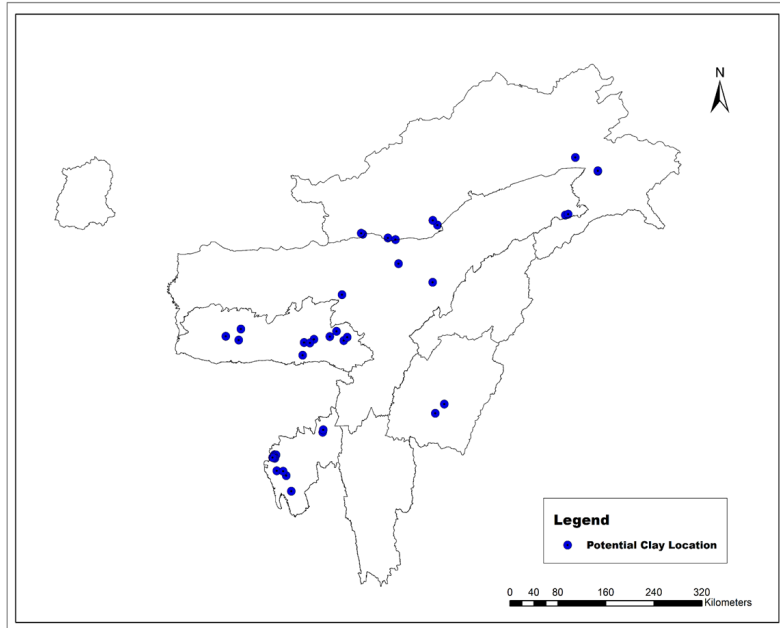
Figure 2.15: Kaolinitic clay deposits in north east
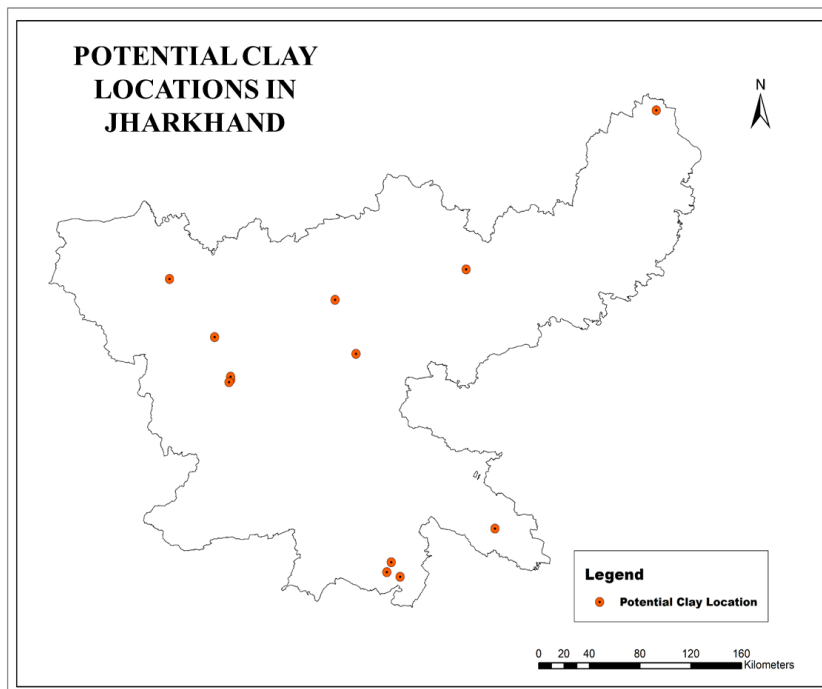
Figure 2.16: Kaolinitic clay deposits in Jharkhand
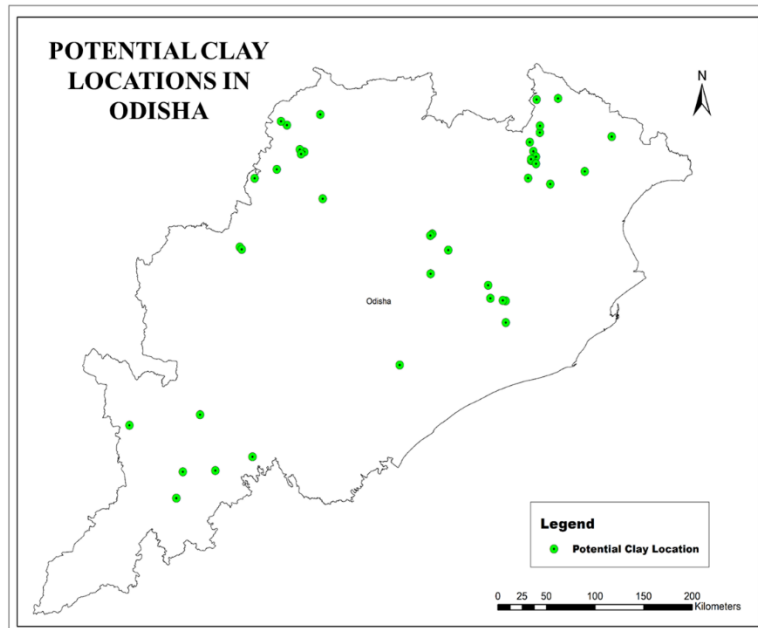
Figure 2.17: Kaolinitic clay deposits in Odisha

In the next step, location of all the major kaolinitic clay areas were plotted on the GIS map as represented in figure 2.18. The data of the locations with kaolinitic clay availability were taken from Indian Minerals Yearbook. The kaolinitic clay areas plotted were based on the district wise data for occurrence of kaolinitic clay resources as reported in the Mineral Yearbook. These were the most authentic reported data available.
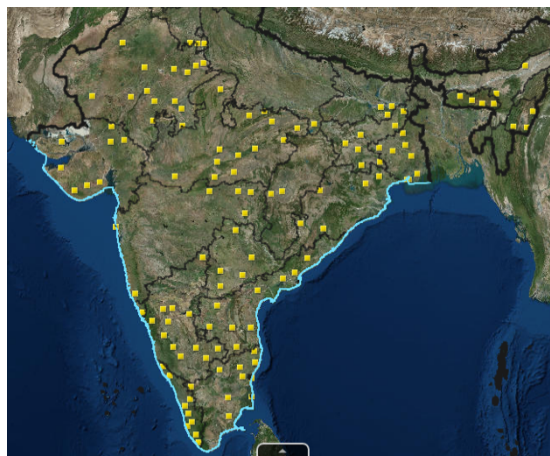
Figure 2.18: Location of kaolinitic clay resources in India according to the Indian Minerals Yearbook

Summary
This chapter discusses the minerology of clays required for LC^3 production and their availability in India. A field and literature survey shows that suitable clays are available throughout the country. A mapping exercise in GIS shows the potential of production of LC^3 almost throughout the country.

Chapter 3: Clay Testing and Suitability Criteria

The raw materials are characterized and their suitability for LC^3 is evaluated using different experimental techniques. Studies have shown that the characteristics of LC^3 depends primarily upon the type of clay. Aluminates in the clay are reactive and form different hydration products that contribute to the early age strength development. The clay processing involves following stages:

1. Drying of samples in an oven to constant weight
2. Grinding and homogenizing in ball mill
3. Finely ground below 90 microns for characterization

The samples for testing are selected using the coning and quartering method. The experimental techniques used for raw clays to know the mineralogical and chemical compositions are as below:

3.1 Testing of raw clays

Figure 3.1 summarises the test methods used to characterise the suitability of clays for use in LC^3.

CHARACTERIZATION TECHNIQUES

X-Ray Diffraction (XRD) — Used to identify mineral phases in a sample appearing as peaks

X-Ray Fluorescence (XRF) — Used to identify composition of oxides in a sample in weight %

Thermo-Gravimetric Analysis (TGA) — Used to infer weight loss correlated with thermal decomposition
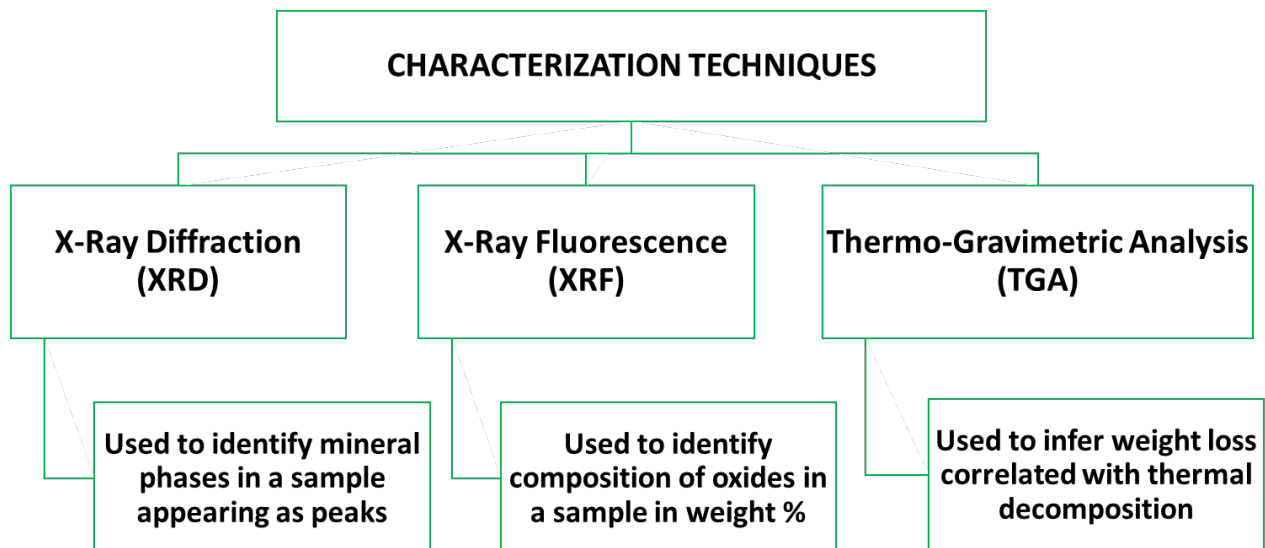
Figure 3.1: Various characterization techniques used in clay testing

1. X-ray florescence (XRF)

XRF is used to determine the oxide composition of the raw materials. Calcium oxide (CaO), Silica (SiO_2) and Alumina (Al_2O_3) are primarily concentrated while carrying out oxide analysis of the samples. The presence of silica and alumina in limestone indicates impurities in the form of quartz or clay minerals. In the case of clays, alumina and silica are the main oxides with minor quantities of CaO. The basic criteria that is used to select the raw clays is identify those clays that have high alumina and LOI content. The chemical requirements that are required for clays to be suitable as SCM are listed in figure 2. This rough screening is made based on the amount of reactive content that is needed so that limestone calcined clay cement shows similar reactive as that of OPC at 7 and 28 days.
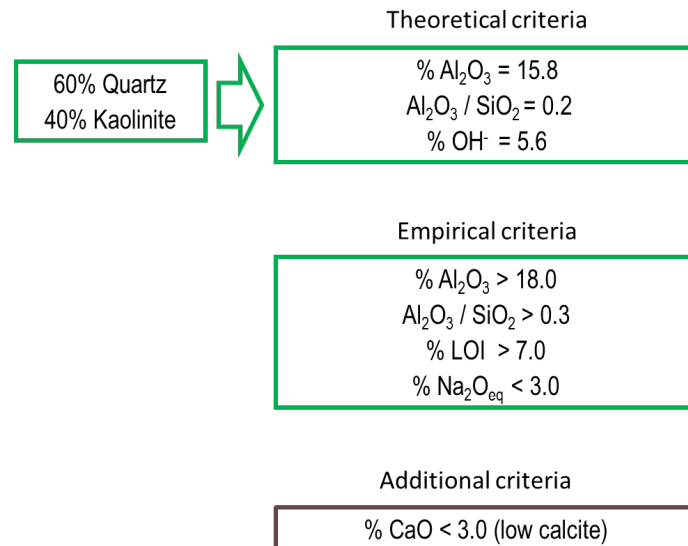
Figure 3.2: Shortlisting criteria for clays using XRF results

2. X-ray Diffraction (XRD)

X-Ray diffraction is one of the important tools that is extensively used to identify the mineral phases present in the sample. When X-rays interact with a material, they form diffraction peaks of varying intensity at different characteristics angles that follows Bragg's law. The position of peaks determines the unit cell parameters and intensity gives information about the nature of atoms in unit cell. The major minerals present in the clay samples are kaolinite, quartz, muscovite, illite and montmorillonite. For our study, the most important mineral is kaolinite. Major kaolinite peaks in XRD analysis are found at these 2θ values: 12°, 19°-22°, 25°, 34°-35°, 38°-39°. Mineral phases that can be present in clay minerals are listed in table 1 below.

Table 1: Various mineral phases present in clay minerals

Phase group	Relevance	Expected phases
Clay minerals 1:1	Highly reactive when properly calcined. Source of reactive Al-rich phases.	Kaolin / dickite / halloysite
Non - kaolinitic clay minerals	Variable pozzolanic reactivity when properly calcined, depending on clay minerals. High chemical and mineralogical variability.	Illite / Montmorillonite / Muscovite
Silicates & Aluminosilicates	Usually thermally inert. Some structural disordered phases or with a high sp. surface (eg: Zeolites) may present moderate to low pozzolanic reactivity.	Quartz / Sanidine / Zeolite / Cristobalite / Bementite / Anorthoclase
Iron (hydro)oxides	Colour modification. May be present as very fine particles.	Hematite / Goethite / Akaganeite / Magnetite
Others	Includes Ti and Mn oxides and other minor phases. Usually inert.	Anatase / Birnessite / Rutile / Gibbsite
Carbonates	May react with thermally activated clay minerals.	Calcite / Dolomite
Sulfides & Sulfates	Potential risk of SOx emmisions. May interfere with proper dehydroxylation.	Jarosite / Natroalunite

3. Thermo-Gravimetric analysis (TGA)

This technique is used for quantification of various mineral phases that decompose at different temperature ranges and also serves as a complementary technique for XRD. This technique measures the weight loss that occurs with increase in temperature. The principle is that the temperature at which reactions occur in minerals and hydrates are known. The measurements are carried out under N_2 atmosphere to prevent oxidation reactions of the specimens. In the case of clays, the typical TGA curve is shown in figure 3. Thermal degradation of kaolinite conversion starts at ~465 °C. The percentage of kaolinite content in the clay can be calculated using the formula shown below:

$$\%\text{Kaolinite content} = \Delta y \times 7.14$$
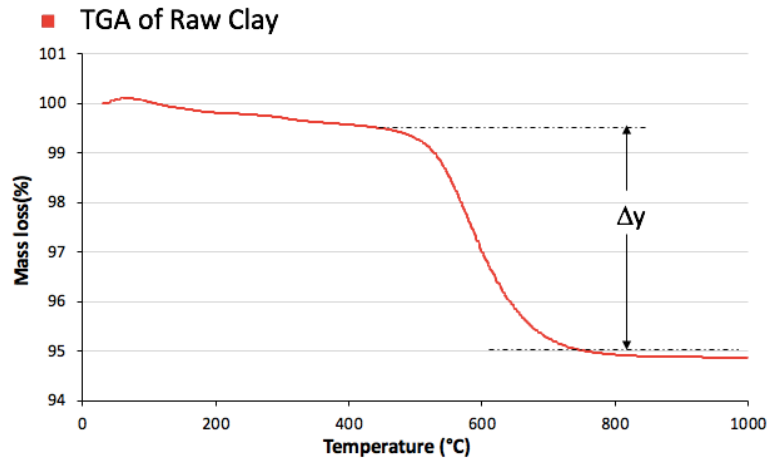
Figure 3.3: Typical TGA curve for kaolinite clay

4. Loss on ignition (LOI) of clays

This is a simple way to know the percentage of kaolinite content in clays. Percentage kaolinite content in a clay sample can be found out be measuring weight loss occurring on heating due to dehydroxylation in the temperature range of 450-650 °C. LOI test is done on the clay samples to find the weight loss occurring in the temperature range of interest. The approximate kaolinite content can be found using the formula above.

After the characterization techniques are performed, analysis is done to determine the amount of kaolinite content present in clay. The selection criteria that is used to find the suitable clays are summarized below in figure 3.4. The clays that pass the selection criteria are then subjected to calcination process to activate the pozzolanic activity.
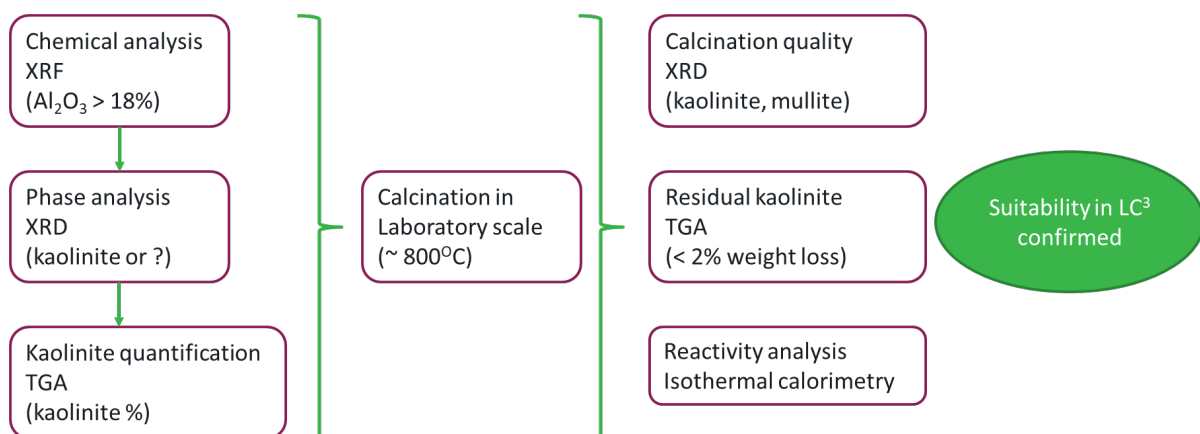
Figure 3.4: Selection criteria for clay

3.2 Suitability test on calcined clays

For a material to be classified as a SCM, first essential criteria is the ability of material to exhibit pozzolanicity. The rate at which calcium hydroxide is consumed by a SCM in presence of water is considered as reactivity indicator. Various test methods are available for assessing the reactivity potential of pozzolan based on either physical or chemical characteristics. Several reactivity tests have been standardized like Frattini test (EN 196-5), Chapelle and Modified Chapelle test (NF P18- 513), lime reactivity test (IS 1727- 1967), etc. Measurement of strength is one of the most common methods for evaluating the performance of pozzolan. Other properties like release of heat due to exothermic reaction, change in volume of hydration product and bound water can also be measured for assessing the reactivity. The test methods can be classified as direct or indirect methods. Direct methods are those in which the CH consumption is recorded, usually using XRD, TGA or titration-based methods. Some of the examples of such tests are such as Frattini test, saturated lime test, modified Chapelle's test, etc. The indirect test methods measure physical properties such as cement mortar compressive strength, heat of hydration, electrical conductivity, strength activity index, lime reactivity test, chemical shrinkage, bound water test, etc. It has been recommended that at least one each of the direct and the indirect tests must be performed to assess the performance of an SCM prior to its use in concrete.

The test methods can also be classified according to the testing duration as shown in table 3.2. The test methods that require less than one day are referred as short-duration ones whereas those requiring 1-day to 10 days are identified as medium duration ones and the ones requiring more than 10 days are classified as long duration ones. Determining the reactivity of SCMs can be complicated since it depends on numerous factors such as temperature, pH and available CH content from clinker hydration. In one study, it is recommended that the particle size of the SCMs need to be below 45 microns for examining the reactivity. But depending on the type of SCMs, and their application, it may not be practical to predict their behaviour after altering the fineness, although this approach can be used to check the variability of the SCM. The testing temperature for the reactivity tests is generally higher than ambient conditions to reduce the test duration.

Table 3.2: Classification of test methods

Duration	Test methods
Short Duration	Modified Chapelle's test
	Amorphous content using XRD
	Dissolution solubility test
Medium Duration	Lime Reactivity
	Electrical conductivity
	Isothermal calorimetry
	Frattini test
Long Duration	Cement mortar strength test
	Strength activity Index
	Chemical shrinkage

3.2.1 Direct testing

In this section, the methods that mainly focus on the CH consumption due to pozzolanic reaction are presented. Modified Chapelle's test, Frattini test and CH consumption measured using XRD, TGA, microscopy or titration methods are explained in the subsections below.

1. Modified Chapelle's test

This method is standardised in French standard NF P 18-513 and is one of the direct test methods to measure reactivity of metakaolin. As per the procedure, 250 ml of water with 1 g of calcined clay and 2 g of CaO are mixed and then heated for 16 hours at 90 °C. The excess amount of water and an

elevated temperature is used to accelerate the dissolution of the SCM in the calcium solution. After that, the hydrated paste is filtered and the filtrate solution is titrated with 0.1N HCL using phenolphthalein as indicator to calculate the milligram of $Ca(OH)_2$ consumed per gram of metakaolin. Chapelle test and modified Chapelle's test are often used to measure the reactivity of SCMs other than metakaolin. In the Chapelle test, 1 g of CaO is used with 1 g of SCMs and boiled for 16 hours. In contrast, the modified Chapelle's test allows for a complete reaction of high purity SCMs by using higher CaO content at 90 °C for 16 hours.

This test is recommended to be more suitable for calcined clay over other methods, but some studies report that the high temperature affects the kinetics of the reaction, which ultimately affects the nature of hydration product formed. Since the hydration of an SCM at 90 °C may not be comparable to the ambient temperature. Further modification of this test is also attempted by reducing the temperature to 40 °C and performing the test for a longer duration of 90 days. The presence of alkalis in SCMs may also affect the results. This test does not give information about the rate of reaction and only determines the final consumption of calcium (Carter et al. 1996). The crystalline quartz present as an impurity in SCMs is reported to have pozzolanic potential when tested at such high temperature. The Chapelle and modified Chapelle's tests are reported to be unsuitable for SCMs such as slag and class C FA. Although the Chapelle test and modified Chapelle's test have been tried for many different SCMs, different studies have reported different test procedures and conditions (Snelling et al. 2018).

Limited studies that investigate the hydration products formed when SCMs hydrate in the accelerated conditions of modified Chapelle's test were found. In the Chapelle's test tried for thermally and mechanically treated kaolinite clays, the formation of C-S-H, C-A-S-H and C3AH6 observed using XRD, TGA and Fourier-transform infrared spectroscopy are reported (Fitos et al. 2015). The quartz peak is reported missing in the XRD data for mechanically activated clay samples either due to the reactivity of quartz at high temperature or a change in the crystalline structure of quartz during grinding. In another study, the XRD analysis of the products from the test carried out at 100 °C on MK, FA, natural pozzolana, slag and quartz show the formation of C-S-H and Hgt phases. Only in the slag sample, silica rich Hgt is also reported. Around 10% of calcium hydroxide is reported consumed by quartz, but XRD data does not indicate the formation of C-S-H phase. The minor consumption of CH was attributed to the carbonation of calcium hydroxide during the test (Snelling and Scrivener 2016 and Parashar 2020).

2. Frattini test

This method is standardised in the British standard BS EN 196-5 and is used for measuring pozzolanicity of pozzolanic cement. A similar procedure for this test is also standardised in Argentina IRAM 1651:03. In this test, 20 g of blended pozzolanic cement is mixed with 100 ml of distilled water and sealed in an airtight container. The sample is then transferred to a 40 °C chamber for testing at 8 and 28 days. At the time of testing, the sample is filtered with the help of a filter paper in a Büchner funnel under vacuum and then cooled down at ambient temperature. Finally, the filtered solution is analysed for hydroxyl ions by titrating against dilute HCL and methyl orange as indicator. After that calcium oxide consumption is measured by re-adjusting the pH of the same solution to 12.5 and titration with 0.03 M EDTA solution using Murexide or Patton and Reeder's indicator. This test measures the Ca^{2+} and OH- ions in the aqueous solution with respect to the solubility curve of CH in alkaline solution at the same temperature (Tironi et al. 2013). If the concentration of Ca2+ and OH- ions for cement is lower than saturation concentration, then the SCM is considered to be reactive as shown in Figure 3.5.
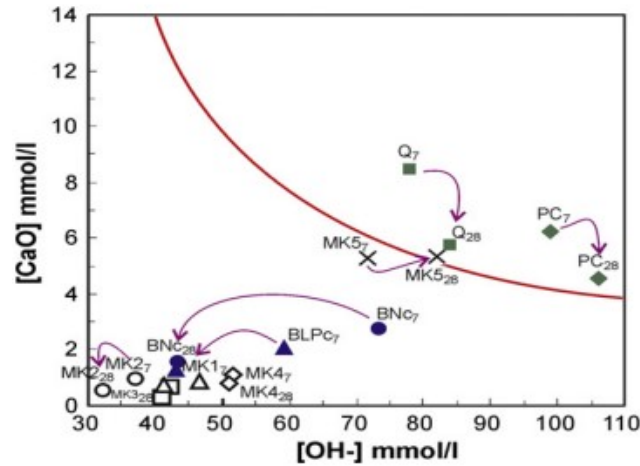
Figure 3.5: Frattini test results (Tironi et al. 2013)

This method is reported sensitive to chemical characteristics of the pozzolana as well as to the alumina content of blended cement. The results are also found dependent on the composition of the cement used (Talero 2005 and Parashar and Bishnoi 2020). As the test is performed with cement, the alkalis present in cement can also influence the activation of SCMs. It has been noted that since EN-196 only reports data between 35 to 90 mmol/l at 40 °C, points outside this range would require additional data for analysis.

3. CH consumption using XRD/TGA and bound water using TGA

The quantity of CH consumed in the pozzolanic reaction is also called fixed lime, which is the amount of CH that has reacted with SCMs for producing hydration products. CH consumption can be measured using different techniques such as quantitative XRD, TGA, titration based methods, etc. But each of these techniques have been found to have limitations. In case of XRD only the crystalline phase can be quantified and the analysis of the result highly depends on the skill of the operator. A few of the studies have also focused on the quantification of available CH in the hydrated samples using XRD. In case of TGA decomposition of other hydration phases could take place in the same temperature range. Moreover, the sample size, quantity, heating rate, surface area etc., also affects the TGA and DTG results. The CH consumption or CH fixation can be calculated corresponding to the temperature range for CH decomposition. The results can be re-normalised for the consumption per g of SCMs/pozzolana added to the cement/CH paste. In different studies, the CH decomposition temperature range can be different depending on the instrument parameters and sample properties (Snelling 2016 and Parashar 2020). Also the quantity of phase quantification can depend on the step method or tangent method used as shown in figure 6.

Similarly, the combined water (also termed as bound water, hydrate water or chemically bound water) can also be calculated using TGA. Similar to CH consumption measurements, the temperature range for measuring the bound water is found to vary in different studies. The bound water in hydrated FA samples has been reported to be used for calculating the rate of reaction of FA at the early ages. In one of the studies, the same approach has been used for calculating the reactivity of carbonates in a hydrated cement system. The results from the mass loss data were not found to be reliable due to the decomposition of other hydration products, such as amorphous products, carbo aluminates, etc. around 600 °C.
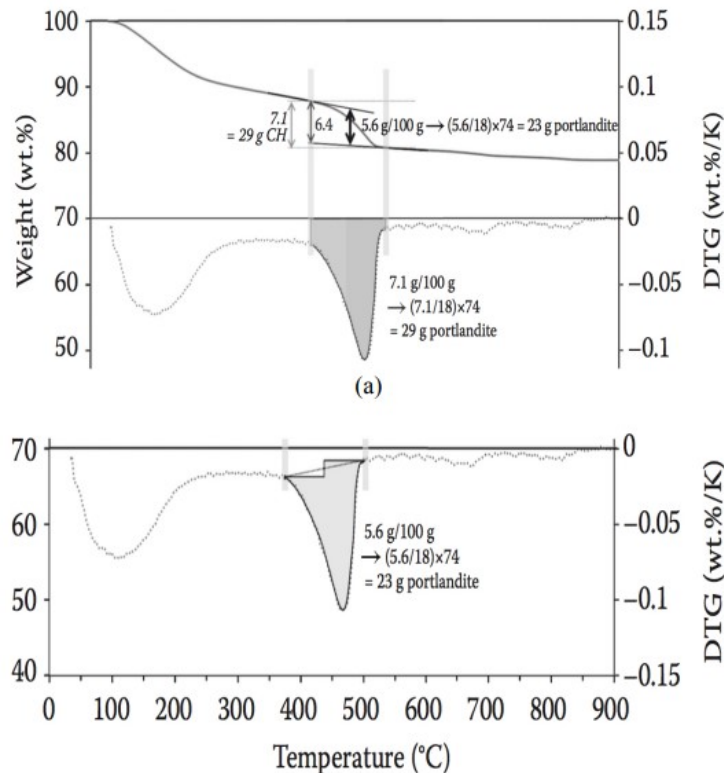
Figure 3.6: Comparison of step method and tangent method for CH quantification using TGA-DTG (Scrivener et al. 2018)

3.2.2 Indirect testing

The tests that measure the influence of the reactions of the SCMs, instead of directly measuring the consumption of CH by the SCM, have been categorised here as indirect tests. Some of the most commonly used indirect tests are discussed in the sub-sections below:

1. Strength activity index

This test is a performance-based test method that is standardised in many countries. As per ASTM C311 "Standard test method for sampling and testing FA or natural pozzolans for use in Portland cement concrete", 20% of OPC is replaced with a pozzolanic material for preparing a blended Portland cement. Mortar cubes of 5 cm size are prepared for both the reference OPC and the blended cement. The water content for 500 g of control OPC is fixed to 242 ml whereas for blends, the water content is controlled so as to achieve the same flow as that of control mix on a flow table. The cubes are air-cured at 23 °C for the first day and then cured in lime saturated solution as per ASTM C 109. The strength activity index (SAI) is calculated using Equation below.

$$SAI=(A/B)\times100$$

where A is compressive strength of test specimens and B is compressive strength of control specimens made with plain OPC.

As per British standard, BS 3892, the blended cement must achieve a minimum of 80% of the compressive strength of plain OPC (CEM1 as per British standard) and as per ASTM C618, the blended cement needs to achieve minimum 75% of the strength of reference cement. In this test, it is assumed that the inert nature of SCMs can reduce the strength by more than 20% due to the dilution effect. One of the advantages of this test method is that it considers the effect of porosity, permeability and hydration reaction kinetics of an SCM in combination with the cement with which it is planned to be used. A modification of this test, with the use of identical w/b ratios on mortar with 20% pozzolana replacement, replacement by volume, other mould types and sizes etc. have been suggested. It is also recommended by the RILEM TC 73 – SBC that the test should have same amount of water and

30

consistency along with similar volume that could be adjusted with sand/binder ratio. Curing at accelerated temperature (not more than 40-50 °C) after one day is also recommended for next 6 days to enhance the pozzolanic reaction. The use of water reducing admixtures to control higher water demand of some SCMs has also been suggested. Along with the reactivity and calcium hydroxide binding capacity of SCMs, the mortar compressive strength also depends on the fineness, packing density and water demand. The results from this test will also be relevant only to the reference OPC since reactivity of SCMs can be different for different cement compositions. Also, the long-term strength of two systems could be similar indicating similar reactivities, due to the complete consumption calcium hydroxide by two different SCMs.

2. Heat of hydration

Calorimetry is the science of heat transfer from a system due to chemical, physical or phase transitions. The use of calorimetry is found helpful in relating the heat of hydration of cement to compressive strength, optimizing the sulphate content, setting behaviour, etc. Heat of solution, adiabatic and isothermal conduction types of calorimeters are commonly used for the cement and concrete. But isothermal conduction calorimetry is the most accurate method to study hydration of cement and pozzolanic materials. The degree of hydration of a cement can be calculated from the heat released measured using a calorimeter under controlled conditions.

Depending on the sensitivity of the instruments, modern calorimeters are capable of measuring heat up to 28 days. The test methods based on isothermal calorimetry are developed for the reactivity assessment of SCMs by measuring the rate of heat evolution by an SCM in the presence of CH. The methods reported in different studies use a high calcium hydroxide to SCM ratio to ensure complete reaction of SCMs and the test conditions are simulated similar to cement pore solution by adding sulphate, alkalis and carbonates. In order to accelerate the reactivity and shorten the testing duration, such tests have been suggested to be performed at elevated temperatures of 40 °C or 50 °C. This approach is also reported to be suitable for testing the reactivity of blend of limestone-calcined clay. The nature of the curve can also be analyzed for assessing the reactivity of different components of ternary blends.

3. Case study on reactivity of clay

The aim of this section is to explain and understand the reactivity of the calcined clay. The first step is to re-characterize the raw clay in order to verify its kaolinite content and to determine the main impurities present in the clay. Then, the clay calcined in India is characterized and compared with the calcination at EPFL. Finally, the reactivity of the calcined clay is tested through the R^3 (Rapid, Relevant, Reliable) pozzolanic test and the measurements of compressive strengths.

The main phases present in this clay are, besides kaolinite, anatase (TiO_2) and gibbsite ($Al(OH)_3$), as shown by X-Ray Diffraction (XRD) in figure 3.7. Thermogravimetric Analysis (TGA) was used to determine the kaolinite content of the clay, as shown in figure 3.8. The dehydroxylation of kaolinite from 450°C to 600°C causes a water loss of 9.9%, corresponding to a kaolinite content of 71.4%. Gibbsite dehydroxylation is also observed at 300 °C.
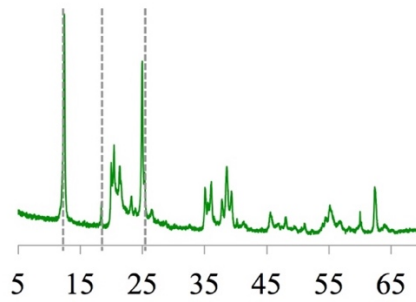
Figure 3.7: XRD pattern of clay. The positions of the main peak of kaolinite (12,3°), gibbsite (18,4°) and anatase (25,4°) are indicated by dashed lines.
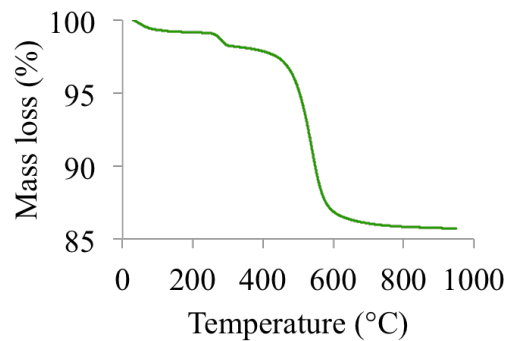
Figure 3.8: TGA of a clay with kaolinite as the main mineral

Clay samples were calcined in India at 600 °C, 700 °C, 800 °C and 900 °C. In addition to these samples, static calcination was carried out at EPFL. It consisted of calcining the clay at 800 °C for 1 hour. Samples were ground at EPFL and then they were analyzed by TGA and XRD to study the efficiency of calcination. From XRD results in figure 3.9, no remaining peaks of kaolinite are observed from a calcination temperature of 600 °C onwards. Moreover, the patterns of clays calcined in India and at EPFL are very similar. This good efficiency of calcination is confirmed by TGA in figure 3.10, where dehydroxylation is already complete at 600°C.
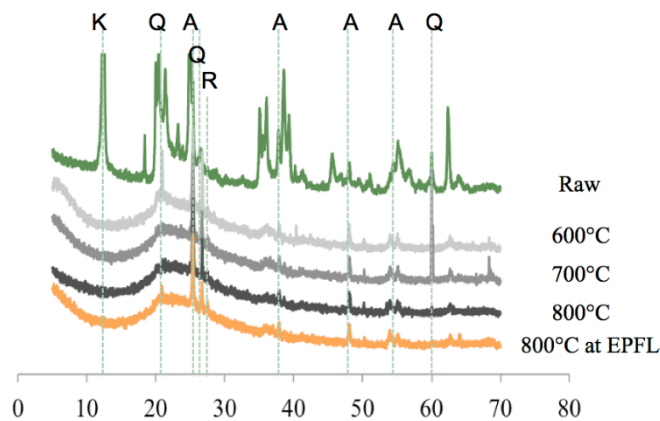
Figure 3.9: XRD patterns of raw and calcined clay
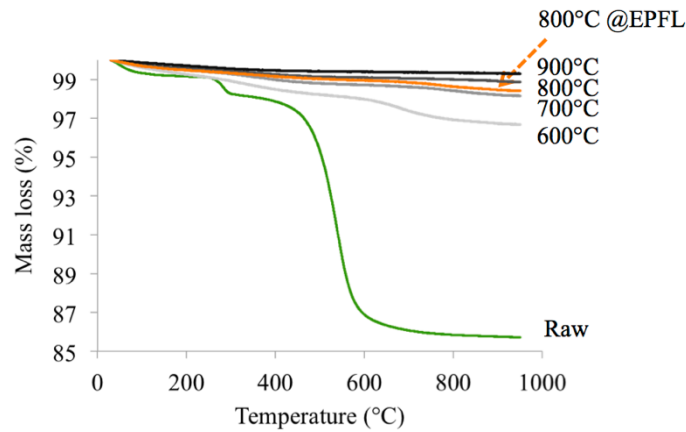
Figure 3.10: TGA of raw clay and clays calcined at 600 °C, 700 °C, 800 °C, and 900 °C.

Reactivity of calcined clay using R3 pozzolanic test

The R^3 pozzolanic test consists of quickly predicting the reactivity of calcined clays by monitoring the heat release of the pozzolanic reaction in portlandite-calcined clay pastes using isothermal calorimetry. Figure 3.11 shows the heat release for clays calcined in India and at EPFL. This heat is slightly higher for the clay calcined at EPFL, showing that the calcination can be better optimized in India. In addition, a significant decrease of reactivity is observed for a calcination temperature of 900°C. For this temperature, rearrangements occur in clay, causing the coarsening of particles.

Compared with the other calcined clays already tested at EPFL, the reactivity of the calcined clay is slightly lower than expected, as shown in figure 3.12. Indeed, similar heats are obtained with the calcined clay containing only 50.8% of calcined kaolinite. However, the slope remains higher for calcined clay 5 from India after 150 hours of test, indicating that the heat release may keep increasing at later age.
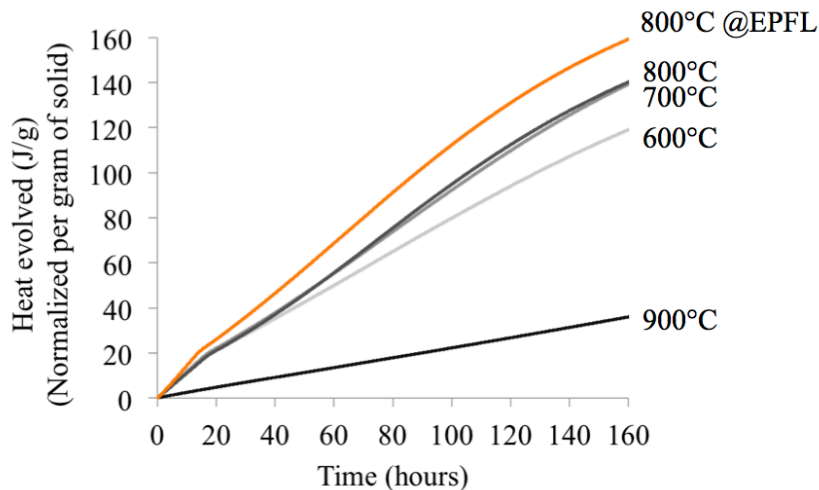
Figure 3.11: Heat release for clay calcined in India and at EPFL
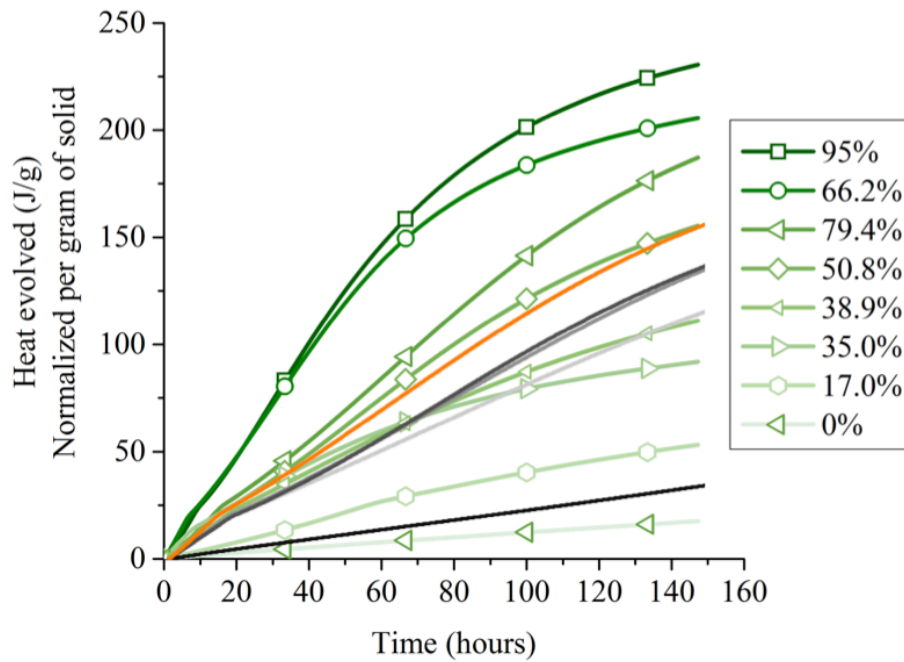
Figure 3.12: Heat release for the different calcined clays tested with the R³ test. The calcined kaolinite content of each calcined clay is indicated (Avet et al. 2016)

Compressive strength tests

For compressive strength tests, mortar bars were cast using water to cement ratio of 0.5 according to EN 196-1. Tests were carried out on mortar cubes of 40x40x40 mm at 1, 3, 7, 28 and 90 days. Only 1- and 3-day results are available now and they are compared with the other calcined clay systems in figure 13. PPC30 refers to systems with 30% of clinker substitution by calcined clays, and LC³-50 corresponds to systems with only 50% of clinker, 5% of gypsum, 30% of calcined clays and 15% of limestone.

Strength results are quite low for the systems containing the calcined clay 5, but they are still acceptable. Results obtained are very close to the strengths of the systems containing the calcined clay with 50.8% of calcined kaolinite. This is in agreement with the results obtained by the R³ test, since the heat release was also very close for these two calcined clays.
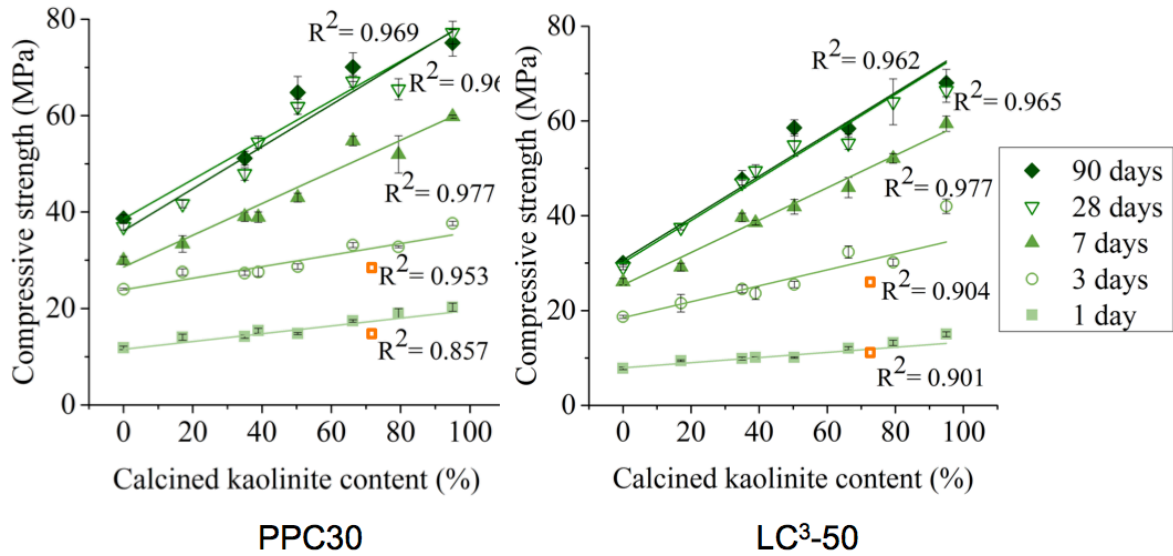
Figure 3.13: Compressive strengths of PPC30 (left) and LC³-50 systems (right). Only results at 1 and 3 days are available for systems containing the calcined clay 5.

The raw clay from India has a kaolinite content of 71%. Its main impurities are anatase and gibbsite. The calcination of clay was properly done, as shown by XRD and TGA. All kaolinite is dehydroxylated for a calcination temperature of 600 °C onwards. Calcination can perhaps be slightly better optimized probably by reducing the calcination time to 1 hour, as done at EPFL.

The heat release and the strength results of the calcined clay are slightly lower than expected. This can be explained by the slower reaction of the calcined clay, as shown by the R^3 test.

4. Lime reactivity

This method is standardized in India (IS 1727 methods of test for pozzolanic materials) and measures the rate of strength development in CH-SCM mortar cube. For this purpose, mortar cubes are cast in a ratio of 1:2M:9 (CH: pozzolan: standard sand) where M is the ratio of specific gravity of pozzolana and the specific gravity of lime. The procedure used for calculating the water demand is based on mortar flow table test and is similar to that of SAI as per ASTM 311. Mortar cubes of 50 mm size are prepared and samples are covered with moist jute cloth for first 48 hours at 27 °C and then cured for next eight days in environmental controller chamber at 50 °C and 90 % RH. The samples are tested for compressive strength at the age of 10 days.

It is reported that the tests that predict reactivity in cement systems are not reliable because the composition of cement phases also influences the performance of the SCM. Therefore, the strength development of an SCM in presence of CH can be more reliable. In addition, the water required based on the flow also gives an indication of the physical characteristics of the SCM. Due to the difference in the specific gravity of SCMs, the total volume of the mix will vary with SCMs. The standard lime reactivity test and other similar approaches (CH mortar strength) are being used for a wide range of SCMs including calcined clay, rice husk ash, pond ash, etc.

This test method is similar to lime reactivity, which was earlier standardized in the ASTM standard - C311. For reasons not known, this test method was later removed from C311. A linear correlation of the measured pozzolanic lime reactivity with the specific surface area of the pozzolan is reported in the results. This method has also been reported to provide a good reactivity indication for rice husk ash depending on its burning conditions and unburned carbon particles. A study on the compressive strength development of calcined clay-lime mortar with varying calcium hydroxide content, water

35

content and type of sand has been reported. Being indirect, this test method provides results that also include the effect of the physical properties of the SCM and, therefore, the influence of the reactivity of the SCM. A RILEM technical committee found that amongst a set of some chosen test methods for pozzolanic reactivity, the results from lime reactivity had one of the best correlations with the strength development in blended mortars, as seen below in table 3.3.

Table 3.3: R^2 index of linear correlation of the reactivity test results to the relative strength at 7, 28 and 90 days for all SCMs tested (Li et al. 2018, RILEM TC 267)

Relative strength at	Standard method					R^3 model					
	Chapelle	Modified Chapelle	IS 1727	Frattini [CaO] reduction	Reactive silica	Bound water	CH consumed	Calorimetry (heat released)			
								0.5 day	1 day	3 days	7 days
7 days	0.20	0.74	0.39	0.54	0.27	0.93	0.89	0.95	0.95	0.90	0.86
28 days	0.03	0.46	0.62	0.31	0.33	0.86	0.74	0.72	0.80	0.91	0.94
90 days	0.04	0.29	0.82	0.17	0.52	0.43	0.51	0.31	0.36	0.50	0.63

Case study on lime reactivity

A set of SCMs was tested using the lime reactivity method to understand the properties of the hydration products formed with this method. The physical and chemical properties of the SCMs studied are listed in table 3.4. K1, K3 and K3 are calcined clays. FA1, FA and FA3 are fly ashes. FA3 was produced by grinding FA1. LS1, LS2 and LS3 are limestone. Q is a quartz produced by grinding standard Indian sand. S1 and S2 are ground granulated blast furnace slags. OPC1 and OPC2 are ordinary Portland cements.

Table 3.4: Physical and chemical properties of SCMs used in this study (Parashar 2020).
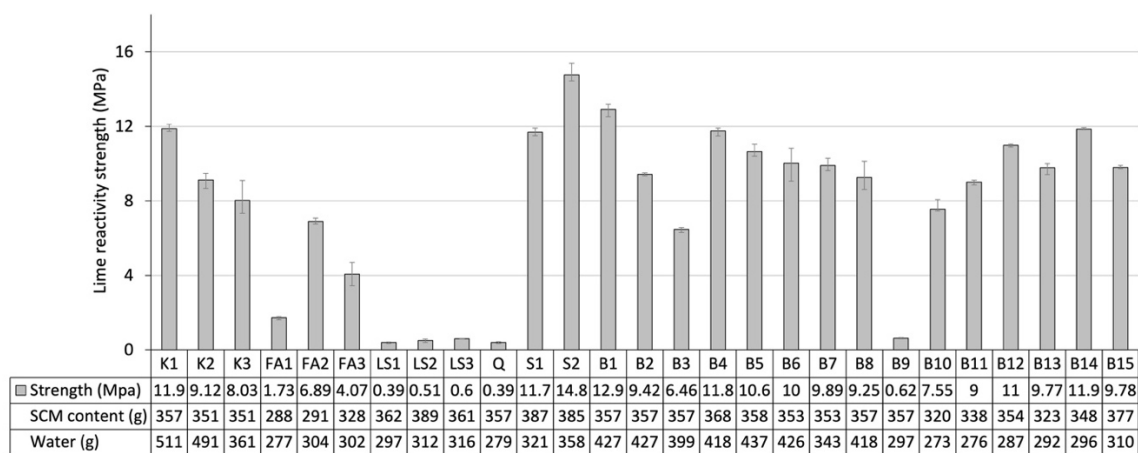
Oxides		K1	K2	K3	FA1	FA2	FA3	LS1	LS2	LS3	Q	S1	S2	OPC1	OPC2
SiO_2		49.6	56.4	73.9	54.3	68.6		11.1	0.7	27.01	95.9	32.3		20.5	20.9
Fe_2O_3		1.5	3.5	1.8	5.9	5.3		1.5	0.6	5.27	0.75	1.93		4.2	3.8
Al_2O_3		46.8	36.8	19.5	31.8	23.2	Same as of FA1	2.5	1.1	9.92	1.88	23.16	Same as of S1	4.5	7.2
CaO		0.2	0.1	0.4	1.6	0.3		45.6	29.8	31.5	0.7	33.9		64.2	55.9
MgO		---	0.1	1	1.7	0.2		1.9	21.8	0.7	0.5	7.1		2.1	3.1
SO_3		0.2	0.03	0.1	0.2	0.02		---	---	0.02	0.2	---		1.9	4.4
Na_2O		---	0.2	---	0.2	0.4		0.5	---	0.2	---	0.3		0.4	0.5
K_2O		---	0.2	---	1.02	1.6		0.3	---	0.7	---	0.6		0.2	0.9
TiO_2		0.8	2.5	2.8	2.3	0.1		---	---	0.8	0.2	---		---	---
P_2O_5		0.01	0.2	---	0.4	0.1		---	---	---	---	0.6		---	---
LOI		3.1	1.6	0.9	0.4	0.8	0.84	35.5	42.1	25.2	0.7	-0.4	-0.5	0.9	1.8
SG		2.64	2.6	2.6	2.22	2.15	2.43	2.64	2.88	2.67	2.64	2.85	2.88	3.17	3.14
PSD, μm	$D_{V\,10}$	1.8	1.6	1.6	6.1	0.6	1.5	1.7	1.9	2.5	3.4	2.3	1.7	3.2	4.7
	$D_{V\,50}$	5.8	5.3	11.3	39	12.2	11.9	11.1	11.1	11.6	12.4	12.7	4.9	17	20.3
	$D_{V\,90}$	21.9	29.7	40.9	150	48.26	42	56.1	49.8	44.9	35.5	45.1	10.8	59.6	57.5

Along with the individual SCMs, their blends were also tested so as to understand the reliability of the lime reactivity test to measure the reactivity of blended pozzolans in composite cements. The list of the blends used is given in Table 3.5. The lime reactivity test was carried out according to the standard IS1727 and the results are shown in figure 3.14. It is seen that the lime reactivity test can also be used to assess the reactivity of blended cements. For example, the lime reactivity values for the blends B1 and B4 are similar to the clay K1. Similarly, B6 and B7 are similar to K2 and K3. The result show that the test can capture the effect of synergy between calcined clay and limestone, due to the sufficient availability of calcium hydroxide in the system. It can also be seen that for all clays and blends of clays with limestone a lime reactivity value of 8 MPa and above was obtained. In cases where a higher

limestone was used, this value was not achieved, clearly showing that the test can also be used to determine the proportions of clay and limestone to be used in LC³ blends. It can be seen in figure 3.15, that the test is able to assess the synergy between calcined clay and limestone as the formation of carboaluminate phases takes place in this test as well. The formation of these phases shows that a reaction between the limestone and the calcined clay is taking place in the system.

Table 3.5: Blends of SCMs and their mix proportions (Parashar 2020)

S. No.	Blend	SCMs used	Blend proportion
1	B1	K1 + LS1	2:1
2	B2	K1 + LS1	1:1
3	B3	K1 + LS1	1:2
4	B4	K1 + LS2	2:1
5	B5	K1 + LS3	2:1
6	B6	K2 + LS1	2:1
7	B7	K3 + LS1	2:1
8	B8	K1 + Q	2:1
9	B9	Q + LS1	2:1
10	B10	FA1 + S1	2:1
11	B11	FA1 + S1	1:1
12	B12	FA1 + S1	1:2
13	B13	FA2 + S1	2:1
14	B14	FA3 + S1	2:1
15	B15	S1 + LS1	2:1

	K1	K2	K3	FA1	FA2	FA3	LS1	LS2	LS3	Q	S1	S2	B1	B2	B3	B4	B5	B6	B7	B8	B9	B10	B11	B12	B13	B14	B15
Strength (Mpa)	11.9	9.12	8.03	1.73	6.89	4.07	0.39	0.51	0.6	0.39	11.7	14.8	12.9	9.42	6.46	11.8	10.6	10	9.89	9.25	0.62	7.55	9	11	9.77	11.9	9.78
SCM content (g)	357	351	351	288	291	328	362	389	361	357	387	385	357	357	357	368	358	353	353	357	357	320	338	354	323	348	377
Water (g)	511	491	361	277	304	302	297	312	316	279	321	358	427	427	399	418	437	426	343	418	297	273	276	287	292	296	310

Figure 3.14: Lime reactivity strength results for SCMs and blends at the end of 10 days (Parashar 2020).

It can be seen in figure 3.16 that the rate of strength development in the lime reactivity test is much faster in the case of calcined clay and limestone calcined clay (LC²) blends. This indicates that for a rough guideline, the duration of the test can be reduced so as to have a faster process of identification and quality control.
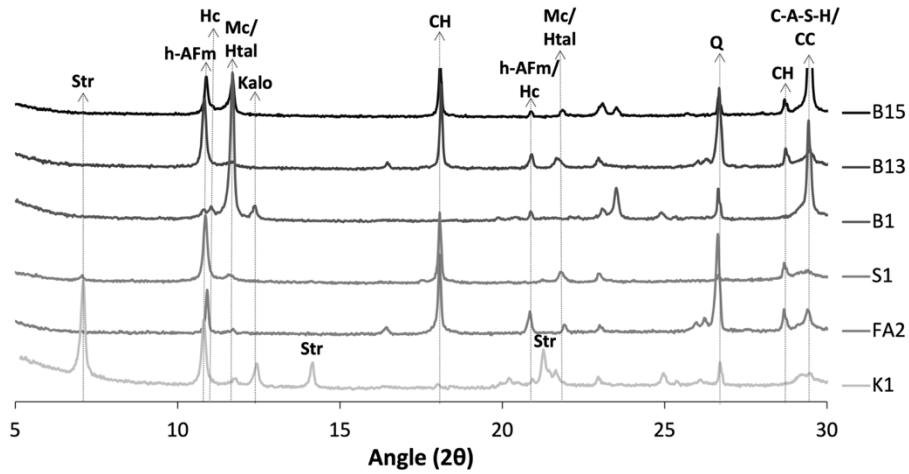
Figure 3.15: XRD plot for K1, FA2, S1, blend B1, B13 and B15 hydrated up to 10 days as per lime reactivity testing conditions (Parashar 2020).
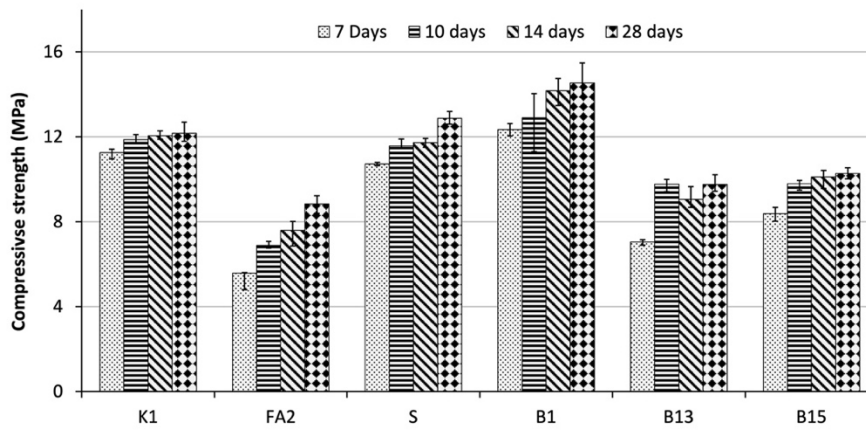
Figure 3.16: Rate of strength development in lime reactivity test at 7, 10, 14 and 28 days (Parashar 2020).

3.3 Summary

The requirements from clays to be suitable for use in LC^3 were discussed in this chapter. Test methods for assessing the reactivity of clays and of the blends of clays and limestone were also discussed. More details about the requirements from limestone will be discussed in a later chapter in this report.

This chapter discusses the production of limestone calcined clay cement (LC^3). The first part of the chapter discusses the identification and processing of the clay and limestone for use in the production of the cement. The second part discusses the production and the properties of the cement.

4.1 Clays for LC^3: Suitability and Calcination
Table 4.1 below shows the some typical elemental composition of clays that have been tested for use in LC^3 and their kaolinite content. It is seen that along with aluminium and silicon, iron, magnesium and calcium make the minority elements. Although the reactivity of the clays is influenced more by the kaolinite content, i.e. the silicon and the aluminium, the minor elements can also impart important properties to the clay. For example, it has been seen that clays with higher iron contents tend to be darker in colour. Most ferrous minerals impart a reddish or brownish colour to these clays.

Table 4.1: Typical elemental compositions of clays used in production of LC^3

|	
Al_2O_3	Between 16% and 39%
SiO_2	Between 35% and 60%
CaO	Not more than 10%
Fe_2O_3	Not more than 12%
MgO	Not more than 3%

4.1.2 Activation of clays
The activation of clays can be carried out through mechanical, chemical and thermal means. In mechanical activation, attrition mills are used to break the bonds between the sheets of clays and to expose more surface of the clay. Alkalis are used in chemical activation to increase the solubility of the alumino-silicates. However, thermal activation is most commonly used for the use of activated clays as cementitious materials.

When exposed to high temperatures, the hydroxyl group in the clay minerals can detach and escape as water vapour. Since the hydroxyl group forms an integral part of the crystalline structure of clay, its removal breaks the crystals and makes the alumino-silicate chains more amenable to dissolution in alkaline conditions.

Illite is known to lose its structural water at temperatures above 900˚C and illitic clays calcined in this way have been used in construction. However, it has been seen that the reactivity of calcined illitic clays is limited. As the temperature is increased above 980˚C, the formation of the unreactive spinel, which is an alumino-silicate phase, starts. This phase is converted into into mullite and cristobalite upon heating further to temperatures above 1050˚C. Mullite is an alumino-silicate that exists as needle-shaped crystals and cristobalite as octahedral crystals. Cristobalite is a phase of silicon dioxide that is formed at temperatures above 1400˚C end exists in a meta-stable state at lower temperatures, slowly converting to quartz. Cristobalite is classified as a carcinogen along with quartz. Mullite and cristobalite are highly stable phases that do not react in the alkalinity provided by cementitious systems. Due to the narrow window available between calcination of the clay and recrystallization of mullite, combined with their relatively lower reactivity, illitic clays are have limited applicability in cements. Smectites are also highly stable clay forms that do not get calcined before the formation of mullite occurs. Due to the difficulty in calcining other clay minerals and, therefore, their limited applicability to LC^3, only kaolinite and its properties are discussed in more detail in this book.

The figure 4.1 below shows weight loss occurring in kaolinitic clays measured using a Thermogravimetric Analyser (TGA).
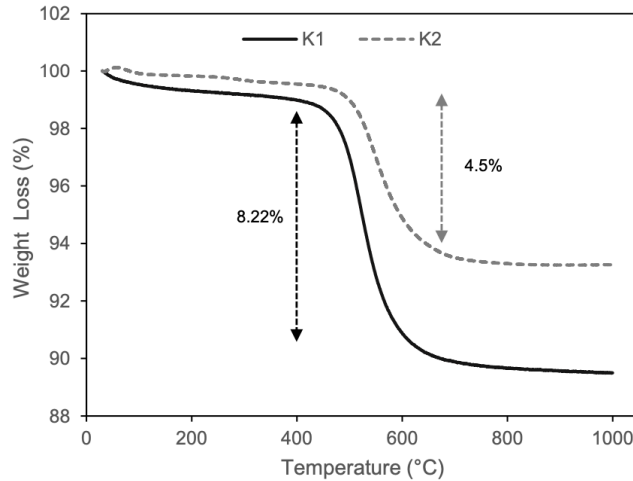
Figure 4.1: TGA analysis of clays with different kaolinite contents (Krishnan 2019, K1 has around 59% kaolinite content and K2 around 32% kaolinite content)

As can be seen in the above figure, the decomposition of kaolinite starts at around 450°C and is complete by 650°C. In the process, 14% of the weight of kaolinite is lost as water vapour in this temperature range, breaking the crystallinity of the kaolinite phase and rendering it amorphous. This amorphous phase is commonly known as metakaolin. A sintering of the particles of metakaolin in known to occur at temperatures above 900°C. Upon further heating to temperatures of around 980°C, metakaolin decomposes into a phase known as spinel, which is a mixture of γ-Al_2O_3 and SiO_2, and amorphous SiO_2. At temperatures around 1100°C, the formation of mullite starts, leading to a sudden reduction in the reactivity of the clay.

In practice, the calcination of clays can be carried out in a variety of ways. Static calcination of clays can be carried out in equipment like muffle furnace by heating them to a temperature that is sufficiently high to ensure calcination throughout the bulk of the clay. In order to improve the efficiency of calcination, clay must first be pressed into thin and dense pellets to ensure a more efficient heat transfer and therefore a more uniform temperature in the clay. The presence of excess air between the particles of clay can reduce the conduction of heat to the inner parts of the pellets and lead to non-uniform calcination. Although the actual temperature required for calculation would depend on the clay and the furnace being used, kiln air temperatures of around 850°C to 900°C have been found to be sufficient for the complete calcination of clays. While lower temperatures can lead to incomplete calcination, the reactivity can be reduced due to sintering and the formation of mullite at higher temperatures. To ensure the uniformity of calcination, the clay pellets should be as thin as possible and must be stacked in a manner that allows the passage of hot air between them. It must also be ensured that the peak temperature is maintained for a sufficiently long time to achieve the calcination temperature in the innermost parts of all the pellets. Most static kilns have the advantage that the clay is isolated from the flame, which allows a more uniform temperature in the air throughout the kiln and prevents the non-volatile matter and unburned organic materials from the fuels from getting incorporated in the clay. However, while static calcination has been found to be useful for laboratory and small-scale trials and productions, it was not found to be useful for industrial scale production. Firstly, since static kilns usually carry out the calcination in batches, the heat in the furnace is lost every time a new batch of clay is loaded, making the process inefficient. Secondly, it is difficult to ensure a uniform temperature distribution inside the clay pellets in larger static kilns, leading to a reduced efficiency of production. The figure 4.2 below shows a trial of clay calcination that was carried out using a static shuttle kiln. It was found in this trial that when clays were dry packed into the containers (known as saggars) before placing in the kiln, while the external air temperature reached more than 1100°C, the temperature in the middle of the containers was less than 450°C,

despite almost 12 hours of residence time. Additionally, it was found that the arrangement of the saggars is crucial to allow a proper flow of hot air throughout the kiln.

Figure 4.2: Saggars arranged in a shuttle kiln

In some static calcination processes, such as vertical shaft kilns, fuel, such as pulverised coal, is mixed with the clays and then fired in order to achieve a more uniform temperature. Attempts using this technique have shown that due to the high combustion temperature of coal, it may be difficult to maintain the temperature of the clay below 900˚C. This may lead to a re-crystallisation of the clay and a reduction in its reactivity.

A continuous calcination of clays can also be carried out in rotary kilns. Rotary kilns are usually hollow steel tubes with lining of refractory materials, usually bricks, on the inner surface of the tube. The kilns are generally mounted with a slight slope to allow an easy flow of the materials. While the raw material is fed at the higher end of the kiln, firing of the fuel is carried out at the lower end. The kiln is continuously rotated to keep turning the material and also to prevent a deformation of the kiln due to the high temperatures. The fuel is either pulverised or gasified and then fired at the other end of the kiln, heating up the air at that end and generating a temperature gradient from the top to the bottom of the kiln, as shown in figure 4.3 below.
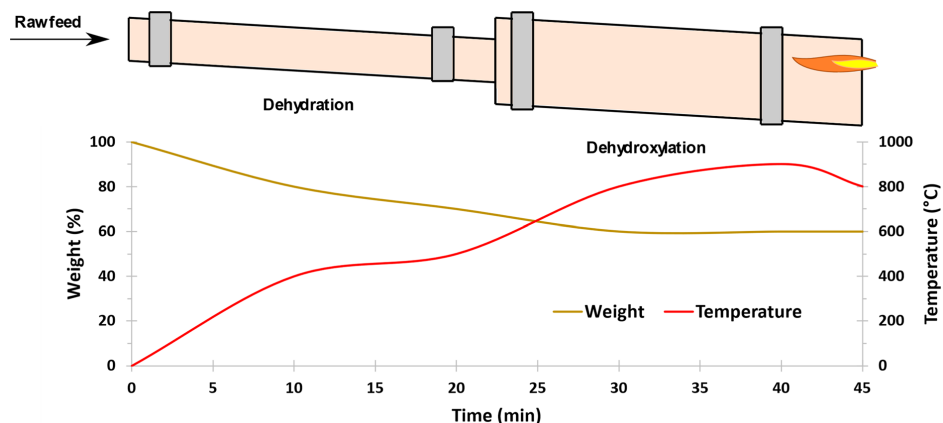
Figure 4.3: Layout of a rotary kiln along with expected loss in moisture along its length (Hanein et al. 2022)

The raw material is generally crushed to lumps of a few centimetres or millimetres size and is continuously fed into the rotary kiln. The size of the lumps has to be controlled in order to ensure proper calcination. If larger lumps of clay are fed, the calcination may not be uniform as the heat may not be able to penetrate throughout the lumps. If much smaller lumps are used, the air in between the lumps can prevent a uniform thermal distribution. Dust in the feed can also reduce the efficiency of calcination. The optimal size of the lumps is usually determined through trial and error and depends on the air temperature, residence time and the rotational speed of the kiln. Figure 4.4 below shows clay lumps just before being fed into a rotary kiln.
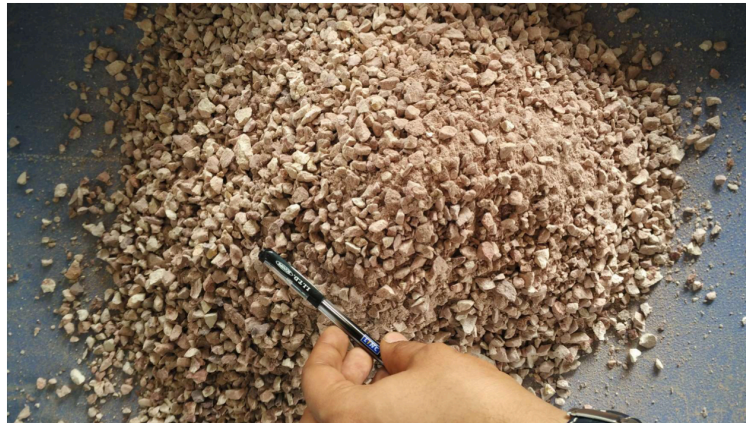
Figure 4.4: Crushed lumps of raw clay

As the lumps move from the relatively cooler zone at the upper end of the kiln towards the hottest lower parts, they slowly their temperature slowly increased, The rotary action of the kiln agitates the materials allowing the entire bulk to be exposed to the hot air. First, as the temperature goes above 100°C, the free moisture content in the clay is lost. Then, as the temperature in the clay goes above 450°C, the hydroxyl groups from the kaolinite crystals start to escape as water vapour, disrupting the crystal structure. While mostly the calcined material exits the rotary kiln in the form of nodules, at times, the loss of water can lead to breaking of the lumps into smaller pieces. The calcined material is collected from openings along the periphery of the kiln. The calcination is generally completed by around 650°C, but a higher temperature of the range of 850°C to 950°C may be required in the air so as to achieve complete calcination of the nodules. The rate of fuel injected into the kiln is controlled in order to achieve this temperature near the exit of the kiln. Care must be taken to not further elevate the temperature in the kiln or to expose the material directly to the flame as this may lead to an over-calcination on the surface of the lumps. The hot air generated near the flames travel upwards through the kiln before exiting from its top end. Due to its continuous nature, the rotary kiln is usually an efficient calcination technique. The efficiency of the rotary kiln is usually improved by recovering a part of the heat in the hot calcined clay that exits the kiln using a cooler and by utilising the residual heat in the air that exits the top end of the kiln. This recovered energy can be used in various ways, such as for drying or preheating raw materials, generating electricity, etc. Such technologies are widely available as it is common for cement plants to recover a majority of heat from the waste gases and the hot clinker.

Although the calcination of clay is almost instantaneous once the required temperature is achieved, sufficient residence time must be ensured to allow the heat to penetrate throughout the lumps. Depending on the size of the kiln, the residence time can vary between a few minutes to an hour. Overall, the length, diameter, rotational speed and the fuel feed of a rotary kiln must be designed in order to ensure proper calcination by controlling the air temperature and the residence time of the feed.

Energy fed into a rotary kiln is consumed in 6 major processes:
-   Increase of chemical energy of the calcined clay with respect to the raw clay,

- Evaporation of water and heating of water and its vapour,
- Combustion of volatile materials,
- Increase in temperature of the calcined clay with respect to the raw clay,
- Increase in the temperature of the output kiln gases with respect to the gases fed into the kiln and
- Heat loss from the surface of a kiln.

The overall energy required for the calcination thus depends on all the above processes. Due to the relatively lower calcination temperatures and energy required, it is expected that the energy consumed in the calcination of clay is 40% to 50% lower than that required for the production of clinker using similar technology. On the basis of trials carried out by the authors and their co-workers, the energy required for the calcination of clays is of the order of 2.5 to 3 MJ/kg of raw clay.

Flash calcination can also be used for the calcination of clays. The principle behind flash calciners is similar to that used in pre-heaters and pre-calciners in clinker plants. In this technology, finely powdered clay is introduced into a stream of air that is heated to temperatures as high as 1100˚C. Depending upon the design of the calciner, the clay can either directly enter the hottest part of the calciner and flow along with the hot gases or could gravitationally move against the flow of air from the cooler to the hottest part. In either case, since the residence time of the particles is limited to a few seconds, the conversion to mullite is significantly reduced despite the high temperatures. The most efficient designs of flash calciners contain several stages of cyclones where the raw clay is fed from the top and it slowly falls against the gyrating flow of hot air allowing a residence time of a few seconds in each stage. The fuel is fired at the bottom, near the exit of the last calciner stage and the speed of flow of the gases is maintained using propellers. One such flash calciner is shown in figure 4.5 below.
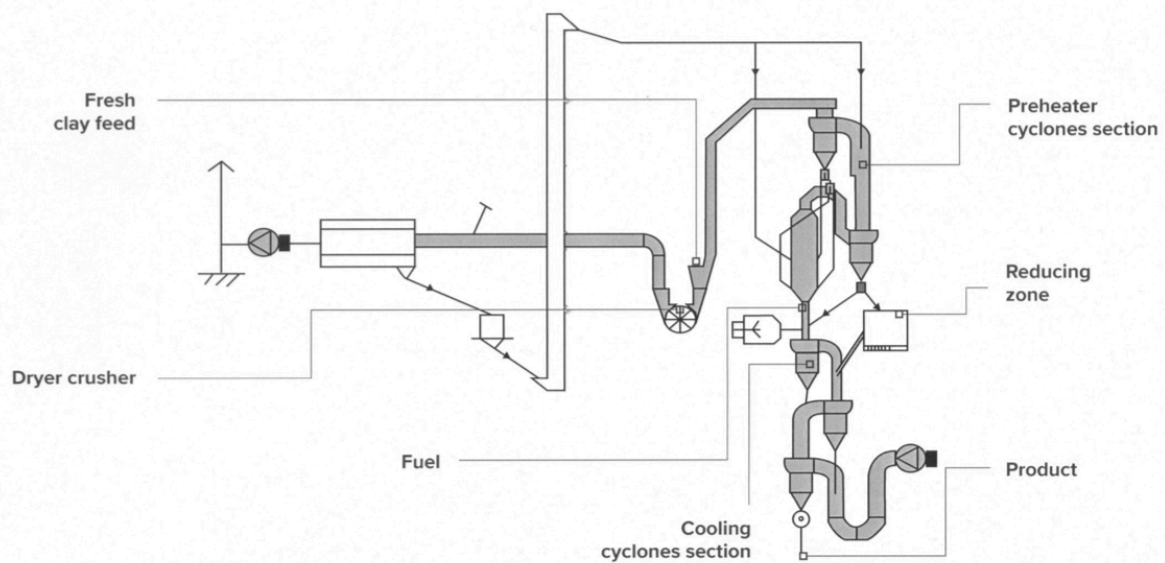
Figure 4.5: Layout of the process in a flash calciner (image courtesy FLSmidth)

Flash calciners consume energy in processes similar to those in a rotary kiln. However, due to the possibility of cycling of gases and the short residence time, higher thermal efficiency can be achieved. For this, flash calciners are generally equipped with pre-heaters that utilise the residual heat in the exit gases to heat the raw clay and with coolers that extract the excess heat in calcined clay for heating of the inlet gases. Similar to rotary kilns, most types of fuels, including coal, petcoke, diesel, furnace oil and alternative fuels can be used to fire flash calciners.

The calcination of clays could also be carried out in fluidised bed reactors where finely powdered clay is fluidised in a high velocity current of hot gases. Fluidised bed reactors function in a manner similar to the flash calciners since they rely on the suspension of the clay particles in hot gases and provide short residence times. Due to the closed circuit circulation of the gases in circulating type reactors, such reactors can be highly efficient. However, no information on instances of clays calcined using this technology were found in the literature.

Smaller scale continuous calcination of clays has also been carried out in vertical shaft brick kilns. While normally such kilns are used for the production of burnt clay bricks, the process can be modified to carry out the calcination of clays. In these kilns, pressed bricks of the clay are fed at the top and the cooled bricks are recovered at the bottom. This process is thermally efficient as it is continuous and residual heat can be recovered from the bricks.

Various types of fuels can be used for the calcination of clays in continuous calciners. Furnace oil and natural gas are commonly used for the calcination of clays used in other industries such as paint and paper. This is because the whiteness of the clay has to be maintained and other solid fuels may leave dark particles in the calcined material since the ash of the fuel would also be incorporated in it. However, for use in LC³, a slight darkness in the colour of the clay is not expected to lead to a significant influence on the properties of the cement. For this reason, fuels like coal and petcoke can be used after pulverisation for firing the kiln. Also, while the introduction of sulphates from fuels like petcoke is often of concern to the clay calcination industry, in the case of LC³, the sulphates that are present in the calcined clay can be compensated for by reducing the sulphates added in the final step of cement production. Alternative fuels like biomass briquettes made from agricultural wastes have also been successfully used for the calcination of clays used in LC³.

The colour of the calcined clay is often a reason of concern for the cement industry. It has been suggested by the industry in most countries that since most of the clays that would be suitable for use in LC³ would contain iron impurities, the calcined clays may be reddish in colour. However, it has been shown that the calcination of clays with higher iron contents in reducing conditions lead to the production of grey coloured calcined clays. Reducing conditions can be achieved in kilns either by adjusting the fuel to air ratio or by introducing reducing gases such as carbon-monoxide into the kiln. Technologies that control the colour of calcined clay are commercially available from many calcination equipment manufacturers.

4.1.3 Characterisation and suitability of clays

Clays containing 40% to 60% kaolinite have been found to be most suitable for the production of LC³. The lower reactivity of clays with lower kaolinite contents has been seen to lead to a reduction in strength development. It has been observed that, due to the limited availability of portlandite in cements with lower clinker contents, there is no significant increase in strength or transport properties of concrete when clays with higher kaolinite content are used. Such clays, however, have been seen to increase the water demand of concrete. It has also been seen that the hydration of clinker, especially of belite, is reduced when clays with higher kaolinite content are used. This is also seen to reduce the long-term strength development of the cement. The ratio of limestone to calcined clay may, therefore, be increased when clays with higher kaolinite contents are used. This is expected to reduce the influence of clays on water demand and on the hydration of clinker phases.

Quartz and other clay minerals, which are known to be commonly present as impurities in kaolinitic clays, are known to not interfere with the performance of the calcined kaolinite in LC³. When present in minor amounts (up to 10% by weight) expansive clay minerals, e.g. montmorillonite and bentonite, are not seen to lead to swelling or unsoundness in the cement. However, the presence of calcite and

dolomite as impurities is known to slightly reduce the reactivity of the calcined clays. Other minerals that may decompose during the calcination process may also interfere in the hydration of cement.

Iron present in the form of hematite is another commonly found impurity in clays. While most other industries avoid the use of clays with an iron content higher than 1% to 2%, such clays have been found to be suitable for use in LC^3. As discussed above, while the colour imparted to the clays by the iron is of importance to many other industries, this colour can be managed during the calcination process for use in LC^3.

Since the clays that are required for the production of ceramics, paints, paper, etc. require clays with high purity and whiter colour, such clays have a higher commercial value and are not widely available. However, clays that are not suitable for use in these industries are often discarded or not mined and, therefore, are available at much lower costs. The lower requirement of purity, thus reduces the cost and increases the availability of clays that are suitable for use in LC^3.

Table 4.2: Composition of raw clays measured using XRF (oxide composition) and TGA (kaolinite content) (All values as in percent by weight)

SiO₂	Al₂O₃	Fe₂O₃	CaO	MgO	Na₂O	K₂O	SO₃	Cl	Kaolinite content
56.24	37.14	1.42	0.54	1.38	0.97	0.68	0.01	0.03	43.1
60.34	32.06	1.93	0.97	1.38	0	0.47	0.02	0.03	47.3
86.26	9.65	1.02	0.55	1.22	0.33	0.21	0.07	0.05	9.2
53.45	38.63	1.33	1.53	1.47	1	0.76	0.02	0.03	65.1
54.94	36.17	1.48	2.48	1.47	1.03	0.9	0.02	0.05	54.3
71.68	19.35	2.73	2.64	1.51	0.54	0.45	0.04	0.05	30.5
56.73	35.71	1.22	1.32	1.4	0.99	0.93	0.03	0.05	53.2
54.46	36.5	1.37	2.54	1.44	1.05	0.87	0.02	0.06	52.2
49.94	19.17	2.42	24.07	1.58	0.58	0.62	0.03	0.08	18.6
38.65	47.4	0.92	12.91	0	0.05	0.06	0	0.01	<50
61.95	22.97	3.21	11.73	0	0.11	0.01	0.02	0	50
44.76	32.25	10.3	12.52	0	0.05	0.12	0	0.01	51
47.34	36.58	3.6	12.37	0	0.08	0.03	0	0	76
16.08	65.73	1.92	15.8	0	0.24	0.05	0.18	0	<50
38.15	49.89	3	7.98	0.72	0.15	0.04	0.07	0.01	2
57.3	25.44	4.37	12.6	0	0.15	0.15	0	0	42
39.01	45.87	1.71	13.19	0	0.15	0.04	0.02	0.01	90
32.37	50.41	2.74	13.59	0	0.33	0.1	0.45	0	83
70.77	14.1	3.86	11.2	0	0	0.05	0	0.01	16
79.11	7.69	2.79	10.29	0	0.1	0.01	0	0	15
57.34	26.72	2.89	11.99	0	0.85	0.05	0.17	0	41

Calcined and raw clays can be characterised by using both traditional and modern techniques. A chemical analysis of the clays in terms of its oxide contents can be carried out either by using chemical analysis techniques such as titration or using the X-Ray fluorescence (XRF) technique. When using XRF, it must be ensured that the equipment is calibrated for clay specimens. This requires the preparation of several calibration standards that have to be first characterised using other techniques or using another XRF equipment that has already been calibrated for clays. The composition of the clays being

used for the calibration must be wide enough to cover the entire range of chemical compositions of clay specimens that are expected to be analysed. Table 4.2 below shows the chemical compositions of some raw clays along with their kaolinite contents.

The chemical analysis results, such as those listed above can be used to estimate the kaolinite content by comparing the alumina and the silica content in the clay. In pure kaolinite (or metakaolin), around Al_2O_3 accounts for 40.5% of the mass, while SiO_2 accounts for 46.5% of the mass; in pure calcined kaolinite (metakaolin), these numbers are 46% and 54% respectively. The alumina content in the clay can be used to estimate the potential kaolinite content. However, since the impurities in the clay, such as clay and other aluminous minerals, may also contain alumina, this method can only provide an upper limit of the kaolinite content in the clay.

X-ray diffraction (XRD) and thermogravimetric analysis (TGA) provide the most accurate means to characterise clays that are suitable for use in LC^3. Since pure kaolinite is known to lose approximately 14% of its weight as water vapour when its temperature is increased from 450˚C to 650˚C, the kaolinite content in a clay can be estimated by measuring its weight loss between these two temperatures using a TGA equipment. The ratio of the weight loss in this temperature range to 14% gives the approximate kaolinite content in the clay. The direct measurement of change of weight in this temperature range can, however, lead to an over-estimation of the kaolinite content in the clay due to the presence of other phases that continue to decompose in the background. The influence of these phases may be eliminated by using the tangent method described in the literature. The temperature range of the decomposition can also be chosen from the DTG graph as shown in Figure 4.6 below.
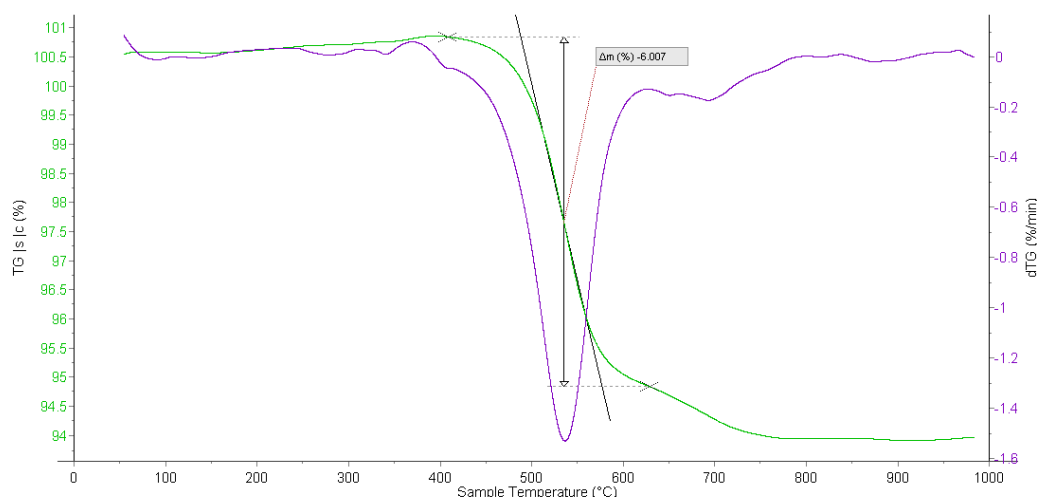
Figure 4.6: Calculation of kaolinite content using TGA: The clay has approximately 43% kaolinite content

The approximate kaolinite content in clays can also be determined using the same principal by static heating of the clay specimens first to 450˚C and then to 650˚C in a furnace. The difference in weights of the specimen at the two temperatures can be used to calculate the fraction of weight lost in the decomposition of kaolinite and thereafter the approximate kaolinite content by dividing this weight loss by 14%. Although specimens that are larger, and hence more representative, than those required for TGA, can be used for this test, it must be ensured that the sufficient time is allowed for a uniform heating of the entire specimen. This can be ensured by using thin specimens, removing the air in the specimen by making a pellet and increasing the soaking time.

At times, the decomposition of minerals other than kaolinite can also take place within the same range of temperatures and additional peaks may be visible in the Differential Thermogravimetry (DTG) graphs. An example of the DTG of one such clay is shown in figure 4.7 below.

46
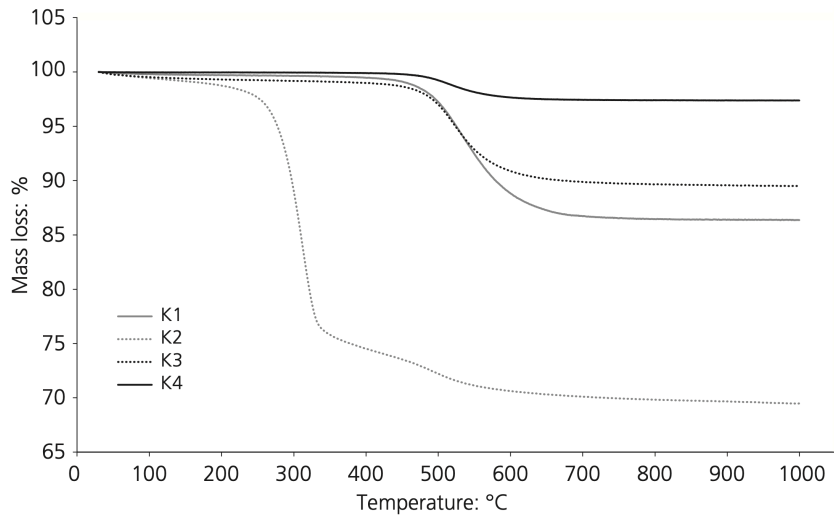
Figure 4.7: DTG of various clays with difference kaolinite contents: K2 has an impurity that decomposes in the same temperature range (Krishnan et al. 2018)

Minerals other than kaolinite that decompose in the same temperature range will also be calcined along with the kaolinite during the calcination process. The decomposition of natural minerals at higher temperatures generally leads to the formation of other more energetic phases that can display reactivity in cementitious systems. The reaction of these phases along with kaolinite in cementitious systems may lead to an influence on the properties of cement. Unless the influence of such impurities is clearly understood, clays that show a decomposition peak in this temperature range, other than that of kaolinite, must be avoided for the production of LC^3.

Quantitative X-ray diffraction analysis can be used in order to verify the content of kaolinite and other minerals in the clay. However, depending on the crystallinity and quantity of the minerals other than kaolinite, they may not be detected in XRD. Such minerals cannot be detected using the static testing method in a furnace discussed above. The presence of such minerals that decompose in this temperature range can be easily detected using TGA. Any additional peaks, changes in the calcination temperature or wider temperature ranges required for calcination could indicate interference in the calcination process from other minerals present in the clay.

Calcined clays can also be characterised using XRD and TGA. Any residual weight-loss in the temperature range of 450˚C to 650˚C using TGA or the static heating method, as a fraction of the original weight loss in this temperature range before calcination represents the uncalcined fraction of the specimen. The figure 4.8 below shows an example of the TGA of an improperly calcined clay, compared to that of a properly calcined one.
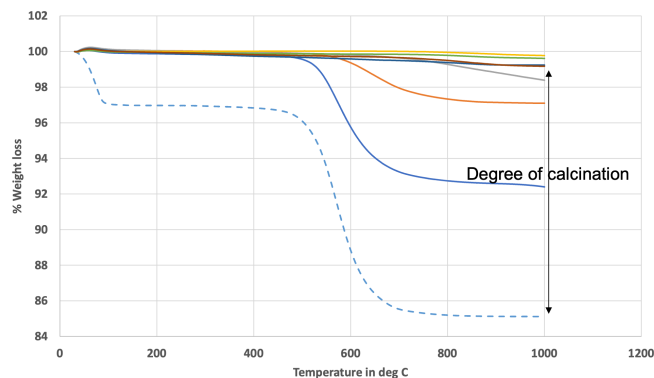
Figure 4.8: TGA of properly and improperly calcined clays

The figure 4.9 below compares the X-ray diffraction (XRD) patterns of uncalcined and calcined kaolinitic clays.
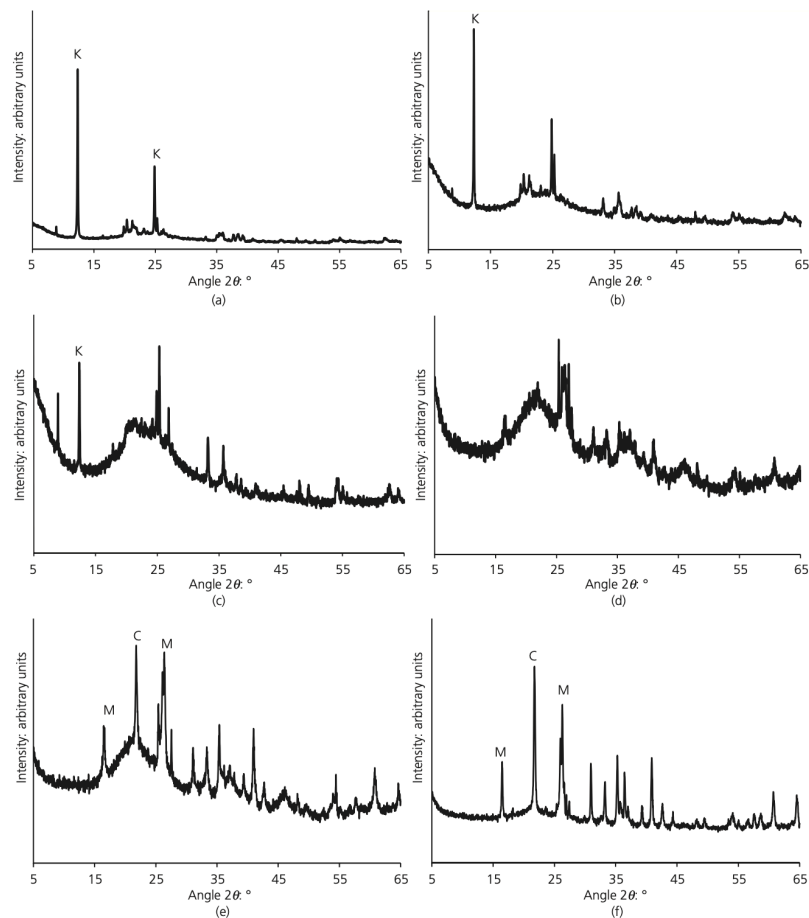
Figure 4.9: X-ray diffractogram of uncalcined (a), undercalcined (b and c), properly calcined (d) and over-calcined clays (e and f) (Krishnan et al. 2018)

It can be seen from the figure above that the quality of calcination of the clays can be assessed using XRD. The table below lists the diffraction angles for some important clay minerals, as observed in X-ray diffraction. It can be seen in the first diffractogram above that that, as is usual, the clay tested contains quartz and some other minerals as impurities. In the diffractogram of the uncalcined clay, the peaks of kaolinite can be observed at 12.326˚ and 24.872˚. As can be seen in the diffractogram for the calcined clay, instead of peaks that were clearly visble earlier, a wide hump is present. The wide hump of diffraction indicates a material that has no well-defined inter-planar distance and is, therefore, amorphous. It can also be observed that there is little influence of the calcination process on the other peaks. The presence of both the amorphous hump and residual peaks of kaolinite indicates incomplete calcination in the third diffractogram. The fourth diffractogram is of a clay that has been exposed to temperatures high enough to cause recrystallization and the formation of mullite. The peaks of mullite can be observed at 25.984˚ and 26.297˚. The absence of the kaolinite peaks in this diffractogram clearly shows that it is the kaolinite that has converted to mullite. Furthermore, the absence of the amorphous hump, which is observed in the second diffractogram, indicates that no amorphous content is remaining in this clay. It can be seen that this clay is over-calcined and is expected to demonstrate no reactivity in cementitious systems.

While the methods discussed above analyse the calcined clays from the chemical point-of-view, their potential performance in LC^3 can be better quantified by looking at either their rate of reaction or

their rate of developing strength. While most of the tests that exist for the assessment of SCMs can also be used for calcined clay and LC^2, a RILEM technical committee [Reference] has found that some tests perform much better than the others. Such tests can either be carried out on the clays or on the blends of the clays with the limestone with which it will be blended in LC^3. The blends of limestone and calcined clay are called limestone calcined clay, or LC^2 in short. Since most SCMs do not react with water on their own, the tests methods require their mixing with alkalis and/or sulphates to activate their hydration.

The figure below shows the chemical composition of cements and SCMs on a ternary phase diagram with CaO, SiO$_2$ and Al$_2$O$_3$ at the nodes.
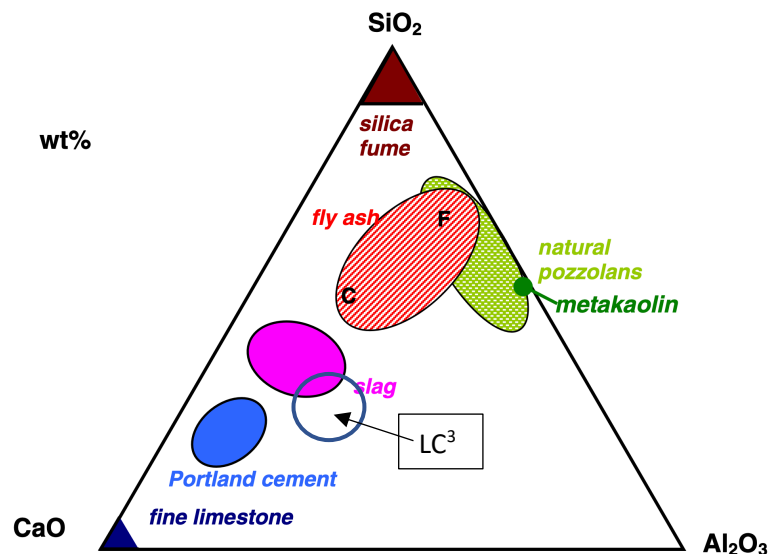

Figure 4.10: Ternary phase diagram for SCMs including LC^2

As can be seen in the figure above, calcined clays and other natural pozzolans lie along the Al$_2$O$_3$-SiO$_2$ axis and have a relatively low CaO content. Quartz being one of the most commonly found materials on the earth's crust, is also the most common impurity in all SCMs. Despite having both alumina and silica in the same crystalline structure, clays are known to react in a non-stoichiometric manner, such that the rate of the reaction of the alumina is independent of the rate of reaction of the silica. The absence of calcium in clays implies that calcium must be provided along with the clay in the test method.

The RILEM technical committee [RILEM TC 267-TRM, Li et al. 2018] has identified two types of tests that give the most reliable correlations with strength potential of an SCM, especially calcined clays.

In the first of these tests, known as the R3 (Rapid, Relevant and Reliable) test, the calcined clay or LC^2, is mixed with calcium hydroxide, potassium sulphate, potassium hydroxide and water and the hydration in the paste is followed using an isothermal microcalorimeter. The calcium hydroxide is added since it is expected to react with the alumino silicates in the calcined clay. Potassium sulphate is added to stimulate the reactions of the aluminates and potassium hydroxide is added to increase the pH to levels similar to those found in cements. Upon mixing these components together, an exothermic reaction that is similar to the reaction of the SCM in cement starts and the heat evolved from the reaction can be measured using a calorimeter. [Avet et al. 2016] presents a detailed study on arriving at the optimal proportions of materials to be mixed in order to obtain the best correlation between the test results and the strength development in mixes containing the clay or LC^2. As can be seen in the figure 4.11 below, the total heat evolved from the paste after one day of hydration has been found to correlate well with the strength development.
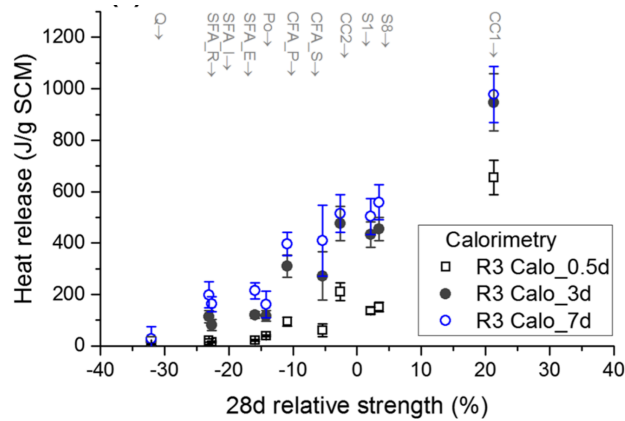
Figure 4.11: correlation between heat evolved in the R3 test and mortar compressive strength (Li et al. 2018)

Although the R3 test is convenient to carry out, it would not be possible to perform without an isothermal calorimeter. A simplified version of the R3 test, that measures the bound water in place of heat of hydration, can be carried out when an isothermal calorimeter is not available. In this test, a paste is prepared in a manner similar to that in the calorimetry method. Thin slices of the paste are cut after 1 day of hydration and the slices are dried at 110˚C to remove all the free water in the paste. The heating is stopped when the weight loss in the specimen is less than 0.5% during the previous 24 hours. The weight of the specimen is then taken and it is heated and kept at 400˚C for 2 hours and then cooled back to 110˚C. The percentage weight of the bound water is then calculated assuming that it is only the bound water that is lost between 110˚C and 400 ˚C. This method is also presented in detail in the literature [Avet et al. 2016].

The strength potential of SCMs is also commonly characterised by measuring the development of strength in pastes containing a blend of the SCM with lime or a cement with standard composition, cured at higher than usual temperatures to accelerate the test. The Indian standard lime reactivity test [IS1727] is one such test. In this test, a paste of lime and the SCM is prepared and 5 cm cubes of the paste are cast. The ratio of lime to SCM is kept as 1:2M, where M is the ratio of the specific gravity of the SCM to the specific gravity of lime. The quantity of water added to the paste is decided by carrying out the flow table test in order to obtain 70% flow after 10 drops of the flow table in 6 seconds. The cubes are left covered with a wet cloth at 27˚C for 48 hours and then demoulded and moved to a chamber with 50˚C temperature and more than 90% relative humidity for 8 days. At the end of 8 days in these conditions, the cubes are cooled back to ambient conditions and their compressive strength is measured. The average compressive strength of three such cubes is called the lime reactivity of the SCM. The suitability of a mixture of limestone with calcined clay (or LC^2) can also be assessed by following the same procedure as above. It has been shown that this test is also able to include the influence of the reaction of the limestone with the calcined clay. Lime reactivity values higher than 6.0 MPa are recommended for clays and LC^2 to be used in LC^3.

Variations of these test methods where cement is used in place of lime are also available. One such test [ASTM C311] recommends measuring the strength activity index, which is the ratio of strength of a mortar with 20% of OPC replaced by the pozzolan with the strength of a control mix without the pozzolan. However, since the results of these tests will be affected by the physical and chemical properties of the cement used, it is difficult to compare the results against defined benchmarks. A more detailed comparison of the performance of various test methods has been presented by Li et al. [2018].

The importance of proper characterisation of a clay before its use in an LC^3 blend cannot be overstated. Not only do the test methods discussed above help in establishing the suitability of a clay, but also in identifying the causes for issues that may be observed once the calcined clays are blended

with cements. The interaction of various components of LC³ and the characterisation of LC³ blends will be discussed in Chapter 6.

4.2 Limestone

This section discusses the geology of limestones, their natural availability and suitability for use in LC³. Test methods to assess their composition and suitability are also discussed.

4.2.1 Geology and use of limestone

Limestone is a sedimentary rock of which at least 50% is calcium carbonate. Limestone is generally formed form the deposition and cementation of the calcareous skeletons and shells of organisms in shallow-water conditions. For this reason, most limestones are of bio-chemical origin. In some cases, chemical limestone can also be formed from the direct precipitation of calcium in water. While the largest deposits of limestone occur in shallow-sea conditions, significant quantities are also present on land. Calcium is the fifth-most abundant element in the earth's crust, making around 3.6% of it. Limestone is the most common form in which this calcium is present.

Depending on their composition, morphology, texture and formation, limestone can be classified into various varieties such as chalk, oolite and tufa. Silica and clay are two of the most common impurities found in limestone.

Although calcium carbonate has three main polymorphs, most of the limestone is present in the form of calcite. Calcite has a hexagonal structure and is stable in the conditions that exist on the earth's crust. Aragonite, an orthorhombic polymorph, is usually associated with metamorphosis of calcite under high pressure and is metastable, and therefore, rare on the earth's crust. While vaterite also has a hexagonal structure, it is the least stable of the three polymorphs in the earth's atmosphere. The specific gravity of pure limestone is of the order of 2.7.

It is common for magnesium to be included in the structure of limestone during its lithification, leading to the formation of dolomite. Although the formation of dolomite is not well understood, it is generally thought that a partial replacement of calcium takes place by magnesium present in the ground water under slightly acidic conditions, leading to a twinning in the structure of calcium carbonate and the formation of calcium magnesium carbonate ($CaMg(CO_3)_2$). The metamorphic recrystallization of limestone and dolomite leads to the formation of marble. Calcite, dolomite and quartz are the main minerals in marble.

Limestone is used for a variety of purposes ranging from medicinal to construction. While high-purity limestone or chalk is used as a calcium supplement for humans and animals, lower purity limestone, along with dolomite and marble, having the important properties of hardness and strength, are used as blocks in load-bearing walls, partition walls and as dimensional stones for flooring, etc. Limestone is also the most important raw material in the production of cement and is the main source of calcium in clinker. Dolomite and limestones with dolomite content are usually avoided for the production of clinker. This is because upon their decomposition, the magnesium in dolomite gets converted to magnesium oxide or periclase. If present in large quantities in clinker, periclase can cause later-age expansion and cracking in cement, known as unsoundness.

Limestone, dolomite and marble are also added as mineral additives to cements and concrete, where they are powdered and mixed with without calcination. It has been shown that there is no risk of unsoundness in cement if magnesium is present in the form of dolomite and not in the form of periclase. Limestone is known to improve the flow of concrete and reduce segregation. As discussed in Chapter 2, limestone also participates in the hydration reactions to a small extent, influencing the microstructure and phase assemblage. Although it has been shown that limestone with calcium

carbonate content lower than that required for clinker production can be used as mineral additives, few standards currently allow this.

4.2.2 Reaction of limestone in Portland cements

Limestone is known to have both physical and chemical effects on cement hydration. A partial replacement of clinker with limestone leads to what is known as the dilution effect, where more water becomes available per unit clinker. Additionally, there is a filler effect where the physical presence of the limestone particles increases the rate of hydration of the clinker phases. A similar effect is also observed with other inert fillers like quartz and rutile.

Despite being sparingly soluble, limestone is known to be reactive in Portland cements (Bonavetti et al. 2001). The presence of calcium carbonates limits the pore-solution concentration of carbonates to a few mmol/l. The availability of carbonates in the solution prevents the conversion of ettringite to monosulphate and any remaining aluminates react to form carboaluminate phases takes place instead. The amount of limestone that reacts depends on the SO_3, Al_2O_3 and CO_2 available in the system (Figure 2.26) (Matschei et al. 2007a). The C_3A and C_4AF phases present in the clinker can act as a source of reactive alumina for the reaction of limestone. Hemicarboaluminate ($C_4A\check{C}_{0.5}H_{12}$) is observed to form first during the early ages of hydration and subsequently get converted to monocarboaluminate ($C_4A\check{C}_{0.5}H_{12}$) at later ages (Ipavec et al. 2011). A complete transformation of hemicarboaluminate to monocarboaluminate has been observed by 90 days in portland-limestone cements.

The formation of carbonate AFm phases prevents the conversion of ettringite into monosulphate (Figure 2.28) in cements incorporating limestone. The stabilisation of low-density ettringite increases the total volume of the solid phases leading to an improvement in compressive strength (Lothenbach et al. 2008b). The impact of limestone on the Ca/Si ratio of C-S-H is still not very clear. However, it has been reported that limestone slightly increases the Ca/Si ratio of the C-S-H compared to the C-S-H formed in OPC (Chowaniec 2012; Péra et al. 1999).

While limestone is known to improve the one day strength of Portland cements, no significant improvement is observed beyond one day when compared to control OPC systems. The strength of the cements is affected by the formation of a well-refined microstructure and the stabilising effect of carboaluminates on the low-density ettringite (Matschei et al. 2007a; Tsivilis et al. 2000).

Limestone is also known to improve the rheology of the concrete mixes and has been used extensively for the production of self-compacting concretes (Alexandra et al. 2018; Elgalhud et al. 2016; Gesoğlu et al. 2012). Limestone is also seen to improve the durability characteristics of portland limestone cement systems due to the refinement of pore structure (Dhir et al. 2007; Elgalhud et al. 2016; Pipilikaki and Beazi-Katsioti 2009).

It has been reported that this prevention of conversion of ettringite increases the solid volume in the microstructure, reducing porosity and increasing strength. The phase changes that occur in the microstructure due to the presence of 4% calcium carbonate are summarised in the results of thermodynamic simulations shown in figure 4.12 below. Due to the limited availability of carbonate ions, hemicarboaluminate ($C_4A\check{C}_{0.5}H_{12}$) is known to form in the early ages and convert to monocarboaluminate ($C_4A\check{C}_{0.5}H_{12}$) with time as more carbonate becomes available.
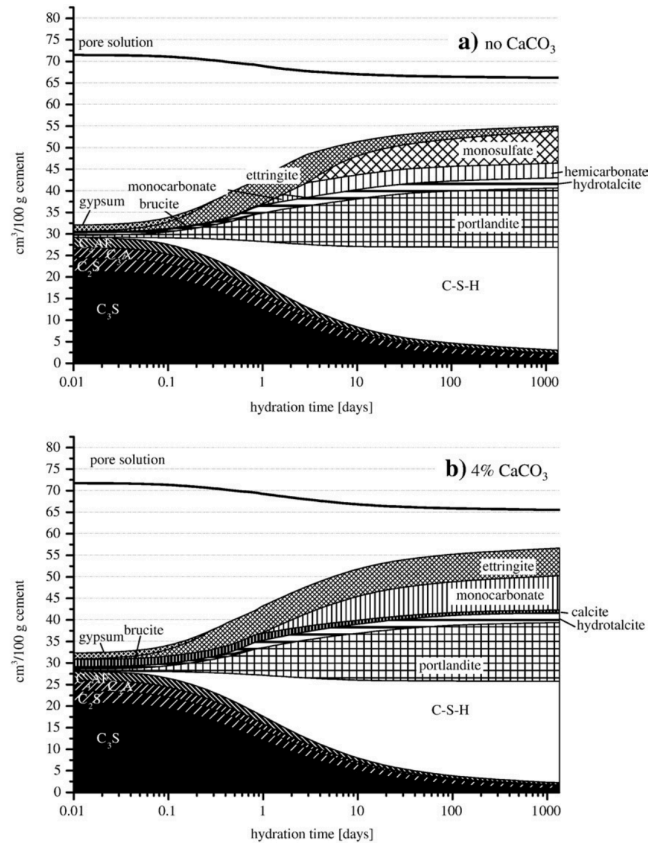
Figure 4.12: Formation of carboaluminate phases in Portland limestone cement due to presence of calcite (Lothenbach et al. 2008)

Due to the limited quantities of alumina available in ordinary Portland cement, the carboaluminate phases usually make a minor contribution to the microstructure. However, the increased availability of alumina from the calcined clay in LC³ increases the proportion of carboaluminates in the microstructure.

4.2.3 Suitability of limestone for LC³

The role of limestone in LC³ is more important than its role as a filler in Portland cements. Not only does it help in reducing the water demand of the cement, it also reacts with calcined clay in alkaline conditions to produce hydration products that contribute to microstructural development.

Despite its limited reactivity, limestone has a complex and important role in LC³. First, the presence of a third component allows LC³ to have a wider particle size distribution, which helps in achieving a better packing of the cement particles and reducing water demand. The smoother surface of the limestone particles also compensates for the increase in water demand due to clay. Secondly, the dissolution of limestone at the higher pH in cement increases the availability of carbonate ions in the solution. This leads to the formation of carboaluminate phases and prevents the conversion of ettringite into monosulphoaluminate.

Although only a limited amount of limestone is known to chemically react in LC³ systems, an assessment of their characteristics is nevertheless important. In the context of LC³, the term limestone covers all the carbonate sources discussed above including limestone, dolomite, marble, etc.

Limestones with a total carbonate content as low as 65% have been used in the production of LC³. Quartz is one of the most commonly found impurities in limestone. The inclusion of quartz in cement

has been widely studied and it is found to be predominantly unreactive material that serves as a hard filler. In LC^3 as well, quartz has been found to neither react nor interfere with the hydration reactions. Therefore, the presence of quartz in limestone is unlikely to have a significant influence on the performance of LC^3. Clays are also commonly found as impurities in limestone. Clays of the smectite type can swell in the presence of water in concrete leading to cracking. However, no swelling has been observed with limestones containing up to 10% of expansive clays.

Like in the case of clays, limestones can also be characterised using chemical analysis techniques such as titration and XRF. Since pure limestone contains 56% CaO by weight, the calcium content in a limestone can be used to estimate its purity. This estimation may be inaccurate due to the presence of impurities such as dolomite. Similar to clays, a proper calibration of the XRF equipment is required in order to obtain reliable chemical composition of limestone containing impurities.

Table 4.3 below shows the composition of some of the limestones that have been used in trial productions of LC^3. Some of the materials listed here are dusts of stones such as marble and quartzitic limestone used as building materials.

Table 4.3: Composition of limestones used in LC^3

	Na$_2$O	MgO	Al$_2$O$_3$	SiO$_2$	SO$_3$	Cl	K$_2$O	CaO	Fe$_2$O$_3$	LOI
Limestone 1	0.32	1.13	8.51	24.31	0.06	0.019	0.62	33.29	4.8	26.9
Limestone 2	0.23	0.035	12.8	31.63	0.02	0.02	0.835	27.65	6.75	22.1
Limestone 2	0.2	0.735	9.925	27.01	0.02	0.019	0.685	31.5	5.275	26.1
Limestone 3	0.255	0.79	9.585	25.94	0.105	0.019	0.81	31.9	4.96	25.9
Limestone 4	0.24	0.055	12.83	32.25	0.06	0.02	0.925	27.37	6.195	21.8
Limestone 5	0.29	1.055	10.12	25.84	0.045	0.019	0.825	31.95	4.805	25.9
Limestone 6	0.625	0.805	6.44	20.61	0.305	0.017	0.575	36.72	3.68	29.1
Limestone 7	0.27	1.39	3.83	13.33	0.19	0.017	0.44	42.85	2.31	35.6

Like in the case of clay, XRD and TGA are the most suitable techniques for the characterisation of limestone. Figure 4.13 below shows the XRD pattern of clinker grade limestone. Figure 4.14 shows the XRD pattern of a low-grade limestone with quartz and clay impurities.
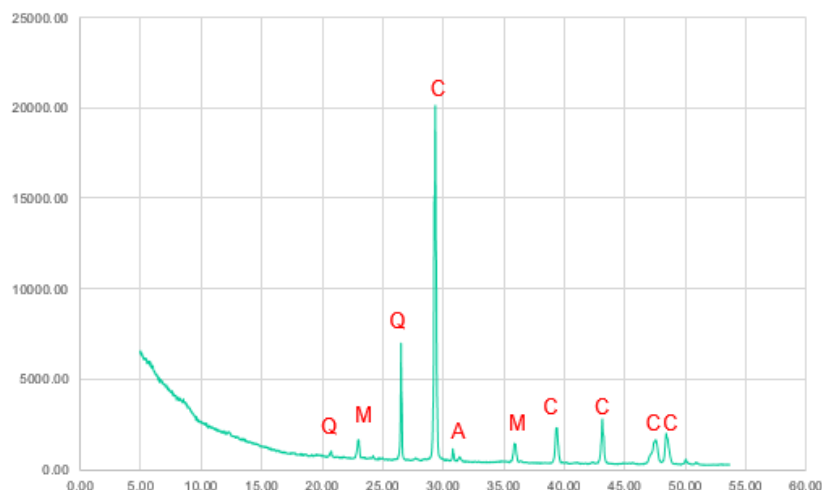

Figure 4.13: XRD patterns of a clinker grade limestone, with quartz, muscovite and ankerite impurity
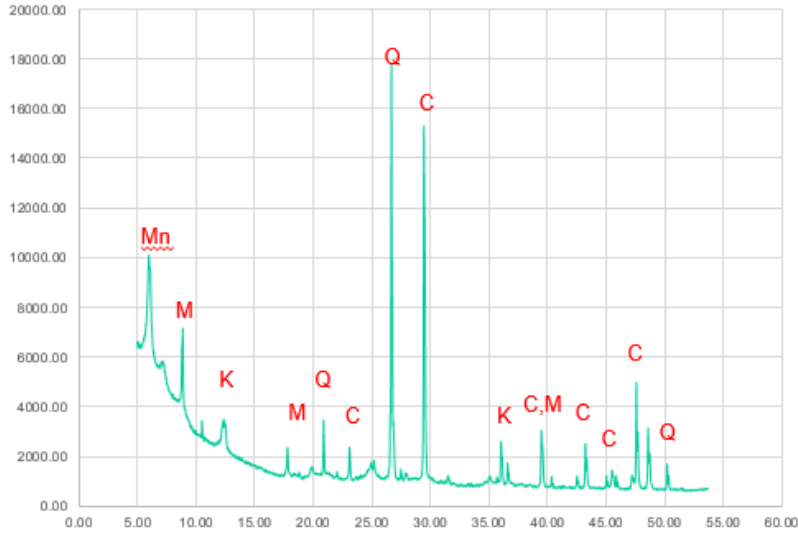
Figure 4.14: XRD patterns of calcitic limestone, with quartz and clay impurity

Rietveld analysis of limestone can not only help in the estimation of its purity, but also in the identification and quantification of the impurities in the limestone. Although Rietveld analysis can be used to quantify the calcite content in a limestone, it is generally easier to measure using TGA. Figure 4.15 below shows the TGA analyses of a pure limestone and a dolomitic limestone, and a low-grade limestone with various other impurities. Figure 4.16 shows the TGA and DTG analysis of a limestone with impurities.
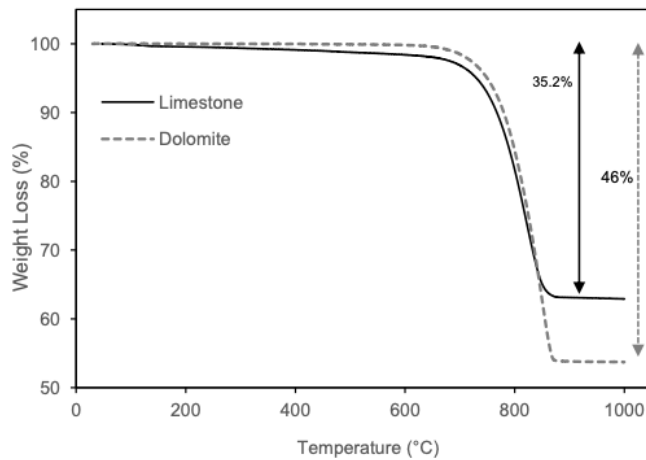
Figure 4.15: TGA analyses of calcitic limestone and dolomitic limestone (Krishnan 2019)
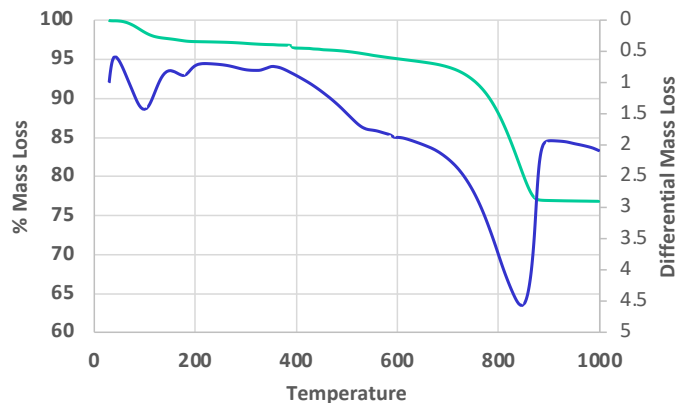
Figure 4.16: TGA and DTG analysis of a limestone with impurities

It can be observed in the figures 4.15 and 4.16 that the decomposition of limestone occurs between 700°C and 950°C. Pure calcium carbonate loses 44% of its weight as CO_2 escapes from the molecule, converting it into calcium oxide. The calcium carbonate content in a limestone can be approximately determined by dividing the fraction of weight lost in this temperature range by 44%. This content is approximate since other minerals, such as dolomite, also decompose in the same temperature range. Dolomite loses approximately 47.7% of its weight when it loses its CO_2 molecules. Some studies have reported that amorphous particles of calcium carbonate may decompose at temperatures as low as 400°C, however, it is not clear if such limestone occurs in nature.

Given the errors in determining the carbonate content in limestone, a combination of chemical analysis, XRD and TGA is usually used required to assess its suitability for LC^3. Usually, limestones with more than 65% carbonate content have been found to be suitable for use in LC^3. Dolomite and limestones with dolomite impurity have been seen to react more slowly than calcite in LC^3 systems. While some studies have advised against the use of dolomite in concrete due to the occurrence of the so-called alkali-carbonate reaction, recent studies have shown that the reaction of dolomite in alkaline conditions does not to expansion or cracking in concrete. More details on the role of carbonates and their influence of hydration and strength development will be discussed in the later chapters.

4.2.4 Summary
Limestone is not only a raw material for the production of clinker, but also an important additive widely used in Portland cements. Despite what has been assumed earlier, limestone is now known to react in cements and to lead to the formation of a finer microstructure. Limestone is also known to contribute to improvind the rheology of cements and concrete. The relatively smaller quantity of aluminates in Portland cements reduces the contribution of limestone to hydration and microstructural development. This report describes the properties of limestone calcined clay cement (LC^3), where the larger quantities of alumina available in calcined clay allow higher reaction of limestone.

4.3 Production and properties of LC^3
The production of LC^3, while similar to the production of Portland and blended cements, requires additional processes to accommodate for its additional components. This chapter discusses the production of LC^3 and its important properties. The design of LC^3 blends and the influence of the constituents on its properties will be discussed later in Chapter 6.

4.3.1 Grinding and blending of LC^3
The production of LC^3 requires the grinding and mixing of the components to yield a homogenised cement. Although the most common way to produce blended cements is to grind all the components together in a mill, also called inter-grinding. For example, PPC can be produced by inter-grinding coarser particles of clinker, fly ash and gypsum using various types of mills such as ball mills, vertical roller mills and roller presses could be used for this process. In such a grinding process, it is usually desirable that all components are ground to a similar particle size and are mixed uniformly. This may, however, be difficult if the relative hardness of various components is different. Given the larger number of components in ternary cements, the likelihood of having different hardness of different components is higher, leading to the preferential grinding of some of the components while the others remain relatively coarser. While the differential hardness of the components can help in achieving a wider particle size distribution, which improves packing of particles and reduces water demand, insufficient grinding of some phases can negatively influence the performance of the cement. Additionally, since clay particles tend to coat the grinding media, the efficiency of grinding has been reported to be reduced.

In the case of LC³, clinker is generally expected to be harder than limestone and calcined clay. This may result in a cement with fine calcined clay and limestone and coarse clinker. Since the hydration and strength development in LC³ relies on the hydration of clinker phases, insufficiently ground clinker would result in a significant reduction in the performance of the cement. Closed-circuit mills with air-classifiers, which send back the coarser particles to the inlet of the mill for further grinding, generally provide a better control over the particle size distribution of cements than normal mills.

In order to optimise the properties of LC³, it is desirable that the clinker grains are ground to a fine state, whereas the clay particles are slightly coarser. While the fine clinker grains will lead to a faster strength development and build up the calcium hydroxide content in the microstructure, a reduction in the fineness of the calcined clay particles will reduce the water demand of the cement and allow for a higher strength development after 7 days of hydration. Figure 4.17 shows the influence of additional grinding on the rate of hydration of LC³. Figure 4.18 shows the influence of additional grinding on strength development of LC³.
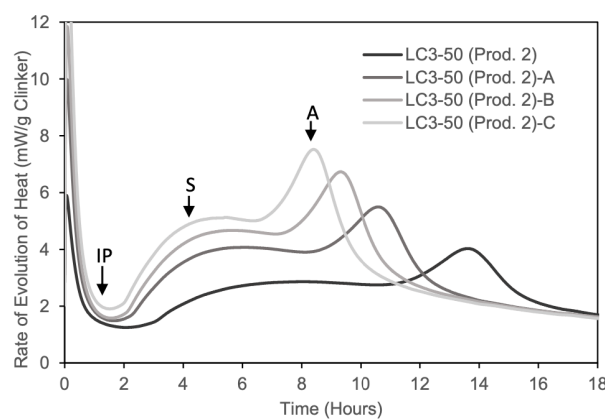

Figure 4.17: Influence of additional grinding on rate of hydration of LC³ (Krishnan 2019)
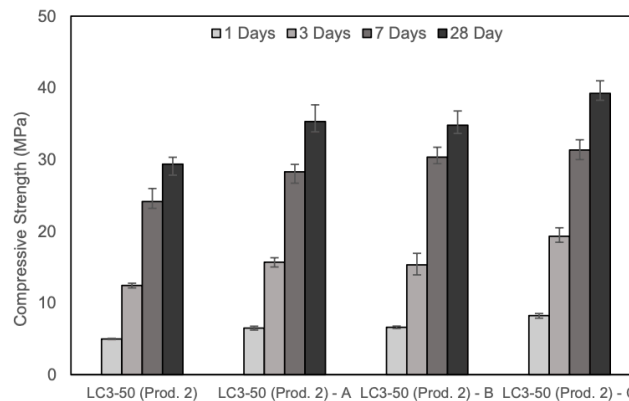
Figure 4.18: Influence of additional grinding on strength development of LC³ (Krishnan 2019)

In the above results, the base LC³ blend has coarser clinker particles and finer clay particles. Further grinding of the cement was carried out in a laboratory ball mill in order to further grind its coarser clinker particles. As can be seen in figure 4.19 below, a further grinding of the cement makes the coarsest of the particle finer, with little effect on the finer particles.
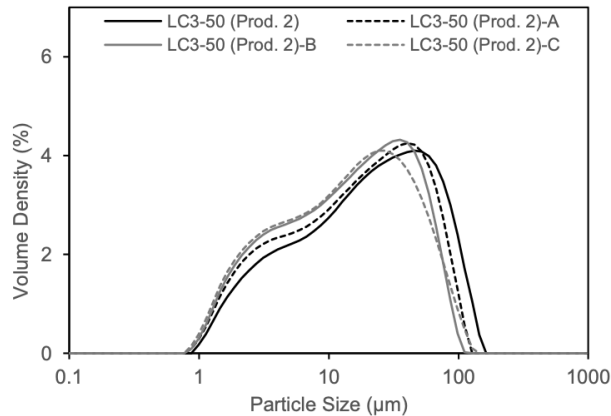
Figure 4.19: Influence of grinding on PSD of LC³

The results above demonstrate the importance of ensuring that the clinker phases in LC³ are well ground. In cases where there is a large difference between the hardness of the components, it may be desirable to separately grind clinker and LC² and to then blend them together. Gypsum can either be ground along with the clinker or partially in both LC² and clinker. This type of blending is common in Portland slag cements, when blast-furnace slags are much harder than the clinker. The Moh's scale of hardness can be used to characterise the relative hardness of minerals on a scale of 1 to 10, where 1 represents the hardness of talc and 10 represents the hardness of diamond. In order to determine the harness of a material, minerals or needles of known hardness are used to scratch the surface of the material. While harder materials leave a scratch, softer ones don't, making it possible to classify the material in between two known standards. Generally, if the hardness of materials is different by more than 2 points on the Moh's scale, it is preferable that they be ground separately and blended together after grinding.

Although there may be some difficulty in blending the pre-ground materials leading to some inhomogeneity in the cement, technology to blend fine powders on the industrial scale is available. The possibility of separately grinding OPC with gypsum and LC² and then blending them together creates the potential of the use of LC² as a separate mineral admixture in concrete.

When LC² is blended separately with OPC or ground clinker, the quantity of sulphates in the final blend must be ensured. This can be done either by adding more gypsum at the time of blending or by inter-grinding gypsum along with calcined clay and limestone at the time of production of LC². As discussed earlier, the quantity of gypsum has an influence on the rate of hydration and strength development.
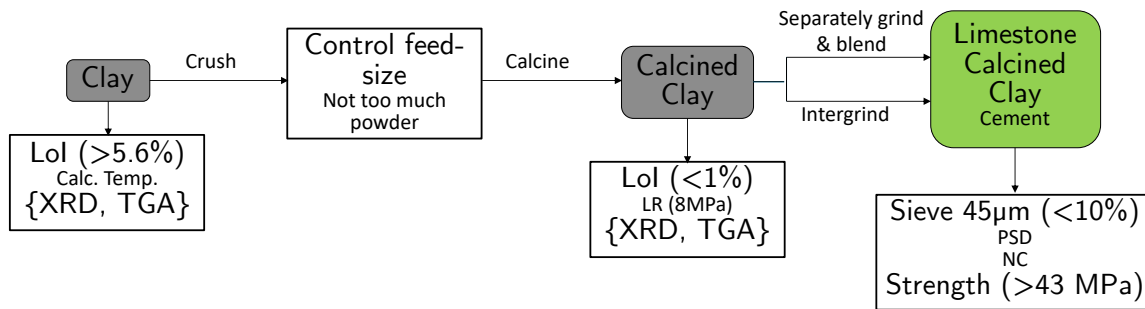
4.3.2 Quality control of LC³

A series of measures are required in order to ensure the quality of the raw materials, the production conditions and the cement produced. A summary of the tests to be carried out on individual components of LC³ and the final product are listed in Table 4.3. Figure 4.20 shows a simplified sketch of some of the important parameters to be checked at the time of production.

Table 4.3: Quality control tests carried out during the production of LC³ and their significance

Test on	Test method	Comments
Clinker	Chemical composition	To compare with usual composition. Clinkers with higher calcium content perform better with LC³.
Clinker	XRD	
Clinker	TGA	To check LoI for quality control. No special requirement for LC³.
Clinker	Hardness	To measure grindability. Softer clinkers are easier to intergrind with calcined clay.

Clinker	Strength potential by making OPC	To check strength potential. It is usually possible to obtain similar 28-day strength as OPC.
Clinker	CH content in hydrated OPC of clinker	To ensure potential for pozzolanic reaction. Clinkers with higher calcium content perform better with LC^3.
Limestone	Chemical composition	To ensure minimum carbonate content and identify impurities. Although requirements in standards may recommend higher contents, around 65% carbonate content is seen to be required. Large amount of clay impurities may be undesirable.
Limestone	XRD	
Limestone	TGA	
Limestone	Hardness	To measure the grindability of the limestone. Harder limestones will give coarser particles on intergrinding and help in reducing overall fineness of LC^3.
Raw clay	Chemical composition	To measure kaolinite content and identify impurities. 40% to 60% kaolinite content is recommended in clays.
Raw clay	XRD	
Raw clay	TGA	In addition to measuring kaolinite content and to determine optimal calcination temperatures.
Calcined clay	XRD	To assess quality and degree of calcination.
Calcined clay	TGA	
Calcined clay	Hardness	To measure grindability of clays and the influence of impurities. The results may be misleading due to coating of grinding media by clay particles.
Gypsum	Chemical composition	To measure sulphate content and to identify impurities.
Gypsum	XRD	
Gypsum	TGA	
LC^3	XRD	To verify composition and uniformity of cement.
LC^3	TGA	
LC^3	Chemical composition	
LC^3	Blaine's fineness	To measure fineness of cement. This test is not recommended for LC^3 due to unreliable results.
LC^3	Laser diffractometry	To ensure proper grinding of the cement and a good distribution of particle sizes.
LC^3	Sieve analysis	To carry out quality control of grinding. Less than 3% is usually retained in 90μm sieve and less than 15% in 45μm sieve.
LC^3	Standard consistency	To measure water demand and assess particle size distribution. The standard consistency is usually higher by up to 0.05 compared to an OPC produced using the same clinker.
LC^3	Setting time	To measure setting time and gypsum optimisation. The setting time is usually shorter than OPC produced using the same clinker.
LC^3	Isothermal calorimetry	To optimise sulphate content and study compatibility of components. The sharp aluminate hydration peak should be after the relatively gentle alite hydration peak.
LC^3	Compressive strength	For quality control. LC^3 can be designed to achieve a similar 28-day strength as an OPC with the same clinker.
LC^3	Soundness	To assess the risk of cracking. Risk of cracking is usually lower compared to OPC due to dilution of clinker with calcined clay and limestone.

Figure 4.20: Key steps in the process of quality control during the production of LC³

Once the cement has been produced, various physical and chemical tests have to be carried out on LC³ in the same manner as they are performed on OPC or PPC for quality control. While most of the physical and chemical properties of LC³ can be tested and interpreted in the same manner as they are for conventional cements, special attention has to be paid to the particle size distribution of the cement.

The Blaine's air permeability apparatus is commonly used as a quality control method to ensure proper grinding of cements in cement plants. In this test, a bed of cement with a standard void ratio is prepared and air is passed through it. However, since this method only represents average fineness of the particles and not their particle size distribution, it is less appropriate for blended cements. In the case of LC³, although the overall fineness of the cement may meet the target range, a possible differential grinding of the cement cannot be identified using this test. The quality of grinding can be checked by either measuring the particle size distribution of the cement or by carrying out a chemical analysis of various fractions of the cement.

Due to the wider particle size distribution of the cement and the nature of the calcined clay particles, the Blaine's fineness of the LC³ cements is generally 50% to 70% higher than OPC made using similar cements. However, the Blaine's fineness should not be interpreted as an indicator of the water demand of the cement. It has been observed that the water demand of LC³ is lower that what is expected from conventional cements with a similar specific surface area. The measurement of standard consistency has been found to be a more reliable measure of the water demand of the cement. Due to the plate-like morphology of calcined clay particles, the packing of the particles may lead to very high values of Blaine fineness being measured. These values are found not to be representative of the true fineness or particle size distribution of the cement.

The interpretation of the loss on ignition (LoI) measurements of LC³ should also be carried out with care. Usually, LoI measurements require measuring the fraction of mass loss in a specimen when heated from just above 100˚C to 1000˚C. LoI represents the amount of volatile materials and materials that decompose releasing gases when heated to higher temperatures. The specimens are pre-conditioned at temperatures slightly above 100˚C to allow for the free water to escape. The LoI values are often used to assess the presence of unfired material or pre-hydration in cements. However, due to the presence of un-calcined limestone, the LoI of LC³ is expected to be higher than that of OPC. The theoretically expected LoI of LC³ can be calculated by multiplying the LoI of the individual components with their proportion in the cement, with the majority of the contribution coming from limestone. While the measurement of LoI up till 1000˚C can be useful to assess the uniformity of blending of the cement, measurements up till 400˚C can be more useful to check if a cement is pre-hydrated. More reliable measurements of mass loss in different temperature ranges can be measured using TGA.

Chapter 5: Limestone mineralogy, purity, effect on properties

5.1 Introduction
This chapter provides a discussion about the geology and mineralogy of the limestone, the effect of limestone on OPC and LC^3 cement hydration mechanism, and characterization techniques for limestone, then moving on to discuss the suitability of limestone use in LC^3, and finally its natural availability across India,

5.2 Geology and Mineralogy of Limestone
Calcium, which is the fifth most abundant element in the earth's crust (after oxygen, silicon, aluminum, and iron) is found mostly in form of the limestone. Limestone is a sedimentary type of rock, primarily consisting of more than 50% calcium carbonate. Impurities in limestone compromise a spectrum of silica, dolomite, gypsum, siderite, iron and manganese oxides, clays, organic matter, etc. Most limestone deposits are formed by organic route, by the accumulation of calcareous remains such as shells and skeletons of organisms at the seabed in shallow water, which was then cemented by the process of diagenesis over the centuries. Another way of formation of limestone deposits is by a chemical process that is by precipitation of calcium carbonate from marine or freshwater. The biological origin limestone deposits are cemented by the precipitation of calcium carbonate from the calcium saturated water which moves through the sediment masses. Depending on their composition, morphology, texture, and formation, limestone can be classified into various varieties such as chalk, oolite, travertine, marble, tufa, etc.

Table 5.1 Minerals commonly associated with limestones (Selley et al. 2005).

Mineral	Formula	Crystal System	Occurrence
Aragonite	$CaCO_3$	Orthorhombic	Some shells and mud, unstable during burial
Calcite	$CaCO_3$	Hexagonal	Some shells and mud, relatively stable during burial
Magnesite	$MgCO_3$	Hexagonal	Rare surface mineral
Dolomite	$CaMg(CO_3)_2$	Hexagonal	Rarely at the surface, more common as a subsurface replacement
Ankerite	$Ca(MgFe)(CO_3)_2$	Hexagonal	A rare cement
Siderite	$FeCO_3$	Hexagonal	As ooliths and cement

Limestone makes 10% of the total volume of the sedimentary rocks and is found across the majority of the countries. Although calcium carbonate has three main polymorphs, most of the limestone is present in the form of calcite. Calcite has a hexagonal structure and is stable in the conditions that exist on the earth's crust. Aragonite, an orthorhombic polymorph, is usually associated with the metamorphosis of calcite under high pressure and is metastable, and therefore, rare on the earth's crust. While vaterite also has a hexagonal structure, it is the least stable of the three polymorphs in the earth's atmosphere. Limestone is relatively soft, having a Mohs hardness of 2 to 4 depending on the conditions of formation. Density of limestone varies in a range of 1.5 to 2.7 g/cm3 depending on its porosity which varies from 0.1% to 40% (Oates 2008). The specific gravity of pure limestone is of the order of 2.7.

During or after the formation of limestone, a certain percentage of magnesia gets added in places of calcium, giving rise to magnesium limestone. When magnesium and calcium limestone are combined in equal molecular proportions, the resulting mineral is called dolomite. Although the formation of

dolomite is not well understood, it is generally thought that a partial replacement of calcium takes place by magnesium present in the groundwater under slightly acidic conditions, leading to twinning in the structure of calcium carbonate and the formation of calcium magnesium carbonate $(CaMg(CO_3)_2)$. Dolomite is a little more stable than calcite, the crystal density of dolomite is about 10 % higher than that of calcite, and dolomitization is accompanied by an increase of porosity. Further, metamorphic recrystallization of limestone and dolomite leads to the formation of marble. Calcite, dolomite, and quartz are the main minerals in marble.
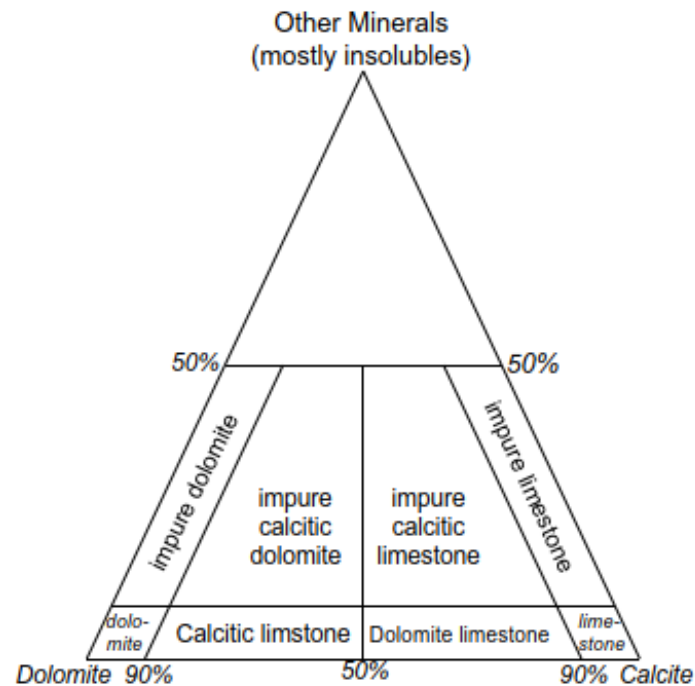
Figure 5.1 Mineralogical classification of carbonate rocks. (Carr and Rooney 1975)

5.2.1 Types of Limestone

Limestone is available in different forms, following is the list of the general form of limestone deposits:

- *Chalk* is a soft, fine grain, and contains very little terrigenous material composed of plates of algae and foraminifera.
- *Marble* is formed by the metamorphosis of limestone under heat and high pressure, resulting in recrystallization. Marble formed from pure limestone consists of white calcite.
- *Dolomite* deposits occur between the limestone beds and sometimes can occur as thick-bedded units, having magnesium present in a crystal lattice of calcium carbonate.
- *Oolitic* limestone is calcite cemented tiny spherical grains formed by algal action, having a resemblance to mass of a fish roe under a lens.
- *Travertine* is calcite deposits formed by chemical precipitation from natural hot springs along their course.
- *Tufa* is calcite deposits formed by chemical precipitation from natural springs water, which is more or less compact.

5.2.2 Limestone in Cement

Limestone is the most important raw material in the production of cement and is the main source of calcium in the clinker. Raw materials comprising limestone, clay, etc. are homogenized by grounding together, which are then heated to a temperature of up to 1450°C forming clinker minerals. After rapidly cooling the clinker, it is mixed with a small percentage of gypsum and grounded together to form the final ordinary Portland cement. Limestone containing dolomite is generally avoided to produce clinker, as upon decomposition the magnesium in dolomite gets converted to magnesium

oxide or periclase. If periclase is present in significant quantities in clinker, it can result in later-age expansion and cracking of cement paste, known as unsoundness.

Limestone, dolomite or marble powder is also added as a mineral additive to the cement, where they may or may not be calcined before. Studies have shown that if the magnesium is present in form of dolomite rather than periclase, it doesn't have the unsoundness effect in cement. Limestone addition as a mineral admixture in cement up to 15% had been allowed in different standards such as European standard: EN 197-1, America standard: ASTM C-595, Canadian standard: CSA A 3001, New Zealand standard: NZS 3125, etc. all around the world. The benefit of limestone addition as a mineral additive can be seen as reducing the clinker factor of cement which in turn reduces the carbon footprint of cement without losing any desirable properties Effect of limestone addition on the hydration process has been discussed in the subsequent sub-sections.

5.2.2 Effect of Limestone addition in Portland cement

Limestone is known to have both physical (filler effect, nucleation effect, and dilution effect) and chemical effects. The filler effect of the limestone is related to its particle size, packing density is higher when limestone is finer than cement is used as it occupies the voids between the cement particles. Thus, reducing the water requirement and increasing the compressive strength and durability of concrete (Martin et al. 2006). However, having very fine limestone can leads to a reduction in flowability as its specific surface area is very high. Additionally, fine limestone particle provides nucleation sites for hydration products to precipitate, accelerates the hydration reaction, and improves the degree of hydration of cement, known as the nucleation effect (Soroka and Setter 1976, Vance et al. 2013, Dale et al. 2015). On limestone addition, keeping the water to binder ratio constant, it increases the amount of available water to react with cement particles as limestone doesn't have cementitious or pozzolanic properties, known as the dilution effect. A higher degree of hydration is observed in cement owning to extra water available for addition. The dilution effect is attributed to the percentage addition of the limestone in the cementitious matrix.
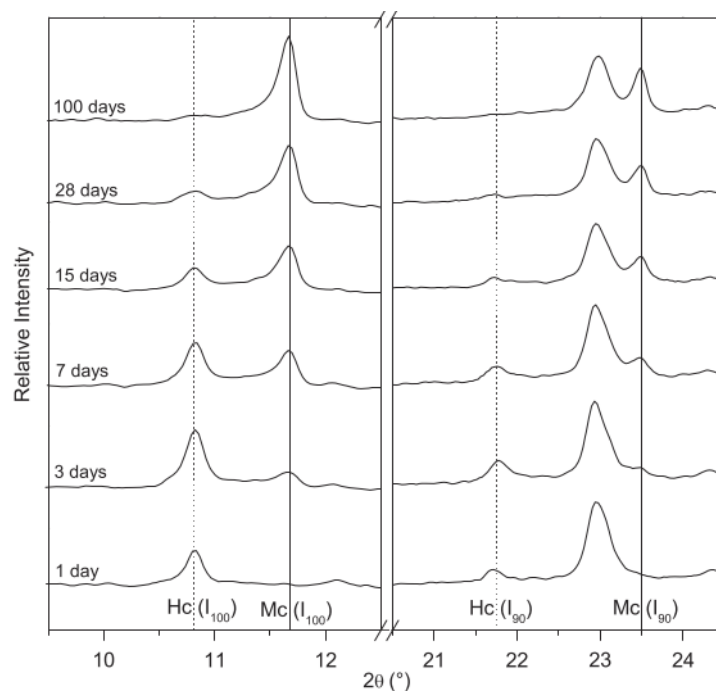

Figure 5.2 XRD pattern of carboaluminate phases in hydrated calcite-containing cement at different stages of hydration. (Ipavec et al. 2011).

63

Limestone is known to be sparingly soluble but still has been found to be reactive in Portland cement (Bonavetti et al. 2001). With the increase in the particle size of limestone, the dissolution rate of limestone increases. As a result, the presence of calcium carbonates increases the pore-solution concentration of carbonates to a few mmol/l. Carbonate ions present in the solution react with the reactive aluminate present in the C_3A and C_4AF phases of the clinker to form hemicarboaluminate ($C_4A\check{C}_{0.5}H_{12}$) and monocarboaluminate($C_4A\check{C}H_{11}$). The formation of carboaluminate phases stabilizes the ettringite and stops its conversion to monosulphate (Kakali et al. 2000). The stabilisation of low-density ettringite, and formation of hemi- and mono-carboaluminate increases the total volume of the solid phases leading to pore refinement, a decrease in porosity, and an improvement in compressive strength (Lothenbach et al. 2008). Hemicarboaluminate ($C_4A\check{C}_{0.5}H_{12}$) is observed to form first during the early ages of hydration and subsequently get converted to monocarboaluminate ($C_4A\check{C}H_{11}$) at later ages (Ipavec et al. 2011), see figure 1.2. A complete transformation of hemicarboaluminate to monocarboaluminate has been observed within 90 days in Portland-limestone cement.
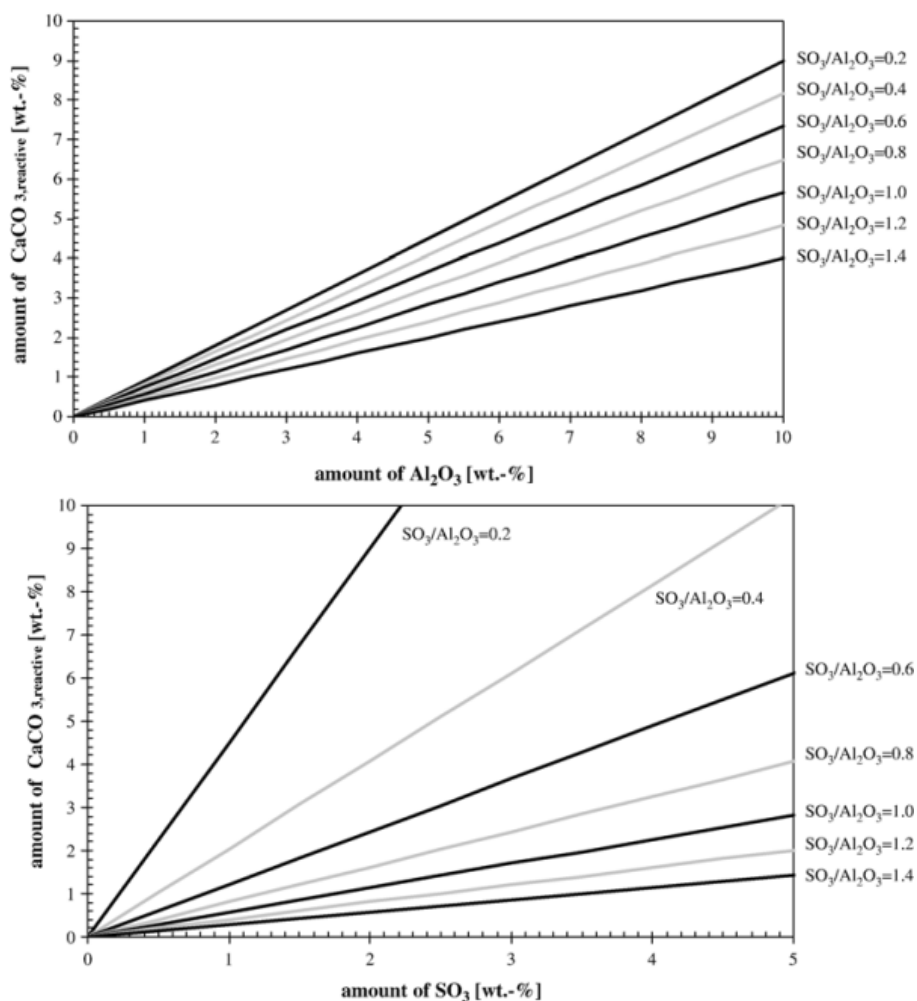
Figure 5.3 Calculated amount of reactive CaCO₃ in dependence of the initial amount of a) initial solid Al₂O₃ content, and b) initial solid SO₃ and bulk SO₃/Al₂O₃-ratio of the paste (data are expressed in weight units) (Matschei et al. 2007)

The amount of limestone that reacts depends on the SO_3, Al_2O_3 and CO_2 available in the system, see figure 1.3 (Matschei et al. 2007). Incorporation of limestone has also changed the morphology of C-S-H into shorter and thicker fibers of C-S-H (Nehdi and Mindness 1996). Although, the impact of limestone on the Ca/Si ratio of C-S-H is still not very clear. However, it has been reported that limestone slightly increases the Ca/Si ratio of the C-S-H compared to the C-S-H formed in OPC

(Chowaniec 2012; Péra et al. 1999).   Since the aluminate phases in the ordinary Portland cement are limited, the chemical effect of the limestone is generally small, however, additional aluminates from SCMs can increase this chemical effect.

While limestone is known to improve the early strength of Portland cement, no significant improvement is observed beyond seven-day when compared to control OPC systems. The strength of the cement is affected by the formation of a well-refined microstructure and the stabilizing effect of carboaluminates on the low-density ettringite (Matschei et al. 2007; Tsivilis et al. 2000; Tsivilis et al. 2002). Limestone addition has been also observed to improve the rheological behavior of the concrete mixes and has been used extensively to produce self-compacting concretes (Alexandra et al. 2018; Elgalhud et al. 2016; Gesoğlu et al. 2012).

5.3 Limestone in LC[3]

LC[3] is a ternary blend of clinker, calcined clay, and limestone. Hydration mechanisms in the LC3 system involve a synergetic reaction between clinker, calcined clay, and limestone, it can be divided into two steps. Firstly, with the addition of the water to the system, alite and belite phases from the clinker starts to react to produce C-S-H and portlandite. Available sulphates from the gypsum, starts reacting with the aluminates from clinker to form ettringite, with the ferrite phases to form hydrogarnet, portlandite and ferrous hydroxide. Initial step of LC3 hydration can be considered similar to the hydration mechanism of the ordinary Portland cement. Here, limestone presence allows having a wider range of particle size distribution which helps in achieving a better packing of the cement particles and reducing the water demand. Additionally, smoother surface of the limestone particles also compensates for the increase in water demand due to addition of calcined clay. Thus, limestone have two roles to play in first step, filler effect which provides better packing density, and nucleation effect which enhances the hydration process.

In the second step, portlandite produced from clinker hydration reacts with the calcined clay and limestone to form an additional C-A-S-H gel and hemi-/mono-carboaluminates, see equation below:

$$AS_2 + C\check{C} + CH + H \rightarrow C_xA_ySH_Z + C_4A\check{C}H_{11}/C_4A\check{C}_{0.5}H_{12}$$
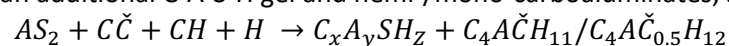
Here, the chemical effect of limestone addition becomes more prominent, the dissolution of limestone at the higher pH in cement increases the availability of carbonate ions in the solution. This results in reaction of carbonate ions with aluminates from calcined clays to form carboaluminate phases. Hemi-carboaluminate which is known to meta-stable phase in ordinary Portland cement, doesn't completely convert to mono-carboaluminate even after 90 days in the LC[3] systems (Krishnan et al. 2019). Consumption of aluminates results in the stabilization of the low-density ettringite and formation of carboaluminates, resulting in refining the pore structure, and compressive strength enhancement at early age. More details on the role of carbonates and their influence of hydration and strength development will be discussed in the later chapters.
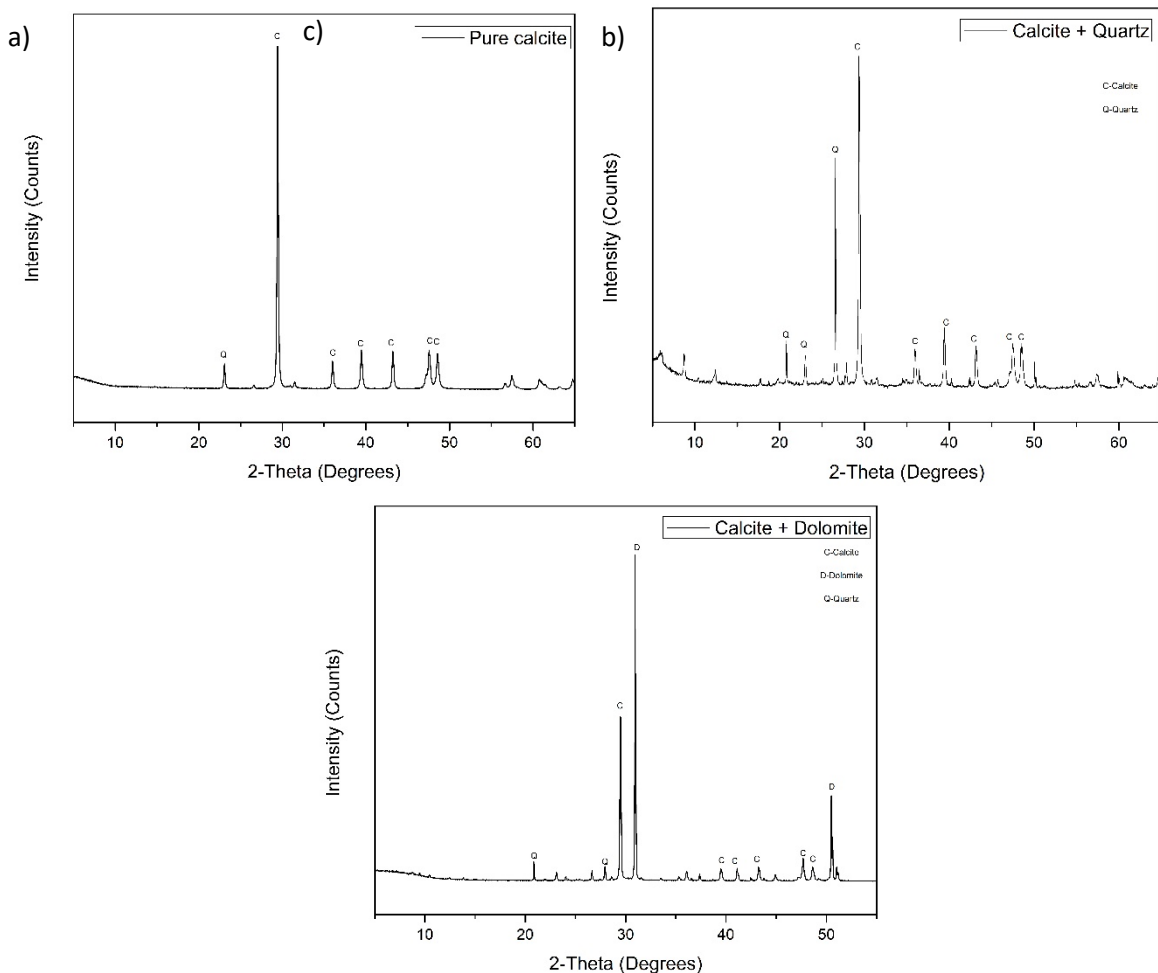
5.4 Characterization of limestone

Although only a limited amount of limestone is known to chemically react in LC[3] systems, an assessment of their characteristics is nevertheless important. In LC3 system limestone is not calcined, used simply for inter grinding or blending in already grounded state. Hence, covering all the carbonate sources and making it possible to use even dolomite, marble, etc. without having any detrimental effect on the cement paste. Just like clays, limestone can be characterized by using chemical and mineralogical techniques like, X-ray fluorescence (XRF), X-ray Diffraction (XRD), and Thermo-gravimetric analysis (TGA).

Table 5.2 XRF data for the composition of limestones that have been used in LC3.

Limestone	Na_2O	MgO	Al_2O_3	SiO_2	SO_3	Cl	K_2O	CaO	Fe_2O_3	LOI
Limestone 1	-	-	-	1.21	0.3	-	0.09	54.64	-	42.54
Limestone 2	0.05	1.46	2.79	9.38	0.04	0.11	0.24	47.46	1.45	36.50
Limestone 3	0.79	1.43	8.53	27.42	0.14	0.10	1.85	34.62	3.94	20.47
Limestone 4	-	0.81	1.90	8.89	0.05	0.02	0.61	47.32	1.03	38.85
Limestone 5	-	0.41	0.68	3.99	0.03	0.07	0.15	54.30	0.66	39.61
Limestone 6	0.09	1.45	3.35	6.20	0.11	0.05	0.42	44.71	4.20	39.40

XRF can be used to determine the oxides present in the raw materials. Primarily oxides of focus are calcium oxide (CaO), Silica (SiO_2), and alumina (Al_2O_3). Presence of silica and alumina in limestones, indicates the possibility of quartz and clay mineral impurities in the limestone. Pure limestone is known to have 56% CaO content by weight. By knowing the calcium oxide content in the limestone helps us to determine the overall calcium carbonate content and its purity. Although, this estimation may be inaccurate sometimes due to the presence of impurities such as dolomite. Hence, to obtain reliable chemical composition of limestone, it is crucial to first properly calibrate the XRF equipment with limestone samples having varying calcium carbonate and impurities in it.


Figure 2.4 XRD pattern of limestone with different impurities a) pure calcite, b) calcite + quartz impurity, and c) calcite + dolomite impurity.

XRD is another suitable technique for the characterization of the limestone, which helps in qualitative and quantitative estimation of the mineral impurities present in the limestone. XRD is performed on the powdered raw materials to find the minerals present in it. Major mineral forms present in limestone are calcite, aragonite, dolomite, and magnesite, while minor minerals are siderite, ankerite,

quartz, muscovite, and kaolinite, etc. Rietveld's analysis of limestone can not only help in the estimation of its purity, but also in the identification and quantification of the impurities in the limestone.

Although Rietveld analysis can be used to quantify the calcite content in limestone, it is generally easier to measure using TGA. It is well known that the decomposition range of limestone occurs between 700℃ to 950℃. Calcium carbonate in pure form is composed of 56% CaO and 44% CO_2 by weight. Thus, heating pure calcium carbonate up to 1000℃ under inert atmosphere results in the loss of 44% of weight as carbon dioxide molecules escape from the system, converting it to calcium oxide. The calcium carbonate content in limestone can be approximately determined by dividing the fraction of weight lost in this temperature range by 44%. Dolomite loses approximately 47.7% of its weight when it loses its CO_2 molecules. Some studies have reported that amorphous particles of calcium carbonate may decompose at temperatures as low as 400˚C, however, it is not clear if such limestone occurs in nature.
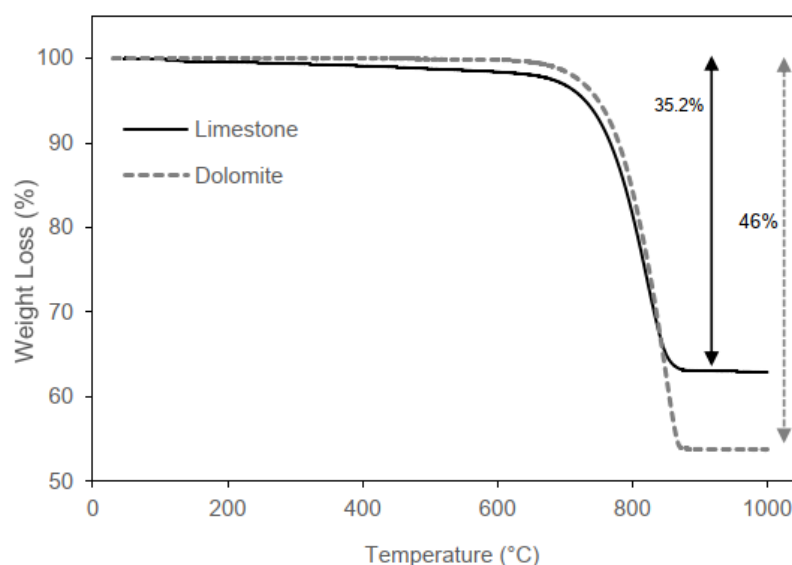
Figure 5.5 TGA of limestone and dolomite (Krishnan 2019).

Given the errors in determining the carbonate content in limestone, a combination of chemical and mineralogical analysis, XRF, XRD, and TGA is usually required to assess its suitability for LC[3]. Quartz is one of the most found impurities in limestone. The inclusion of quartz in cement has been widely studied and it is found to be a predominantly unreactive material that serves as a hard filler. In LC[3] as well, quartz has been found to neither react nor interfere with the hydration reactions. Therefore, the presence of quartz in limestone is unlikely to have a significant influence on the performance of LC[3]. Clays are also commonly found as impurities in limestone. Clays of the smectite type can swell in the presence of water in the concrete leading to cracking. However, no swelling has been observed with limestones containing up to 10% of expansive clays. Magnesium carbonate is another impurity found in the limestone. If magnesium is present in periclase form it causes unsoundness of cement, however, in the dolomitic form it doesn't have any such effect. Generally, limestones with dolomite impurity have been seen to react more slowly than calcite in LC[3] systems. While some studies have advised against the use of dolomite in concrete due to the occurrence of the so-called alkali-carbonate reaction, recent studies have shown that the reaction of dolomite in alkaline conditions does not lead to expansion or cracking in concrete. Limestones up to 65% of calcium carbonate content have been suitably used in the production of LC[3].

### 5.5 Suitability of Limestone for LC³

We know that only a small part of calcium carbonate reacts chemically in the system to form carboaluminates and the rest of it predominantly acts as inert filler material. This indicates the fact that not a very high grade of limestone is required to produce LC³. Additionally, carbonate sources are easier to replace than clinker or clay, provided there are no deleterious effects caused by the addition or replacement. Two different studies which have been performed to check the suitability of using low-grade limestone for LC3 production are described in the subsequent sub-sections.

5.5.1 Study I: Natural limestones of different grade

From major cement manufacturers in India, 4 different types of limestone have been procured namely, old mine reject (heap of limestone discarded from use in clinkerisation for years), new mine reject (recently discarded limestone from the bulk of sample being used from clinker production), low-grade limestone (used to adjust lime saturation factor when high purity limestone is being used for clinker production), and feed grade (used in clinker making process). Oxide composition of these four grades of limestone is provided in table 1.3. XRD scan of raw limestone samples is provided in figure 1.6. TGA curves for the different limestone grades are provided in figure 1.7.

Table 5.3 Oxide composition of limestone samples in study I

Limestone	Na$_2$O	MgO	Al$_2$O$_3$	SiO$_2$	SO$_3$	Cl	K$_2$O	CaO	Fe$_2$O$_3$	LOI
Old Mine Reject	0.2	0.74	9.93	27.01	0.02	0.02	0.69	31.50	5.28	26.10
New Mine Reject	0.29	1.06	10.12	25.84	0.05	0.02	0.83	31.95	4.81	25.9
Low-grade	0.63	0.81	6.44	20.61	0.31	0.02	0.58	36.72	3.68	29.1
Feed-grade	0.27	1.39	3.83	13.33	0.19	0.02	0.44	42.85	2.31	35.6
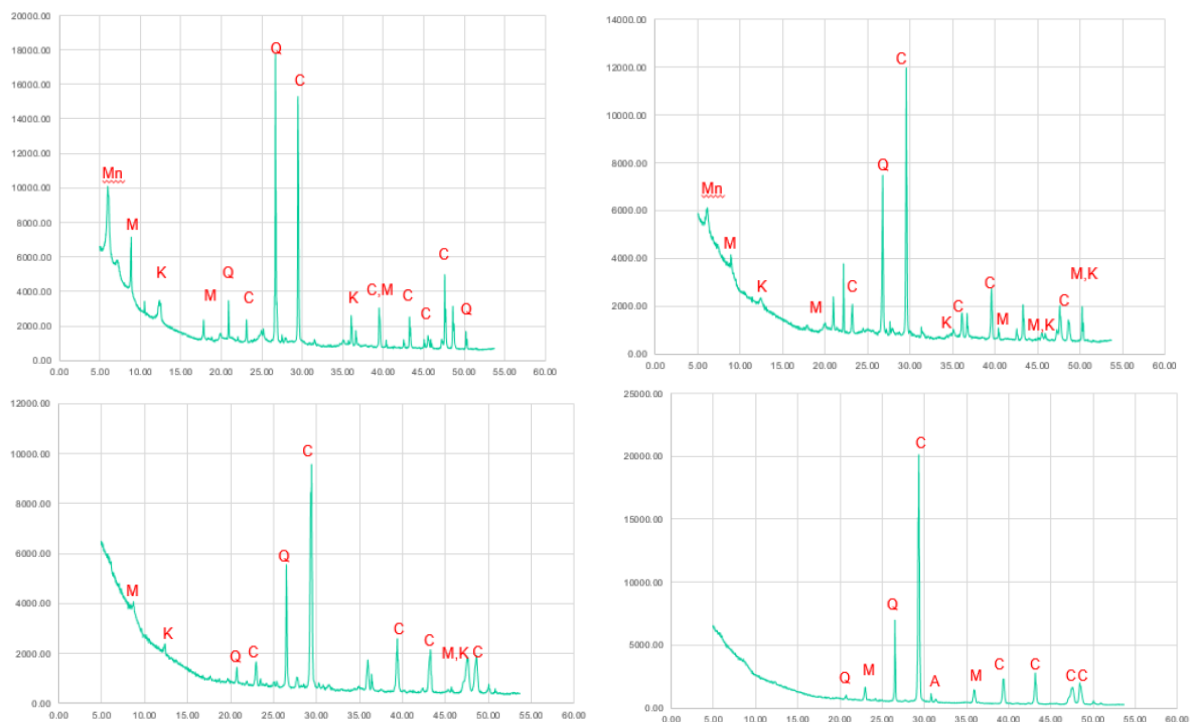
Figure 5.6 XRD scan of old mine reject (top-left), new mine reject (top-right), low-grade limestone (bottom-left), and feed grade limestone (bottom-right). (Q-Quartz, K-Kaolinite, C-Calcite, M-Muscovite, Mn-Montmorillonite and A-Ankerite).
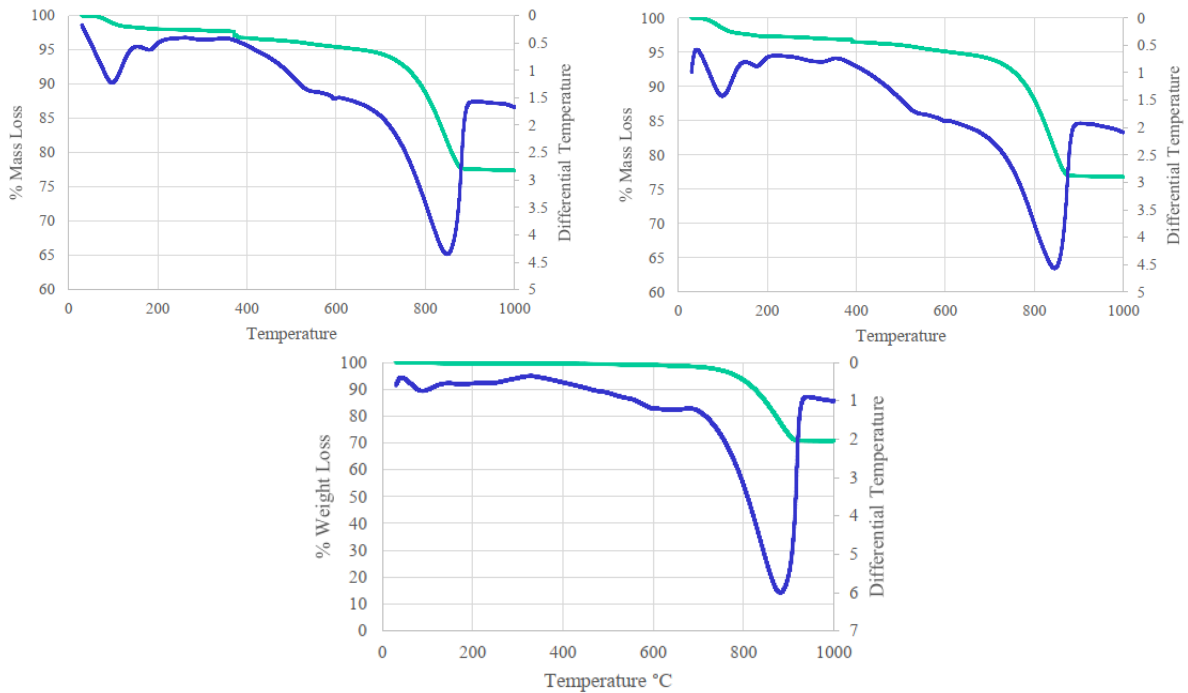
Figure 5.7 TGA of old mine reject (top-left), new mine reject (top-right), and low-grade limestone (bottom-left).

5.5.1 Isothermal calorimetry of LC3 blends

The composition of LC^3 used in carrying out isothermal calorimetry was 50% clinker, 30% calcined clay, 15% limestone, and 5% gypsum. The paste was prepared using water to binder ratio of 0.45. Four different LC3 blends were prepared using different types of limestone while keeping the same clinker, calcined clay, and gypsum.

Calorimetric results for the blends are provided in figure 1.8, irrespective of the limestone type, the hydration curve for LC3 blends doesn't change much. Although the peak corresponding to aluminate reaction is higher in low grade and feedable grade limestone as compared to old and new reject limestone, the difference in heat evolution is relatively less. The cumulative heat evolution curve shows that the mix containing old mine reject has the highest heat evolution whereas feedable grade contributed to the lowest. The total heat evolution is majorly contributed by the reaction of aluminates in the system, and it can be observed that the difference in the heat is contributed by the aluminates present in each limestone mix and not due to the difference in the calcite content in the limestones.
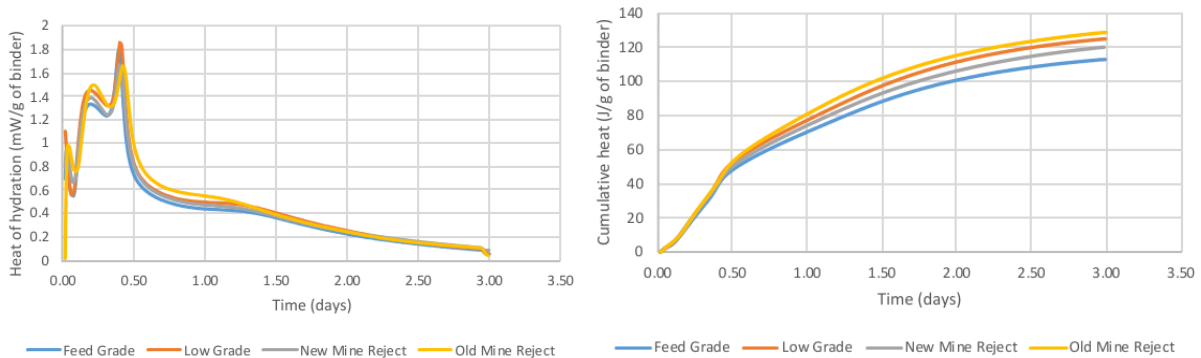
Figure 0-8 Calorimetry result for LC3 blends with different grade of limestone, left – Heat of hydration curve, right – cumulative heat released.

Compressive strength of LC³ blends

The compressive strength of LC³ blends prepared with four different grades of limestone having the same clinker, calcined clay, and gypsum in the standard proportion described above, was measured on mortar cubes cast at a water to cement ratio of 0.45 with sand to cement ratio of 3:1. The compressive strength results show that the highest strength is obtained in the LC³ sample cast using feedable grade limestone. However, there is little difference in the compressive strength obtained in LC³ mixes cast using different limestone grades. The results indicate that high-quality limestone does not significantly increase the strength and even lower-grade limestone contributes to similar strength.
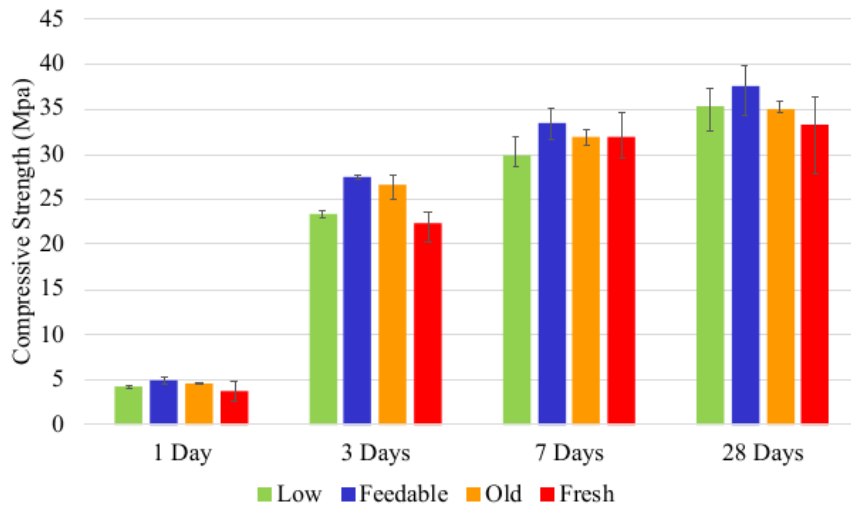
Figure 5-9 Compressive strength of the LC3 made with the different grades of the limestones.
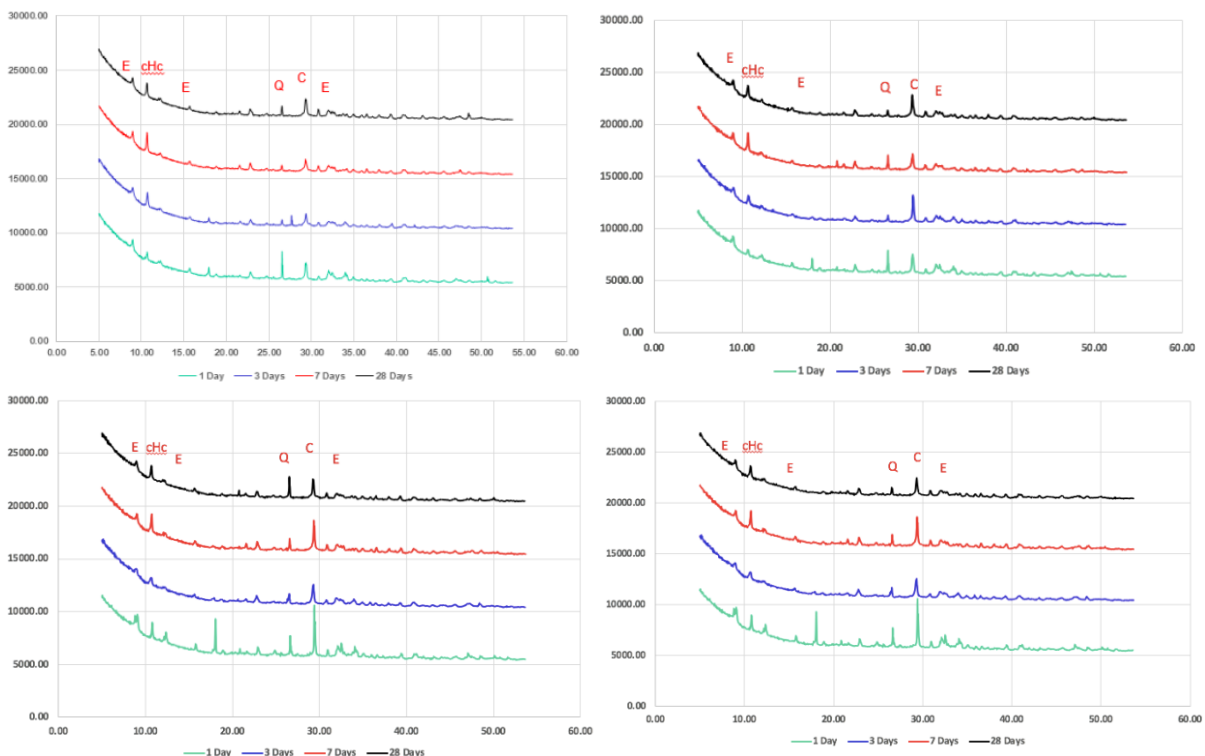
Figure 5-10 XRD scan of hydrated LC3 at different ages cast using feed grade limestone (top-left), low-grade limestone (top-right), old mine reject (bottom-left), new mine reject (bottom-right). (E-Ettringite, cHc: Hemicarboaluminate, Q-Quartz, C-Calcite)

Progress of hydration in LC3 blends using XRD

XRD was employed to understand the effect of limestone on the presence of the hemi- and mono-carboaluminates phases in the cement paste. Paste samples were cast using LC3 with different grades of limestone at a water to cement ratio of 0.45. XRD was done on hydrated samples at ages 1, 3, 7, and 28 days. Figure 1.10, shows the XRD scans at different ages for the LC3 mixes cast with different limestone samples. The XRD scans of hydrated LC3 samples show that irrespective of the type of limestone used the carboaluminate phases are formed at all ages. This indicates that calcite quantity in the limestone doesn't affect the formation of hydration products and even lower grade limestones having a lower quantity of calcite can be used in preparing LC^3.

Study II: Blended Low-grade and High-grade limestone

From a major cement manufacturer in India, 2 different types of limestone have been procured namely, high-grade limestone (having high calcium carbonate percentage) and low-grade limestone (basically reject limestone which can't be used for clinkerization). Two different grades of limestone were mixed in different ratios to form 5 different grades of limestone i.e 100%HG, 75%HG + 25%LG, 50%HG + 50%LG, 25%HG + 75%LG, and 100%LG. Material characterization results of these two grades of limestone is provided in table 1.4.

Table 5-4 Limestone characterization results using XRF, XRD and TGA

XRF	Na_2O	MgO	Al_2O_3	SiO_2	SO_3	K_2O	CaO	Fe_2O_3	LOI	$CaCO_3$
Low-grade	0.31	2.34	8.84	22.09	0.05	0.89	32.20	5.03	26.1	57.5
High-grade	0.08	4.09	1.93	10.40	0.03	0.44	44.64	1.04	35.6	79.71

XRD	Major minerals	Minor Minerals	$CaCO_3$
Low-grade	Calcite, Quartz	Kaolinite, Muscovite	79.54%
High-grade	Calcite	Quartz, Dolomite	60.25%

TGA	Mass loss (750-950℃)	$CaCO_3$
Low-grade	19.39%	54.73%
High-grade	35.31%	80.24%

Isothermal calorimetry of LC3 blends

The composition of LC3 used in carrying out isothermal calorimetry was 52.8% OPC, 28.8% calcined clay, 14.4% limestone, and 4% gypsum. The paste was prepared using water to binder ratio of 0.4. Five different LC3 blends were prepared by mixing two different types of limestone in various ratios while keeping the same clinker, calcined clay, and gypsum.

Calorimetry results for the 5 different blends prepared are provided in figure 1.11, irrespective of ratios in which limestones were mixed, the hydration curve for LC3 blends doesn't change much. Although the peak corresponding to aluminate reaction is higher in 100% low-grade and 100% high-grade limestone as compared to other ratios of mixing, the difference in heat evolution is relatively less. The cumulative heat evolution curve shows that there isn't much significant difference in cumulative heat at the end of 24 hours. The highest cumulative heat is observed in 100% high-grade and 100% low-grade limestone, while others show a marginally lower cumulative heat. The difference in the heat arises from the reaction of the aluminates phases in the system rather than the calcite present in the limestone.

Figure 5-11 Calorimetry result for LC3 blends with different mixing proportions of limestone, left – Heat of hydration curve, right – cumulative heat released.

Compressive strength of LC3 blends

The compressive strength of LC3 blends prepared with five different mixing proportions of limestone having the same clinker, calcined clay, and gypsum in the standard proportion described above, was measured on mortar cubes cast at a water to cement ratio of 0.52 with sand to cement ratio of 3:1. The compressive strength results show that the highest strength is obtained in the LC3 sample cast using low-grade limestone. However, there is little difference in the compressive strength obtained in LC3 mixes cast using different mixing proportions of limestones, as all the results lie within the error bar of each other. The results indicate that high-quality limestone does not significantly increase the strength and even lower-grade limestone contributes to similar strength.
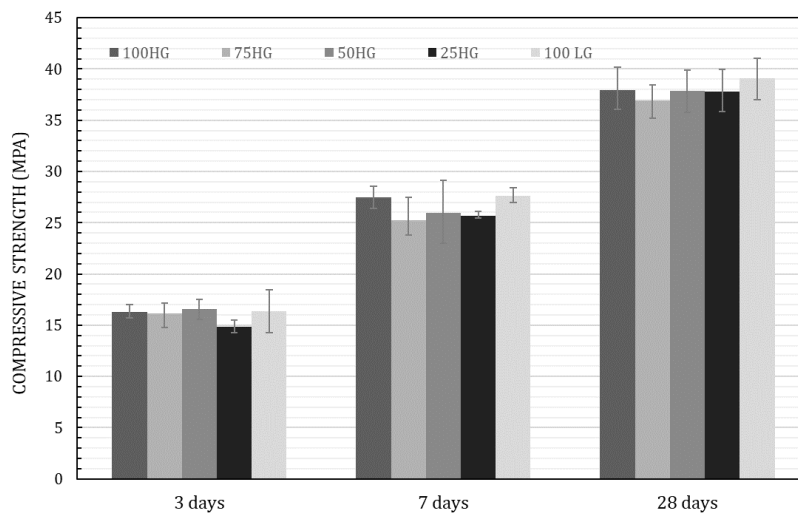
Figure 5-12 Compressive strength of the LC³ made with the different mixing proportions of the limestones.

5.6 Systematic study on the influence of limestone purity

In this section, the effect of using different grades of limestone (by blending low-grade and high-grade limestone in different proportion) on strength development and hydration characteristics has been investigated. Details of the study which have been performed to check for the suitability of using low-grade limestone in LC³ production has been described in the subsequent sub-sections. The work undertaken covers limestones with CaO contents in the range of 32.2% to 44.64%.

5.6.1   Experimental Work

Materials

Composition of LC³ used to carry out the current study was 50% clinker, 30% calcined clay, 15% limestone, and 5% gypsum. 2 different types of limestone have been procured namely, high-grade

limestone (HG) (having high calcium carbonate percentage) and low-grade limestone (LG) (basically reject limestone which can't be used for clinkerization). Study performed involved intermixing of low-grade and high-grade limestone to achieve the different calcium carbonate content for limestone, which has been used to make LC3. Oxide content of various raw materials used in the study is given in table 5-5.

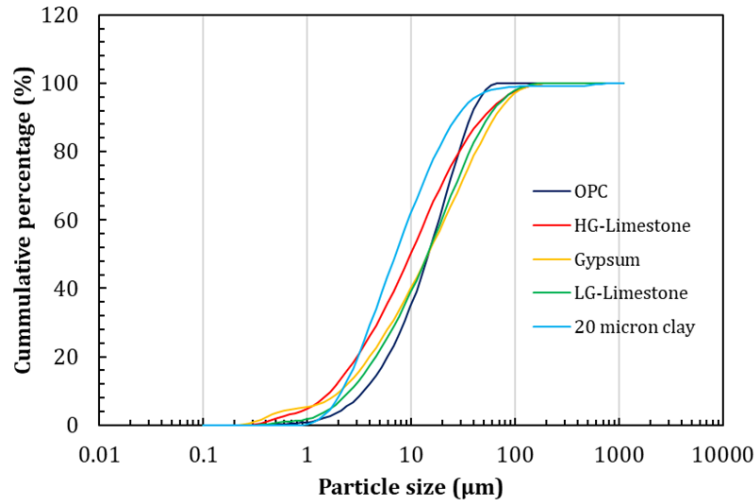**Table 5-5 Oxide composition from XRF for different raw materials used in the study**

Oxides	Calcined Clay	Gypsum	OPC-53	HG Limestone	LG Limestone
SiO_2 (%)	47.73	19.65	19.18	10.40	22.09
Fe_2O_3 (%)	1.35	2.10	6.38	1.04	5.03
Al_2O_3 (%)	38.85	4.04	4.49	1.93	8.84
CaO (%)	1.81	23.75	62.34	44.64	32.20
MgO (%)	3.79	1.44	1.33	4.09	2.34
SO_3 (%)	0.13	28.21	2.53	0.03	0.05
Na_2O (%)	0.99	0.13	0.15	0.08	0.31
K_2O (%)	0.00	0.58	0.51	0.44	0.89
TiO_2 (%)	0.67	0.23	0.84	0.00	0.46
LOI (%)	4.49	18.24	1.32	37.17	27.14

Additionally, calcium carbonate percentage obtained from thermogravimetric analysis for high-grade limestone was 80.24%, and for low-grade limestone was 54.73%. Protocol for making LC^3 involved limestones ground in laboratory ball mill using charge to ball ratio of 1:5 for 6000 revolutions. Grounded low-grade and high-grade limestones were blended in together to have 5 different grades of limestone, i.e 100%HG, 75%HG + 25%LG, 50%HG + 50%LG, 25%HG + 75%LG, and 100%LG. Grounded raw materials were blended together in as above-mentioned ratios to make LC^3 blends having different calcium carbonate content. Particle size distribution curve for the raw materials is shown in figure 1 and 10%, 50%, and 90% percentage passing fraction is given in table 5-6.

Table 5-6 Particle size at different passing fractions for raw materials used in the study

Raw Material	D_{10} (µm)	D_{50} (µm)	D_{90} (µm)
Ordinary Portland cement (OPC)	4.01	16.7	42.4
High grade Limestone (HG)	1.92	11.2	55.9
Low grade Limestone (LG)	2.92	16.3	62.4
Calcined clay (CC)	2.46	8.03	30.9
Gypsum (G)	2.38	16.6	72.0

Figure 5-13 Particle size distribution of various raw materials used in the study.

Experiment methods

Normal consistency and Setting time **–** IS 4031 has been used to determine the standard consistency of the blends, followed by initial and final setting time determination. Water demand is affected by the fineness of the calcined clay used.

Isothermal calorimetry - Calorimetry studies were carried out to understand the effect of limestone grade on the heat of hydration and cumulative heat realized up on hydration at 27℃. Tests have been performed on the paste samples made at water to binder ratio of 0.40 up to 24 hrs using Calmetrix I-Cal 8000. Isothermal calorimetry is useful in understanding the reaction kinetics as it records the heat release signature of the hydrating cement paste and process involved in hydration are well known to be exothermic.

Compressive strength development - Compressive strength of the blends was measured on 70.6 mm*70.6 mm *70.6 mm mortar cubes with a fixed water/binder ratio of 0.52. Standard sand conforming to IS 650 was used to prepare the mortar. The ratio of cement to sand was kept 1:3 by weight. The cubes were demoulded after one day and stored under water till the time of testing. Average of three cubes were taken as the compressive strength at that age.

Results

Normal consistency and setting time for different blends is given table 5-7. It can be observed that there has been no difference in the normal consistency of the all the 5 blends. Although consistency values for all blends have come high, which can be attributed to the higher water demand of the calcined clay which has been used, as it has very high kaolinitic content and was fineness. Additionally, initial setting time for all blends has been between 112-118 minutes and final setting time has been between 187-201 minutes. As, it can be seen there is no effect on the setting behaviour and dormant period of the cement blends upon addition of different grades of limestone.

Table 5-7: Normal consistency and setting time of different blends.

S. No.	Blend	Sp. Gravity	Normal Consistency	IST (hr:min)	FST (hr:min)
1.	100HG	2.96	40%	1:52	3:07
2.	75HG + 25LG	2.96	40%	1:55	3:12
3.	50HG + 50LG	2.96	40%	1:58	3:21
4.	25HG + 75LG	2.96	40%	1:52	3:15
5.	100LG	2.96	40%	1:55	3:14

Calorimetry results for the 5 different blends prepared are provided in figure 5-14, irrespective of ratios in which limestones were mixed, the hydration curve for LC³ blends doesn't change much. Although the peak corresponding to aluminate reaction is higher in 100% low-grade and 100% high-grade limestone as compared to other ratios of mixing, the difference in heat evolution is relatively less. The cumulative heat evolution curve shows that there isn't much significant difference in cumulative heat at the end of 24 hours. The highest cumulative heat is observed in 100% high-grade and 100% low-grade limestone, while others show a marginally lower cumulative heat. The difference in the heat arises from the reaction of the aluminates phases in the system rather than the calcite present in the limestone.

Figure 5-14: Calorimetry result for LC³ blends with different mixing proportions of limestone

Table 5-8: Chemical composition of clinker, calcined clay, limestone and dolomite used in the study (Krishnan and Bishnoi 2018)

Oxide composition (%)	Clinker	Calcined Clay	Dolomite	Limestone
CaO	65.16	0.06	29.68	44.24
SiO_2	21.07	54.93	0.75	11.02
Al_2O_3	4.65	39.75	1.02	2.53
Fe_2O_3	4.32	4.16	0.64	1.55
MgO	2.13	0.02	21.26	1.96
Na_2O	0.38	0.18	0.1	0.5
K_2O	0.20	0.17	0.05	0.28
SO_3	0.77	0.1	–	–
LOI	0.96	0.24	46.09	36.96
Specific gravity (g/cm³)	3.1	2.60	2.88	2.64

Table 5-9: Properties of materials used in the study with stone dusts (Krishnan et al. 2018)

Oxide (%)	OPC	Calcined Clay	Banswara limestone (BA)	Kishangarh limestone (KG)	Kota stone dust (KS)
SiO_2	22.07	55.11	4.99	7.45	21.96
Fe_2O_3	4.69	4.18	1.55	0.47	0.76
Al_2O_3	3.75	39.89	0.32	0.62	2.98
CaO	63.35	0.09	31.89	42.29	39.40
MgO	1.08	0.02	27.15	5.44	0.67
SO_3	2.09	0.104	0.84	0.10	-
Na_2O	0.32	0.18	0.09	3.57	0.90
K_2O	0.71	0.19	0.09	0.18	0.67
LOI	1.14	-	42.85	39.32	32.94
D_{50} (μm)	18.6	19.8	8.13	10.2	7.58

The XRD measurements on hydrating pastes in both systems show the formation of carboaluminate phases, similar to the systems containing calcitic limestone. The results can be seen in figures 5-17 and 5-18. It can be seen in figure 5-19 and 5-20 that LC^3 prepared with limestone or stone dust containing a large amount of dolomite impurity, or even pure dolomite have a similar strength development as the one using a relatively pure calcite limestone. It can also be seen in figure 5-21 that there is very little influence of the replacement of limestone by dolomite on the pore-refinement of the cement and therefore on the durability performance of the cement.
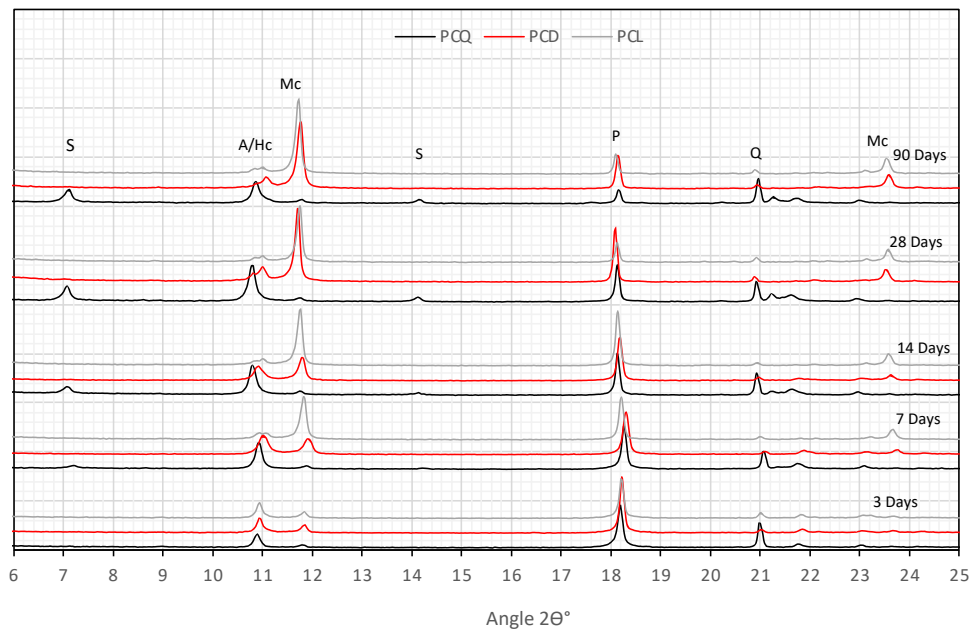
Figure 5-17: XRD measurements on pastes prepared using LC^3 containing limestone (PCL), dolomite (PCD) and quartz (PCQ) (Krishnan and Bishnoi 2018)
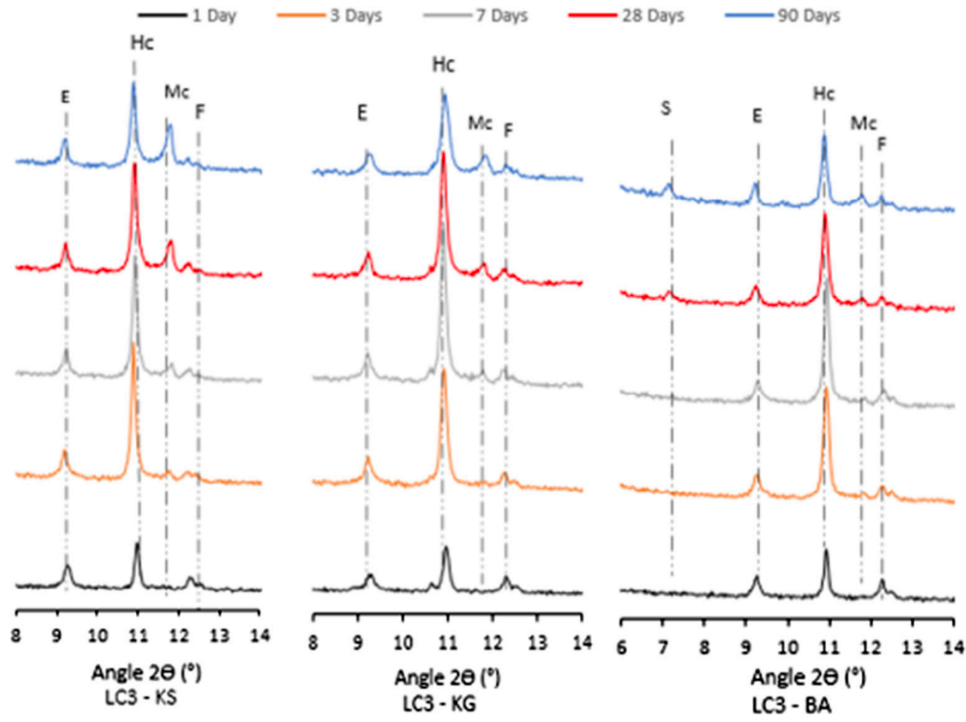
Figure 5-18: XRD measurements on pastes prepared using LC³ containing Kota stone (KS), Kishangarh (KG) and Banswara (BA) stone dusts (Krishnan et al. 2018)

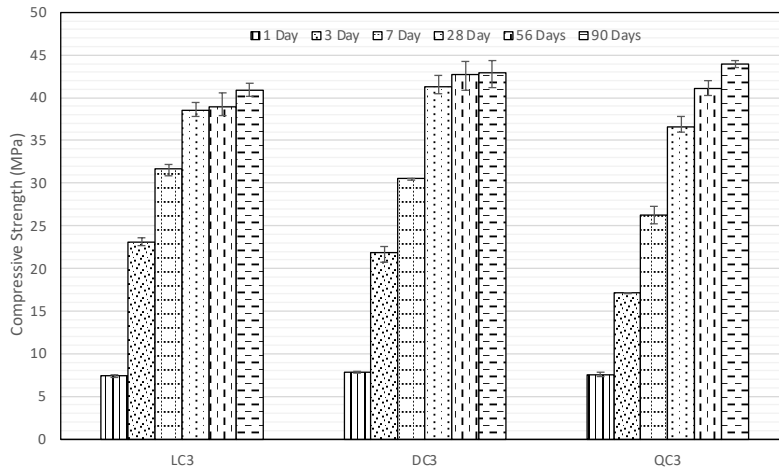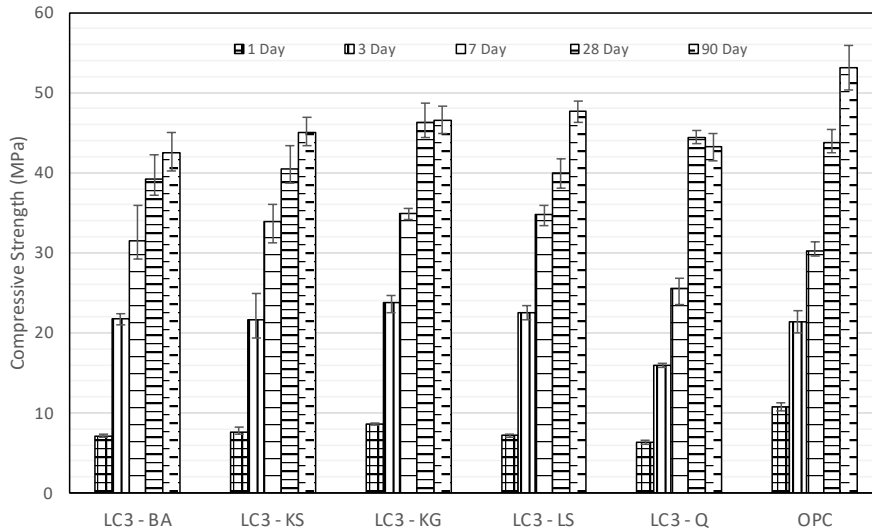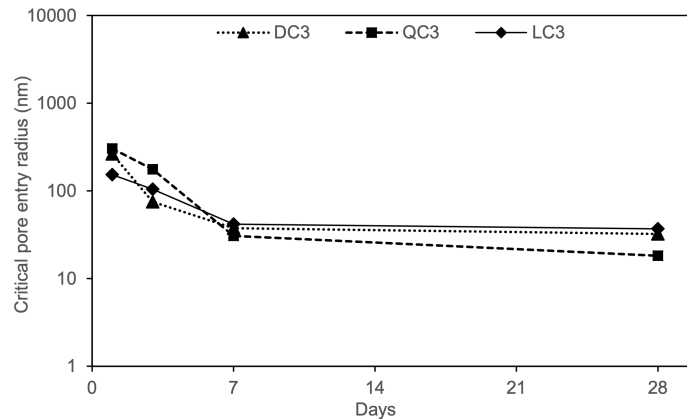**Figure 5-19: Compressive strength measurements on mortars prepared using LC³ containing limestone (LC3), dolomite (DC3) and quartz (QC3) (Krishnan and Bishnoi 2018)**

Figure 5-20: Compressive strength measurements on mortars prepared using LC^3 containing Kota stone (KS), Kishangarh (KG) and Banswara (BA) stone dusts (Krishnan et al. 2018)

Figure 5-21: Critical pore-entry radius (MIP) measurements on pastes prepared using LC^3 containing limestone (LC3), dolomite (DC3) and quartz (QC3) (Krishnan 2019)

The above results clearly demonstrate the potential of the use of impure limestone containing dolomite impurity in LC^3. It may be noted here that since this limestone is not calcined, there is no risk of formation of periclase (MgO) that may lead to unsoundness in the cement. The de-dolomitisation reaction has also been shown to not lead to expansion or unsoundness.

5.8 Availability of Limestone in India

The economics and growth of the cement industry depend entirely on the easy availability of cement-grade limestone. Fortunately, India has large deposits of limestone and calcareous materials. Geologically they range from Archean to Recent in the stratigraphic sequence and geographically occur in almost 23 states of India. However, the distribution is not uniform. The total reserves/resources of limestone of all categories and grades as per national mineral inventory (NMI) data based on the United Nations Framework Classification for Resources (UNFC) system as of 2015 have been estimated at 203,224 million tonnes, of which 16,336 MT (about 8%) are placed under the reserves category.

Karnataka is the leading state having 27% of the total resources. This is followed by Andhra Pradesh and Rajasthan (12% each), Gujarat (10%), Meghalaya (9%), Telangana (8%), Chhattisgarh, and Madhya Pradesh (5% each), and the remaining 12% by other states (Soni and Nema 2021). Cement grade has

a leading share of about 70%, followed by unclassified grades at 12%, and BF grade at 7%. The remaining 11% are various different grades. As per IBM, the total cement grade limestone resources is 124,539.551 million tonnes, out of which the total cement grade limestone reserves is 8948.926 million tonnes (UNFC), and the total remaining resources is 115,590.625 million tonne. As per a study conducted by National Council for Cement and Building Materials (NCCBM), 97% of total cement-grade limestone resources is concentrated in only 10 states. Marly and miliolitic limestone are found near the seacoast, and karsty limestone is mined at some places of north-eastern India, where different geological ages of rock have been reported. Seabeds (marine topography) and lake beds also contain significant limestone and carbonate rock.

A brief on the limestone availability (Indian Bureau of Mines 2014) in emerging states are given below.

Andhra Pradesh: Majority of limestone deposits are concentrated in the district of Adilabad, Kadapa, Guntur, Kurnool, Nalgonda, Khammam and Krishna. The total cement grade limestone resources of Andhra Pradesh is 34,281.763 million tonnes.

Rajasthan: Cement grade limestone deposits are mainly available in the districts of Ajmer, Chittorgarh, Jaisalmer, Jhunjhunu, Pali, Sirohi, Nagaur, Jaipur and Udaipur. Deposits of Bundi and Kota districts are reportedly of low grade limestone. The total cement grade resources of the state is estimated at 18,537.900 million tonnes.

Karnataka: The limestone deposits are mainly distributed in the districts of Gulbarga, Belgaum, Bijapur and Chitradurga. The total cement grade limestone resource of the state is 25,614.440 million tonnes.

Himachal Pradesh: Cement grade limestone is available in the districts of Bilaspur, Chamba, Kangra, Kullu, Mandi, Sirmaur, Shimla, Solan, Lahul & Spiti, and Kinnaur. The total cement grade limestone in the state as estimated is 3,617.220 million tonnes. The geographical condition and general topography has restricted the growth of cement industry in the state. However, due to continued scarcity of cement in the northern states and rapid growth of construction activities in neighboring states, there is enough potential for the growth of cement industry in the state for utilizing the available limestone reserves.

Gujarat: Cement grade limestone is available in the districts of Amreli, Banaskantha, Bhavnagar, Junagarh, Kutch, and Jamnagar. The total cement grade limestone resource is 8,958.119 million tonnes.

Meghalaya: Major limestone deposits are reported in three districts of West Garo Hills, East Khasi Hills and Jaintia Hills. The total cement grade limestone resource of the state are 13944.435 million tonnes.

Jammu and Kashmir: The limestone deposits are mainly distributed in the districts of Anantnag, Srinagar, Kathua, Baramula and Rajauri. The total cement grade limestone resources in the state are 601.932 million tonnes.

Chhattisgarh: Limestone bearing districts of Chhattisgarh are Bastar, Bilaspur, Janjgir, Durg, Raipur and Raigarh. The total cement grade limestone resources of the state are 7903.208 million tonnes.

Madhya Pradesh: Majority of limestone deposits are concentrated in the districts of Damoh, Dhar, Neemuch, Sheopur, Rewa, Satna and Sidhi. The total cement grade limestone resources of the state are 4326.3 million tonnes.

Maharashtra: Limestone-bearing districts of Maharashtra are Chandrapur and Yavatmal. The total cement grade limestone resources of the state are 1361.244 million tonnes.
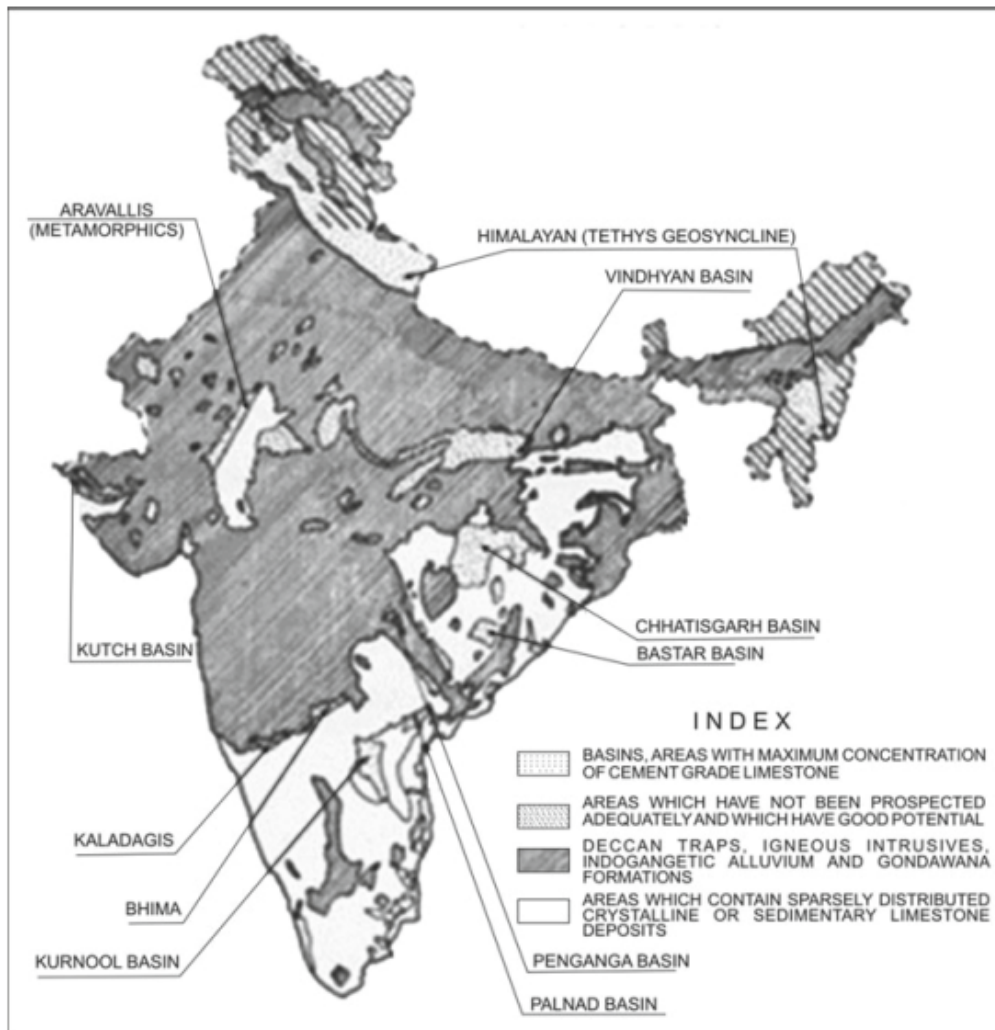
Figure 5-22 Map of India showing geological horizons containing limestone deposits (source: NCCBM)

5.9 Summary

Limestone is not only a raw material for the production of clinker but also an important additive widely used in Portland cement as a performance enhancer. Despite what has been assumed earlier, limestone is now known to chemically react with aluminates in cement and leading to the formation of a finer microstructure. Limestone is also known to contribute to improving the rheology of cement and concrete. The relatively smaller quantity of aluminates in Portland cement reduces the contribution of limestone to hydration and microstructural development. However, in limestone calcined clay cement (LC^3), where the larger quantities of alumina available in calcined clay allow higher reaction of limestone and finer microstructure. Additionally, only a small part of limestone is consumed for chemical effect, and the rest of it acts as filler. This further provides an opportunity to use low-grade limestones in the production of LC^3 without having any detrimental effects on the strength and durability properties of concrete. Finally, a discussion about the wide availability of limestone reserves throughout India is provided, which makes it possible to produce LC^3 in different regions.

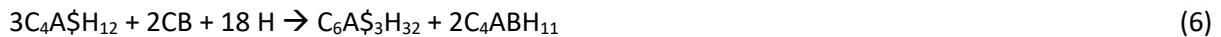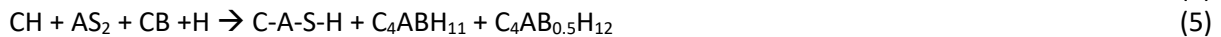# Chapter 6: Hydration and microstructural development of LC³

6.1 Introduction

Cement cannot act as a binding material without the addition of water in it. Cement acquires adhesive properties with the addition of water, due to which the chemical reaction between the cement and water takes place that results in the formation of various hydration products This chapter discusses the hydration mechanisms, and microstructure development, as well as phase assemblage of the hydrating LC³ system.

Hydration of Portland Cement is a complex process where several ionic species react in an aqueous medium. The addition of SCMs makes the process more complex and changes the properties of the products that are formed. Ionic species from each of the components in LC³ interact with the species from the other components, creating a synergistic system. The process of hydration in the LC³ occurs in two steps; in the first step, the alite and aluminates from the cement clinker react with water to produce C-S-H, portlandite and ettringite, as shown in Equations 1&2. Once a significant amount of clinker phases had reacted, the calcined clay and limestone start to react. The silicate in the calcined clay reacts with portlandite to produce calcium alumino-silicate hydrate (C-A-S-H). While some of the alumina in the clay is seen to get incorporated in this product, the remaining alumina reacts with the carbonate phases to form carboaluminates.

$$C_3S + 5.3H \rightarrow C_{1.7}SH_4 + 1.3\ CH \tag{1}$$
$$C_2S + 4.3H \rightarrow C_{1.7}SH_4 + 0.3\ CH \tag{2}$$

The ettringite that is formed from the hydration of aluminate and gypsum (eq. 3) gets converted to monosulphate (eq. 4) upon the exhaustion of the sulfates (in the case of OPC) but in LC³ presence of carbonate ions from limestone prevents this conversion. Free aluminate ions from the clinker phases and the calcined clay react with the carbonate ions producing the carboaluminate phases (eq. 5).

$$3C\$H_2 + C_3A + 26H \rightarrow C_6A\$_3H_{32} \tag{3}$$
$$C_6A\$_3H_{32} + 2C_3A + 22H \rightarrow 3C_4A\$H_{12} \tag{4}$$
$$CH + AS_2 + CB + H \rightarrow C\text{-}A\text{-}S\text{-}H + C_4ABH_{11} + C_4AB_{0.5}H_{12} \tag{5}$$
$$3C_4A\$H_{12} + 2CB + 18\ H \rightarrow C_6A\$_3H_{32} + 2C_4ABH_{11} \tag{6}$$

> $\$$= Sulphates, C=Calcium oxide, S= Silicate, B = Carbonate, A = Aluminate, H= Water (H₂O)
> CH= Calcium Hydroxide (Portlandite), C₄ABH₁₁=Mono Carboaluminate
> C₄AB₀.₅H₁₂=Hemi carboaluminate, C₆A$₃H₃₂= Ettringite (Aft), 3C₄A$H₁₂= Monosulphate(Afm)

The consumption of the aluminate ions for the production of the carboaluminate phases prevents the conversion of ettringite to monosulphate. Mature LC³ pastes, therefore, contain a higher volume of ettringite and carboaluminates than other cement (equation 6).

6.2 Hydration Products

AFt, AFm, Ettringite and C-A-S-H are the major hydration products that are formed because of the hydration reaction of the LC³. XRD graphs have shown the evolution of these hydration products with the passage of time. Aluminates from the clinker in LC³ react with sulphates to produce ettringite (an AFt phase), the ettringite content depends only on the initial amount of sulfate and the availability of sufficient reactive alumina in the cement clinker. The amount of C₃A present in the clinker is usually sufficient to consume the gypsum present in the blends, Once the availability of sulfates in the solution reduces, the aluminates start to react with the carbonates present in LC³ The presence of CO3²⁻ ions further modifies the hydration reaction, with the monosulphate phase combining with the CO3²⁻ ions to produce monocarboaluminate and additional ettringite. Therefore, the presence of the carboaluminate phases stabilizes the ettringite (Equation 6).
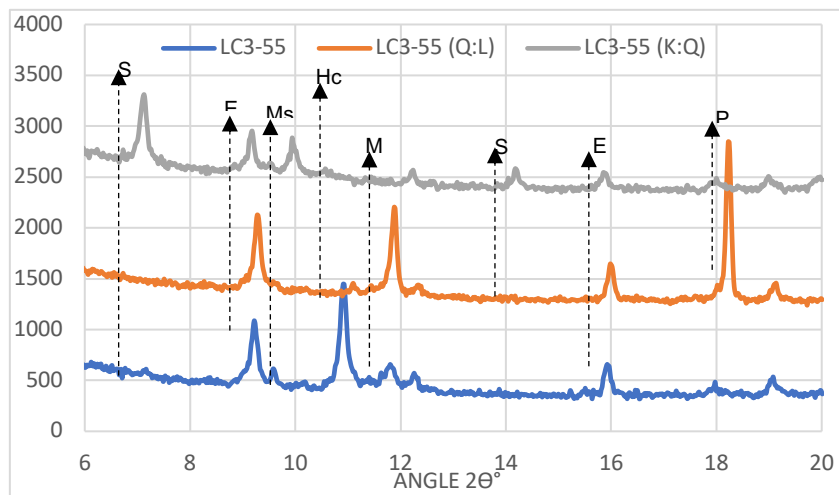
The hemicarboaluminate and monocarboaluminate are the carboaluminate phases that are formed in the LC³ because of the reaction of the carbonates from the limestone and aluminates of the clinker and calcined clays. The development of AFt/AFm phase assemblage was studied by XRD measurements and as shown in figure 6.1 at 1, 7, 28, and 90 days of hydration, as the hydration proceeds the reduction of ettringite peak intensities was observed as well as the formation of monosulphate peaks observed in the diffractograms of LC³-55(K:Q). In the calcite-containing blends, the formation of the carboaluminate phases prevents the conversion of ettringite to monosulphate. It was observed that the complete conversion of hemicarboaluminate (Hc) to monocarboaluminate (Mc), was not observed in the LC³ system, Minor peaks of Mc were visible in the diffractograms after 28 days. However, it was observed that Hc peak intensities were significantly higher than that of Mc. As the Hc-Mc transformation is subject to the availability of the carbonate ions (CO_3^{2-}), the partial conversion of the Hc to Mc indicates reduced reactivity of calcite in the LC³-55 blend. In the blend LC³ – 55(Q: L) where there is no calcined clay, the complete transformation of the Hc phase to Mc phase with time is clearly visible. Hc is the dominant carboaluminate phase in the system for up to 7 days The Hc to Mc conversion has already started by this time, with minor peaks of Mc being detected in the diffractograms. The transformation is, for the most part, complete by the end of 28 days, which was confirmed by the significant reduction in the peak intensity of the Hc phase.

By the end of 90 days, the Hc peak was seen to vanish entirely with Mc being the dominant carboaluminate phase. The complete transformation of the Hc to Mc in the blend LC³-55(Q:L), as shown in figure 6.2, suggests that a higher amount of calcite can react in LC³-55(Q:L). It has been reported that the amount of alumina available for the formation of the carboaluminate phases (Zajac et al. 2014b, 2018) controls the reactivity of calcite. The results suggest that there are parameters other than the aluminate content that affects the kinetics of calcite dissolution, as there is sufficient alumina available in the LC³-55 for the Hc to Mc conversion. Hydrated gehlenite (stratlingite or C_2ASH_8) was seen to form instead of carboaluminates in the absence of CO_3^{2-} ions in the blend LC³-55(K: Q); Stratlingite was observed at 28 days and remained stable even after 90 days. Stratlingite is a low-density AFm phase that improves the space-filling in cementitious systems.
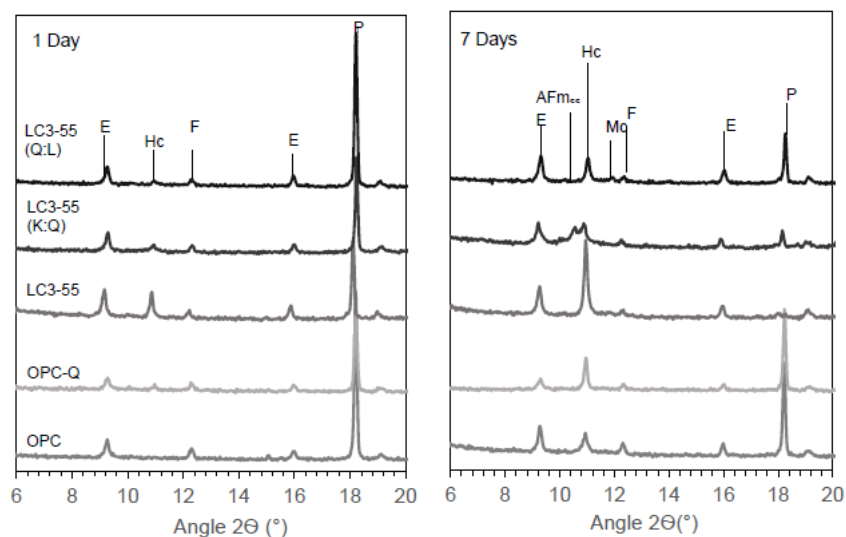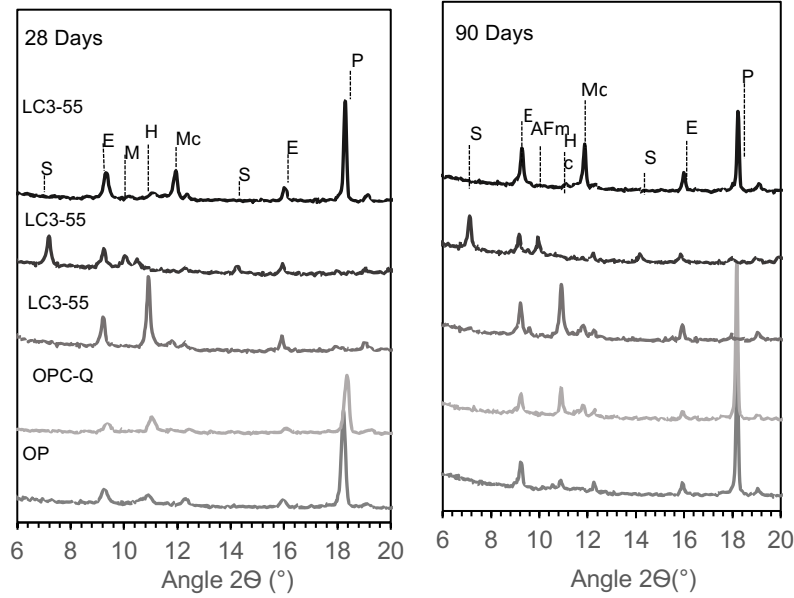
Figure 6.1: XRD Spectra of LC³at 1, 7, 28, and 90 days of hydration

Figure 6.2: XRD Spectra of LC³-55, LC³-55(Q:L), and LC³-55(K:Q) at 90 days of Hydration

Ettringite and monosulphate are sulfate-based AFt/AFm phases formed from the reaction of SO_3^{2-} available in the hydrating cement systems, whereas the carboaluminates are formed by the reaction of CO_3^{2-} ions. The most common source of SO_3^{2-} ions is the gypsum, which is added as a set regulator, while the CO_3^{2-} ions come from the calcite added as a performance enhancer. The solubility of the gypsum (2.4g/L) is significantly higher than calcite (0.014g/L) (Klemm and Adams 1990). Therefore, the sulfate ions will go to the solution rapidly and precipitate as ettringite by combining with the CaO, Al_2O_3, and OH^- ions. Ettringite has the least solubility among the AFt/AFm phases and hence would be the most stable phase. The ettringite formed will combine with the reactive Al_2O_3 (if available) to form monosulphate. The presence of CO_3^{2-} ions further modifies this reaction, with the monosulphate phase combining with the CO_3^{2-} ions to produce monocarboaluminate and additional ettringite. Therefore, the presence of the carboaluminate phases stabilizes the ettringite. It is clear that the monocarboaluminate and ettringite combination would be the most favoured among various possibilities, In the absence of calcite, hydrogarnet and stratlingite were formed in the portlandite and calcined clay system, there is no reaction between the calcite and portlandite in the absence of calcined clay.
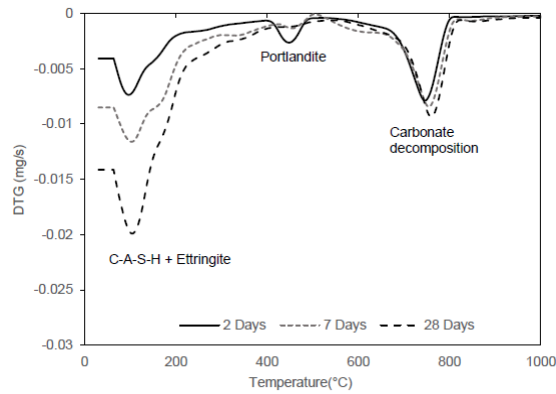
Figure 6.3 DTG of LC³ at various ages

Figure 6.3 shows the DTG curves of the hydrated LC³-55 specimens after 2, 7, and 28 days confirming the observations made using X-ray diffraction. No portlandite decomposition peak was observed between 400°C and 550°C at 7 and 28 days by thermal analysis. In LC³-55 (K: Q), the complete consumption of portlandite was observed only after 28 days. The portlandite present in the LC³-55 (Q: L) was lower than OPC-Q at all ages, which is due to carboaluminate formation and the Hc-Mc transformation.

6.3 Nature of C-A-S-H in LC³

C-A-S-H is the hydration product that is formed because of the reaction of additional alumina from the calcined clays. The composition of C-A-S-H in hydrated LC³ differs from OPC depending on the degree of hydration, metakaolin content of clay, and content of limestone and clay. The microstructure of OPC and the LC³-50 (17.0%), LC³-50 (50.3%), and LC³-50 (95.0%), blends is shown in figures 6.4 and 6.5 in Bright Field (BF) mode and in High Angle Annular Dark Field (HAADF) mode, in all systems, a fibrillar C-A-S-H morphology is observed. These images show that neither the reaction of the calcined clay nor the calcined kaolinite content of the calcined clay influences the morphology of C-A-S-H. In addition to C-A-S-H, ettringite (AFt) is also observed in the LC³-50 (17.0%) and unreacted metakaolin in the case of LC³ (95%).

**Table 6.1 Al/Ca and Si/Ca atomic ratios of C-A-S-H obtained by SEM-EDS and STEM-EDS [Avet et al. 2018]**

	SEM-EDS		STEM-EDS	
	Al/Ca	Ca/Si	Al/Ca	Ca/Si
PC	0.06 ±0.01	1.96±0.06	0.08±0.01	1.89±0.10
LC3-50 (17%)	0.07±0.02	1.61±0.05	0.08±0.03	1.75±0.08
LC3-50 (50.3%)	0.13±0.02	1.49±0.05	0.16±0.01	1.54±0.07
LC3-50 (95.0%)	0.26±0.03	1.49±0.10	0.24±0.01	1.37±0.12

Figures 6.6 and 6.7 show the SEM-EDS analysis of the C-A-S-H in hydrated OPC and LC³ OPC systems after 1 and 28 days of hydration [Krishnan 2019]. The compositions of the C-A-S-H are very similar for OPC ($C_{1.98}A_{0.08}SH_x$ and LC³ ($C_{1.96}A_{0.098}SH_x$) after 24 hours, indicating that it is mostly the clinker that reacts in all these systems during the initial stages. However, the C-A-S-H compositions of OPC, and LC³ are seen to differ significantly after 28 days. At 28 days, these compositions are found to be close to $C_{1.61}A_{0.23}SH_x$, and $C_{1.76}A_{0.095}SH_x$ for LC³, and OPC respectively. LC³ has a higher Ca/Si ratio and lower Al/Ca ratio compared to OPC. The higher alumina content in the case of LC³ is due to higher aluminium content in the pore solution incorporated by the dissolution of metakaolin at later ages. Therefore, the alumina uptake increases with increasing metakaolin content and increasing calcined clay content.

The lower Ca/Si ratio in LC^3 can be attributed to the pozzolanic reaction that consumes calcium-rich portlandite. A comparison of Figures 6 and 7 also shows a higher scattering of the data points in the case of LC^3. This indicates that the C-A-S-H is more intermixed with other products in the case of LC^3.
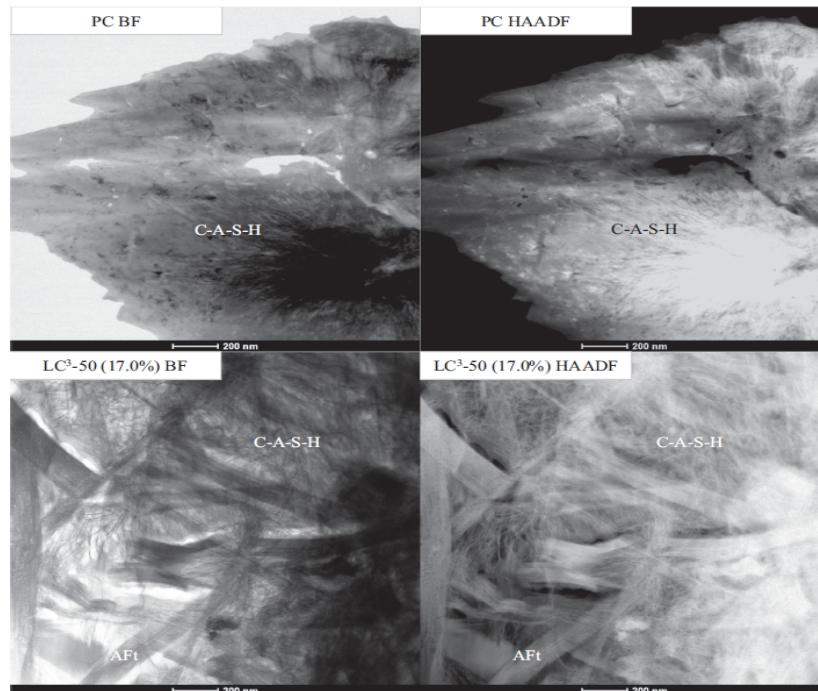

Figure 6.4: Microstructure of PC and LC^3-50 (17.0%) at 28 days of hydration in Bright Field (BF) and High Angle Annular Dark Field (HAADF) modes. [Avet et al. 2018]
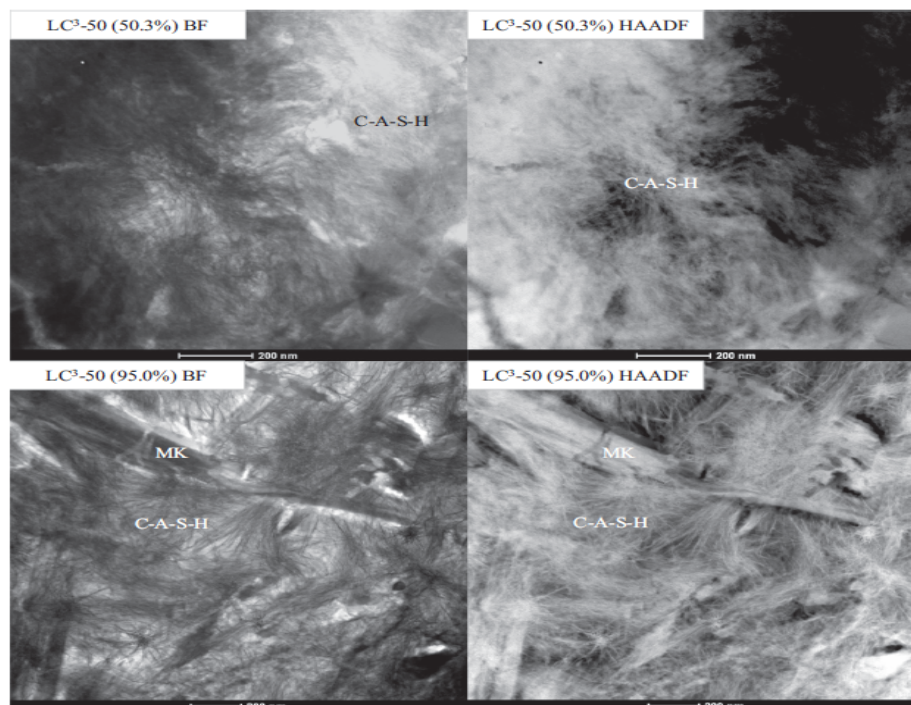
Figure 6.5: Microstructure of LC^3-50(50.3%) and LC^3-50 (95.0%) at 28 days of hydration in Bright Field (BF) and High Angle Annular Dark Field (HAADF) modes. [Avet et.al. 2018]
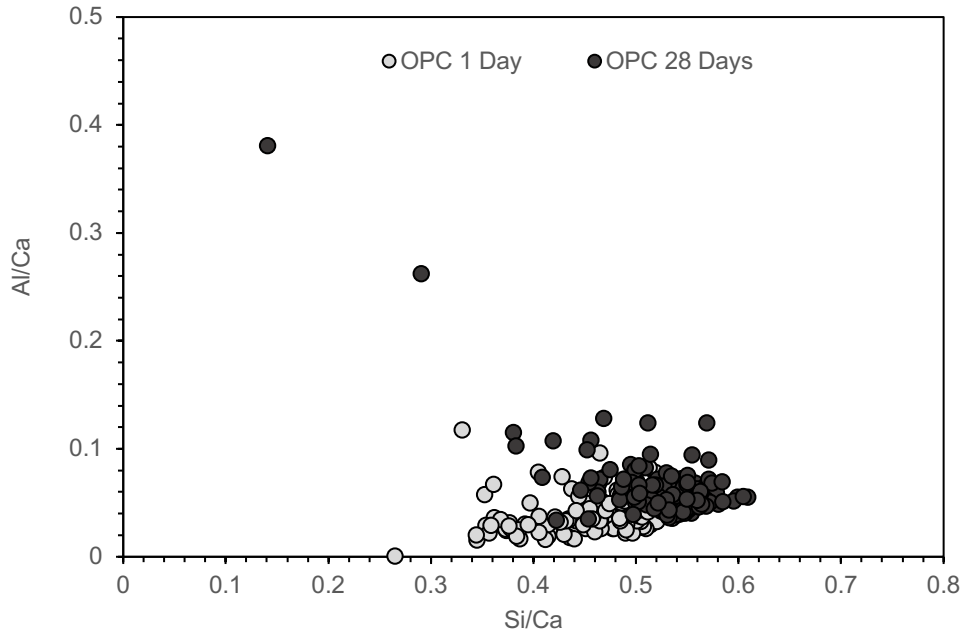
Figure 6.6: The SEM-EDS analysis of the C-A-S-H in hydrated OPC paste at 1 day and 28 days. The average composition of the C-A-S-H was estimated to be $C_{1.98}A_{0.04}SH_x$ and $C_{1.76}A_{0.0475}SH_x$ [Krishnan 2019]
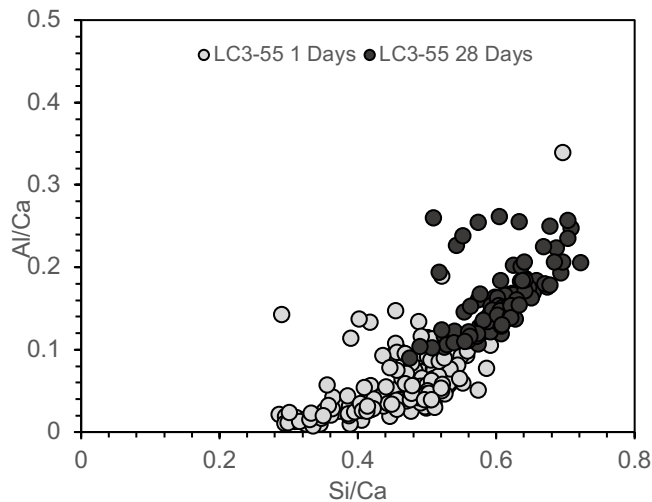
Figure 6.7 The SEM-EDS analysis of the C-A-S-H in hydrated LC^3 paste at 1 day and 28 days. The average composition of the C-A-S-H was estimated to be $C_{1.96}A_{0.049}SH_x$ and $C_{1.61}A_{0.115}SH_x$ respectively [Krishnan 2019]

Table 6.1 summarizes the Al/Ca and Si/Ca atomic ratios obtained for the different systems using both SEM-EDS and STEM-EDS techniques. Similar aluminium incorporation is observed for the reference PC and LC^3-50 (17.0%). The aluminium incorporation in C-A-S-H significantly increases with the calcined kaolinite content of the calcined clay. According to [Avet, Scrivener (2018)] This increase in aluminium incorporation is due to the increase of the aluminium concentration of the pore solution with the increase of the calcined kaolinite content. The Si/Ca ratio is higher for the LC^3 -50 blends than for PC. This can be due to the pozzolanic reaction of the metakaolin in the calcined clay, providing aluminium and silicon to the system. This leads to the consumption of portlandite and a decrease in the calcium concentration in the pore solution [Lothenbach, et.al 2011]. It is observed that the Si/Ca ratio increases with the calcined kaolinite content for STEM-EDS results.
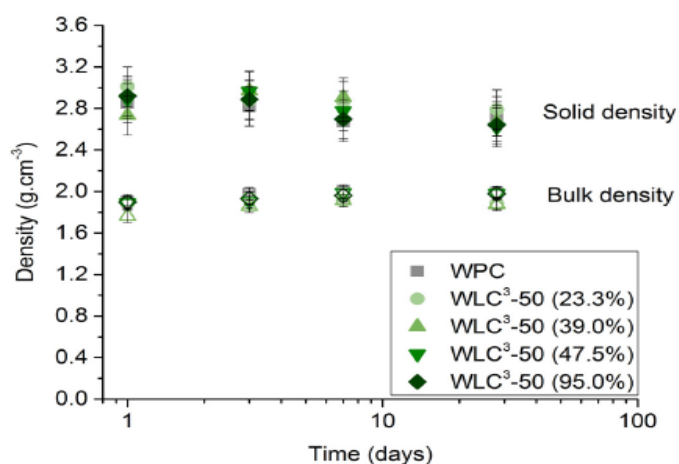
Figure 6.8: C-A-S-H density for WPC and WLC3-50 blends: plain and hollow symbols, WPC-White Portland cement, WLC³-White. LC³ [Avet et al. 2018]

The solid density of C-A-S-H (excluding gel water) slightly decreases from about 2.9 gm·cm⁻³ to 2.7 gm·cm⁻³ from 1 to 28 days of hydration. There is a spread between the different systems, but the variations are in the range of error. Thus, there is no major change in C-A-S-H solid density for reference WPC and for the WLC³-50 blends. The slight decrease of the solid density observed with time for all systems is because of the increase of the C-A-S-H layers with time [Muller AC et al. 2012]. The water present at the C-A-S-H surface is in direct contact with the gel water and shows a longer relaxation time than the interlayer water. For a number n of calcium silicate layers, n-1 interlayers of water are detected by 1H NMR [Avet et al. 2018]. Thus, with the increase of the number of layers n of the C-A-S-H, the average solid density slightly decreases since the ratio $n/n-1$ decreases with n. The determination of the bulk density of C-A-S-H (including gel water) also shows very similar results for WPC and for WLC³-50 blends. The values slightly increase from 1.85 gm-cm⁻³ at 1 day to 1.92 gm-cm⁻³ at 28 days of hydration. The small variations observed between the different systems are in the range of error. Thus, neither the calcined clay nor the calcined kaolinite content of the calcined clay impacts the density of C-A-S-H significantly. The slight increase in density with time observed for all systems corresponds to the densification of the C-A-S-H, with the slowing down/stopping of gel pore formation from 1 to 7 days, depending on the system.

Statistical nano-indentation and quantitative electron dispersive spectroscopy (SNI-QEDS) confirms the high levels of inter-mixing of the products and a denser microstructure in LC³. The space between the anhydrous cement grains and calcined clays was found to be filled with hydration products which partially embeds the anhydrous calcined clay, limestone, and quartz with Al-rich AFt/AFm phases displaying higher mechanical properties than C-A-S-H gel.
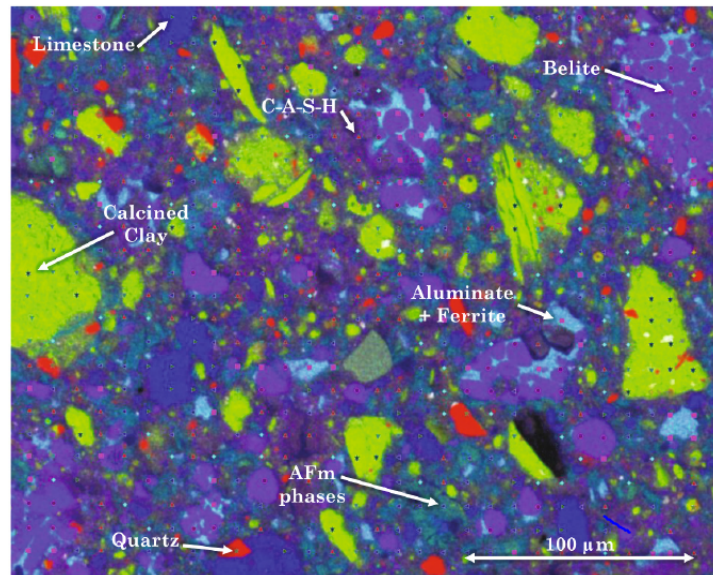
Figure 6.9 SNI-QEDS analysis of the hydrated LC3 paste (Wilson et al. 2018)

6.4 Rate of Hydration

The cement clinker reacts with water to acquire stable, low-energy states, and this process of acquiring low-energy states results in the release of energy in the form of heat, this release of heat is known as the heat of hydration, in the case of supplementary cementitious materials (SCMs) this heat of hydration was found to be lower because they have finer particle size and increased surface area. SCMs are known to increase the rate of clinker reaction, which aids in nucleation and growth reactions, SCMs accelerate the hydration of clinker phases due to the filler effect (Lothenbach et al. 2011), which provides an additional surface area for the C-S-H gel to nucleate. A reduced induction period was observed in blends with limestone and calcined clay, which is due to the acceleration of the clinker hydration; it has been reported that limestone contributes additional Ca^{2+} ions to the hydrating cement systems, which accelerate the hydration of clinker phases and shorten the induction period. Figure 10 (a) shows isothermal calorimetry measurements of LC^3 and OPC measured at 27°C. After the initial rapid dissolution, a gentle acceleration reaching a peak within a few hours is seen, which is similar to that of alite in OPC. Within a few hours after the first peak, a second, sharper peak, similar to that of aluminate hydration in OPC is observed. A comparison of the heat of hydration of OPC with LC^3 indicates that most of the hydration during the first day is that of C_3S and C_3A. Similar to OPC, a third broad peak, associated with the formation of AFm phases, is observed around 48 hours to 60 hours in LC^3. However, compared to OPC, this peak in LC^3 signifies the synergic reaction of limestone and metakaolin that converts ettringite to carboaluminates.
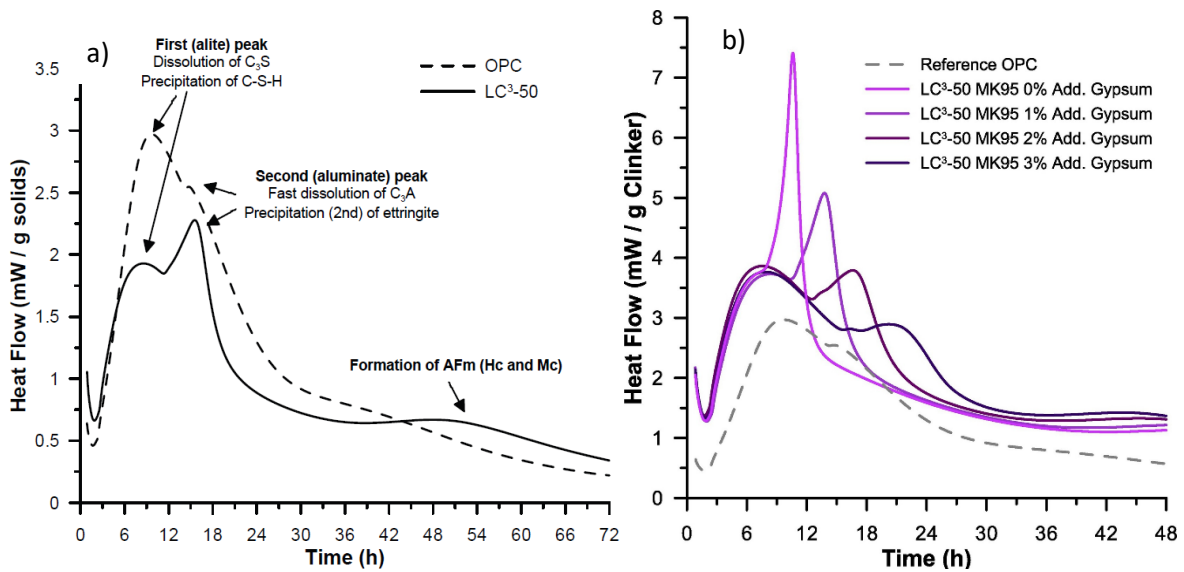
Figure 6.10: (a) Typical Heat of Hydration of LC³, (b) Influence of sulfate content on hydration
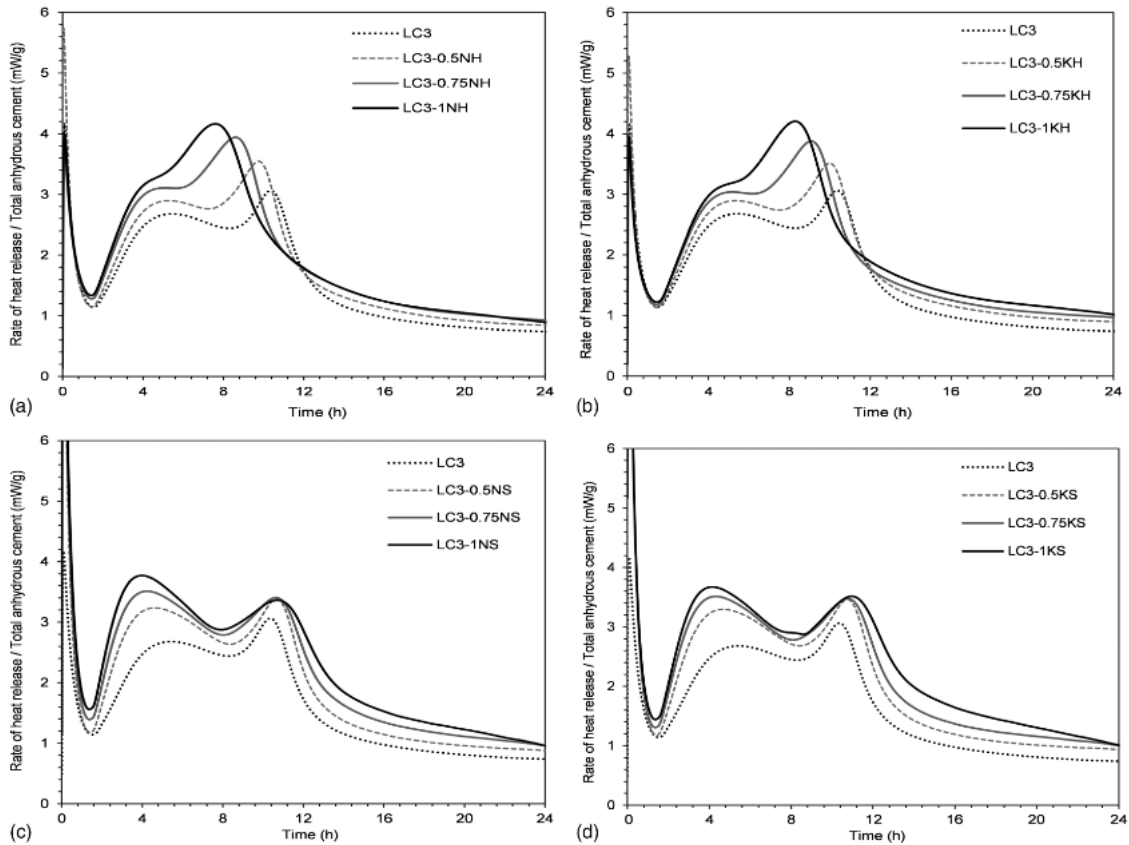

Figure 6.11: (a) Effect of NaOH on the rate of heat evolution in LC³; (b) effect of KOH on the rate of heat evolution in LC³; (c) effect of Na₂SO₄on the rateof heat evolution in LC³; and (d) effect of K₂SO₄on the rate of heat evolution in LC³

A lower degree of hydration of alite and belite was observed at later ages in blends that incorporate calcined clay when compared with other blends as shown in fig. 6.12 and 6.13. The lower degree of hydration was more for belite compared to the other phases. There is higher reduction in the hydration of belite when limestone was present with calcined clay than when quartz was present along with calcined clay. In fact, there is no significant hydration of alite and belite after 7 days in blends LC³-55 and LC³-55(K:Q), which implies that the major strength development is expected to

89

happen during the early ages. The reduction in the belite hydration as shown in fig. 13 was said to be caused by the formation of a dense CSH gel layer that covers the belite particles, which prevents the further reaction of belite. Figure 10 (b) compares the heat of hydration of LC^3 pastes produced with different sulfate contents. An increase in the sulfate content does not appear to significantly influence the hydration of C_3S, as the first peak appears to be mostly unchanged. The second peak, however, gets delayed with the increase in the sulfate content. The above observation can also be used to optimize the sulfate content in LC^3. It has been observed that in order to have proper hydration of the clinker phases in LC^3, the sharper peak of alumina hydration must be sufficiently delayed so that it occurs only after the deceleration of the C_3S hydration has started. Systems with lower sulfate content tend to develop lower early and long-term strengths.
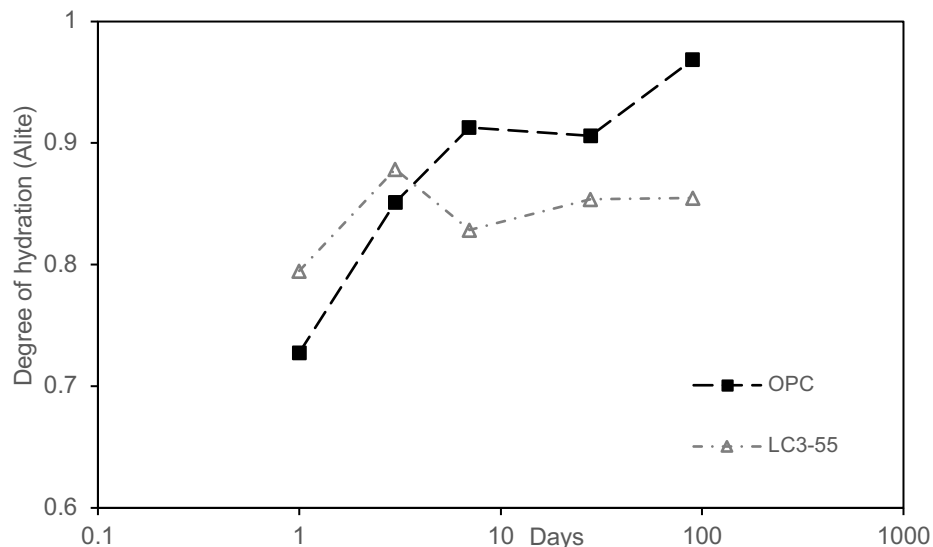

Figure 6.12 Degree of Hydration of alite [Krishnan 2019]
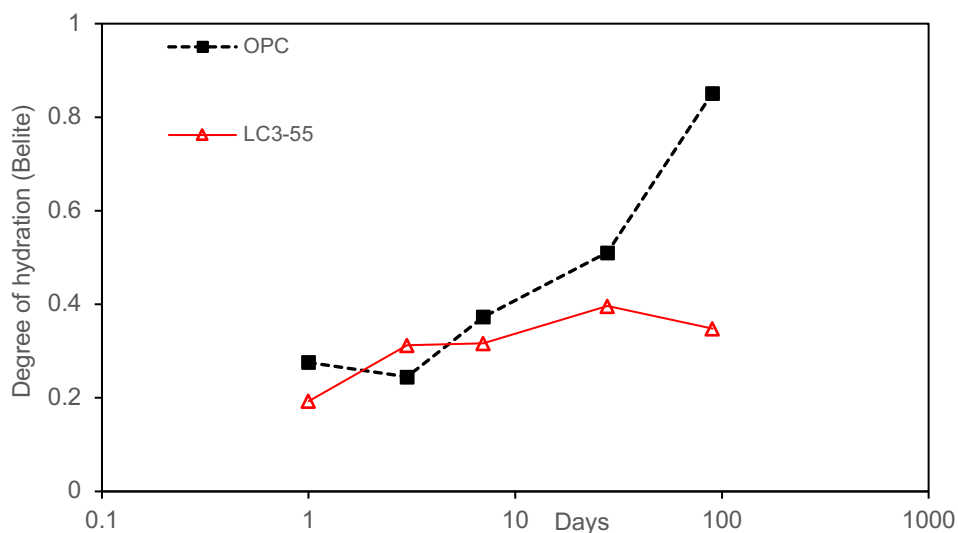
Figure 6.13 Degree of Hydration of Belite [Krishnan 2019]

Figure 6.11 shows the isothermal calorimetry results of the LC^3 systems with additional alkalis. A typical calorimetry curve of LC^3 has two distinct peaks during the first 24hr of hydration, i.e., silicate peak and aluminate peak that appear after the induction period (Krishnan et al. 2019b ; Scrivener et al. 2018). The aluminate peaks in the LC^3 systems are more intense and easily distinguishable when compared to OPC systems. The cations (Na^+ and K^+) appear to have similar effects on the reaction kinetics of LC^3. In contrast, the anions (OH^- and SO_4^{2-}) seem to affect the hydration curves significantly, which is similar to the hydration behavior observed in the OPC systems. Identical hydration curves are

observed for KOH and NaOH as well as K_2SO_4 and Na_2SO_4 at the same Na_2O_{eq} values. As the alkalinity increases, a reduction in the induction period is observed irrespective of the alkali used. The reduction in the induction period is more apparent in the case of LC^3 when compared to the OPC systems. Reduction in the induction period can lead to faster setting times, which can be undesirable in many applications. Acceleration of the silicate hydration is observed as the alkali content increases, with a higher value for silicate peak found for alkali sulfates compared to alkali hydroxides at similar Na_2O_{eq} values. Therefore, early age hydration of the calcium silicate phases in LC^{3}appears to be similar to the trends observed in OPC when alkalinity is increased, The addition of the calcium sulfate appears to have a different effect on the LC^3 hydration curves compared to the addition of alkali sulfates. Increasing the calcium sulfate content in the LC^3 systems does not seem to affect the silicate peak. However, a significant delay in the occurrence of the aluminate peak has been reported (Krishnan et al. 2019a)

6.5 Pore structure Evaluation in LC^3

Pore size distribution is an important factor that affects the permeability and moisture diffusion properties of cement-based materials. The development of pore structure in the cementitious system depends on many factors, such as water-cement ratio, reaction kinetics, degree of hydration, temperature, curing, volume efficiency of hydrate products, and amount of Supplementary Cementitious Materials (SCMs). The OPC system results are shown in Fig. 6.14 (a), The total intruded volume reported as permeable pore volume in percentage decreases with the hydration period due to continuously decreasing pore space with the hydration, critical pore size shifts with age, and further, the total pore size range is continuously reduced to a narrow range of pore sizes with an increase in curing duration. The continuous space-filling occurred throughout the system until a specific inter-particle (or interhydrate) space was attained. The use of supplementary cementitious materials is known to influence the reaction process from an early age and hence, alter the kinetics of microstructure development. The effect can vary depending on the dissolution rate and amount of the replacement materials. Fig. 6.14 (b) shows that FA30 (PPC) is having a higher threshold than the OPC at an early age because of a less amount of clinker, which is an actively participating constituent in the reaction process to produce hydrates. In contrast to FA30 (PPC) and OPC, the LC^3 system showed a greater reduction in the threshold size Fig 6.14 (c) and critical pore size at an early age because of the early reaction of the alite and aluminate phases present in the LC^3.

The total intruded pore volume of LC^3, OPC, and PPC as shown in figure 6.15, it was observed that the volume of pore in the LC^3 was found to be comparable to FA30 but higher than OPC. Concretes with fly ash showed lower strength gain at early ages and better durability at later ages; as seen from the pore structure development, a major part of the pores is reduced in the paste phase only beyond 14 days. In the case of LC^3 the pore sizes were certainly shifted in the system, The pore volume up to 1 mm was nearly 5 mm^3/g in LC^3 compared to about 60 mm^3/g in the OPC at 3 days. The early drop in pore size is mainly associated with the better hydration characteristics of the LC^3 system, apart from the fineness of materials and packing. The pore structure results indicate that the LC^3 system could potentially have higher resistance against ionic/fluid transport due to reduced permeability caused by the finer pore structure.
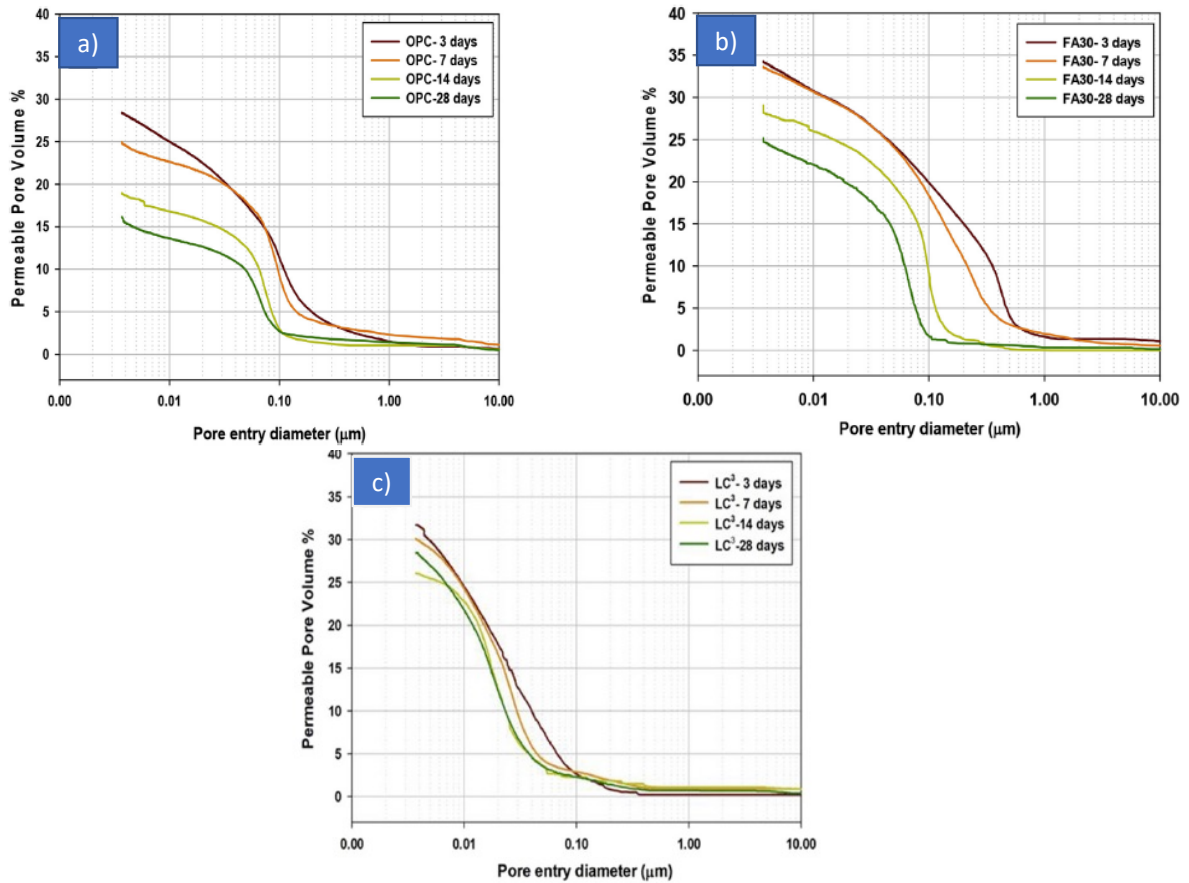
Figure 6.14: Permeable Pore Volume (%) (a) OPC (b) PPC (c) LC^3 [Yuvaraj Dhandapani, Manu Santhanam 2017]
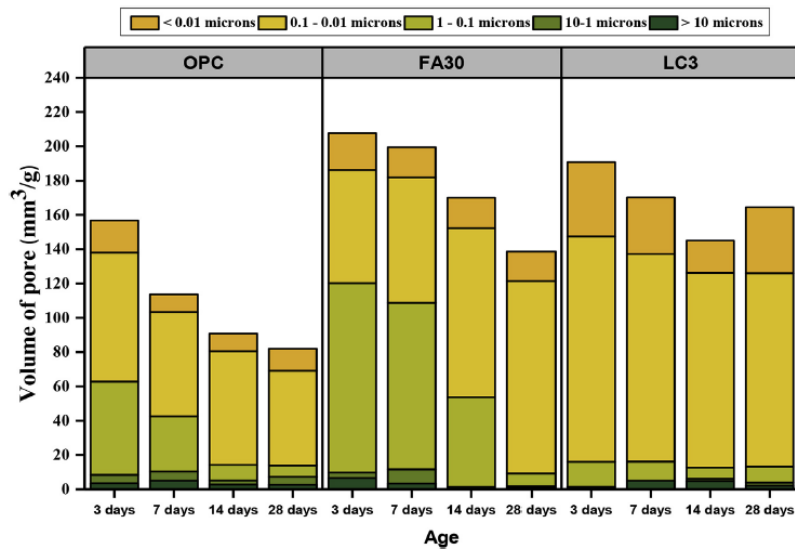
Figure 6.15: Shift in pore size of OPC, PPC, and LC^3 [Yuvaraj Dhandapani, Manu Santhanam 2017]

6.6 Design of LC^3 blends

Understanding the hydration and microstructural development of LC^3, Krishnan and Bishnoi (2020) proposed a simple numerical method to design LC^3 blends. Based on the stoichiometry of the reactions that take place in LC^3, the amount of calcined clay and limestone that can react in the cement was

calculated on the basis of the alite and belite content in the cement (figures 6.16 and 6.17). Assumptions regarding the composition of C-A-S-H are made to arrive at these relationships. At the same time, it is recognised that not all phases can be present at the same location and therefore the actual amount of phases required will be higher than those calculated from the figures below.
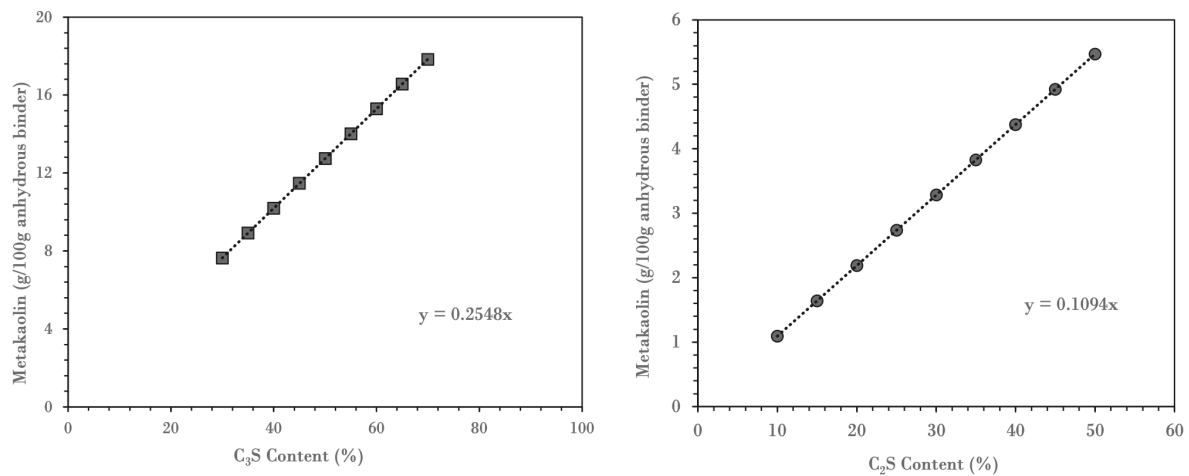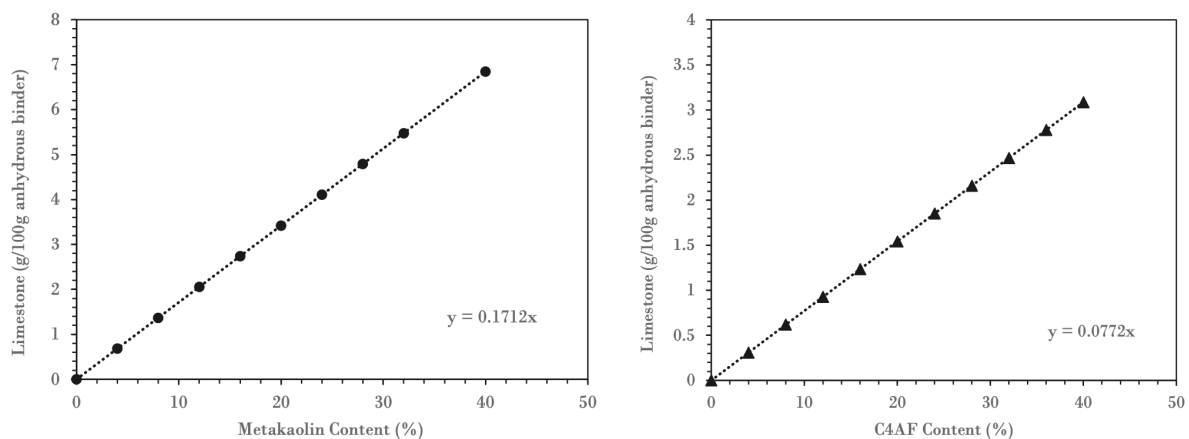

Figure 6.16: Mass of metakaolin phase that can react in an LC^3 containing 50% clinker

Figure 6.17: Mass of calcite phase that can react in an LC^3 containing 50% clinker

The above calculations also take into account the reduction in the hydration of alite and belite phases that take place upon the increase in calcined kaolinite content in the cement. In general, it can be seen that when clays of higher kaolinite content are available, a higher limestone content can be used in LC^3. This is because, the calcium hydroxide available for reaction with the calcined clays will be limited by the amount of alite and belite available in the cement. Also, since calcined clay has a higher embodied energy and increases water demand, its quantity should be minimised based on the amount that can react in the system. The relationships discussed above can be used as thumb-rules to design the initial blends for carrying out a trial-and-error based optimisation of LC^3 blends.

6.7 Summary
This chapter presents the hydration and microstructure development in the limestone calcined clay cement (LC^3). The key points reported in this chapter are listed below:
- The critical pore size evolution and conductivity suggest that the LC^3 binder system reaches greater refinement in the pore structure by 7 days. X-ray diffraction confirms a higher portlandite consumption at an early age due to the high reactivity of calcined clay during the same period. Further, monocarboaluminate and hemicarboaluminate phases were also observed within 3 days contributing to the progressive microstructure development.

- In terms of morphology, STEM provides unique information on the morphology of the C-A-S-H, where a fibrillar morphology is observed for all systems. There is no significant influence of the calcined clay or of the calcined kaolinite of the calcined clay on the C-A-S-H morphology.
- A reduction in the long-term clinker hydration was observed in the LC^3. Among the clinker phases, it is seen that the hydration of belite is affected the most. It has been shown that the reason for the slow-down is due to the presence of calcined clay.
- The maximum strength development in LC^3 systems takes place during early ages with no significant strength gain beyond 28 days due to the reduction in the degree of hydration of clinker.
- Alkali addition accelerated the early-age hydration of clinker but reduced the long-term clinker hydration in both OPC and LC^3 systems.

7.1 Introduction

Workability of fresh concrete is crucial for transportation, pumping, placement, and proper finishing of the cast surfaces. With the increasing utilization of high-strength concrete to build massive block-type structures, concrete with very low water-to-cement ratios needs to be produced. In such cases the workability is severely affected, and chemical admixtures must be added in order to facilitate comfortable handling of the concrete. Even in the cases where concrete in small amounts is manually transported and placed, the concrete must be sufficiently workable in that duration to ensure that it can be easily placed within the reinforcement grid and thoroughly compacted. There are two broad aspects of workability of fresh concrete viz. consistency and slump retention. Both of these aspects of workability are vital to safeguard the structure from issues related to strength and durability arising out of poor workmanship and improper finishing.

7.2 Workability & LC3

As mentioned in the previous chapters, Limestone Calcined Clay Cement (LC^3) is a ternary blended cement produced using calcined clays, limestone, clinker and gypsum. Even though with a clinker factor of as less as 0.5, it portrays comparable mechanical performance with that of Ordinary Portland Cement (OPC) as well as other blended cements. However, it is a well-known fact that the use of LC3 poses a difficulty in achieving desired workability in concretes and mortars. The primary reason for reduction of workability of LC3 is the morphology of calcined clay. The clay particles are flaky and angular in nature provide greater resistance to interparticle movement during the concrete mixing process. Moreover, the high fineness, the sheet-like microstructure and the narrow particle size distribution in clays causes an increase in the water demand (Cassagnabère et al. (2013)). Therefore, to obtain the desired workability, the superplasticizer dosage has to be enhanced (Batis et al. (2005), Paiva et al. (2012), and Perlot et al. (2013)). Clay particles can have positively charged edges and negatively charged faces that contribute to the flocculation (Lorentz et al. (2020)). As a result, clays have a tendency to readily exchange cations in order to balance the inherent electrical charges on the surface. When chemical admixtures are added to cement systems containing clays, the cations in the clay particles get exchanged with the organic chains present in the admixture molecules. This results in a reduced dispersion and facilitates the adsorption of the admixture molecules on the surface of the clay. Therefore, a large part of the admixture added is consumed by the clay particles and higher dosages are required to attain the required workability. The high admixture requirement not only increases the cost and but also results in a longer setting time, delay in strength gain and removal of formwork (Nehdi et al. (2014)). The following sections discuss the various phenomena influencing the workability and rheology of LC^3 systems in more detail.

7.3 Compatibility with chemical admixtures

The interaction between clays and poly-carboxylate ether (PCE)-based chemical admixtures has been widely studied owing to the severe loss of dispersion efficiency that is observed which leads to the requirement of higher dosages of these dispersants. It has been found that, especially in the case of aggregates which are not washed thoroughly and contain natural clays, the workability of concrete is severely affected (Nehdi et al. (2014), and Lei et al. (2014)). Studies suggest that polycarboxylate-based superplasticizers (PCEs) in particular, are more sensitive to clays than poly-condensate superplasticizers (Nehdi et al. (2014)). PCE superplasticizers are a group of cement dispersants that exhibit a comb or brush like structure. Their structure consists of a trunk chain carrying carboxylate groups and of pendant chains that comprise of polyethylene or polyethylene/polypropylene glycols (Lei et al. (2014)). These PCE molecules get incorporated within the interlayer spaces of the clay minerals and depending on the type and amount of clay contaminant in the aggregates, the dispersing ability of PCEs can be vigorously hindered or even totally inhibited (Lei et al. (2014)). The effect of various clay minerals on workability and water demand varies widely. It has been reported that

montmorillonite has a more pronounced negative effect on concrete fluidity as compared to other clay minerals such as kaolinites owing to the expansion of lattices of montmorillonite enabling intercalation, swelling and cation exchange (Jeknavorian et al. (2003)). Table 7.1 shows the water and superplasticizer demand of variety of naturally occurring clay minerals and that of similar sized particles of non-clayey nature (Nehdi et al. (2014)). The water or superplasticizer requirement is obtained for mortar samples which had a constant flow of 110 ± 5.

Apart from natural clays present as impurities in aggregates, calcined clays have been popularly used as supplementary cementitious materials in the recent times. They are obtained by high temperature calcination and dehydroxylation of argillaceous minerals of clays, and consist of amorphous aluminosilicate phases (AS2, AS4) (Alujas et al. (2015)). These amorphous phases, when substituted in cement, can react with Portlandite or calcium hydroxide (CH), which a cement hydration product, to form compounds with cementitious properties like C-S-H. The reactivity of calcined clays is governed primarily by their specific surface, and the chemical and mineralogical composition of the amorphous phases (Tironi et al. (2013), & Plank et al. (2015)).

Table 7.1: Water and superplasticizer demand of clay minerals and similar-sized non-clayey particles (Nehdi et al. (2014))

Type of Mineral	Water Demand (b/c requirement)	Superplasticizer dosage (mL) (b/c = 0.42)
Control: Granite sand	0.47	4.5
Clay mineral		
1% Kaolinite	0.50	6.0
4% Kaolinite	0.60	8.0
1% Illite	0.49	5.5
4% Illite	0.51	10.0
1% Montmorillonite	0.62	18.5
4% Montmorillonite	0.90	186.0
Clay sized particles		
1% Fine calcium carbonate (60% < 2 µm)	0.48	-
4% Fine calcium carbonate (60% < 2 µm)	0.48	4.0
1% Ultrafine calcium carbonate (90% < 2 µm)	0.49	-
4% Ultrafine calcium carbonate (90% < 2 µm)	0.49	4.0
1% Ground silica (96% < 5 µm)	0.47	-
4% Ground silica (96% < 5 µm)	0.47	2.5

Clays samples in which dehydroxylation is not properly achieved, could experience some of these same incompatibility issues. The primary mechanism of PCE consumption has been widely attributed to the intercalation of macromolecules in the interlayer space of phyllosilicates, also named as chelation mechanism (AIt-Akbour et al. (2015), & Ng (2012)). Even if small amounts of surface adsorption could be measured, it appears that intercalated PCE induces a deformation of the clay sheet-like structure, easily observed by X-ray diffraction through increasing the interlayer thickness. This indicates that the clay platelet stacked structure deforms to accommodate large molecules.

Most authors observed that only the side grafts of the PCE macromolecules, namely poly(ethylene oxide) (PEO) chains, produce an intercalation effect. However, a study reported in demonstrated that this intercalation induces a decrease of the interlayer water amount, according to a dehydration-like mechanism (AIt-Akbour et al. (2015)). It has also been proposed that the units of the PEG chains interact with interlayer cations in a crown-ether-like fashion, replacing the hydration water of the said ions. It was shown that intercalation is more pronounced for longer PEO chains than for the shorter ones, which led to the design of very short sidegraft PCE molecules to improve clay tolerance. Other

modifications involved the insertion of amide groups or substitution of PEO by β-cyclodextrin, leading to mixed results in mitigating the intercalation, the total polymer consumption and the cementitious material workability. No intercalation of PCE was reported for kaolinite and illite; it is argued that their structure naturally leads to such behavior. The kaolinite interlayer space is devoid of any cation, which eliminates the basic PEO chelation mechanism described previously. This leads to the conclusion that most PCE interactions with kaolinite or illite would merely involve surface adsorption. It was indeed shown that PCE molecules are efficient dispersants of kaolinite suspensions.

Intercalations are controlled by many factors, such as polymer structure, molecular weight and charge density of PCE, types of clays and so on (Ma et al. (2020)). Reduction in the number of active sites of clays and optimization of structure of PCEs are the main methods for the enhancement of the tolerance of PCEs to clays.

Interaction of PCE superplasticizers with raw and calcined clays are dominated by two mechanisms namely, physisorption and chemisorption and is determined by the internal structure of clays.

7.3.1   Physisorption

The structure of PCEs is anionic in nature which can get adsorbed onto the clay surface with positive charges through uptake of Ca^{2+} cations. They have large adsorption capacity and form an adsorption layer on the surface of clays simultaneously (Plank et al. (2015)). Physisorption exhibits (a) hydrogen bonding or/and (b) electrostatic adsorption, as illustrated in figure 7.1 and plays an important role at low PCE dosages (Ma et al. (2020)).
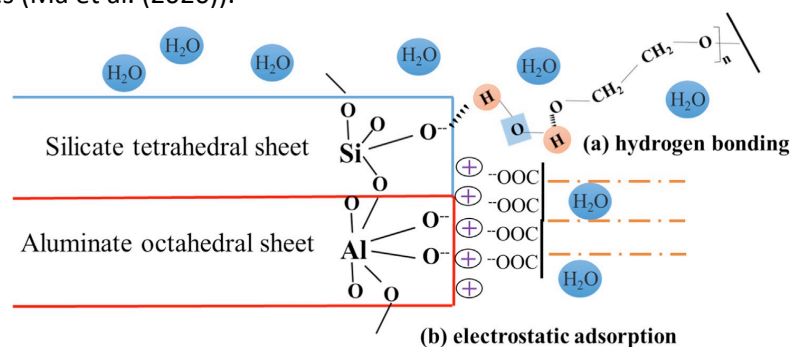
Figure 7.1: Illustration of physisorption of PCEs on clays (Ma et al. (2015))

Interactions of PCEs with kaolinite and illite are predominantly electrostatic adsorption due to their non-expandable structure and internal stability (Lei et al. (2014)). They adsorb much more PCEs in contrast with Portland cement. It was reported that about 45% of PCE is adsorbed by kaolinite while that by Portland cement is only 11% (Wang et al. (2014)). The strong electrostatic interactions between PCE and clays cause a partial depletion of superplasticizers available for cement dispersion. However, the PCEs absorbed on clays still have dispersion and water-reduction capability provided by steric hindrance of side chains.

The adsorption behavior of PCE onto calcined clay is determined by the presence of multivalent cations in the medium (Akhlagi et al. (2014)). To achieve the same flowability, the dosage of PCE required for calcined clay cement system has been observed to be greater than that for pure Portland cement system. Dhandapani et al. reported that the optimum superplasticizer dosage was related to the fineness of calcined clay (Dhandapani et al. (2012)). More calcium sulphoaluminate hydrate (AFm) was produced with the addition of metakaolin. It meant that electrostatic adsorption favors the interactions between PCE and metakaolin. Calcined clay (~metakaolin of 42%) hardly interacts with PCE directly due to the absence of multivalent cations (e.g., Ca^{2+}) and its low negative zeta potential (-21 mV) in water. It can be concluded that the amount of PCE getting physisorbed into the clay layers

after calcination is reduced, however, interactions are fairly similar as that with the slightly different structure prior to calcination.

7.3.2   Chemisorption

Chemisorption refers to chemical intercalation of side chains of PCEs into the interlayer region of clays. This phenomenon is takes precedence when PCE side chains with high affinity for the aluminosilicate layers comes in contact with clay, without destroying the structure of silicate and aluminate layers (Nehdi et al. (2014), Tan et al. (2016) & Tan et al. (2015)).

Due to the structural characteristics in layers of kaolinite, montmorillonite and illite, intercalation cannot occur between PCE and kaolinite or illite. The negative charge of the basal surface in montmorillonite generated by extensive isomorphous substitutions of Si^{4+} by Al^{3+} need to be balanced by intercalation and adsorption of cations. The d (0 0 1) value of montmorillonite in the presence of PCE solution (~1.863 nm) is higher than that of original montmorillonite (~1.43 nm) and the increment is consistent with width of side chain unit (EO) in PCEs, meaning that montmorillonite has strong intercalation effects besides surface adsorption (Antoni et al. (2012)), & (Wang et al. (2014)). Partially polarized oxygen atoms inside chains bond with water molecules that are anchored by the silanol groups in the aluminosilicate layers, then side chains enter into interlayers and results in intercalation, as shown in Fig. 7.2 (Ma et al. (2020)). There are three types of montmorillonite in the system, i.e., partially intercalated, fully intercalated, and non-intercalated montmorillonite. Both the partial or full intercalation of montmorillonite leads to the invalidation of PCEs, thereby negatively affecting the workability of cement and concrete seriously (Lei et al. (2012)).
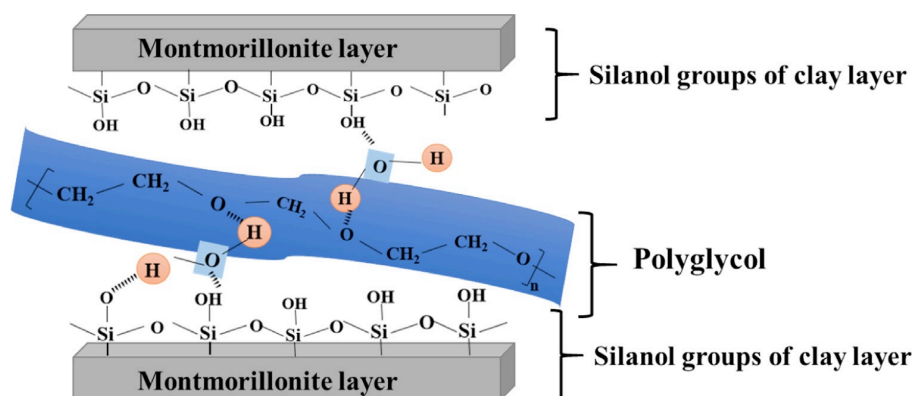

**Figure 7.2: Illustration of chemisorption of PCE onto clays (Ma et al. (2015))**

Calcined montmorillonite can also interact with PCEs by the chemisorption apart from physisorption according to the intercalation mechanism. The formation of hydrogen bond between interlayer is related to the OH⁻ groups of clays and partially polarized oxygen atoms of the side chain in PCE. Such groups can be provided by interlayer and absorbed water of montmorillonite, because the absorbed water still remains in its interlayers even after the complete dehydroxylation due to its water-absorbing tendency. It means that intercalation of side chain of PCE is hardly affected by the calcination.

7.4 Effect of clay content and clay type

The rheological performance of Portland cement-based systems containing clay have been have studied in the past by various researchers, however, that of LC3 systems with varying clinker substitution has been little explored. Kawashima et al. investigated the effect of small additions of highly purified attapulgite clays on the rheology of cement pastes. From the trend of the peak force of the tack test, it was inferred that clay increases the cohesion and viscosity of the pastes. In another study, Kawashima et al. reported that purified attapulgite clays significantly accelerate the rate of recovery of pastes, especially at early ages, and that this accelerating effect diminishes at longer

resting times as hydration of cement begins to dominate. Li et al. (2021) evaluated the increase in water demand of OPC blended with increasing substitution levels of calcined clay. At first, the fluidity of the pastes was measured at a constant water-to-binder ratio of 0.5 and compared. Fig. 3 (a) compares the flow spread at a constant w/b ratio of 0.5 while Fig. 3 (b) compares the w/b ratio required to achieve a particular slump spread for cement blends with calcined clay content increasing from 0% to 40% by weight. No superplasticizer was used to study only the water demand specifically.

It was found that increased additions of CC significantly affect paste fluidity. For example, already at a clinker substitution rate of 30% the paste flow had decreased from ~19 cm to 8 cm (Fig. 3 (a)) which signifies a complete loss of fluidity since the diameter of the Vicat cone is 8 cm. This effect was attributed to the much-increased specific surface area of the composite cements. It is in line with findings from other literature that the yield stress of a cement paste increases exponentially with the increase of the specific surface area. Furthermore, also the solid volume fraction of the composites will influence the yield stress of the cement paste. Here, as the water-to-binder ratio was kept constant at 0.5, the solid volume fraction in OPC and the OPC-CC blends varied from 38.99% (for the neat OPC) to 40.04% (for the 60:40 OPC/CC composite). However, such an increase is relatively minor and therefore of limited impact on workability.
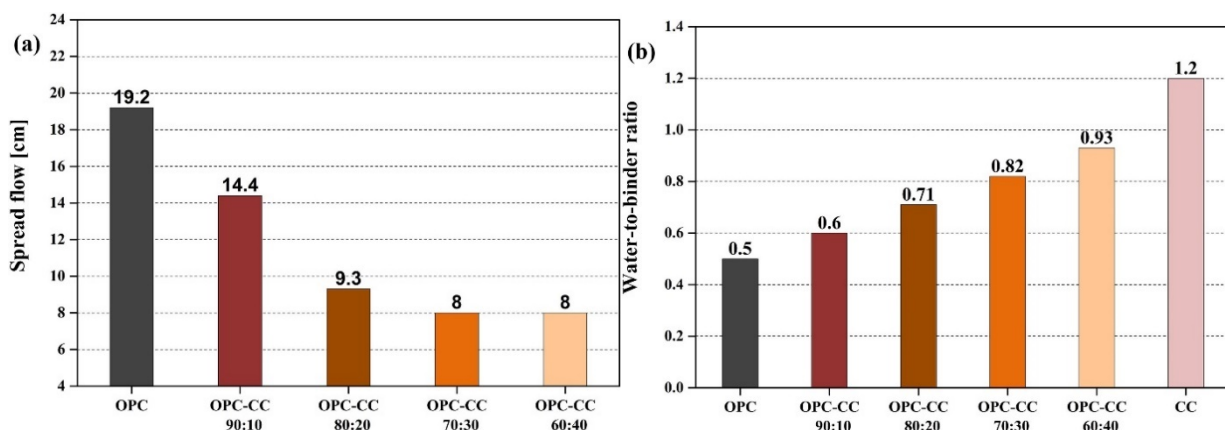
Fig. 7.3: (a) Spread flow of OPC/CC blended cements representing different substitution rates for the clinker, w/b ratio = 0.5, no PCE polymer added, (b) Water demand of composite cements containing OPC and CC at different substitution rates; no PCE polymer added (Li et al. (2021))

The results from Fig. 7.3 (a) suggest that the water demand of CC is much higher than of OPC. To confirm, the water demand of thxe different OPC/CC blends was determined. In this series of tests, the w/b ratios at which a paste spread flow of 18 ± 0.5 cm was obtained for different OPC/CC blends were determined. The results are displayed in Fig. 7.3 (b). There it can be seen that the amount of water required increases linearly with ascending substitution rate for the cement clinker. For example, at 40% replacement of cement clinker by CC (OPC:CC 60:40), the water demand had almost doubled from 0.5 for neat OPC to 0.93 for the 60:40 blend. For the neat calcined clay sample, the water demand raised to an even much higher value of 1.2 to achieve the targeted spread flow. This indicates that the water demand of the CC sample investigated here is particularly high, presumably resulting from the high content of fine meta kaolin.

In another similar study, Li et al. (2021) investigated the fluidity retention by the variation of mini-slump spread with time for OPC as well OPC substituted with increasing amount of calcined clay mixtures. A ready-mix HPEG PCE was used to study the slump retention. Fig. 4 below shows the mini-slump spread variation of the cements with time.
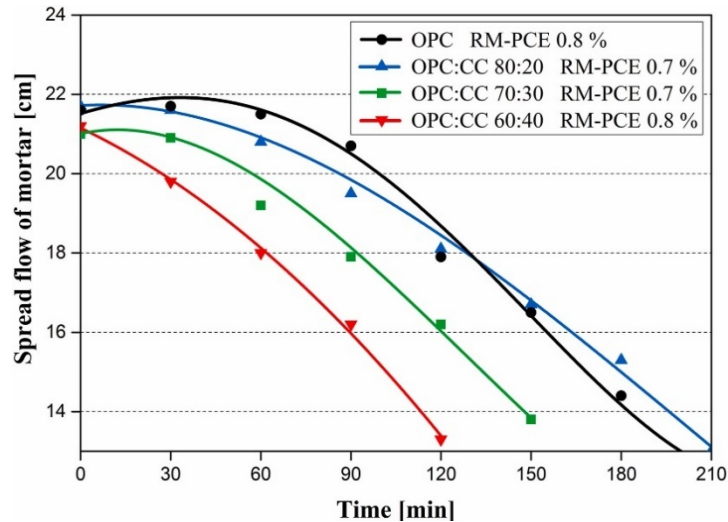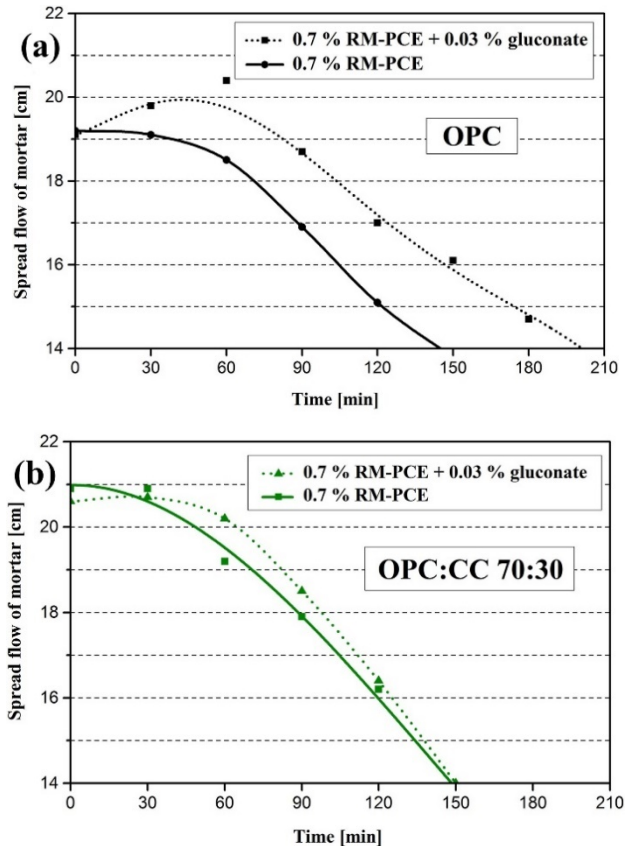
Fig.7.4: Fluidity retention of mortars prepared from neat OPC or OPC/CC blends admixed with different dosages of a commercial benchmark ready-mix HPEG PCE (w/b ratio = 0.4) (Li et al. (2021)

As is shown in Fig. 7.4, in neat OPC the ready-mix HPEG PCE produced excellent slump retention over a period of ~90 min, and then fluidity gradually decreased over a period of 2 h until it reached the spread flow value of the non-treated mortar. It was highlighted that, the mechanism behind the slump retaining effect of this PCE relies on continuously produced carboxylate groups as a result of ester hydrolysis occurring under the highly alkaline conditions of the cement pore solution.

However, with increasing content of calcined clay in the composite cement, the slump retaining ability of this ready-mix PCE deteriorated steadily. For example, at 20 wt % substitution rate (clinker factor 0.8), fluidity retention lasted only for 60 min as compared to 90 min for the neat OPC sample. Moreover, for the 30 and 40 wt % calcined clay blended cements, workability could be retained for 45 and 30 min only, respectively, thus signifying an extremely negative effect of the calcined clay on fluidity retention. In the 60: 40 OPC/CC blend, even an increase in the dosage of PCE to 0.8% could not remedy the problem. The results signify that when a threshold value of ~20 wt % of this calcined clay in the binder is exceeded, then slump retention becomes a serious issue for such concretes, and conventional PCE admixtures fail to solve this problem.

To alleviate this issue, Li at al. (2021) used sodium gluconate retarder along with the commercial ready-mix PCE to study the efficacy of this combination on the fluidity retention of OPC as well as OPC-calcined clay composite cement. Fig. 5 (a) and (b) show the comparison between the effect of only PCE addition and PCE+gluconate addition on fluidity of OPC and OPC+30% CC combinations respectively.

Fig. 7.5: Fluidity retention of mortars prepared from (a) neat OPC or (b) OPC:CC 70:30 blend admixed with an industrial benchmark ready-mix PCE (RM-PCE), with or without sodium gluconate (w/b ratio = 0.4) (Li et al. (2021))

As is shown Fig. 7.5 (a), in neat OPC at a dosage of 0.7% of this PCE a spread flow of 19 cm is reached and initial fluidity is maintained for around 60 min. Dosing in of additional 0.03% of sodium gluconate (such addition rate is commonly used in practice) prolonged the fluidity retention time from 60 to ~ 100 min, thus demonstrating the well-known synergistic effect between the PCE and this retarder. Such slump retaining effect of sodium gluconate has been studied extensively before and was found to rely on postponed ettringite formation. However, as is evident from Fig. 7.5 (b), the presence of calcined clay severely impedes slump retention, for the system based on the individual PCE as well as for the PCE/gluconate combination. Moreover, the effect of sodium gluconate as auxiliary slump retaining admixture is almost completely lost.

The results signify that in calcined clay blended cements fluidity retention is difficult to achieve when using the conventional concepts established on OPC. However, a solution to this problem is crucial to enable a more widespread use of calcined clay blended cements in the future.

Muzenda et al. (2020) carried out rheological measurements of cement pastes with varying composition of limestone, calcined clay and clinker content to study the individual and combined effect of substitution of these SCMs. A total of 7 blends and 1 reference Portland cement were characterized for rheological performance by preparing cement pastes at a w/b ratio of 0.45. Fig. 7.6 compares the statis yield stress variation of these blends with time of resting between trials. The nomenclature can be read as 'REF' meaning 95% clinker and 5% gypsum while for the blends, it can be read as 'Cx/Ccy/Lz' meaning x% of clinker, y% of calcined clay and z% of limestone.
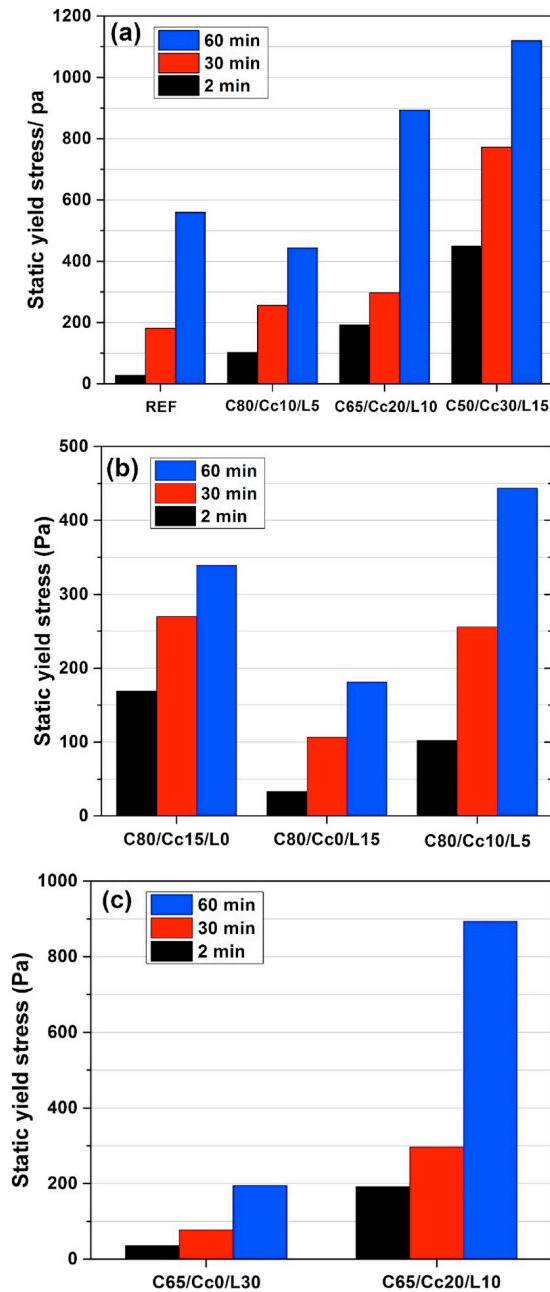
Fig. 7.6: (a) The variation of SYS with resting time, and comparison of the effect of limestone and calcined clay on SYS at (b) 80 wt% substitution and (c) 65 wt% substitution (C65/Cc30/L0 did not flow at the rheometer's maximum torque of 200 mNm). (Muzenda et al. (2020))

A clear increase can be noticed in the static yield stress (SYS) from the REF to C50/Cc30/L15, with the SYS of C50/Cc30/L15 being over 15 times that of the REF. SYS increased with resting time for all samples (Fig. 6a) but at different rates which reflects the different mechanisms at work in the different systems. In generalized terms, the SYS of C80/Cc10/L5 and C65/Cc20/L10 were greater than that of C80/Cc0/Cc30/L0 at all resting times, respectively. Therefore, in general, it is calcined clay that is responsible for the increase in SYS with increase in SCM content in the LC3 system. However, there was an exception when C80/Cc10/L5 was greater than C80/Cc15/L0 at 60 min resting time. This is likely because the combined effect (synergy) of CC and LS on cement hydration supersedes that of calcined clay and limestone when employed separately, resulting in greater increase in SYS for C80/Cc10/L5. The authors further investigated the flow curves of these different LC³ and REF samples at different resting times were obtained and used to determine the Bingham model parameters,

namely dynamic yield stress (DYS) and plastic viscosity as shown in Fig. 7.7. Results show that DYS and plastic viscosity both increase with increase in SCM content and resting time. Clays are well known to act as viscosity modifiers to enhance flocculation strength, therefore an increase in calcined clay content is expected to increase both DYS and plastic viscosity. Additionally, although limestone can act as a filler to increase viscosity at certain addition levels, from the results of the SYS measurements, it is expected that the effect of calcined clay governs here. Also, the increase over time for all mixes is consistent with REF, as this is primarily tied to the progression of cement hydration. In addition to the above observations, clays can exhibit significant shear thinning, as seen in Fig. 7.7 (b).

It is interesting to note the sharp increase in plastic viscosity for REF as compared to the other three blends (Fig. 7.7b), similar to SYS and DYS. Plastic viscosity changes by 183%, 136%, 129% and 125% from 2 min to 60 min for REF, C80/Cc10/L5, C65/Cc20/L10 and C50/Cc30/L15, respectively. Even though the plastic viscosity of REF at 60 min was still far lower than that of C50/Cc30/L15, the increase from 2 min for each of the REF shows that, for early ages, its hydration process is faster than that of the LC3 system. This is due to the relative amounts of clinker in each sample and the fact that calcined clay is not very reactive in the early stages of cement hydration. It has been reported that LC3 blends usually have a low 1- or 3-day compressive strength than that of REF. This is also mirrored in the lower effect of resting time (and hence the hydration mechanism) on the plastic viscosity for high clinker substitutions. This reflects that the increasing effect of calcined clay on static and dynamic yield stress, as well as plastic viscosity, does not primarily hinge on their hydration effect but instead on their high-water adsorption, or possible interaction between the clays and hydration products like ettringite.
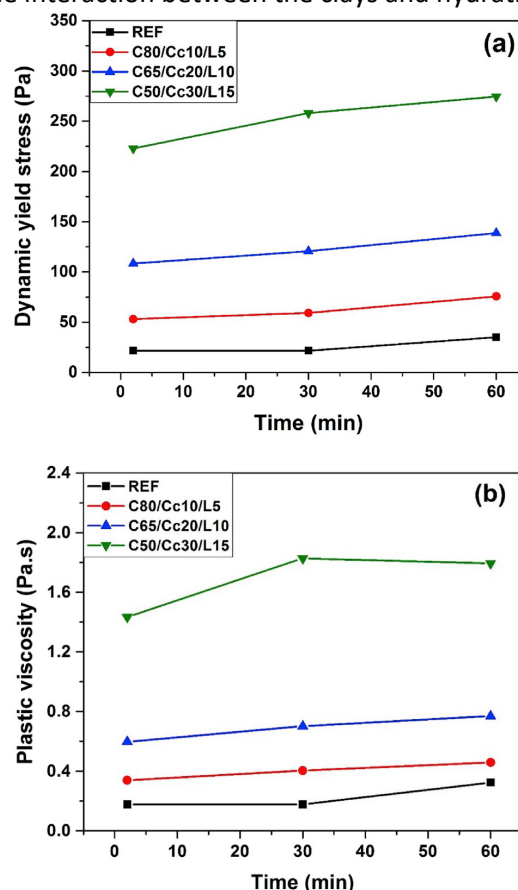

Fig. 7.7: Effect of resting time on (a) dynamic yield stress and b) plastic viscosity, as determined from the flow curves. (Muzenda et al. (2020))

7.5 Effect of limestone filler

Limestone has been known to be used as a SCM to produce blended cements like the Portland-limestone cement and even LC[3]. Apart from the filler effect resulting from the addition of limestone,

which results in the pore structure refinement in LC^3 systems, limestone also provide nucleation sites for cement hydration as well as participates in the reaction leading to the formation of carboaluminate phases. Although very limited studies have been conducted to study the effect of limestone on the workability and flow characteristics of LC^3 systems, researchers have suggested that limestone can have a neutral-to-positive impact on the cement paste and concrete rheology. Santos et al. (2017) studied the effect of limestone on the segregation resistance. It was highlighted that limestone filler alone is not able to assist in enhancing the segregation or bleeding resistance, and no difference was found between the rheology of cement pastes with limestone filler and that of OPC pastes. On the other hand, Muzenda et al. (2020) reported that, apart from its contribution to hydration, limestone also moderately affects statis yield stress (SYS) increase over time due to dissolution-precipitation processes leading to the formation of links between grains. A case in point is that only C65/Cc20/L10 and C65/Cc0/L30 are shown in Fig. 6c because the torque required to reach the SYS for C65/Cc30/L0, even after a short resting time (2 min), exceeded the rheometer's maximum limit of 200 mNm. This highlights the marked effect of CC on SYS. C50/Cc30/L15 has the same content of CC as C65/Cc30/L0 (30%) but the former flowed while the latter did not. This can be attributed to the 15% LS content in C50/Cc30/L15. At 2 min resting time, C80/Cc15/L0 yielded a 67% increase in SYS while C80/Cc0/L15 yielded a 69% decrease in comparison to C80/Cc10/L5. Therefore, it could be concluded that limestone significantly reduces SYS, while calcined clay has an opposite effect. One reason for this observation is the difference in the particle shapes of the two SCMs. Limestone has a somewhat round or circular shape that provides a 'bearing effect' in the paste and thus increasing flowability whereas calcined clay has a layered structure which contributes to its high-water demand.

In another interesting study, Vance et al. (2013) evaluated the rheological properties of ternary binders containing Portland cement, limestone, and metakaolin or fly ash. Combinations of OPC, limestone (10 and 20% replacement with different particle sizes of 0.7, 0.3 and 15 mm) and metakaolin (5 and 10% substitution by mass) with volumetric water-to-solid ratio (w/s) of 0.40 and 0.45 were used in the study. The rheological studies of binary blend combination of coarser limestone of size 15 mm (5% replacement) and OPC showed that there was reduction in yield stress and plastic viscosity with respect to the control mix (Fig. 7.8). For limestone particles coarser than cement, there was a decrease in particle packing and specific surface area. This reduced the ability of the paste to resist shear, thus explaining the reduced yield stress. When fine limestone powder (0.7 and 0.3 mm) was used as replacement and OPC, there was increase in yield stress and plastic viscosity. Therefore, replacement with limestone particles coarser than OPC decreased the yield stress and plastic viscosity, whereas particles finer than OPC increased the yield stress and plastic viscosity. In the case of metakaolin replaced Portland cement paste, yield stress and plastic viscosity were significantly increased because of the high surface area and the tendency of particles to agglomerate. The rheology of the ternary blend combination of limestone and metakaolin is quite complex. For ternary blends with fine limestone addition and metakaolin, with increase in limestone content, the plastic viscosity also increased, similar to that of binary blend with fine limestone particles and OPC (Fig. 7.9). However, for ternary blend with coarser limestone addition, the plastic viscosity remained unchanged, as the viscosity is predominately affected by the fine metakaolin particles. The plastic viscosity increased with an increase in metakaolin content and was invariant with the limestone content. On the other hand, in the case of ternary blends with the increase in finer limestone additions at fixed metakaolin content, there was decrease in yield stress. Even though the addition of fine limestone reduces the particle spacing and increases the yield stress, the electrostatic attraction between the negatively charged metakaolin and positively charged limestone particles increased the interparticle spacing and thereby reduced the yield stress.
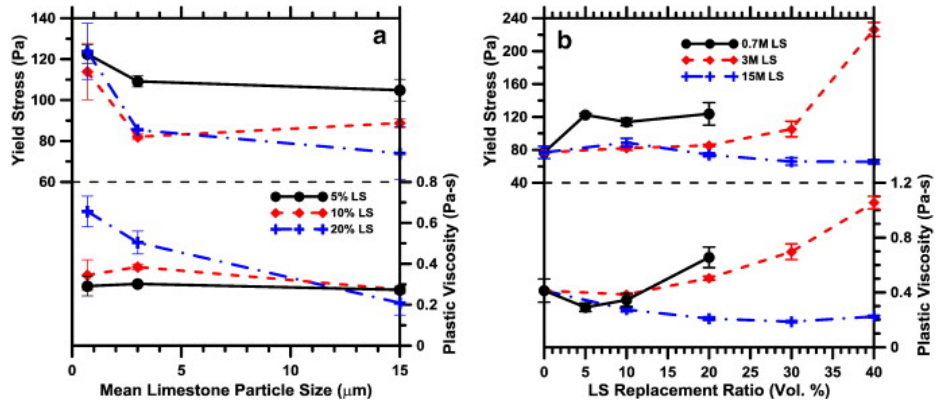
Figure 7.8: influence of (a) limestone particle size and; (b) level of replacement of OPC by limestone (volume basis) on the yield stress and plastic viscosity of pastes
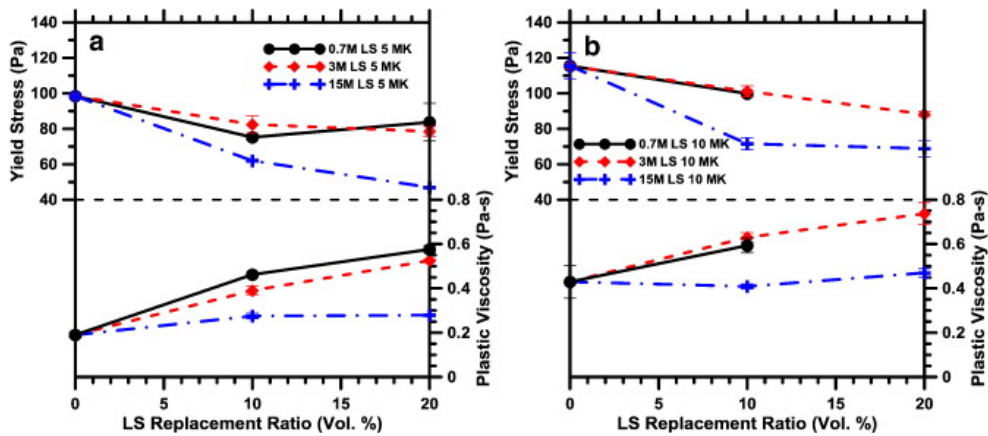

Figure 7.9: Influence of limestone dosage on the measured rheological properties of metakaolin blended pastes for: (a) 5% metakaolin, (b) 10% metakaolin. (Vance et al. (2013))

7.6 Effect of binder content and water-to-binder ratio

The workability of LC^3 cement pastes have been compared with that of OPC and the pastes of other blended cements to understand the water and superplasticizer demand of the LC^3 systems without the influences of aggregates. Nair et al. (2020) compared the saturation dosage of two types of commercially available superplasticizers, viz., SNF and PCE for OPC, PPC and LC^3 cement pastes prepared at varying w/b ratios. The w/b ratios were varied between 0.35 to 0.45. Marsh cone flow and mini-slump spread tests were carried out for the various paste samples by increasing the admixture content to arrive at the saturation dosage required for each admixture for a given type of cement and w/b ratio. Table 2 below lists the saturation dosage as well as the corresponding marsh cone flow time and mini-slump spread obtained for OPC, PPC and LC^3 paste samples.

It was observed that the w/b ratio has significant influence on the flow time. The flow time was found to decrease with the increase in w/b ratio as expected. It was highlighted that at low w/b ratios, the availability of water is less, which decreases the relative fluidity and increases the flow time. Comparing the behavior of cement types, it was reported that OPC showed much lower flow times at saturation dosage for all w/b ratios. At w/b ratios of 0.35, 0.40, and 0.45, PPC and LC3 showed comparable flow times at saturation dosage. As for the performance of the types of superplasticizers, it was observed that, the saturation dosage saturation was higher for SNF as compared to PCE for all w/b ratios. This effect was attributed to the mechanism of action of both the superplasticizers. For PCE admixtures, the dispersion is caused by both steric and electrostatic repulsion mechanisms, whereas for SNF based admixtures, the dispersion is only due to electrostatic repulsive forces. Due to this reason, higher dosage of SNF is required for better dispersion. Apart from this, it was also noted that the saturation dosage required for LC^3 is greater compared to OPC and PPC at all w/b ratios. This

was attributed to the intercalation of superplasticizer molecules between layers of clay and to the higher fineness of LC3 particles as compared to that of other cement types. The mini-slump spread values were found to increase up to saturation dosage. Beyond the saturation dosage, there was no significant change in the spread value. Bleeding was observed at very high dosages of superplasticizer. It was understood from the results that LC^3 can achieve similar spread as OPC at the saturation dosage at higher water-to-binder ratios.

Table7.2: Summary of saturation dosage determined from Marsh cone tests and mini-slump spread. (Nair et al. (2020))

Type of Binder	w/b ratio	SP saturation dosage (%b)		Flow time at saturation dosage (s)		Mini-slump spread at saturation dosage (mm)	
		PCE	*SNF*	*PCE*	*SNF*	*PCE*	*SNF*
OPC	0.35	0.15%	0.40%	26	21	165	200
PPC	0.35	0.20%	0.50%	47	43	180	200
LC3	0.35	0.40%	0.70%	50	49	180	175
OPC	0.40	0.10%	0.20%	11	8	180	150
PPC	0.40	0.15%	0.30%	16	19	200	150
LC3	0.40	0.30%	0.40%	14	16	180	175
OPC	0.45	SP not required	SP not required	-	-	-	-
PPC	0.45	0.05%	0.10%	11	10	150	160
LC3	0.45	0.20%	0.30%	10	8	150	170

Full scale concrete workability studies have been undertaken by various researchers to understand the actual rheological behaviour of LC^3 for use in concrete. In an elaborate study, Nair et al. (2020) evaluated the influence of water content reduction with respect to the superplasticizer dosage and the variation in water content and PCE superplasticizer requirement for each of the different LC^3 concrete mixes as listed in Table 7.3 (Nair et al. (2020)). Fig. 8 shows a plot of the water and superplasticizer requirement for these mixes.

Table 7.3: Summary of concrete mix proportions for evaluating the influence of mix water on LC^3 concrete (Nair et al. (2020))

Mix ID	Binder content (kg/m^3)	Water content (kg/m^3)	w/b ratio
MIX 1	300	180	0.60
MIX 2	350	175	0.50
MIX 3	370	167	0.45
MIX 4	400	160	0.40
MIX 5	420	147	0.35
MIX 6	450	135	0.30

It was observed that for a reduction in water content from 180 kg/m^3 (MIX 1) up to 167 kg/m^3 (MIX 3), there was no increment in the SP dosage required to produce the target workability. However, for water content lesser than 167 kg/m^3 (i.e., for MIX 4, MIX 5 and MIX 6), the PCE dosage required increased drastically with the reduction in water content.
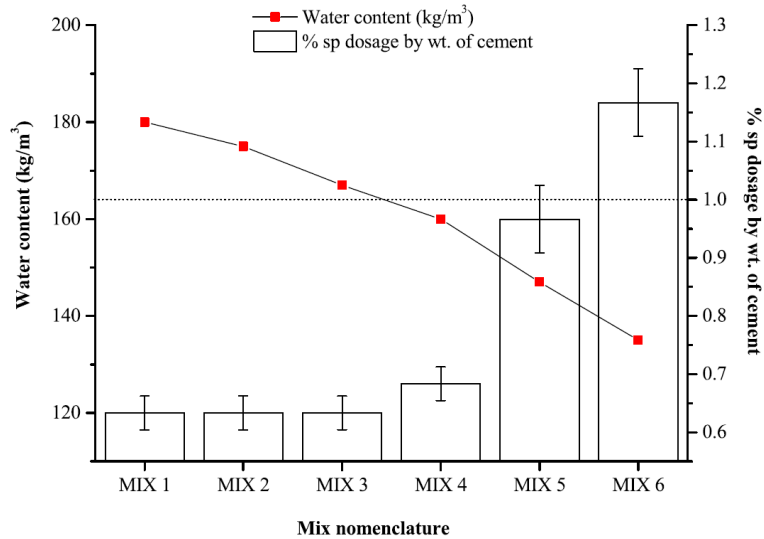
**Fig. 7.10: Water content and PCE superplasticizer dosage requirement for each mix (Nair et al. 2020)**
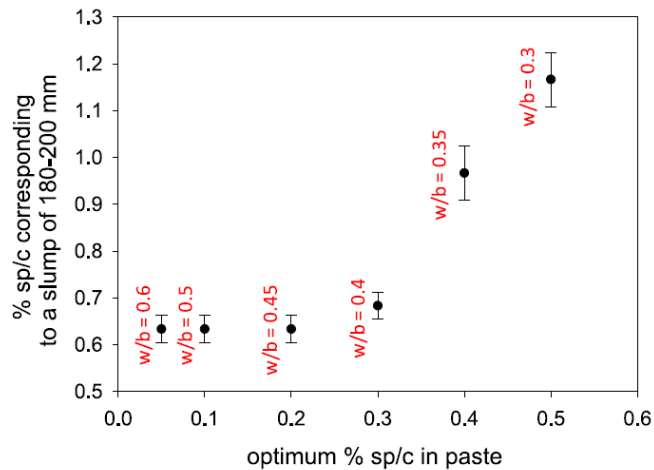
Fig. 7.11: Correlating saturation dosage of PCE superplasticizer from paste studies with the finalized dosages from concrete (Nair et al. (2020))

In terms of the water-to-binder (w/b) ratio, this issue of workability and the massive increase in superplasticizer requirement is noticed between 0.4 to 0.3 w/b ratio, which is in conformity with the LC^3 cement paste studies as well. Furthermore, the admixture requirement in LC^3 concrete and cement paste were correlated as shown in Fig. 7.11. From Fig. 7.11, it can be observed that in both LC^3 cement paste and concrete studies, when the w/b ratio was reduced below 0.40, there was a sudden increase in the requirement of superplasticizer. As seen from Fig. 7.11, while the saturation dosage of PCE superplasticizer in the paste increases steadily with a decrease in the w/c, the corresponding dosage to produce a high slump of 180–200 mm in concrete does not significantly change until a w/c of less than 0.40. Below this w/c, there is a major increase in the PCE dosage required for achieving the target slump. Apart from this, it was also mentioned that the requirement of SNF to achieve the target slump was significantly higher compared to PCE. At w/b ratio of 0.30 and 450 kg/m^3 binder content, the SNF superplasticizer dosage was even greater than 1.6% by weight of cement and the target slump was not achieved. Therefore, the LC^3 – SNF combination for w/b ratio below 0.40 was deemed incompatible. From the slump tests, it can be concluded that PCE based admixture is better suited for LC3 systems as compared to SNF (Nair et al. (2020)).

In another similar study by researchers at IIT Delhi, the variation of the mini slump spread and the Marsh cone flow time of LC3 cement pastes prepared at varying water-to-cement (w/c) ratios was evaluated. The corresponding superplasticizer requirement was also obtained. As shown in Fig. 12, the slump spread values decreased with the decreasing w/c ratio of the paste samples. Apart from this, the superplasticizer requirement increased significantly while moving from 0.45 to 0.35w/c ratio. As can be seen in Fig. 13., the flow times achieved at higher w/c ratios like 0.5 to 0.6, are quite low and the SP demand is less, which indicate that a good workability can be achieved. However, a drastic increase in the flow times can be observed for the pastes with w/c ratios between 0.45 and 0.35. Additionally, at 0.35 w/c ratio the flow time varies abruptly with the increasing SP dosage and no clear trend can be found. Therefore, it can be understood that, the workability of LC^3 systems can be similar to that of other cement when sufficient water is available, however, this severely hampered as we move towards lower w/c ratios, especially below 0.45.
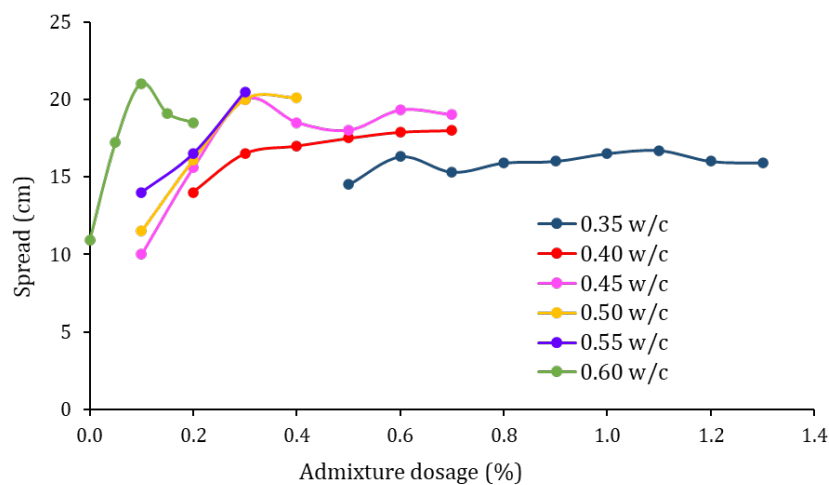
Figure 7.12: Variation of mini-slump spread with admixture dosage for LC^3 cement pastes at different w/c ratios
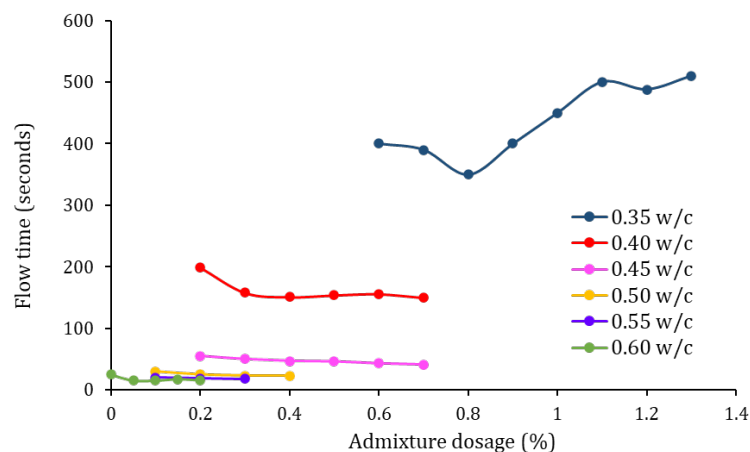
Figure 7.13: Variation of Marsh cone flow time with admixture dosage for LC3 cement pastes at different w/c ratios

7.7 Summary

The workability of LC3 systems is influenced by a variety of factors. From the previous sections, it can be understood that PCE superplasticizers are better suited and more effective with LC^3 systems as compared to the other commercially available admixture types. However, the intercalation of PCE superplasticizer in the clay interlayers is higher which raises concerns. Admixture formulations better suited for LC3 systems need to be produced in order restrict the intercalation and adsorption effect.

It can be understood that the issues with achieving desired workability in both concrete as well cement pastes of LC3 are more pronounced at lower water-to-cement ratios, i.e., below 0.45. Apart from this, the calcined clay content substituted in the blends seems to be a factor dominating the rheological characteristics of LC^3. With increase in calcined clay substitutions both yield stress as well as viscosity tend to shoot up. Even though limestone filler provides a ball-bearing effect and aids in alleviating the workability issues, the fineness of limestone can play a role in this respect.

Chapter 8: Mechanical properties of LC^3 mortar and concrete

8.1 Introduction

To establish the acceptability of LC^3 cement as an alternative binder system in comparison to widely adopted OPC and fly ash based PPC cementitious systems, the mechanical performance is the key parameter. The influence of the kaolinite content, effect of particle size of the individual components and different types of limestone on the compressive strength are already covered in the previous chapters of clay testing, grinding and limestone respectively. Also, how microstructure of a cement matrix in LC^3 mortar and concrete affects the compressive strength is also covered in the previous chapter.

This report includes the detailed investigation on the comparison of LC^3 mortar and concrete with OPC and PPC systems, the composition of the clinker, curing temperature, relative humidity, alkali content on the mechanical performance of the LC^3 systems.

8.2 Compressive strength

Compressive strength is the most crucial parameter among all other parameters necessary for achieving the required mechanical performance of a structure. The mechanical performance of LC^3 systems with low clinker factor of 40% to 50% is comparable with the OPC and Fly ash based systems. The LC^3 mixes has marginally lower 3-day strength in comparison to OPC mixes but it is higher than that of fly ash or slag based blended cements and at 7 and 28 day, LC^3 mix achieves similar strength as OPC mix (Yuvraj et.al. 2018). Fig. 8.1 shows that after 28 days, the compressive strength increase in the LC^3 system is negligible (Zunini 2020, Krishnan et. al. 2019), due to suppressed alite and belite hydration in the presence of calcined clay (Krishnan 2019).

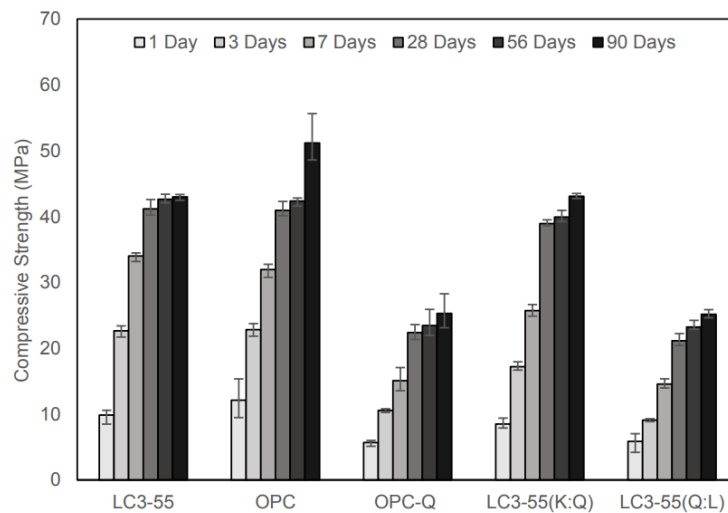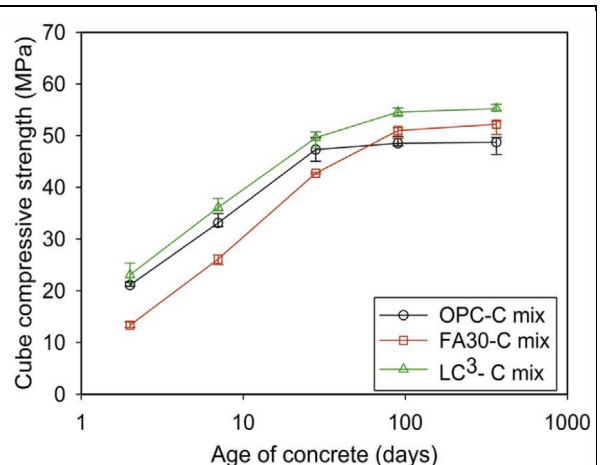**Fig. 8.1: The compressive strength development in the LC^3 and OPC systems**

Whereas, Yuvraj et.al. reports that similar to fly-ash based system (FA30), 28-day strength of LC3 mixes increases between 28 to 90 days (Figure 8.2). He also reported (Figure 8.3), that if we keep the mix proportion same i.e. same binder content and w/b ratio for LC^3, OPC and FA30, LC^3 mixes shows highest compressive strength at all ages.
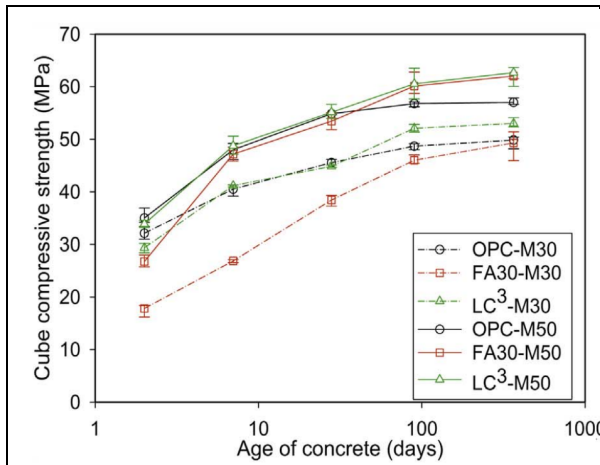
| Figure 8.2: Comparison b/w LC3, OPC and FA30 | Figure 8.3: Same binder content and w/b ratio |

Krishnan et. al. 2018 highlight that fineness of individual components is dominant in case of low alite clinker, here clinker fineness is of prime importance in comparison to clay and limestone fineness, this will lead to faster hydration rate of clinker and thereby availability of calcium hydroxide for reaction with clay and limestone. Calcium ions are rapidly consumed during second hydration reaction which increases the early clinker hydration rate, hence reduces the unhydrated clinker in the system which leads to strength development reduction at later ages.

8.3 Elastic modulus

The static elastic modulus of the different concrete mixes is shown in Figure 8.4(a). The results indicate that the elastic modulus was similar for concretes wth all the binder systems. This indicates that concrete made with LC^3 can have similar mechanical performance characterisics for structural applications as the other conventional binder systems. The correlation between elastic modulus and compressive strength (presented in figure 8.4(b)) shows a linear trend (R^2= 0.89), independent of the binder used for the concrete. For reference, the predicted moduli from the Indian standards (IS 456 2000) and FIB Model Code 2010 (Fédération Internationale du Béton 2010) are also plotted (Yuvraj et.al. 2018). Figure 8.5 also shows that portland cement and LC3-50 have similar trend (Scrivener, Avet, Maraghechi et al. 2019)
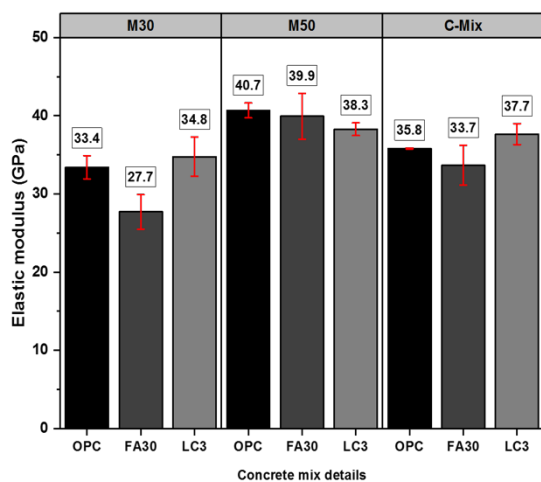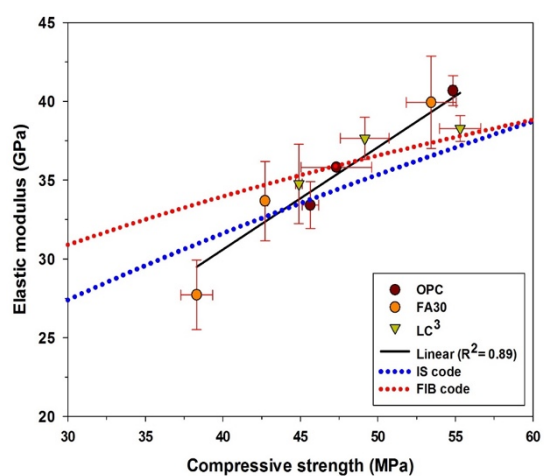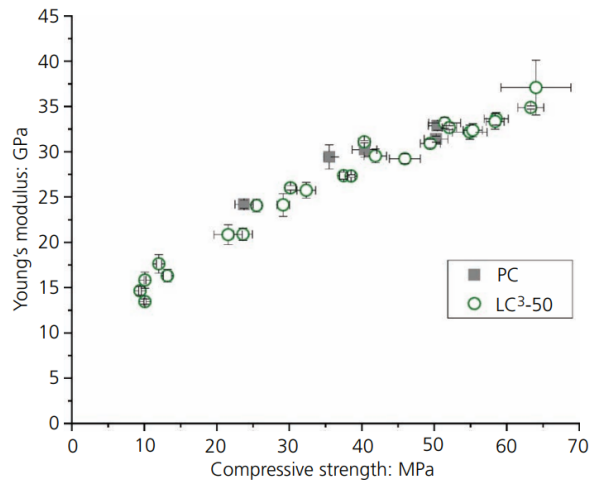

(a)   (b)

Figure 8.4 (a) Elastic moduli of concretes made with OPC, FA30, and LC^3 and (b) correlation between elastic modulus and compressive strength

Fig 8.5: Young' modulus as a function of compressive strength for LC³-50 and Portland Cement

8.4 Shrinkage

The autogenous and drying shrinkage influence cracking in concrete structures, as the binder phase continues to deform amidst the restraint offered by the aggregates in the hardened concrete. Autogenous shrinkage is controlled by the change in the internal RH (due to consumption of free water) of the system due to self-desiccation at low water-cement ratio, whereas the loss of moisture (due to drying) from the concrete leads to drying shrinkage. Bissonnette et al. 1999 reported that the influencing parameters affecting the shrinkage measurement were water-cement ratio, size of specimen, relative humidity, and paste volume. A more detailed classification of factors are listed in ACI Committee 209 2005.

The evolution of shrinkage strains in cylindrical and prismatic specimens are shown in Figure 8.6 to 8.8. The autogenous shrinkage strains measured for all the concretes were lower compared to the values reported in literature. In this study, the specimens were wrapped with aluminum adhesive tape only after 28 days of curing. The autogenous shrinkage from casting until 28 days (t_0) is neglected in this measurement. The drying shrinkage is presented as total shrinkage as it also includes a part of autogenous shrinkage.

For M30 concrete mixes, the measured autogenous shrinkage strains after 28 days were comparable for the OPC and LC³ systems (figure 8.6). However, FA30 showed a higher shrinkage (autogenous) due to lower water-cement ratio in the concrete mix. In contrast, for the same reason of the lower water content, drying shrinkage results suggest that FA30 has lower shrinkage than the OPC and LC³ concretes. Figure 8.7 reports the results of the M50 grade concretes, and it is seen that the drying shrinkage of FA30-M50 concretes was comparatively lower (than M30 concretes) due to the lower water-binder ratio (0.35) opted for the FA30-M50 concrete mixes. The initial shrinkage of FA30-M50, which occurs at a faster rate was also found to be lower in both types of specimens. In the C-mix (with the same binder content and w/b), the measured shrinkage strains in the different binder systems were comparable (figure 8.8). From the results, it is seen that the influence of water-cement ratio dominates the effects of shrinkage development in concrete, which is evident from the difference in the shrinkage strains noted in the two sets of equivalent grade concrete mixes. However, the concretes with the same binder content and w/b ratio showed minimal difference between the different binder systems.

The shrinkage behaviour can be further rationalised by dissociating the effect of water-binder ratio, pore sizes, and degree of hydration at varying water-binder ratio for the three binder systems. The governing mechanisms causing shrinkage in the different cementing matrices are controlled by these factors. First and foremost, a lower water-binder ratio (typically less than 0.4) leads to reduced

112

hydration degree due to a more packed capillary space. This causes a reduction in the amount of hydrates and thereby, the medium which is shrinking in the concrete is also reduced. Alternatively, at lower water-binder ratios, there is an increase in the amount of the finer pores (more specifically in the blended systems) which increases the shrinkage per unit mass loss due to higher capillary pressure during drying.

This difference can be explained by taking a closer look at the shrinkage strain and mass loss of the different binder systems (figure 8.9). The shrinkage performance in fly ash mixes can be attributed to the lower hydration degree, lower water-binder ratios and coarser pores in FA30 systems from the slow reaction of fly ashes which reduces the amount of hydrates. This results in lower shrinkage strain, even at similar amount of mass loss due to drying. In contrast, a higher water content, finer pores (details of pore sizes are discussed in Table 6) and higher hydration extent due to early reactivity of calcined clay in the LC^3 systems (M30 and M50 mixes) collectively increases the shrinkage strain (marginally), despite lower or similar amount of mass loss from drying (figure 8.9).

In previous studies on metakaolin addition on shrinkage evolution, Brooks and Megat Johari 2001, reported that increasing metakaolin content from 5% to 15% lowered the early age autogenous shrinkage and drying shrinkage, and increased the long term autogenous shrinkage. Metakaolin has been reported to reduce free drying shrinkage (Ding and Li 2002; Güneyisi et al. 2007). Literature on limestone addition also shows that increasing amounts of limestone replacing the Portland cement results in similar (or lower) drying shrinkage for up to 10% substitution (Camiletti et al. 2013; Dhir et al. 2007), whereas higher replacement level (20% or above) can lead to increase in the drying shrinkage (Bederina et al. 2011; Varhen et al. 2016). From this study, it can be concluded that combined substitution of limestone and calcined clay resulted in similar or marginally higher shrinkage in concretes as compared to OPC and FA30. The effect of water-binder ratio (the amount of free water) and mixture proportioning (paste volume) had a more dominant effect on the evolution of shrinkage strains between the different binders.
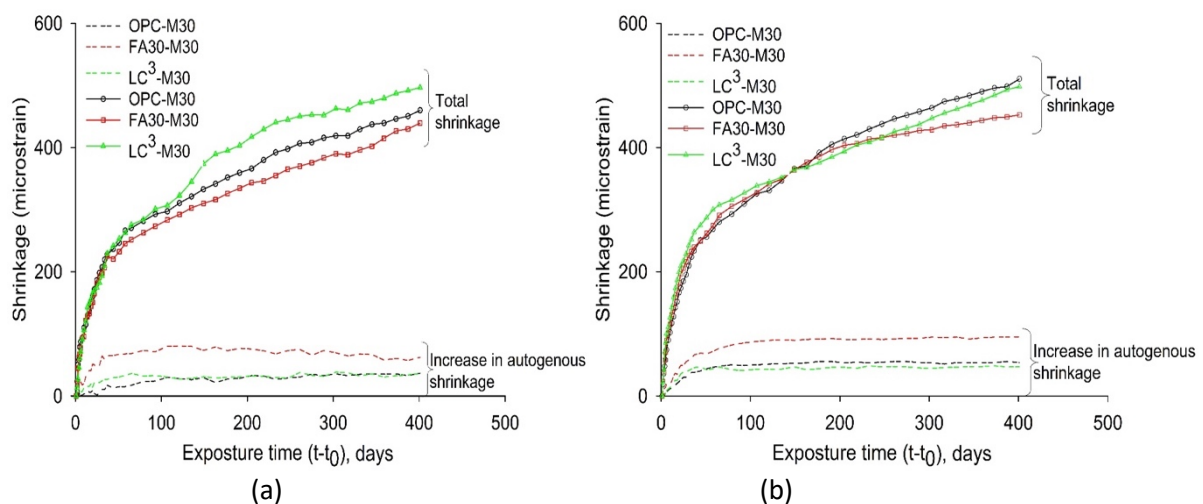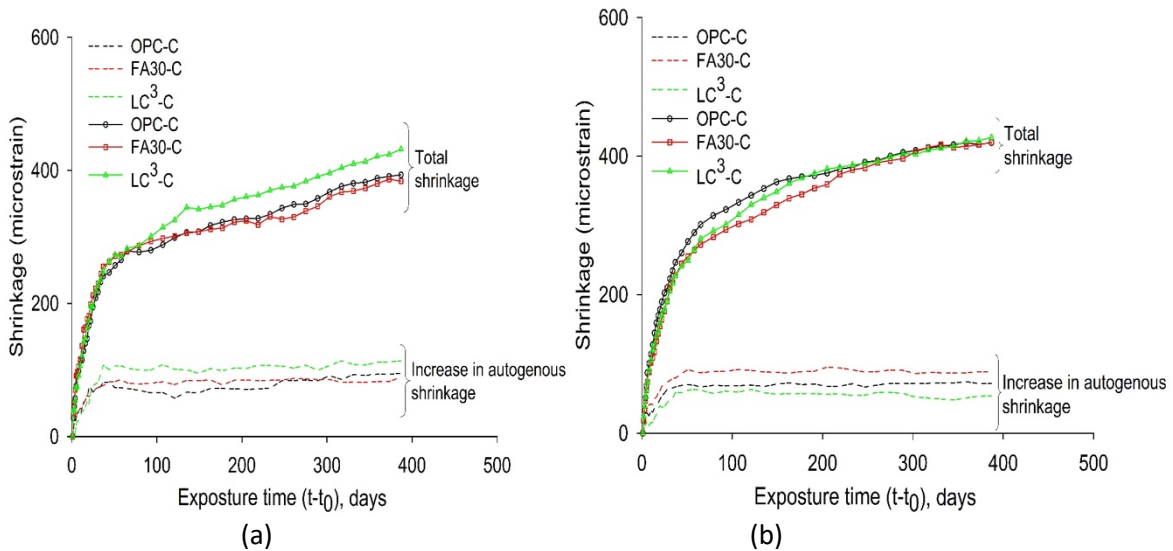

Figure 8.6: Shrinkage strain in M30 concretes (a) Cylindrical specimens and (b) Prismatic specimens
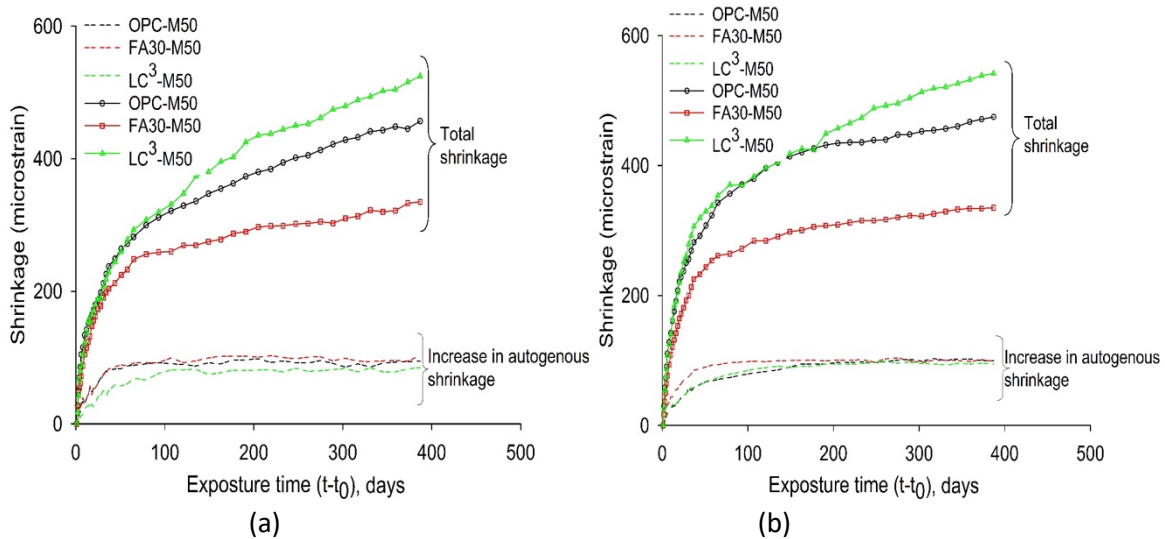
Figure 8.7 Shrinkage strain in M50 concretes (a) Cylindrical specimens and (b) Prismatic specimens

Figure 8.8 Shrinkage strain in equivalent binder content and w/b concretes (a) Cylindrical specimens and (b) Prismatic specimens

The measured shrinkage strains and the prediction by existing shrinkage models are summarized in table 8.1. From the results, it can be seen that the shrinkage strains predicted by B4 model (Bažant 2015) were nearly consistent with the experimental observation for the three binder systems (except for LC[3]- M50). FA30 mixes had a higher deviation from the predictions with ACI model (ACI 209R-92 1997) and FIB - Model code (Fédération Internationale du Béton 2010) in all the cases. The deviations were comparatively less in LC[3] than FA30 concrete mixes in equivalent strength category. This is mainly due to the lower water-binder ratio opted for FA30 mixes to achieve the target 28 day strength. In the case of C-mix, B4 model could give a closer prediction to the experimental values with the three binder systems.

To explain the difference in the shrinkage performance observed in the three binder systems, the evolution of the total shrinkage strain is plotted against the mass loss observed (as weight loss %) in figure 8.9. It is noted that the maximum weight loss (%), at the drying period of 400 days, was higher in the prismatic specimens than cylindrical specimens. The prismatic specimens have a greater surface area (per unit volume) leading to faster rate of weight loss in these specimens. However, the observed

shrinkage strains were similar (or marginally lower in cylindrical specimens) between both the specimens.

Table 8.1 Comparison of experimentally measured shrinkage with available models

Concrete grade			M30			M50			C-Mix		
Binder			OPC	FA30	LC^3	OPC	FA30	LC^3	OPC	FA30	LC^3
Shrinkage (microstrain) at (1 year)		Cylindrical specimens	450	430	490	450	330	520	390	380	430
		Prismatic specimens	500	450	490	470	330	540	420	420	430
	B4 Model	Cylinders	410 (-40)	370 (-60)	410 (-80)	390 (- 60)	380 (+ 50)	360 (-160)	430 (+ 40)	410 (+ 30)	430 (0)
		Prisms	430 (-70)	390 (- 60)	430 (-60)	410 (-60)	400 (+ 70)	380 (-160)	460 (+40)	420 (0)	450 (+ 20)
	ACI model	Cylinders	440 (-10)	440 (+10)	430 (- 60)	450 (0)	480 (+150)	470 (- 50)	450 (+60)	450 (+ 70)	470 (+ 40)
		Prisms	500 (0)	500 (+50)	480 (-10)	500 (-60)	545 (+215)	520 (- 20)	500 (+ 80)	500 (+ 80)	530 (+ 100)
	CEB Fib 2010 model	Cylinders	471 (+ 20)	520 (+ 90)	490 (0)	450 (0)	440 (+ 110)	450 (- 70)	480 (+ 90)	490 (+ 110)	460 (+ 30)
		Prisms	540 (+ 40)	600 (+ 150)	560 (+ 70)	510 (+ 40)	500 (+ 170)	510 (- 30)	550 (+ 130)	560 (+ 140)	530 (+ 100)

Note: The values in the parenthesis indicate the difference between the experimental and predicted shrinkage strain.
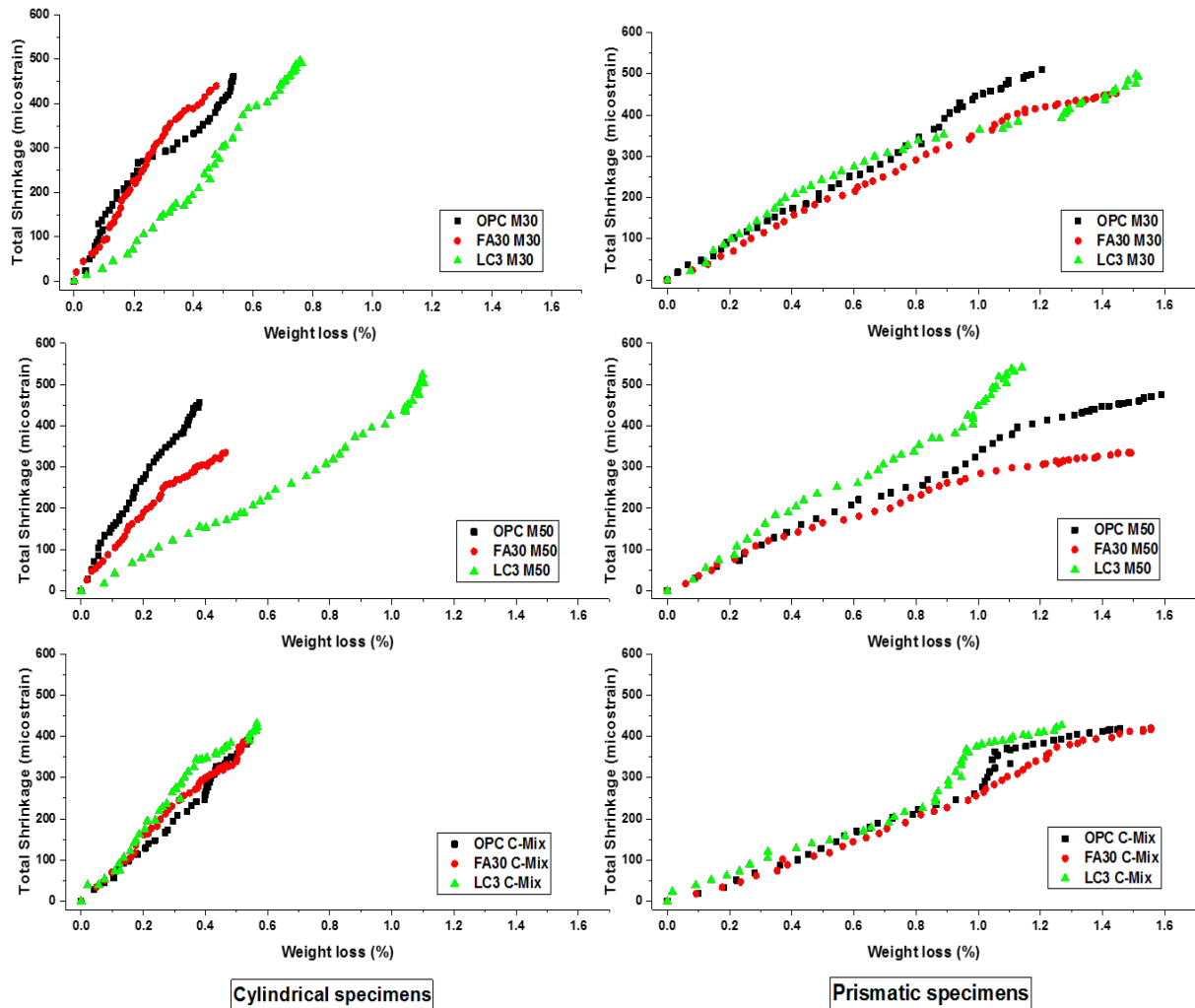
Figure 8.9: Relationship between Total shrinkage and Weight loss (%) for the different binder systems (Mass losses in the prismatic specimens are higher due to higher surface area)

In the case of cylindrical specimens, the ultimate weight loss is higher due to higher water-binder ratio and lower binder content in M30 and M50 concrete mixes of LC^3 than OPC and FA30. This confirms that the amount of free water predominantly affects the shrinkage development in the equivalent grade concretes mixes, despite the variation in the capillary pressure (which leads to shrinkage) due to difference in the pore sizes. Results also suggest that for the same extent of moisture loss, LC^3 binders showed lesser shrinkage at an equivalent strength level. However, the concrete made with similar mixture proportion shows that the mechanism of shrinkage development due to loss of moisture can be similar between concretes made with the three binder systems.

The results of the prismatic specimens suggest that drying was marginally higher for the LC^3 concretes in all the categories, which in turn, results in higher shrinkage strain of the LC^3 as observed in table 8.1.

8.5 Influence of Curing Conditions on Strength Development

Curing temperature is one of the critical factors that determine the early and later age performance of cement-based construction materials. In real field conditions, the curing temperature differs from the normal laboratory conditions significantly. The construction industry often uses various heat curing methods for maintaining the project schedule. Due to global warming, the rise in atmospheric temperature is also a concern, especially in tropical countries. During mass concreting, the

temperature of the fresh concrete often rises due to the heat evolution from cement hydration. Hence, it is imperative to understand how the temperature and time of exposure influence the performance of cement.

In general, the increase in temperature accelerates the cement hydration and subsequently increases the early age strength. However, it is observed that the high temperature curing adversely affects the later age performance (Kim et al. 1998; Saul 1951). Although the ultimate degree of hydration (DoH) of clinker is found to be independent of curing temperature (within 5°C to 60°C), the density of the main hydration product, C-S-H increases with temperature which subsequently increases the porosity of the microstructure that leads to reduction in strength (Escalante-García and Sharp 2001; Gallucci et al. 2013). The temperature regime also has a significant impact on the performance of the blend (Sajedi 2012; Zhang 2007).

Hydration of cement requires water for the hydration reactions to take place. The process of curing ensures the presence of water in the system during the hydration process, by providing moisture externally or stopping evaporation of water from the specimen. Generally, the rate of hydration is high at early ages and then decreases, making the early age critical from the curing point of view. The curing requirement may be different for different types of cement. It is expected that cements with high early age strength demand a high amount of water. Ternary cements using alternative raw materials may influence the curing requirements. Many studies have shown that the effect of curing conditions is more influential on blended cements. A study on fly ash based cement indicated that effect of curing depends on physical and chemical properties of clinker and w/b ratio rather than that of fly ash properties and replacement factor (Termkhajornkit et al. 2006).

In this study, the effect of curing temperature and relative humidity were tested for LC^3 and compared to that of OPC, FA30 and composite cement (CC).

8.5.1 Materials
Raw materials for this study (clinker, calcined clay, limestone, fly ash, slag and gypsum) were procured and ground individually in a laboratory ball mill. The particle size distribution of the raw materials is shown in figure 8.10. The blends were prepared by interblending the ground raw materials in a turbo blender. The composition of the blends is shown in Table. Three different temperatures: 10°C, 27°C and 50°C were selected for the experiment.
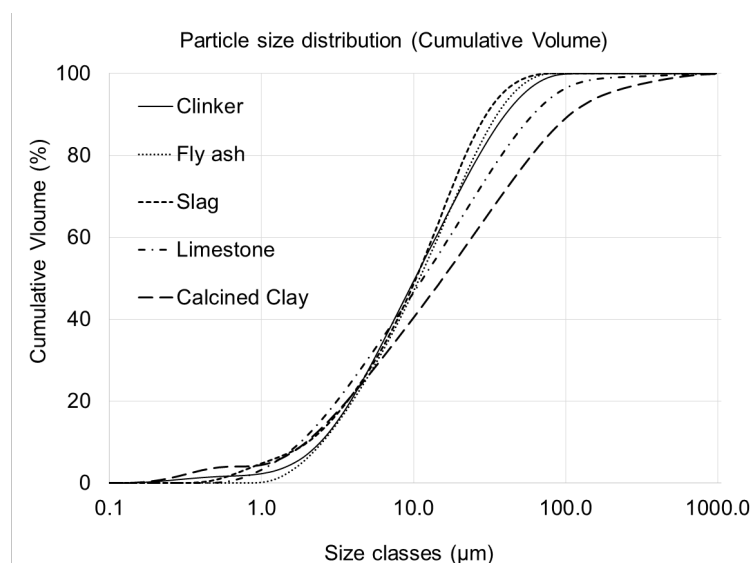

Figure 8.10: The particle size distribution of raw materials

Table 8.2. The raw material composition of blends (weight %)

Blend	Clinker	Fly ash	Slag	Calcined Clay	Limestone	Gypsum
OPC	50	-	45	-	-	5
FA30	65	30	-	-	-	5
LC^3	50	-	-	30	15	5
CC	50	15	30	-	-	5

8.5.2 Methods

Isothermal calorimetry

Rate of heat evolution was measured using isothermal conduction calorimetry. Before the start of the experiment, materials, and accessories: the dry blend, deionised water, calorimetric cups, mixing cups, spoons were preconditioned by placing the samples inside a temperature-controlled chambers set at the required temperature for 24 hours. A fresh paste of blends was prepared by thoroughly with water for three minutes using a paste mixer. The mixed paste was then weighed in calorimetric cups up to 72.5 gms and placed in an I-Cal HPC-2000 from Calmetrix. The same weight of dry powder (50gm) with constant water to binder ratio of 0.45 was used for all the calorimetric experiments.

Mercury Intrusion Porosimetry (MIP)

MIP was performed using Thermo Fischer Pascal 440 porosimeter. At the age of testing, i.e. 28 days in this study, the paste slice samples were immersed in isopropanol for 5 days and then stored in a vacuum desiccator till 28 days. About 1.5 to 2 grams of samples were cut from the slices after removing the edges. MIP was carried out by measuring the volume of mercury intruded in the specimen as the pressure was incrementally increased to 400 MPa. A contact angle of 120 degree assumed for the calculation of overall porosity and pore entry diameter. The total percolated pore volume (total/overall porosity) represents the total accessible pore volume at 400 MPa applied pressure and critical pore-entry diameter is the pore size where steepest slope of the cumulative intrusion curve is recorded.

Mortar compressive strength

Mortar cubes of 70.6 mm size were prepared, cast and tested as per Bureau of Indian Standards (IS: 4031 (Part 6) 1988). Indian standard sand (IS: 650 1991) was used for making the mix at a sand to cement ratio of 1:3. The water to cement ratio was kept constant at 0.45. The materials (blend, standard sand, and distilled water) were preconditioned at the specified temperature for 24 hours before casting. The specimens were placed in an environmental chamber immediately after casting for one day, followed by demoulding the specimens and cured in lime saturated water in a temperature-controlled water bath till the time of testing. Cubes were also cured at different temperature regimes by shifting the specimens at 1 and 3 days from 27 to 50°C based on required temperature regimes. The strength test was performed in a compression testing machine of capacity 500kN with a loading rate of 2.40kN/s. Average compressive strength of 3 cubes was considered for representation.

8.5.3 Results

Influence of temperature on hydration kinetics

Heat flow curve was obtained by plotting thermal power as a function of time and expressed as milli-watt per unit weight of the binder. Total heat was calculated from heat flow curve by integrating thermal power with time from the dormant period and expressed as Joule per unit weight of binder. The heat generation till dormant period was not considered since it is predominantly from initial dissolution. Heat flow vs time was plotted for the blends and the cumulative heat released was plotted against time after omitting heat till dormant period.
 (see figure 8.11 to 8.13).
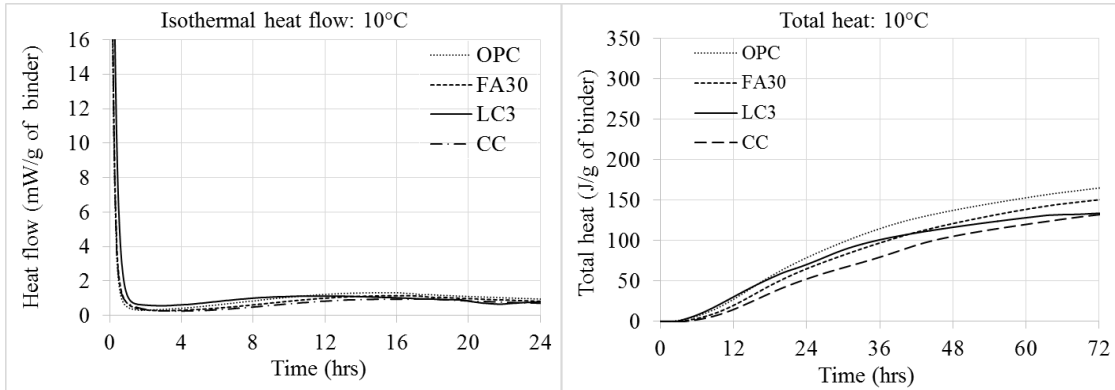
Figure 8.11: Isothermal heat flow and total heat of hydration of blends at 10°C
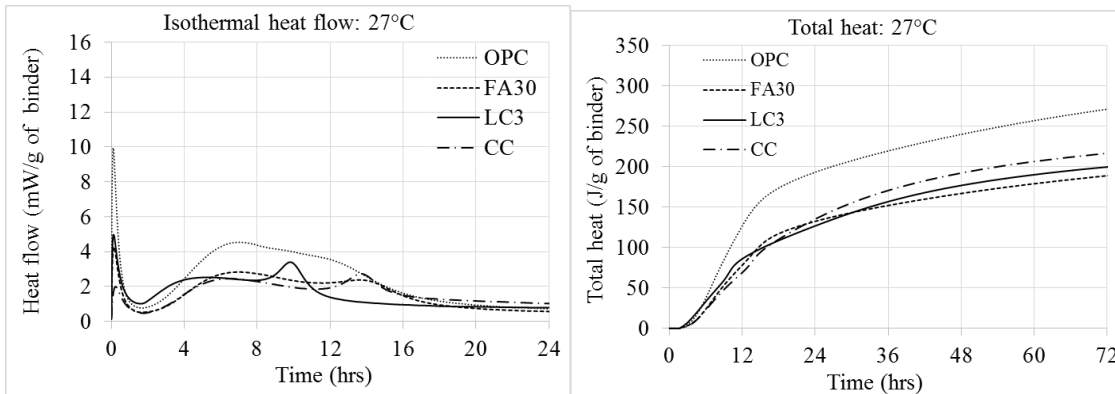
Figure 8.12: Isothermal heat flow and total heat of hydration of blends at 27°C
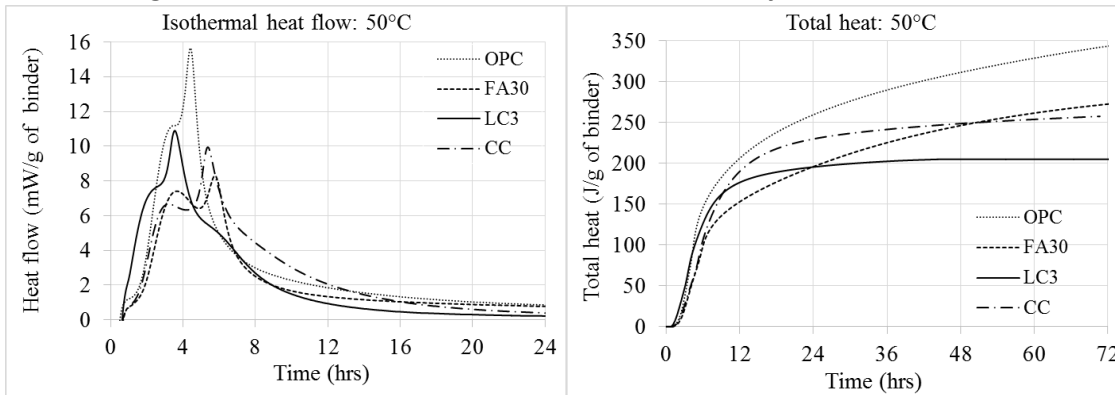

**Figure 8.13: Isothermal heat flow and total heat of hydration of blends at 50°C**

Isothermal heat flow and total heat of hydration of blends cured at 10 °C (Figure) show a much lower rate of hydration at this temperature when compared with 27 °C and 50 °C. It is difficult to distinguish between the silicate and aluminate peak at this temperature. The heat of hydration of OPC is higher than that of blended cements. However, the difference is not very significant.

The calorimetric curves for the samples cured at 27°C are shown in Figure. Although the clinker content in the blended cements is approximately half that of OPC, the hydration of LC³ systems was found to be faster and the induction period was shorter as compared to OPC and CC systems. In OPC, acceleration started at around 2 hours, and in LC³, it started around 1 hour 30 minutes. This can be attributed to the high alumina content in the clay. Whereas in CC, the acceleration was found to start later than OPC and the peak hydration was lower than OPC, mainly due to lower clinker content and slow pozzolanic activity of both slag and fly ash. A clear aluminate hydration peak was visible in both blended systems, with calcined clay and slag contributing to aluminates in the solution. It can

119

be seen in the LC³ blends that the addition of gypsum delays the onset of this peak; however, this appears to have little influence on the hydration after 24 hours.

The calorimetry curves at 50°C curing (Figure) emphasises that the heat of hydration increases significantly with the increase in temperature. Unlike at 27˚C, the peak corresponding to aluminate hydration was clearly visible in the OPC system at this temperature. In LC³, there appears to be an acceleration in the formation of ettringite and also its conversion to monosulphate, visible as a shoulder after the aluminate peak. It can be observed that, when cured at 50˚C, there is very little additional heat of hydration in the LC³ and CC systems after 24 hours of hydration, probably, leading to a substantial reduction in the rate of clinker hydration after one day.

Influence of temperature of porosity and pore size distribution
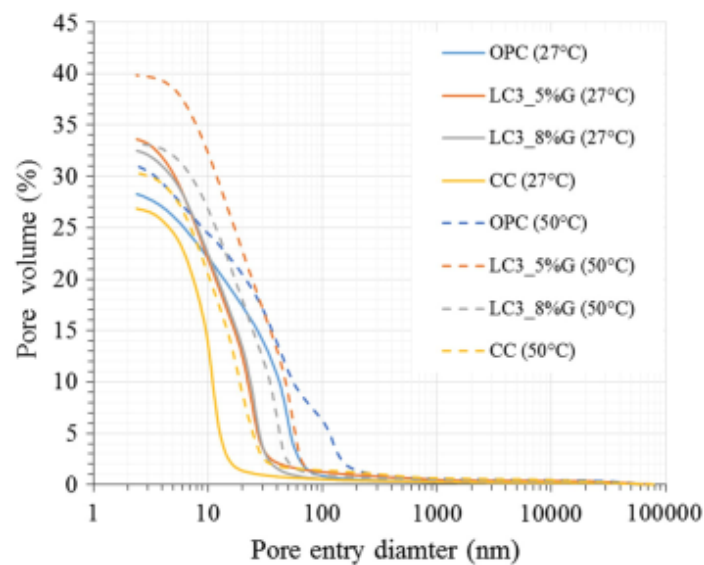
Figure 8.14: Porosity graph for different blends cured at 27 and 50℃ at 28 days

Figure 8.14 shows how the temperature influences the pore structure of hydrated cement paste at 28 days using mercury intrusion porosimetry. With increase in curing temperature from 27 to 50℃, an increase in total pore volume for all types of blends can be from the peak value on y axis. Although increase in volume for CC and OPC blend is not as much as for LC³ with 5 percent gypsum content. However, with addition of gypsum in LC³ a decrease in increased total pore volume had been observed due to increased formation of ettringite. Additionally, it can be observed that the threshold pore diameter increase due to temperature rise is more in OPC and CC blends as compared with the LC³ blends. Similar results have been observed by Hanpongpun and Scrivener, 2020 although temperature difference was not much high, Figure 8.15. These coarser pores are known to affect the compressive strength at later ages since the hydration of the clinker and pozzolanic reaction are promoted since early age of hydration.
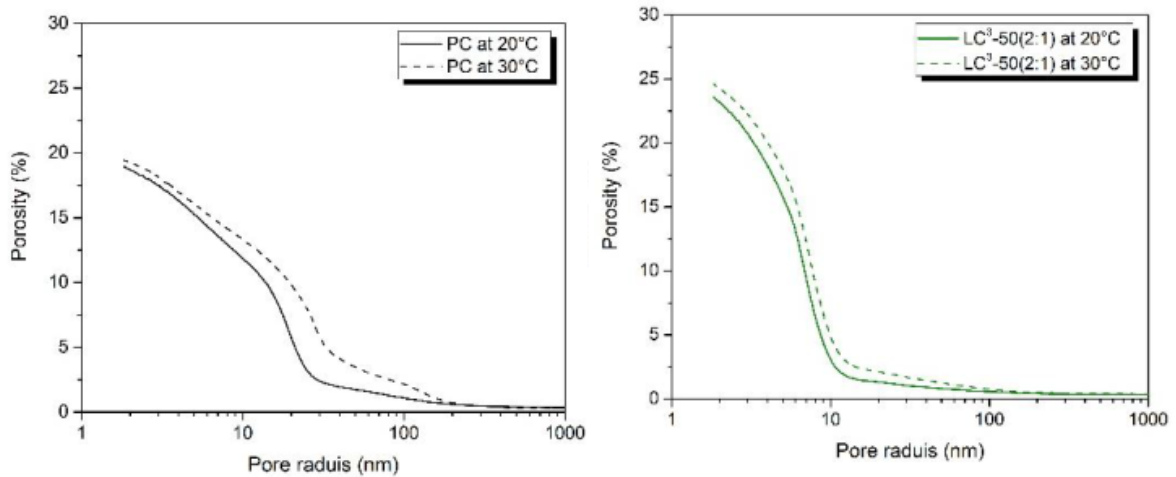
Figure 8.15: Pore size distribution of PC and LC3 cured at 20 and 30℃ for 28 days (Hanpongpun and Scrivener, 2020)

Influence of temperature on compressive strength

Figure 8.16 shows the compressive strength of the mortar cubes of LC³, OPC, FA30 and calcined clay cured at 10 °C, 27 °C and 50 °C up till 90 days. The performance of LC³ at 10°C at 90 days was found significantly higher than other blended cements and is comparable to that of OPC. However, when the curing temperature is increased from 27°C to 50°C, a reduction in the strength of mortars was observed (except FA30). This reduction in strength is the least in OPC, while it is the highest in LC³. Although the increase in gypsum content slows down the strength development at 27 °C, the strength at 50°C is higher than the blend with 5% gypsum as shown in Figure . The strength gain observed after three days in all the low clinker blends is insignificant when cured at 50 °C except fly-ash blend.
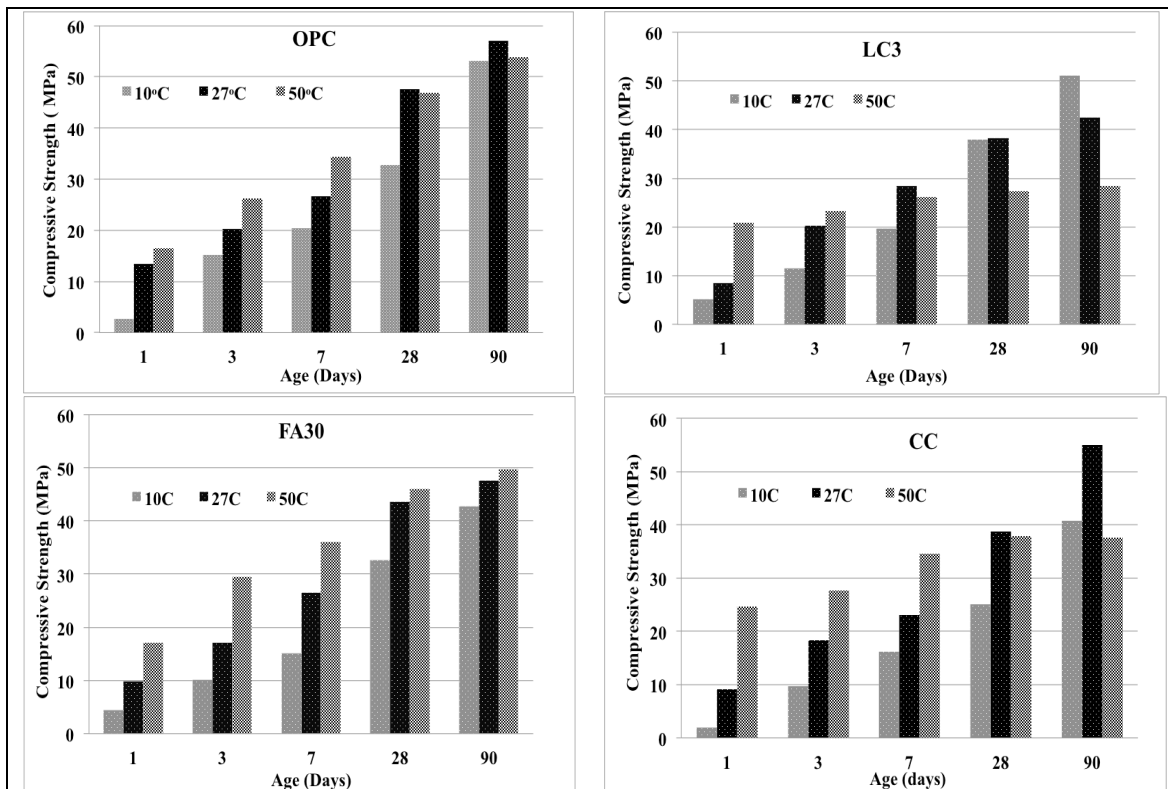
Figure 8.16: The compressive strength of LC³, OPC, FA30 and CC at different temperature
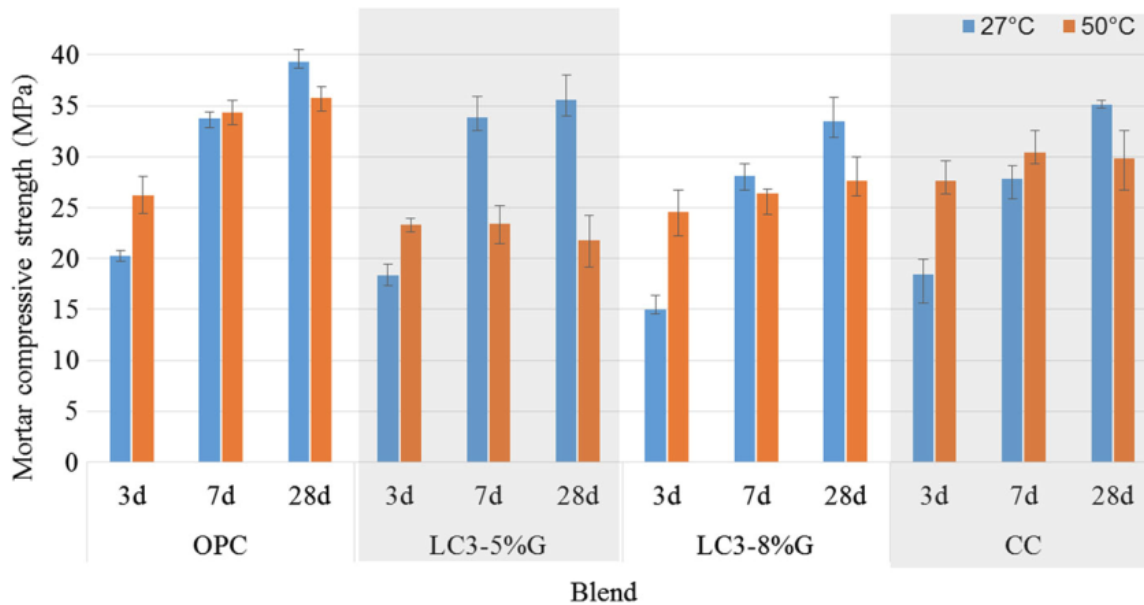
Figure 8.17: Compressive strength of mortars cured at different temperatures. (Mishra et al. 2019)

Influence of temperature regime on the performance of LC³

The influence of temperature regime on LC³ was studied using two temperatures: 27 °C and 50 °C. The performance of LC³ was compared to that of CC at different temperature regimes. OPC and FA30 were avoided in this study as it was observed that the influence of temperature on final strength was lower in both these cases. The temperature regimes considered in this study is shown in table 8.3. 28 days compressive strength of mortar samples exposed at at different temperature regimes for both the blends are compared in Figure.

Table 8.3: Temperature regimes for the specimens

Temperature regime	Notations
Samples cured at 50°C till 28 days	h28
Samples cured at 27°C for one day and exposed to 50°C till 28 days	m1.h28
Samples cured at 27°C for three days and exposed to 50°C till 28 days	m3.h28
Samples cured at 27°C till 28 days	m28
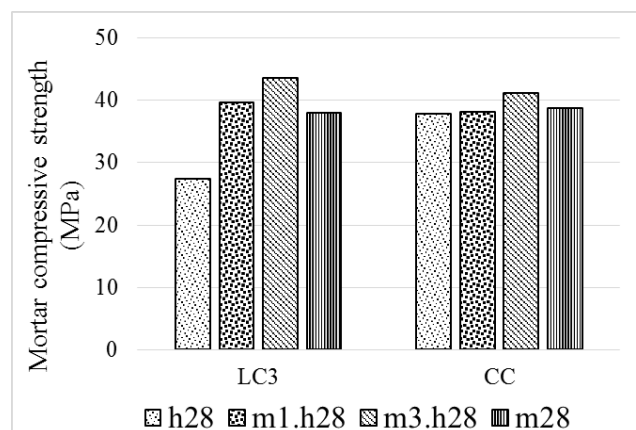
Figure 8.18: 28 days mortar compressive strength of blends cured at different temperature regimes

Though the strength of LC³ cured isothermally at 27 °C has shown similar performance to that of CC, the samples exposed to 50 °C isothermal condition observed a significant reduction in 28 days

122

compressive strength. However, it can be seen that by delaying the exposure to higher temperature by one day or further could potentially improve the 28-day compressive strength of LC^3.

Influence of short-term heat curing on the performance of LC^3

Recently, Vaasudeva et al. 2021 compared the LC^3 concrete subjected to short term heat curing and compared it with the Portland cement and fly-ash based binder at water to binder ratio of 0.4 and 0.45. Curing regime adopted in the study is given in figure 8.19. After 24 hrs specimens were demoulded and placed in moist curing room at 27℃ and 95-100% relative humidity until respective age of testing.

1 – Precuring at ambient temperature
2 – Specimen moved to steam condition
3 – Maximum temperature of heat curing (60°C)
4 – Specimen cooling period
5 – Ambient conditioning duration
6 – Demoulded for ambient curing (or) 24 hour testing
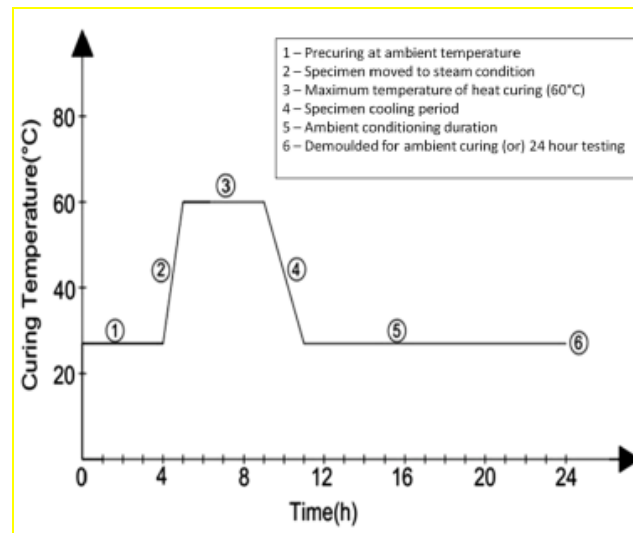
Figure 8.19: Steam curing regime followed in study performed by Vaasudevaa et al. 2021

LC^3 have been observed to show a similar improvement in strength as of OPC after the short-term heat treatment. Increase in LC^3 strength is for two reasons: i) Acceleration of the clinker reaction at the higher elevated temperature, and ii) Enhancement in the reactivity of calcined clay at elevated temperature curing at early age. 1 day strength gain observed is higher for higher water to binder ratio. LC^3 have been observed to show better strength at all ages as compared to 30% fly-ash replaced steam cured concrete at both w/b.

Early age strength development of concrete with LC^2 admixture and improved performance of LC^3 systems subjected to steam curing could be advantageous for the adoption of sustainable binder systems in applications of high early strength requirements where other conventional SCMs like fly ash may not be suitable. This also suggests the suitability of using LC^3 in precast manufacturing plants to satisfy the early-age compressive strength requirements.
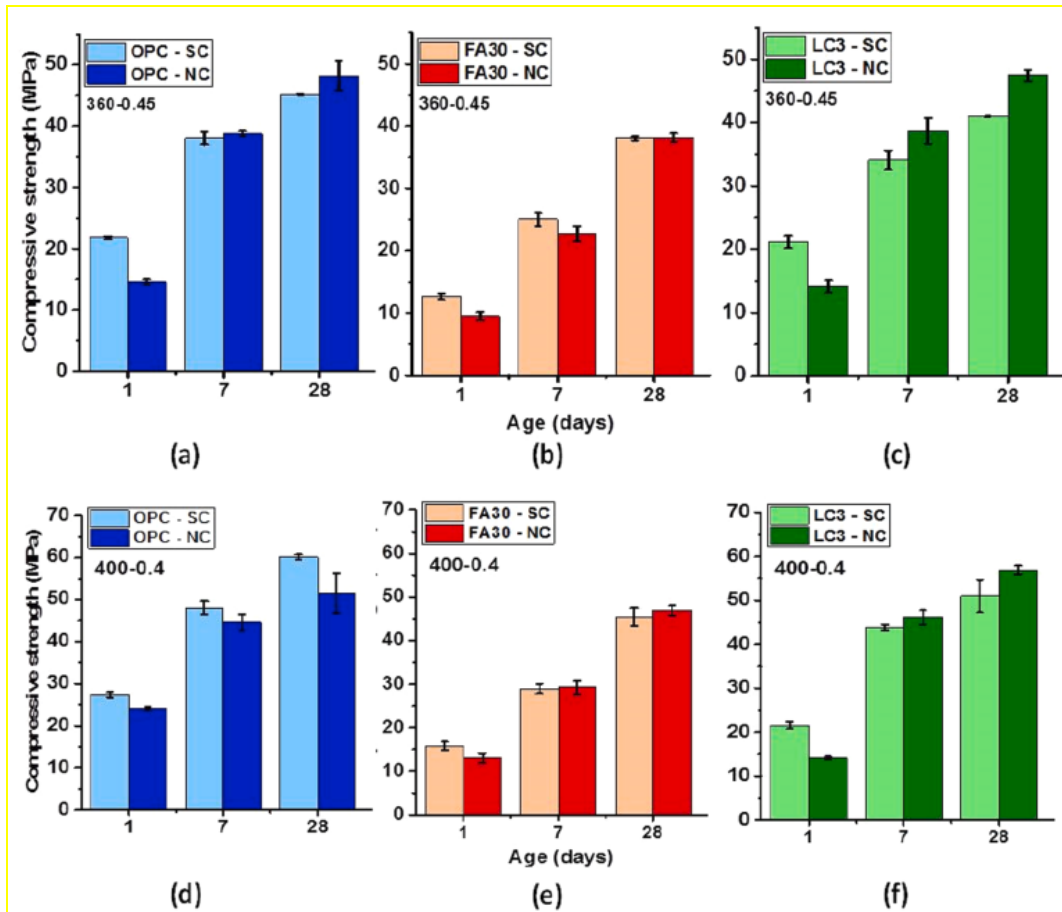
Figure 8.20: Compressive strength of concrete under steam cured and normal cured (NC) concrete conditions

Effect of relative humidity (RH)

Specimens were cured at different humidity regimes at standard temperature (27 °C). Two RH conditions were used to construct the regimes: A higher RH of 100% (HH) and a lower RH of 10-20% (LH) were considered in this study. Curing regimes and respective notations are given in Table 0-1. The compressive strength of LC[3], OPC, FA30 and CC at RH conditions is shown in Figure.

Table 0-1. Curing regime and their respective notations

Curing regime	Notation
Specimen cured in HH	HH
Specimen cured in HH till 3 days and shifted to LH after 3 days	HH(3d)_LH
Specimen cured in HH till 7 days and shifted to LH after 7 days	HH(7d)_LH
Specimen cured in LH	LH
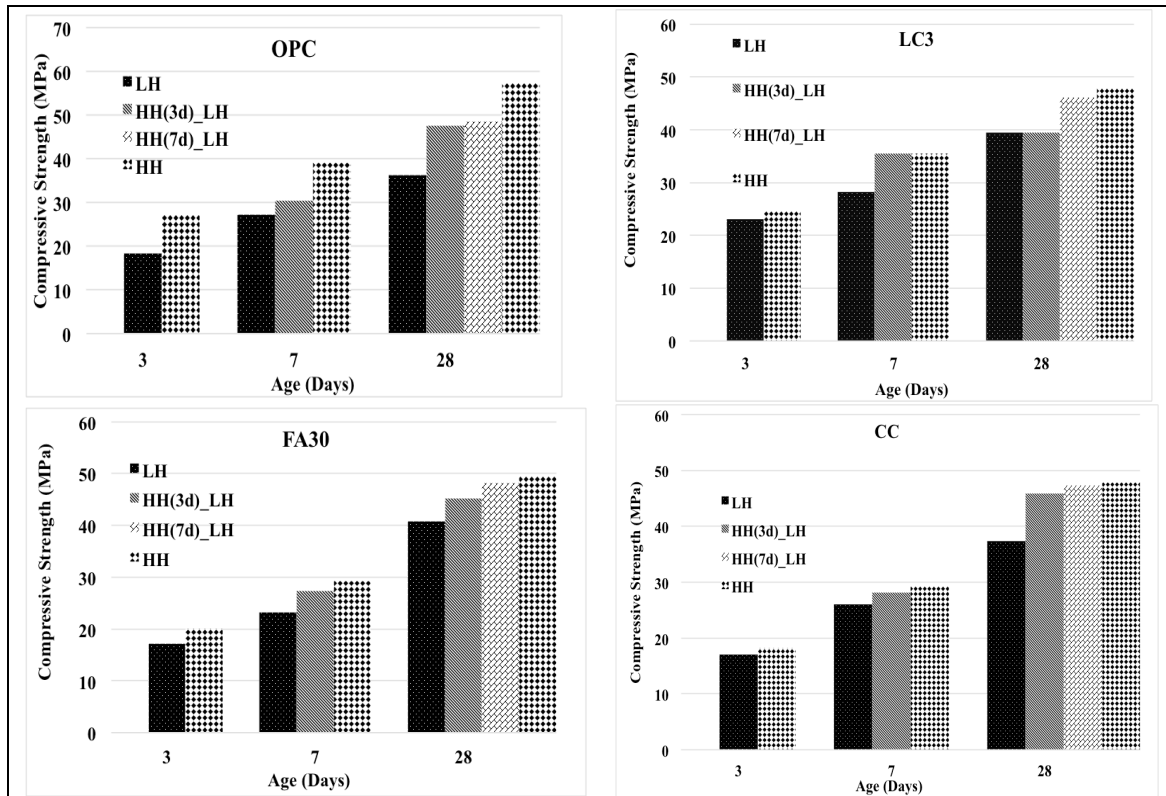
Figure 8.21: The compressive strength of LC³, OPC, FA30 and CC at RH conditions

Phung et al. 2021 performed a curing sensitivity tests on the multi-binder systems which consist of cement (OPC), calcined clay (CC), fly ash (FA), and limestone powder (LP). Three series of mortar with different water to binder ratios by weight (w/b) of 0.35 and 0.55 and different paste ratios of 1.2 and 1.4 were produced for testing compressive strength. The specimens of each binder system were put under two conditions of curing water curing (water-cured) and no curing (air-cured at temperature and RH of 28 ± 2°C and 80 ± 5%, respectively) after demoulding. To compare different mixes curing sensitivity, curing sensitivity index (CSI_{fc',t}) was used as the parameter, which was calculated as:

$$CSI_{fc,t} = \frac{(fc'(t)_{WC} + fc'(t)_{NC})}{fc(t)_{WC}} \times 100\%$$

where, where fc'(t)WC and fc'(t)NC are the compressive strengths of water-cured and no-cured (or air-cured) specimens at t days of ages, respectively.

Figure 8.22: Curing sensitivity index for test mortars with different paste content a) CSI_{fc} at 28 days, and b) CSI_{fc} at 91days

Figure 8.23: Curing sensitivity index for test mortars with different w/b a) CSI_{fc} at 28 days, and b) CSI_{fc} at 91days

Numbering value before the notation for SCM used, specify the percentage of replacement by that SCM in figures 8.22 and 8.23. Blends with calcined clay, and limestone had been observed to show lower low curin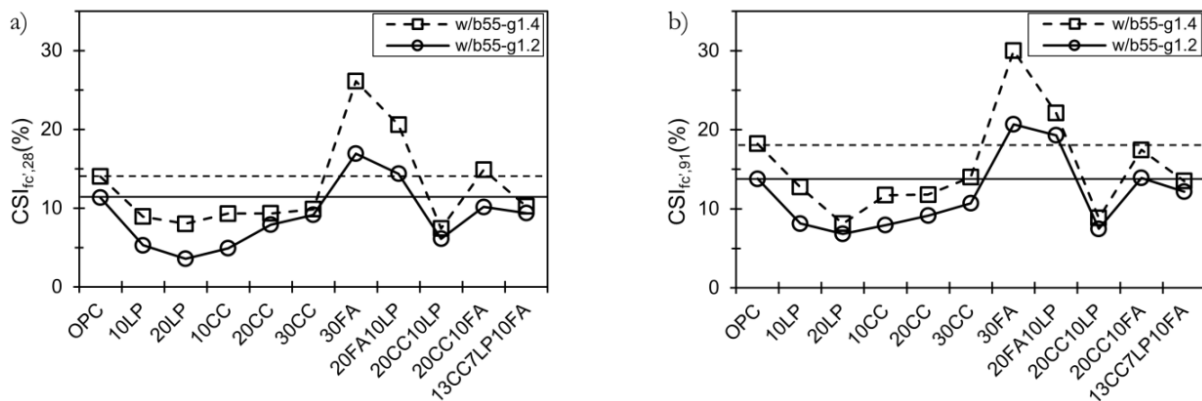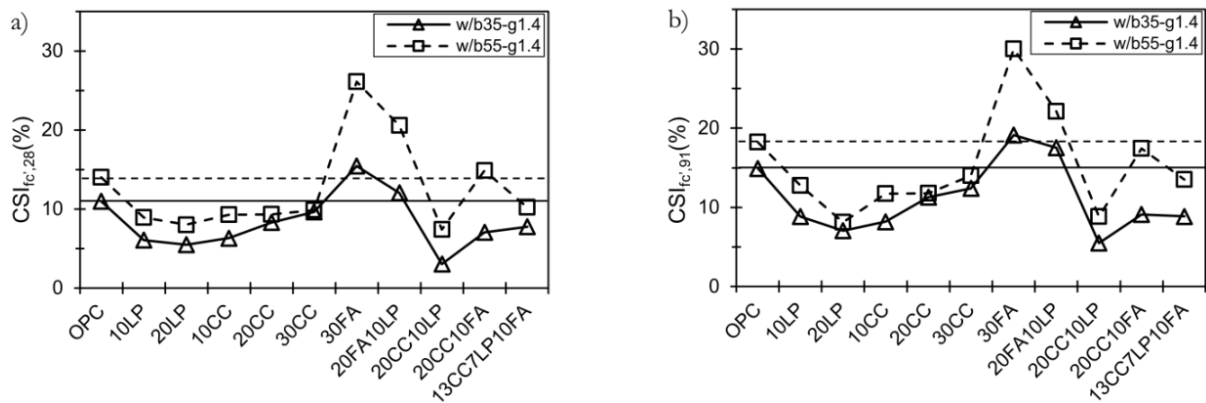g sensitivity index. Least curing sensitivity index had been observed for the LC^3 blend where calcined clay and limestone are used as combination. This effect is attributed to the fast reaction of calcined clay at early age and filler effect of the limestone which accelerate the initial hydration of the cement.

Influence of fineness of clinker on strength development at higher temperatures
Recent results, shown in figure 8.24 below, show that the potential negative effect of high temperature curing on strength development can be overcome by having a sufficiently fine clinker in LC^3. In this figure, cement has been produced by grinding the same clinker for 3000, 6000 and 9000 rotations in a laboratory ball mill. The results show that the strength development is much higher with the finer clinker phase. This indicates that it is important for the clinker phases to hydrate before a rapid hydration of calcined clay starts.
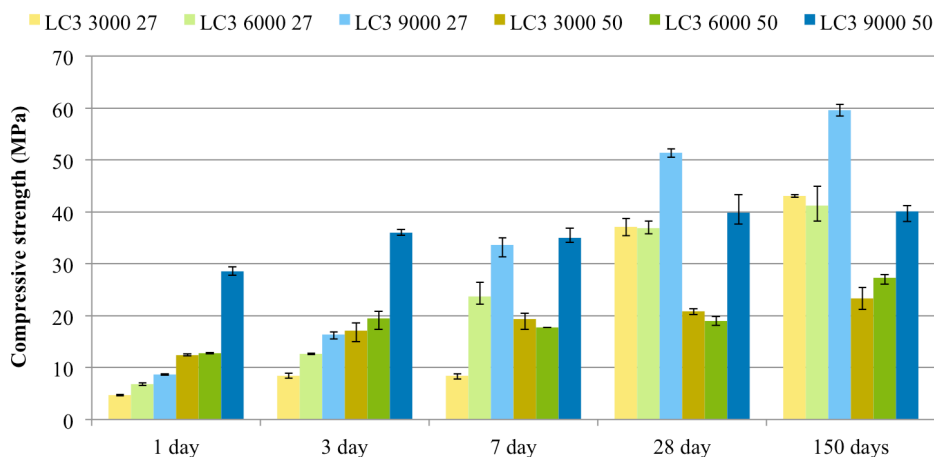
Figure 8.24: Influence of fineness of clinker on strength development in LC^3 containing clinker of various fineness.

8.6 Summary
- At lower temperatures, the early age strength of LC^3 (3 day) is better than other blended cements studied. Moreover, LC^3 shows comparable later age strength development to that of OPC and significantly higher strength than FA30 and CC.
- High-temperature curing increases the early age strength of all the blends. For both LC^3 and CC, high-temperature curing reduces the later age strength. However, one day delay in exposure at

high temperature could potentially improve the adverse effect of high temperature curing for LC^3. Better results are expected when LC^3 is produced in an industrial ball mill.

- Short-term heat curing of LC^3 study suggests the suitability for early precast manufacturing plants to satisfy the early-age compressive strength requirements.
- Relative humidity at early ages influences the performance of all the systems. However, all the blended cement showed lesser influence on compressive strength than OPC at different curing conditions. Additionally, blends where combination of limestone and calcined clay had been used, curing sensitivity index has been observed to be very low.
- The effect of high temperature on strength development can be overcome by properly grinding the clinker in LC^3 to a sufficiently fine level.

Chapter 9: Durability

After understanding the LC³ hydration and microstructure development, this chapter provides a discussion on effect of altered hydration products on the durability of the LC³ concrete. Starting with the pore structure characteristics of LC³ and its influence on the transport properties such as oxygen permeability, water absorption, and resistivity, this chapter explores performance of LC³ concrete when exposed to various environmental conditions such as carbonation, chlorides, sulphates, and alkali-silica. Since LC³ is a relatively new developed cement, field data on the long-term performance of concrete using the cement is not available. Therefore, results from microstructural analysis and accelerated tests are used to assess the expected durability performance of the cement.

9.1 Porosity and Pore Structure

Pore size distribution in hardened cement paste is very wide ranging from 1nm to 1 cm, i.e., seven orders of magnitude. As per Mindness et al. 2002, pores are classified as interlayers spaces (< 2.5 nm), gel pores (2.5 - 10 nm), capillary pores (10 nm to 10 µm) and air voids (10 µm up to few mm). Pore structure and porosity of concrete plays a significant role on its durability properties. For pore characterization, commonly used parameters in cementitious materials are, permeable pore volume (total porosity), critical pore size and threshold pore size. Commonly used pore characterization techniques include mercury intrusion porosimetry (MIP), nuclear magnetic resonance (NMR), vacuum saturation, gas adsorption, etc.
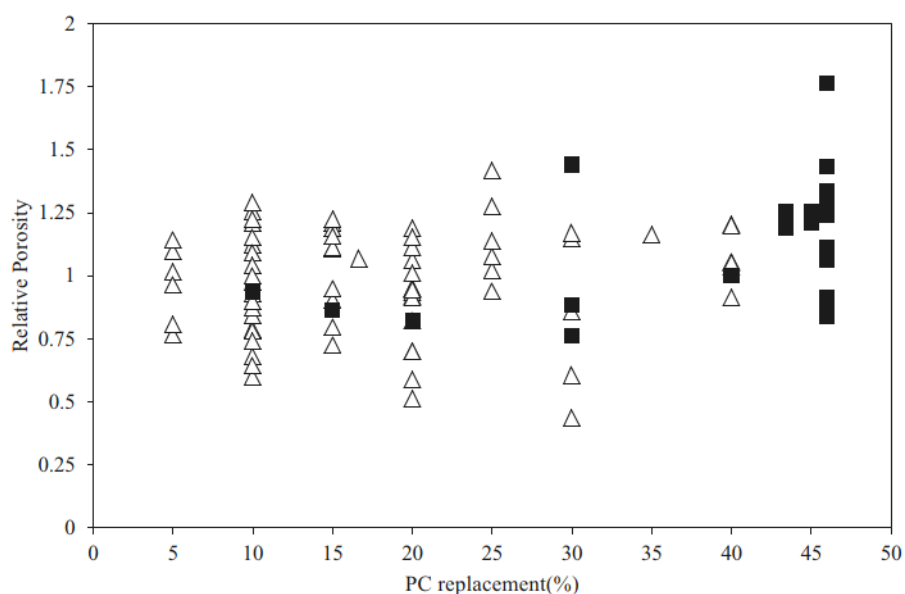
Figure 9.1: Relative porosity of cementitious system with changing calcined clay + limestone replacement level. (triangles – OPC + Calcined clay, squares – OPC + Limestone + Calcined clay) (Dhandapani et al. 2022)

In literature, there are conflicting results regarding the effect of limestone calcined clay combination on the porosity, some researchers have reported the lower porosity while many others have reported higher porosity, see figure 9.1. It can be concluded from graph that total porosity isn't sufficient parameter to understand overall impact on durability and transport properties of LC³ concrete.

Significant refinement in the pore structure of cement paste at early age in blended cements with calcined clays has been observed (Jiang et al. 2015, Tironi et al. 2014, 2015) due to fineness of clay and rapid pozzolanic reaction. In figure 9.2, it can be observed that the critical pore size entry of OPC is lower than all the LC³ blends. By 2 days already the critical pore size of high purity clay MK95 has

reduced significantly due to early formation of the hemi and mono carbo-aluminates formation. At 3 days, clays with purity more than 60% are already showing critical pore diameter smaller than OPC and others are tending towards it. By end of 7 days, all the LC³ systems have smaller critical pore size than its counter OPC.
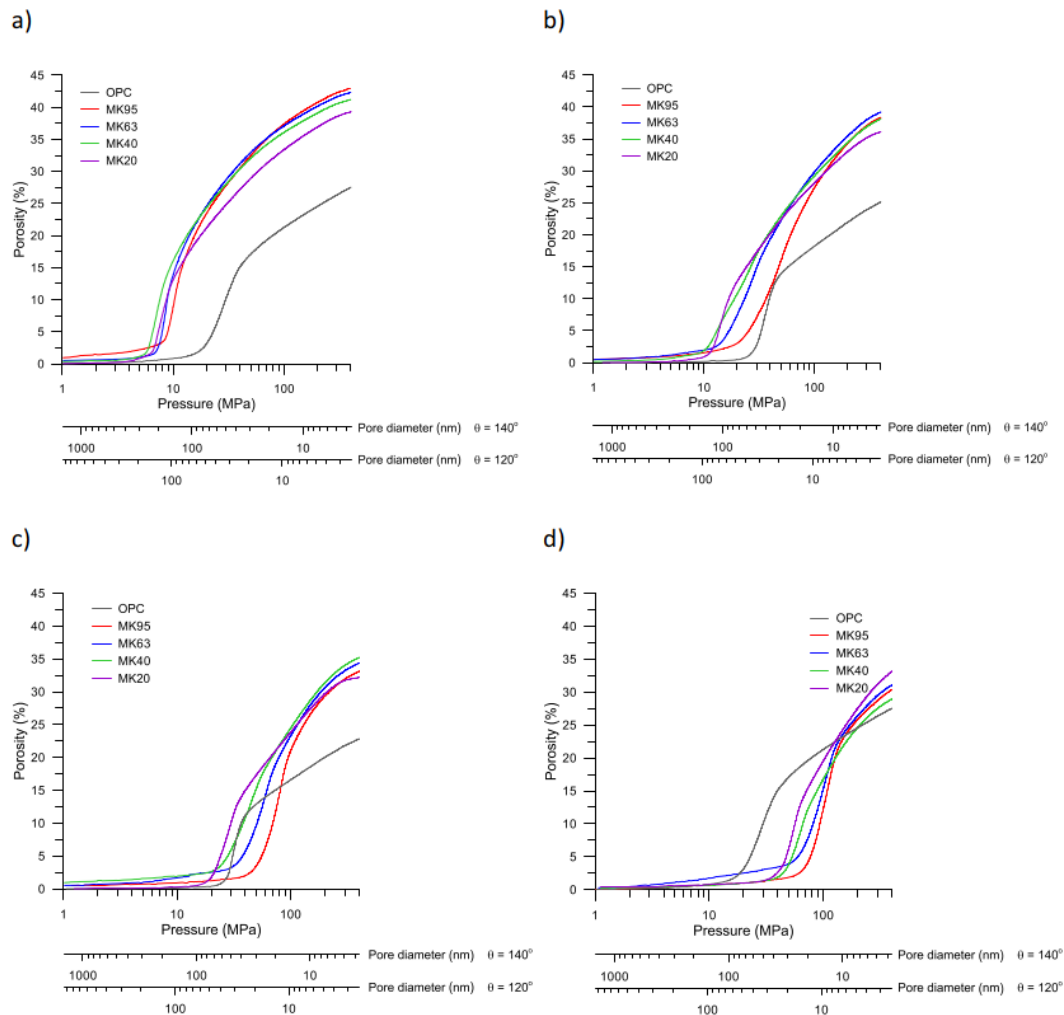
Figure 9.2: Total porosity verses applied pressure measured by MIP on OPC and LC³ with different grade of clay after a) 1, b) 2, c) 3 and d) 7 days of hydration. (Zunino and Scrivener 2021).

In another study pore structure characteristics of OPC, fly ash based PPC, and LC³ systems were studied by Dhandapani and Santhanam (2017), where a clear reduction in the volume of finer pores (<1µm) was observed in LC3 systems at early ages (Figure 9.3). Rate of this pore refinement in LC³ is dependent on the grade of calcined clay that is used. If a calcined clay with more than 65% kaolinite content is used, the critical threshold porosity is achieved by 3 days. There is a significant pore refinement between 3 and 28 days if the kaolinite content of the calcined clay is less than 50% (Avet and Scrivener 2018). LC³ systems well-defined pore structure at early age is important from the point of view of strength development and durability characteristics as well.
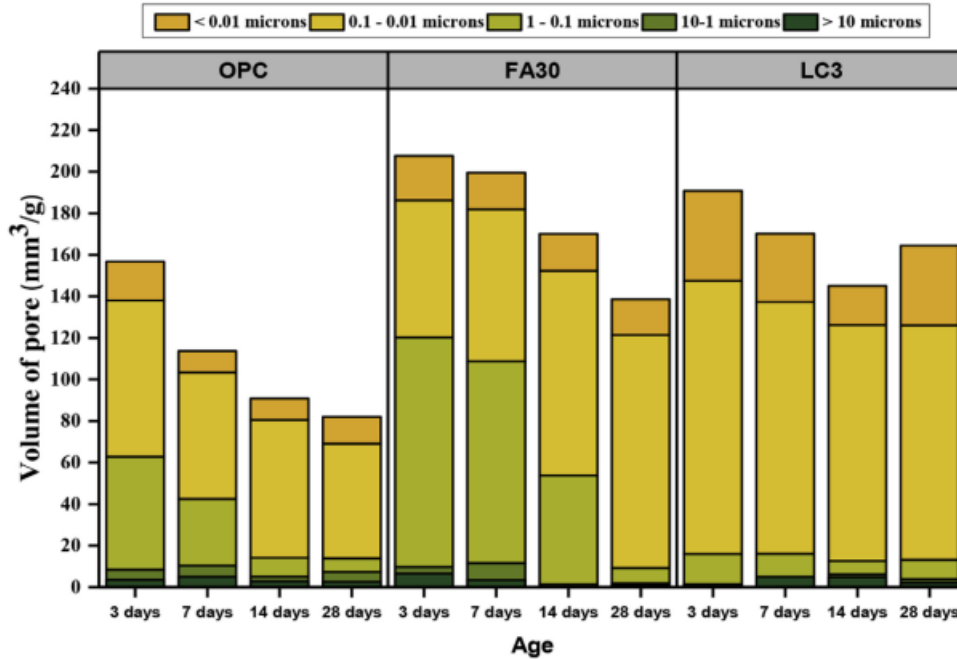
Figure 9.3 Comparison of total porosity in OPC, FA30 and LC3 systems (Dhandapani and Santhanam 2017).

9.1.1 Transport properties

Gases like oxygen, carbon dioxide, etc. and liquids like water with dissolved ions like chlorides, sulphates, etc can penetrate through its connected pore network. Phenomena which result in degradation and deterioration of reinforced concrete depend on the processes which allows the transport of moisture, sulphate and chloride ions, carbon dioxide, oxygen, charged ions, etc within the concrete. Transport mechanism of these species can happen as per four basic mechanisms: capillary suction – due to capillary pressure from connected capillary pores in concrete, permeation – due to flow under pressure gradients, diffusion – due to concentration gradient of species, and migration – due to electrical potential gradients. Diffusion, permeation, and capillary absorption are major transport mechanism. Discussion on the performance of LC^3 systems related to these transport mechanisms is given below.

9.1.2 Water sorptivity

Under environment where frequent saturation or splashing of water on concrete surface happens, absorption of water is predominant transport mechanism. Water absorption is governed by capillary pores and connectivity of the pores in the system. Positive impact of pore refinement with limestone calcined clay increases the tortuosity of the system and is expected to lower the absorption rate in concrete. Shah et al. 2020 varied the percentage addition of limestone calcined clay up to 20% and observed that with increasing replacement level, rate of water absorption is reducing. In recent RILEM TC2 CCL review paper by Dhandapani et al. 2022, a compilation of data from literature on influence of calcined clay and calcined clay plus limestone on absorption rate has been done (Figure 1-4). Even after a lot of scatters due to varied cement type, water to cement ratio, calcination method, etc. in LC3 systems a 30 and 50% reduction in absorption rate compared to the reference concrete was observed. Goncalves et al. 2009 in their study observed that high grade metakaolin was more effective in reducing sorptivity at lower replacement levels (< 20%) while low grade metakaolin was more effective in reducing sorptivity at higher replacement levels (30-40%).
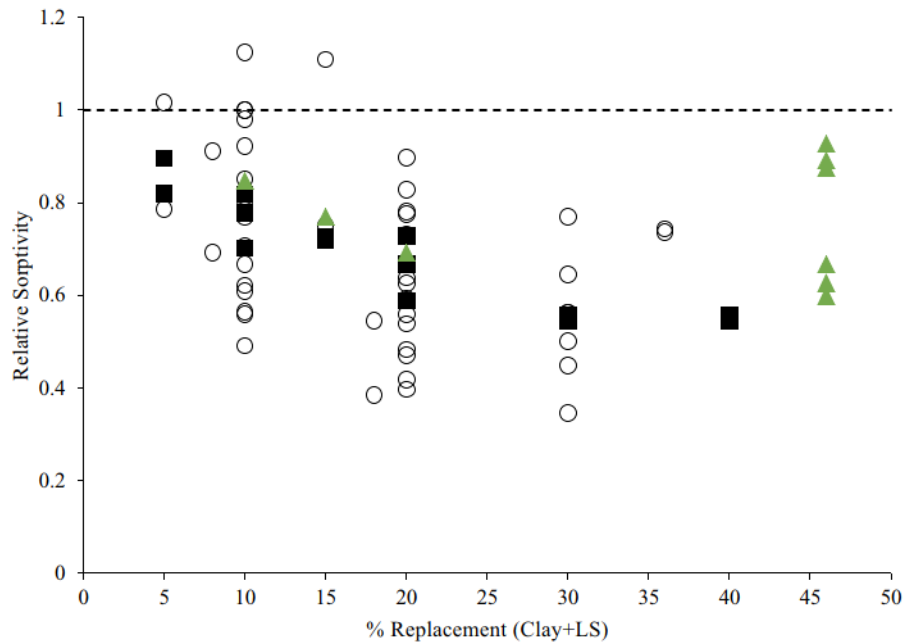
Figure 9.4: Influence of calcined clay replacement level on the absorption rate, where Circles - metakaolin, squares - calcined clays and triangles- OPC + limestone + calcined clay systems (Dhandapani et al. 2022).

9.1.3   Gas permeation – Oxygen Permeability Test

To compare the oxygen permeability between various concretes, South African Durability Index manual procedure for oxygen permeability test has been followed. Four specimens of 69mm diameter and 30 ± 2mm thickness were conditioned as per guidelines and test using the falling head permeability cell apparatus as described in Alexander et al. 2005. The negative logarithm of the Darcy's permeability coefficient is represented as Oxygen permeability index.

Figure 9.5, shows the results obtained for testing concrete made for two different grades with 3 types of cement, OPC, PPC and LC³. The results show that all concretes considered in the study had low permeability as per the classification (i.e., excellent permeability resistance category) suggested by Alexander et al. 1999. The results suggest that both FA30 and LC3 attain higher resistance than OPC. Notably, M50 concretes attain higher resistance than M30 grade of concrete within a particular binder system due to better concrete mix design. At equivalent strength, FA30 mixes attain higher resistance than LC3. However, w/c was lowered in the FA30 mixes to produce equivalent strength concrete, as against OPC and LC3. The C-mix with equivalent binder and water-cement ratio shows higher OPI in FA30 and LC³ than concrete made with OPC.
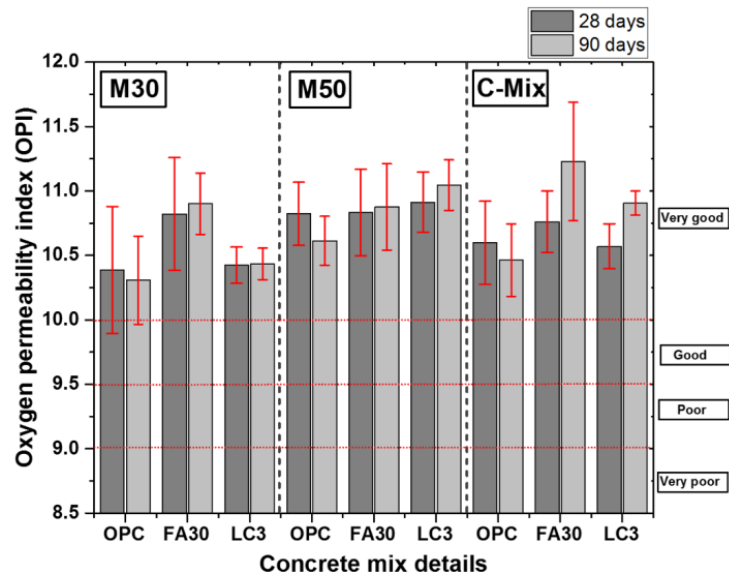
Figure 9.5: OPI values for different grades of concrete at 28 and 90days (Dhandapani and Santhanam 2018).

9.1.4 Resistivity

Electrical resistivity of concrete is known as its ability to resist the transfer of charges when an electric field is imposed. Electrical resistivities of concrete specimens are attributed to their microstructure properties like pore size, pore shape of interconnections, pore solution characteristics, etc. Therefore, resistivity values are an indication of the interconnectivity of pores and thus an indication to resistance of ionic ingress as well.

Figure 9.6 depicts the surface resistivity value for all the concrete mixes studied at 28 days, 56 days, and 90 days. Among all the systems studied, LC^3 concrete systems are observed to attain highest resistivity, irrespective of the range of concrete mixes. As discussed in previous section, due to presence of calcined clay in the system early age refinement of pore structure happens and thus leading to an increase resistivity of LC^3 systems. Due to improved kinetics of microstructure development in LC^3 systems, by end of 28 days it have a denser microstructure. For fly-ash mixes an increase in resistivity has been observed after 28 days due to additional pozzolanic reaction and extended curing. OPC shows minimal resistivity as clinker phases undergo maximum reaction at early ages (within 7 days) and there is a slowdown in their contribution over time. Similar observation has been made by others in their work as well such as Nguyen et al. 2018, Martiena et al. 2018, and Canbek et al. 2022. Muni et al. 2020 has also documented such results and have shown have the at different water to cement ratio and cement content resistivity development occurs over the age, LC^3 is observed to have high resistivity from early age itself.
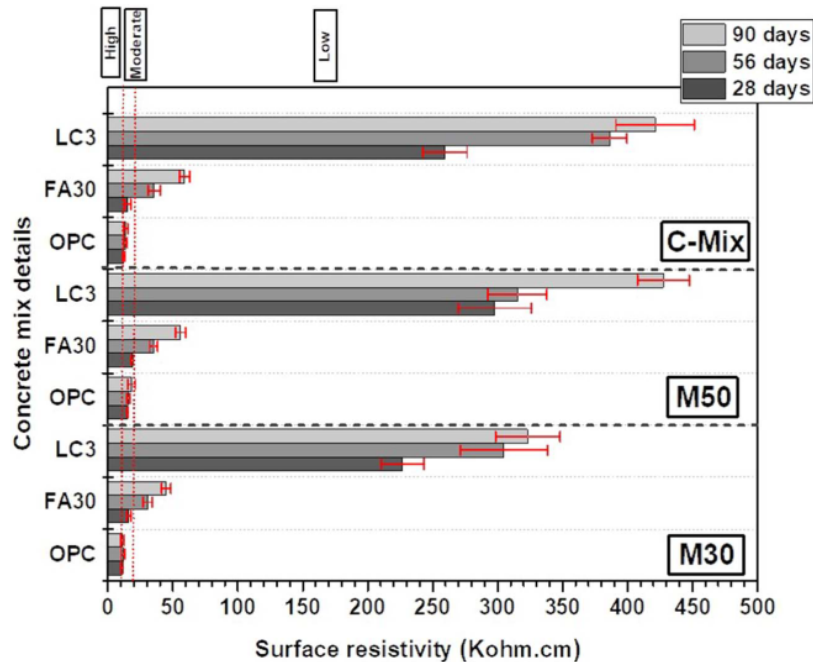
Figure 9.6 Surface resistivity of different concretes at 28, 56, and 90 days. (Dhandapani et al. 2018)

The ACI classification (ACI-222R-01 2010) on corrosion rate (High, Moderate, and Low) based on surface resistivity values is indicated in Figure 1-6 to show the relative quality of different concretes. The results clearly show that concretes made with LC3 binder can have excellent resistance to ions transport in concrete.

9.2 Durability under different environmental exposures
9.2.1 Carbonation
Concrete made with SCMs have been observed to be more vulnerable to carbonation in comparison with concrete made from ordinary Portland cement. Extent of carbonation can be seen as depth up to which the pH has fallen due to reaction between dissolved carbon dioxide and alkalis present in the system. Colorimetry is most commonly used for the measurement of carbonation depth, using suitable indicator. Carbonation is a complex physio-chemical process which results in physical and chemical pore characteristics of the system depending on the system as OPC, binary or ternary blends. The carbonation rate depends on several factors, including the reserve alkalinity, distribution of hydration products, permeability (porosity & pore size distribution), relative humidity, temperature, among others.

Carbonation is an extremely slow natural process which takes decades for the concrete cover to carbonate. Under lab conditions, accelerated carbonation test have been developed and continuously used for characterizing carbonation resistance of concrete where the concentration of carbon dioxide is almost 25 to 2500 times (1% to 100%) higher as compared to natural concentration. Castellote et al. 2008 and Leemann and Moro 2017 reported that accelerated carbonation at 3% and 4% of concentration of CO_2 does not cause drastic alterations in microstructure as compared to naturally carbonating systems. Carbonation coefficient or carbonation rate is slope of the plot between carbonation depth versus square root of time, which is a measure of comparison of carbonation performance between different cement systems. Discussion about effect of carbonation on LC[3] microstructure and carbonation rate in LC3 is given in subsequent sections.

Effect of carbonation on LC[3] microstructure
To understand the changes happening in microstructure on carbonation techniques like X-ray diffraction (XRD), mercury intrusion porosimetry (MIP), thermos-gravimetric analysis (TGA), scanning

electron microscope (SEM), etc. are employed. From the XRD scans of the uncarbonated hydrated cement paste it has been observed that major crystalline phases in OPC and PPC samples are portlandite and ettringite, however in LC3 samples, ettringite, monocarboaluminate (M_c) and hemicarboaluminate (H_c) were the major crystalline hydrate phases. From XRD scan b f the carbonated samples, it can be inferred that all the hydrate phases carbonate simultan ly i.e monocarboaluminate, ettringite, portlandite, etc. and the total amount of crystalline hydration products up on carbonation is reduced to low/insignificant quantities (Figure 9.7). Even a reduction in total amorphous content in carbonated samples has been observed which indicates towards the carbonation of amorphous high calcium bearing phases like C-S-H. Additionally, all the polymorphs of calcium carbonate are observed to be forming upon carbonation. Although, in the figure below they are collectively shown as calcium carbonate only.
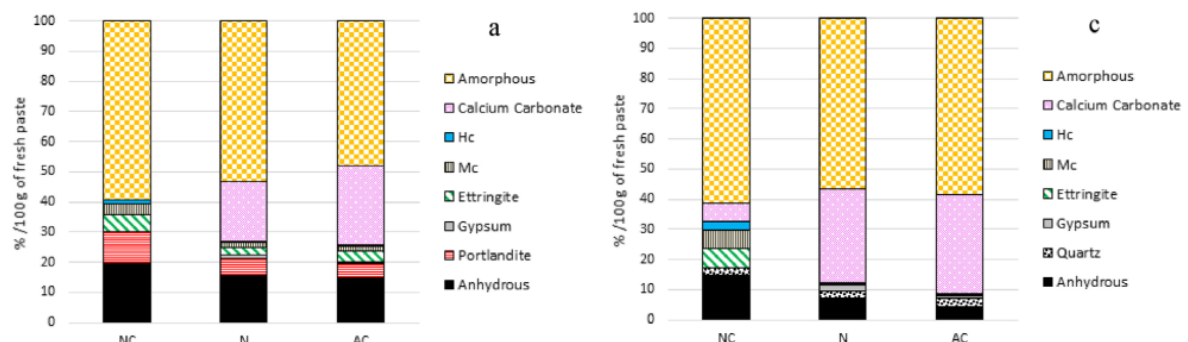

Figure 9.7: Quantification of XRD results for non-carbonated, natural carbonated and accelerated carbonated a) OPC, and b) LC3 samples (Shah et al. 2018)
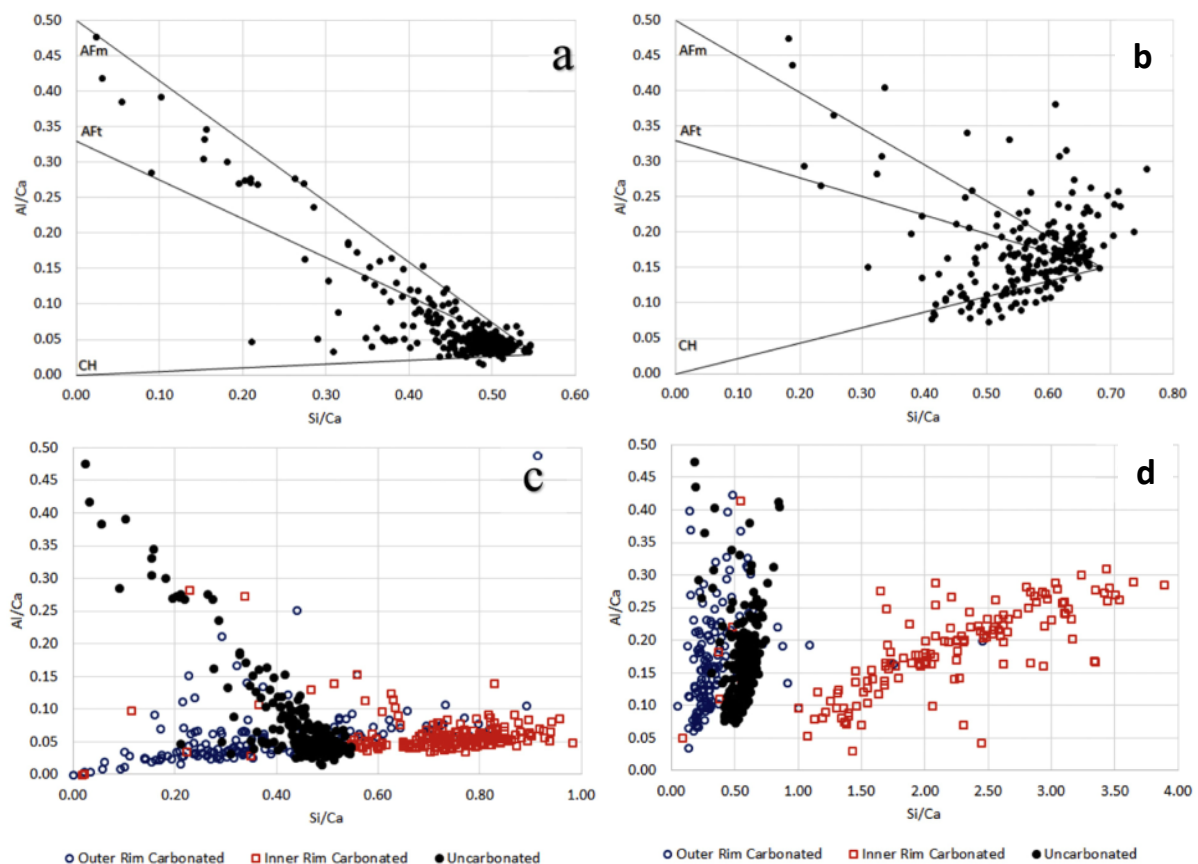

Figure 9.8: EDS point analysis of OPC uncarbonated - a, LC3 uncarbonated - b, OPC carbonated – c, and LC3 carbonated – d. (Shah et al. 2018)

134

Carbonation of the high-calcium rich C-S-H is evident from the back-scatter electron (BSE) image from SEM as well, a fine mix of the calcium carbonate intermixed with the de-calcified C-S-H or silica gel is observed. Groves et al. 1991 also identified a fine mix of calcium carbonate and decalcified C-S-H in carbonated sample using Transmission Electron Microscopy (TEM). To further understand this effect, EDX point analysis on the uncarbonated, and carbonated inner and outer C-S-H has been performed. The Ca/Si ratio of C-S-H decreases with increase in replacement level by SCMs i.e. OPC has the higher Ca/Si ratio whereas LC[3] has the lower. In the carbonated samples, the data points collected through EDS have a large degree of spread. EDS analysis of the points collected from the inner rim and the outer rim of the carbonated samples show a clear difference in their elemental composition. Data points collected on dark inner rim i.e. rim closer to cement grain have higher Si/Ca whereas points collected from the outer rim show lower Si/Ca. Figure 9.8 shows point analysis results of all the samples obtained by plotting atomic ratio of Si/Ca against Al/Ca, where higher Si/Ca and Al/Ca implies decalcification of C-S-H and conversion into silica and alumina gel.

With carbonation of the hydrated phases of cement paste and formation of new products, a change in the pore structure characteristic is inevitable. To understand the change in the pore characteristics MIP is most commonly employed technique. MIP results give two valuable information, one total pore volume and second being threshold pore or critical pore radius. The MIP curves of the uncarbonated samples measured at the end of the curing regime i.e. 120 days and before exposure to carbonation are shown in figure 9.9. Before carbonation LC[3] has a smaller critical pore diameter as compared to OPC even with a clinker replacement level of 50%, however higher total pore volume. After carbonation an overall reduction in the total porosity of OPC is noted whereas an increase in total porosity was observed for LC[3]. This can be explained as up on carbonation portlandite converts to the calcium carbonate, which is well known to have higher solid volume, no matter the type of polymorph formed. While the carbonation of phases like ettringite, releases lots of water upon carbonation and have a low solid volume upon carbonation. Even carbonation of C-S-H results in leaching of calcium ions and formation of less volume occupying silica gel or decalcified C-S-H.
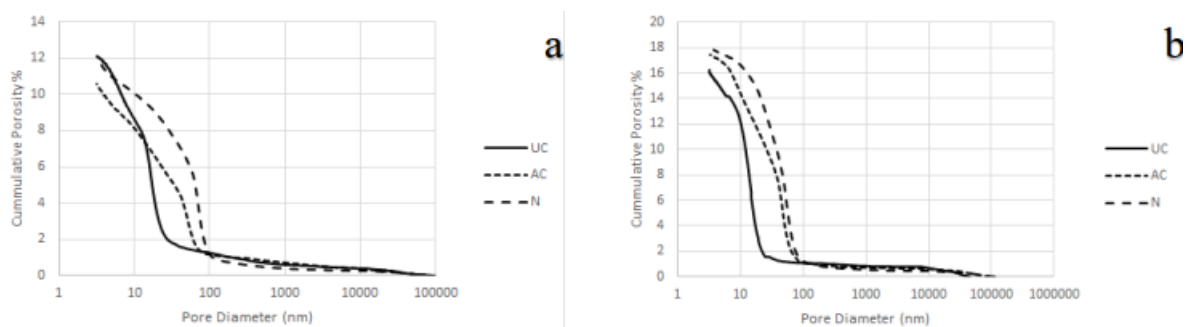
Figure 9.9: MIP curves for carbonated and uncarbonated a) OPC and, b) LC[3] (Shah et al. 2018)

Shi et al. 2016 in their study showed that with addition of the metakaolin the percentage of the ink bottle pores (pores connected with narrow neck to the external surface) increase as compared to the OPC. To measure the inked bottle, two MIP were performed and subtraction between gave volume of ink bottle pores. Figure 9.10 shows the intruded pore volumes and threshold pore sizes for the studied blends. It had been observed that carbonation resulted in an increased volume of percolated pores in the range 10–100 nm for the metakaolin and metakaolin & limestone blended mortars. In contrast, a small decrease in the volume of percolated pores combined with an increase in pore size of the percolated pores is observed for the OPC and PLC mortars after carbonation.
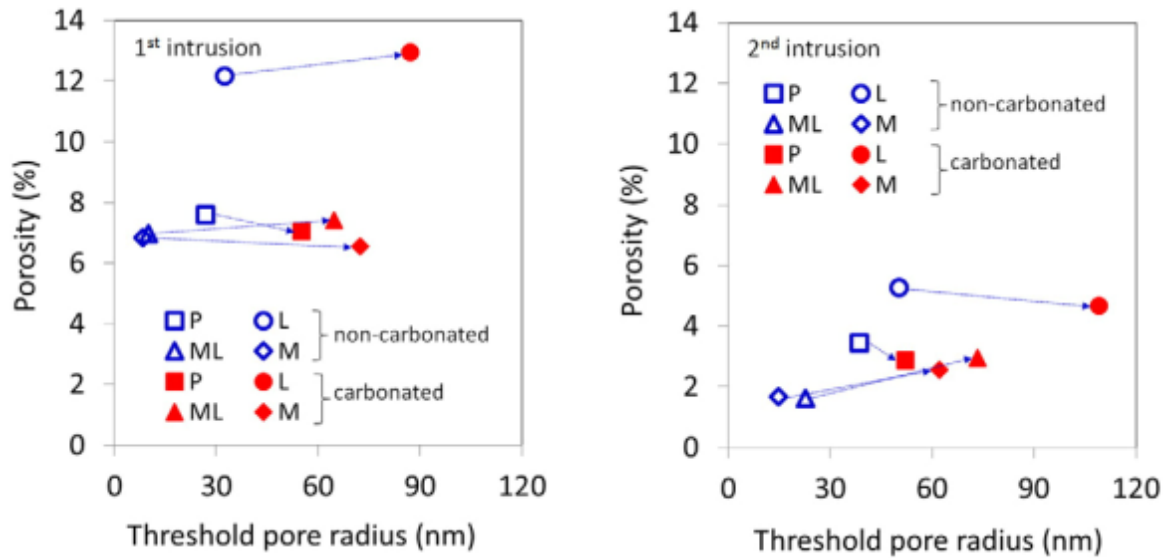
Figure 9.10: Impact of carbonation on the microstructure based on the first (left) and second (right) MIP intrusion cycles for the four studied mortars. (P–OPC, L–OPC +Limestone, M – OPC + Metakaolin, and ML – OPC + Limestone + Metakaolin) (Shi et al. 2016).

Thermal decomposition provides another method for the quantification of the carbonation of hydrates and calcium carbonate formation (figure 9.11). Mass loss between 30 to 300 °C is related to decomposition of C-S-H, AFt and AFm phases. The intensity of the decomposition peak occurring in this range decreases on carbonation indicating that the phases are carbonating. Portlandite is characterized by weight loss in the temperature range of 400–500 °C. Peak of portlandite decomposition is almost flat in case of the LC^3 indicating almost complete consumption of portlandite partially by secondary hydration reaction and partially upon carbonation. Carbonated samples show weight loss due to decomposition of calcium carbonate at around 700–800 °C. The continuous decomposition from 400 -800°C indicates that the presence of amorphous or poorly crystalline calcium carbonate that can decompose at lower temperatures (Sevelsted and. Skibsted 2015).
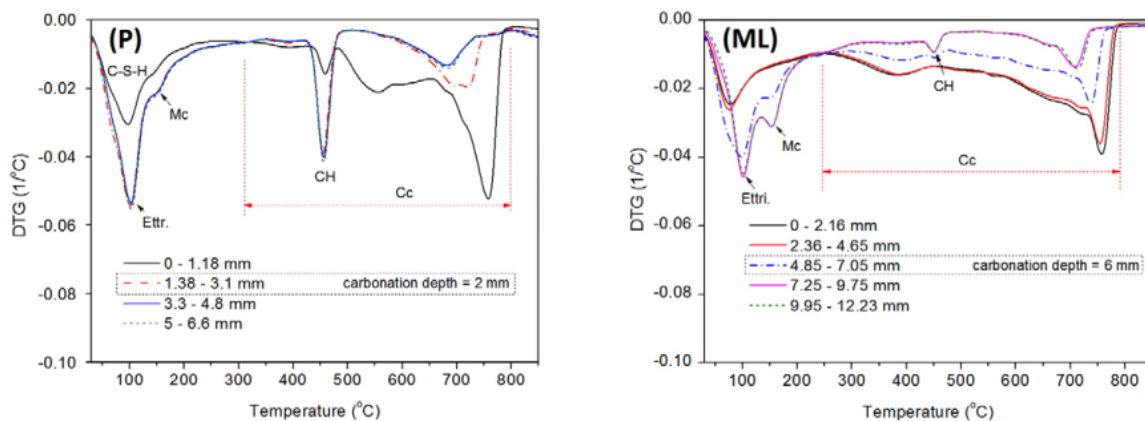
Figure 9.11: DTG curves for left) OPC, and right) LC3 at different depths upon carbonation for 91 days (Shi et al. 2016).

Carbonation rate in LC^3

As we keep on increasing the replacement level of clinker with calcined clay or calcined clay and limestone system, it has been found that the carbonation rate increases as compared to ordinary Portland cement. Not just replacement level, in fact the grade of clay as in reactivity of clay also have an influence on the carbonation rate as it is directly related to the degree of hydration of clinker as well as the overall system. Higher grade clays are known to hamper the belite hydration and higher

consumption of calcium hydroxide and thus resulting in the faster carbonation with higher grade kaolinitic clays (Krishnan 2019, Shah et al. 2018).
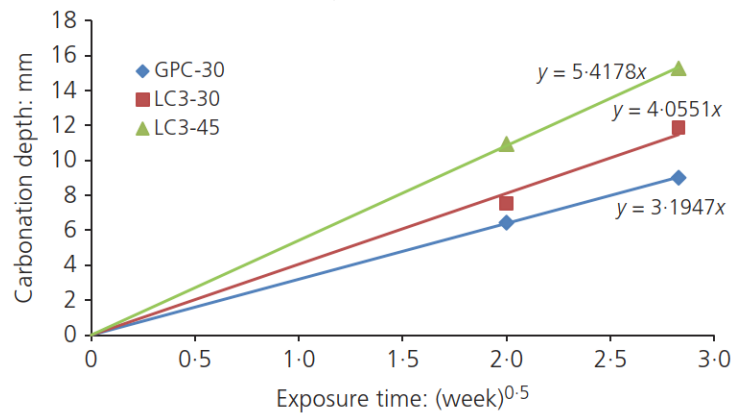
Figure 9.12 Carbonation depth of concrete at 1% carbon dioxide concentration (Khan et al. 2019) (GPC -30: OPC, LC3-30: OPC + 30% calcined clay +limestone, and LC3-45: OPC + 45% calcined clay + limestone).

With increasing the water to cement ratio, the carbonation rate is higher for all the different cement. At very low water to cement ratios OPC outperforms other cements by wide margin because of very dense microstructure and wide availability of portlandite and even non hydrated clinker. From figure 9.13, it can be observed that LC^3 have higher carbonation depth as compared to PPC and OPC.
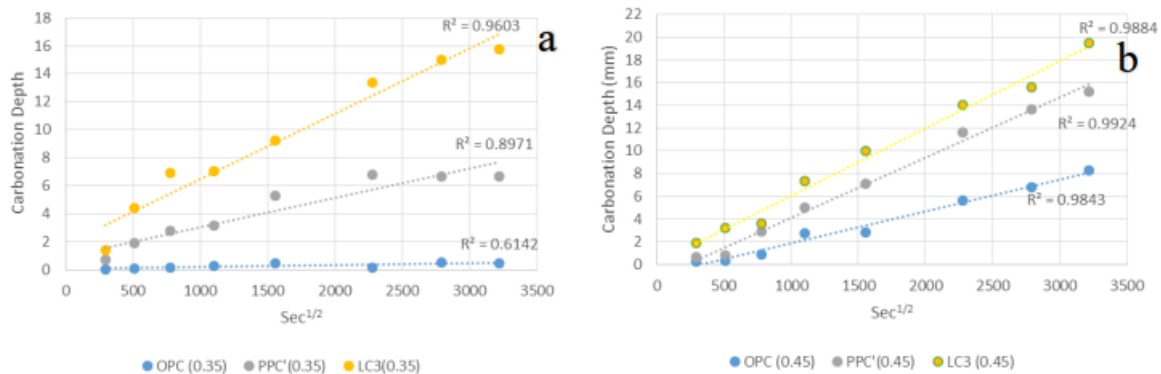
Figure 9.13: Carbonation depth measured in samples placed in accelerated carbonation condition a: Samples exposed in 3% CO_2 concentration, b: Samples exposed in 1% CO_2 concentration

Effect of relative humidity on carbonation is well known for OPC, thus its effect on LC^3 has also been investigated at different relative humidity. Samples were exposed in 40%, 60%, and 80% relative humidity at 3% carbon dioxide concentration and 27°C. Effect of temperature on progress of carbonation was also studied at carbon dioxide concentration of 3% and relative humidity of 60% and at 27°C and 45°C. It has been observed that the carbonation depth measured in LC3 is higher than OPC and PPC at all relative humidity levels. Additionally, the depth of carbonation was observed to be higher for samples exposed to higher temperatures.
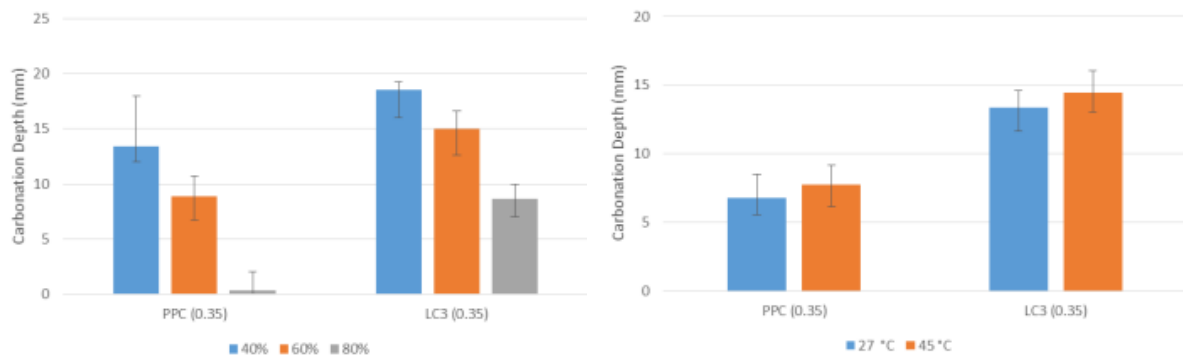
Figure 9.14: Carbonation depth of samples exposed in different relative humidity conditions a: Carbonation depth after 3 months exposure in different relative humidity, b: Carbonation depth after 2 months exposure in different temperature

Recently, Rathnarajan et al. 2022 in their study showed that the blended cement like LC^3 has change in carbonation rate after a certain period of time, which can be credited to the more refined microstructure of the interior concrete compared to surface and the favourable rate of changes in the humidity conditions inside the concrete. In addition, the low penetrability of concretes with SCMs, especially at a depth inside the concrete than at the surface, could be another reason for the reduction in the carbonation rate at the later ages.

9.2.2 Chloride ingress

For marine exposures and cold countries where de-icing salts are used chloride ingress in the reinforced concrete structures is a major challenge. Chlorides owning to high external concentration diffuses through the connected pore network of concrete and reaches up to reinforcement level. Once a critical threshold chloride concentration of these ions has reached around reinforcement, passivating film de-stabilizes and active corrosion of rebars begin. Pore structure and chloride binding capacity of governs the hindrance to chloride ingress in the concrete. Chloride ingress in concrete depends on several factors, including porosity, pore size distribution, pore connectivity, pore solution composition, physical and chemical chloride binding, temperature, and relative humidity (degree of saturation) (Pillai et al. 2019, Ueli et al. 2009).

Chloride concentration in is sea water is about 0.55 mol/litre, which takes long time to ingress in concrete. However, in lab conditions to check the chloride ion resistance of concrete accelerated tests are performed such rapid chloride penetration test (ASTM C 1202), rapid chloride migration test (NT Build 492), etc. To check the ingress profile development and chloride binding other tests which use high concentration of chlorides are salt ponding test (AASHTO T259), bulk diffusion test (NT Build 443), etc. Apparent diffusion coefficient of chloride in concrete is a measure used for evaluating performance comparison between different binder systems. Discussion about chloride binding and chloride ingress rate in LC^3 is given in subsequent sections.

Chloride binding in LC^3

Cement hydrates have an ability to bind with the chlorides ingressing in the concrete. Chloride binding is of two types, chemical binding and physical binding. For OPC cement, amount of the calcium aluminate decides the amount of the chemical binding potential as they chemically found the chloride from pore solution to form Friedel's salt. In LC3 system due to the synergic effect, more of AFm phases are formed i.e formation of hemi-carboaluminate and mono-carboaluminates. Apart from the chemical binding, another way by which chlorides can be bound is by physical adsorption on the C-S-H layer, which also plays a significant role. Although it's the free chlorides in the system that causes the de-passivation, however the bound chlorides can act as reservoir and may present a corrosion risk.

Sui et al. 2019 studied the binding capacity of the different blends which is summarised in figure 9.15. It can be seen that considering the experimental error, limestone + calcined clay, slag, and fly-ash all have the similar chloride binding capacity. However, looking at the percentage of AFm phases that are formed in the different systems, it can be seen that calcined clay and limestone system have considerably higher AFm phases compared to slag and fly-ash systems. That reflects on the amount of Friedel's salt formed, LC^3 systems form highest amount of the Friedel's salt. It can be observed that the trend of total Friedel's salt formed is different from the total bound chloride profile, which underlies the importance of the physical absorption of chloride on C-S-H. Effect of calcined clay kaolinitic content on chloride binding has been investigated by Marghechi et al. 2018, it has been found that maximum binding happens in the clays which have kaolinitic content of 40-80% (figure 9.16).
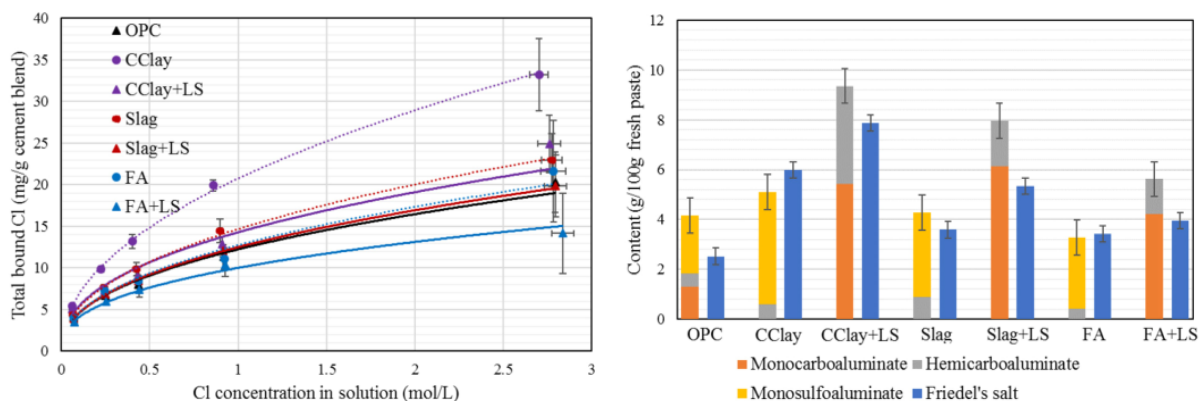
Figure 9.15: left) binding isotherms of different systems, and right) AFm phases and Friedel's salt content from XRD Rietveld analysis
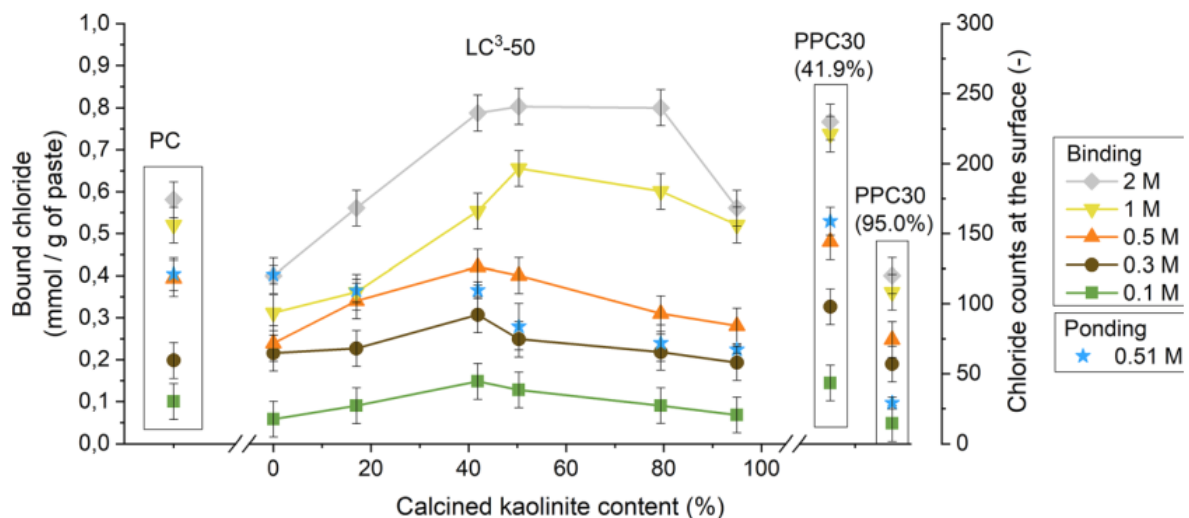
Figure 9.16: Total bound chloride as a function of clay grade in LC3-50 and PPC30 pastes after exposure to 0.1to 2 M NaCl solutions (Marghechi et al. 2018)

Maraghechi et al. 2018, characterized the porosity and pore structure of the LC^3 systems before and after chloride ingress. It has been found that interaction of the binders with chloride ions did not significantly affect the porosity (Figure 9.17). In fact, the trend in the chloride ingress test results were in good agreement with the measured pore structure, i.e. the finer the pore connectivity, the more resistant the cementitious system to chloride ingress.

139
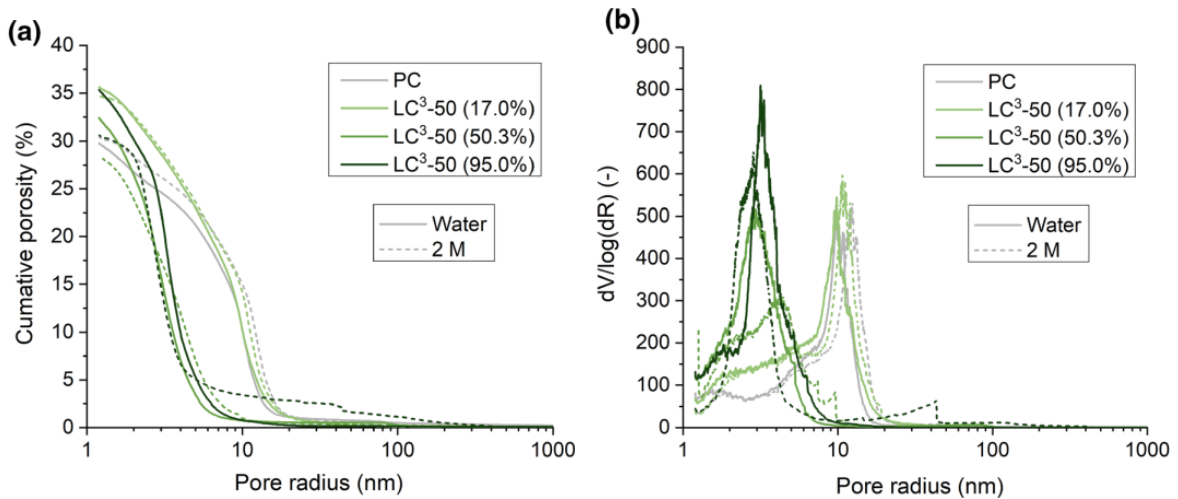
Figure 9.17: Porosity distribution of PC and LC³-50 paste samples after 6 m exposure to water or 2 M NaCl solution

Chloride ingress rate

Rapid chloride penetration test (RCPT) provides an indirect estimate of the chloride resistance of the concrete. ASTM C 1202 specifies the protocol for the testing and classification of concrete based on charged passed through concrete. Lesser is the charge passed, more is the chloride resistance of the concrete. From figure 1-18, it can be seen that at all grades LC³ concrete offers the highest resistance to the chloride ingress. Charge passed through LC³ concrete is either very low or negligible, showing its suitability for being used in chloride ingress prone areas.
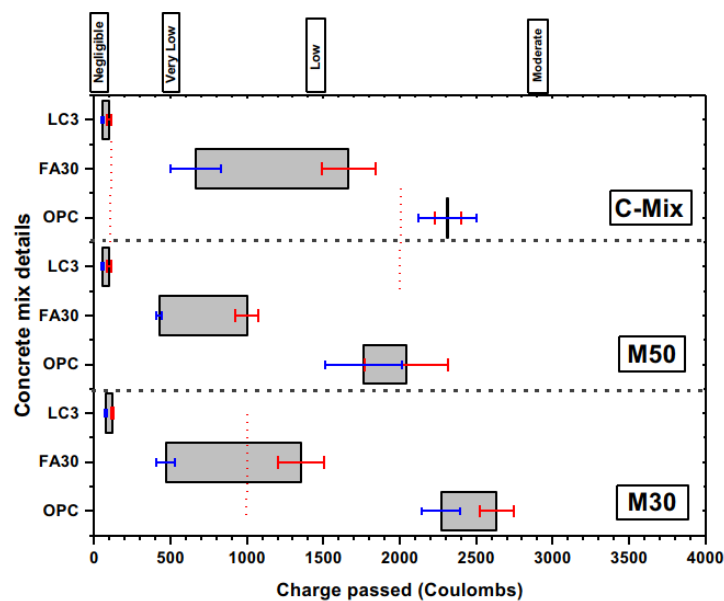
Figure 9.18 RCPT - total charge passed in the different concretes at 28 days (red) and 90 days (blue) (Dhandapani et al. 2018)

RCPT is widely used for concrete quality assessment more specifically in chloride ingress environment, rapid chloride migration test (NT Build 492) offers a quantitative measure for the chloride resistance in terms of migration coefficient i.e chloride ingress rate under externally applied potential. RCMT results are affirmative of the RCPT tests, (Figure 9.19). It can be seen that concrete made with LC³ have chloride migration coefficient values an order lower as compared to concrete made with OPC. Additionally, it can be observed that LC³ offers better resistance from early age itself, this is attributed to early age pore refinement observed in LC³. Furthermore, addition of calcined clay along with

limestone improves the chloride binding as well in the system due to secondary hydration products, as discussed above.
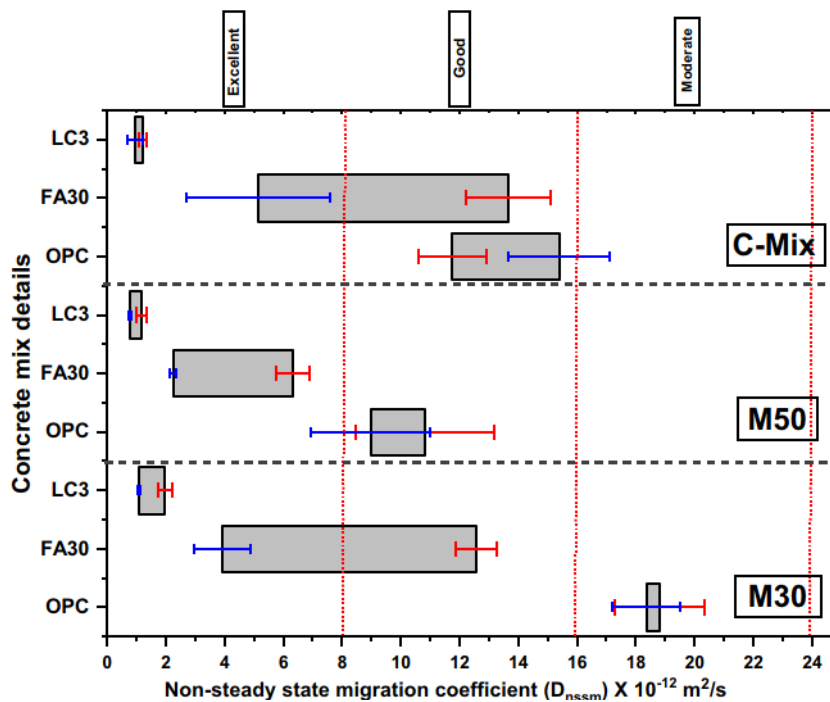
Figure 9.19: Chloride migration coefficient of the different concretes at 28 days (red) and 90 days (blue) (Dhandapani et al. 2018)

Pillai et al. 2019 performed bulk diffusion test on 7 different concrete mixes and obtained chloride profile. Figure 9.20, highest chloride ingress rate can be clearly seen in the OPC mixes for both grades of concrete followed by PFA and LC³. LC³ and PFA show lower ingress rate due to their improved microstructure and high ionic resistance offered by binder phases. Lower surface concentration in LC³ and PPC is owning to their lower porosity and smaller pore sizes near the exposed surface, inspite of same exposure. Additionally, chloride threshold values for OPC, PPC and LC³ has also been evaluated and a reversal in trend has been observed, OPC having highest chloride threshold and LC³ having the lowest (Figure 9.21). Which can be due to high alkalinity and buffering capacity of portlandite at the interface of concrete and steel in OPC system. Whereas for the blended systems, consumption of portlandite takes places during the secondary hydration reactions. Thus, it can be concluded that LC³ system does offer higher chloride resistance but lower chloride threshold values.
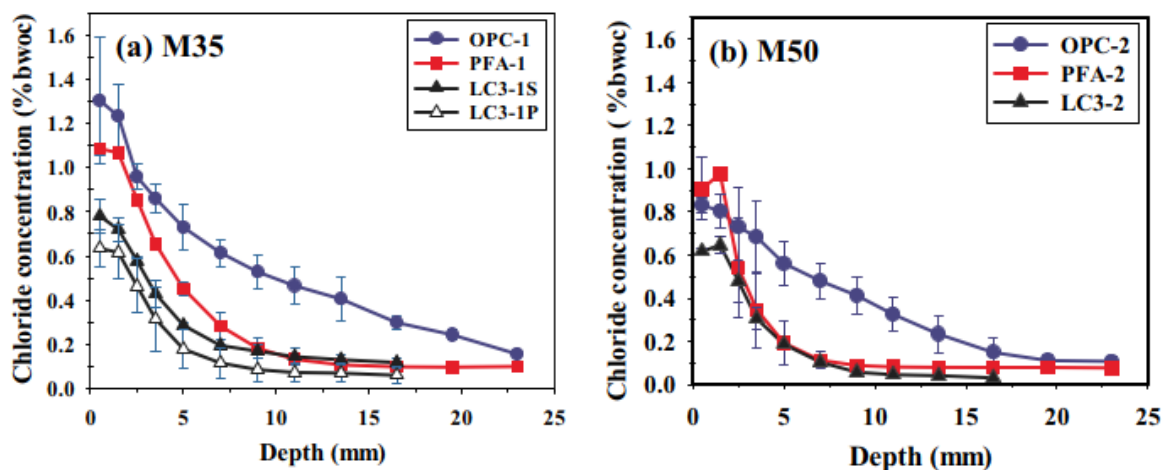
Figure 9.20 Chloride profiles in the concrete mixes after 56 days of exposure to chloride solution, (a) M35 and (b) M50 concrete (%bwoc = % by weight of concrete)

141
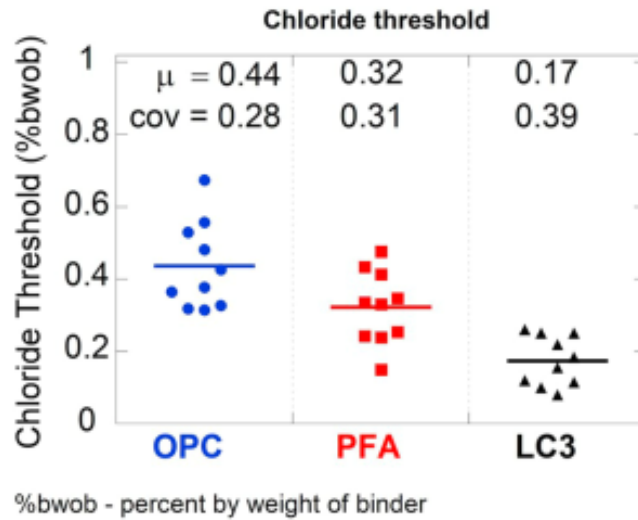
Figure 9.21 Chloride threshold for corrosion initiation of the rebar in OPC, PFA and LC3 mortar (Pillai et al. 2019)

Maraghechi et al. 2018 further compared the effect of the grade of calcined clay being used in LC^3-50 preparing on apparent chloride diffusion coefficient. Apparent diffusion coefficient was calculated based on the Fick's 2nd law of diffusion after getting the chloride profile from ponding tests. The apparent diffusion coefficient decreased as the kaolinite content of the calcined clay increased and was about two orders of magnitude lower for LC^3-50 (95.0%) compared to PC system (Figure 9.22). For preferred kaolinitic content of 40-60% in LC^3 production, apparent diffusion coefficient is about 1-1.5 orders lower than ordinary Portland cement systems.
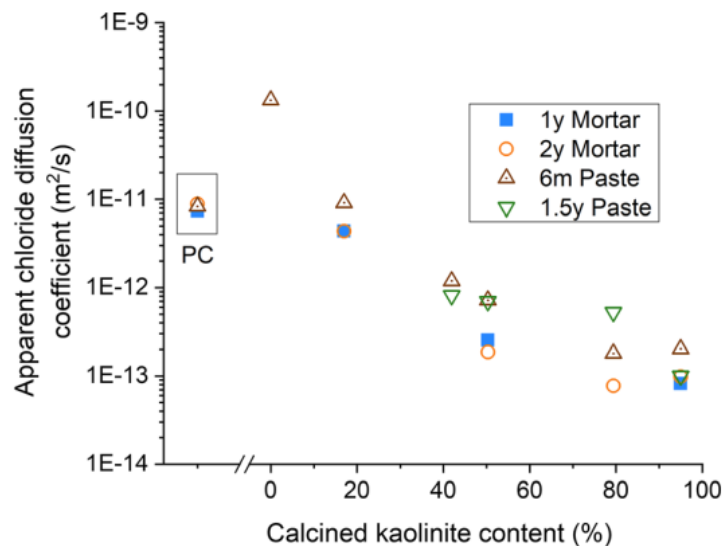
Figure 9.22: Apparent diffusion coefficients for PC and LC3-50 mortar and paste samples, calculated using Fick's law of diffusion (Maraghechi et al. 2018)

9.2.3   Sulphate attack
Under sulphate attack reaction between the aluminate phases or portlandite and sulphate ions takes place, leading to formation of either softer or expansive products which causes failure of the binder component of matrix (concrete). Sulphate attack can be internal due to sulphate adsorption in C-S-H at high temperature curing or due to external sulphate ingress, here we will be focusing on the external sulphate attack. Under external sulphate attack sulphate ions ingress in concrete and react

with AFm phases or portlandite forming ettringite, gypsum, and even thaumasite if carbonates are present in the system at low temperatures.

Magnitude of sulphate attack is attributed to physical factors like porosity, pore size distribution, connectivity, etc and chemical factors like alkalis, portlandite, AFm phases, etc of concrete. Physical factors are about the resistance to sulphate ions ingress and chemical factors are more about amount of final reaction products which cause the expansion, cracking, strength loss, jeopardizing the engineering properties. Like other environments to study the sulphate attack, accelerated tests are performed, ASTM C 1012 outlines the procedure for the sulphate attack study and evaluation. Subsequent section provides the details about the microstructural changes and sulphates ingress resistance & expansion of LC^3 when subjected to sulphate environment.

Microstructural changes

In the presence of externally ingressed sulphate ions, the hydration products like monosulphate, hemi-carboaluminates, mono-carboalumintes, hydrogarnets etc. are unstable and they start reacting with sulphate ions to form ettringite. Formation of ettringite in paste causes local expansion resulting in micro-cracking an exposing of large surface to the aggressive solution (Irassar 2009). However, addition of metakaolin and limestone together in the system helps in three different ways. Firstly, by reducing the overall amount of C_3A per gm of cement paste, secondly by consumption of portlandite in secondary hydration reaction (reducing potential of ettringite and gypsum formation), and lastly by the pore refinement that starts from early age itself (increase ingress resistance).

Suma and Santhanam 2017, performed the XRD on mortar samples of LC^3, OPC and PPC after exposing the mortar specimens to 5% sodium sulphate solution and observed that intensity of gypsum and ettringite peaks is higher and clear than the blended cements which clearly indicate severe sulphate attack in OPC only. Thaumasite peak is hard to identify because of its overlap with ettringite. Another, interesting observation made during their work was that, although monocarbolaluminate peak was present for 26 weeks saturated lime curing but had been absent by 66 weeks of LC^3 sample immersed in sodium sulphate solution, indicating to the conversion of monocarboaluminate to ettringite. Additionally, peaks of portlandite were absent in LC^3 from early age itself due to complete consumption owning to high reactivity of calcined clay. That also means, that the potential of gypsum and ettringite formation is further reduced.
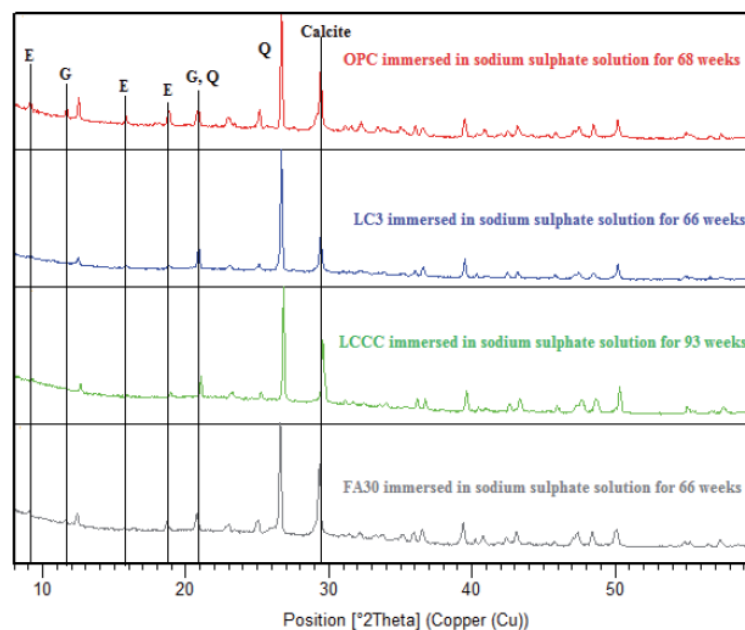
Figure 9.23: XRD patterns for the different mortars after 60 – 90 weeks of exposure in the sodium sulphate solution (Suma and Santhanam 2017)

143

When the same samples are exposed to the magnesium sulphate solution, it is seen that the deterioration in LC^3 is faster as limited portlandite availability readily reacts to forms brucite and post which magnesium directly attacks C–(A–)S–H forming the non-cementitious magnesium silicate hydrates (M–S–H) and gypsum. Which results in the mass loss and disintegration of cementing matrix.
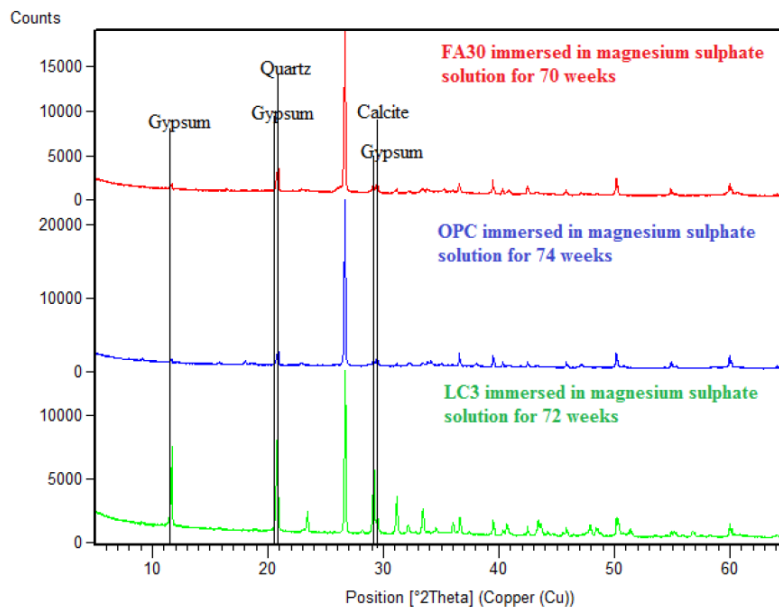
Figure 9.24: XRD pattern of samples immersed in magnesium sulphate solution
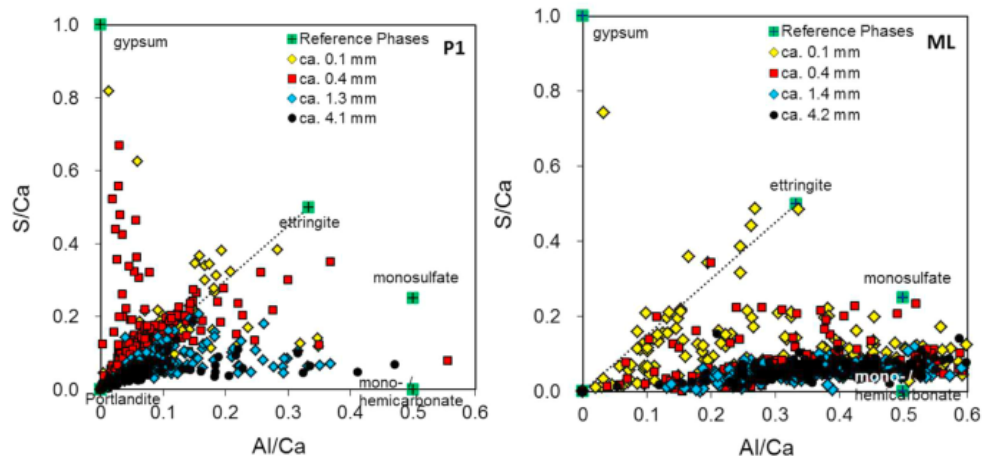
Figure 9.25: EDX dot plots of S/Ca versus Al/Ca atomic ratios at different depths from the exposing surface of the P1 (OPC), and ML (LC3) mortars (Shi et al. 2019)

Shi et al. 2019 performed SEM-EDX analysis on mortar samples exposed to 16g/l of sodium sulphate solution for 42 days and have observed that although the metakaolin limestone mortar is rich in Al, no expansion is observed for this mortar because of the lack of calcium. In fact, ingress of sulphate has been observed to be much deeper in OPC as compared to the LC3 systems which is visible from the points cloud been more concentrated towards mono and hemi carboaluminates (Figure 9.25).

Sulphate ingress resistance and expansion in LC^3
Suma in her Ph.D thesis studied the sulphate attack on the LC^3 and compared it with the OPC and PPC (30% - fly ash). Figure 9.26, shows the results of the expansion percentage that is happening different specimens when they are subjected to sodium sulphate and magnesium sulphate solution for 94 and 72 weeks respectively. It can be seen that the expansion ratio is almost negligible in the case of PPC and LC3 when subjected to the sodium sulphate solution, in comparison to OPC which have 1% of

144

expansion. Synergic effect of LC^3 provides a positive impact on the sodium sulphate resistance of system.
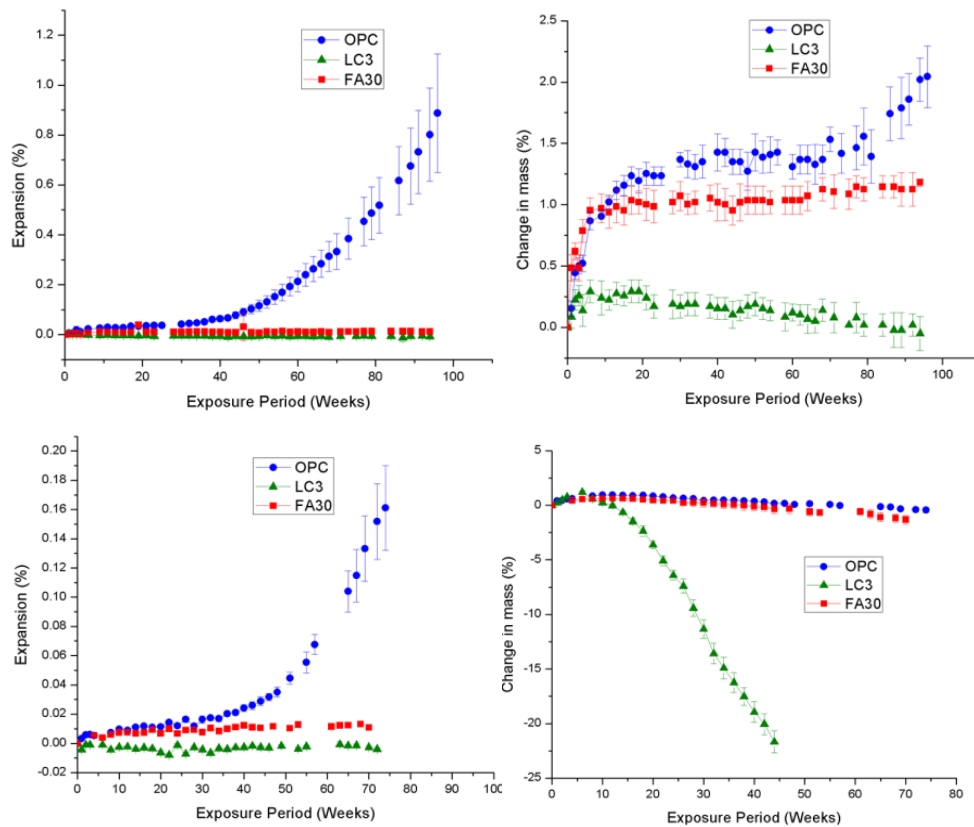
Figure 9.26: a) expansion of specimen, b) mass loss of specimen immersed in sodium sulphate, c) expansion of specimen, and d) mass loss of specimen immersed in magnesium sulphate

Whereas loss of dimension of LC^3 specimens had begun from early age itself on exposing them to magnesium sulphate, which can be seen as continuous loss of mass from 8 weeks onwards. Shi et al. 2019 in their study on subjection of different blends to sodium sulphate at different temperature observed that on addition of calcined kaolin and calcined montmorillonite the change in less and change in mass is negligible. Rossetti et al. 2020 used illitic calcined clay in their work and directly subjected specimens to sodium sulphate immersion without curing. It had been observed that the pozzolanic reaction of illitic calcined clay in mortars consumed the CH and blocked the sulphate ingress due to pore size refinement. Additionally, even though mono and hemi carbonate phases formed during hydration did convert to ettringite in exposed pastes, however the mortar showed no expansion and retained the compressive strength even at 6 months in these ternary systems. Wang et al. 2021 in their work concluded that the LC^3 cement paste offers a good resistance to sodium sulphate attack even in cyclic and high sulphate concentration environment, showing slower ingress and slight expansion. Favier and Scrivener 2018 performed experiment at different replacement level of clinker and found that a minimum amount of calcined clay and limestone was required (around 30%) to mitigate the expansion caused by sulphate attack.
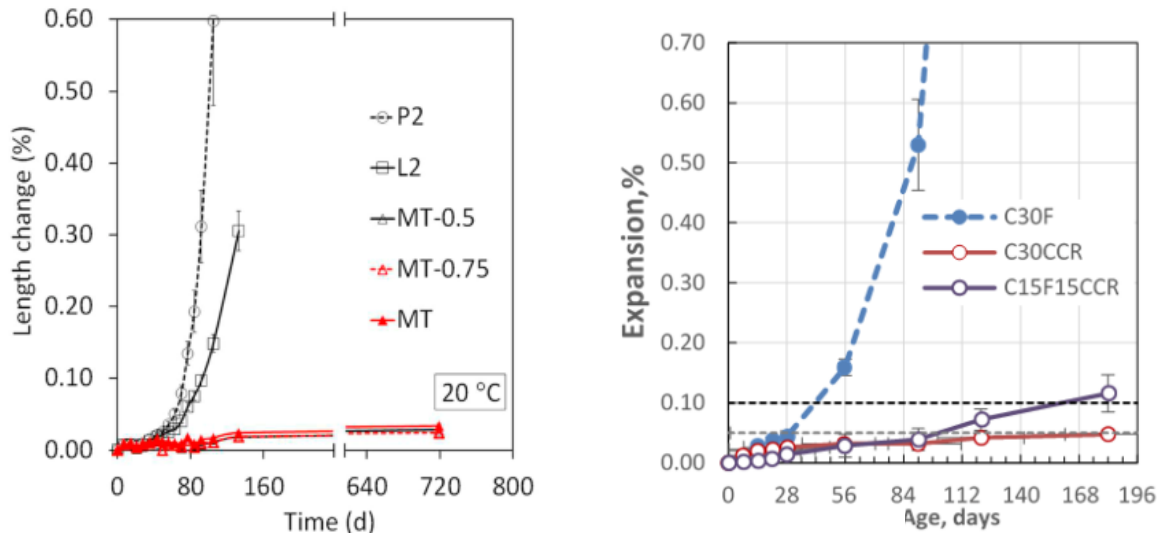
Figure 9.27: left) Length change in specimen exposed to sodium sulphate when calcined montmorillonite clay is used, and right) expansion in specimen exposed to sodium sulphate when calcined illitic clay is used.

9.2.4 Alkali silica reaction

Alkali silica reaction (ASR) is a deleterious swelling reaction that occurs in concrete between reactive amorphous silica present in aggregates and highly alkaline pore solution, given enough moisture is available. ASR is a serious problem where non-reactive aggregates are limited, and cost of transport is significantly elevated. To mitigate ASR, focus is mainly on reducing the amount of ASR gel formed by changing the chemical environment inside cement paste. These include (i) usage of the low-alkali cement, (ii) usage of SCMs and (iii) usage of chemical admixtures such as lithium-based admixtures (Xu et al. 1995, Kim and Olek 2016). ASTM C 1293, ASTM C 1260, ASTM C 1567 provides protocols for determining the potential for alkali silica reactivity of SCMs, cementitious materials and aggregates as well as limits for the expansion.

Scrivener et al. 2018 performed an accelerated mortar bar test to access the potential for alkali-silica reactivity using LC^3 cement and Jobe reactive aggregates. Test was performed at two different clinker factors 0.5 and 0.65 using 50% calcined kaolinite. The mortar bars were cured in fog condition for 28 days and were soaked in 0·32 M sodium hydroxide solutions at 38°C. It has been found that calcined clay and limestone combination was effective in in preventing alkali silica reaction in concrete, owning to low alkalinity and presence of high alumina in the pore solution (Figure 9.28). Favier et al. 2015 showed how ASR can be mitigated using the ternary blend of LC^3 because of the positive effect of the alumina in mitigating ASR. Favier and Scrivener performed their experiment at sodium hydroxide concentration of 0.32mol/l at 38°C and analysed results as per ASTM C 1293 limits and have found that LC^3-50 doesn't expand much and passed the requirements.
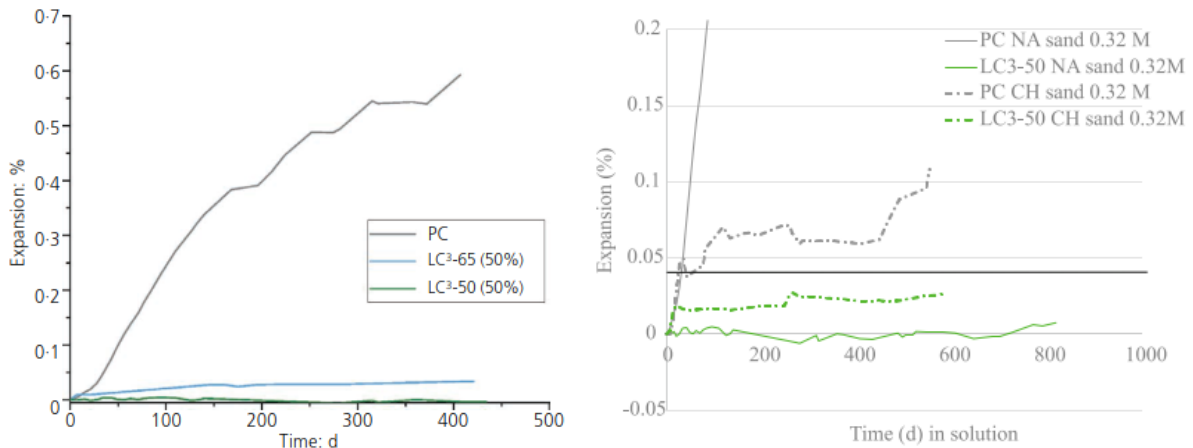
Figure 9.28: left) Expansion measured for PC and LC3-65 and LC3-50. (Scrivener et al. 2018), and right) Expansion measured for PC, LC3-50 (Favier and Scrivener et al. 2018) both performed at 38℃ with 0.32 mol/l NaOH

Nguyen et al. 2020 performed AMBT using the calcined clay and limestone at a substitution rate of 20% and 30% with the ratio of 2:1. Expansion of the mortar bars were compared with the limit of Australian Standard 1141.60.1 at 10 days and 21 days for specimens with 30 wt% replacement and have been found to be below the specified limits (Figure 9.29). Additionally, apart from rapid pozzolanic reaction, calcium-rich phases in LC3 have been found to delay the ASR gel formation or to produce high Ca/Si ASR gels that have the less expansive capability.
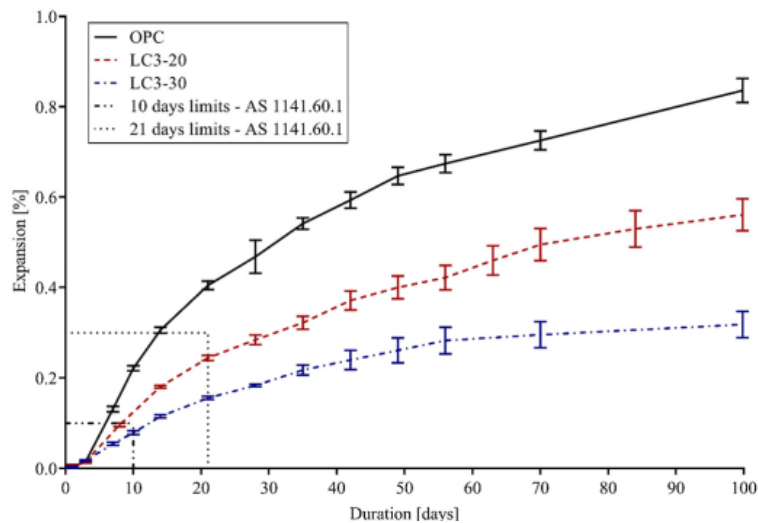
Figure9.29: ASR expansion of mortar bars for AMBT (Nguyen et al. 2020)

The exact mechanisms of mitigation of ASR expansion in LC3 systems are not fully understood. However, considering the pozzolanic reaction of calcined kaolinite in system, one can believe that LC3 would have similar effects to typical SCMs (such as fly ash and slag) on the mitigation of ASR expansion. These include (i) reduction in alkalis in system owning to dilution effect, (ii) reduction in the alkali concentrations in the pore solution owning to the alkali fixation by secondary hydration products forming, (iii) having a denser microstructure which slows down the diffusion or migration of ions taking part in ASR reaction, and (iv) limiting the silica dissolution because of aluminium presence in the pore solution (Chappex and Scrivener 2012, Li et al. 2015, Nguyen et al. 2020).

9.3 Corrosion in LC³

Corrosion in presence of water in liquid state happens by an electrochemical mechanism, oxidation and reduction taking place simultaneously. Ordinarily a rebar embedded in concrete is under protective condition due to presence of the passivating film which forms over it under alkaline conditions of pore solution. However, this passivating film can be lost owning to carbonation of concrete cover which brings down the pH below 9.0 (carbonation induced corrosion) or by ingress of the chlorides up to rebar which when crosses the critical chloride concentration results in loss of thermodynamic stability of passivating film (chloride induced corrosion). Once, passivating film has been lost, anode and cathodes start forming on the rebar. If oxygen and sufficient moisture is present around rebar to complete the cell, an anodic site is formed at point of heterogeneity where iron gets oxidised. Electrons realised are transferred through metal rebar toward the cathodic zone where reduction of oxygen and water takes place to form hydroxide ions. Hydroxide ions combine with ferrous ions to form ferrous hydroxide, ferrous hydroxide in the presence of the oxygen converts to ferric hydroxide, rust. Corrosion in the structure leads to the cracking, loss of bond between concrete and steel interface, spalling, loss of stiffness, etc.

Corrosion rate in a cementitious system depends on several factors like, degree of saturation, total pore volume, pore solution ions, temperature, resistivity of concrete, distribution of cathode and anodes on rebar, etc. To evaluate the condition of reinforcement embedded in cementitious materials commonly employed techniques are resistivity measurement, half-cell potential, linear polarization resistance, etc. Subsequent sections provide the performance evaluation of LC³ in both carbonation and chloride induced corrosion.

9.3.1 Carbonation induced corrosion

Accelerated carbonation is used to induce corrosion. Carbonation of cement blended with calcined clay and limestone result in the coarsening of the porosity. Carbonation of cement paste alters the microstructure, oxygen and moisture availability around the rebar, making the carbonation induced corrosion a debating subject which requires more attention for comprehension. In general observation corrosion rate values obtained for the carbonation induced corrosion are much lower than that obtained under chloride induced environment (Stefanoni et al. 2018). Recent studies by Cabrera et al. 2020, have demonstrated that changing calcined clay to limestone ratio doesn't have much effect on the corrosion rate, although with increasing water to cement ratio, corrosion rate value increases in high relative humidity environment (Figure 9.30).
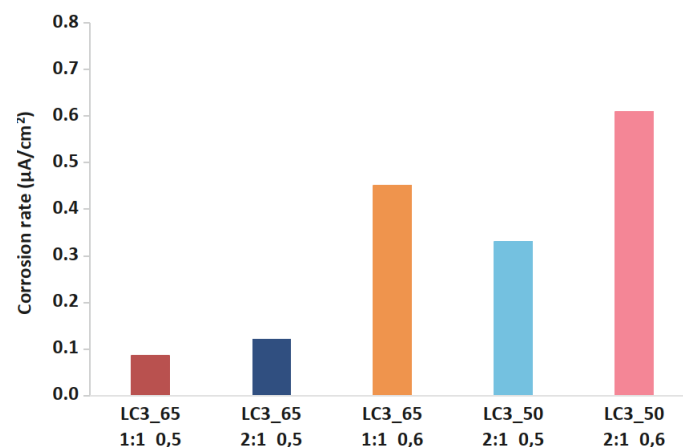
Figure 0-1 Corrosion rate in LC3 mortar at 95% relative humidity (Cabrera et al. 2020)

A study was performed at IIT-Madras for carbonation induced corrosion using 3 electrode method. Open circuit potential and linear polarization resistance values have been obtained for carbonated cementitious systems of OPC, PPC and LC3 (Figure 9.31). Open circuit potential values been observed

to more negative for the SCMs blended systems. Polarisation resistance values were converted to corrosion rate using the Stern-Geary equation. Corrosion rate values obtained in LC^3 system was higher than those obtained in the OPC system. Possible reason for the higher corrosion rate was thought to be because of nature of rust-products formed and pH level at steel-concrete interface.
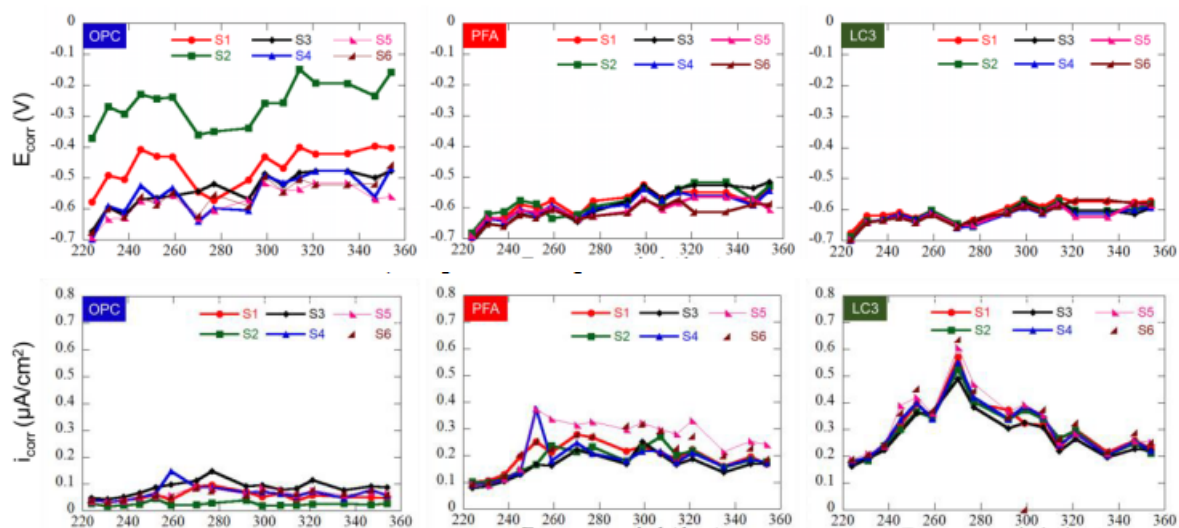
Figure 9.31: Electrochemical measurements in different types of binders

In another recent study, Nguyen and Castel 2020, the performance of reinforced LC^3 concrete specimens was comparable to traditional OPC concrete in corrosion propagation phase, despite the higher resistivity. Although the trends for the open circuit potential have been same in the OPC and LC^3 concrete, however a significant variation had been observed in the Tafel constant which is used to calculate the corrosion rate from the polarization resistance. For LC^3 concrete value of B parameter was observed to be 47 mV, which is higher in comparison with traditionally used value of 26 mV for OPC concrete. Increased value of B can be due to refined pore structure of LC^3 concrete, resulting in slow oxygen renewal at the cathodic site. More data is required to have conclusive comments, still from available literature data it is advisable to have higher cover depths in structure prepared with LC^3 to have an overall sufficient design life.

9.3.2   Chloride induced corrosion

Studies related to chloride ingress have revealed slower chloride ingress and lower chloride threshold values in LC3 cementitious systems. Propagation phase of corrosion is dependent on the oxygen and moisture availability, ionic concentration in the system, cathode and anode distribution over rebar, etc. In recent studies performed at IIT-Madras during S. Rengaraju thesis work, LC^3 blends have been realised to be having high surface resistivity. Inverse polarization resistance obtained for the systems showed low corrosion rates values in LC^3 as compared to OPC and PPC blends (Rengaraju et al. 2019). Furthermore, it had been realised that in highly resistive systems it was difficult to check the onset of corrosion using the linear polarization technique. Results from the alternate wetting and drying cycles of chloride admixed samples are shown in figure 9.32, it can be seen that the inverse polarization resistance rates values obtained were in similar range as compared to ordinary Portland cement.
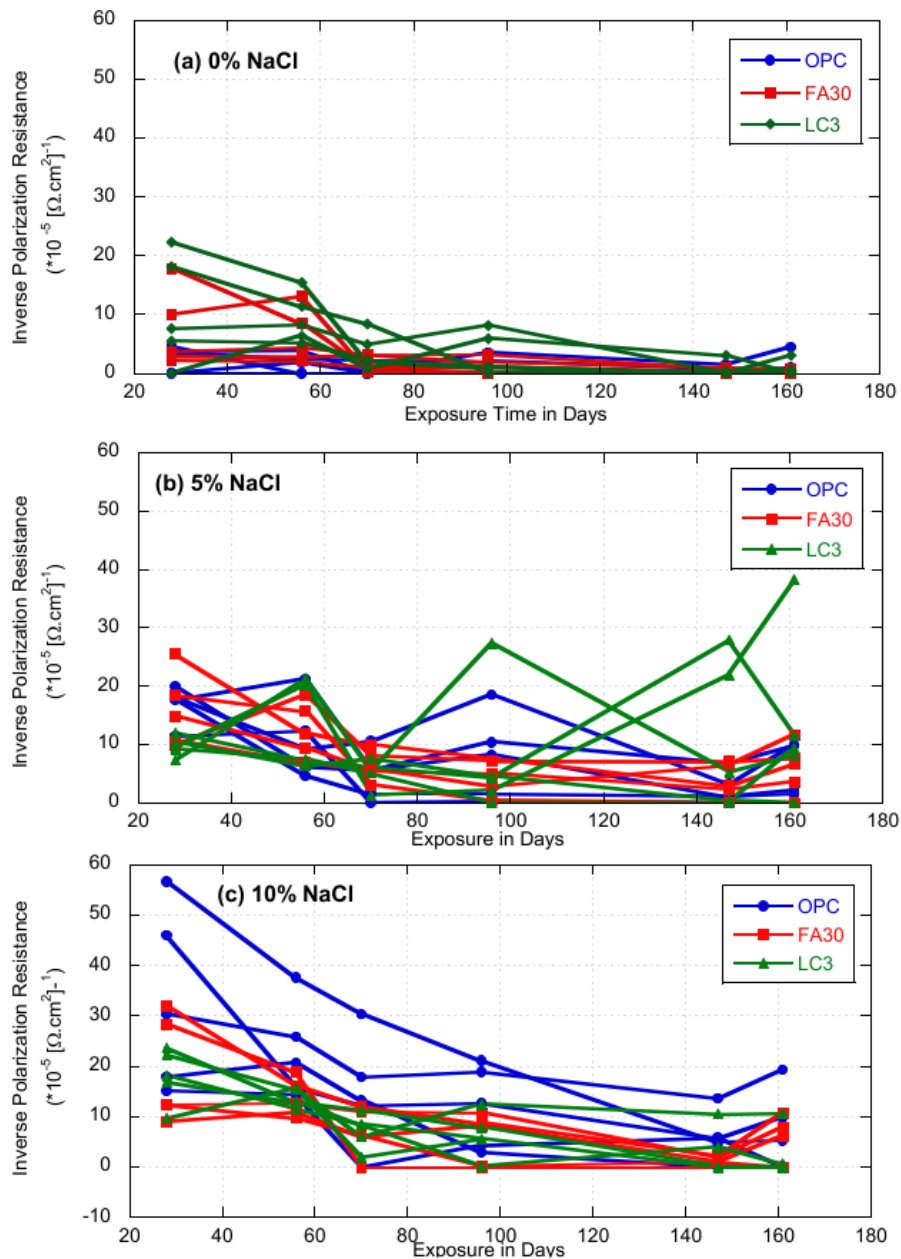
Figure 9.32: Inverse polarization resistance for the samples admixed with different chloride percentage.

In another study by Nguyen and Castel 2020, similar observation has been made that although polarization resistance obtained were higher in LC^3 concrete, consequently propagation phase performance after the re-calibration of Tafel's constant had been found similar or better to the conventional OPC cement (figure 9.33).
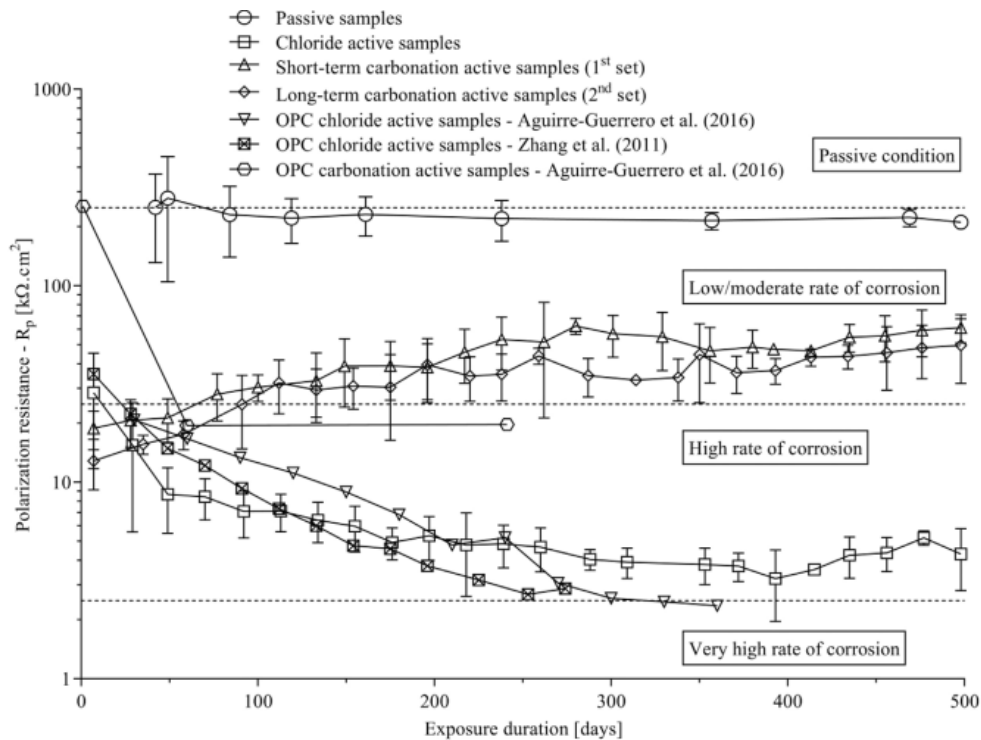
Figure 9.33: Evolution of polarization resistance over time, reference bench marks are as per OPC (Nguyen and Castel 2020)

9.4 Summary

- While LC^3 has higher total porosity than (Ordinary Portland Cement) OPC and (fly-ash based Portland Pozzolanic Cement) PPC, the intrinsic permeability and the RCPT values are significantly lower than OPC and PPC. Mercury intrusion porosimetry (MIP) results have shown that the pores in LC^3 are significantly finer than those in OPC and PPC.

- The carbonation of low-clinker LC^3 is faster than concretes containing cements with higher clinker content such as OPC and PPC. However, the carbonation rates appear to be similar to concretes prepared using other composite cements, such as those containing slag and fly ash, having a similar clinker content.

- Chloride ingress is significantly lower in LC^3 compared to OPC and PPC. While this is primarily due to the lower permeability of LC^3, the higher alumina content in LC^3 also increases chloride binding in the cement.

- Due to the significantly lower alkali content in the cement, expansion due to alkali silica reaction is significantly lower in LC^3, with respect to OPC and PPC. In the case of sulphate attack, it is seen that the performance of the cement is better at lower clinker contents of cement.

- The sulphate resistance of LC^3 mortars is seen to be better than other cements.

Limestone calcined clay cement (LC³) is a blended cement that combines clinker, calcined clay, limestone, and gypsum. It takes advantage of the high reactivity of calcined clay and the synergistic reaction between limestone and clay, offering equivalent mechanical performance to Ordinary Portland Cement (OPC), with the benefit of decreasing clinker factors to 50%. LC³, while retaining the mechanical behaviour of OPC, also significantly improves some relevant properties such as resistance to chloride ingress and alkali silica reaction as compared to other cements. Furthermore, limestone and calcined clays are among the few raw materials available in the quantities required to constitute a technology suitable for coping with the projected worldwide demand for cement.

In addition to these technical advantages of LC³, this technology also allows significant CO^2 emission savings. A detailed assessment of the environmental benefits of the LC³-50 formulation, as compared to OPC, shows that this technology can offer up to 40% CO^2 savings beyond that of the technology used to produce calcined clay and clinker.

However, the advantages of LC³ will not allow for its world- wide propagation if its production does not prove financially attractive. A deciding factor is which cement should be used for the financial benchmark. Since the cement type having the closest performance to LC³ is OPC, the benchmark should be done with cement composed of 95% clinker and 5% gypsum.

10.1 Initial study on economy

The work by Joseph et al. (2016) showed that the financial feasibility of LC³ depended on various factors such as the cost of fuel, the cost of other supplementary cementitious materials, the cost of clinker production, the distance for which the materials are to be transported, etc. An economic feasibility study was carried out from the initial industrial scale production in West Bengal. The production cost of LC³ is compared with OPC and PPC from a cement plant and on a grinding unit. The different factors affecting the economy of LC³ is also in the scope of this study. It is observed that LC³ is far more economical than OPC and it could be more economical than PPC in many scenarios.

Data and assumptions for the study

The Compositions for various cements used for the study have assumed as follows:

- OPC: 95% clinker and 5% gypsum
- PPC: 60% clinker, 35% fly ash and 5% gypsum
- LC³: as 50% clinker, 30% calcined clay, 15% low grade limestone and 5% gypsum (18% weight loss, including moisture, is assumed for calcination of clay)

The cost of materials were provided by Cement companies in India. The electricity requirement for production of clinker and calcination of clay are assumed to be same and the fuel requirement for calcination of clay is assumed to be 50% of clinkering. The electricity requirement for grinding could be lower for LC³ than PPC and OPC, as calcined clay being one of the major raw material need not be ground and a basic grinding would only be needed for the better performance by intergrading. In a large scale production unit, a separate grinding could be made use to get better efficiency for LC³ production. The limestone is assumed to be near by the plant which would be transported by a belt conveyor and other clinkering materials such as iron and alumina base fluxes, gypsum and coal are at a distance of 50, 200 and 500 km. respectively.

Cost Analysis

Comparison of cost of production in a cement plant

The cost of production of OPC, PPC and LC³ is compared and shown in figure 10.1. It is assumed that the source of fly ash and clay is 100 km away from the cement plant and they have been transported by road. It is evident that LC³ is much more economically viable than OPC. The reduction is primarily due to the low clinker factor and the fact that calcination of clay would require much less fuel and electricity compared to production of clinker. Even for a similar thermodynamic system, calcination of clay will have lower heat loss as the generated temperature also is low. As per Newton's law of cooling, the heat loss will be proportional to temperature difference between the surface and the ambient temperature.
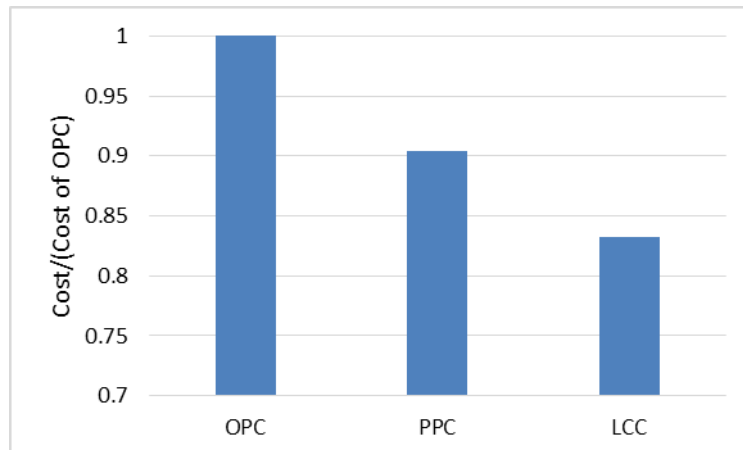
Figure 10.1: Comparison of production cost of PPC and LC³ with OPC

One of the main variables that affects the production cost of PPC is the cost of fly ash available in India which varies from location to location depending on the availability and quality. In this analysis the cost variable of fly ash is coupled with the distance between the source of fly ash and clay from the cement plant. The results have been summarized in figure 10.2. The source of fly ash which is mainly from the thermal power plant could be far away from the cement plants as cement plants would be more concentrating on selecting a site near the limestone deposits. It is evident from this investigation that depending on the locations of cement plant, thermal power plant and clay deposits, irrespective of the cost of fly ashes there could be many possibilities that LC³ could be made cheaper than PPC.

In this analysis, the mode of transportation is selected as road. It must be noted that there is an added advantage of clay over fly ash for the possibility of transporting clay to the cement plant in train, which would be a much cheaper mode of transportation compared to road. Most already existing cement plants will be having a railway line connecting to the plant for the transportation of coal.
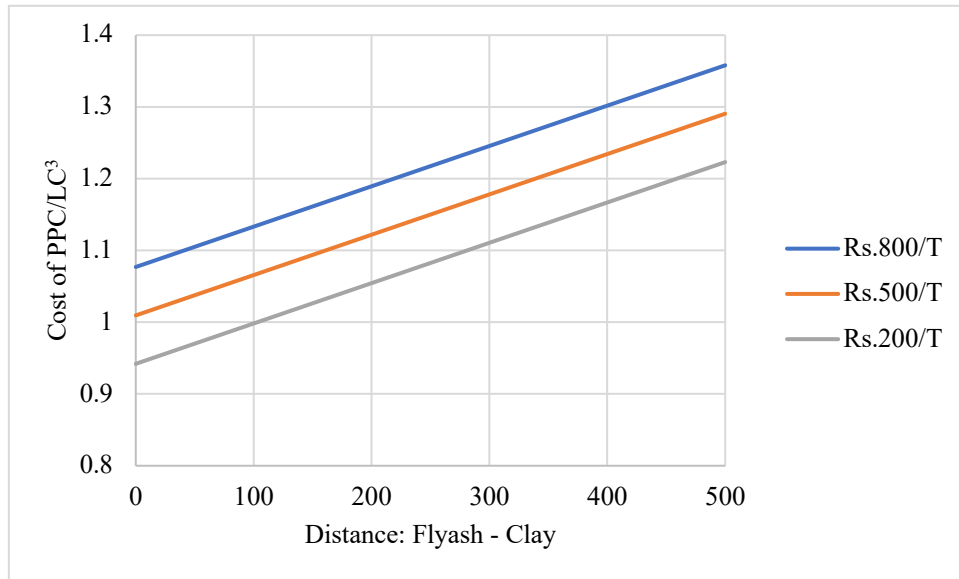
Figure 10.2: Cost comparison between PPC and LC³ with variable cost of fly ash and variable distance of source of fly ash and clay from the cement plant

Effect of clinker factor on the economy between LC³ and PPC

In this scenario, the effect of clinker factor of LC³ is compared with different replacement values of fly ash. For this particular analysis, the cost of fly ash is assumed to be Rs.500/T and both the source of fly ash and clay is at equal distance. The possible clinker factor of LC³ is still not fixed, though 50% is a viable option, however as per the available literature, it would depend on lot of factors from availability of suitable raw materials and the required grade of cement and the recommendations from the standard committee. The percentage replacement of clinker would be an indicative of how much savings this technology could make. From the previous research carried out in EPFL and India, it could be said that a clinker factor as low as 40% can be achieved.

The amount of replacement of clinker by fly ash for PPC also depends on the quality of fly ash. Most fly ashes which are available in India are of lower quality than specified in the standards for replacing clinker and are dumped in ash ponds (Dhadse et al. 2008). There is also a lot of variability in the fly ash properties leading to variation in the performance of concrete (Kaur et al. 2017). Quality of fly ashes could be improved upon processing but would result in higher cost (Bouzoubaâ et al. 1997; Lee et al. 2012; Payá et al. 1995; Shi and Day 2001). Figure 10.3 indicates the savings in LC³ technology compared to PPC especially when the clinker factor of LC³ could be made low.

154
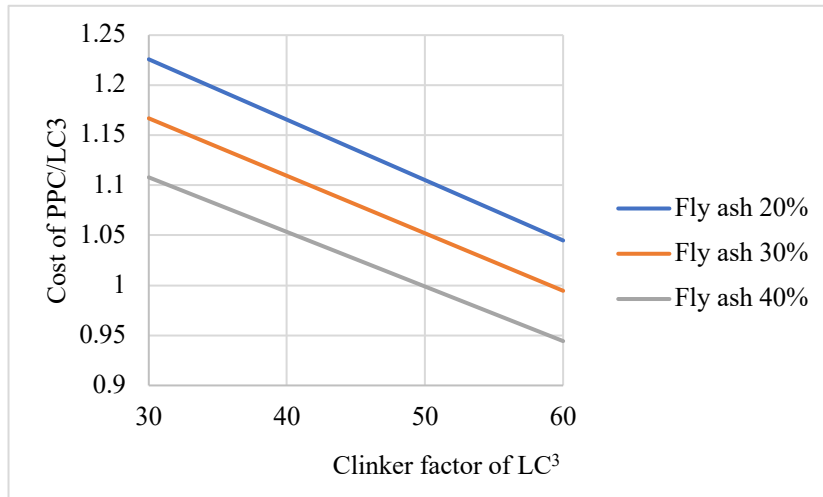
Figure 10.3: Effect of clinker factor of LC³ on the production cost ratio of PPC and LC³ for different fly ash replacement values

Economy for a grinding unit

In the case of a grinding unit, the case is different. The main cost is the cost of clinker which would be as much as double the production cost by including transportation costs. And the most fluctuating factor for the economy would be the cost of calcined clay (see Figure 10.4). Unlike the cement plant, a grinding unit may not be able to acquire clay mines and mine themselves. And the calcination could be also done in some other place and the mode of calcination could be different and the cost of calcination could also vary on the type of calcination used. So in this study, the cost of calcined clay, including transportation is kept varying from Rs.1000/Ton to Rs.3000/Ton.

As the main cost in the grinding unit is the cost of clinker, the cost effectiveness of LC³ and PPC is much higher. So the comparison is only done with PPC and LC³. The analysis done for the part is, a control has been selected with the following assumptions as given below and has been called 'C'. A parameter each is changed viz 'V1', 'V2' and 'V3'. It shows the trend in the variation by changing a single parameter.

Control (C)

OPC	95% clinker, 5% gypsum	
PPC	65% clinker, 30% fly ash, 5% gypsum	
LC³	50% clinker, 30% Calcined Clay, 15% Limestone, 5% gypsum	
Cost	Rs.800/tonne of Fly Ash	

Parameters

C	Control
V1	Clinker Factor of LC³ = 0.35
V2	Cost of Fly Ash = Rs.1500/tonne
V3	Fly ash Replacement = 20%
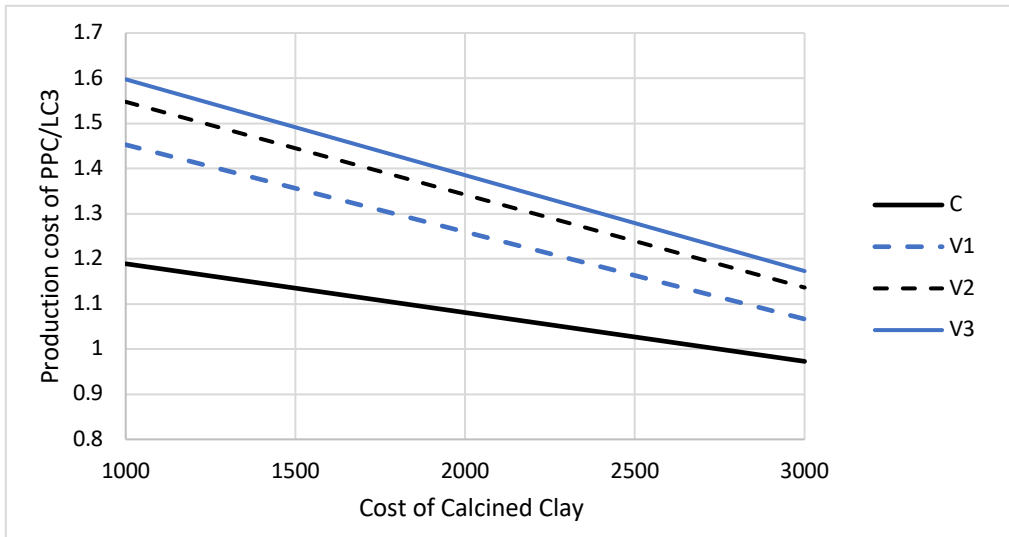
Figure 10.4: Estimation of calcination cost

Grinding units would be more localized in nature and the cost does vary a lot. But what it is evident from this study is that the potential of LC^3 to have an substantial reduction in cost over PPC. The combination of the three could even give higher economy or lower. It shows that for a grinding unit, the potential savings would be much more than that for a cement plant.

Return on Investment

The return on additional investment required due to LC^3 is analysed for different % of savings. It is assumed that the production cost of cement is Rs.1800/T. The savings are given in million $ (Figure).
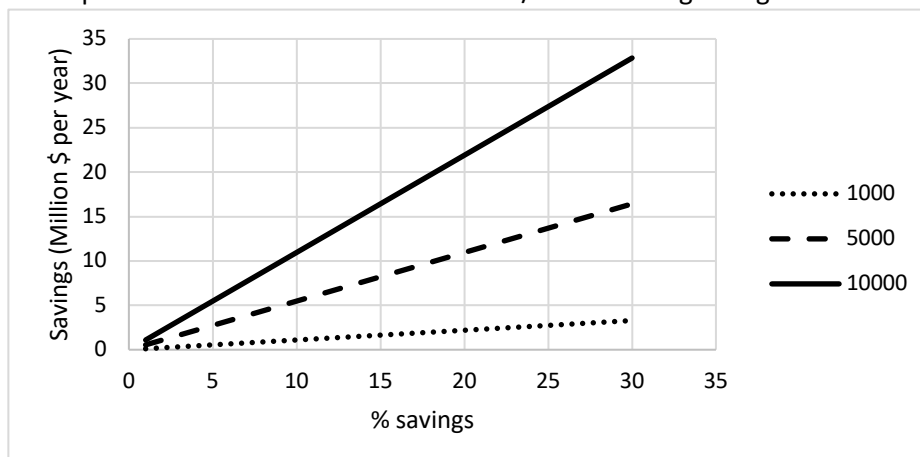
Figure 10.5: Annual savings for different capacities of cement plant

From the data obtained from FLSmidth (LC^3 meeting in Switzerland on 20 December 2013), the cost for a flash calciner to produce calcined clay of capacity 1000tonnes/day is around $24 million (un-negotiated, $12 million for equipment cost and $12 million for installation). With this data, the different scenarios for justification of the additional investment to turn to LC^3 technology is summarized in the Figure 10.6: (for a cement plant of 3300T/day capacity) and for different payback period and different rate of return. It is to be noted that the annual return is kept fixed and is not affected by inflation and growth.
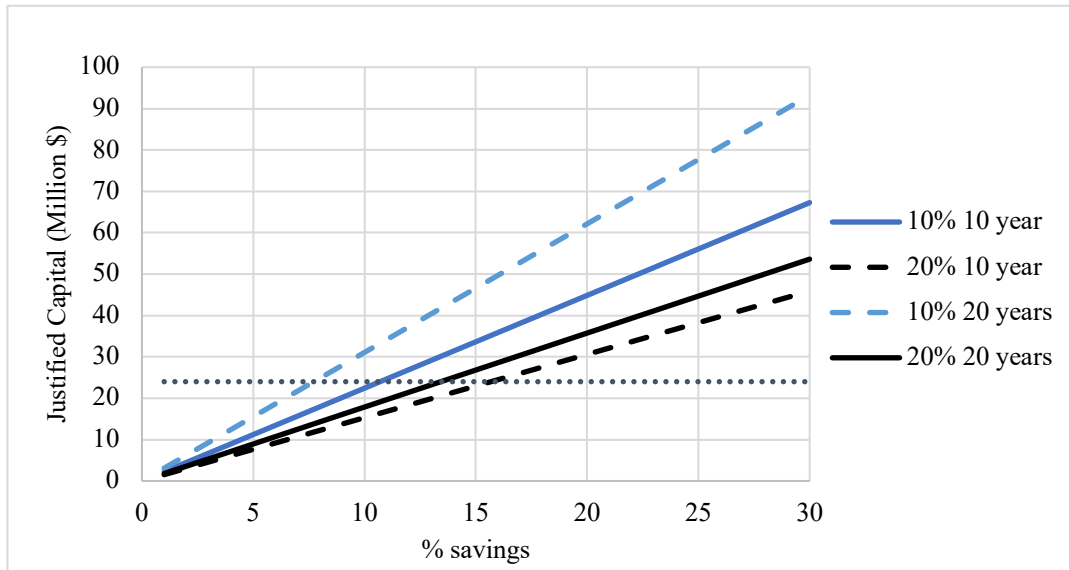
Figure 10.6: Justified capital investment for 3300tonne/day capacity plant for different rate of returns and payback period (dotted line shows the investment required as per FLSmidth)

Factors not considered

Sustainability of cement plant

With low clinker contents in LC^3, the sustainability of cement plant is increased as with the same available resources the cement plant will be able to sustain more years. As the limestone used in LC^3 is of lower quality, the good quality of limestone could be kept as a resource for the future. Which also means that the new installation cost of cement plants which would be needed to relocate when the current resources get depleted will be needed after longer time. Some cement plants invest on fuels which are more costly which would bring down the economy of production cost just to increase the sustainability of their limestone deposits.

Increased capacity

The increased capacity has mainly two advantages. One is that it can generate more profits with the existing equipment and resources and it make sure the additional investment required is waved off for an increased production for the market requirements using the current technology.

Carbon credit

LC^3 ensures less carbon dioxide emissions which could be benefited to the cement industry internationally and nationally with the policies.

Selling cost

The selling cost or the cost required for the marketing is not accounted in this study. This could go either way depending on how public take this cement. Initially the selling cost could be higher and in the long run it could be cheaper with the proven track record.

10.2 Recent study on economy

Three different implementation scenarios were analysed:
  i. An existing integrated cement plant willing to replace some of its OPC production with LC^3
  ii. A grinding station willing to do the same using its imported clinker
  iii. An investor willing to produce LC^3 out of a greenfield grinding station project also with imported clinker.

Flash calciner and rotary kiln were assessed as alternatives for clay calcination. Additionally, the location of a suitable clay close to (10km) or far from (200 km) the production site was considered.

Location significantly impacts project profitability, because cost differential of transport is estimated at USD 13/T of clay. All considered scenarios assume the use of coal; fuel costs, such as diesel, would make LC3 production economically unviable unless such combustion is heavily subsidised. The cost of OPC to be benchmarked with is estimated at USD 30/Ton cement if produced in a cement plant, and USD 47/Ton if produced with imported clinker.

For industrial-scale installation production of calcined clay, three basic scenarios were assumed and the clay's material properties were clearly defined to enable design and dimension the required equipment accordingly.

The three scenarios are as follows:
Scenario 1– Clay thermal processing solution of 960 tons per day (tpd) suitable for 1 mtpa LC^3 cement production. Utilisation, to the greatest extent possible, of infrastructure and production assets at an existing integrated cement production plant, including fuel preparation, integrated cement grinding and inventories.

Scenario 2– Clay thermal processing solution of 400 tpd suit- able for 0.4mtpa LC^3 cement production. Utilisation, to the greatest extent possible, of infrastructure and production assets of an existing cement grinding station, including integrated cement grinding and inventories. A thermal fuel prepa- ration (coal based) grinding plant complete with Just In Time (JIT) dimensioned inventories is provided.

Scenario 3– A 0.4mtpa LC^3 greenfield cement grinding plant which considers a complete clay thermal processing solution, dimensioned for 400tpd, thermal fuel preparation (coal based), and a cement grinding for intergrinding LC^3 cement complete with relevant JIT dimensioned inventories.
The following sub-criteria were considered for each scenario:
- Clay calcination with (1) flash calciner and (2) rotary kiln
- Clay sourcing with (1) clay available close to the production facility and (2) at a distance of 200 km

It is noted that access to low-cost thermal fuel, such as natural gas, would also make Scenario 1 suitable for implementation at a larger capacity stand-alone, or satellite, cement grinding station. The objective of these case studies is to compare LC^3 production cost with OPC. The OPC has been selected because it performs closest to LC^3.

In all scenarios, OPC is considered to be made of 95% clinker and 5% gypsum. For integrated cement plants, both clinker and OPC costs have been estimated based on average pro- duction costs in emerging countries.
- Estimated cash production clinker: USD 23.9 /T
- Estimated cash production cost OPC: USD 30.0 /T
- In the absence of clinker production an average import price for clinker has been estimated.
- Estimated import cost clinker: USD 40.0 /T delivered
- Estimated cash production cost OPC with imported clinker: USD 47.0 /T

LC^3 is made of 50% clinker, 30% calcined clay, 15% limestone and 5% gypsum. Other assumptions include:
- Kaolinite content in clay: minimum 40%
- Particle size: < 25mm
- Moisture content: < 12%
- Calcination temperature of clay: 800°C

Fuel: All scenarios are based on coal as the combustible, with a delivered cost of USD 80 per ton coal and a lowest heat value of 26 MJ /kg. If petcoke is used for clinker production in the integrated cement plant, either an additional, easy to burn "ignition fuel" must be used, and thus guarantee safe ignition and complete petcoke combustion in the clay calcining system, or a separate grinding of petcoke solid fuels with easier ignition behaviour. Due to higher volatilities, including additional equipment like storage bins should be considered, particularly if available secondary air temperatures are low because of low system recuperation efficiency of the from the hot finished product. Other fuel types like natural gas and diesel could be considered, but unless these are heavily subsidised their international market price makes LC^3 production less financially attractive when compared to OPC.

- Limestone is assumed at USD 2.8 /T limestone (poor quality or reject limestone from existing quarry)
- Gypsum cost: USD 20 /T gypsum

NOTE: These scenarios are only estimations. They are based on average numbers applicable in emerging countries. These numbers should be revised on a case per case basis. However, the overall conclusion remains valid in most cases except two:

- If very cheap mineral components, like natural Pozzolanic material, fly ash, or slag, available at competitive cost, or
- If clay is located more than 200 km from the plant.

Profitability compares producing LC^3 with OPC. This indirectly implies that the sales price of LC^3 is aligned to the sales price of OPC.
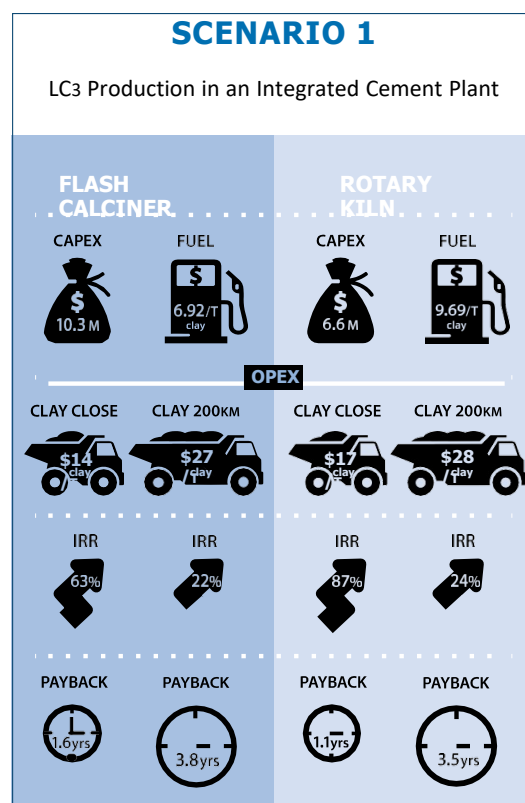
Scenario 1: LC^3 Production in an Integrated Cement Plant

SCENARIO 2

LC3 Production in a Grinding Plant

FLASH CALCINER . . . . **ROTARY KILN** . . . . . .

FLASH CALCINER		ROTARY KILN	
CAPEX	FUEL	CAPEX	FUEL
$8.15M	8.65/T clay	$6.1M	10.4/T clay

OPEX

CLAY CLOSE	CLAY 200km	CLAY CLOSE	CLAY 200km
$16.5/clay	$29/clay	$18/clay	$31/T.
IRR	IRR	IRR	IRR
75%	55%	98%	71%
PAYBACK	PAYBACK	PAYBACK	PAYBACK
1.3yrs	1.8yrs	1yr	1.4yrs
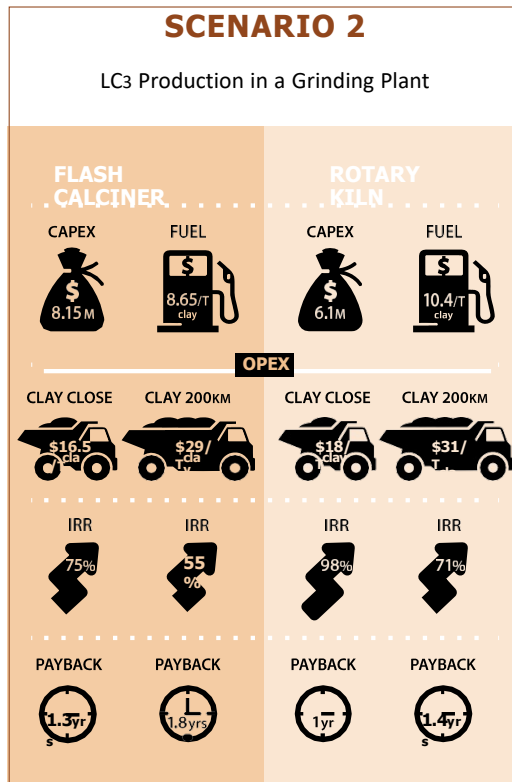
Scenario 2: LC³ produced in a Grinding Station Plant

SCENARIO 3

LC3 Production in a Greenfield

FLASH CALCINER . . . . **ROTARY KILN** . . . . . .

FLASH CALCINER		ROTARY KILN	
CAPEX	FUEL	CAPEX	FUEL
$27M	8.65/T clay	$26M	10.4/T clay

OPEX

CLAY CLOSE	CLAY 200km	CLAY CLOSE	CLAY 200km
$16/clay	$29/clay	$18/clay	$31/clay
IRR	IRR	IRR	IRR
17%	9%	17%	9%
PAYBACK	PAYBACK	PAYBACK	PAYBACK
4.4yr	6yrs	4.4yr	6yrs
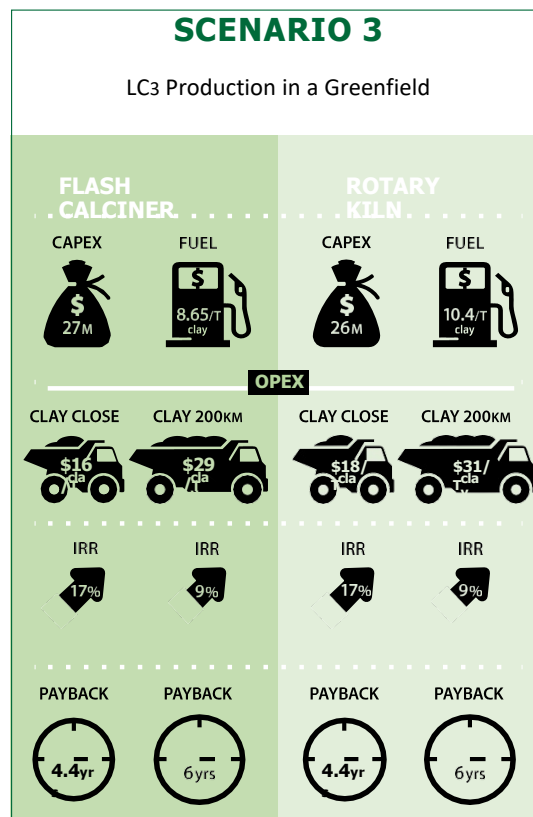
Scenario 3: Greenfield for Production of Calcined Clay and Cement

LC^3 has been used in many different regions and different scales in India and aborad. Several trial productions of LC^3 ranging from a few tens of tonnes, to thousands of tonnes of LC^3 have been carried out around the world. In these trails, the calcination was carried out using different technologies such as a muffle furnace, and small and large cement kilns. In some of the productions, clinker kilns were temporarily used for the calcination of clays. Fuels of various types such as coal, petcoke, biomass, furnace oil and diesel have been used in these trials. Grinding of the cements has been carried out using ball mills and vertical roller mills of various types. After the production of cement at each of these trials, the cement has been used to build various demonstration structures. The key learning from these trials was that LC^3 can replace any cement on the site, without any prior retraining of the construction workers. Minor modifications in the mixture design may be required to take into account the local weather and materials.

Some of the projects where LC^3 has been used in India and abroad are listed below.

i. In India, the first practical project of LC^3 was the model house in Jhansi in 2014. This house is made up of 98% LC^3 and it used 26.6t of industrial waste i.e., 192kg/sqm and saved 15.5t of CO$_2$ i.e., 114kg/sqm. This house is being continuously monitored to assess corrosion of reinforecement and the behaviour of the concrete in hot climates.

LC^3 house in Orchha, Madhya Pradesh, India

ii. The other prominent application of LC^3 in India was done at the offices of the Swiss Agency for Development and Cooperation in the compound of the Swiss Embassy in Delhi in 2017. The walls of this building were built using autoclave aerated concrete blocks produced using LC^3 at the JK Lakshmi AAC block plant at Jhajjhar, Haryana.

Office of the Swiss Agency for Development and Cooperation at Swiss Embassy, New Delhi, India

iii. LC³ has also been used to construct a 75m long road at TARA campus in Ghitorni, New Delhi. This road was constructed in the year 2016 and to this date the performance has been exceptional and no visible signs of degradation on this road have been seen.

Road built at Ghittorni, New Delhi, India

iv. Road built at the truck exit gate of the JK Lakshmi Cement plant, Jhajjhar, Haryana using LC³ produced in a trial at the same cement plant in 2017. The road is being regularly monitored and despite the heavy traffic over it, there are no signs of cracking or abrasion in this road. A picture of the pavement after 5 years of use can be seen below. The segment cast using LC³ is in the middle and the abrasion in the adjoining panels of the pavement can be compared with the lack of abrasion in the panel made using LC³.

Road being built at the truck exit gate of JK Lakshmi cement plant

A comparison of the lack of abrasion in the road panel in the middle produced using LC^3 with the panel using other cement

v.   A small check-dam was built using LC^3 produced at a cement plant in western India at the Orchha facility of TARA in 2018. The dam is being monitored and has shown no sign of deterioration in the last 3 years.

Check-dam built at Orchha by TARA

vi.   A pavement was built using LC^3 in Leh, Ladakh, India jointly by IIT Madras and TARA in 2018. This pavement is exposed to extreme cold conditions. The pavement was inspected in 2022 and no signs of deterioration due to freeze-thaw were found.

Inspection of pavement made using LC^3 in Leh, Ladakh, India

vii.   Our project partners at Indian Institute of Technology, Madras (IIT-M) constructed a sea-side structure using LC^3 at a place near the coast of Chennai. The objective of constructing this structure is to study the impact of seawater on the performance of LC^3.

viii.   In 2022, IIT-M project team has developed tetropods which will be placed at a breakwater structure near Kudankulam nuclear power plant in Tamil Nadu, India. Tetropods of sizes ranging from 2 tons to 20 tons have been developed using a mixture of 70% PPC and 30% LC^2.

Tetrapods made using LC^3 by IIT Madras team

i. In Latin America, several applications of LC^3 have been built. These applications are mainly in Cuba but also present in some other countries. Amongst those applications is a LC^3 house, testing sites in the sea, art sculptures and pavements.

A small cabin made using LC^3 in Cuba

A house made using LC^3 in Cuba

A pavement made using LC^3 in Cuba

Artwork using LC^3 in Cuba

Use of LC^3 in industrial casting in Cuba

LC^3 has been used in many more applications around the world. This chapter lists only a few of these applications of various types so as to demonstrate that LC^3 can be used in all types of applications where other cements can be used.

References

A. G. A. Saul. "Principles underlying the steam curing of concrete at atmospheric pressure." *Magazine of concrete research 2, no. 6, (*1951): 127-140*.*

Achparaki, M., Thessalonikeos, E., Tsoukali, H., Mastrogianni, O., Zaggelidou, E., Chatzinikolaou, F., J. Poesen Additional. "Basics of Clay Minerals and Their Characteristic Properties ", (2012).

Ait-Akbour, Rachid, Pascal Boustingorry, Fabrice Leroux, Frédéric Leising, and Christine Taviot-Guého. "Adsorption of PolyCarboxylate Poly (ethylene glycol)(PCP) esters on Montmorillonite (Mmt): Effect of exchangeable cations (Na+, Mg2+ and Ca2+) and PCP molecular structure." *Journal of Colloid and Interface Science* 437, (2015): 227-234.

Akhlaghi, Omid, Tunahan Aytas, Buse Tatli, Dilek Sezer, Amin Hodaei, Aurélie Favier, Karen Scrivener, Yusuf Z. Menceloglu, and Ozge Akbulut. "Modified poly (carboxylate ether)-based superplasticizer for enhanced flowability of calcined clay-limestone-gypsum blended Portland cement." *Cement and Concrete Research* 101, (2017): 114-122.

Alexandra, Coșa, Hegheș Bogdan, Negruțiu Camelia, and Kiss Zoltan. "Mix design of self-compacting concrete with limestone filler versus fly ash addition." *Procedia Manufacturing* 22, (2018): 301-308.

Almenares, R. S., Vizcaíno, L. M., Damas, S., Mathieu, A., Alujas, A., and Martirena, F. "Industrial calcination of kaolinitic clays to make reactive pozzolans". *Case Studies in Construction Materials*, (2017): 225–232.

Alujas, A., Roger, D., Reyes, S. A., Hanein, T., Irassar, E. F., Juenger, M., … Santos, K. "Properties and occurrence of clay resources for use as supplementary cementitious materials : a paper of RILEM TC 282-CCL". *Materials and Structures*, *2*, (2022).

Alujas, Adrian, Rodrigo Fernández, Rafael Quintana, Karen L. Scrivener, and Fernando Martirena. "Pozzolanic reactivity of low grade kaolinitic clays: Influence of calcination temperature and impact of calcination products on OPC hydration." *Applied Clay Science* 108, (2015): 94-101.

Analysis of Cementitious Materials, (2018): doi:10.1201/b19074.

Angst, Ueli, Bernhard Elsener, Claus K. Larsen, and Øystein Vennesland. "Critical chloride content in reinforced concrete—A review." *Cement and concrete research* 39, no. 12 (2009): 1122-1138

Antoni, Mr, J. Rossen, F. Martirena, and K. Scrivener. "Cement substitution by a combination of metakaolin and limestone." *Cement and concrete research* 42, no. 12 (2012): 1579-1589.

ASTM Standard C595. Standard specification for blended hydraulic cements. West Conshohocken, PA: ASTM International, (2012)

Avet, F. "Investigation of the grade of calcined clays used as clinker substitute in Limestone Calcined Clay Cement (LC^3)". *8143*, (2017): 169.

Avet, F., Snellings, R., Alujas Diaz, A., Ben Haha, M., and Scrivener, K. "Development of a new rapid, relevant and reliable (R3) test method to evaluate the pozzolanic reactivity of calcined kaolinitic clays". *Cement and Concrete Research*, *85*, (2016):1–11.

Avet, François, and Karen Scrivener. "Investigation of the calcined kaolinite content on the hydration of Limestone Calcined Clay Cement (LC^3)." *Cement and Concrete Research* 107 (2018): 124-135.

Avet, François, Emmanuelle Boehm-Courjault, and Karen Scrivener. "Investigation of CASH composition, morphology and density in Limestone Calcined Clay Cement (LC^3)." *Cement and Concrete Research* 115 (2019): 70-79.

Batis, G., P. Pantazopoulou, S. Tsivilis, and E. Badogiannis. "The effect of metakaolin on the corrosion behavior of cement mortars." *Cement and concrete composites* 27, no. 1 (2005): 125-130.

Bazant, Zdenek Pavel, MIlan Jirasek, M. H. Hubler, and Ignacio Carol. "RILEM draft recommendation: TC-242-MDC multi-decade creep and shrinkage of concrete: material model and structural analysis. Model B4 for creep, drying shrinkage and autogenous shrinkage of normal and high-strength concretes with multi-decade applicability." *Materials and structures* 48, no. 4 (2015): 753-770.

Bederina, Madani, Zoubir Makhloufi, and Tayeb Bouziani. "Effect of limestone fillers the physic-mechanical properties of limestone concrete." *Physics Procedia* 21 (2011): 28-34.

Bentz, Dale P., Ahmad Ardani, Tim Barrett, Scott Z. Jones, Didier Lootens, Max A. Peltz, Taijiro Sato, Paul E. Stutzman, Jussara Tanesi, and W. Jason Weiss. "Multi-scale investigation of the performance of limestone in concrete." *Construction and Building Materials* 75 (2015): 1-10.

Bergaya, F., and Lagaly, G. "General Introduction : Clays , Clay Minerals , and Clay Science". *5*, (2013): 1–19.

Bishnoi, S., Maity, S., Mallik, A., Joseph, S., and Krishnan, S. "Pilot scale manufacture of limestone calcined clay cement : The Indian experience". *Indian Concrete Journal*, *88*(7), (2014): 22–28.

Bishnoi, S. "RILEM Bookseries Calcined Clays for Sustainable Concrete Proceedings of the 3rd International Conference on Calcined Clays for Sustainable Concrete".(2020).

Bissonnette, Benoît, Pascale Pierre, and Michel Pigeon. "Influence of key parameters on drying shrinkage of cementitious materials." *Cement and Concrete Research* 29, no. 10 (1999): 1655-1662.

Blatt H, Middleton GV, and Murray RC. "Origin of sedimentary rocks". Prentice Hall, Englewood Cliffs, N.J., United States, (1972)

Bonavetti, V. L., V. F. Rahhal, and E. F. Irassar. "Studies on the carboaluminate formation in limestone filler-blended cements." *Cement and Concrete Research* 31, no. 6 (2001): 853-859.

Bratoev, B., Doykov, I., Ninov, J., and Lenchev, A. "Pozzolanic activity assessment of calcined clays with complex minerals content". *Advances in Cement Research*, *30*(3), (2018): 103–112.

Brooks, J. J., and MA Megat Johari. "Effect of metakaolin on creep and shrinkage of concrete." *Cement and concrete composites* 23, no. 6 (2001): 495-502.

Cabrera, Elizabeth, Adrián Alujas, Bernhard Elsener, and Jose Fernando Martirena-Hernandez. "Preliminary Results on Corrosion Rate in Carbonated LC^3 Concrete." In *Proceedings of the International Conference of Sustainable Production and Use of Cement and Concrete*, pp. 293-298. Springer, Cham, (2020).

Camiletti, Jessica, Ahmed M. Soliman, and Moncef L. Nehdi. "Effect of nano-calcium carbonate on early-age properties of ultra-high-performance concrete." *Magazine of Concrete Research* 65, no. 5 (2013): 297-307.

Canbek, Oğulcan, Newell R. Washburn, and Kimberly E. Kurtis. "Relating LC³ microstructure, surface resistivity and compressive strength development." *Cement and Concrete Research* 160 (2022): 106920.

Carr, D. D., and L. F. Rooney. "Limestone and dolomite in Industrial Minerals and Rocks: American Institute of Mining." *Metallurgical and Petroleum Engineers* (1975): 757-789.

Cassagnabère, Franck, Paco Diederich, Michel Mouret, Gilles Escadeillas, and M. Lachemi. "Impact of metakaolin characteristics on the rheological properties of mortar in the fresh state." *Cement and Concrete Composites* 37 (2013): 95-107.

Castellote, Marta, Lorenzo Fernandez, Carmen Andrade, and Cruz Alonso. "Chemical changes and phase analysis of OPC pastes carbonated at different CO_2 concentrations." *Materials and Structures* 42, no. 4 (2009): 515-525.

Cedria, T. B., and Hammam, B. P. "Evolution of thermal transformation of tunisian kaolinite". (2009): 70–77.

Chakraborty, A. K. "Phase transformation of kaolinite clay*.*" (2014):(Vol. 9788132211).

Chappex, Théodore, and Karen Scrivener. "Alkali fixation of C–S–H in blended cement pastes and its relation to alkali silica reaction." *Cement and Concrete Research* 42, no. 8 (2012): 1049-1054.

Chowaniec, Olga. *Limestone addition in cement*. No. THESIS. EPFL, (2012).

CSA A3001. Cementitious materials for use in concrete. Toronto, Ontario: Canadian Standards Association, (2008)

Cyr, Martin, Philippe Lawrence, and Erick Ringot. "Efficiency of mineral admixtures in mortars: Quantification of the physical and chemical effects of fine admixtures in relation with compressive strength." *Cement and concrete research* 36, no. 2 (2006): 264-277.

Dhandapani, Yuvaraj, and Manu Santhanam. "Assessment of pore structure evolution in the limestone calcined clay cementitious system and its implications for performance." *Cement and Concrete Composites* 84 (2017): 36-47.

Dhandapani, Yuvaraj, Shiju Joseph, Shashank Bishnoi, Wolfgang Kunther, Fragkoulis Kanavaris, Taehwan Kim, Edgardo Irassar et al. "Durability performance of binary and ternary blended cementitious systems with calcined clay: a RILEM TC 282 CCL review." *Materials and Structures* 55, no. 5 (2022): 1-29.

Dhandapani, Yuvaraj, T. Sakthivel, Manu Santhanam, Ravindra Gettu, and Radhakrishna G. Pillai. "Mechanical properties and durability performance of concretes with Limestone Calcined Clay Cement (LC³)." *Cement and Concrete Research* 107 (2018): 136-151.

Dhir, R. K., M. C. Limbachiya, M. J. McCarthy, and A. Chaipanich. "Evaluation of Portland limestone cements for use in concrete construction." *Materials and structures* 40, no. 5 (2007): 459-473.

Ding, Jian-Tong, and Zongjin Li. "Effects of metakaolin and silica fume on properties of concrete." *Materials Journal* 99, no. 4 (2002): 393-398.

Donatello, S., Tyrer, M., and Cheeseman, C. R. "Comparison of test methods to assess pozzolanic activity". *Cement and Concrete Composites*, *32*(2), (2010):121–127.

Drits VA, Besson G and Muller F. "An improved model for structural transformations of heat-treated aluminous dioctahedral 2:1 layer silicates". *Clays Clay Minerals* 43 (1995): 718–731.

Elgalhud, Abdurrahman A., Ravindra K. Dhir, and Gurmel Ghataora. "Limestone addition effects on concrete porosity." *Cement and Concrete Composites* 72 (2016): 222-234.

Emmanuel, A., Halder, P., Joseph, Maity, S. & and., Bishnoi, S. (2016). "Second pilot production of limestone calcined clay cement in India". *Indian Concrete Journal*, *90*(11), (2016): 22–27.

Escalante-Garcıa, J. I., and J. H. Sharp. "The microstructure and mechanical properties of blended cements hydrated at various temperatures." *Cement and Concrete Research* 31, no. 5 (2001): 695-702.

European Committee for Standardization EN 197-1, ''Cement – part 1'', composition, specifications and uniformity criteria for common cements, Brussels, Belgium, (2000).

Favier, A.; Scrivener, K. Alkali silica reaction and sulfate attack: expansion of limestone calcined clay cement. En *Calcined Clays for Sustainable Concrete*. Springer, Dordrecht, (2018): 165-169.

Favier, Aurélie R., Cyrille F. Dunant, and Karen L. Scrivener. "Alkali–silica reaction mitigating properties of ternary blended cement with calcined clay and limestone." *Calcined Clays for Sustai nable Concrete* (2015): 577-578.

Fernandez R, Martirena F and Scrivener KL. "The origin of the pozzolanic activity of calcined clay minerals: a comparison between kaolinite, illite and montmorillonite". *Cement and Concrete Research* 41 (2011) :113–122.

Fitos,M., Badogiannis, E.G.,Tsivilis, S.G.,and Perraki, M., "Pozzolanic activity of thermally and mechanically treated kaolins of hydrothermal origin", *Applied Clay Science*. (2015):116–117, 182–192.

Frías, M., Rodríguez, O., Vegas, I., & Vigil, R. "Properties of calcined clay waste and its influence on blended cement behavior". *Journal of the American Ceramic Society*, *91*(4),(2008): 1226–1230.

Gallucci, E., X. Zhang, and Karen L. Scrivener. "Effect of temperature on the microstructure of calcium silicate hydrate (CSH)." *Cement and Concrete Research* 53 (2013): 185-195.

Garg N and Skibsted J. "Thermal activation of a pure montmorillonite clay and its reactivity in cementitious systems". *The Journal of Physical Chemistry* 118 (2014):11464–11477.

Gesoğlu, Mehmet, Erhan Güneyisi, Mustafa E. Kocabağ, Veysel Bayram, and Kasım Mermerdaş. "Fresh and hardened characteristics of self-compacting concretes made with combined use of marble powder, limestone filler, and fly ash." *Construction and Building Materials* 37 (2012): 160-170.

Groves, Geoffrey W., Adrian Brough, Ian G. Richardson, and Christopher M. Dobson. "Progressive changes in the structure of hardened C3S cement pastes due to carbonation." *Journal of the American Ceramic Society* 74, no. 11 (1991): 2891-2896.

Güneyisi, Erhan, Mehmet Gesoğlu, and Kasım Mermerdaş. "Improving strength, drying shrinkage, and pore structure of concrete using metakaolin." *Materials and structures* 41, no. 5 (2008): 937-949.

Gupta, J. Sen, & Rao, A. V. R. "Production of clay pozzolana by fluidized bed technique". *Transactions of the Indian Ceramic Society*, *37*(4), (1978):165–171.

Hanpongpun W. and Scrivener K. "The effect of curing temperature on the properties of limestone calcined clay cement (LC^3)" *Calcined Clays for Sustainable Concrete,* RILEM 25 (2020): 293-298.

Hemalatha, M. S., and Santhanam, M. "Characterizing supplementary cementing materials in blended mortars". *Construction and Building Materials*, *191*, (2018): 440–459.

Hollanders, S., Adriaens, R., Skibsted, J., Cizer, Ö., and Elsen, J. "Pozzolanic reactivity of pure calcined clays". *Applied Clay Science*, *132–133*, (2016):552–560.

Huang, Y., Deng, J., Wang, W., Feng, Q., and Xu, Z. "Preliminary investigation of pozzolanic properties of calcined waste kaolin". *24*(2), (2018): 177–184.

Indian Bureau of Mines. (2014). "Part-III: Mineral Reviews." Indian Minerals Yearbook 2012

Ipavec, Andrej, Roman Gabrovšek, Tomaž Vuk, Venčeslav Kaučič, Jadran Maček, and Anton Meden. "Carboaluminate phases formation during the hydration of calcite-containing Portland cement." *Journal of the American Ceramic Society* 94, no. 4 (2011): 1238-1242.

Irassar, E. F. "Sulfate attack on cementitious materials containing limestone filler—A review." *Cement and Concrete Research* 39, no. 3 (2009): 241-254.

Jeknavorian, A. A., L. Jardine, C. C. Ou, H. Koyata, and K. Folliard. "Interaction of superplasticizers with clay-bearing aggregates." *Special Publication* 217 (2003): 143-160.

Jiang, Guang, Zhidan Rong, and Wei Sun. "Effects of metakaolin on mechanical properties, pore structure and hydration heat of mortars at 0.17 w/b ratio." *Construction and Building Materials* 93 (2015): 564-572

Kakali, G., S. Tsivilis, E. Aggeli, and M. Bati. "Hydration products of C3A, C3S and Portland cement in the presence of CaCO$_3$." *Cement and concrete Research* 30, no. 7 (2000): 1073-1077.

Kawashima, Shiho, Mohend Chaouche, David J. Corr, and Surendra P. Shah. "Influence of purified attapulgite clays on the adhesive properties of cement pastes as measured by the tack test." *Cement and Concrete Composites* 48 (2014): 35-41.

Kawashima, Shiho, Mohend Chaouche, David J. Corr, and Surendra P. Shah. "Rate of thixotropic rebuilding of cement pastes modified with highly purified attapulgite clays." *Cement and concrete research* 53 (2013): 112-118.

Khan, Mohammad SH, Quang Dieu Nguyen, and Arnaud Castel. "Performance of limestone calcined clay blended cement-based concrete against carbonation." *Advances in Cement Research* 32, no. 11 (2020): 481-491.

Kim, J-K., Y-H. Moon, and S-H. Eo. "Compressive strength development of concrete with different curing time and temperature." *Cement and Concrete Research* 28, no. 12 (1998): 1761-1773.

Kim, Taehwan, and Jan Olek. "The effects of lithium ions on chemical sequence of alkali-silica reaction." *Cement and Concrete Research* 79 (2016): 159-168.

Klemm, Waldemar A., and Lawrence D. Adams. *An investigation of the formation of carboaluminates*. West Conshohocken: ASTM International, (1990).

Krishnan, Sreejith, and Shashank Bishnoi. "A numerical approach for designing composite cements with calcined clay and limestone." *Cement and Concrete Research* 138 (2020): 106232.

Krishnan, Sreejith, Arun C. Emmanuel, and Shashank Bishnoi. "Hydration and phase assemblage of ternary cements with calcined clay and limestone." *Construction and Building Materials* 222 (2019): 64-72.

Krishnan, Sreejith. "Hydration and microstructure development in limestone calcined clay cement." PhD diss., IIT Delhi, 2019.

Lázaro, B. B."Halloysite and kaolinite: two clay minerals with geological and technological importance", (2015):7–38.

Leemann, Andreas, and Fabrizio Moro. "Carbonation of concrete: the role of CO_2 concentration, relative humidity and CO_2 buffer capacity." *Materials and Structures* 50, no. 1 (2017): 1-14.

Leemann, Andreas, Peter Nygaard, Josef Kaufmann, and Roman Loser. "Relation between carbonation resistance, mix design and exposure of mortar and concrete." *Cement and Concrete Composites* 62 (2015): 33-43.

Lei, L., and J. Plank. "A study on the impact of different clay minerals on the dispersing force of conventional and modified vinyl ether based polycarboxylate superplasticizers." *Cement and concrete research* 60 (2014): 1-10.

Lei, L., and J. Plank. "Synthesis, working mechanism and effectiveness of a novel cycloaliphatic superplasticizer for concrete." *Cement and Concrete Research* 42, no. 1 (2012): 118-123.

Lei, Lei, and Johann Plank. "Synthesis and properties of a vinyl ether-based polycarboxylate superplasticizer for concrete possessing clay tolerance." *Industrial & Engineering Chemistry Research* 53, no. 3 (2014): 1048-1055.

Li, Chang, Jason H. Ideker, and Thanos Drimalas. "The efficacy of calcined clays on mitigating alakli-silica reaction (ASR) in mortar and its influence on microstructure." In *Calcined clays for sustainable concrete*, Springer, Dordrecht, (2015): 211-217.

Li, Ran, Lei Lei, Tongbo Sui, and Johann Plank. "Approaches to achieve fluidity retention in low-carbon calcined clay blended cements." *Journal of Cleaner Production* 311 (2021): 127770.

Li, Ran, Lei Lei, Tongbo Sui, and Johann Plank. "Effectiveness of PCE superplasticizers in calcined clay blended cements." *Cement and Concrete Research* 141 (2021): 106334.

Li, X., Snellings, R., Antoni, M., Alderete, N. M., Ben Haha, M., Bishnoi, S., … Scrivener, K. L. "Reactivity tests for supplementary cementitious materials: RILEM TC 267-TRM phase 1". *Materials and Structures, 51,* (2018):6.

Lorentz, Brandon, Hai Zhu, Dhanushika Mapa, Kyle A. Riding, and Abla Zayed. "Effect of clay mineralogy, particle size, and chemical admixtures on the rheological properties of CCIL and CCI/II Systems." In *Calcined Clays for Sustainable Concrete*, Springer, Singapore, (2020):211-218

Lothenbach, Barbara, Karen Scrivener, and R. D. Hooton. "Supplementary cementitious materials." *Cement and concrete research* 41, no. 12 (2011): 1244-1256.

Lothenbach, Barbara, Thomas Matschei, Göril Möschner, and Fred P. Glasser. "Thermodynamic modelling of the effect of temperature on the hydration and porosity of Portland cement." *Cement and Concrete Research* 38, no. 1 (2008): 1-18.

Ma, Yihan, Caijun Shi, Lei Lei, Shengnan Sha, Beibei Zhou, Yi Liu, and Yuchong Xiao. "Research progress on polycarboxylate based superplasticizers with tolerance to clays-a review." *Construction and Building Materials* 255 (2020): 119386.

Mackenzie, R. C., and Caillere, S. "The Thermal Characteristics of Soil Minerals and the Use of These Characteristics in the Qualitative and Quantitative Determination of Clay Minerals in Soils", (1975): 529–571.

Maraghechi, Hamed, Francois Avet, Hong Wong, Hadi Kamyab, and Karen Scrivener. "Performance of Limestone Calcined Clay Cement (LC^3) with various kaolinite contents with respect to chloride transport." *Materials and structures* 51, no. 5 (2018): 1-17.

Martirena, F., Almenares, R., Zunino, F., Alujas, A., and Scrivener, K. "Color control in industrial clay calcination". *RILEM Technical Letters*, *5*, (2020): 1–7.

Martirena, Fernando, Ernesto Díaz, Dayran Rocha, Hamed Maraghechi, and Karen Louise Scrivener. "Performance of Concrete Made with a Calcined Clay–Limestone-Portland Cement Exposed to Natural Conditions." (2019).

Matschei, Thomas, B. Lothenbach, and Fredrik P. Glasser. "The role of calcium carbonate in cement hydration." *Cement and concrete research* 37, no. 4 (2007): 551-558.

Mbey, J. A., Thomas, F., Razafitianamaharavo, A., Caillet, C., and Villiéras, F. "A comparative study of some kaolinites surface properties". *Applied Clay Science*, *172* (2019): 135–145.

McCarter W and J, Tran D. "Monitoring pozzolanic activity by direct activation with calcium hydroxide". *Construction and Building Materials*, 10 (1996): 179–184.

Minerals, C. "Clay Minerals". In *Encyclopedia of Geology, 2nd edition*,(2019).

Mishra, Geetika, Arun C. Emmanuel, and Shashank Bishnoi. "Influence of temperature on hydration and microstructure properties of limestone-calcined clay blended cement." *Materials and Structures* 52, no. 5 (2019): 1-13.

Moore DM, and Reynolds RCJ. "X-ray diffraction and the identification and analysis of clay minerals". *Oxford University Press* (OUP) (1989).

Muni, Hareesh, Yuvaraj Dhandapani, K. Vignesh, and Manu Santhanam. "Anomalous early increase in concrete resistivity with calcined clay binders." In *Calcined Clays for Sustainable Concrete*, Springer, Singapore, 2020: 749-757

Murray, H. H. "Overview - clay mineral applications". *5*, (1991): 2016379–395.

Nair, Nithya, K. Mohammed Haneefa, Manu Santhanam, and Ravindra Gettu. "A study on fresh properties of limestone calcined clay blended cementitious systems." *Construction and Building Materials* 254 (2020): 119326.

NCCBM (1985) Comprehensive appraisal of cement grade limestone deposits of India, July, SP 15-85, National Council for Cement and Building Materials (NCCBM), New Delhi, 160

Neeraj, K., and Mohan, C., "Basics of clay minerals and their characteristics properties", (2021).

Nehdi, M. L. "Clay in cement-based materials: Critical overview of state-of-the-art." *Construction and Building Materials* 51 (2014): 372-382.

Nehdi, Moncef, Sidney Mindess, and Pierre-Claude Aïtcin. "Optimization of high strength limestone filler cement mortars." *Cement and concrete research* 26, no. 6 (1996): 883-893.

Ng, Geok Bee Serina. "Interactions of Polycarboxylate based Superplasticizers with Montmorillonite Clay in Portland Cement and with Calcium Aluminate Cement." PhD diss., Technische Universität München, (2013).

Nguyen, Quang Dieu, and Arnaud Castel. "Reinforcement corrosion in limestone flash calcined clay cement-based concrete." *Cement and Concrete Research* 132, (2020): 106051.

Nguyen, Quang Dieu, Mohammad Shakhaout Hossain Khan, and Arnaud Castel. "Engineering properties of limestone calcined clay concrete." *Journal of Advanced Concrete Technology* 16, no. 8, (2018): 343-357.

Nguyen, Quang Dieu, Taehwan Kim, and Arnaud Castel. "Mitigation of alkali-silica reaction by limestone calcined clay cement (LC^3)." *Cement and Concrete Research* 137, (2020): 106176.

Oates, Joseph AH. Lime and limestone: chemistry and technology, production and uses. John Wiley & Sons, (2008).

Odom, I. E., Trans, P., and Lond, R. S."Smectite clay Minerals : Properties and Uses", (1984), 391–409.

Paiva, H., A. Velosa, P. Cachim, and V. M. Ferreira. "Effect of metakaolin dispersion on the fresh and hardened state properties of concrete." *Cement and Concrete Research* 42, no. 4, (2012): 607-612.

Parashar, A., and Bishnoi, S. "A comparison of test methods to assess the strength potential of plain and blended supplementary cementitious materials". *Construction and Building Materials*, *256*, (2020): 119292.

Péra, Jean, Sophie Husson, and Bernard Guilhot. "Influence of finely ground limestone on cement hydration." *Cement and Concrete Composites* 21, no. 2, (1999): 99-105.

Perlot, Céline, Patrick Rougeau, and Sylvain Dehaudt. "Slurry of metakaolin combined with limestone addition for self-compacted concrete. Application for precast industry." *Cement and concrete composites* 44, (2013): 50-57.

Phung, C. M., Kaewmanee, K., & Tangtermsirikul, S. "Curing Sensitivity of Mortars Containing Cement, Calcined Clay, Fly Ash, and Limestone Powder." *Engineering Journal*, 25(6), (2021), 87-96.

Pillai, Radhakrishna G., Ravindra Gettu, Manu Santhanam, Sripriya Rengaraju, Yuvaraj Dhandapani, Sundar Rathnarajan, and Anusha S. Basavaraj. "Service life and life cycle assessment of reinforced concrete systems with limestone calcined clay cement (LC^3)." *Cement and Concrete Research* 118, (2019): 111-119.

Pipilikaki, P., and M. Beazi-Katsioti. "The assessment of porosity and pore size distribution of limestone Portland cement pastes." *Construction and Building Materials* 23, no. 5, (2009): 1966-1970.

Plank, Johann, Etsuo Sakai, C. W. Miao, Cheng Yu, and J. X. Hong. "Chemical admixtures—Chemistry, applications and their impact on concrete microstructure and durability." *Cement and concrete research* 78, (2015): 81-99.

Pruett RJ (2016) "Kaolin deposits and their uses: Northern Brazil and Georgia, USA". *Applied Clay Science* 131, (2016) :3–13.

Rathnarajan, Sundar, B. S. Dhanya, Radhakrishna G. Pillai, Ravindra Gettu, and Manu Santhanam. "Carbonation model for concretes with fly ash, slag, and limestone calcined clay-using accelerated and five-year natural exposure data." *Cement and Concrete Composites* 126, (2022): 104329.

Rengaraju, Sripriya, Lakshman Neelakantan, and Radhakrishna G. Pillai. "Investigation on the polarization resistance of steel embedded in highly resistive cementitious systems–An attempt and challenges." *Electrochimica Acta* 308, (2019): 131-141.

Rengaraju, Sripriya. "Electrochemical response and chloride threshold of steel in highly resistive concrete systems." *Indian Institute of Technology Madras*, (2019).

Rosetti, Agustín, Tai Ikumi Montserrat, Ignacio Segura Pérez, and Egardo Fabián Irassar. "Sulfate resistance of blended cements (limestone illite calcined clay) exposed without previous curing." In *Current Topics and Trends on Durability of Building Materials and Components: proceedings of the XV edition of the International Conference on Durability of Building Materials and Components (DBMC 2020), Barcelona, Spain, 20-23 October 2020*: 1625-1632.

Sajedi, Fathollah. "Effect of curing regime and temperature on the compressive strength of cement-slag mortars." *Construction and Building Materials* 36, (2012): 549-556.

Santos, Fabiano Nazário, Sara Raquel Gomes de Sousa, Antonio José Faria Bombard, and Sheila Lopes Vieira. "Rheological study of cement paste with metakaolin and/or limestone filler using mixture design of experiments." *Construction and Building Materials* 143, (2017): 92-103.

Schulze, S. E., and Rickert, J. "Suitability of natural calcined clays as supplementary cementitious material". *Cement and Concrete Composites*, *95*, (2019): 92–97.

Scrivener, K., Martirena, F., Bishnoi, S., and Maity, S. "Calcined clay limestone cements (LC^3)". *Cement and Concrete Research*, (2018): *114*, 49–56.

Scrivener, K., Snellings, R., and Lothenbach, b., "A Practical Guide to Microstructural

Scrivener, Karen, François Avet, Hamed Maraghechi, Franco Zunino, Julien Ston, Wilasinee Hanpongpun, and Aurélie Favier. "Impacting factors and properties of limestone calcined clay cements (LC^3)." *Green Materials* 7, no. 1, (2018): 3-14.

Selley, Richard C., Leonard Robert Morrison Cocks, and Ian R. Plimer. *Encyclopedia of geology*. Elsevier Academic, (2005).

Sevelsted, Tine F., and Jørgen Skibsted. "Carbonation of C–S–H and C–A–S–H samples studied by 13C, 27Al and 29Si MAS NMR spectroscopy." *Cement and concrete research* 71, (2015): 56-65.

Shah, V., Parashar, A., Medepalli, S., and Bishnoi, S. "Prediction of carbonation using reactivity test methods for pozzolanic materials". *Advances in Cement Research*, *32*(7), (2020):297–306.

Shah, Vineet, Karen Scrivener, Bishwajit Bhattacharjee, and Shashank Bishnoi. "Changes in microstructure characteristics of cement paste on carbonation." *Cement and Concrete Research* 109 (2018): 184-197.

Shi, Zhenguo, Barbara Lothenbach, Mette Rica Geiker, Josef Kaufmann, Andreas Leemann, Sergio Ferreiro, and Jørgen Skibsted. "Experimental studies and thermodynamic modeling of the carbonation of Portland cement, metakaolin and limestone mortars." *Cement and Concrete Research* 88, (2016): 60-72.

Shi, Zhenguo, Sergio Ferreiro, Barbara Lothenbach, Mette Rica Geiker, Wolfgang Kunther, Josef Kaufmann, Duncan Herfort, and Jørgen Skibsted. "Sulfate resistance of calcined clay–Limestone–Portland cements." *Cement and Concrete Research* 116, (2019): 238-251.

Snellings R., K.L. Scrivener. "Rapid screening tests for supplementary cementitious materials: past and future", *Materials and Structure*, 49, (2016): 3265–3279

Soni, A. K., and P. Nema. *Limestone Mining in India*. Springer Singapore, (2021).

Soroka, I., and N. Stern. "Calcareous fillers and the compressive strength of Portland cement." *Cement and Concrete Research* 6, no. 3, (1976): 367-376.

Stefanoni, M., Ueli Angst, and Bernhard Elsener. "Corrosion rate of carbon steel in carbonated concrete–A critical review." *Cement and Concrete Research* 103, (2018): 35-48.

Sui, Shiyu, Fabien Georget, Hamed Maraghechi, Wei Sun, and Karen Scrivener. "Towards a generic approach to durability: Factors affecting chloride transport in binary and ternary cementitious materials." *Cement and Concrete Research* 124, (2019): 105783.

Suma, M. Fathima & Santhanam, Manu. "Performance of limestone calcined clay blends in sodium sulphate attack on mortars", (2016).

Tan, H., C. Qi, B. Ma, X. Li, and S. Jian. "Effect of polycarboxylate superplasticiser adsorption on fluidity of cement–clay system." *Materials Research Innovations* 19, no. sup5, (2015): S5-423.

Tan, Hongbo, Xin Li, Min Liu, Baoguo Ma, Benqing Gu, and Xiangguo Li. "Tolerance of clay minerals by cement: effect of side-chain density in polyethylene oxide (PEO) superplasticizer additives." *Clays and Clay Minerals* 64, no. 6, (2016): 732-742.

Termkhajornkit, Pipat, Toyoharu Nawa, and Kiyofumi Kurumisawa. "Effect of water curing conditions on the hydration degree and compressive strengths of fly ash–cement paste." *Cement and Concrete Composites* 28, no. 9, (2006): 781-789.

Tironi, A., Cravero, F., Scian, A. N., and Irassar, E. F. "Pozzolanic activity of calcined halloysite-rich kaolinitic clays". *Applied Clay Science*, *147*(July), (2017): 11–18.

Tironi, A., Trezza, M. A., Scian, A. N., and Irassar, E. F. "Assessment of pozzolanic activity of different calcined clays". *Cement and Concrete Composites*, *37*(1), (2013): 319–327.

Tironi, A., Trezza, M. A., Scian, A. N., and Irassar, E. F. "Potential use of Argentine kaolinitic clays as pozzolanic material". *Applied Clay Science*, *101*, (2014):468–476.

Tironi, Alejandra, Claudia C. Castellano, Viviana Bonavetti, Mónica A. Trezza, Alberto N. Scian, and Edgardo F. Irassar. "Blended cements elaborated with kaolinitic calcined clays." *Procedia Materials Science* 8, (2015): 211-217.

Tironi, Alejandra, Claudia C. Castellano, Viviana L. Bonavetti, Mónica A. Trezza, Alberto N. Scian, and Edgardo F. Irassar. "Kaolinitic calcined clays–Portland cement system: Hydration and properties." *Construction and Building Materials* 64, (2014): 215-221.

Tournassat, C., Bourg, I. C., and Steefel, I. *"Surface Properties of Clay Minerals"*. 5–31.

Tsivilis, S., E. Chaniotakis, E. Badogiannis, G. Pahoulas, and A. Ilias. "A study on the parameters affecting the properties of Portland limestone cements." *Cement and concrete composites* 21, no. 2, (1999): 107-116.

Tsivilis, S., G. Batis, E. Chaniotakis, Gr Grigoriadis, and D. Theodossis. "Properties and behavior of limestone cement concrete and mortar." *Cement and concrete research* 30, no. 10, (2000): 1679-1683.

Tsivilis, Set al, E. Chaniotakis, G. Kakali, and G. Batis. "An analysis of the properties of Portland limestone cements and concrete." *Cement and concrete composites* 24, no. 3-4, (2002): 371-378.

Vaasudevaa, B. V., Dhandapani, Y., & Santhanam, M. "Performance evaluation of limestone-calcined clay (LC2) combination as a cement substitute in concrete systems subjected to short-term heat curing." *Construction and Building Materials*, *302*, (2021), 124121.

Vance, Kirk, Aditya Kumar, Gaurav Sant, and Narayanan Neithalath. "The rheological properties of ternary binders containing Portland cement, limestone, and metakaolin or fly ash." *Cement and Concrete Research* 52, (2013): 196-207.

Vance, Kirk, Matthew Aguayo, Tandre Oey, Gaurav Sant, and Narayanan Neithalath. "Hydration and strength development in ternary portland cement blends containing limestone and fly ash or metakaolin." *Cement and Concrete Composites* 39, (2013): 93-103.

Varhen, Christian, Dilonardo, Isabela, de Oliveira Romano, Roberto C., Pileggi, Rafael G., and Antonio D. de Figueiredo. "Effect of the substitution of cement by limestone filler on the rheological behaviour and shrinkage of microconcretes." *Construction and Building Materials* 125, (2016): 375-386.

Wang Ziming, Wu Hao, Xu Ying, et al. Inhibition mechanism of clay on the application performance of polycarboxylate superplasticizer [J]. Journal of Building Materials 17(2),279, (2014): 234-238.

Wang, Qiao, William Wilson, and Karen Scrivener. "Unidirectional sulfate ingress in limestone calcined clay cement (LC^3) pastes under cyclic exposure." (2021).

White, W. A., and Pichler, E. "State of Illinois Water-Sorption Characteristics of Clay Minerals", (1959).

Wilson, William, Luca Sorelli, Sreejith Krishnan, Shashank Bishnoi, and Arezki Tagnit-Hamou. "Micro-chemo-mechanical characterization of a limestone-calcinated-clay cement paste by statistical nanoindentation and quantitative SEM-EDS." In *Calcined Clays for Sustainable Concrete*, Springer, Dordrecht, (2018): 494-499.

Xu, George JZ; Watt, Daniel F.; HUDEC, Peter P. Effectiveness of mineral admixtures in reducing ASR expansion. *Cement and Concrete Research*, vol. 25, no 6, (1995): 1225-1236.

Yi, Z., Huang, L., Liu, F., Kuang, M., Ling, Q., and Zhu, J. "Characteristics of clay minerals in soil particles of two Al fi sols in China". *Applied Clay Science*, *120*, (2016): 51–60.

Yuan, S., Han, Y., Li, Y., Gao, P., & Yu, J. "Effect of calcination temperature on activation behaviors of coal-series kaolin by fluidized bed calcination". *Physicochemical Problems of Mineral Processing*, *54*(2), (2018): 590–600.

Zajac, Maciej, Anne Rossberg, Gwenn Le Saout, and Barbara Lothenbach. "Influence of limestone and anhydrite on the hydration of Portland cements." *Cement and Concrete Composites* 46, (2014): 99-108.

Zajac, Maciej, Pawel Durdzinski, Christopher Stabler, Jan Skocek, Dominik Nied, and Mohsen Ben Haha. "Influence of calcium and magnesium carbonates on hydration kinetics, hydrate assemblage and microstructural development of metakaolin containing composite cements." *Cement and Concrete Research* 106, (2018): 91-102.

Zunino, Franco, and Karen Scrivener. "Microstructural developments of limestone calcined clay cement (LC^3) pastes after long-term (3 years) hydration." *Cement and Concrete Research* 153, (2022): 106693.

Annexures

Annex I – Suitability of low-grade limestone for use in LC³
Report by Indian Institute of Technology Delhi

I. INTRODUCTION

With population boom and globalization, 21st centuries demand for infrastructure and housing units is being all time high. Which has been seen as an exponential growth in the construction industry over the last few decades, though it has started putting a strain on the global environment as well as on the available natural resources that are continuously mined to meet the growing needs. Last year over 4 billion metric tonnes of cement have been produced worldwide, this volume has increased by almost 2 times in the last decade and half itself. Such enormous cement consumption quantities mean substantial carbon dioxide emissions (currently 8% of global carbon dioxide emissions are from cement industry) and fast depleting natural reserves of limestone, gypsum, etc. Limestone is the most important raw material in the production of conventional cement and is the main source of calcium in the clinker for over a century.

Currently, the cement industry is facing two major issues, one being carbon dioxide emissions related to cement production and other being the depleting cement-grade limestone reserves. Recently developed limestone calcined clay cement (LC3) provides an effective way to tackle the above-mentioned issues. LC3 is a ternary blend of ordinary Portland cement (clinker + gypsum), calcined clay, and limestone, having a common clinker factor of 0.5. The reduced carbon footprint of LC3 is due to bringing down the clinker factor, calcination of clays at 800-900℃ which is much lower than clinker formation temperature and adding limestone by simply grinding it. LC3 has up to 30% percent less carbon emission as compared to ordinary Portland cement (Gettu et al. 2019). It is known that only a small part of calcium carbonate reacts chemically in the LC3 system to form carbo-aluminates and the rest of it predominantly acts as an inert filler material (Krishnan and Bishnoi 2020). This indicates towards the fact there is no need for cement-grade limestone to be used for LC3 production. Additionally, carbonate sources are easier to replace than clinker or clay, provided there are no deleterious effects caused by the addition or replacement. Hence using low-grade limestone will be more economical and eco-friendlier. The incorporation of low-grade limestone will even increase the possibility for LC3 production in the regions where such high-quality limestone is not available but other raw materials are available. In the present work, the effect of using different grades of limestone (by blending low-grade and high-grade limestone in different proportion) on strength development and hydration characteristics has been investigated. Details of the study which have been performed to check for the suitability of using low-grade limestone in LC3 production has been described in the subsequent sections.

II. SCOPE

The work undertaken covers the following points:

- Limestone purity (CaO: 32.20 – 44.64%)
- Isothermal calorimetry – 24hrs
- Compressive Strength (3, 7, 28 days)

III. Experimental Work

a. Materials

Composition of LC3 used to carry out the current study was 50% clinker, 30% calcined clay, 15% limestone, and 5% gypsum. 2 different types of limestone have been procured namely, high-grade limestone (HG) (having high calcium carbonate percentage) and low-grade limestone (LG) (basically reject limestone which can't be used for clinkerization). Study performed involved intermixing of low-grade and high-grade limestone to achieve the different calcium carbonate content for limestone, which has been used to make LC3. Oxide content of various raw materials used in the study is given in table 1.

Table 2 Oxide compoition from XRF for different raw materials used in the study

Oxides	Calcined Clay	Gypsum	OPC-53	HG Limestone	LG Limestone
SiO_2 (%)	47.73	19.65	19.18	10.40	22.09
Fe_2O_3 (%)	1.35	2.10	6.38	1.04	5.03
Al_2O_3 (%)	38.85	4.04	4.49	1.93	8.84
CaO (%)	1.81	23.75	62.34	44.64	32.20
MgO (%)	3.79	1.44	1.33	4.09	2.34
SO_3 (%)	0.13	28.21	2.53	0.03	0.05
Na_2O (%)	0.99	0.13	0.15	0.08	0.31
K_2O (%)	0.00	0.58	0.51	0.44	0.89
TiO_2 (%)	0.67	0.23	0.84	0.00	0.46
LOI (%)	4.49	18.24	1.32	37.17	27.14

Additionally, calcium carbonate percentage obtained from thermogravimetric analysis for high-grade limestone was 80.24%, and for low-grade limestone was 54.73%. Protocol for LC3 making involved limestones grounding in laboratory ball mill using charge to ball ratio of 1:5 for 6000 revolutions. Grounded low-grade and high-grade limestones were blended in together to have 5 different grades of limestone, i.e 100%HG, 75%HG + 25%LG, 50%HG + 50%LG, 25%HG + 75%LG, and 100%LG. Grounded raw materials were blended together in as above-mentioned ratios to make LC3 blends having different calcium carbonate content. Particle size distribution curve for the raw materials is shown in figure 1 and 10%, 50%, and 90% percentage passing fraction is given in table 2.

Table 3 Particle size at different passing fractions for raw materials used in the study

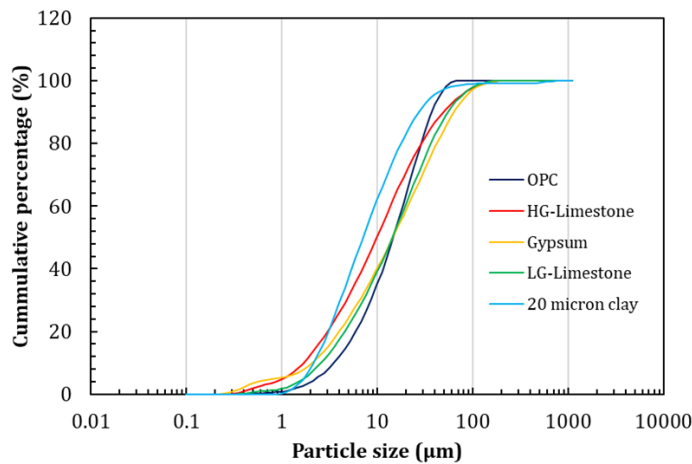| Raw Material	D_{10} (µm)	D_{50} (µm)	D_{90} (µm)
Ordinary Portland cement (OPC)	4.01	16.7	42.4
High grade Limestone (HG)	1.92	11.2	55.9
Low grade Limestone (LG)	2.92	16.3	62.4
Calcined clay (CC)	2.46	8.03	30.9
Gypsum (G)	2.38	16.6	72.0

Figure 2 Particle size distribution of various raw materials used in the study.

b.   Experiment methods

Normal consistency and Setting time – IS 4031 has been used to determine the standard consistency of the blends, followed by initial and final setting time determination. Water demand is affected by the fineness of the calcined clay used.

Isothermal calorimetry - Calorimetric studies were carried out to understand the effect of limestone grade on the heat of hydration and cumulative heat realized up on hydration at 27°C. Tests have been performed on the paste samples made at water to binder ratio of 0.40 up to 24 hrs using Calmetrix I-Cal 8000. Isothermal calorimetry is useful in understanding the reaction kinetics as it records the heat release signature of the hydrating cement paste and process involved in hydration are well known to be exothermic.

Compressive strength development - Compressive strength of the blends was measured on 70.6 mm*70.6 mm *70.6 mm mortar cubes with a fixed water/binder ratio of 0.52. Standard sand conforming to IS 650 was used to prepare the mortar. The ratio of cement to sand was kept 1:3 by weight. The cubes were demoulded after one day and stored under water till the time of testing. Average of three cubes were taken as the compressive strength at that age.

IV.   Results

Normal consistency and setting time for different blends is given table 3. It can be observed that there has been no difference in the normal consistency of the all the 5 blends. Although consistency values for all blends have come high, which can be attributed to the higher water demand of the calcined clay which has been used, as it has very high kaolinitic content and was fineness. Additionally, initial setting time for all blends has been between 112-118 minutes and final setting time has been between 187-201 minutes. As, it can be seen there isn't any effect on the setting behaviour and dormant period of the cement blends upon addition of different grades of limestone.

Table 4 Normal consistency and setting time of different blends.

Sr. No	Blend	Sp. Gravity (g/cc)	Normal Consistency	Initial Setting Time (hr:min)	Final Setting Time (hr:min)
1.	100HG	2.96	40%	1:52	3:07
2.	75HG + 25LG	2.96	40%	1:55	3:12
3.	50HG + 50LG	2.96	40%	1:58	3:21
4.	25HG + 75LG	2.96	40%	1:52	3:15
5.	100LG	2.96	40%	1:55	3:14

Calorimetric results for the 5 different blends prepared are provided in figure 2, irrespective of ratios in which limestones were mixed, the hydration curve for LC3 blends doesn't change much. Although the peak corresponding to aluminate reaction is higher in 100% low-grade and 100% high-grade limestone as compared to other ratios of mixing, the difference in heat evolution is relatively less. The cumulative heat evolution curve shows that there isn't much significant difference in cumulative heat at the end of 24 hours. The highest cumulative heat is observed in 100% high-grade and 100% low-grade limestone, while others show a marginally lower cumulative heat. The difference in the heat arises from the reaction of the aluminates phases in the system rather than the calcite present in the limestone.

Figure 3 Calorimetry result for LC3 blends with different mixing proportions of limestone, left – Heat of hydration curve, right – cumulative heat released.

Compressive strength development for the different blends is shown in figure 3, which was cast at w/c 0.52. The compressive strength results show that the highest strength is obtained in the LC3 sample cast using low-grade limestone. However, there is very little difference in the compressive strength obtained in LC^3 mixes cast using different mixing proportions of limestones, as all the results lie within the error bar of each other. The results indicate that high-quality limestone does not significantly increase the strength and even lower-grade limestone contributes to similar strength development.

Figure 4 Compressive strength of the LC3 made with the different mixing proportions of the limestones (w/b – 0.52)

Figure 5 Compressive strength of the LC3 made with different mixing proportions of the limestones (w/b – 0.42)

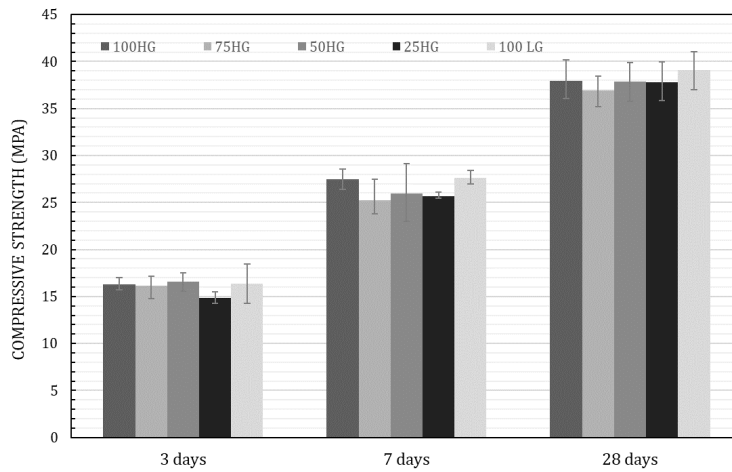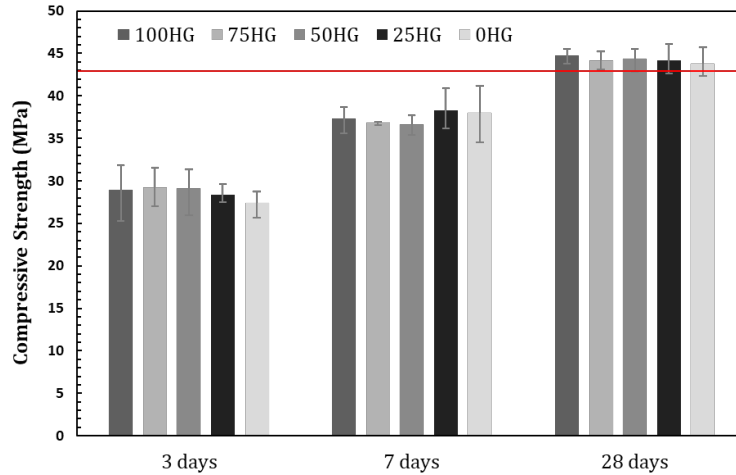Compressive strength development has been repeated at lower water to binder ratio of 0.42 with admixture dosage of 0.4%, results of which are shown in figure 4. Similarly, as in previous case, here again there had been no significant difference and the results were within the error bar of each other at all ages. Thus, reinforcing the observation that addition of low-grade limestone does not hamper the initial hydration kinetics and compressive strength development of LC^3.

V.   Conclusion

Present study has demonstrated how even low-grade limestone is suitable for the production of LC^3 by comparing the hydration rate and compressive strength development of different limestones. From the study performed, a conclusion can be drawn that limestone having a calcium carbonate content of as low as 60% is good enough, if it doesn't contain any other deleterious substance. As it has been observed that excess calcite in the system doesn't help in the strength development. Hence, using limestone having lower purity but enough calcite for carbo-aluminate formation is good enough for LC^3 production. This provides an opportunity to use the reject limestone present around the cement plants and lessen the burden of cement-grade limestone reserves.

Annex II – Mechanical properties of concrete prepared using LC³
A report by Indian Institute of Technology Delhi

1 Introduction

In the present era, the importance of the word "Global Warming" needs no exaggeration. According to the International Energy Agency (IEA), every year approximately 33.5 billion tonnes of CO_2 are emitted. Almost 72% of the emitted greenhouse gases is carbon dioxide of which 7% is produced during the manufacturing of cement. This process is therefore harmful to the environment. It has become a challenge for the construction industry to emphasize this matter for further research. The current level of partial replacement of clinker with conventional supplementary cementitious materials (SCMs) has its limitations in the Portland system as, beyond a certain proportion of substitution, the properties of the blended cement get affected. Further, the availability of these SCMs is also going to reduce, as the world is shifting towards the adoption of renewable energy. The use of limestone calcined clay cement reduces carbon emission of the cement industry by 30-40%. It makes it comparatively eco-friendly and economic to reduce the clinker-content by up to fifty percent which is expected to reduce the carbon foot-print of cement industry.

Therefore, it becomes essential to evaluate the performance of LC³ w.r.t to the popular conventional cements to assess the adoptability of this promising cement. This work compares the mechanical properties of LC³ with Ordinary Portland cement (OPC) and fly-ash based Pozzolana Portland Cement (PPC) as per the Indian Standards to assess the suitability of the cement in India conditions as India is a very large consumer of cement.

2 Objective

The primary objectives of this report are to evaluate and compare the mechanical performance of the OPC, PPC, and LC³ cement concretes. The tests include compressive, flexural, split tensile strength tests, modulus of elasticity, and bond properties with reinforcement. The procedure of design mix, casting and testing was carried out as per Indian Standard (IS) code specifications.

3 Properties of materials

THE THREE TYPES OF CEMENT USED WERE AS FOLLOWS:
1) OPC- grade 43
2) PPC- Fly-ash based
3) LC³- Prepared by blending 50% of OPC 43 grade with 50% LC2 containing 63.3 % of calcined clay,31.7% of lime, and 5% of gypsum.

Aggregates used were crushed angular quartzitic stones of 20 mm and 10 mm nominal sizes. Whereas, the fine-aggregates used were river-sand.

3.1 Specific Gravity
3.1.1 Cement
Specific gravity was determined using Le Chatelier's flask as per IS 2720, Part-3. Table 1 shows the values of the specific gravity of various types of cement used in this study.

Table 5 Specific Gravity of different types of cement

Cement type	Value
OPC	3.17
PPC	2.81
LC³	3.00

3.1.2 Aggregates

Specific gravity was determined using as per IS2386. Table2 shows the values of specific gravity of aggregates used in this study.

Table 6 Specific Gravity of Aggregates

Aggregates type	Value
Coarse (20mm)	2.81
Coarse (10mm)	2.68
Sand	2.62

3.2 Sieve Analysis

3.2.1 Coarse aggregates

Sieve analysis was performed using as per IS 2386. Table 3 shows the particle size distribution of aggregates used in this study and is found to satisfy the gradation requirements in IS 383.

Table 7 Sieve Analysis of Coarse Aggregates

Size (cm,mm)	Weight Retained (20 mm)	Cummulative retained	% passed	Weight Retained (10 mm)	Cummulative retained	% passed
20 cm	250	250	95	0	0	100
12.5 cm	3960	4210	15.8	150	150	97
10 cm	440	4650	7	790	940	81.2
4.75 mm	320	4970	0.6	3570	4510	9.8
2.36 mm	0	4970	0.6	470	4980	0.4
PAN	30	5000	0	20	5000	0
Total	5000	5000	0	5000	5000	0

3.2.2 Fine aggregates

Fine aggregates were sieved, and particle size analysis was done as per IS 383. The sand was found to be conforming to zone 2.

Table 8 Sieve Analysis of Fine Aggregates

Size (μm, mm)	Weight Retained In gms (FA)
4.75 mm	180
2.36 mm	220
1.18 mm	240
600 μm	140
300 μm	960
150 μm	200
PAN	60

3.2.3 Cement

Malvern Mastersizer 3000E was used for determining the particle size of cements. Isopropyl alcohol was used as a dispersion medium. The particle size is mentioned in the table below.

Table 9 Particle Size of Different types of cement

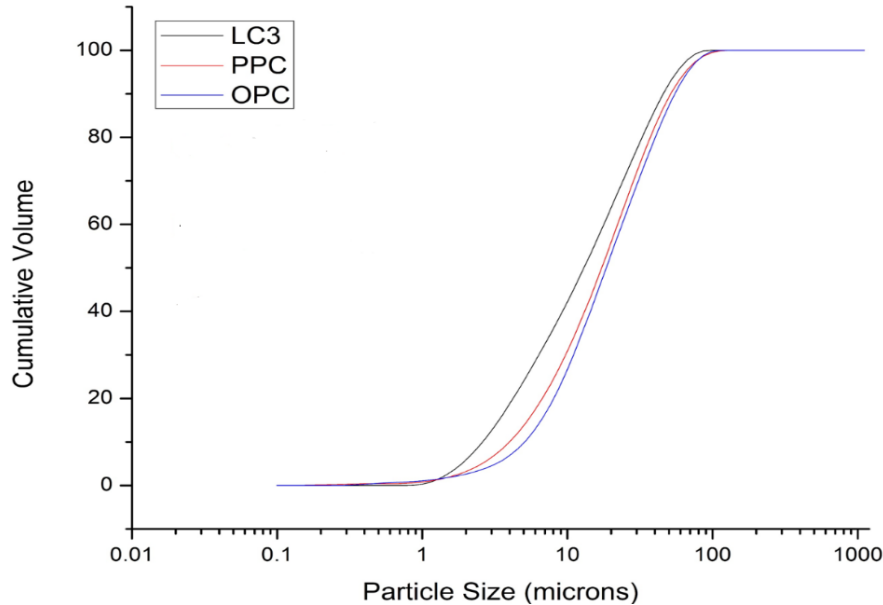| D_x	OPC Particle Size (µm)	PPC Particle Size (µm)	LC^3 Particle Size (µm)
D_{10}	5.76	4.53	2.96
D_{50}	21.0	19.6	14.8
D_{90}	62.5	58.5	51.9

Figure 6: Particle Size Distribution of Different types of cement

3.3 Oxide composition of cements

X-ray Fluorescence of different types of cement was done to determine the oxide composition of the cements.

Table 10: X-ray Fluorescence of different types of cement

Oxides Component	OPC (%)	PPC (%)	LC^3 (%)
SiO_2	20.69	35.22	29.70
Fe_2O_3	5.26	5.54	3.86
Al_2O_3	4.03	12.92	19.10
CaO	59.90	34.51	32.21
MgO	0.98	1.20	1.36
SO_3	2.53	2.86	2.74
Na_2O	0.09	0.42	0.48
K_2O	0.57	0.82	0.46
TiO_2	0.4	1.09	1.39
LOI	4.3	4.1	7.9

4 Mixing procedure

Initially, the concrete materials were weighed as per the mix design of the three types of mixes. The w/b ratio and c/a ratio were kept the same for all these mixes of a particular grade. The materials were dry mixed for 5 minutes after which the mix attained homogeneity. One-third of the calculated amount of water was first poured into the concrete mixer, and then the remaining water was mixed with chemical admixtures to obtain a homogenous mixture.

Figure 7 Slump test in progress

5 Testing of fresh concrete

After successfully mixing the concrete before casting the specimens, the workability of mixes was tested by performing a slump-cone test as per IS 1199 as shown in figure 2.

6 Sample preparation

6.1 Casting and Curing of Specimens

The inside portion of the steel cube mould was oiled and kept on a plain solid platform. After performing the slump test, the concrete was put into the mould in three equal layers which were tamped using a tamping rod as per IS 516. Samples of pull-out tests were prepared as per IS 2770. The finishing was done by using a trowel. After 24 hours when the concrete specimen attains enough strength to be in the desired shape, it was de-moulded carefully. Lastly, the samples were put for curing in the curing tank for the desired period.

Figure 8 Casting of samples for pull-out test

7 Results and discussion

7.1 Measurement of compressive strength

This test was performed using UTM in which the specimen was kept in its proper position as shown in figure 4. The procedure for testing was carried out as per IS: 516. Testing was conducted over 7 days & 28 days. The strength of concrete depends upon the kind of cement and its chemical components, duration of curing, measurements of aggregates, compaction degree, w/b ratio, voids present in concrete, and temperature while curing.

The results of the tests are presented in table 7 and 8 and are compared in figure 5. The compressive strength of LC^3 M-25 grade of concrete for 7 days was found higher than that of OPC and PPC by around 24% and 5.5%. For 28 days, the compressive strength was higher than PPC by approx. 3.6%. But when compared to OPC, it was lower by 3.3%. The compressive strength of M-50 grade of LC^3 had shown superior compressive strengths at both 7 and 28 days when compared to OPC and PPC. At 7 days, the strength was 24.8% higher than PPC and 7.6% higher than OPC. Whereas, at 28 days, the compressive strength of LC^3 concrete showed higher compressive strength than OPC and PPC by 23.1 % and 24.5%. From the above data, it was concluded that LC^3 performed better in uniaxial compressive strength.
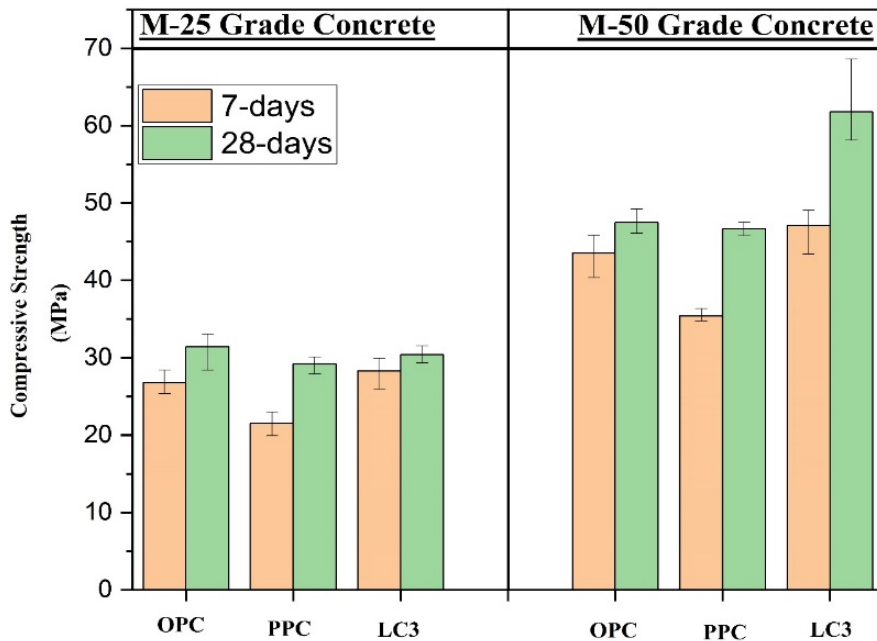
Figure 9 Test for compressive strength in progress

Figure 10 Comparison of Uniaxial compressive strengths of samples

Table 11 Uniaxial Compressive Strengths (MPa) of samples for M-25 concrete

Sample (M-25)	LC³		PPC		OPC	
No.	7-days	28-days	7-days	28-days	7-days	28-days
1.	26.66	29.21	20.056	28.34	25.07	29.78
2.	27.55	30.52	21.364	28.99	27.03	30.00
3.	30.66	31.40	23.108	30.52	28.12	34.45
Avg.	**28.29**	**30.374**	**21.509**	**29.28**	**26.74**	**31.41**

Table 12 Uniaxial Compressive Strengths (MPa) of samples for M-25 concrete

Sample (M-50)	LC³		PPC		OPC	
No.	7-days	28-days	7-days	28-days	7-days	28-days
1.	45.12	54.93	34.45	45.78	41.20	45.70
2.	45.34	64.96	35.53	46.65	42.72	47.90
3.	50.79	65.40	36.18	47.52	46.65	48.80
Avg.	**47.08**	**61.76**	**35.39**	**46.65**	**43.52**	**47.46**

7.2 Measurement of Flexural Strength

The flexural strength of the concrete was measured by using 4-point loading method on beams cast. The procedure was carried out as per IS 516. The values of tested samples were recorded and compared.

The flexural strength of LC³ M-25, at 7 days, was found to be higher than PPC and OPC by 42.4% and 18.6%. A similar trend was observed for 28 days, where it exceeded the strength of PPC and OPC by 17.8% and 18.1%. For LC³ M-50 concrete, the flexural strength was observed to be higher than PPC and OPC. For 7 days, the strength was 27.2% higher than PPC and 12.3% than OPC. The 28-day flexural strength of LC³ was 29.9% higher than PPC concrete. When compared to OPC, it was only 4.8% higher.

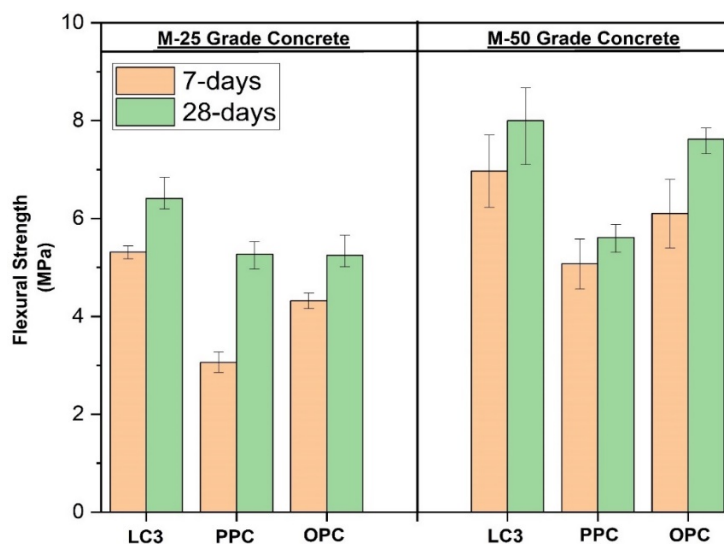*Figure 11 Flexure test in progress*

Figure 12 Comparison of flexural strengths of sample

Table 13 Flexural strength of samples (MPa) for M-25 concrete

Sample (M-25)	LC³		PPC		OPC	
No.	7-days	28-days	7-days	28-days	7-days	28-days
1.	5.18	6.2	2.87	4.97	4.17	5.01

2.	5.31	6.2	3.05	5.32	4.31	5.10
3.	5.44	6.84	3.27	5.53	4.48	5.66
Avg.	**5.31**	**6.41**	**3.06**	**5.27**	**4.32**	**5.25**

Table 14 Flexural strength of samples (MPa) for M-50 concrete

Sample(M-50)	LC^3		PPC		OPC	
No.	7-days	28-days	7-days	28-days	7-days	28-days
1.	6.23	7.10	4.49	5.31	5.275	7.32
2.	6.97	8.24	5.14	5.66	6.234	7.71
3.	7.71	8.67	5.58	5.88	6.80	7.85
Avg.	**6.97**	**8.00**	**5.07**	**5.61**	**6.10**	**7.62**

7.3 Measurement of Split Tensile Strength

This test was performed as per IS 5816. As a result, the specimen undergoes a high magnitude of stress close to the loading zone.

The split tensile strength of LC^3 concrete was higher for both M-25 and M-50 grades of concrete. For M-25, at 7 days, the strength was 38.6% and 18.0% higher than PPC and OPC. After 28 days, LC^3 showed higher strength by 20.2% and 27.2% than PPC and OPC. The LC^3 M-50 grade concrete surpassed the PPC and OPC by 8.18% and 0.7% for 7 days. The same implies for 28 days as it achieves higher split tensile strength by 18.7% and 8.7% than PPC and OPC respectively at 28 days.

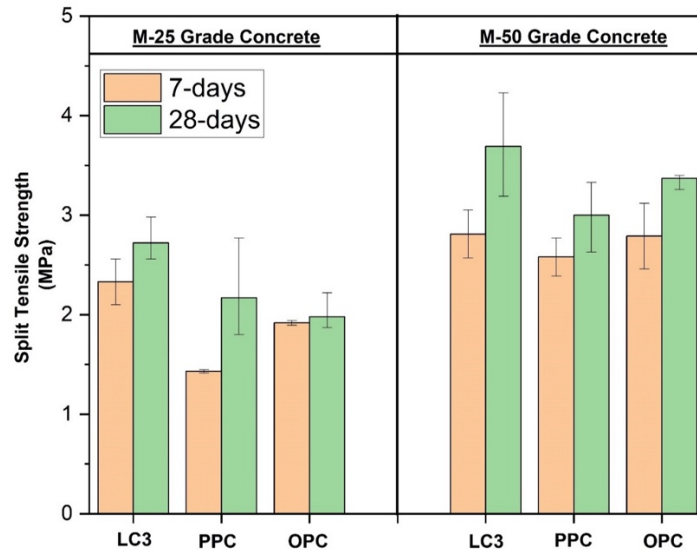*Figure 13 Split-tensile test in progress*

Figure 14 Comparison of split-tensile strengths of samples

Table 15 Split-tensile of samples (MPa) for M-25 concrete

Sample (M-25)	LC³		PPC		OPC	
No.	7-days	28-days	7-days	28-days	7-days	28-days
1.	2.08	2.56	1.39	1.80	1.73	1.87
2.	2.36	2.63	1.45	1.94	1.80	1.87
3.	2.56	2.98	1.45	2.77	1.94	2.22
Avg.	**2.33**	**2.72**	**1.431**	**2.17**	**1.917**	**1.98**

Table 16 Split-tensile of samples(MPa) for M-50 concrete

Sample (M-50)	LC³		PPC		OPC	
No.	7-days	28-days	7-days	28-days	7-days	28-days
1.	2.63	3.19	2.22	2.63	2.56	3.26
2.	2.77	3.67	2.77	3.05	2.70	3.40
3.	3.05	4.23	2.77	3.33	3.12	3.47
Avg.	**2.81**	**3.69**	**2.58**	**3.00**	**2.79**	**3.37**

7.4 Measurement of Modulus of Elasticity

The test of modulus of elasticity of concrete was performed as per the IS 516 using a data logger. Modulus of elasticity was found to increase with compressive strength, except for the OPC M-50. For M-50: At 7 days, this modulus was found 13.5% higher for LC³ than PPC and 0.6% higher than for OPC. At 28 days, Young's modulus was higher for LC³ by 5.9% and 17.4% than that of PPC and OPC respectively.

For M-25: The 7days value of Young's modulus of PPC was higher than LC³ by 3.7%. Whereas, when compared to OPC, the LC³ had a higher modulus of elasticity than OPC by 4.6%. The modulus of elasticity of LC³ at 28 days had a higher value than OPC and PPC by 5.3% and 4.2% respectively.

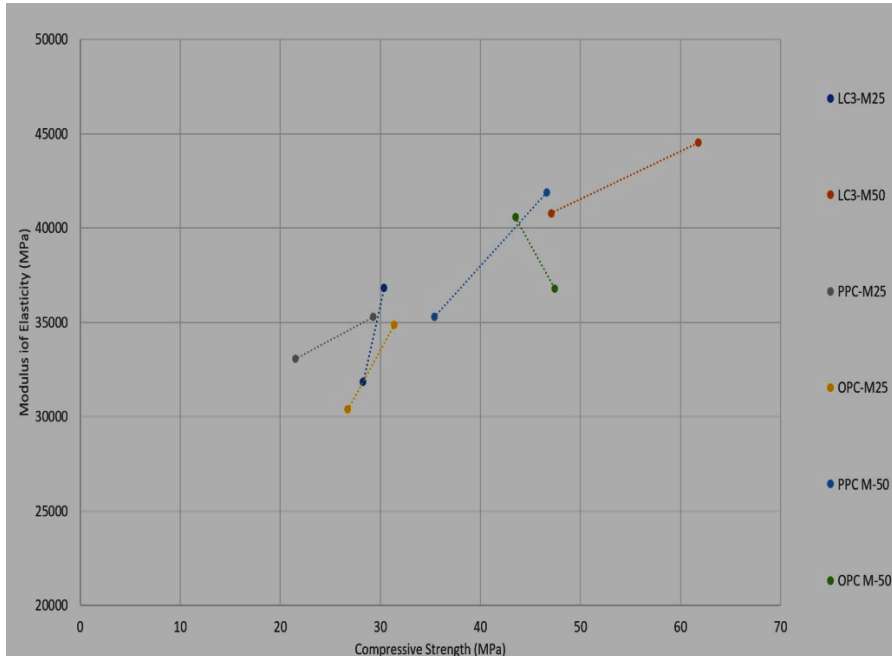Figure 15 Arrangement of test for Modulus of elasticity using a data-logger

Figure 16 Elastic Modulus Vs compressive strength of the samples at 7 & 28 days

Table 17 Modulus of elasticity (MPa) of the samples for M-25

Sample (M-25)	LC³		PPC		OPC	
No.	7-days	28-days	7-days	28-days	7-days	28-days
1.	33514	37463	36443	34706	31037	36001
2.	27364	34360	31794	33860	30668	31413
3.	34690	38672	30987	37327	29471	37255
Avg.	**31856**	**36832**	**33074**	**35298**	**30392**	**34890**

Table 18 Modulus of elasticity (MPa) of the samples for M-50

Sample (M-50)	LC³		PPC		OPC	
No.	7-days	28-days	7-days	28-days	7-days	28-days

1.	37031	42010	31504	48055	36601	35724
2.	41972	47160	35917	Rejected	41975	38305
3.	43491	44401	38492	35771	43168	36354
Avg.	**40831**	**44523**	**35304**	**41913**	**40581**	**36794**

7.5 Measurement of Pull-out strength

The test for measuring pull-out strength with reinforcement was carried out as per IS 2770. The pull-out strength of OPC concrete of M-25 grade was observed to be the highest at 7 and 28 days, and the pull-out strength of LC^3 M-25 with 12 mm diameter rebar was found to be lower by 19.2% and 24.8%, respectively that of the OPC specimens. Similarly, the PPC-M-25 specimens with 12 mm rebar portrayed a pull-out strength lower than that of OPC-M-25 specimens by 17.96% and 21.6% at 7 and 28 days respectively. On the other hand, when 25 mm diameter rebars were used, the 7-day and 28-day pull-out strength of LC3-M-25 was lower than that of the OPC-M-25 specimens by a margin of 16.8% and 9.2%, respectively. The 7-day and 28-day pull-out strength of PPC-M-25 were lower than that of the OPC-M-25 specimens by 25.7% and 4.0%, respectively.

In the case of M-50 grade concrete, while OPC-M-50 specimens with 12 mm dia rebars did not show any remarkable change in the pull-out strength values, the LC3 and PPC specimens portrayed substantial improvement in performance. The LC3-M-50 specimens with 12 mm rebars depicted the highest pull-out strength at both 7 days as well as 28 days, the values being greater than the reference OPC-M-50 specimens by 12.5% and 13.0%, respectively. The 7-day pull-out strength of PPC-M-50 specimens with 12 mm rebars was observed to be lesser than the corresponding OPC-M-50 specimens by 6.4% whereas, the 28-day strength was found to exceed that of the OPC-M-50 specimens by 10.9%. For the specimens cast with 25 mm rebars, LC3-M-50 and PPC-M-50 portrayed similar pull-out performances while the OPC-M-50 values were marginally lower. The 7-day and 28-day pull-out strength of LC3-M-50 specimens with 25 mm rebars were observed to be higher than that of the control OPC-M-50 specimens by 10.7% and 16.8%.

Figure 17 (a) Test arrangement for Pull-out strength, (b) failed specimens
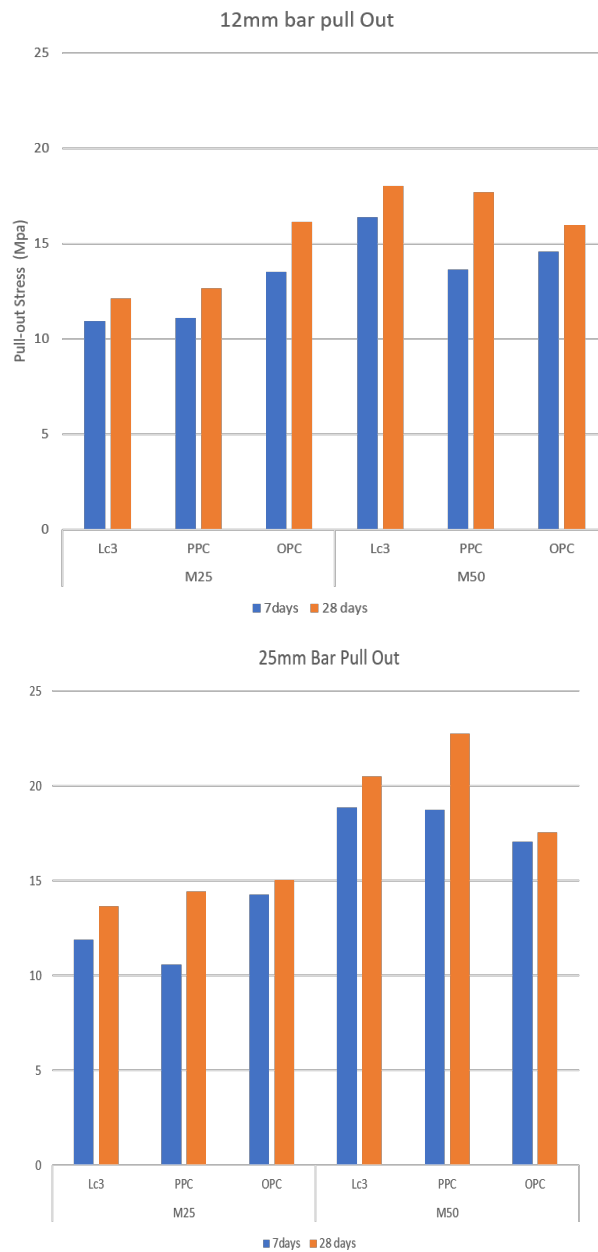

Figure 18 Comparison of Pull-out strength of the samples

Table 19 Pull-out strength of 12mm , M-25 sample

No.	LC³ (Strength (MPa) and slip (mm))				PPC(Strength (MPa) and slip (mm))				OPC (Strength (MPa) and slip (mm))			
	7 Days	Slip (7Days mm)	28 Days	Slip (28Days mm)	7 Days	Slip (7Days mm)	28 Days	Slip (28 Days mm)	7 Days	Slip (7Days mm)	28 Days	Slip (28Days mm)
1	9.37	0.50	9.89	0.00	9.37	0.85	10.93	2.00	13.53	0.80	17.70	1.60
2	10.41	0.60	11.97	1.50	11.97	1.00	13.03	1.60	13.53	1.00	15.10	1.80
3	13.01	0.30	14.57	1.80	11.97	1.10	14.05	1.30	13.53	1.20	15.62	1.60
Avg.	10.93	0.45	12.14	1.65	11.10	0.99	12.66	1.64	13.53	1.00	16.14	1.67

Table 20 Pull-out strength of 25mm , M-25 sample

No.	LC³ (Strength (MPa) and slip (mm))				PPC(Strength (MPa) and slip (mm))				OPC (Strength (MPa) and slip (mm))			
	7 Days	Slip (7Days mm)	28 Days	Slip (28Days mm)	7 Days	Slip (7Days mm)	28 Days	Slip (28 Days mm)	7 Days	Slip (7Days mm)	28 Days	Slip (28Days mm)
1	10.66	1.20	7.16	1.50	10.16	1.20	14.66	1.50	13.49	1.30	16.16	2.60
2	12.33	2.30	13.99	1.50	10.33	1.50	14.49	1.10	14.32	2.00	12.66	4.50
3	12.66	2.20	13.32	0.55	11.33	1.50	14.16	2.00	15.00	1.20	16.32	4.10
Avg.	11.88	1.9	13.65	1.18	10.60	1.4	14.43	1.54	14.27	1.5	15.04	3.73

Table 21 Pull-out strength of 12mm, M-50 sample

No.	LC³ (Strength (MPa) and slip (mm))				PPC(Strength (MPa) and slip (mm))				OPC (Strength (MPa) and slip (mm))			
	7 Days	Slip (7Days mm)	28 Days	Slip (28Days mm)	7 Days	Slip (7Days mm)	28 Days	Slip (28 Days mm)	7 Days	Slip (7Days mm)	28 Days	Slip (28Days mm)
1	15.62	1.50	17.70	1.00	10.41	0.60	18.74	1.40	12.50	1.10	12.49	1.00
2	16.40	1.30	18.22	1.20	16.14	1.20	17.70	1.30	15.62	1.00	16.67	1.20
3	17.18	1.30	18.22	1.30	16.40	1.00	16.66	0.65	15.62	1.50	18.74	1.00
Avg.	16.40	1.37	18.04	1.17	13.65	0.93	17.70	1.11	14.58	1.20	15.96	1.06

Table 22 Pull-out strength of 25mm, M-50 sample

	LC³ (Strength (MPa) and slip (mm)			
No.	7 Days	Slip (7Days mm)	28 Days	Slip (28Days mm)
1	17.91	2.50	20.82	0.80
2	18.32	1.30	20.49	2.00
3	20.41	1.20	20.16	0.55
Avg.	18.88	1.67	20.49	1.11

	PPC(Strength (MPa) and slip (mm)			
No.	7 Days	Slip (7Days mm)	28 Days	Slip (28 Days mm)
1	17.49	1.50	23.16	1.20
2	17.91	1.50	21.49	1.00
3	20.82	1.00	23.66	1.10
Avg.	18.74	1.34	22.77	1.10

	OPC (Strength (MPa) and slip (mm)			
No.	7 Days	Slip (7Days mm)	28 Days	Slip (28Days mm)
1	16.83	1.50	18.32	1.50
2	16.83	2.00	17.66	1.50
3	17.49	2.00	16.66	1.00
Avg.	17.05	1.83	17.54	1.34

Further information

Mix Designs Used

Materials' weight (kg/m³)	OPC		PPC		LC³	
	M-25	M-50	M-25	M-50	M-25	M-50
Water Content	165	165	165	165	165	165
Cement Content	366.67	590	366.67	590	366.67	590
Fine Aggregate	638.45	523.87	623.19	501.49	627.41	507.67
Coarse Aggregate (10mm)	495.74	466.41	483.89	446.49	487.16	451.99
Coarse Aggregate (20mm)	743.6	699.62	725.84	669.73	730.74	677.99
Chemical Admixture	3.67	5.9	3.67	5.9	3.67	5.9

Abbreviations

OPC	Ordinary Portland cement
PPC	Portland Pozzolana cement
LC³	Limestone calcined clay cement
MOE	Modulus of Elasticity
CTM	Compression testing machine
UTM	Universal testing machine
SP	Superplasticizer
PSD	Particle size distribution
XRF	X-ray fluorescence
CA	Coarse aggregate
FA	Fine aggregate

Annex III – Effect of iron impurity in clay on performance of LC³
Report by Indian Institute of Technology Delhi

1. Introduction

The emission of greenhouse gases like carbon dioxide is a major concern for climate change and global warming. The cement industry is the second largest source of carbon emissions and is responsible for generating more than 3GT of carbon dioxide annually. This comes from the burning of limestone between 750 °C to 850 °C and fuel consumption to attain a clinker temperature of 1450 °C. Therefore, a key strategy is to find alternative materials to minimize the carbon footprints of cement industry without compromising on its strength and durability characteristics [1,2]. This is achieved by the reaction which takes place between the portlandite (by-product of cement hydration) and supplementary cementitious material to form additional hydration products. Widespread availability and low initial costs are prerequisites and clay appear to be one such potential material [3,4,5].

Previous studies have shown that kaolinite is an excellent pozzolan when calcined between 700 °C to 850 °C. In the field, kaolinite mineral is often combined with several impurities like calcite, gibbsite and ferrite. Such clays are often being discarded as the removal of impurities increases the initial cost of pozzolan. To avoid the treatment process and expand the range of material to be accepted as SCM, few studies have been done that extensively investigated the effect of gibbsite and calcite on the properties of calcined kaolinite [6,7]. Zunino et al. [6] studied the influence of calcite on kaolinite clay and reported that the decomposition of calcite during calcination temperature reduces the specific surface area and influences the reactivity of kaolinite clays. Nonetheless, it was found that clay with calcite content upto 10% can be used as pozzolan material. While, Danner et al. [7] studied the impact of calcite content (15 % and 25 %) on smectite and illite clays. They also reported an appreciable reduction in specific surface area of clays, but observed higher compressive strength for clays that contained greater percentage of calcite. While, another study conducted by Zunino et al. [7] showed that gibbsite does not interfere with the metakaolin formation as it was found to be in an unreactive phase after calcination.

Iron is one of the major elements and is often encountered with the kaolinite mineral. It can exist either as iron hydroxide, or in the structure of clay mineral itself by substitution of cations. Iron is usually known only for imparting color to the clay that hinders its application in paper pulp and ceramics industries. Thus, vast resources of such clay exist and can serve as a suitable pozzolan for blended cement. Musbau et al. [9] compared the performance of laterite with kaolinite clay and noticed no change in the workability and strength characteristics. Extensive research has been carried out on kaolinite clay in cement industry but there is limited data available on the interaction of iron with the kaolinite clay during the calcination process. This study explores the influence of iron ranging from 5 % to 20 % on the properties and pozzolanic reactivity of calcined clay. The finding will enable us to understand more about the thermal behavior of low-grade kaolinite clay and an effort to use new low-cost material with contains not only kaolinite but other minerals as well.

2. Material and methods
2.1 Materials

In this study, both natural and model clay compositions were used. In natural clays, seven different clay samples were selected from clay deposits of Gujrat, India. While, for model clays, medium grade clay was mixed with laterite in different amount. All the clay samples were investigated for the chemical composition using X-ray fluorescence (Bruker S2 Puma) with pressed pellet method. The mineralogical analysis was carried out on Bruker D8 Advance Eco diffractometer with configuration of θ- θ type. The instrument was operated at 40 KW and 20V and diffraction pattern was measured between 2θ values of 5° to 65°. The thermogravimetric analysis was done using SETERAM Labsys

Instrument with alumina crucible. The sample was heated from 30 °C to 1000 °C at heating rate of 20 K/ min in nitrogen environment. The results are presented in Table 1.

Table 1: Characteristics of natural raw clays

Chemical composition							
Oxides(wt%)	A2	A3	B1	B2	B3	C2	C3
SiO_2	43.3	42.8	39.5	40.7	41.8	38.1	35.9
Al_2O_3	23.3	15.3	21.07	24.07	25.9	25.2	24.8
Fe_2O_3	10.2	9.44	12.64	20.64	5.80	4.87	7.20
CaO	0.51	4.02	0.16	0.61	0.36	0.25	0.23
MgO	0.62	1.22	0.57	0.57	0.39	0.34	0.41
Na_2O	0.60	0.86	4.27	4.27	1.01	1.32	0.81
K_2O	0.34	2.13	0.28	0.28	0.29	0.25	0.32
TiO_2	3.12	1.36	3.79	3.79	3.78	3.67	4.02
MnO	0.28	0.20	0.35	0.35	0.10	0.08	0.14
P_2O_5	0.04	0.04	0.024	0.024	0.03	0.04	0.02
SO_3	0.89	6.78	0.57	0.57	2.76	6.34	8.01
Cl	0.56	0.68	1.60	1.6	0.62	0.68	0.21
LOI	16.2	15.1	15.1	3.32	17.1	18.8	17.9
TGA Analysis							
Kaolinite content	55.9	25.1	48	53.8	45.9	88.2	78.9

From the oxide composition, one can observe that the chemical criteria adopted for kaolinite clays to be used as SCM: Al_2O_3 > 18 % and LOI > 7 % were fulfilled by all raw clays except A3. Moreover, criteria mentioned in ASTMC618 for natural pozzolan N (Al_2O_3+SiO_2+Fe_2O_3 > 70%) was also satisfied by all raw clays except A3. Clays selected for this study, have varying iron content ranging from as low as 5 % in B3 to as high as 20 % in B2. Kaolinite present in raw clays was quantified from the thermogravimetric analysis by determing the weight loss due to dehydroxylation process. The temperature range was selected from the first derivative of the weight loss curve. Kaolinite content was found to be greater than 40 % for all raw clays except A3, that is within the recommended criteria for use in cement.

Since, the purpose of this study is to analyze the effect of iron content on low grade kaolinite. It was decided to select A2 and B2 clays for further investigation as kaolinite content of both clays lies in the same range, but have a considerable difference in iron content. A2 clay has kaolinite content of 55.9 % while B2 clay has kaolinite content of 53.8 %. Iron content was found to be 10.2 % and 20.64 % for A2 and B2 clay respectively. As expected, XRD analysis also showed that Kaolinite and Quartz were present in major mineral phases and iron bearing phases were present in minor phases.

Model clays were prepared in the laboratory by mixing kaolinite clay with quartz and laterite as impurities. D1 clay was made with 75% kaolinite clay, 25% quartz and is considered reference clay. While, D2 clay was prepared by mixing 75 % kaolinite, 12.5% laterite and 12.5 % quartz. Similarly, D3 clay has 75 % kaolinite and 25 % laterite. The iron content found in D1,D2 and D3 was 3%, 12.5 and 22 % respectively.

Table 2: Chemical composition of model clays

Oxides	D1	D2	D3
SiO_2	58.55	48.04	37.53
Al_2O_3	30	29.93	29.86
Fe_2O_3	3	12.49	21.99
CaO	0.35	0.35	0.36
MgO	1.22	1.12	1.01
Na_2O	0.84	0.84	0.83
K_2O	0.22	0.2	0.17
TiO_2	1.73	1.73	1.74
MnO	0.01	0.13	0.24
P_2O_5	0	0.02	0.03
SO_3	0.62	0.75	0.88
Cl	0.08	0.09	0.09

2.2 Methods

Raw materials were subjected to several stages of processing before their use as a source of SCM. Firstly, they were first dried in an oven at 105 °C to remove moisture and then crushed to reduce the size of feed to 2mm and below. Afterwards, calcination was carried out in static method using the laboratory muffle furnace. The calcination temperature was selected from the thermogravimetric curves to make sure that the temperature is sufficiently high to transform all raw kaolinite into a reactive phase. Once the target temperature is reached in muffle furnace, it was maintained for two hours so that uniform heating is achieved in the entire sample. After calcination process, samples were taken out from furnace and cooled at room temperature. Calcined clays were then ground to very fine levels using laboratory ball mill.

Natural clays were calcined at two different temperatures (750 °C and 850 °C) to understand the influence of iron impurities on the transformation process. The quality of calcination was assessed with the thermogravimetric curves and weight loss was found to be less than 0.5 %, indicating the efficient treatment at 750 °C and 850 °C. Moreover, peaks of high temperature stable crystalline phases like mullite were also absent in diffractogram of calcined clays.

The calcination temperature of 750 °C was found to be sufficient as the dehydroxylation process was complete and thus, model clays were heated at this temperature only. Two approaches were adopted for the formation of model clay system to investigate its impact on the properties of calcined clays. In one method, calcination of individual clay component was done separately and then mixed in different proportions to obtain model clays as listed in table 2. While, in the second method, model clay was mixed in raw state and then subjected to calcination treatment.

The pozzolanic activity of calcined clays were assessed using lime reactivity test method which is standardized as per IS 1727. In this test method, reactivity is determined from the compressive strength of mortar cubes prepared by mixing lime: SCM: standard sand in the ratio of 1:2M:9 by weight. The water content is fixed by hit and trial approach and the amount of water shall be equal to that required to give a flow of 65 % to 75 % in mortar table test. Mortar cubes of 50 mm size are prepared and samples are covered with moist jute cloth for first 48 hours at 27 °C and then cured for next eight days in an environmental controller chamber at 50 °C and 90 % RH. The samples are tested for compressive strength at the age of 10 days.

3. Results and Discussion
3.1 Effect of iron on physical properties of clay

The presence of iron phases affects the appearance as it imparts red color to the clay. The extent of color change depends on the amount of iron content present in the clay. The notable difference is observed when iron content exceeds 2 %. The color of clay becomes darker with a higher level of iron content as depicted in figure 2. D3 clay has maximum iron content which is evident from its dark brown color and explains the presence of goethite phases. The calcination process also brings about change in the color of calcined clay when compared to the raw clay. This is because goethite present in raw clay transforms into hematite (red color) and magnetite (grey color) phases upon heating. And, during the cooling process in an oxygen rich environment, magnetite becomes unstable and transforms into hematite phase and gives dark color to clay.
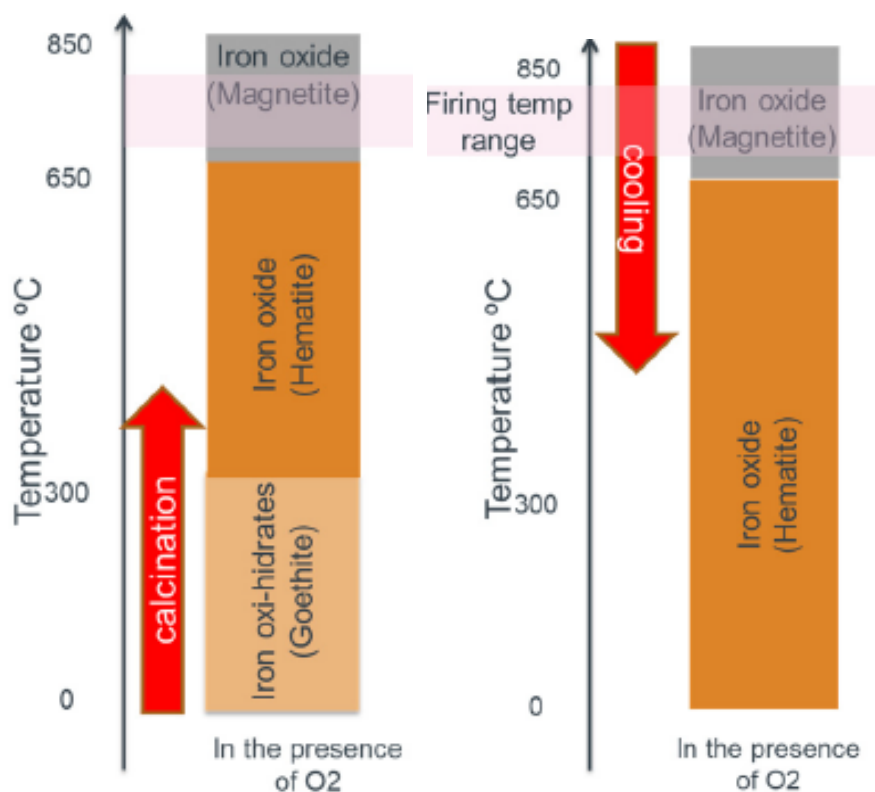
Figure 1: Transformation of iron rich phases during calcination process

Figure 2: Clays with different iron contents

3.2 Effect of Iron on calcined clay reactivity

The compressive strength results obtained from lime reactivity test of A2 and B2 clays calcined at two temperatures are plotted in figure 3. All calcined clay samples achieved higher strength than the minimum requirement of 8 MPa after 10 days. Even though, iron content of A2 clay was 10 % and B2 clay was 20 %, the reactivity of both clays was observed to be in same range. This indicates that kaolinite content governs the reactivity and the presence of iron impurity does not affect the performance of clays. Increasing calcination temperature from 750 °C to 850 °C does not seem to impact the reactivity as lime reactivity values are similar for both clays. This is because the degree of dehydroxylation was complete at 750 °C itself and increasing temperature would not further enhance the reactivity potential.

Figure 4 represent lime reactivity values obtained for model clays. D1- C1, D2- C1 and D3- C1 represents model clays that were made after calcination of individual components. While, D1- C2, D2- C2 and D3- C2 represent model clays that were prepared in raw state and then calcined. The compressive strength of lime mortar cubes was found to be high enough for a material to be classified as a pozzolan. It was noticed that method adopted for the preparation of model clays does not have any impact on reactivity. There was roughly 15% increase in reactivity of clay when 12.5 % of iron was present as compared to reference sample. With further in iron content to 22 %, 8% reduction in reactivity values was observed when compared to clay with 12.5 % iron content, but nonetheless still higher than the reference sample.
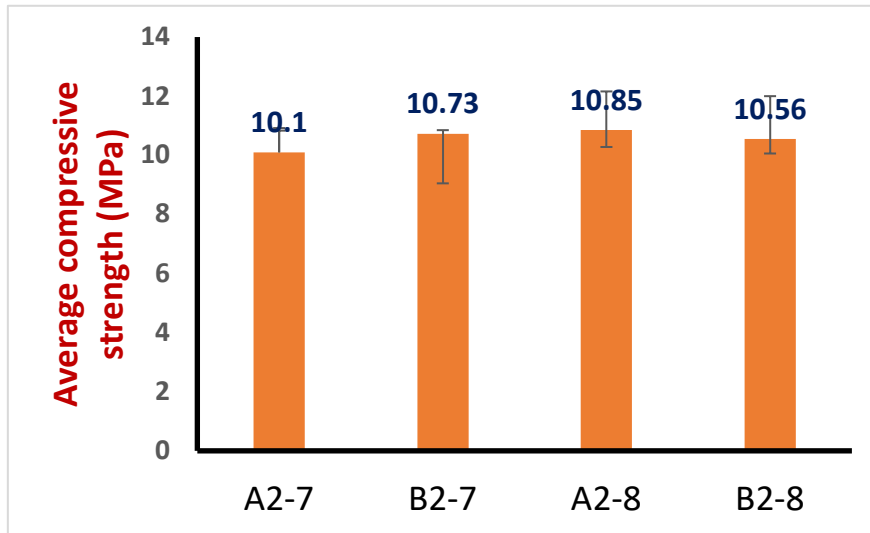
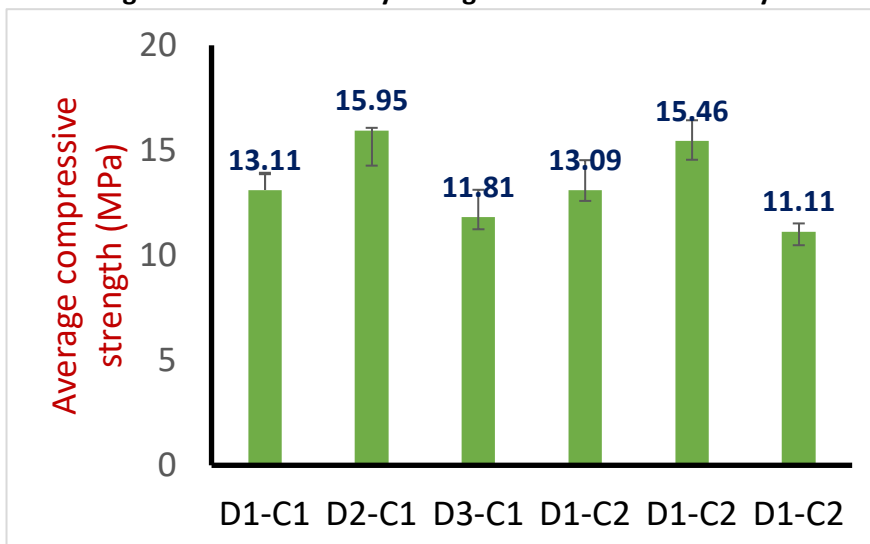**Figure 3: Lime reactivity strength results of natural clays**

Figure 4: Lime reactivity strength results of model clays

3.3 Effect of iron on properties of cement

For the preparation of ternary binder, limestone and calcined clay were used to replace 45 % clinker in the ratio of 1:2 by weight. For each clay, limestone calcined clay cement was produced and properties like specific gravity, setting time and water demand were measured. The impact of clay composition on the compressive strength of mortar was also evaluated.

3.3.1 Impact on setting time

Table 3 presents the results of setting time of cement with different types of clay compositions and all values are within the permissible limits. It can be observed that increasing the iron content from 10 % to 20 % in case of A2 and B2 clays respectively, does not change either the initial or final setting time. This is primarily because the iron is present in the phase that is not soluble in cement system and thus will not influence the reactions and would rather remain in an unreactive phase. As expected, changing the calcination temperature of natural clay also does not have any impact on the setting values of cement. Cement prepared with model clays using two different approaches, showed similar values of setting time as well. From the setting time results, it can be concluded that the presence of iron upto 22% does not influence the setting behavior of cement.

Table 3: Setting time results of limestone calcined clay cement made with iron rich clays

Cement	Initial setting time (mins)	Final setting time (mins)
A2-7-LC3	106	174
B2-7-LC3	115	182
A2-8- LC3	113	175
B2-8-LC3	117	180
D1-C1- LC3	125	178
D2-C1- LC3	96	168
D3-C1-LC3	103	165
D1-C2-LC3	110	186
D2-C2-LC3	98	172
D30-C2-LC3	107	178

3.3.2 Impact on specific gravity

Incorporating low grade kaolinite with iron impurities increases the specific gravity of blended cement as shown in Figure 4. As expected, cement with higher iron impurity shows higher gravity than the one with lower impurity. There was 2.39 % increase in density values of cement made kaolinite clay containing 22 % iron impurity as compared to reference cement (3% iron content).
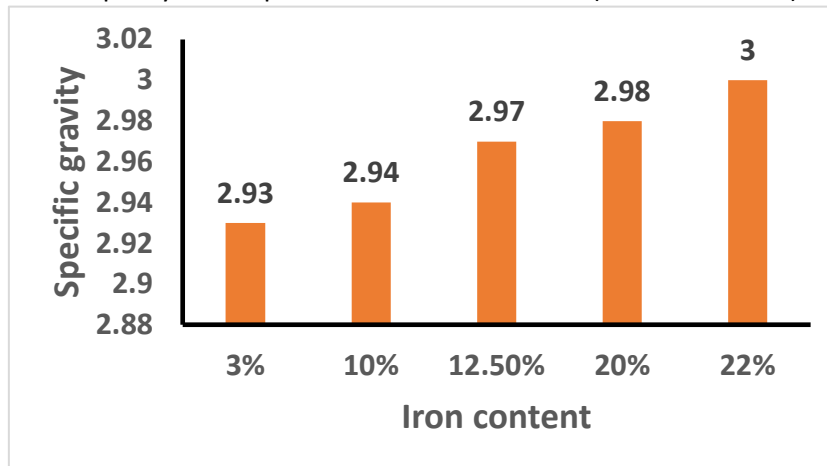
Figure 5: Specific gravity at different iron content

3.3.3 Influence on water demand

Tests were performed on cement prepared with different clay compositions to determine the amount of water required to get standard consistency and study the change in water demand. The data on normal consistency as listed in table 4, showed no significant change in water demand despite huge variation in the amount of iron content.

Table 4: Normal consistency of LC^3 prepared with impure clays

Cement	Water demand
A2-7-LC3	35.5
B2-7-LC3	34.5
A2-8- LC3	35
B2-8-LC3	34.5
D1-C1- LC3	35
D2-C1- LC3	36
D3-C1-LC3	35.5
D1-C2-LC3	35.5
D2-C2-LC3	36
D30-C2-LC3	35

3.3.2 Compressive strength

The measurements of compressive strength of mortar mixes at 3,7 and 28 days are presented in figure 6. Cement made with A2 clay containing 10 % iron content showed 31.48 % and 16.86 % increase in strength values from 3 days to 7 days and from 7 days to 28 days respectively. While, cement made with B2 clay that contains 20 % iron content, exhibited 37.35% higher strength from 3 days to 7 days and 24.6 % from 7 days to 28 days. This could imply that cement made with higher iron content achieves marginally greater strength values at 28 days. The impact of an increase in calcination temperature of clays from 750 °C to 850 °C, on strength values was not noticeable like in lime reactivity results, as a similar trend was observed for both cement.
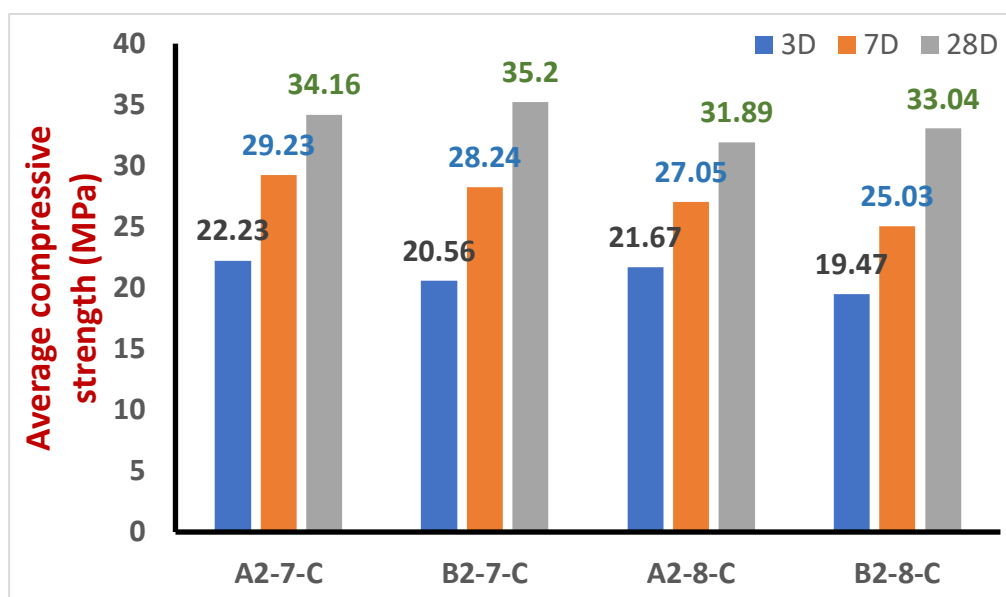
Figure 6: Compressive strength of mortar made with natural clays

Figure 7 shows the compressive strength results of mortar mixes prepared using model clays at 3, 7 and 28 days. Irrespective of the age of testing, lowest compressive strength was observed for D1 mix as compared to D2 and D3 mixes. This is mostly because the substitution of iron in the lattice of kaolinite structure imparts the higher degree of disorder. And, it is well known that disordered kaolinite are more reactive than ordered structure [9,11]. Interestingly, D2 mix composed of clay with 12.5 % iron content, showed significantly higher strength at 7 days, as compared to D3 mix made with clay containing 22 % iron content. However, at 28 days, difference between the strength values of D2 and D3 mixes was not significant. The approach by which the model clays were made do not influence the strength properties as similar behavior was exhibited by both mixes.

Investigation of the compressive strength with varying iron content (figure 8) shows that the results are dependent on the type of clay (natural or model composition). In case of natural clays, strength results were found to be similar at 3,7 and 28 days even though iron content changed from 10 % to 20 %, highlighting that the higher amount of iron has not negative impact on the performance. While, for model clays, there seems to be an optimum percentage beyond which strength was found to reduce slightly at 7 days. Clay with 12.5 % iron content showed higher strength at 7 days and as compared to clay with 22% iron content. Therefore, from this study, clays upto 12.5 % iron content can be considered as suitable material for the use of SCM.
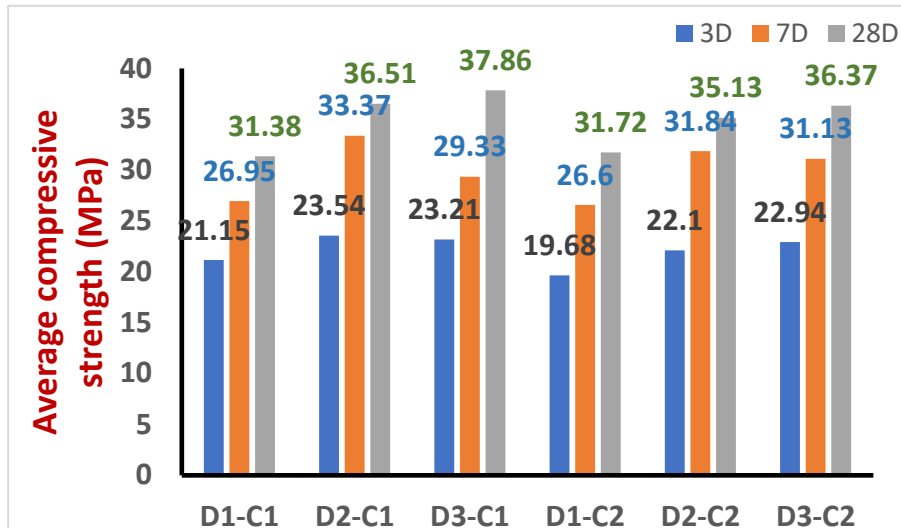
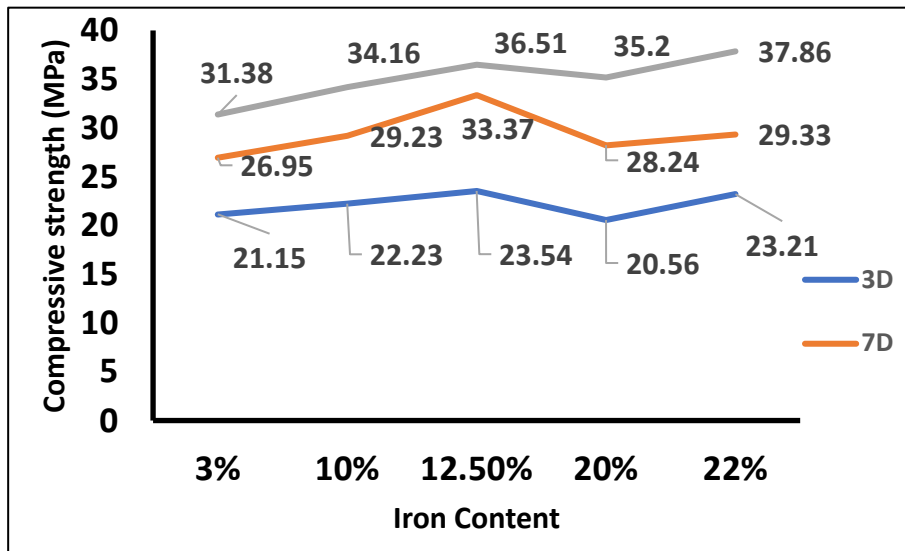**Figure 7: Compressive strength of mortar made with model clays**

Figure 8: Compressive strength at different iron content

4. Conclusions

This study explored the influence of iron contaminated kaolinite on the reactivity of limestone calcined clay cement. From these investigations, the following conclusions can be made:

1. Iron impurities do not influence the reactivity of calcined clays as lime reactivity values were found to be higher for all clays and qualified as pozzolan in cement-based industry.

2. No significant change was noticed in the properties of cement like water demand and setting time while using clays, even though iron content changed from 3 % to 22 %.

3. The method adopted for the formation of model clays does not impact the reactivity and compressive strength.

4. Increasing the calcination temperature from 750 °C to 850 °C does not affect the performance of clay.

5. The behavior of model clay was found to be different from natural clays. There seems to be an optimum iron content of 12.5 % from lime reactivity and compressive strength results. While, natural clays with iron content upto 20 % were found to be suitable for use as SCM.

xxx

References

[1] Scrivener, K. L., (2014). Options for the future of cement. *Indian Concr. J*, *88*(7), 11-21.

[2] Scrivener, K., Martirena, F., Bishnoi, S., & Maity, S. (2018). Calcined clay limestone cements (LC3). *Cement and Concrete Research*, *114*(March), 49–56. https://doi.org/10.1016/j.cemconres.2017.08.017

[3] Taylor-Lange, S. C., Lamon, E. L., Riding, K. A., & Juenger, M. C. G. (2015). Calcined kaolinite-bentonite clay blends as supplementary cementitious materials. *Applied Clay Science*, *108*, 84–93. https://doi.org/10.1016/j.clay.2015.01.025

[4] Alujas Diaz, A., Almenares Reyes, R. S., Hanein, T., Irassar, E. F., Juenger, M., Kanavaris, F., … Snellings, R. (2022). Properties and occurrence of clay resources for use as supplementary cementitious materials: a paper of RILEM TC 282-CCL. *Materials and Structures/Materiaux et Constructions*, *55*(5). https://doi.org/10.1617/s11527-022-01972-2

[5] Rakhimova, N. R., Rakhimov, R. Z., Bikmukhametov, A. R., Morozov, V. P., Eskin, A. A., & Gubaidullina, A. M. (2020). Calcined low-grade multimineral clays as supplementary cementitious materials: a feasibility study. *Geosystem Engineering*, *23*(3), 168–173. https://doi.org/10.1080/12269328.2020.1713911

[6] Zunino, F., Boehm-Courjault, E., & Scrivener, K. (2020). The impact of calcite impurities in clays containing kaolinite on their reactivity in cement after calcination. *Materials and Structures/Materiaux et Constructions*, *53*(2). https://doi.org/10.1617/s11527-020-01478-9

[7] Bishnoi, S. (2020). RILEM Bookseries Calcined Clays for Sustainable Concrete Proceedings of the 3rd International Conference on Calcined Clays for Sustainable Concrete. Retrieved from http://www.springer.com/series/8781

[8] Kaze, C. R., Lecomte-Nana, G. L., Kamseu, E., Camacho, P. S., Yorkshire, A. S., Provis, J. L., … Melo, U. C. (2021). Mechanical and physical properties of inorganic polymer cement made of iron-rich laterite and lateritic clay: A comparative study. *Cement and Concrete Research*, *140*(December 2020). https://doi.org/10.1016/j.cemconres.2020.106320

[9] Musbau, K. D., Kolawole, J. T., Babafemi, A. J., & Olalusi, O. B. (2021). Comparative performance of limestone calcined clay and limestone calcined laterite blended cement concrete. *Cleaner Engineering and Technology*, *4*(April). https://doi.org/10.1016/j.clet.2021.100264

[10] Martirena, F., Almenares, R., Zunino, F., Alujas, A., & Scrivener, K. (2020). Color control in industrial clay calcination. *RILEM Technical Letters*, *5*, 1–7. https://doi.org/10.21809/RILEMTECHLETT.2020.107

[11] Peys, A., Isteri, V., Yliniemi, J., Yorkshire, A. S., Lemougna, P. N., Utton, C., … Hanein, T. (2022). Sustainable iron-rich cements: Raw material sources and binder types. *Cement and Concrete Research*, *157*(May), 106834. https://doi.org/10.1016/j.cemconres.2022.106834

[12] Fernandez, R., Martirena, F., & Scrivener, K. L. (2011). The origin of the pozzolanic activity of calcined clay minerals: A comparison between kaolinite, illite and montmorillonite. *Cement and Concrete Research*, *41*(1), 113–122. https://doi.org/10.1016/j.cemconres.2010.09.013

[13] Sharma, M., Bishnoi, S., Martirena, F., & Scrivener, K. (2021). Limestone calcined clay cement and concrete: A state-of-the-art review. *Cement and Concrete Research*, *149*(August), 106564. https://doi.org/10.1016/j.cemconres.2021.106564

Annex IV – Medium term field performance of LC³ concrete
Testing of LC³ house in Orchha and LC³ and PPC columns placed in different weather zones across India
Report by Indian Institute of Technology Delhi

I. INTRODUCTION

Vast consumption of cement leads to equivalently vast emission of carbon dioxide, which makes cement industry a major cause of global emission. To cut down the carbon dioxide emission and to move toward global sustainability, we need to bring down the clinker factor of the cement using natural resources which are widely available to meet our cement demand even in coming future. LC3 is new ternary cement blend which uses a clinker factor of 0.5 and is a combination of ordinary Portland cement, calcined clay, and limestone, both of which are widely available throughout world. This new cement has comparable 28-day strength with Ordinary Portland cement and have almost 40% lesser carbonation emissions coming per tonne of final product. However, for any new cement just strength is not sufficient enough parameter, we need durability studies also to show the capabilities of this new product in the industry.

This report covers the durability testing of the LC³ building in TARAgram Orchha, Madhya Pradesh as well as testing of the LC3 and PPC columns that have been cast and placed all throughout India in different weather zones. TARAgram Orchha building has been constructed in 2015-16 using LC3 cement from the first pilot production. Also, 9 column each of PPC and LC3 has been cast in the same year and has been placed at different location across the India covering major weather zones of nation. This report has been divided into different section and sub-sections, starting with the scope of the work undertaken. Further, the observation made, and experimental results obtained for the above-mentioned building and columns are discussed.

II. SCOPE

The work undertaken covers the following points:

- Carbonation depth
- Resistivity of the concrete
- Half-cell potential
- Corrosion rate observations
- Visual inspections

PART A: INSPECTION OF LC3 BUILDING ORCHHA, JHANSI, M.P

Figure: 1 a) Front view, and b) back view of LC3 building TARAgram Orchha (near Jhansi), Madhya Pradesh, India

Building construction has been done during year 2014 using the LC^3 from the first pilot production in India. All the structural members have been made with the LC^3 cement, even the roof tiles and plaster has been done using the LC^3 cement. Construction has been unmonitored and expected to have high water to binder ratio of 0.6. Additionally, the clay used in the cement was not properly calcined and the cement used was coarse, thus properties of concrete can be expected to be poor. The properties of the clays used and the properties of the cements are shown in the tables below from Bishnoi et al. 2014.

S.No.	Chemical Constituents	Clay 1	Clay 2
1	Silica (SiO_2)	43.30%	55.78%
2	Alumina (Al_2O_3)	36.35%	17.46%
3	Ferric Oxide (Fe_2O_3)	2.56%	8.89%
4	Calcium Oxide (CaO)	0.46%	4.84%
5	Loss on Ignition (LOI)	13.94%	9.49%
6	Colour	White	Red
7	Lime reactivity	9.25 MPa	1.38 MPa

Property	LC3 A	LC3 B	LC3 C	LC3 D
Standard consistency (%)	32.5	33	34	34
Initial setting time (min.)	34	33	101	105
Blaine fineness (m^2/kg)	534	534	520	462
Mortar cube strength (MPa) (Water-cement ratio)	34.4 (0.445)	40.8 (0.45)	24.7 (0.46)	27.2 (0.46)

The building is currently under use by TARAgram Orchha for various office purposes such as video recording and session recording for Bundelkhand Radio. Over the years, building has been regularly monitored and inspected by IIT Delhi as well as TARA. During Jan, 2022 some durability tests were performed on the building and the results of the same are compiled below.

I. pH OF THE CONCRETE – on observing that the carbonation depth has reached up to the rebar level, a decision has been made to check the pH of the plaster, concrete at interface of plaster and column, and around the rebar. A bit higher pH values can be expected because of mixing of uncarbonated cement paste while powdering the samples for testing. Results obtained show that, concrete has been carbonated and loss of passivating can be expected.
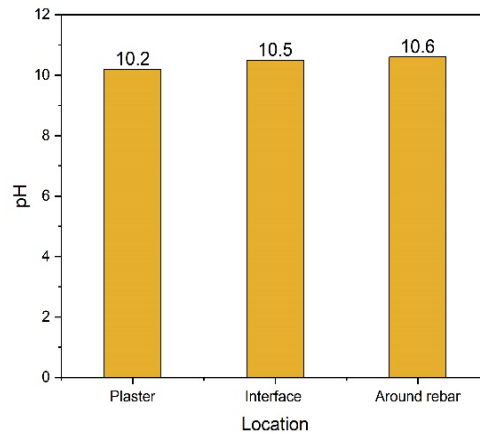
Figure: 2 pH of sample collected from different locations

II. RESISTIVITY OF THE CONCRETE – surface resistivity of concrete has measured after splash wetting the surface of column for 15 minutes and ensuring saturated surface dry conditions. Readings for surface resistivity were taken in direction parallel as well as perpendicular to main rebar. In both direction average resistivity values coming are falling in low corrosion risk range.
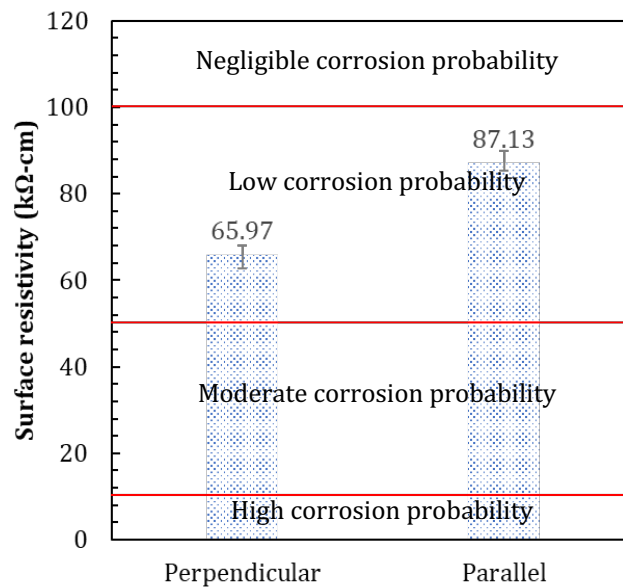

Figure: 3 Resistivity values for the column tested in direction perpendicular and parallel to main rebar.

III. HALF-CELL POTENTIAL OF THE CONCRETE-STEEL SYSTEM – half-cell potential readings were taken on the middle and corner main rebar. To ensure the proper connection, rebar was first cleaned with the sandpaper. Results obtained shows the half-cell potential values are in uncertain range to make any comment on corrosion probability.
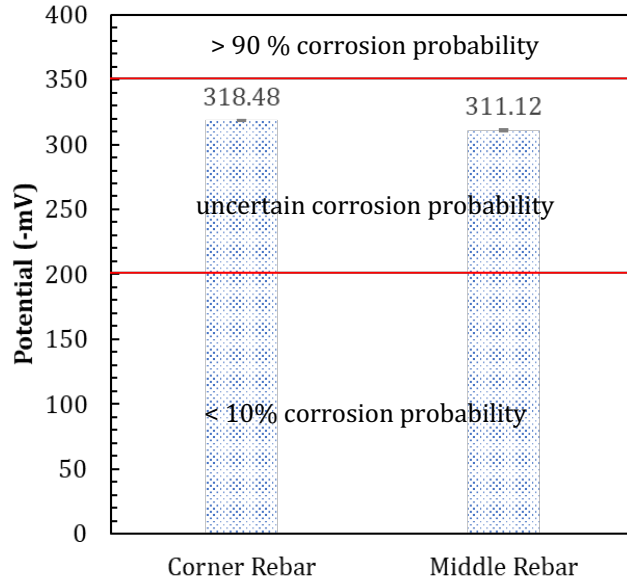
Figure: 4 Half-cell potential values for the column tested for corner and middle main rebar.

IV. LINEAR POLARISATION RESISTANCE VALUE - to monitor the corrosion in the structure, linear polarization resistance experiment has been performed on the corner and middle rebar of the column using the ACM field machine under IR compensation mode and while using guard rings for better results. Corrosion rate observed in the middle bar was $0.7\mu A/cm^2$ ($8.12\mu m/year$), while corrosion rat observed in corner rebar is $0.43\mu A/cm^2$ ($4.99\mu m/year$) which shows the indeed de-passivation has occurred. However, the corrosion rate is falling under very low range i.e less than $1\mu A/cm^2$ and can't be considered that detrimental to the structure.
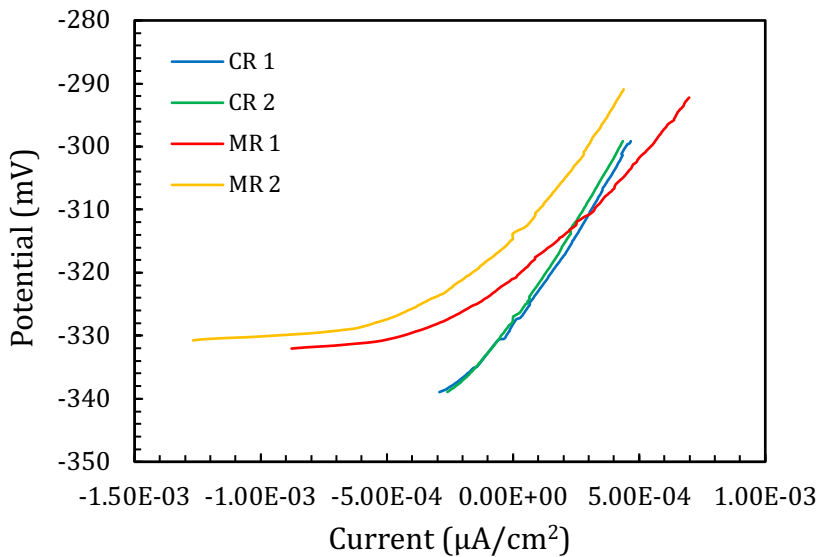
Figure: 5 Linear polarization resistance graph about the open cell-potential.

Figure: 6 left) breaking of the plaster from over the concrete and right) resistivity measurement on the exposed column surface.
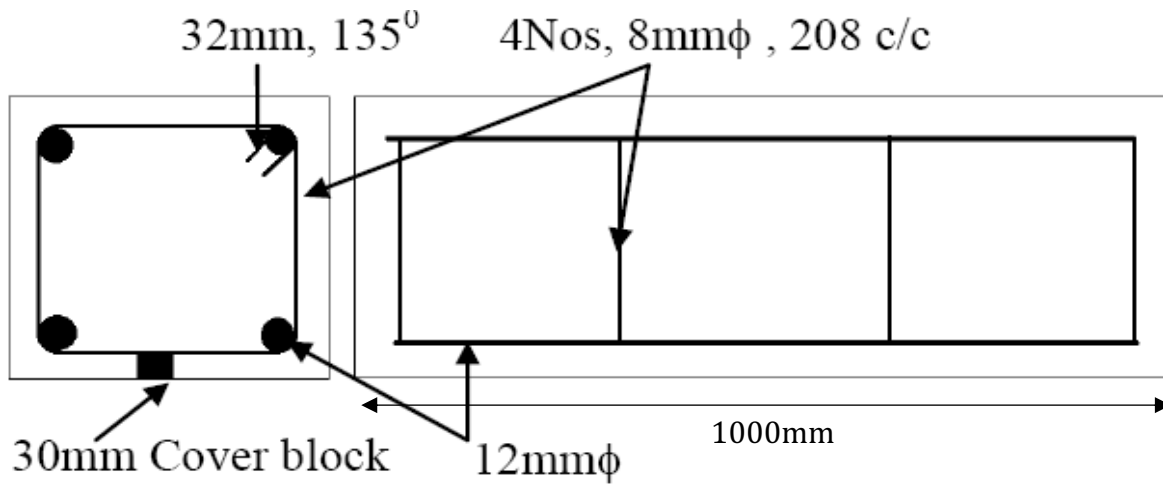
Figure: 1 Dimensions and reinforcement distribution of LC3 column placed across India.

The properties of the materials used in this study are shown in the table below.

Chemical Composition	Clinker	Gypsum	Fly ash	Calcined Clay	Limestone
SiO_2	21.07	2.77	67.66	54.67	11.02
Al_2O_3	4.65	0.62	22.18	27.69	1.55
Fe_2O_3	4.32	0.36	5.32	4.93	2.53
CaO	65.16	32.62	0.32	0.06	44.24
MgO	2.13	1.2	0.18	0.13	1.96
SO_3	0.77	38.75	0.02	0.1	0
Na_2O	0.38	0.06	0.43	0.12	0
K_2O	0.2	0.037	1.6	0.25	0
LOI	0.96	23.02	1.74	10.28	36.96

The mixes were prepared at a water to cement ratio of 0.45 and the mix designs used are shown in the table below.

| Blend | Water | Clinker | Fly Ash | Coarse Agg. | | Fine Agg. |
				10mm	20mm	(zone-II)
PPC	162	252	108	467.1	700.6	693.7
LC^3	162	360(LC^3)		470.2	705.2	698.2

9 sets of LC3 and PPC columns had been cast at IIT-Delhi and then placed across India at Delhi, Chennai, Kolkata, Srinagar, Orchha, Jodhpur, Bangalore, Surathkal and Meghalaya. A detailed description of the location and the weather zone is given in the table 1.

Table 23 Location and weather zones of the place where columns were placed.

Sr. No	State	Location	Climatic Condition (NBCI)	Climatic Condition (Koppen)
1	Delhi	IIT Delhi	Composite	Semi-Arid
2	Tamil Nadu	IIT Madras	Warm Humid	Tropical Wet and Dry
3	J & K	Srinagar Airport	Cold	Mountain
4	Rajasthan	IIT Jodhpur	Hot and Dry	Arid
5	Karnataka	IISc Banglore	Temperate	Semi-Arid
6	Karnataka	NIT Surathkal	Marine Exposure *	Marine exposure*
7	M. P	TARAgram,Jhansi	Composite	Humid Subtropical
8	Meghalaya	Adhunik Cements	Warm Humid	Humid Subtropical
9	West Bengal	Kolkata (Maity)	Warm Humid	Tropical wet and dry

These columns were partially buried under the soil and left out in open where no obstruction from any nearby trees or manmade construction was there for natural exposure. During this summer many of these columns were tested and results have been complied for the same which are discussed in subsequent section.

I. HALF-CELL POTENTIAL OF CONCRETE-STEEL SYSTEM – Half cell values obtained from copper-copper sulphate solution are reported below. Readings were taken along the rebar at step size of 6cm, away from the point where connection to the rebar has been made. Potential has been observed to be dropping as we move further away from the connection point. Reading obtained were mostly greater than -200mV and some lying in between -200mV to -350mV.
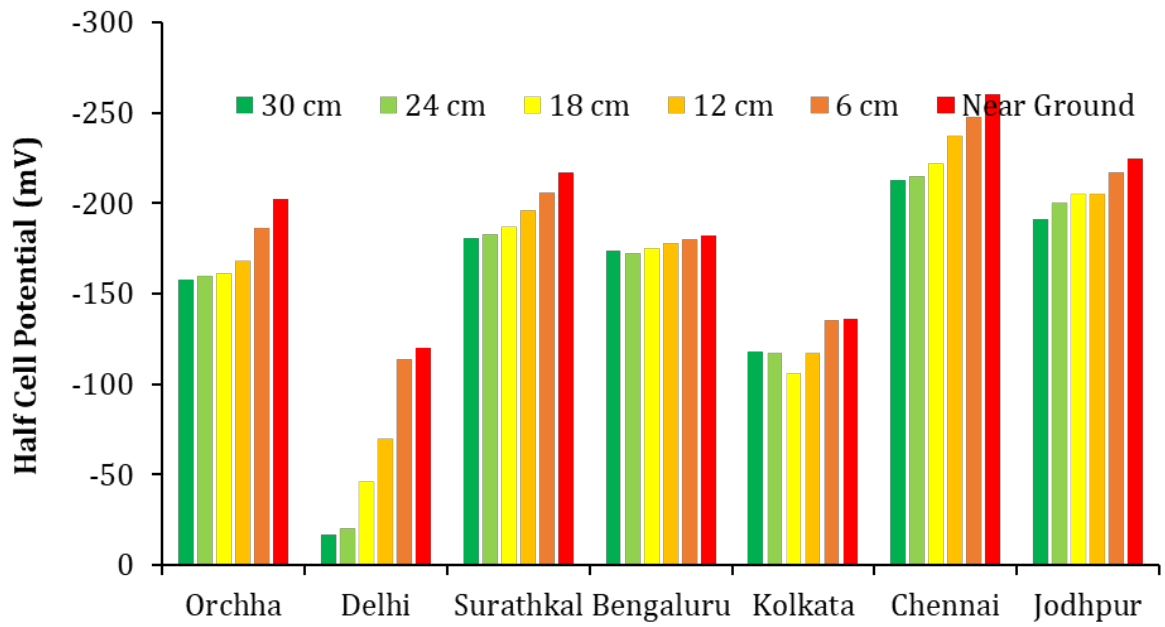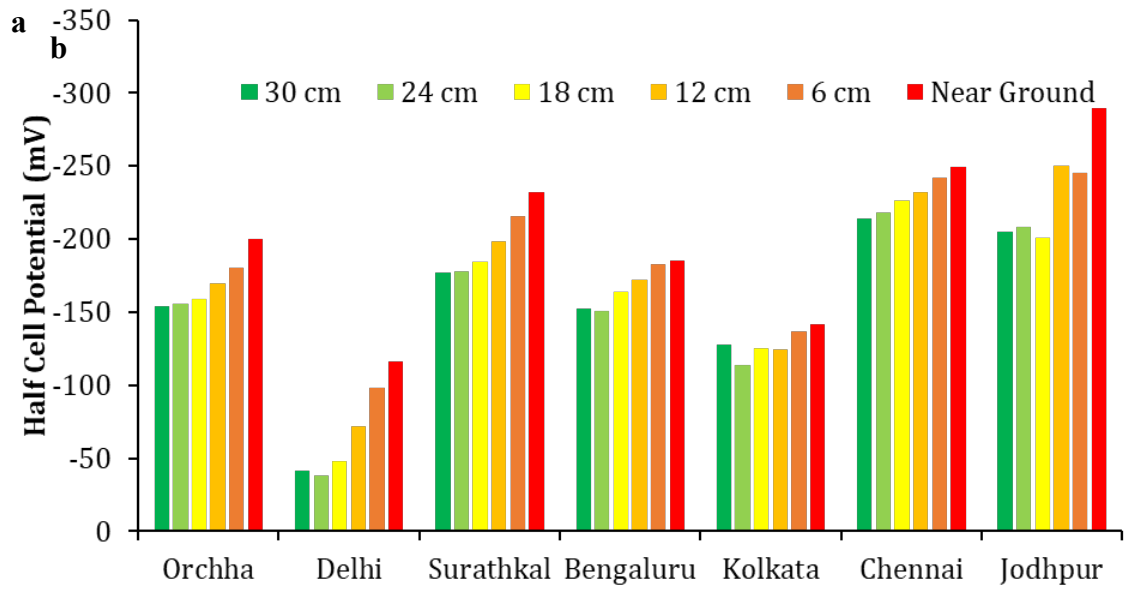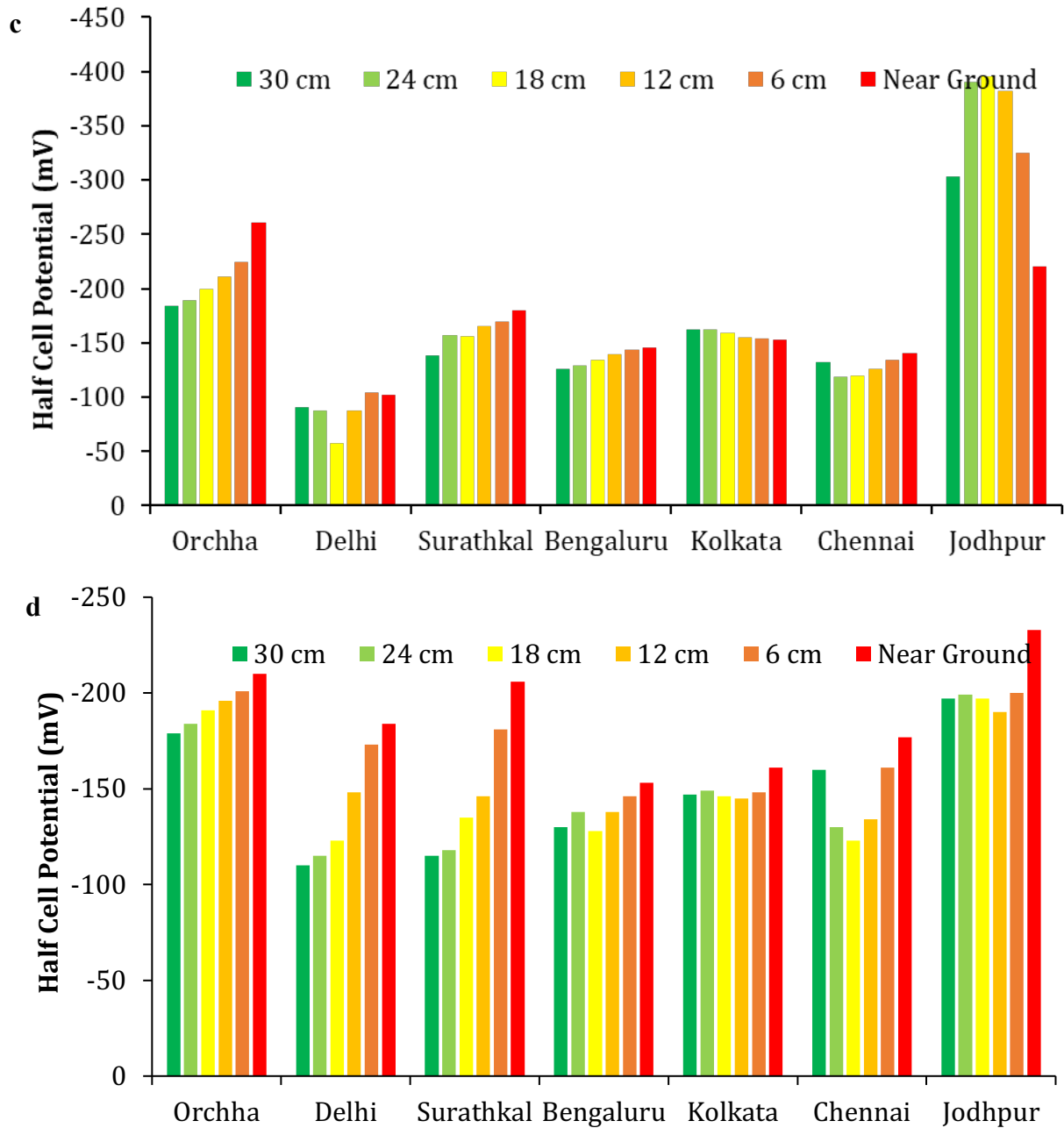
Figure: 7 Half -cell potential readings obtained along the rebar for different location of PPC and LC3 columns. a) PPC column face 1, b) PPC column face 2, c) LC3 column face 1, and d) LC3 column face 2.

II. SURFACE RESISTIVITY OF CONCRETE – surface of the column has been first saturated by splashing water on the column and leaving wet gunny bag over it, after which surface resistivity measurements had been taken. Surface resistivity of LC3 concrete has been found to be sustainability higher than PPC concrete at all the locations due to the significant pore refinement in LC3.
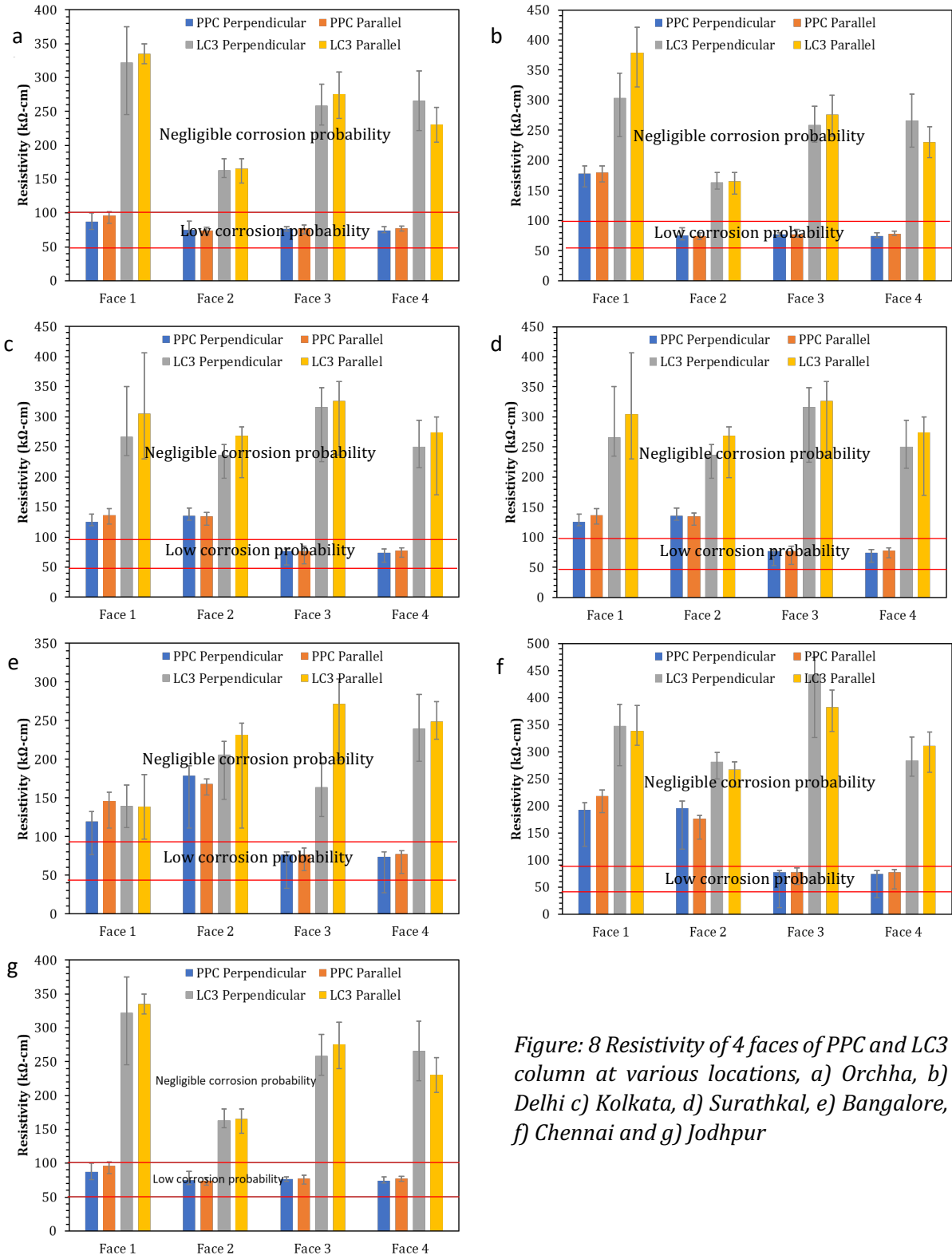
Figure: 8 Resistivity of 4 faces of PPC and LC3 column at various locations, a) Orchha, b) Delhi c) Kolkata, d) Surathkal, e) Bangalore, f) Chennai and g) Jodhpur

III. CORROSION RATE IN REINFORCED CONCRETE – Rapicorr machine has been used for the field investigation of corrosive state of these columns. Rapicorr works on principle of monitoring potential change after imposing galvanostatic current through counter electrode. Depending upon the corrosion rate values, half-cell potential and resistivity readings, comments about corrosion level can be provided as per table 2. For most of the cases observed corrosion rate values had been in negligible range while for few it was under low range.

Table 24: Criteria for classification of corrosion level (Luping and Utgenant 2007).

Corrosion level		Corrosion rate [μm/yr]	Half-cell potential [mV$_{(CSE)}$]	Resistivity [kΩ·cm]	Criteria
1	Negligible	$< X_L$	-	-	$X_L = 1$ μm/yr
		$X_L \sim X_M$	$\geq E_{cr}$	$\geq \rho_{cr}$	$X_M = 3 \sim 5$ μm/yr*
2	Low	$X_L \sim X_M$	$< E_{cr}$	$< \rho_{cr}$	$X_H = 10$ μm/yr
		$X_M \sim X_H$	$\geq E_{cr}$	$\geq \rho_{cr}$	$E_{cr} = -200$ mV$_{(CSE)}$
3	Moderate	$X_M \sim X_H$	$< E_{cr}$	$< \rho_{cr}$	$\rho_{cr} = 100 \sim 120$ kΩ·cm†
		$> X_H$	$\geq E_{cr}$	$\geq \rho_{cr}$	
4	High	$> X_H$	$< E_{cr}$	$< \rho_{cr}$	

* 3 for average measurement and 5 for single measurement.
† depending on the type of concrete, surface treatment, weather, etc.

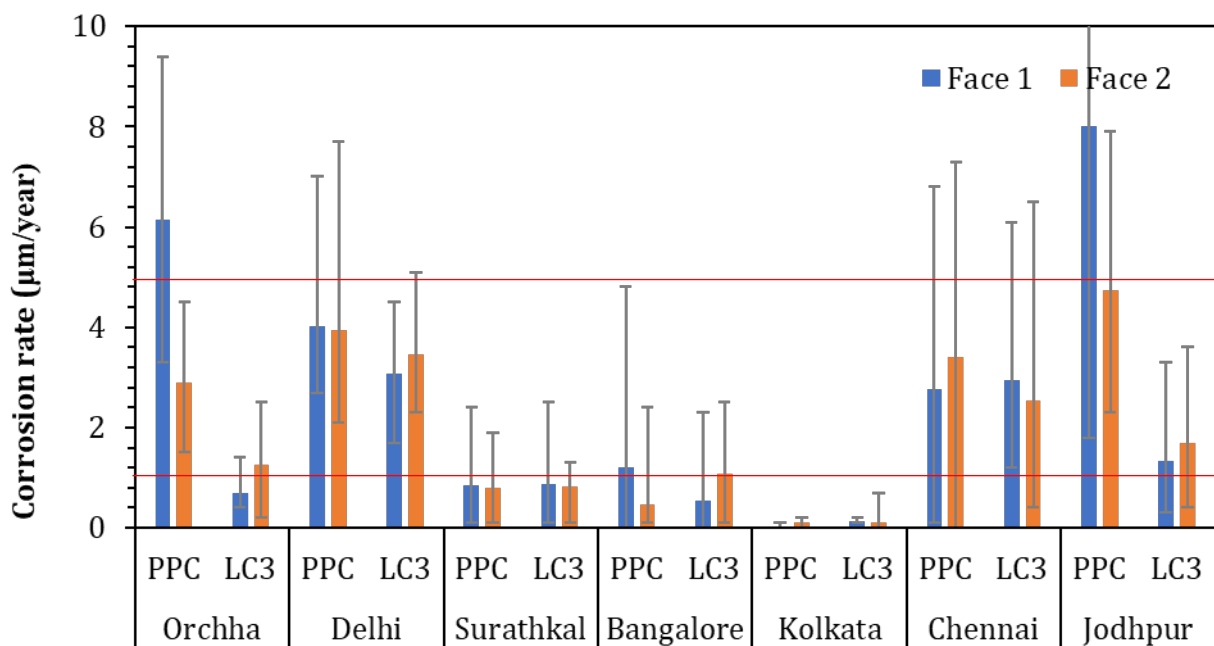*Figure: 9 Corrosion testing of PPC and LC3 columns with Rapicorr machine.*
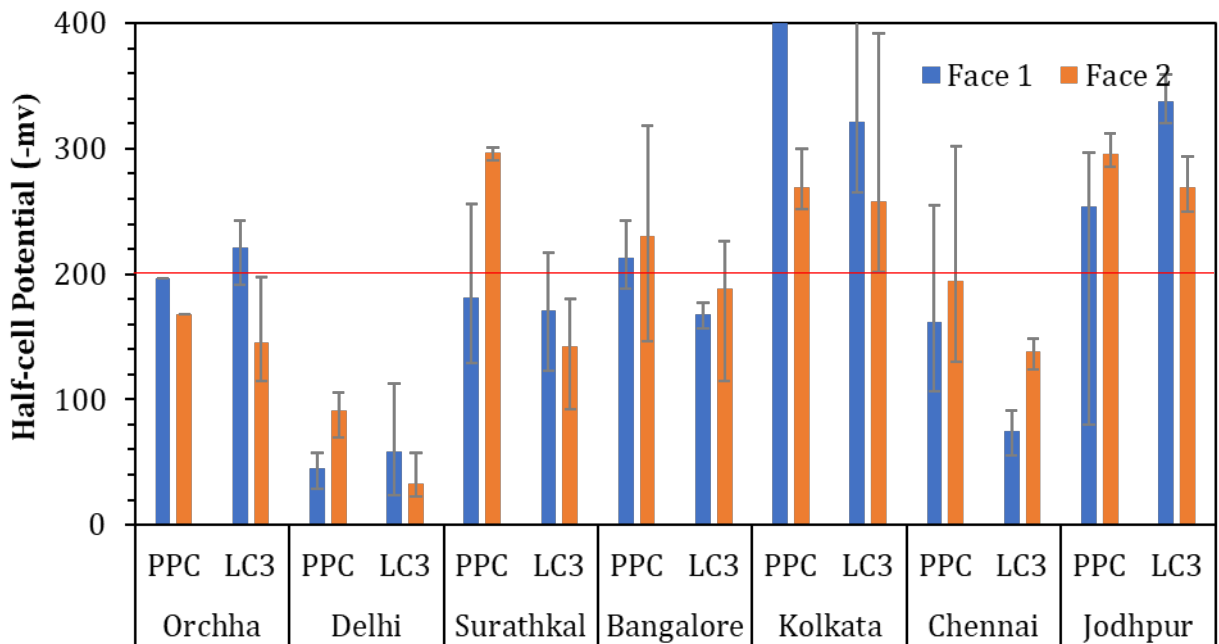
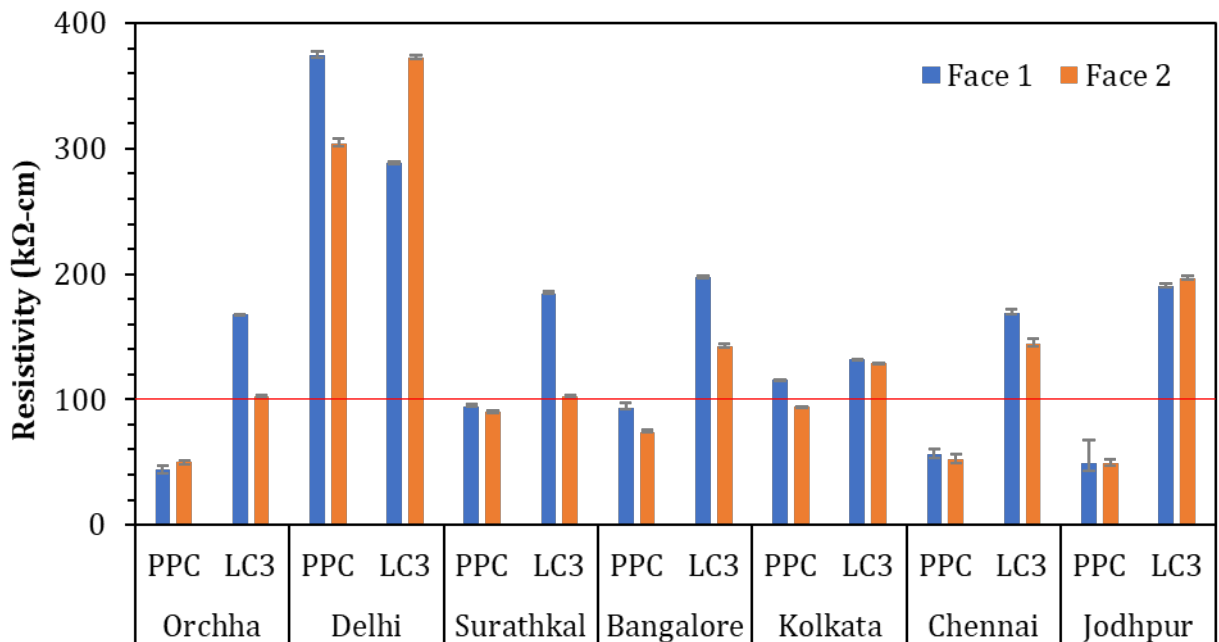*Figure: 11 Half- cell potential values obtained from Rapicorr.*

Figure: 12 Resistivity values obtained from Rapicorr.

IV. CARBONATION DEPTH OF THE CONCRETE - carbonation depth was checked by spraying phenolphthalein on freshly chipped off concrete and then letting it be for few minutes. Interesting observation was that at almost all the places PPC was showing higher carbonation depth as compared

to the LC3 concrete. Additionally, carbonation depth hasn't been observed to reach rebar level in any of the location, which means rebar is still protected by the passivating film.
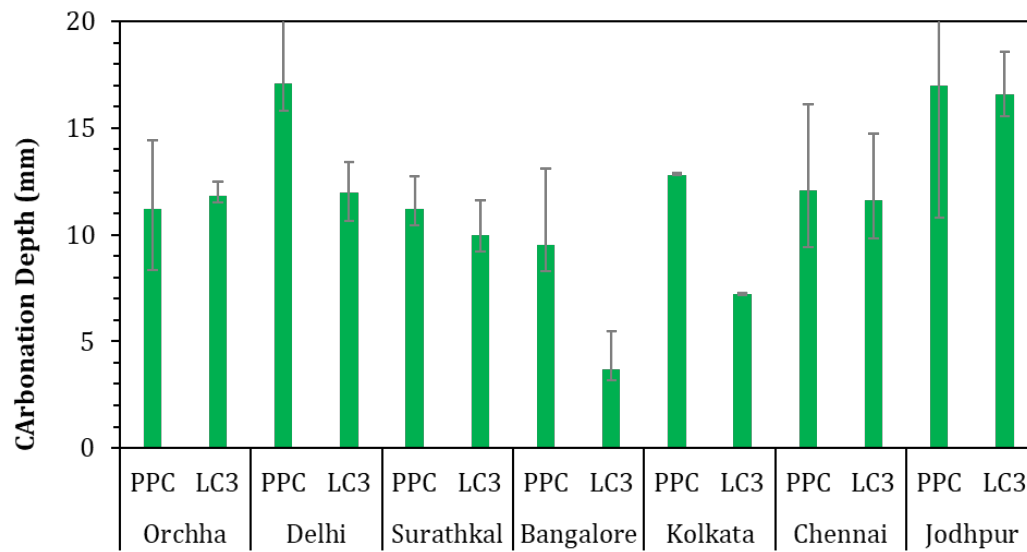

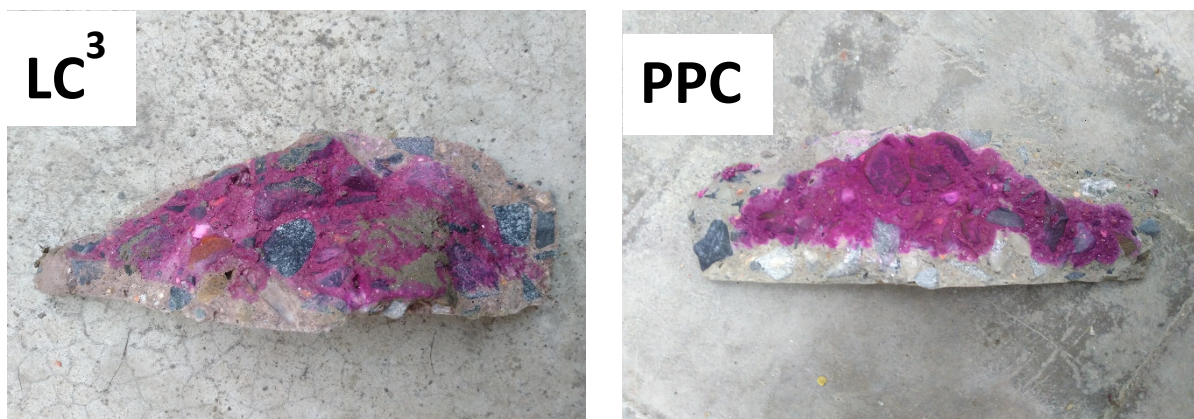*Figure: 13 Carbonation depth at various location across India for columns.*

Figure: 14 Carbonation depth measured on-site for the columns.

Protocol for Testing
**Carbonation Depth Protocol**
* Main aim here is to check if the concrete around rebar is carbonated or not.
Protocol to be followed to determine Carbonation Depth (IS-516: Part 5/Sec 3):

- Extract a concrete sample from over the rebar at the cornered location.
- Soon after recovering the sample, spray it with the phenolphthalein solution and leave it for some time.
- After colour has stabilized (5-10min), the demarcation between the region, which turns into magenta and the region showing no change in colour will indicate the carbonation front.
- Note down the carbonation depth values of the sample in the data sheet.
- Take minimum of three readings and collect about 50-80 grams of the powdered sample from around the rebar location.
- Seal the sample in zip lock as soon as possible to avoid any further carbonation.

Instruments and Reagents required:

- Phenolphthalein solution
- Chisel and hammer
- De-ionised water
- Zip locks
- Measuring scale or vernier calliper
- Marker
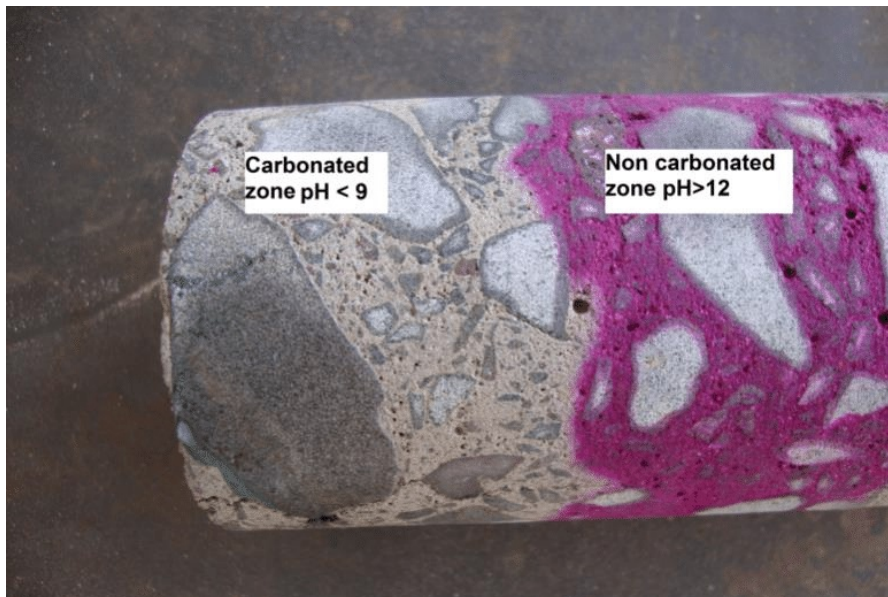
Half-Cell Potential Protocol
* Take reading on two adjacent faces keeping connection made at rebar in middle of grid.
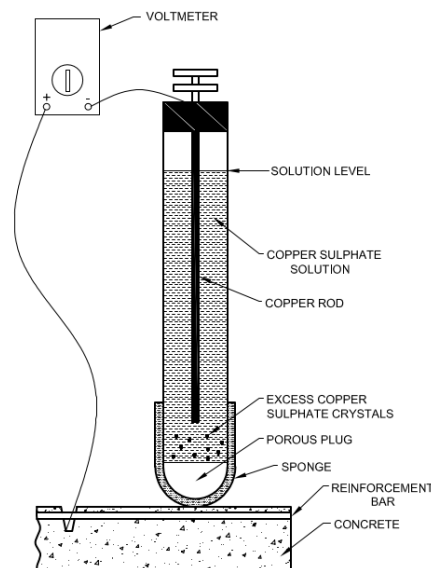*Protocol to be followed to determine Half-cell potential (IS-516: Part 5/Sec 2):*

- Prepare a grid around of dimension 24x24cm with 4cm sub-divisions, around the corner rebar.
- Expose the rebar at a corner location and clear it with help of sandpaper to ensure proper connection.
- Make a connection at rebar with electrical wire and connect that to the positive terminal of voltmeter and other connection of voltmeter should be made with the half-cell.
- Place the half-cell on the surface of concrete at various grid locations and observe the voltmeter reading.

- If the readings are not stable, you can pre-wet the surface. Please, avoid having any free surface water when taking the reading.
- Take down reading on the two adjacent faces beside the rebar exposed.
- Note down the temperature on the day of testing as well, see note.

NOTE: If the half-cell temperature is outside the range of 22.2 ± 5.5 °C. The temperature coefficient correction of about 0.000 91 V more negative per °C for the temperature range from 0 to 49 °C shall be applied.

Instruments and Reagents required:
- Half-cell
- Electrical junction device
- Copper sulphate crystals
- Voltmeter
- Electrical lead wires
- De-ionised water
- Chisel, scale, and hammer

**Surface Resistivity Protocol**

* Cover all the four faces of the column, 5 reading in each direction
Protocol to be followed to determine surface resistivity:
- Splash water on the concrete surface and leave it for some time and then splash some water again, try to ensure saturation of concrete.
- Meanwhile, calibrate the Resipod with the provided calibration strip.
- Once, concrete appears to be saturated and the surface doesn't show any signs of the free water, you can start taking the measurements.
- Gently press the Resipod, such that all the 4 probes are in contact with surface and note down the reading.
- Take 5 reading in both directions (perpendicular and parallel to main rebar)
- Ensure a gap of minimum 4cm between consecutive readings.
- If a certain resistivity value appears to be drastically low in comparison to other, mark it and cross check if there is possibility of rebar falling directly below at the location, take another reading in place of it.

Instruments and Reagents required:

- Resipod
- Water
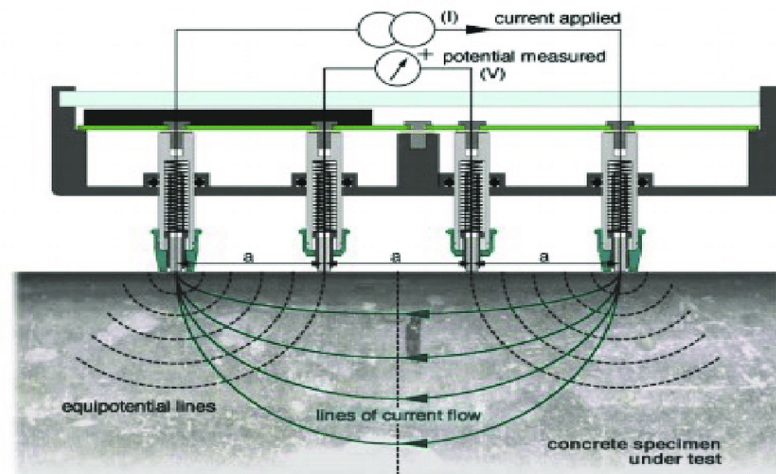
Corrosion rate measurement Protocol

Protocol to be followed to determine corrosion rate by RapiCorr Machine:
- First calibrate the RapiCorr with the check box provided along with it and with the half-cell provided for reference potential. (Procedure for calibration is provided in manual kept in briefcase)
- Expose the rebar at a corner location and clear it with help of sandpaper to ensure proper connection.
- Now make the connections one directly with the rebar and the RapiCorr terminal and other to the electrode's configuration and RapiCorr terminal.
- Place a wet sponge on the concrete surface right over the rebar to ensure a proper connectivity.
- Now place the electrodes configuration right over sponge over the rebar and hold it gently.
- Mention the length as 10 cm and area of the rebar.
- Run for the corrosion rate measurement and note down the value reported on screen such that half-cell potential, resistivity, and corrosion rate.
- Repeat the procedure for minimum 10 times at each location and on both faces.

Instruments and reagents:
- Check box and Half-cell for calibration
- Electrical junction device and lead wires
- Electrode configuration
- Wet sponge
- Chisel and hammer
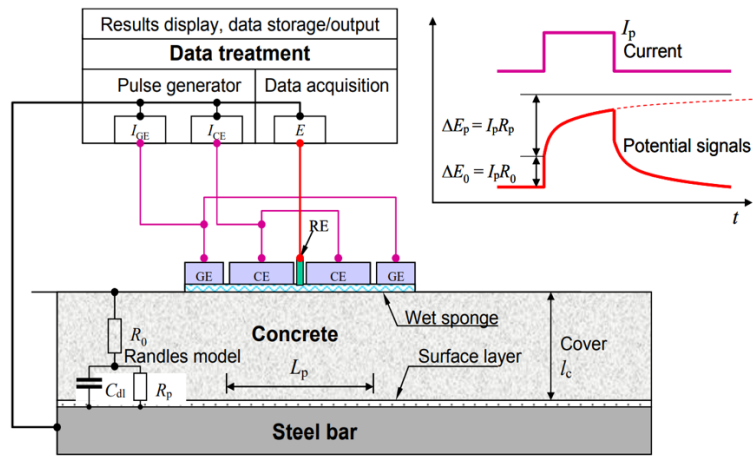
Annex V – Mix design of concrete using LC³
Report by Indian Institute of Technology Delhi

Introduction

The incorporation of different supplementary cementitious materials has been going on for a long time to reduce the impact of carbon emissions associated with cement production. Mineral admixture like fly ash has the potential to reduce clinker content, but high replacement levels have an adverse effect on early age strength. Moreover, quantity is limited as the production process is controlled by a specific industry [1,2]. In this context, it is necessary to identify new sources of material and the potential SCMs that are available in massive quantities are clay and limestone.

Kaolinite clay is composed of octahedral aluminate and tetrahedral silicate sheets in which adjacent layers are held together by a strong hydrogen bond. The calcination process results in the dehydroxylation reaction between the temperature range of 650 °C to 800 °C, and makes the disordered aluminosilicate phases. Metakaolin shows a high reaction with the calcium hydroxide when mixed with water and functions as an effective SCM [3,4]. However, calcined clays have a high specific surface area due to layered structure, that results in higher water demand for achieving the desired workability. While, in presence of limestone, the reactivity of calcined clays further enhances due to the formation of additional hydrates (carboaluminate phases). The loss in workability due to the clay is also compensated to some extent by the incorporation of limestone in the system [1,8].

LC³ is a ternary blended cement made up of clinker and two types of pozzolans i.e, calcined clay and limestone. This binder shows similar mechanical characteristics as that of ordinary Portland cement with a clinker factor of only 50 %. Numerous research works have been carried out that demonstrated the excellent properties exhibited by LC³ with regards to strength and durability [5-7]. However, just a few studies have investigated the effect of variables involved in the mix design of the LC3 system [9,10]. The present study focuses on the influence on workability and compressive strength by changing three parameters i.e., water content, coarse aggregate to total aggregate and water to cement ratio. The results of this study are expected to provide some insights into the influence of these parameters on concrete performance in terms of fresh and hardened properties.

Selection of raw materials and characterization

Limestone calcined clay cement was prepared by blending 55 % clinker and gypsum, 30 % clay and 15 % limestone. The characteristics of cement were determined according to the IS 4031:2019. The chemical composition of cementitious binder is provided in table 1.

Table 1: Chemical composition of cement

Oxides	SiO_2	Al_2O_3	Fe_2O_3	CaO	MgO	Na_2O	K_2O	TiO_2	MnO	P_2O_5	SO_3
(wt.%)	23.67	13.19	5.49	49.45	1.38	0.23	0.45	1.10	0.08	0	4.10

Locally available manufactured sand confirming to Zone II gradation as per IS 383:2016 was used. The specific gravity and fineness modulus was found to be 2.64 and 2.35 respectively. The water absorption of sand was found to be 0.81 % while bulk density was 2.65 g/cm³. The third generation polycarboxylic ether-based superplasticizer was added to improve the fresh properties of concrete with 46.5 % solid content. Tap water that was free from deleterious impurities was used for concrete mixing and curing. The natural coarse aggregates are collected from locally available crushing plants. The nominal maximum size of coarse aggregates used in this study were 20 and 10 mm. The properties of coarse aggregates are given in table 2.

Properties	C.A (10 mm)	C.A (20 mm)
Specific gravity	2.79	2.70
Water absorption	1.13 %	0.49 %

Methodology

This study investigates the influence of three parameters i.e. water content, coarse aggregate to total aggregate ratio and water cement ratio on the performance of limestone calcined clay cement. To study the effect of water content, three different values of 165 kg/m^3, 180 kg/m^3 and 190 kg/m^3 were selected and concrete mixes were designed as Mix A, Mix B and Mix C respectively. Coarse aggregate to total aggregate ratios of 0.68, 0.66 and 0.64 were used and mixes were named as Mix D, Mix E and Mix F respectively. Seven concrete mixes named as Mix G, Mix H, Mix I, Mix J, Mix K, Mix L and Mix M were prepared with water cement ratio of 0.6, 0.55, 0.5, 0.45, 0.4, 0.35 and 0.30 respectively. Trials were done for concrete mixes to determine the volume of admixture required to achieve the slump value of 80 mm and above. The workability of concrete mixes was assessed by determining the slump values as prescribed in IS code. The compressive strength was obtained by loading the sample in the universal testing machine at 14M-Pa/m. Cubes of 150 mm size were used to measure the crushing strength confirming to IS 516 at the age of 1, 7, 28 and 56 days.

Results and Discussions

1. Effect of water content

Three mixes (Mix A, Mix B and Mix C) were prepared with the water content of 165 kg/m^3, 180 kg/m^3 and 190 kg/m^3 respectively as shown in table 3, while water- cement ratio and c/a ratio of 0.4 and 0.66 was kept fixed. The mix made with water content of 165 kg/m^3 appeared to be stiff and required a higher admixture dosage to attain the target slump value as compared to mixes made with water content of 180 kg/m^3 and 190 kg/m^3. The results of fresh properties of different mixes are listed in table 4. It was found that admixture dosage increased by 41 % as water content was reduced from 180 kg/m^3 to 165 kg/m^3. However, decreasing the water content from 190 kg/ m^3 to 180 kg/m^3 resulted in only a minor change in the volume of admixture dosage. Nonetheless, it was observed that mix with water content of 190 kg/m^3 showed bleeding tendency. It could be concluded that water content influences the workability as the change in volume of admixture dosage was required to achieve desired slump values.

Table 3: Mix proportions of the concrete mix at different water content values

Mix Design (kg/m^3)	Mix A	Mix B	Mix C
Water content	165	180	190
Cement content	412.5	450	487.5
Chemical admixture	4.95	4.05	3.90
Fine aggregate	629.93	605.91	581.88
Coarse aggregate – 10mm	511.44	491.93	472.43
Coarse aggregate – 20mm	767.16	737.90	708.64

Table 4: Fresh properties of mixes with different water content

	Mix A (165 kg/m^3)	Mix B (180 kg/m^3)	Mix C (190 kg/m^3)
SP dosage (%)	1.2	0.85	0.8
Slump	140	90	110

Figure 1 displays the effect of water content on the compressive strength of LC^3 concrete mixes at different ages. In general, it was observed that strength values lie in a similar range by changing water content. At 1, 7 and 28 days, the compressive strength of mixes with the water content of 165 kg/m^3 is almost similar to mix with water content of 190 kg/m^3. While, lower strength was reported for mix

with 190 kg/m³ at 56 days as compared to other mixes. Nonetheless, no appreciable difference is noticed between the strength values of concrete mixture with 165 kg/m³ and180 kg/m³ of water content.
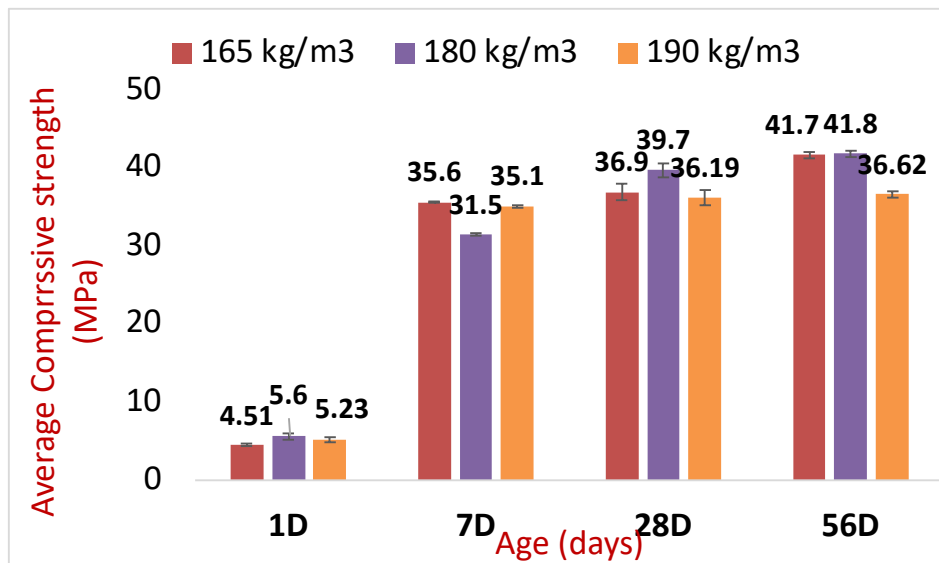

Figure 1: Compressive strength of LC3 mixes with varying water content

2. Effect of coarse aggregate to total aggregate

Three concrete mixes designated as Mix D, Mix E and Mix F were prepared using mix proportions given in table 5. The effect of c/a ratio on freshly mixed concrete was assessed by measuring the slump values as shown in figure 2. It was found that the volume of admixture dosage required for achieving the target slump of concrete remained unaffected as the coarse aggregate to total aggregate ratio was changed from 0.68 to 0.66. While, mix with c/a ratio of 0.64 showed a reduction in slump value by 15 mm for the same admixture dosage as compared to the other two mixes (Table 6). Further, none of the concrete mixes showed segregation or bleeding tendency.

Table 5: Mix proportion of the concrete mixes at different c/a ratios

Mix Design (kg/m³)	Mix D (0.68)	Mix E (0.66)	Mix F (0.64)
Water content	180	180	180
Cement content	450	450	450
Chemical admixture	4.05	4.05	4.05
Fine aggregate	570.26	605.91	641.55
Coarse aggregate – 10mm	506.80	491.93	477.027
Coarse aggregate – 20mm	760.30	737.90	715.54

Figure 2: Concrete slump for mixes with c/a ratio of 0.68, 0.66 and 0.64

Table 6: Slump values of concrete mix with (a) c/a= 0.68; (b) c/a= 0.66; (c) c/a= 0.64

	Mix D (0.68)	Mix E (0.66)	Mix F (0.64)
SP dosage (%)	0.85	0.85	0.85
Slump	90	90	75

Compressive strength values of concrete mixes with different c/a ratios at 1,7, 28 and 56 days are represented in figure 4. At 7 days, strength values of 29.35 MPa, 30.01 MPa and 28.34 MPa were noticed for concrete mixes with c/a of 0.68, 0.66 and 0.64 respectively, which doesn't reflect any a significant difference. Likewise, no appreciable difference in strength values were observed at 28 and 56 days.

Thus, it can be concluded that varying c/a ratio from 0.68 to 0.64 does not result in significant change in workability as the same volume of admixture was used. Likewise, compressive strength results were also found to be similar at all ages.
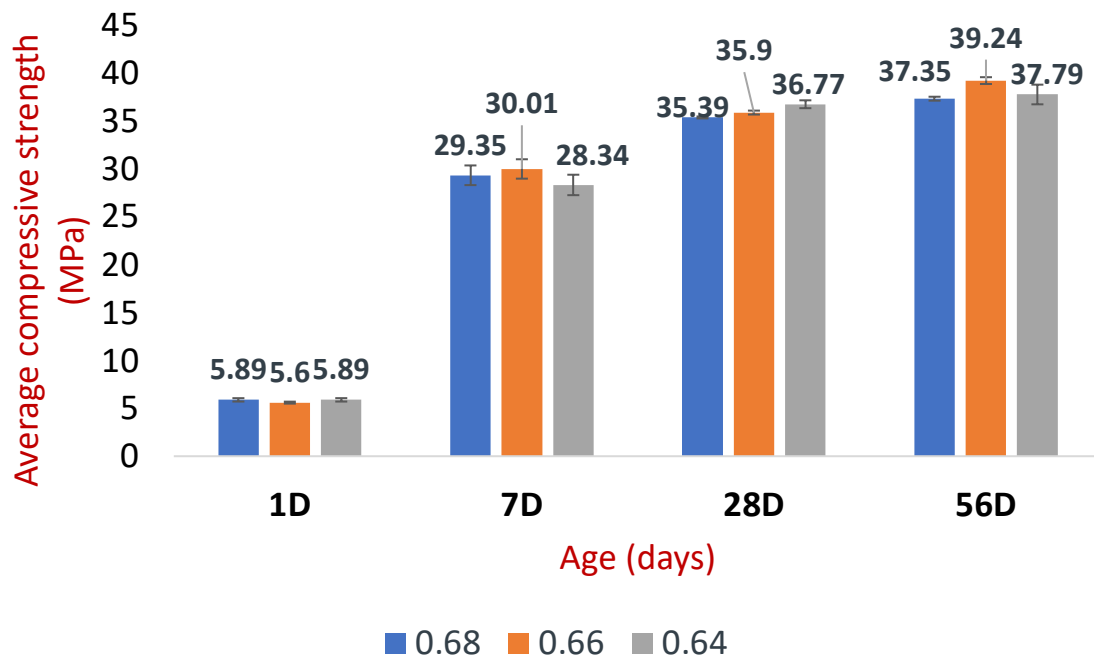

Figure 3: Compressive strength of LC3 mixes with varying c/a ratio.

3. Effect of water to cement ratio

Six concrete mixes with water- cement ratios ranging from 0.6 to 0.3 were made using the designed mix proportions given in table 7, to study their influence on workability and mechanical characteristics. The admixture demand of different mixes with slump values is presented in table 8. Despite having water- cement ratio of 0.6, 0.15 % admixture was added in Mix G due to the cohesive nature and high fineness of LC^3. Mix at lower water to cement ratios had greater demand for superplasticizer to achieve high workability. It was possible to attain a slump value of 120 mm at w-c ratio of 0.3 with an admixture dosage of 0.45 %. Further, increasing admixture dosage caused no segregation or bleeding in any mix.

Table 7: Mix proportion of the concrete mix at different water to cement ratio

Mix Design (kg/m^3)	Mix G (0.6)	Mix H (0.55)	Mix I (0.50)	Mix J (0.45)	Mix K (0.40)	Mix L (0.35)	Mix M (0.30)
Water content	180	180	180	180	180	180	180
Cement content	300	327.27	360	400	450	514	600
Fine aggregate	628.55	620.30	610.4	598.31	583	568.06	537.81
Coarse aggregate – 10mm	510.8	504.1	496	486.2	473.9	461.6	437
Coarse aggregate – 20mm	766.16	756.1	744	729.3	710.8	692.4	655.5

Table 8: Fresh properties of mixes at different water to cement ratio

	Mix G (0.6)	Mix H (0.55)	Mix I (0.5)	Mix J (0.45)	Mix K (0.4)	Mix L (0.35)	Mix M (0.3)
SP dosage (%)	0.15	0.20	0.25	0.30	0.35	0.40	0.45
Slump	100	80	80	115	85	140	120

The compressive strength results of LC3 mixes at different water to cement ratio are shown in figure 4. The decrease in water to cement ratio obviously enhances the compressive strength of LC^3 that is consistent with the research results of the literature. At 7 days, strength was found to increase by 14.89 %, 38.52 % and 40.62 % by reducing w-c ratio from 0.6 to 0.5 ,0.4 and 0.3 respectively. While at 28 days, 22.7 %, 25.64 % and 28.52 % higher strength were achieved by decreasing w-c ratio from 0.6 to 0.3 at 0.1 intervals. This happens because the lower the water- cement ratio, faster is the hydration reaction and more hydration products are formed that makes the microstructure compact. Beyond 28 days, strength gain was found to be low particularly for mixes made at low w-c ratio because almost all cement particles have contributed to hydration reactions.
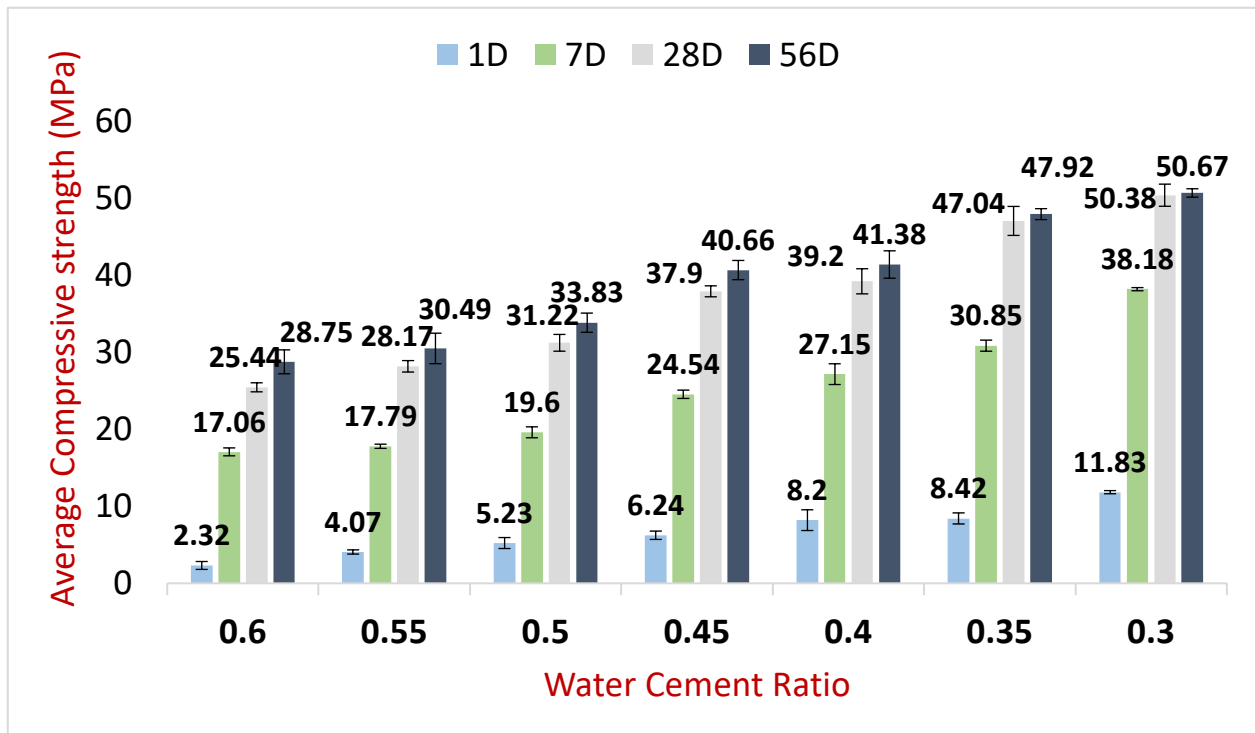
Figure 4: Compressive strength of LC3 mixes with varying water-cement ratio

Conclusions

The effect of water content, coarse aggregate to total aggregate ratio and water to cement ratio on the performance of LC^3 concrete were studied through concrete slump test and mechanical test. Based on the experimental results, following conclusions were drawn:

1. The slump value obtained is related to the water content, so it is necessary to design the concrete mixture with suitable water content to ensure the fluidity of LC3. The increase in water content of concrete mix leads to a decrease in admixture requirement, but mix with water content higher than 180 kg/m3 showed segregation and bleeding tendency.

2. Coarse aggregate to total aggregate ratio seems to influence the volume of admixture needed to achieve the desired workability marginally. This is because, at the same admixture dosage, only 15 mm reduction in slump value was observed for the mix with c/a ratio of 0.64 as compared to mix with c/a ratio of 0.66 and 0.68.

3. The admixture requirement of LC3 mixes increased with the reduction of water to cement ratio to achieve similar workability in all mixes. High slump values were observed at a lower water cement ratio by increasing superplasticizer dosage and no segregation and bleeding were noticed in any of the mixes.

4. The influence of water content on the compressive strength results of LC3 was marginal as similar strength was shown by concrete mix with water content of 165 kg/m3 and 180 kg/m3, but slightly lower strength by concrete mix with the water content of 190 kg/m3.

5. The compressive strength was found to be unaffected by the coarse aggregate to total aggregate ratio as similar results were observed by all concrete mixes. While, strength improves significantly by the reduction of water to cement ratio from 0.6 to 0.3. The increase in strength values between 28 days and 56 days was less especially at the lower water to cement ratio.

References

[1] Dhandapani, Y., Sakthivel, T., Santhanam, M., Gettu, R., & Pillai, R. G. (2018). Mechanical properties and durability performance of concretes with Limestone Calcined Clay Cement (LC3). *Cement and Concrete Research*, *107*(February), 136–151. https://doi.org/10.1016/j.cemconres.2018.02.005

[2] Scrivener, K. L., (2014). Options for the future of cement. *Indian Concr. J*, *88*(7), 11-21

[3] Alujas, A., Fernández, R., Quintana, R., Scrivener, K. L., & Martirena, F. (2015). Pozzolanic reactivity of low grade kaolinitic clays: Influence of calcination temperature and impact of calcination products on OPC hydration. *Applied Clay Science*, *108*, 94–101. https://doi.org/10.1016/j.clay.2015.01.028

[4] Fernandez, R., Martirena, F., & Scrivener, K. L. (2011). The origin of the pozzolanic activity of calcined clay minerals: A comparison between kaolinite, illite and montmorillonite. *Cement and Concrete Research*, *41*(1), 113–122.https://doi.org/10.1016/j.cemconres.2010.09.013

[5] Scrivener, K., Martirena, F., Bishnoi, S., & Maity, S. (2018). Calcined clay limestone cements (LC3). *Cement and Concrete Research*, *114*(March), 49–56. https://doi.org/10.1016/j.cemconres.2017.08.017

[6] Sharma, M., Bishnoi, S., Martirena, F., & Scrivener, K. (2021). Limestone calcined clay cement and concrete: A state-of-the-art review. *Cement and Concrete Research*, *149*(August), 106564. https://doi.org/10.1016/j.cemconres.2021.106564

[7] F. Avet, L. Sofia, K. Scrivener, Concrete Performance of Limestone Calcined Clay Cement (LC3) Compared with Conventional Cements, *Advances in Civil Engineering Materials*, ASTM, 8 (2019), DOI: 10.1520/ACEM20190052

[8] Aramburo, C., Pedrajas, C., Rahhal, V., González, M., & Talero, R. (2019). Calcined clays for low carbon cement: Rheological behaviour in fresh Portland cement pastes. *Materials Letters*, *239*, 24–28. https://doi.org/10.1016/j.matlet.2018.12.050

[9] Liu, J., An, R., Jiang, Z., Jin, H., Zhu, J., Liu, W., … Sui, T. (2022). Effects of w/b ratio, fly ash, limestone calcined clay, seawater and sea-sand on workability, mechanical properties, drying shrinkage behavior and micro-structural characteristics of concrete. *Construction and Building Materials*, *321*(November 2021), 126333. https://doi.org/10.1016/j.conbuildmat.2022.126333

[10] Ferreiro, S., Herfort, D., & Damtoft, J. S. (2017). Effect of raw clay type, fineness, water-to-cement ratio and fly ash addition on workability and strength performance of calcined clay – Limestone Portland cements. *Cement and Concrete Research*, *101*(August), 1–12. https://doi.org/10.1016/j.cemconres.2017.08.003

[11] Aramburo, C., Pedrajas, C., Rahhal, V., González, M., & Talero, R. (2019). Calcined clays for low carbon cement: Rheological behaviour in fresh Portland cement pastes. *Materials Letters*, *239*, 24–28. https://doi.org/10.1016/j.matlet.2018.12.050

[12] Nair, N., Mohammed Haneefa, K., Santhanam, M., & Gettu, R. (2020). A study on fresh properties of limestone calcined clay blended cementitious systems. *Construction and Building Materials*, *254*. https://doi.org/10.1016/j.conbuildmat.2020.119326

Annex VI – Ingress of chloride in carbonated LC³ concrete
Report by Indian Institute of Technology Delhi

1. Introduction
1.1. General
Corrosion of rebars in concrete is a major issue which leads to deterioration of concrete and if it becomes worst the structural integrity gets affected. Carbonation and presence of chloride in the concrete has been known to cause the rebar corrosion embedded in concrete. The carbonation is more homogenised phenomenon as it is due to ingress of CO_2 from the environment to the concrete, reacting with hydration products of concrete leading to lowering the pH of concrete. Lowering of pH can lead to loss of stability of passive layer around the rebar and resulting into initiation of corrosion. On the other hand, in case of presence of chlorides in concrete rebar passive layer becomes unstable and corrosion may start even at higher pH value. Since carbon dioxide is present in the air and the process of carbonation is almost inevitable. However, rate of diffusion of moisture with detrimental ions (Chlorides) from surface to the bulk of concrete depends on pores structure.

Owing to carbonation microstructural changes occur in concrete. Hence, to better understand how carbonation phenomenon may affect the chloride resistance of concrete this study has been carried out. Test that may give insight of chloride resistance of concrete such as RCPT and RCMT have been performed in the study.

2. Materials and Methods
2.1. Materials
Types of cements used in this study are Portland Pozzolanic cement (PPC-30%FA+70%OPC), Lime stone calcined clay (LC³- 55%OPC + 30%Calcined clay + 15%Limestone). River sand has been used as fine aggregate and crushed stone as coarse aggregate with specific gravity 2.7. Table 1 shows the physical properties. Specific gravity of three blends was determined according to IS 4031 part 2. To find out the normal consistency of three blends IS 4031 part 4 has been followed. Initial setting and final setting time has been performed in compliance with IS 4031 part 5.

Table 25: Physical properties

Sr. No	Cement Type	Specific Gravity	Normal Consistency (%)	Initial Setting time (min)	Final Setting time (min)
1	PPC	2.9	31.5	190	295
2	LC³	2.9	34.5	151	229

2.2. Sample preparation
Cylinder specimen of diameter 100 mm and height 200 mm were cured for 56 days. The control specimens were left under extended curing and rest samples were sent to the carbonation chamber. Before sending to the carbonation chamber discs having diameter 100 mm and thickness 50 mm were sliced out of the cylinder specimen. Epoxy was applied on curved surface of these disc samples and were left to dry. Extra epoxy on the exposed surface was removed by grinding. The samples were then send to the Plexiglass carbonation chamber for a period of 90 days and under 3% CO_2 concentration. The humidity in the chamber was low. After 90 days the effect of carbonation on chloride ingress in concrete was observed by performing various test that give indication of chloride ingress into the concrete.

3. Experimental Program
3.1. Compressive strength
Compressive strength of PPC and LC^3 concrete has been determined at 7 and 28 days. Mix proportion of materials has been given in Table 2. Both Concrete mixes have been cast at same proportion and similar w/c ratio.

Table 26: Mix Proportion of LC^3 and PPC

Sr. No	Blend	w/c	Cement (kg)	Sand (kg)	Aggregates (kg)	Water (ltr)
1.	LC^3	0.4	465	592	1123.2	186
2.	PPC	0.4	465	592	1123.2	186

3.2. Accelerated Carbonation
Concentration of CO_2 in environment is approximately 0.03% hence rate of carbonation will be very slow. Therefore, in laboratory the concentration of CO_2 is increased hundred folds in order to get faster results of carbonation. In this study CO2 concentration of 3% was used. The plexiglas carbonation chamber has been used to keep the samples as shown in Fig. 3.1.

Fig. 3.1: Carbonation Chamber

3.3. Carbonation depth and pH
Carbonation depth is determined in order to know the extent of reaction of CO_2 with the hydration products. Carbonation front can be determined by the spraying phenolphthalein on the broken samples.

The pH of the pore solution of the carbonated and non-carbonated concrete has been determined using potentiometric titration technique. Powder of concrete is obtained from the core using a drilling machine. The powder is then collected and sieved through 150µm sieve. A solution of 1:10 is prepared using this powder and distilled water. pH of solution is measured when the electrode of pH meter is dipped in the solution. The electrode of pH meter should be cleaned and pH meter must be calibrated before determining the pH meter.

3.4. Rapid Chloride Permeability Test
Rapid Chloride permeability test (RCPT) is performed in lab to know the resistance to the penetration of chloride ions in concrete. This test is carried out in compliance with ASTM C1202 or AASHTO T277. Concrete disc samples are saturated first in water for around 18±2 hours. Concrete specimen of diameter 100 mm and thickness 50 mm is taken and subjected to a voltage of 60V DC for a period of

6 hours. On one side of 3% NaCl is filled and the other end contains 0.3 M NaOH. The total charge passed is calculated and evaluated as per standard given in the above mentioned code.

3.5. Accelerated Chloride Migration Test (ACMT)

Unlike rapid chloride permeability test where resistance to chloride ingress is gauged in terms of total charge (coulombs) passed under a high potential, migration test gives insight of actual movement of chloride ions under a small applied voltage. Nord Test BUILD-492 has been followed to perform this test in the laboratory. Disc specimen of diameter 100 mm and thickness 50 mm are used in this test. Under external electrical field chlorides are forced to enter the specimen for a specified duration. After completion of test, solution of silver nitrate is spread over specimen to see the depth of chlorides. White coloured precipitates appear on the surface of specimen on the portion where there is presence of chlorides. The depth is measured for calculation of steady state migration coefficient.

4. Results and Discussions

4.1. Compressive strength

Compressive strength was determined at 7 day and 28 days. LC3 concrete exhibits higher strength to that of PPC at both 7 and 28 days.
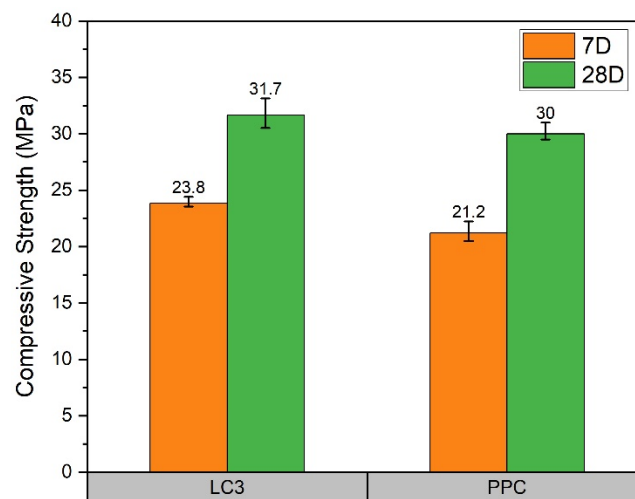
Fig. 4.1: Compressive strength

4.2. Carbonation depth and pH

Carbonation depth test results shows that after 90 days of carbonation and at 3% carbon dioxide concentration LC^3 concrete exhibits higher carbonation depth than PPC. Carbonation front can be visibly seen after spraying phenolphthalein in LC^3 (Fig. 4.1) and PPC (Fig. 4.2). In case of LC^3 carbonation depth of 5.8 has been observed and in PPC 2.9 depth was observed, shown in Fig. 4.3. LC^3 exhibits twice the carbonation depth than PPC for same duration and under similar ambient conditions. Determination of pH of the carbonated and non-carbonated samples has been done and shown in Fig. 4.4. pH of samples under 90 days carbonation is lower than the non-carbonated samples as expected because of the reaction of CO2 with portlandite leads to lowering of pH. It is apparent that in case of carbonated sample pH of LC^3 is lower than the PPC whereas in non-carbonated samples pH of LC^3 and PPC is quite similar.

Fig. 4.1: Carbonation depth front in LC³   Fig. 4.2: Carbonation depth front in PPC
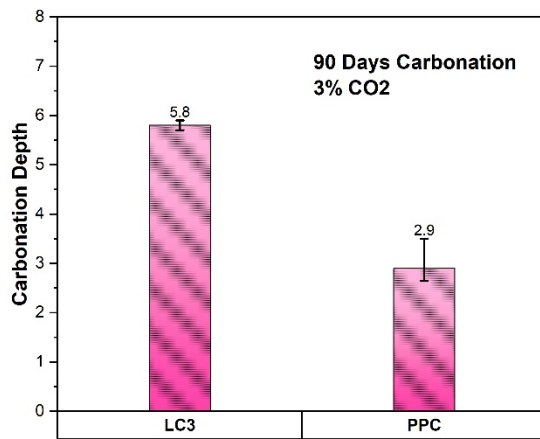

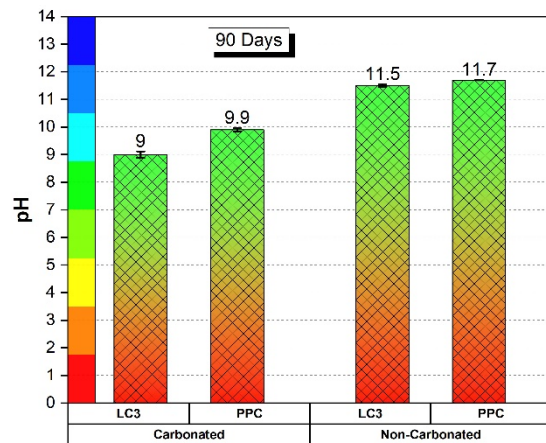
Fig. 4.3: Carbonation depth   Fig. 4.4: pH in LC3 and PPC

4.3. Rapid Chloride Permeability Test

The resistance to chloride ion by concrete can be grouped according to charge passed and shown in Table. 3. RCPT result has been presented in Fig. 4.5. It is apparent that lower charge has been passed in case of non-carbonated LC³ concrete as compared to carbonated concrete, similarly in non-carbonated PPC concrete lower charge is observed as compared to carbonated PPC concrete. Due to the coarsening of pore structure because of carbonation the total porosity increases which may be the cause for higher charge pass in case of carbonated concretes whether LC³ or PPC. Whereas between PPC and LC³ carbonated concrete, LC³ carbonated concrete exhibits lower amount of charge passed. This can be attributed to the refined pores in LC³ and the chloride binding due to presence of higher aluminates in LC³. Additionally, very small difference is observed in charge passed by PPC concrete with carbonation and without carbonation. Whereas charge passed by carbonated LC³ is significantly higher than LC³ with non-carbonated concrete. However, the charge passed in LC³ both carbonated and non-carbonated concrete still is lower than carbonated and non-carbonated PPC concrete.

Table 27: RCPT Rating as per ASTM C1202

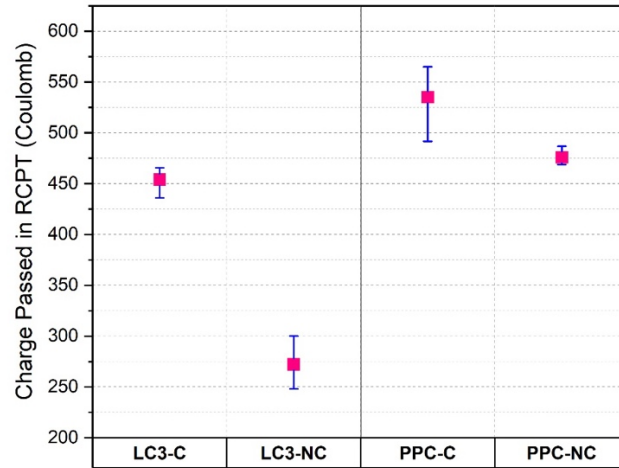| Charge passed (Coulomb)	Chloride Ion Penetrability
> 4000	High
2000-4000	Moderate
1000-2000	Low
100-1000	Very Low
<100	Negligible

Fig. 4.5: Chloride penetration resistance by RCPT

4.4. Rapid Chloride Migration Test

After breaking specimens of chloride migration test depth of chloride ingressed has been noted down. The broken specimens of carbonated LC^3 (Fig. 4.6), carbonated PPC (Fig. 4.7) and non-carbonated LC^3 (Fig. 4.8), PPC (Fig. 4.9) show the interface up to which the chlorides have ingressed.
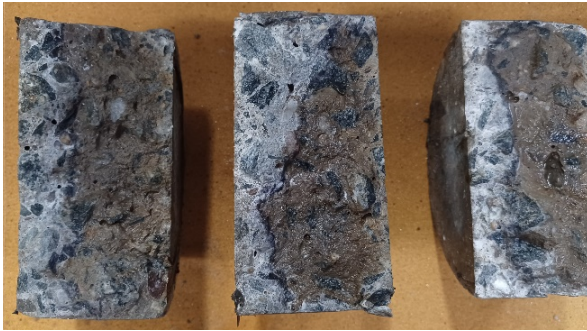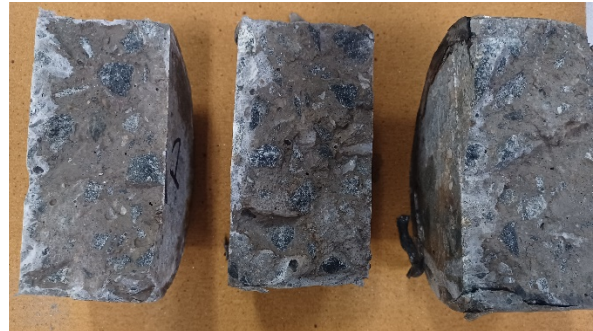

Fig. 4.6: Carbonated- LC^3

Fig. 4.7: Non-Carbonated- LC^3

Fig. 4.8: Carbonated-PPC

Fig. 4.9: Non-Carbonated-PPC

Depth of chloride penetration can be detected by the formation of white precipitates on the broken core concrete upon spraying silver nitrate. The rest portion which exhibits brown colour is devoid of chlorides. Chloride penetration depth has been listed in Table. 4. From the figures it can be observed that the carbonated concretes both LC^3 and PPC show higher chloride ingress as compared to non-carbonated ones (LC^3 and PPC).

Table 28: Chloride penetration Depth

Sr. No	Specimen	Chloride penetration depth (X_d)
1.	Carbonated-LC3	15.8
2.	Non-Carbonated-LC3	7.2
3.	Carbonated-PPC	10.3
4.	Non-Carbonated-PPC	5.4

The Non-steady state chloride migration coefficient has been demonstrated in Fig. 4.10. Non steady state coefficient (D_{nssm}) goes well with the results obtained from RCPT test. From the results it can be noticed that the D_{nssm} for non-carbonated concretes is low both in PPC and LC^3. Whereas in carbonated LC^3 and PPC concrete D_{nssm} tend to increase. The reason can be stated that coarsening of pores due to carbonation lead to the higher chloride migration. However, it can be observed that D_{nssm} for LC^3 carbonated concrete is still lower than the PPC carbonated concrete. Even if the presence of carbonation is there chloride migration in LC^3 is lesser as compared to carbonated PPC.
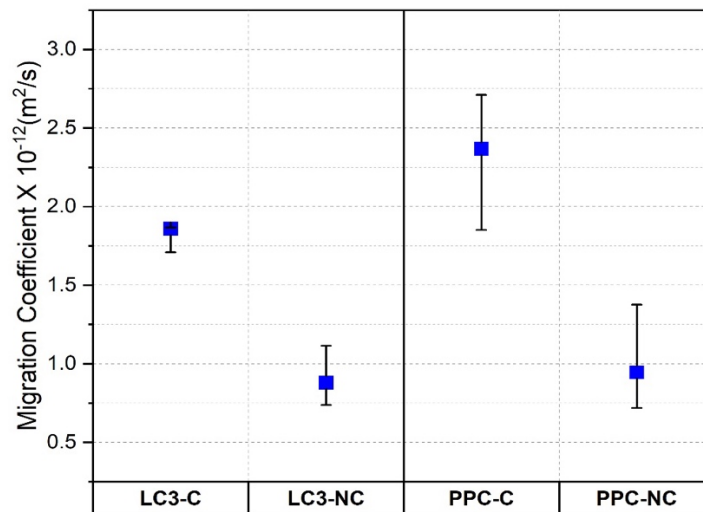

Fig. 4.10: Chloride Migration Coefficient

5. Conclusion

From the study carried out to understand the influence of carbonation on chloride ingress in LC^3 following conclusions can be drawn

- Carbonation depth was observed to be high in LC^3 concrete after 90 days of carbonation than in PPC concrete
- pH reduces significantly after carbonation in LC^3 concrete than in PPC concrete
- Resistance to chloride is observed to reduce in LC^3 as well as in PPC as a result of carbonation, however, influence of carbonation on chloride ingress is less significant in LC^3 than in PPC concrete
- Chloride resistance of LC^3 concrete is higher even after carbonation as compared to PPC concrete
- Chloride migration coefficient of LC^3 remains lower than PPC concrete even after carbonation indicating better resistance against chlorides in LC^3

Annex VII – Manual use of LC³ by construction workers
Report by Indian Institute of Technology Delhi

1. Introduction

Cement is the most consumed building material and plays a key role in building our infrastructure and used for all types of construction, including housing, roads, schools, hospitals, dams etc. Concrete is a versatile and reliable construction material with a wide range of applications. In production of Ordinary Portland Cement, huge amount of CO_2 is emitted. When looking at possible pathways to reduce the carbon footprint,Limestone Calcined Clay Cement (LC³) is a good alternative to the Ordinary Portland cement. LC³ can reduce CO_2 emissions related to manufacturing by 30% as compared to ordinary Portland cement by reducing the amount of clinker, replacing it with limestone and calcined clays.The main components of LC³ are clinker, calcined clay, limestone, and gypsum.

Since a sizeable amount of cement is consumed in the unorganised sector, where concrete is produced manually, without the use of mechanised equipment, it is important to understand the performance of LC³ in such conditions. To study this, concretes were prepared by construction workmen using usual manual techniques, without the use of mechanised equipment or chemical admixtures. The water content in the concrete was controlled by the workmen as per the required workability. The workability and strength of the concrete was assessed.

2. Materials

In this study, two types of cement i.e. LC³ and PPC were used. LC³ was made by replacing 45 % of OPC with 30 % of clay and 15% of limestone. 10 mm and 20mm coarse aggregate and river sand were used. Two nominal mix designs were adopted. In first case, Cement: Sand: Coarse Aggregate was 1:1.5:3 and in second case Cement: Sand: Coarse Aggregate was 1: 2: 2. The 10 mm coarse aggregates and 20 mm coarse aggregates were taken in ratio of 1:1. Water cement ratio was around 0.55. Details of mixes are given in Table 1.

Table 29: Mix proportion

Mix Design	Cement Type	Cement: Sand: Coarse Aggregate	Water: Cement
1	LC³	1:1.5:3	As required to produce a workable mix
	PPC	1:1.5:3	
2	LC³	1:2:4	
	PPC	1:2:4	

3. Methodology

The concrete was mixed by hand in such a manner that loss of water or other materials were avoided. The concrete batch was mixed on a water tight platform with a shovel and trowel. Immediately after mixing, Slump was taken to test the workability of concrete. Then, the cubes of size 150mm × 150mm × 150mm were cast for compressive strength.

Fig. 1: Dry Mixing of mix design 1:1.5:3

Fig. 19: Wet mixing and Trowel movement of mix design 1:1.5:3

Fig. 20: Slump measurement of mix design 1:1.5:3

Fig. 21: Slump measurement of mix design 1:1.5:3

Fig.22: Cast cubes of PPC of mix design 1:1.5:3

Fig.23:Cast cubes of LC3 of mix design 1:1.5:3

Fig.24: Dry Mix of Mix design 1:2:2   *Fig.25: Dry Mix of Mix design 1:2:2*

Fig.26: Slump measurement of Mix design   *Fig. 27: Slump measurement of Mix design 1:2:2*
1:2:2

Fig. 28: Cast cubes of mix design 1:2:2

4. Results
Compressive strength results are presented in table 2.

Table 30: Compressive strength of PPC and LC³ cubes

Sr. No.	Mix Design	Slump (in mm)		Compressive Strength(in MPa)			
				LC³		PPC	
		LC³	PPC	7-Days	28-Days	7-Days	28-Days
1	1:1.5:3	40	40	15.2	20.86	11.86	19.40
2	1:1.5:3	55	155	12.86	14.8	10.17	18.4
3	1:1.5:3	30	85	12.72	15.3	9.37	15.3
4	1:2:2	130	180	13.2	17.95	12.64	20.50
5	1:2:2	190	120	8.86	13.74	9.34	15.84
6	1:2:2	165	140	7.94	12.57	8.4	13.98

5. Comments from masons
The observations made by the masons are listed below:
- Water demand in LC³ is higher as compared to PPC.
- LC³ mixes were stiffer than PPC at same water content.
- No difference was observed in dry mixing of LC³ and PPC.
- No difference was observed in trowel movement during finishing.
- There was a clear colour difference between LC³ and PPC.
- The 7 and 28 day strengths of the mixes were similar in most cases.
- It is desirable to reduce the sand content in the mixes to achieve a lower water demand and higher workability in the LC³ mixes.

Annex VIII – Use of LC³ for plastering a wall
Report by Indian Institute of Technology Delhi

Introduction

Cementitious plaster is a versatile and weather-resistant cladding material for interior and exterior use. Cement plaster can be applied to flat, curved or rough substrates of concrete, clay masonry, concrete masonry, etc. Cement plaster has shown excellent performance in a variety of environments. The workability of plaster allows for a variety of shapes, designs and textures. When the plaster hardens, these features remain in a solid, permanent form.

Desirable properties of Plaster

Cementitious plaster must have desirable properties for plastic and hardened state to permit proper application and long-term use. Freshly mixed plaster should have good adhesion and cohesion properties and remain workable long enough to produce the desired finish. Cured plaster should be weather resistant, durable, and meet specified appearance (colour and texture) criteria.

Fresh or *plastic* plaster should have the following desirable properties: Adhesion, Cohesion and Workability. *Hardened* state of plaster should have weather resistance, freeze thaw resistance, sulphate resistance, bond and tensile strength

Objective

Our main aim for this work is to understand and evaluate the initial performance of a new ternary blend of limestone calcined clay cement when used as a rendering material in an externally faced brick wall. The evaluation of the plaster would be based on its properties shown during its fresh or plastic state and later on in the hardened state.

Raw Materials and methods

The mortar mix for the plaster was made with a new ternary blend LC³ that constitutes a premixed LC² - Bhuj (Limestone to calcined clay 1:2), which is used as a mineral admixture to substitute and obtain a 55% clinker ratio with OPC – 43 grade. Well-graded river sand (passed with a 4.5mm sieve) is used in 1:4 (cement to sand ratio). Manual proportioning and mixing were performed with local labour. The location of the plaster site is at a newly made brick wall (exterior side) in IIT Delhi civil engineering department.

Figure 1: The picture above shows the manual mixing performed with manual labor of the plaster mix (left). The application of mortar mixes on the surface of the brick wall (right)

Results and observation

The workability of the fresh state plaster mix was good as it showed the ease of applicability on the surface. No segregation or bleeding was observed in the mix. The adhesion of the plaster mix was better as the mortar mix adhered well to the substrate, lowered the rebound fall of the mix and was quite easily sticking on the brick wall surface as clearly seen in *Fig 1.* The cohesion in the mix was effective as no sign of sagging, sloughing, or delaminating was detected. The finish of the plaster surface was smooth without any significant marks as observed in *Fig 3*. Overall assessment made based on the mason review and physical observation collected is shown below in *Fig 2*.
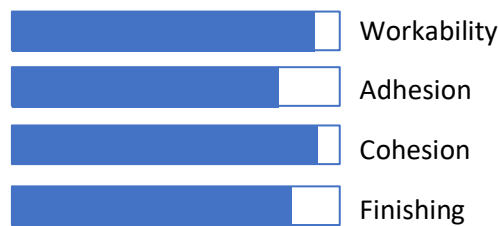
Figure 2: Assessment made for the desirable properties for fresh or plastic plaster state.

Figure 3: The finish state of the plaster on the brick wall surface.

Once the plaster was cured and observations were made periodically on the behavior of plaster during the hardened state, firstly we observed no sign of efflorescence on the plaster surface. The plaster has withstood weathering including resistance to wind and rain penetration till date. No penetration of external water was noticed through the plaster. The bond and tensile strength look good as no sign any delamination or peel-off of the plaster and no visible cracks on the surface were observed as seen in *Fig 4*. The freeze and thaw resistance were not part of the study as the climate in Delhi do not have extreme low temperature.

Figure 4: The current state of hardened plaster made with LC^3 cement
.

Overall, the plaster done with the new cement limestone calcined clay cement was a successfully study, The mason and observer at site clearly mentioned that application during fresh state showed far better adhesion and cohesion compared with conventional cements plaster (OPC and PPC). Also, the workability was good with a small increase in water content. The hardened state currently shows no signs of efflorescence even after a year of withstanding weather and rain.

Annex IX – Use of LC³ for repair of concrete
Report by Indian Institute of Technology Delhi

1. Introduction
1.1. General
Corrosion of reinforcement in concrete is a serious issue which can manifest cracks in the concrete leading to spalling of concrete and if the corrosion happens at a significant rate integrity of structures can be at peril. One of the major cause of reinforcement corrosion is the presence of chlorides in concrete. Chlorides lead to loss of stability of passive layer of rebar. Chlorides induce localized corrosion also known as pitting corrosion [1]. A very common repair strategy is to apply a patch of new material at the affected area however, this leads to another problem called incipient anode wherein the patched area becomes cathode making the possibility for the unrepaired area to becomes anode. This can further aggravate the situation as new anodic sites are formed in the rebars and new corrosion starts [2]. In such case it is recommended to remove all the concrete containing chlorides.

In this study application of repair material has been done all over the substrate concrete which is admixed with chlorides in order to see whether a new material can bind the free chlorides causing the rebar corrosion. This study incorporates LC³ that tend to have good chloride binding capacity [3]. Besides LC³ is considered to have good resistance against transport of moisture which is a necessary condition for corrosion process. This study highlights how the corrosion rate varies with time after application of a layer of such a new repair material on concrete which is having chlorides. An apt repair strategy for reinforced concrete structure deteriorating due to corrosion of reinforcement can be suggested if the status of rebar corrosion is known. Hence, it is also imperative to know the rate at which the corrosion is occurring in the rebar. Various techniques for assessment of corrosion rate along with other non-destructive test that can aid to tell additional information have been incorporated in this study. The study compares the suitability of three different materials as repair material. Comparison of these materials on various ground have been done and efforts have been made to identify the behaviour of these material to act as good repair work.

2. Materials
This study has been conducted on three types of blends viz. ordinary Portland cement (OPC-grade 43), Pozzolanic Portland cement (PPC-30%FA+70%OPC), Lime stone calcined clay (LC³-55% OPC + 30%Calcined clay + 15%Limestone). The materials were prepared in the laboratory by blending the raw material. River sand has been used as fine aggregate and crushed stone as coarse aggregate to prepare mortars and concrete respectively. The properties of these blends have been given below.
2.1. Characterisation of material
2.1.1 Chemical Properties of the three types of cements studies has been shown in Table 1.

Table. 31: XRF of blends

Oxides (%)	OPC	PPC	LC3
SiO_2	21.39	32.49	23.16
Fe_2O_3	6.17	5.85	5.66
Al_2O_3	4.78	14.17	12.09
CaO	62.33	41.3	51.14
MgO	1.27	1.51	1.35
SO_3	2.02	1.63	4
Na_2O	.15	.42	.18
K_2O	.5	.76	.46
LOI	1.76	1.95	9

2.1.2. Particle size distribution
Particle size distribution of the three blends is presented in the Table. 2 below.

Table. 32: Particle size distribution of Blends

	OPC	PPC	LC3
D10 (µm)	4.49 µm	4.73 µm	3.12 µm
D50 (µm)	18.3 µm	19.9 µm	15.4 µm
D90 (µm)	50.5 µm	62.4 µm	51.7 µm

2.1.3. Physical Properties

Specific gravity of three blends was determined according to IS 4031 part 2. To find out the normal consistency of three blends IS 4031 part 4 has been followed. Initial setting and final setting time has been performed in compliance with IS 4031 part 5. These properties have been listed in Table. 3. Among three blends, LC³ exhibited highest value of normal consistency indicating higher water demand as compared to OPC and PPC. Initial set and final set in case of LC³ is observed earlier than OPC and PPC blends. Therefore, for applications where early setting is needed especially quick repair works this property of LC³ can be a boon.

Table. 33: Physical properties of Blends

Sr. No	Cement Type	Specific Gravity	Normal Consistency (%)	Initial Setting time (min)	Final Setting time (min)
1	OPC	3.2	30.5	194	254
2	PPC	2.9	31.5	190	295
3	LC3	2.9	34.5	151	229

2.2. Specimen preparation

Slab samples of size (300 × 300× 56) mm were cast for corrosion rate monitoring as shown in Fig. 2.1. A rebar of diameter 16 mm has been placed in the slab with cover of 20 mm. Two types of control specimens were cast, one having OPC and PPC concrete (O-CS and P-CS) and second similar specimens were cast with admixed chloride (O-Cl and P-Cl). Another type of specimens was cast with concrete as substrate and was designed at high w/c ratio simulating low strength concrete. OPC and PPC concrete slabs were cast with 3% admixed chloride up to half rebar depth with this low strength concrete. The cast surface of the concrete was scraped using a wire brush to prepare a rough surface in order to form a good bond between new material and the substrate concrete. After 24 hours the rebars were cleaned using wire brush and sand paper. The application of three different types of mortar i.e. OPC, PPC and LC³ was done on the remaining half slabs. The slabs were named as OPC substrate with OPC as O-OPC and PPC substrate with PPC as P-PPC similarly the first syllable means substrate and name after hyphen indicate type of repair mortar applied. The samples have been cured for 28 days. After 28 days the corrosion rate monitoring has been done one these slab specimens as shown in Fig. 2.2 along with half-cell potential and surface resistivity measurement.
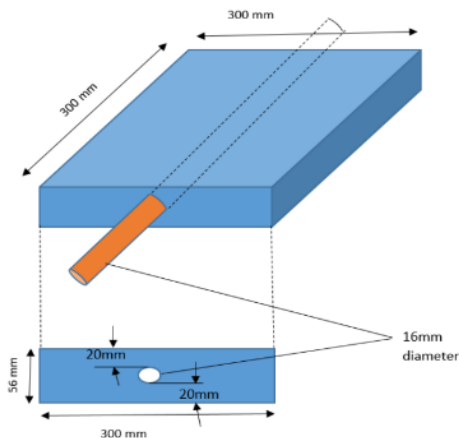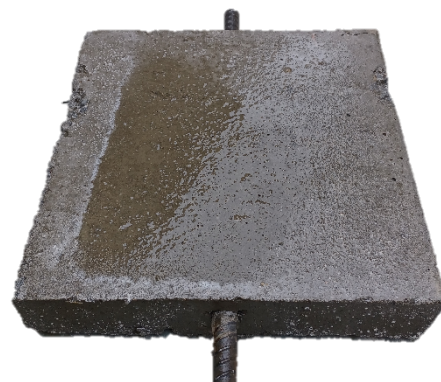

Fig. 2.1: Slab specimen dimensions

Fig. 2.2: Slab specimen after casting

3. Experimental method

3.1. Compressive strength

Compressive strength of three different mortars was determined at 3, 7, 28 and 56 days in compliance with IS 4031 part 6. Mortar cubes of size 70±.6 mm were cast at a w/c ratio of 0.4. By fixing the one parameter i.e. w/c ratio strength and other properties in the mortars have been studied. Mix proportion of the mortars is given in the Table 4. Two substrate concrete have been caste i.e. OPC and PPC concrete. Substrate concrete is simulating the low strength concrete, thus caste at higher w/c ratio. Strength determination was done at 28 days only Mix proportioning of substrate concrete is given in Table 5.

Table. 34: Mortar mix proportion

Sr. No	Blend	w/c	Cement (kg)	Sand (kg)	Water (ltr)
1	OPC	0.4	540	1621	216
2	PPC	0.4	530	1591	212
3	LC3	0.4	530	1591	212

Table 35: Mix Proportioning of Substrate concrete

Sr. No	Blend	w/c	Cement (kg)	Sand (kg)	Aggregates (kg)	Water (ltr.)
1	OPC	0.58	300	748.98	1222	174.8
2	PPC	0.51	364	702.81	1146.7	186

3.2. Bond strength

In order to determine the bonding behaviour of different mortars on the substrate concrete bond test studies have been performed. Bond strength between new repair material and substrate concrete has been evaluated in terms of split tensile strength and slant shear test. Spilt tensile and slant shear tests have been performed in compliance with the ASTM C496 and ASTM C882 respectively. For split tensile test, half cylinder substrate concrete specimen of size (150×300) mm were cast.
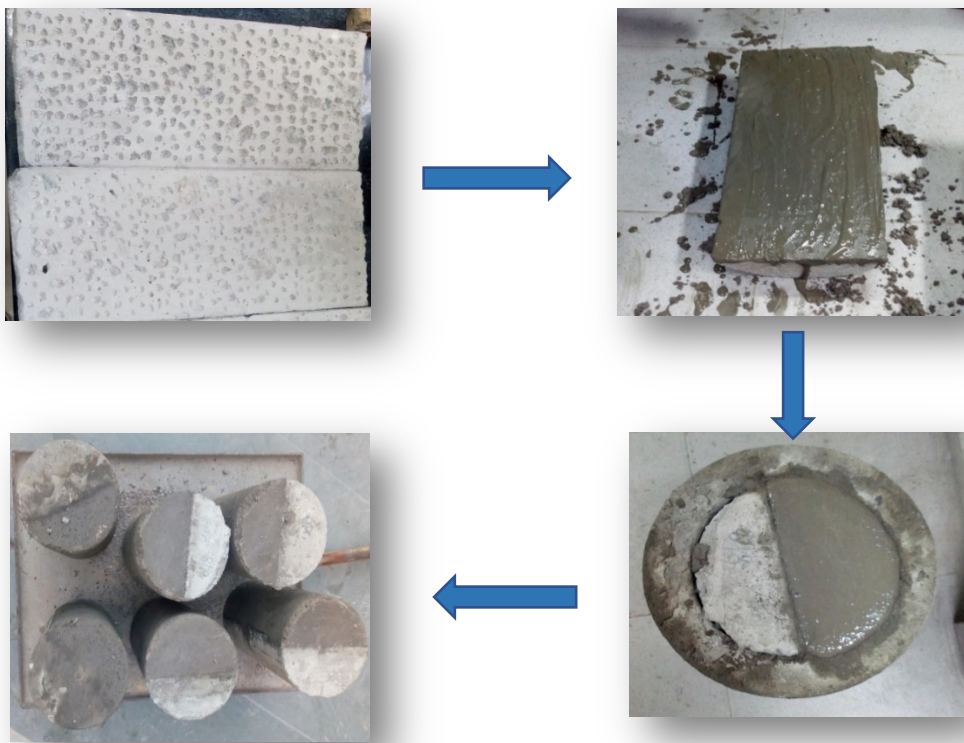

Fig. 3.1: Preparation of sample for split tensile test

Surface of concrete half cylinders was made rough using a chisel. After 28 days curing, half cylinders were placed in the mould and remaining half was filled with the mortar. Before filling the mortar, the half substrate concrete cylinder was applied with cement slurry paste. Systematic representation of specimen preparation has been shown in Fig. 3.1. Similar procedure was followed for slant shear test except of cylinders, beams of size 100×100×300 were cast. Half beams of substrate concrete were cast at specified angle mentioned in the ASTM C882. Surface was made rough using chisel and cement slurry was applied before filling repair mortar in the moulds. Fig.3.2 demonstrates the process of sample preparation of slant shear test.
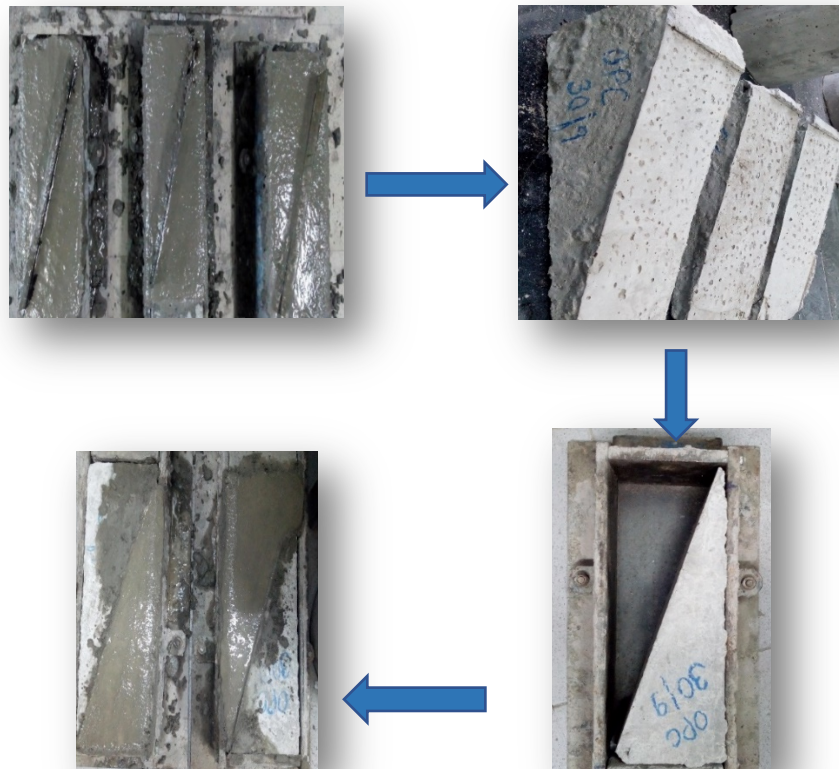
Fig.3.2: Preparation of specimens for slant shear test

3.3. Transport Properties

Availability of moisture and oxygen are two essential conditions for the corrosion to take place. In worst cases, detrimental species of ions such as chloride can also penetrate inside concrete along with water through different transport mechanisms such as capillary suction, diffusion, hydraulic gradient. Primarily, diffusion is the dominant phenomenon however, diffusion rate depends upon the pore structure. New repair material either applied as patch repair or used all over should be able to shield the substrate structure from further deterioration by slowing down the rate of moisture movement. This can be ensured by studying how the pore structure of new repair material can resist the ingress of moisture. Therefore, how the pore structures of three different blends can influence the transport mechanism can be studied through various laboratory tests. Tests for determination of transport properties of the repair mortar have been performed and evaluated in the section later.

3.3.1. Water Boiling Test

Water boiling test gives an indication of percentage of voids present in the system which play a significant role in the transportation of moisture and ions from the external environment to the core of the concrete up to the reinforcement level. Water absorption test is done in accordance with the ASTM C642-06. Disc specimens of size 100mm diameter and 50mm thickness were taken under

observation. Samples were oven dried at 100°C until the difference between the mass of two specimens is less than the .5% of the lesser mass of the specimen. After oven drying, samples were immersed in water for not less than 48h unless increase in mass of the specimen was less than 0.5% of the larger value. Samples were placed in boiling water for a period of 5hours and mass of specimen was measured after cooling. Mass of specimens immersed in water or apparent mass was then noted down. In compliance with the mentioned ASTM code tests on mortar specimen were performed at 28 and 56 days.

3.3.2. Sorptivity

This test method is done in order to assess the rate of absorption of water of the specimen. Detrimental ions species are transported through Capillary action in the concrete. Hence this test method can give an indication of the penetrability of the system. ASTM C1585 was followed to perform this test. The specimens of size 100mm diameter and 50mm thickness were sliced and kept in 50°±2°C and 80±3% relative humidity for 3 days. Afterwards specimens were place inside a container at 23±2°C for at least 15 days. The curved surface of the specimens was covered with epoxy in order to allow only one dimensional absorption and top surface covered with plastic sheet in order to avoid any moisture loss.

3.3.3. Oxygen Permeability Test

Oxygen permeability Index gives an idea of the compaction, degree of interconnectedness of pore structure which could be a deciding factor in transportation of ions from outside to the level of reinforcement. South African Durability Index code was followed to perform the test. The samples of 70 mm diameter and 30 mm thickness were sliced and kept in oven at 50°±2°C for 7 days. After this, samples were placed in oxygen permeability cell and a pressure of 100±120 kPa was applied. The drop in pressure was measured for a duration of 6h or until the pressure drops to 50% whichever is earlier.

3.4. Corrosion Rate measurement and monitoring

Corrosion rate is expressed in terms of penetration rate i.e. μm/year and in laboratory experiments it is expressed in electrochemical units as mA/m^2 or $μA/cm^2$. Corrosion rate determination has been done using lab instrument called RapiCor shown in Fig. 3.3. This instrument is quite handy and gives quick measurement. Corrosion rate along with potential and resistivity values are indicated on the screen and polarisation curves are visible too. Values of resistivity and half-cell potential are complementary. Principle of working of RapiCor is that it measures half-cell potential and generates galvanostatic pulses to measure corrosion rate and resistivity. Principle of RapiCor has been demonstrated with help of diagram in Fig. 3.4.
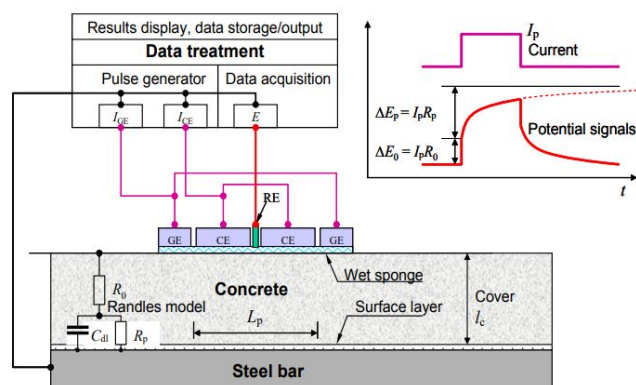

Fig.3.3: RapiCor   Fig. 3.4: Principle of RapiCor

Before measurement of corrosion rate, the slab specimen was saturated by splashing water and covering with the gunny bags. Such treatment is necessary before taking measurements so that half-cell potential values do not get influenced by the high resistivity of concrete.

4. Results and Discussion

4.1. Compressive strength

Compressive strength of repair mortars was determined at 3, 7, 28 and 56 days demonstrated in Fig. 4.1. At 3, 7, 28-days compressive strength of OPC is noticeably higher as compared to the PPC and LC^3 mortars. However, at 56 days the difference between compressive strength of the three mortars has been mitigated. PPC and LC^3 tend to show increase in strength at later ages due to the pozzolanic reaction.

Compressive strength of substrate concrete is shown in Fig. 4.2 OPC concrete gained 23.8 MPa while PPC gained 21.4 MPa. Both the concrete are representatives of low strength deteriorating concrete. Repair mortar application is to be done on this low strength concrete.
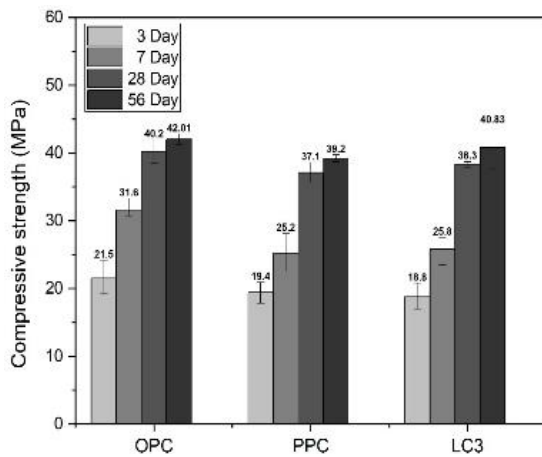
Fig. 4.1: Compressive strength of mortars
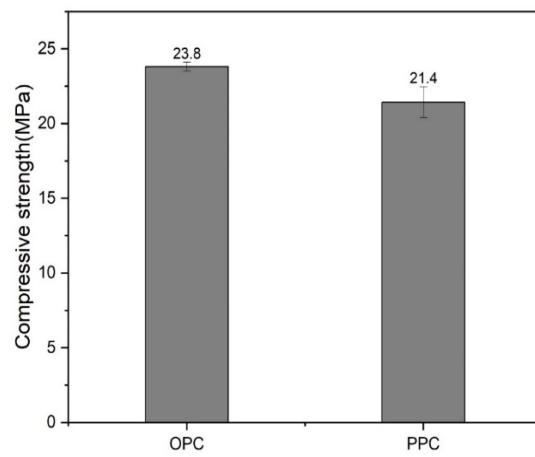
Fig. 4.2: Compressive strength of substrate concrete

4.2. Bond strength

Bond strength studies were done in order to know the strength of bonding between new mortar and the existing concrete. Split tensile test results shown in Fig. 4.3 indicate that LC^3 mortar makes a good bond with substrate OPC and PPC concrete. Split tensile strength test of LC^3 mortar shows almost similar range of strength with the OPC and PPC substrate concrete as that of the PPC and OPC mortar.
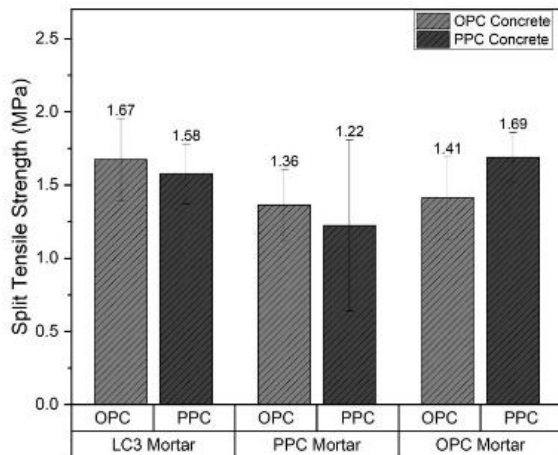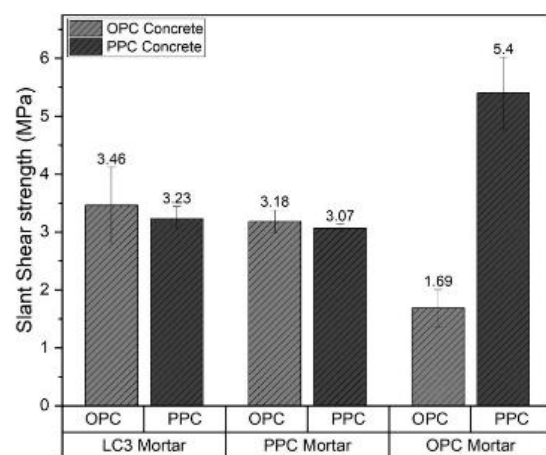
Fig. 4.3: Split tensile strength

Fig. 4.4: Slant Shear strength

Similarly, in case of slant shear test, LC^3 mortar manifests same bonding with the substrate as that that OPC and PPC mortar shown in Fig. 4.4. Overall, it can be concluded that the LC^3 mortar is capable of achieving similar bond with OPC and PPC substrate concrete as that the conventional OPC or PPC mortars.
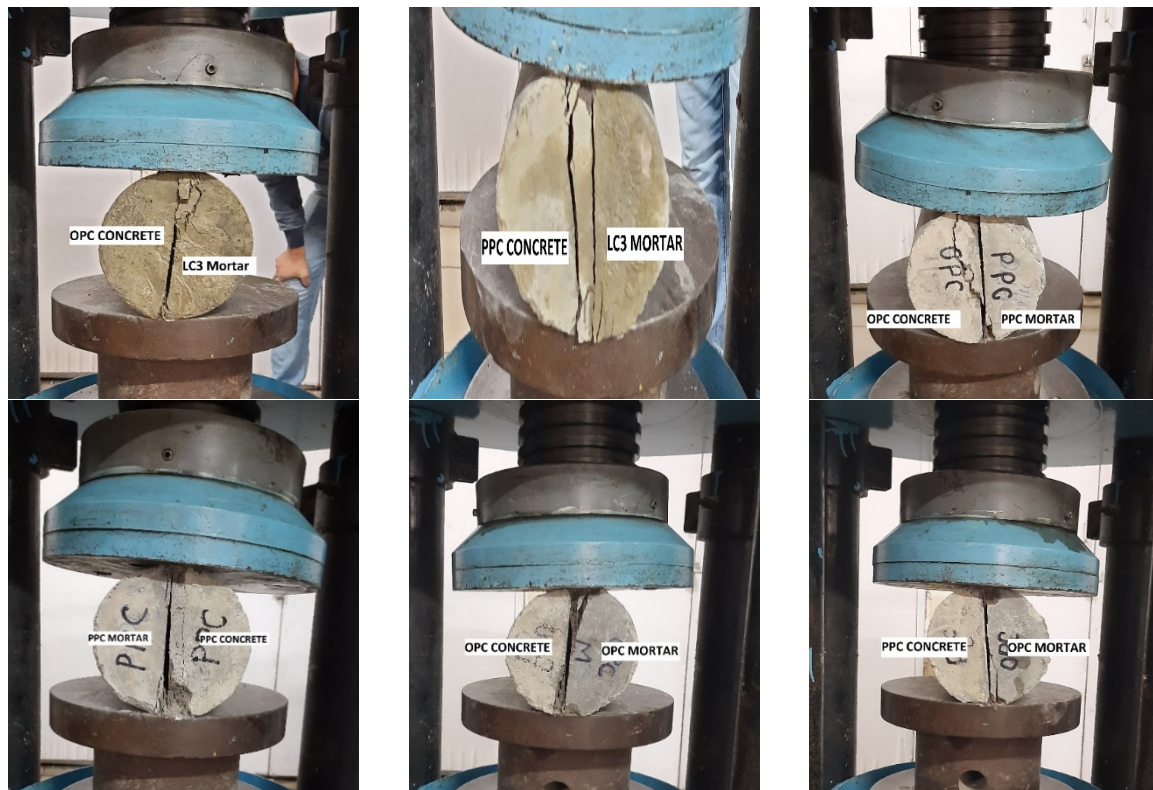

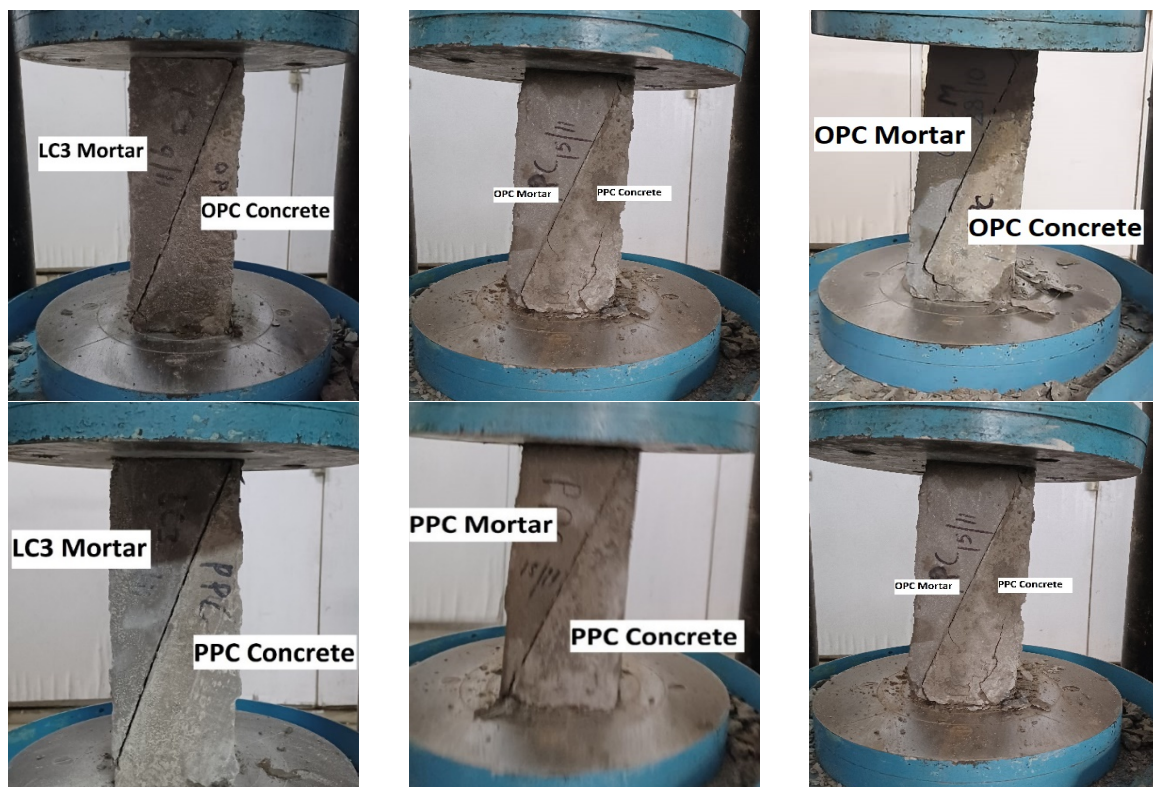Fig. 4.5 : Split tensile test failure pattern

Fig. 4.6: Slant shear test failure pattern

Failure patterns of the split tensile and slant shear tests are shown in Fig.4.5 and Fig. 4.6. It can be observed that two types of failure pattern have occurred, one through the interface, one through the substrate concrete. In most cases the failure has happened by cracking in the substrate concrete. In few specimen failure has been observed at the interface of the bonds [4].

4.3. Transport Properties
4.3. Water Boiling

Porosity determined at 28 days show highest porosity for LC^3, which is quite similar to that of PPC porosity whereas for OPC minimum value for porosity is observed. At 56 days, porosity results as shown in Fig. 4.7 exhibit maximum value for OPC and lowest in case of PPC and LC^3. The reduction in porosity of the LC^3 and PPC is the formation of solids and refinement of pores as a result of pozzolanic reaction which takes place at later stage when sufficient alkalinity is present in the system to carry out the reaction with the Fly ash and calcined clays in PPC and LC^3 respectively.
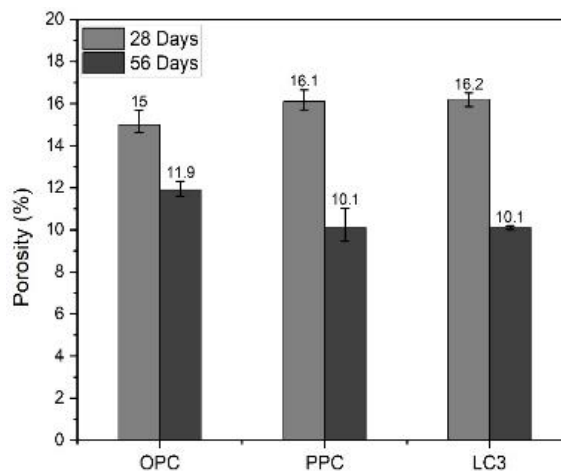

Fig. 4.7: Total Porosity

4.3.2. Oxygen permeability

Oxygen permeability index gives insight about degree of compaction, interconnection of pores which is a deciding factor in the migration of ions from external environment to the inside of concrete. OPT results at 28 days show that OPI value is highest for PPC followed by OPC and lowest for LC^3. However, according to OPI classification all three mortars lie in the range of good to excellent shown in Fig.8.
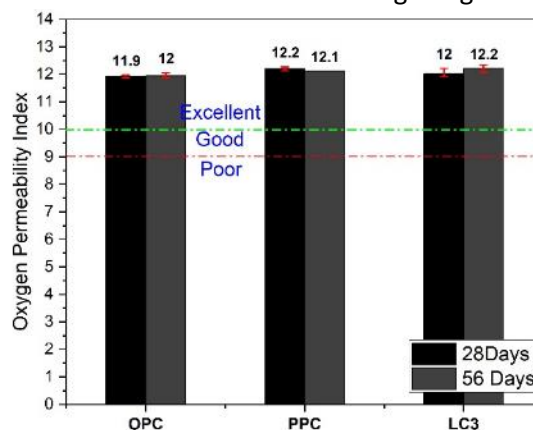

Fig.4.8: Oxygen permeability index value of mortars at 28 day and 56 day

4.4. Corrosion rate monitoring

Non-destructive techniques to evaluate the status of corrosion in the slab specimens has been discussed in the Table. 6.

Table 36: Criteria for classification of corrosion level [5]

Corrosion level		Corrosion rate [μm/yr]	Half-cell potential [mV(CSE)]	Resistivity [kΩ·cm]	Criteria
1	Negligible	$< X_L$	-	-	$X_L = 1$ μm/yr
		$X_L \sim X_M$	$\geq E_{cr}$	$\geq \rho_{cr}$	$X_M = 3 \sim 5$ μm/yr*
2	Low	$X_L \sim X_M$	$< E_{cr}$	$< \rho_{cr}$	$X_H = 10$ μm/yr
		$X_M \sim X_H$	$\geq E_{cr}$	$\geq \rho_{cr}$	$E_{cr} = -200$ mV(CSE)
3	Moderate	$X_M \sim X_H$	$< E_{cr}$	$< \rho_{cr}$	$\rho_{cr} = 100 \sim 120$ kΩ·cm†
		$> X_H$	$\geq E_{cr}$	$\geq \rho_{cr}$	
4	High	$> X_H$	$< E_{cr}$	$< \rho_{cr}$	

4.4.1. Half-Cell Potential (mV)

Half-cell potential indicates the likelihood of corrosion at the time of measurement. Half-cell potential readings have been obtained complementary with RapiCor instrument. Half-cell potential readings have been taken over the rebar somewhere at the centre of the rebar. In RapiCor the reference electrode is silver-silver chloride electrode, this potential has been converted to copper-copper sulphate electrode potential as shown in Fig. 4.9 According to ASTM C876, numeric magnitude technique has been followed to interpret the results. The above mentioned code states that potential more positive than -200mV indicate no corrosion activity (<10% risk) and potential more negative than -350mV indicate greater than 90% corrosion risk, between -200mV and -350mV there is an uncertainty over the corrosion activity. In OPC and PPC control specimen without chlorides (O-CS and P-CS) HCP values lie in low corrosion risk zone however after a period of six months hike in corrosion risk appears in these samples. This could be attributed to the high w/c ratio, perhaps leading to high porosity which makes the oxygen and moisture available from the ambient environment. OPC (O-Cl) and PPC (P-Cl) concrete specimen with chlorides exhibit high negative potential at all measurement. Due to presence of high amount of chloride (3%) and high w/c ratio a high risk of corrosion is observed. In case of specimen having repair mortar application, HCP values lie in the range of uncertain and above 90% risk of corrosion. This is an indication that there is formation of anode on rebar. It can be observed that HCP value after 6 months for OPC, PPC and LC3 repair mortar have appear to become more positive than the initial values that were more negative. This might be due to the hindrance provided by the repair mortars to the ingress of moisture and oxygen from the atmosphere.
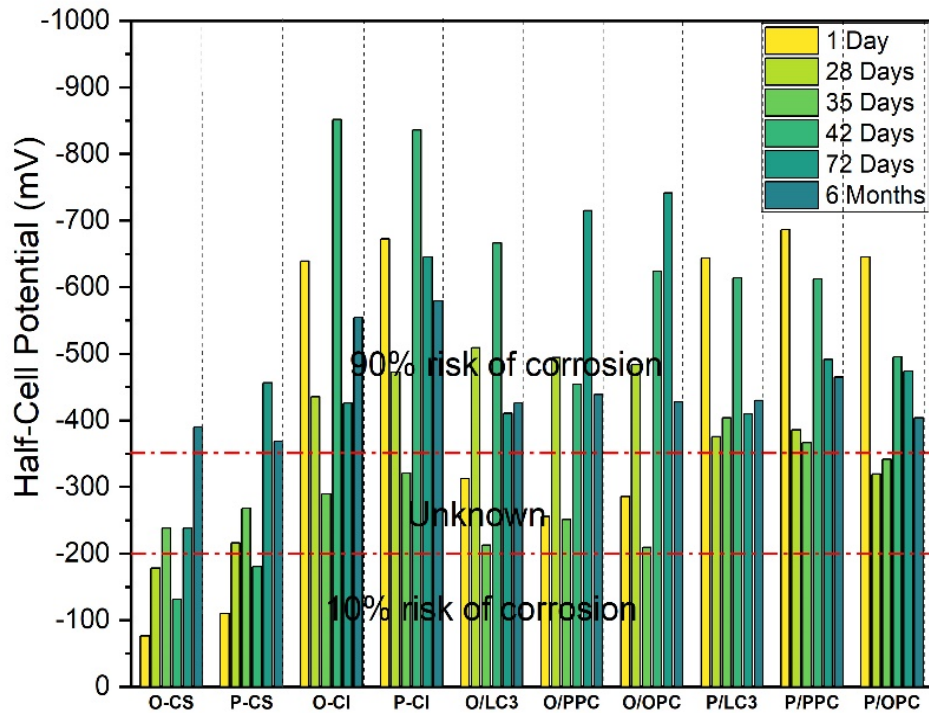
Fig.4.9: Half-Cell potential

4.4.2. Resistivity (k ohm-cm)

Electrical resistance depends upon the microstructure of paste and moisture content of concrete. Electrical resistance is useful in conjunction with half-cell potential results. Surface resistivity values have been shown in Fig. 4.10. According to ACI 222R 01 corrosion rate can be grouped as high, moderate and low based on the surface resistivity values (blue text in Fig. 4.12). High resistivity values indicate that even if the rebar is corroding as indicated by the half-cell potential values, the rate of corrosion may be low. High resistivity values are indicated in control specimen with OPC and PPC concrete at every measurement taken. Resistivity for concrete specimens with chlorides are lowest, imposing that a high or moderate corrosion rate may be going on. The presence of chloride ions in the bulk concrete increases the conductivity. Resistivity values for LC^3 repair mortar are high at each time of measurement giving an indication of low corrosion activity. However, there may be anode formation as indicated by the HCP values. In case of PPC, most values indicate having low to moderate corrosion rate and resistivity values seems to increase with increasing time. In OPC repair mortar resistivity values are low as compared to PPC and LC^3 repair mortar indicating high or moderate corrosion rate. Overall it can be noticed that resistivity values seem to be increasing for last two readings. This may be due to the fact that moisture availability in the pores of the mortar may be reducing with increasing time and resistivity is controlled by the moisture condition of the sample.
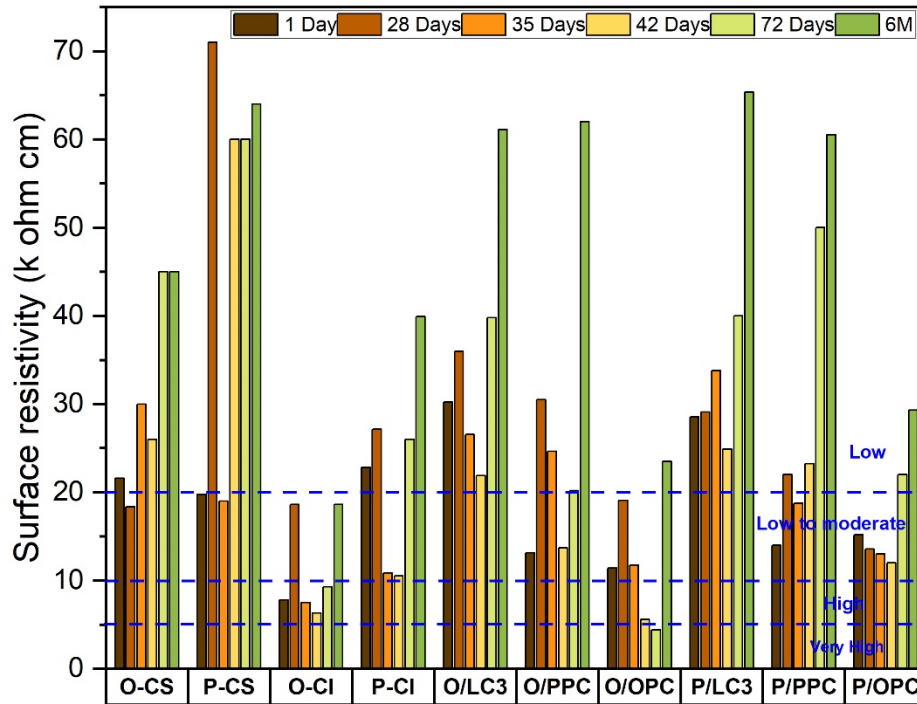
Fig. 4.10: Surface resistivity (kohm-cm)

The LC[3] repair mortar whether applied on OPC or PPC concrete seem to attain the high resistivity values almost similar to that of concrete after 6 months. Thus, repair mortar application instead of concrete where cover is low can be done to shield the substrate concrete from further deterioration. Hence, corrosion rate can provide more clear idea about corrosion activity in the rebar and a correlation can be established between these two parameters.

4.4.3. Corrosion Rate (µm/yr)

Corrosion rate monitoring has been done at various time intervals. First reading of corrosion rate was taken after 28 days of curing hence it has been written as 1 day. Corrosion rate can be considered negligible when it is below 2 µm/yr, low between 2 and 5 µm/yr, moderate between 5-10 µm/yr, intermediate between 10-50 µm/yr, high between 50-100 µm/yr and very high above 100 µm/yr. It can be inferred from Fig. 4.11 that corrosion rate lies in negligible range for PPC and OPC concrete control specimen. Despite having high w/c ratio corrosion rate is low in these specimen. In case of PPC and OPC concrete specimen with chloride corrosion rate lies in the category of low however after 6 months corrosion rate seems to increase as compared to the previous values. This is attributed to the presence of large amount of free chloride ions in the complete concrete specimen. Unlike this, in case of LC[3] cast on OPC concrete corrosion rate lies in low range though but after 6 months slight increase has been observed whereas corrosion rate in LC3 on PPC substrate after 6 months is negligible. In case of PPC mortar corrosion rate is in low category and with time seems to decrease. Similarly, in OPC corrosion rate tends to decrease with time and fall in low to negligible range.
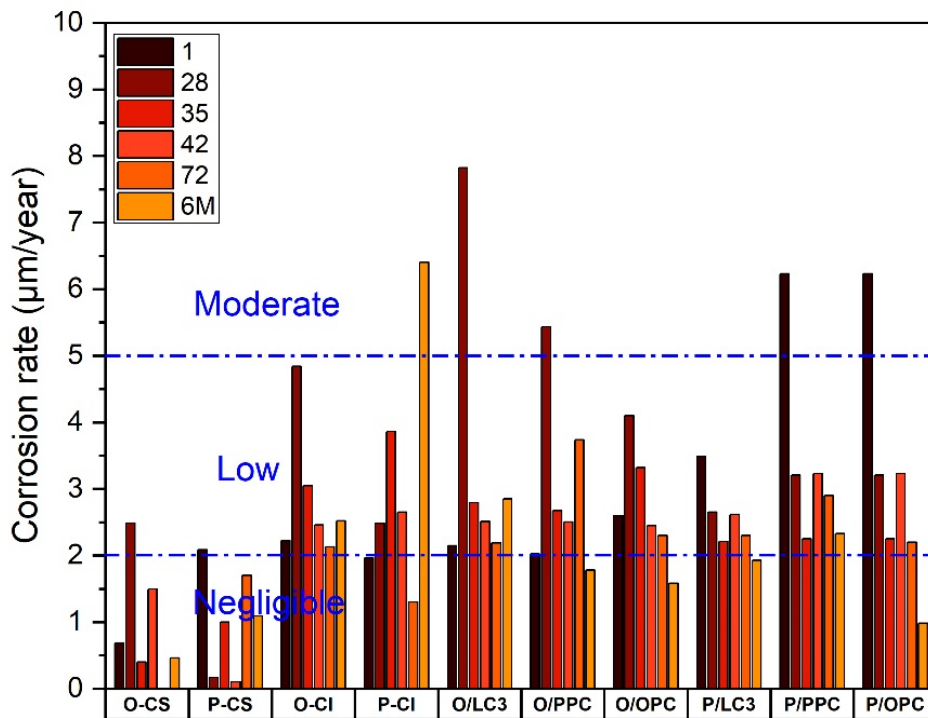
Fig. 4.11: Corrosion rate (µm/year)

5. Conclusion

This study was proposed fundamentally to determine the rate of corrosion in reinforced concrete where application of repair mortar has been done. The following conclusion has been made based upon the results obtained through various experiments performed.

- LC^3 mortar achieves similar strength as that of the OPC at later ages, thus can be used as a substitute to the PPC and OPC mortars even in repair work applications
- LC^3 mortar is compatible with the substrate concrete and exhibits similar bond strength with OPC and PPC substrate concrete as that of the PPC and OPC mortars
- Transport properties study of LC^3 mortar indicate that
    - the porosity is reduced at later ages thus susceptibility to the ingress of moisture and detrimental ions is reduced too
    - Rate of water absorption test indicates that LC^3 has lower initial water absorption rate at later ages and similar results has been observed in secondary water absorption concluding that LC^3 will ingress water from the environment at a slower rate thus taking more time for moisture to reach the rebar level
    - Oxygen permeability index of LC^3 lies in excellent range thus indicating lesser interconnected pores and slower ingress of moisture up to the rebar
- Results of corrosion rate monitoring in slab specimens has been depicted the by half-cell potential, resistivity, corrosion rate.
    - Half-cell potential indicate that there is the formation of anode in the rebar for all specimen after 6 months of time duration however, these values seems to be moving slight on positive sides as compared to readings taken at earlier age, indicating lower moisture and oxygen availability
    - Surface resistivity of LC^3 mortar is higher than the PPC and LC^3 mortar, however the surface resistivity is sensitive to the moisture level in the mortar. High resistivity values of LC^3 are an indication of the fact that corrosion is ongoing at a low rate despite the formation of anode as indicated by the half-cell potential.

- Corrosion rate in slab specimens with LC^3 mortar is in negligible to low range. The rate of corrosion appears to decrease with time (after 6 months) for all types of specimen including LC^3. Corrosion rate

References

[1] Montemor, M. F., Simoes, A. M. P., & Ferreira, M. G. S. (2003). Chloride-induced corrosion on reinforcing steel: from the fundamentals to the monitoring techniques. *Cement and concrete composites*, *25*(4-5), 491-502.

 [2] Alexander, M. G., Beushausen, H. D., Dehn, F., & Moyo, P. (Eds.). (2008). *Concrete Repair, Rehabilitation and Retrofitting II: 2nd International Conference on Concrete Repair, Rehabilitation and Retrofitting, ICCRRR-2, 24-26 November 2008, Cape Town, South Africa*. CRC Press.

[3] Avet, F., & Scrivener, K. (2020). Influence of pH on the chloride binding capacity of Limestone Calcined Clay Cements (LC3). *Cement and Concrete Research*, *131*, 106031.

[4] Zanotti, C., Borges, P. H., Bhutta, A., & Banthia, N. (2017). Bond strength between concrete substrate and metakaolin geopolymer repair mortar: Effect of curing regime and PVA fiber reinforcement. *Cement and Concrete Composites*, *80*, 307-316.

[5] Luping, T., & Utgenannt, P. (2007). Chloride Ingress and Reinforcement Corrosion in Concrete under De-Icing Highway Environment-A study after 10 years' field exposure.